

IFIP AICT 419



Daoliang Li
Yingyi Chen
(Eds.)

Computer and Computing Technologies in Agriculture VII

7th IFIP WG 5.14 International Conference, CCTA 2013
Beijing, China, September 18-20, 2013
Revised Selected Papers, Part I

1 Part I

 Springer

Editor-in-Chief

A. Joe Turner, Seneca, SC, USA

Editorial Board

Foundations of Computer Science

Mike Hinchey, Lero, Limerick, Ireland

Software: Theory and Practice

Michael Goedicke, University of Duisburg-Essen, Germany

Education

Arthur Tatnall, Victoria University, Melbourne, Australia

Information Technology Applications

Ronald Waxman, EDA Standards Consulting, Beachwood, OH, USA

Communication Systems

Guy Leduc, Université de Liège, Belgium

System Modeling and Optimization

Jacques Henry, Université de Bordeaux, France

Information Systems

Jan Pries-Heje, Roskilde University, Denmark

ICT and Society

Jackie Phahlamohlaka, CSIR, Pretoria, South Africa

Computer Systems Technology

Paolo Prinetto, Politecnico di Torino, Italy

Security and Privacy Protection in Information Processing Systems

Kai Rannenber, Goethe University Frankfurt, Germany

Artificial Intelligence

Tharam Dillon, Curtin University, Bentley, Australia

Human-Computer Interaction

Annelise Mark Pejtersen, Center of Cognitive Systems Engineering, Denmark

Entertainment Computing

Ryohei Nakatsu, National University of Singapore

IFIP – The International Federation for Information Processing

IFIP was founded in 1960 under the auspices of UNESCO, following the First World Computer Congress held in Paris the previous year. An umbrella organization for societies working in information processing, IFIP's aim is two-fold: to support information processing within its member countries and to encourage technology transfer to developing nations. As its mission statement clearly states,

IFIP's mission is to be the leading, truly international, apolitical organization which encourages and assists in the development, exploitation and application of information technology for the benefit of all people.

IFIP is a non-profitmaking organization, run almost solely by 2500 volunteers. It operates through a number of technical committees, which organize events and publications. IFIP's events range from an international congress to local seminars, but the most important are:

- The IFIP World Computer Congress, held every second year;
- Open conferences;
- Working conferences.

The flagship event is the IFIP World Computer Congress, at which both invited and contributed papers are presented. Contributed papers are rigorously refereed and the rejection rate is high.

As with the Congress, participation in the open conferences is open to all and papers may be invited or submitted. Again, submitted papers are stringently refereed.

The working conferences are structured differently. They are usually run by a working group and attendance is small and by invitation only. Their purpose is to create an atmosphere conducive to innovation and development. Refereeing is also rigorous and papers are subjected to extensive group discussion.

Publications arising from IFIP events vary. The papers presented at the IFIP World Computer Congress and at open conferences are published as conference proceedings, while the results of the working conferences are often published as collections of selected and edited papers.

Any national society whose primary activity is about information processing may apply to become a full member of IFIP, although full membership is restricted to one society per country. Full members are entitled to vote at the annual General Assembly, National societies preferring a less committed involvement may apply for associate or corresponding membership. Associate members enjoy the same benefits as full members, but without voting rights. Corresponding members are not represented in IFIP bodies. Affiliated membership is open to non-national societies, and individual and honorary membership schemes are also offered.

Daoliang Li Yingyi Chen (Eds.)

Computer and Computing Technologies in Agriculture VII

7th IFIP WG 5.14 International Conference, CCTA 2013
Beijing, China, September 18-20, 2013
Revised Selected Papers, Part I



Springer

Volume Editors

Daoliang Li
Yingyi Chen
China Agricultural University
China-EU Center for Information
and Communication Technologies in Agriculture (CICTA)
17 Tsinghua East Road, Beijing 100083, P.R. China
E-mail: {dliang, chenyingyi}@cau.edu.cn

ISSN 1868-4238

e-ISSN 1868-422X

ISBN 978-3-642-54343-2

e-ISBN 978-3-642-54344-9

DOI 10.1007/978-3-642-54344-9

Springer Heidelberg New York Dordrecht London

Library of Congress Control Number: 2014931263

© IFIP International Federation for Information Processing 2014

This work is subject to copyright. All rights are reserved by the Publisher, whether the whole or part of the material is concerned, specifically the rights of translation, reprinting, reuse of illustrations, recitation, broadcasting, reproduction on microfilms or in any other physical way, and transmission or information storage and retrieval, electronic adaptation, computer software, or by similar or dissimilar methodology now known or hereafter developed. Exempted from this legal reservation are brief excerpts in connection with reviews or scholarly analysis or material supplied specifically for the purpose of being entered and executed on a computer system, for exclusive use by the purchaser of the work. Duplication of this publication or parts thereof is permitted only under the provisions of the Copyright Law of the Publisher's location, in its current version, and permission for use must always be obtained from Springer. Permissions for use may be obtained through RightsLink at the Copyright Clearance Center. Violations are liable to prosecution under the respective Copyright Law.

The use of general descriptive names, registered names, trademarks, service marks, etc. in this publication does not imply, even in the absence of a specific statement, that such names are exempt from the relevant protective laws and regulations and therefore free for general use.

While the advice and information in this book are believed to be true and accurate at the date of publication, neither the authors nor the editors nor the publisher can accept any legal responsibility for any errors or omissions that may be made. The publisher makes no warranty, express or implied, with respect to the material contained herein.

Typesetting: Camera-ready by author, data conversion by Scientific Publishing Services, Chennai, India

Printed on acid-free paper

Springer is part of Springer Science+Business Media (www.springer.com)

Preface

First of all, I must express my sincere thanks to all authors who submitted research papers to support the 7th International Conference on Computer and Computing Technologies in Agriculture (CCTA2013) held in Beijing, China, during September 18–20, 2013.

The conference was hosted by the China Agricultural University; the IFIP TC5 Work Group (WG) on Advanced Information Processing for Agriculture (AIPA); the Agricultural Engineering Information Committee, Chinese Society of Agricultural Engineering. It was organized by the China-EU Centre for Information & Communication Technologies (CICTA).

Proper scale management is not only a necessary approach for agro-modernization and agro-industrialization but it is also required for the development of agricultural productivity. Thus, the application of different technologies in agriculture has become especially important and “informatized agriculture” and the “Internet of Things” have been sought out by many countries recently in order to scientifically manage agriculture so as to achieve low costs and high income. CICTA aims at boosting research on advanced and practical technologies applied in agriculture and promoting international communication and cooperation, and has successfully held seven international conferences since 2007.

The topics of CCTA2013 cover a wide range of interesting theory and applications of all kinds of technology in agriculture, including: the Internet of things and cloud computing; simulation models and decision-support systems for agricultural production; smart sensor, monitoring, and control technology; traceability and e-commerce technology; computer vision, computer graphics, and virtual reality; the application of information and communication technology in agriculture; and universal information service technology and service system development in rural areas.

We selected the 115 best papers among all those submitted to CCTA2013 for these proceedings, and all the papers are divided into two thematic sections. In this volume, creative thoughts and inspirations could be discovered, discussed and disseminated. It is always exciting to have experts, professionals, and scholars getting together with creative contributions to share inspiring ideas and hopefully accomplish great developments in these technologies of high demand.

Finally, I would like to express my sincere thanks to all the authors, speakers, session chairs, and attendees, both local and international for their active participation and support of this conference.

January 2014

Daoliang Li
Chair of CCTA2013

Conference Organization

Sponsors

- China Agricultural University
- The IFIP TC5 Work Group (WG) on Advanced Information Processing for Agriculture (AIPA)
- Agricultural Engineering Information Committee, Chinese Society of Agricultural Engineering

Organizer

- China-EU Center for Information & Communication Technologies in Agriculture (CICTA)

Chair

- Daoliang Li

Conference Secretariat

- Lihong Shen

Table of Contents – Part I

The Application Study of Electronic Farming in the Ecology Construction in Chinese Tropical Area	1
<i>Meng Meng, Xiaofei Zheng, and Jiabin Wang</i>	
Developments on Informatization Technology in Agricultural Operations in China	10
<i>Qiuping Zhou and Guohua Fu</i>	
The Parameter Optimization and Performance Analysis of the Suspension System in the Cab of a Heavy Truck	16
<i>Jihai Gu, Hui Wang, Chengwen Wang, Ming Pang, and Xiangyang Jin</i>	
Evolution of Growing Season Precipitation Series in the West Region of Heilongjiang Province Based on Wavelet Analysis	25
<i>Wensheng Zheng, Sijia Shi, and Zhenping Gong</i>	
The Matching Research of Strawberry Diseases Image Features Based on KD-Tree Search Method	32
<i>Jianshu Chen, Jianlun Wang, Shuting Wang, and Hao Liu</i>	
Research on Automatic Irrigation Algorithm of Strawberry Greenhouse Based on PLC	41
<i>Jianlun Wang, Shuting Wang, Jianshu Chen, Hao Liu, and Dongbo Xu</i>	
A Dynamic Knowledge Models of Nitrogen Fertilizer and Computer System for Cotton	52
<i>ChunJing Si</i>	
Research and Design of One Webpage System for Each Village in Shandong Province	61
<i>Wenjie Feng, Huaijun Ruan, Yan Tang, Wenxiang Zhao, Qingfu Kong, and Fengyun Wang</i>	
Simulation Study of Winter Wheat Photosynthate Distribution Effect on Controlled Water and Fertilizer Measure	69
<i>Yan Li, Yang-ren Wang, and Shuhong Sun</i>	
Secure Gateway of Internet of Things Based on AppWeb and Secure Sockets Layer for Intelligent Granary Management System	78
<i>Rong Tao, Senbin Yang, Wei Tan, and Changqing Zhang</i>	
Feature Based Hole Filling Algorithm on Triangular Mesh	90
<i>Bin Xu, Zhongke Li, and Ying Tan</i>	

Design and Implementation of Aquarium Remote Automation Monitoring and Control System	102
<i>Yinchi Ma and Wen Ding</i>	
Study on Conditional Autoregressive Model of Per Capita Grain Possession in Yellow River Delta	109
<i>Yujian Yang, Huaijun Ruan, Yan Tang, Wenxiang Zhao, and Xueqin Tong</i>	
Agent-Based Simulation of Rural Areas and Agriculture Information of 11 Country Units in Shandong Province	117
<i>Yujian Yang, Lili Wang, Qingyu Chen, and Jingling Li</i>	
Influence of Digital Computer Technology on Architectural Design Teaching Mode	123
<i>Huang Ting and Jiang Sicheng</i>	
Optimization Design on Deep-Fertilization Fertilizer Amount Adjusting Mechanism for Paddy Field	128
<i>Jinfeng Wang, Detang Zou, Jinwu Wang, and Xinlun Yang</i>	
Testing and Analysis of the Shear Modulus of Urea Granules	137
<i>Jinfeng Wang, Detang Zou, Jinwu Wang, and Wei Zhou</i>	
Analysis and Evaluation the Websites of Agridata Base on Link Analysis	145
<i>Jian Wang and Ding-feng Wu</i>	
Discussion on Fruiter Professional Information Service Mode of Shandong Province	152
<i>Zhi-jun Wang, Meng Jiang, and Shu-han Cheng</i>	
The Application of Image Retrieval Technology in the Prevention of Diseases and Pests in Fruit Trees	160
<i>Zhi-jun Wang, Xin Liu, Meng Jiang, and Shu-han Cheng</i>	
Advances in the Application of Image Processing Fruit Grading	168
<i>Chengjun Fang and Chunjian Hua</i>	
Using Memcached to Promote Unified User Management System	175
<i>Zuliang Zhao, Xiaodong Zhang, Lin Li, Zhe Liu, De-Hai Zhu, and Shao-Ming Li</i>	
A Growth Measuring Approach for Maize Based on Computer Vision . . .	183
<i>Chuanju Wang, Boxiang Xiao, Xinyu Guo, and Sheng Wu</i>	
The Comprehensive Assessment of Planting Elements Based on Analytic Hierarchy Process	190
<i>Yujian Yang, Huaijun Ruan, Jingling Li, and Lei Wang</i>	

The Monitoring of Rare Earths Mining from the Gannan Area of Southern China Using Remote Sensing Technology	197
<i>Baoying Ye, Zhenghui Chen, Nisha Bao, and Ying Li</i>	
A Survey on Farmland Crop Information Acquisition	206
<i>Danqin Yi and Haiyan Ji</i>	
Self-tuning PID-type Fuzzy Adaptive Control for CRAC in Datacenters	215
<i>Junwen Deng, Liu Yang, Xinrong Cheng, and Wu Liu</i>	
Spatio-temporal Variability Analysis of Soil Volumetric Moisture Content on the Field Scale	226
<i>Xueqin Tong, Yujian Yang, and Wei Dong</i>	
Taxonomy of Source Code Security Defects Based on Three-Dimension- Tree	232
<i>Yan Zhang, Guowei Dong, Tao Guo, and Jianyu Yang</i>	
Path Recognition for Agricultural Robot Vision Navigation under Weed Environment	242
<i>Peidong Wang, Zhijun Meng, Changhai Luo, and Hebo Mei</i>	
Application of LS-SVM and Variable Selection Methods on Predicting SSC of Nanfeng Mandarin Fruit	249
<i>Tong Sun, Wenli Xu, Tian Hu, and Muhua Liu</i>	
A Novel Robust Method for Automatic Detection of Traffic Sign	263
<i>Bo Peng and Juan Wu</i>	
The Vulnerability Assessment Method for Beijing Agricultural Drought	269
<i>Lingmiao Huang, Peiling Yang, and Shumei Ren</i>	
Application of Modbus Protocol Based on μC /TCPIP in Water Saving Irrigation in Facility Agricultural	281
<i>Jin-lei Li, Wen-gang Zheng, Chang-jun Shen, and Ke-wu Wang</i>	
The Soil Heavy Metal Information Accurate Collection and Evaluation about <i>Lycium Barbarum</i> Cultivation in Western China	289
<i>Ming Xiao, Wenjun Yang, Ze Zhang, Xianglin Tang, Xin Lv, and Dezhao Chi</i>	
Research on the Optimization of Agricultural Supply Chain Based on Internet of Things	300
<i>Guangsheng Zhang</i>	
Measurement and Study on Drying Shrinkage Characteristic of Tobacco Lamina Based on Computer Vision	306
<i>Wenkui Zhu, Zhaogai Wang, Delong Xu, and Jinsong Du</i>	

Research of PID Algorithm for Valve Controlled Hydraulic Motor Variable Rate Fertilizer Control System	315
<i>Chunying Liang, Xi Wang, Jianwei Ji, Qianhui Xu, and Peng Lü</i>	
OAPRS: An Online Agriculture Prescription Recommendation System	327
<i>Qingtian Zeng, Zhichao Liang, Weijian Ni, and Hua Duan</i>	
Study of Rice Identification during Early Season Using Multi-polarization TerraSAR-X Data	337
<i>Lin Guo, Zhiyuan Pei, Shangjie Ma, Juanying Sun, and Jiali Shang</i>	
Color Image Segmentation in RGB Color Space Based on Color Saliency	348
<i>Chen Zhang, Wenzhu Yang, Zhaohai Liu, Daoliang Li, Yingyi Chen, and Zhenbo Li</i>	
Water-Landscape-Ecological Relationship and the Optimized Irrigation Strategy for Green-Roof Plants in Beijing, a Case Study for <i>Euonymus</i> <i>japonicus</i>	358
<i>Caiyuan Wang, Peiling Yang, Yunkai Li, and Shumei Ren</i>	
Design and Implementation of Agro-technical Extension Information System Based on Cloud Storage	371
<i>Leifeng Guo, Wensheng Wang, Yong Yang, and Zhiguo Sun</i>	
Analyzing Thermal Infrared Image Characteristics of Maize Seedling Stage	380
<i>Zilong Chen, Dazhou Zhu, Xiangrong Ren, Hua Cong, Cheng Wang, and Chunjiang Zhao</i>	
Modeling Design and Application of Low-Temperature Plasma Treatment Test Stand for Seeds before Sowing	393
<i>Changyong Shao, Yong You, Guanghui Wang, Zhiqin Wang, Yan Li, Lijing Zhao, Xin Tang, Liangdong Liu, and Decheng Wang</i>	
Research on Rapid Identification Method of Buckwheat Varieties by Near-Infrared Spectroscopy Technique	401
<i>Fenghua Wang, Ju Yang, Zhiyong Xi, and Hailong Zhu</i>	
The Characteristic of Hyperspectral Image of Wheat Seeds during Sprouting	408
<i>Jiayu Chen, Honghui Chen, Xiaodong Wang, Chunhua Yu, Cheng Wang, and Dazhou Zhu</i>	
Control Software Design of Plant Microscopic Ion Flow Detection Motion Device	422
<i>Lulu He, Fubin Jiang, Dazhou Zhu, Peichen Hou, Baozhu Yang, Cheng Wang, and Jiuwen Zhang</i>	

Interactive Information Service Technology of Tea Industry Based on Demand-Driven	434
<i>Xiaohui Shi and Tian'en Chen</i>	
Design and Development of Intelligent Monitoring System for Plastic Tea Greenhouse	443
<i>Fengyun Wang, Jiye Zheng, Lin Mei, Zhaotang Ding, Wenjie Feng, and Lei Wang</i>	
Research on the Method of Simulating Knowledge Structure of the Information Searchers — Illustrated by the Case of Pomology Information Retrieval	450
<i>Ding-feng Wu, Guo-min Zhou, Jian Wang, and Jian Wang</i>	
Strategies for High Yield Inferred through Path Analysis of Major Economical Traits in Yongyou 8, a Hybrid Late Season Japonica Rice	458
<i>Weiming Liu, Enguo Wang, Shanyou Huang, and Xianbiao He</i>	
Mathematical Modeling and Optimization of Schemes of Major Agronomic Factors for Hybrid Rice ‘Yongyou 17’	464
<i>Weiming Liu and Zuda Bao</i>	
Segmentation of Small Animal Computed Tomography Images Using Original CT Values and Converted Grayscale Values	470
<i>Guoqiang Ma, Naixiang Li, and Xiaojuan Wang</i>	
Design and Implementation of Laiwu Black Information Management System Based on ExtJS	478
<i>Dong Chen, Pingzeng Liu, Yunfan Zhang, and Hongjian Ma</i>	
Fresh Tea Picking Robot Based on DSP	486
<i>Heng Li, Chao Li, Liming Xu, Guangming Qin, Xin Lu, and Ying Zhao</i>	
Study on Cloud Service Mode of Agricultural Information Institutions	497
<i>Xiaorong Yang, Neng-fu Xie, Dan Wang, and Li-hua Jiang</i>	
Impact of Simulated Irrigation with Treated Wastewater and Saline- Sodic Solutions on Soil Hydraulic Conductivity, Pores Distribution and Fractal Dimension	502
<i>Fangze Shang, Shumei Ren, Tian Zou, Peiling Yang, and Nuan Sun</i>	
Author Index	517

Table of Contents – Part II

Maize Seed Embryo and Position Inspection Based on Image Processing	1
<i>Yingbiao Wang, Liming Xu, Xueguan Zhao, and Xingjie Hou</i>	
Greenhouse Irrigation Optimization Decision Support System	10
<i>Dongmei Zhang, Ping Guo, Xiao Liu, Jinliang Chen, and Chong Jiang</i>	
Study on Pear Diseases Query System Based on Ontology and SWRL	24
<i>Qian Sun and Yong Liang</i>	
Applications and Implementation of Decomposition Storage Model (DSM) in Paas of Agricultural	34
<i>Shuwen Jiang, Tian'en Chen, Jing Dong, and Cong Wang</i>	
Estimation of Pig Weight by Machine Vision: A Review	42
<i>Zhuo Li, Cheng Luo, Guanghui Teng, and Tonghai Liu</i>	
Agricultural Field Environment High-Quality Image Remote Acquisition	50
<i>Junqian Fu, Deqin Xiao, and Xiaohui Deng</i>	
Study on Consultative Agricultural Knowledge Service System	61
<i>Xiguang Wang</i>	
Stochastic Simulation and Application of Monthly Rainfall and Evaporation	70
<i>Nana Han and Yang-ren Wang</i>	
Elimination Method Study of Ambiguous Words in Chinese Automatic Indexing	79
<i>Dan Wang, Xiaorong Yang, and Jie Zhang</i>	
Analysis and Evaluation of Soil Fertility Status Based on Weighted K-means Clustering Algorithm	89
<i>Guifen Chen, Lixia Cai, Hang Chen, Liying Cao, and Chunan Li</i>	
Effect of Website Quality Factors on the Success of Agricultural Products B2C E-commerce	98
<i>Ping Yu and Dongmei Zhao</i>	
Importance of Information Systems in the Evaluation and Research of Nutrition and Health of Key Groups in China's Rural Areas	114
<i>Liqun Guo, Bo Peng, and Zhenxiang Huang</i>	

The Classification of Pavement Crack Image Based on Beamlet Algorithm	129
<i>Aiguo Ouyang, Qin Dong, Yaping Wang, and Yande Liu</i>	
Research on the Construction and Implementation of Soil Fertility Knowledge Based on Ontology	138
<i>Li Ma, Helong Yu, Guifen Chen, Liying Cao, and Yue Wang</i>	
Virtual Prototype Design of Double Disc Mower Drive Bracket Based on ANSYS Workbench	145
<i>Ning Zhang, Manquan Zhao, Yanhua Shi, and Yueqin Liu</i>	
Research on 3G Terminal-Based Agricultural Information Service	152
<i>Neng-fu Xie and Xuefu Zhang</i>	
Study on Semantic Heterogeneity Elimination of Agricultural Product Price Information in Multi-source Network	158
<i>Jing Zhang, Guo-min Zhou, Jian Wang, Jie Zhang, and Fangli Xie</i>	
Study on the Application of Information Technologies on Suitability Evaluation Analysis in Agriculture	165
<i>Ying Yu, Leigang Shi, Heju Huai, and Cunjun Li</i>	
Research of the Early Warning Analysis of Crop Diseases and Insect Pests	177
<i>Dengwei Wang, Tian'en Chen, and Jing Dong</i>	
Study on the Way of Production, Life and Thinking of Farmers in Mobile Internet Era	188
<i>Yong Yang, Wensheng Wang, Leifeng Guo, Zhiguo Sun, and Xiufeng Li</i>	
Studies on Domestic and Overseas in Research Progress of Agricultural Information Technologies	198
<i>Ying Yu, Cunjun Li, Leigang Shi, Heju Huai, and Xiangyang Qin</i>	
Research and Design of Peanut Diseases Diagnosis and Prevention Expert System	212
<i>Kun Zhang, Benjing Zhu, Fengzhen Liu, and Yongshan Wan</i>	
Filling Holes in Triangular Meshes of Plant Organs	222
<i>Zhihui Sun, Xinyu Guo, Shenglian Lu, Weiliang Wen, and Youjia Chen</i>	
Semantic-Based Reasoning for Vegetable Supply Chain Knowledge Retrieval	232
<i>Xinyu Liu, Lifan Hou, and Yonghao Wang</i>	

Spectral Characteristics of Tobacco Cultivars with Different Nitrogen Efficiency and Its Relationship with Nitrogen Use	239
<i>Taibo Liang, Jianwei Wang, Yanling Zhang, Jiaqin Xi, Hanping Zhou, Baolin Wang, and Qisheng Yin</i>	
Research on Agricultural Products Cold-Chain Logistics of Mobile Services Application	247
<i>Congcong Chen, Tian'en Chen, Chi Zhang, and Guozhen Xie</i>	
The WSN Real-Time Monitoring System for Agricultural Products Cold-Chain Logistics	255
<i>Chen Liu, Ruirui Zhang, Tian'en Chen, and Tongchuan Yi</i>	
The Construction of Agricultural Products Traceability System Based on the Internet of Things—The Cases of Pollution-Free Vegetables in Leping of Jiangxi Province	262
<i>Fang Yang</i>	
Key Technologies and Algorithms' Application in Agricultural Food Supply Chain Tracking System in E-commerce	269
<i>Lijuan Huang and Pan Liu</i>	
Evaluation of EPIC Model of Soil NO ₃ -N in Irrigated and Wheat-Maize Rotation Field on the Loess Plateau of China	282
<i>Xuechun Wang, Shishun Tao, Jun Li, and Yongjun Chen</i>	
Three-Dimensional Reconstruction and Characteristics Computation of Corn Ears Based on Machine Vision	290
<i>Jianjun Du, Xinyu Guo, Chuanyu Wang, Sheng Wu, and Boxiang Xiao</i>	
Application of RMAN Backup Technology in the Agricultural Products Wholesale Market System	301
<i>Ping Yu and Nan Zhou</i>	
Effects of Water and Nutrition on Photoassimilates Partitioning Coefficient Variation	309
<i>Jianhua Jin and Yang-ren Wang</i>	
Effect of Water and Nitrogen Stresses on Correlation among Winter Wheat Organs	316
<i>Xin-yang Zhou and Yang-ren Wang</i>	
Application of a Logical Reasoning Approach Based Petri Net in Agriculture Expert System	326
<i>Xia Geng, Yong Liang, and Qiulan Wu</i>	
Fermentation Condition Optimization for Endophytic Fungus BS002 Isolated from <i>Sophora Flavescens</i> by Response Surface Methodology	342
<i>Na Yu and Lu He</i>	

Daily Sales Forecasting for Grapes by Support Vector Machine	351
<i>Qian Wen, Weisong Mu, Li Sun, Su Hua, and Zhijian Zhou</i>	
Research on Text Mining Based on Domain Ontology	361
<i>Li-hua Jiang, Neng-fu Xie, and Hong-bin Zhang</i>	
Accuracy Loss Analysis in the Process of Cultivated Land Quality Data Gridding	370
<i>Lingling Sang, De-Hai Zhu, Chao Zhang, and Wenju Yun</i>	
Research and Application of Variable Rate Fertilizer Applicator System Based on a DC Motor	381
<i>Honglei Jia, Xianzhen Feng, Jiangtao Qi, Xinhui Liu, Chunxi Liu, Yongxi Yang, and Yang Li</i>	
Brief Probe into the Key Factors that Influence Beijing Agricultural Drought Vulnerability	392
<i>Lingmiao Huang, Peiling Yang, and Shumei Ren</i>	
Chinese Web Content Extraction Based on Naïve Bayes Model	404
<i>Jinbo Wang, Lianzhi Wang, Wanlin Gao, Jian Yu, and Yuntao Cui</i>	
Research on the Vegetable Trade Current Situation and Its Trade Competitiveness in China	414
<i>Shasha Li</i>	
A Fault Data Capture Method for Water Quality Monitoring Equipment Based on Structural Pattern Recognition	423
<i>Hao Yang, Daoliang Li, and Yong Liang</i>	
The Analysis of County Science and Technology Worker Internet Usage and Its Influence Factors	434
<i>Huiping Chen, Zhihong Tian, Yubin Wang, and Xue Han</i>	
A Smart Multi-parameter Sensor with Online Monitoring for the Aquaculture in China	444
<i>Fa Peng, Jinxing Wang, Shuangxi Liu, Daoliang Li, Dan Xu, and Yang Wang</i>	
An Intelligent Ammonia Sensor for Livestock Breeding Monitoring	453
<i>Yang Wang, Zetian Fu, Lingxian Zhang, Xinxing Li, Dan Xu, Lihua Zeng, Juncheng Ma, and Fa Peng</i>	
Research on the Knowledge Based Parameterized CAD System of Wheat and Rice Combine Chassis	461
<i>Xingzhen Xu, Shuangxi Liu, Weishi Cao, Peng Fa, Xianxi Liu, and Jinxing Wang</i>	
An Intelligent Search Engine for Agricultural Disease Prescription	469
<i>Weijian Ni, Mei Liu, Qingtian Zeng, and Tong Liu</i>	

Design of Animal Myocardial Contractile Force Detection System Based on Tissue Engineering	478
<i>Guiqing Xi, Ke Han, Ming Zhao, Caojun Huang, and Feng Tan</i>	
Analysis of Airflow Field of Toss Device of Yellow Corn Forage Harvester	486
<i>Yan Huang, Manquan Zhao, and Hantao Liu</i>	
A GPRS-Based Low Energy Consumption Remote Terminal Unit for Aquaculture Water Quality Monitoring	492
<i>Dan Xu, Daoliang Li, Biaoqing Fei, Yang Wang, and Fa Peng</i>	
The Model for the Agricultural Informationalization Benefit Analysis . . .	504
<i>Lifeng Shen, Xiaoqing Yuan, and Daoliang Li</i>	
Strategic Optimal Path and Developmental Environment on Photovoltaic Industry in China Based on an AHP-SWOT Hybrid Model	513
<i>Yiding Zhang and Songyi Dian</i>	
Design of the Unmanned Area Fetching Trolley	523
<i>Xuelun Hu, Licai Zhang, Yaoguang Wei, and Yingyi Chen</i>	
Intelligent Ammonia-Nitrogen Sensor Which Based on Ammonia Electrode	534
<i>Fan Zhang, Yaoguang Wei, Yingyi Chen, and Chunhong Liu</i>	
Dissolved Oxygen Prediction Model Which Based on Fuzzy Neural Network	544
<i>Yalin Liu, Yaoguang Wei, and Yingyi Chen</i>	
Flexible Embedded Telemetry System for Agriculture and Aquaculture	552
<i>André Weiskopf, Frank Weichert, Norbert Fränzel, and Manuel Schneider</i>	
Author Index	561

The Application Study of Electronic Farming in the Ecology Construction in Chinese Tropical Area

Meng Meng, Xiaofei Zheng^{*}, and Jiabin Wang

Institute of Scientific and Technical Information, CATAS, 571737, Danzhou Hainan, China
{Mengmengsir, zs-xf, jia_bin_na}@163.com

Abstract. In this paper, which takes Hainan as an example, analyze the application of Electronic agriculture affairs in the process of building ecology, and aims at proposing the application strategy of Electronic agriculture affairs. The paper points out the advantages of applying electronic agriculture affairs in building ecology and the ways to carry it out. It takes the application of electronic agriculture affairs of Hainan as the focal point and analyzes its application mode. Together with the analysis of the application situation in other areas, it summarizes the problems in the process of applying electronic agriculture affairs. At last, it proposes the countermeasures and solutions in application of electronic agriculture affairs.

Keywords: Ecology Construction, Electronic Farming, Agricultural Informatization, Chinese Tropical Area.

1 Introduction

Information technology has greatly changed the mode of agricultural development and reform, in particular, had a huge impact on the interaction between the markets for agricultural products and agricultural production.

The core to build a new socialist ecology is to develop the agricultural economy and increase rural incomes. It is undoubtedly an effective way to reform the traditional management of agriculture for building new ecology. Electronic agriculture affairs, as an advanced commercial pattern, has great advantages in improving the industrialization degree of agriculture, adjusting agriculture structure, reducing the transaction cost, and expanding the market of the sale of agricultural products.

As the country's largest special economic zone and international tourism island, Hainan is an agricultural province; agricultural information degree of market determines the level of results and to play the role of bridgehead of the new socialist ecology construction in Hainan. Although the province's agricultural information market in recent years has made great progress, especially one-year term of Hainan Winter Fair, rural economic development of Hainan and the surrounding provinces and cities of the more advanced market demand, technology and industrial development

^{*} Corresponding author.

agricultural information. Hainan agricultural market development status, the market is not mature, the trading behavior is not standardized, even the existence of low-quality information, false information events.

The Hainan is a major agricultural province; therefore, to the establishment of a sound, comprehensive agricultural information system to promote rural economic development of Hainan is the urgent task of the agricultural province.

2 New Socialist Ecology Farm Applications Countermeasures

To become boosters of the socialist new socialist ecology construction, the implementation of e-agriculture is very complex system engineering. E-agriculture in the new socialist ecology construction applications may encounter a variety of problems, for the problems that may arise, as well as the construction of a new socialist ecology in the case of successful application of e-agriculture, domestic socialist ecology building applications for electronic farm to make some suggestions.

2.1 The Establishment of Agricultural Information Service System

The establishment of agricultural information service system and gradually establish agricultural means of production and supply system; processing of agricultural products, sales system; agricultural research, teaching, technology extension system; crop seeds, poultry livestock cultivation, breeding, processing, marketing system and agricultural quality inspection and supervision system, a series of agricultural information service system.

2.2 Government Supports

To guide the development of the advanced countries of agricultural products e-commerce demonstration system experience shows that without government involvement and support in e-commerce of agricultural products is difficult to smooth progress. The construction of e-agriculture as the main government departments, and deregulation operating services, promote the diversification of service model, and the promotion of e-agriculture targeted. Government to the grassroots agricultural sites, below the county grass-roots promotion of agricultural technology organizations, rural information service enterprises, farmers, professional and technical associations and intermediary organizations to provide support in all aspects, so that they can on the joint network, the second line people. To strengthen the Government's efforts to support the provision of public information products and services to the majority of farmers, the provision of fiscal and monetary policy support, standardize the order of the information services market.

2.3 Train a New Generation of "Electrical Farmers"

To take various measures to train a new generation of "electrical farmers" the quality of farmers is the key to China's agricultural modernization, but also an important factor in the development of e-commerce of agricultural products. The long-term goal of the departure from the modernization of agriculture, to develop detailed planning to take concrete measures to step-by-step phases, get down to improve farmers' cultural knowledge and agricultural technology.

2.4 Establish the Appropriate Supply Chain and Logistics Systems

To establish the appropriate supply chain and logistics systems agriculture has obvious regional and seasonal characteristics of the different regions, different seasons of the agricultural products to be linked between agriculture and e-commerce platform, which requires the establishment of effective supply chain system, as well as agricultural database. Establish the agricultural supply chain of agricultural logistics system.

2.5 Determine the E-farm Demonstration Sites to Comprehensively Promote Information Technology in Rural Areas Provide a Demonstration Effect

The limited local finance, promote e-agriculture construction impossible to carry out large-scale. Therefore, local governments in promoting informatization construction, make sure that the construction of demonstration sites, building on a small scale. Leading enterprises, agricultural cooperative organizations, large breeding, as the focus of information construction. In the demonstration sites should be taken to the idea of rapid application of high standards of quality, low-input, and to adopt a unified program, unified standards, unified integrated, hierarchical implementation approach, the accumulation of experience in the construction. This information construction in rural areas is very important, and helps to reduce the blind investment and resource conservation, and can find the information on the real needs of rural residents.

2.6 Market-Oriented Operation Mechanism for E-agriculture Construction Refueling

E-agriculture has a strong public interest, and to highlight the social benefits is a long-term task, you must combine government promotion, guidance and market mechanisms. In addition to government departments, various social or business organizations can become direct information service principal, the Government can play an organization to promote and oversee the manager's role, and insisted that the government-led emphasis on the basic role of the market, accelerating the development of the information technology market players, play to their enthusiasm; the role of government to gradually Go to actively create a favorable policy environment for up to encourage and support all kinds of social forces to carry out the socialization of information services for the majority of farmers, to promote e-agriculture.

As long as the governmental organizations, to co-ordinate the planning, funds, technical support. Development of low-cost, high-tech, systems-oriented integrated innovation; e-agriculture will be able to achieve brilliant results. Which is conducive to narrow the urban-rural digital divide, break the urban-rural dual structure; conducive to the promotion of farmers to change their ideas and improve quality; conducive to modern technology and the combination of agriculture, strengthen the comprehensive agricultural production capacity-building, the construction of these e-agriculture, promote rural economic and social development played an important role of government is a way of building a new socialist ecology.

3 A New Socialist Ecology E-farm Application of Innovative Solutions

3.1 Overall Program Architecture

After a large number of requirements analysis, in-depth study on the construction of agricultural information, a comprehensive plan to provide a set of agricultural information technology solutions, mainly from three aspects:

First offers a range of hardware and software products for the agricultural production information to meet the agricultural prenatal, delivery, postpartum and other aspects of the high-tech needs, enhance scientific and technological content of agricultural production, and enhance the market competitiveness of agricultural products.

Followed by agriculture-related enterprises to provide information technology solutions, from simple to complex embodiment, a comprehensive plan for the gradual implementation of agriculture-related enterprises gradually increase the level of information, meet agricultural production, operation in science and technology, market, management, personnel and other information needs.

Again to provide information services for the government, enterprises, scientific research institutions, farmers, build modern rural information service system. Vast amounts of technology and market data sources as the basis of all the modern means of communication, build a convenient, fast, intelligent, high-speed two-way information channel and trading platform to meet all aspects of the information needs of all levels.

3.2 Agricultural Production Information-Precision Agriculture System Solutions

Precision agriculture by 10 system, namely, global positioning systems, field information collection system, agricultural remote sensing monitoring system, irrigation and geographic information systems, agricultural expert systems, intelligent farm machinery systems, environmental monitoring systems, system integration, network management systems and training system, its core is a perfect farmland geographic information system (GIS), can be said that the full integration of a new type of agricultural information technology and agricultural production. Precision agriculture is not too much emphasis on high-yield, and the main emphasis on

effectiveness. It agriculture into the digital information age is an important direction of development of agriculture in the 21st century.

Precision agriculture is based on information technology support, based on the spatial variability, positioning, timing, quantitative implementation of a set of modern farming operations technology and management system, a new type of agriculture is fully integrated information technology and agricultural production. Precision agriculture technology system, including the different levels of the system, based on the application software.

System Software: Average common Windows operating system software;

Basic software: Can be used for secondary development of GIS software such as MapInfo, Arc / Info; application programming software, such as VB, VC, the underlying database software;

Applications: Spatial information management and analysis software; farmland GIS precision agriculture as the foundation of the database; software and data exchange software, software and hardware interface software; GPS and GIS interface software, GPS, GIS and intelligent agricultural interface software, field information collection and GIS interface software; analysis and decision software and agricultural expert systems, crop growth and numerical simulation, farm management decision-making software.

3.3 Agricultural Production Management Program

Analog agricultural experts ponder the reasoning process to solve the farmers' problems in the production process a set of utility software. Can also be run separately to run on a computer to solve due to the usual fertilization irrigation, pest and disease control, information understanding timely grasp inaccurate not the right response to the losses caused by integration with the local agricultural site. Agricultural expert system to guide scientific farming, science and sprinkle the medicine, scientific fertilization, scientific pest control, reduce the dangers of instability and improve the economic efficiency of the agricultural industry. Agricultural expert system has a unique intelligent reasoning, the use of multimedia information technology, graphic audio and Mao popularization of agricultural production technology guidance of scientific farming.

The main features of the system:

Fool: The color of the man-machine interface, style design with the current mainstream WINDOWS XP interface style; method of operation, the choice of the list (such as a drop-down list, combined list), greatly reducing the user manual input operation; the form of a Windows Explorer on the system to use interface enables users to easily get started operation; tree structure in the form of knowledge representation, knowledge system a clear at a glance.

Intelligent: The system according to the relevant parameters of the user-selected pest and disease onset of symptoms, body characteristics, automatic judgment, analysis, results given by the inference engine, such as the name of the pest and disease control methods.

Interactivity: Agriculture and animal husbandry expert professional interaction through the system with the user, with a professional online conversation function module, the user of the problem and reply to the experts in this line docking.

Simple: The system comes with a data management system that provides a simple maintenance platform, according to the instructions to fill in the data, the system can automatically and immediately to knowledge extraction and interpretation, the required knowledge stored in the underlying database maintenance The process is very simple.

3.4 Pest Control Forecasting System

Solve local plant protection departments pest forecast forecasts of information technology, it is a combination of software technology, network technology and plant protection technology intelligence software, specifically designed for plant protection forecasting, for all aspects of the plant protection work process design, effectively reduce the workload of the plant protection of forecasting, improve work efficiency.

This system is fully functional, related to all aspects of plant protection, the system consists of ten subsystems, namely: pest data upload and release system, the pest database management system, integrated pest and disease information inquiry system, reporting and management systems, pest and disease forecasting Statistical Analysis System, pest and disease forecast data mining system, pest prediction visual modeling system, pest multimedia data management systems, pest and disease forecasting model simulation system and disaster fuzzy evaluation system. The function of each system is described as follows:

(1) Under the network environment pest data upload and release system

The system through the Internet site of data to collect, collates, publishes, uploads and issued. Around the state, counties and cities statistics and other materials to document form on the aggregated upload. The provincial stations under the local cities and counties can also be down directly send text notifications.

(2) Pest and disease information query system

The data management module embedded in a strong data query functions. Query objects include: data table fields, data sheet describes the information, data sheet classification, data tables, fields, field descriptions. You can query data tables, fields, and records. Comparison include: equal, not equal, fuzzy comparison, equal to the null value is not equal to a null value.

(3) Reporting and management system

Report Manager free report table-like design to achieve a good header of the freedom to customize, easy to use and powerful. Users according to the actual need to design a report header, select the matching data sheet and select the corresponding field for each column, then a simple parameter settings to the preview of the report, print.

(4) Pest forecasting Statistical Analysis System

The statistical analysis of regression prediction method is the prediction of agricultural pests and diseases has important practical significance. System and multiple linear regression modeling and prediction function, intuitive modeling guide makes the model easy to use, standardized and rigorous. Save the establishment of a

good model, forecasts, select the data table corresponding to the model library model input argument value, you can calculate the predicted value and the predictive value of interval estimation.

3.5 Agricultural Enterprise Information Solutions ----- Supply and Demand of Agricultural Products Information Intelligent Service System

Based on fully research the current agricultural enterprises informatization construction features of the core of enterprise resource plan (ERP) agricultural enterprises informatization construction program, including the construction of network infrastructure, enterprise Internet (LAN and wide-area network), Enterprise Resource Management and e-commerce in order to achieve full sharing and utilization of information resources. Using Internet resources to establish an online order service platform, logistics and distribution system, to achieve the full range, removable, integrated centralized management and real-time process control; fully tap the business information resources, and provide an important basis for management decisions.

Agricultural supply and demand information intelligent service system integration with local rural network to forecast the trend of prices of agricultural products through intelligent analysis, analysis of market conditions, to automatically search market supply and demand information, analysis and retrieval, automatic matching of supply and demand of agricultural products. Agricultural supply and demand information intelligent service system is a data acquisition, data cleansing, data mining analysis, intelligent prediction, visualization, display and other subsystems organic whole, mining analysis and intelligent prediction from each other, complement each other to form a comprehensive smart trends predictive analysis methods, and ultimately the formation of an integrated system.

Agricultural supply and demand information intelligent service system main function is to: show the prices of major agricultural spatial distribution, the timing variation trends of the market price, supply and demand information intelligent docking; market-oriented agricultural structure adjustment for government departments; agriculture and animal husbandry enterprises, large, Association, and even ordinary farmers show the dynamic and intelligent analysis.

(1) The prices of agricultural data mining method

Based on the prices of agricultural data warehouse, variety, price, quality, production, origin, property, classification, clustering, association, timing and other mining analysis, reveal price trends influencing factors and reasons, such as: the impact of high prices, , low distribution area characteristics, population characteristics, the analysis of the seasonal characteristics of inter-city price fluctuation relationship between varieties prices ebb and flow, and the industrial structure, price and agro-meteorological relationship analysis.

(2) Commodity price trends analysis and forecasting methods

Price data and spatial distribution of the data according to the timing of agricultural products, the establishment of a data mart, through statistical analysis, support vector machines, neural network and wavelet chaotic prediction method for trend analysis, timing analysis and cycle analysis, forecast the trend of prices of agricultural products.

(3) Agricultural supply and demand information intelligent docking method

The use of Ontology-based Web information mining, extraction, semantic analysis technology, combined with the price, quantity, quality, location and other attributes intelligent docking of supply and demand information for the user or request information, the priority of the request or for competitiveness automatic docking to the user. Information is available through the means of transmission, such as: voice systems, portals, SMS platform, customization and broadcast push.

3.6 Rural Information Technology Solutions - The Rural Market Service System

Existing agricultural market information collection channels and collection points, unified and standardized information collection system of various types of agricultural products, as well as market supply and demand and prices of agricultural commodities (including fertilizers, pesticides, plastic sheeting and other agricultural markets, food, vegetables, livestock, aquatic products and other agricultural products market information). In the data acquisition system based on the integration of existing information media, real-time information released by e-mail, pager, SMS, etc. In addition to real-time information on the Internet, information is automatically released. Processing, sorting and analysis of information resources, analysis and forecast the agricultural main varieties of domestic and international market conditions, production and marketing situation. Use the web to provide the means of communication in the online transaction an exchange of information between the two sides, trading contact stylized system; take online auction as the main mode of trading Contact by e-mail, mobile phone text messages and paging intelligent an exchange of information. Create an online agricultural trade information service platform, to achieve real-time online deliberation trading conditions.

4 Conclusions

In this paper, some of the problems of e-farm applications in the construction of new socialist ecology, some countermeasures, and launched on the basis of the application of innovative solutions for e-agriculture, including agricultural information technology, the agriculture enterprise information and rural information of the solution.

References

- [1] Chen, X.: The evolution of agricultural informationization and countermeasures. *Science and Technology Management Research* (7), 437–03 (2009)
- [2] Yong, C.: To speed up the agricultural informationization construction to promote agricultural modernization development. *Journal of Inner Mongolia Science and Technology and Economy* (9), 63–64, 18 (2009)
- [3] Zhao, C.: Henan province rural informatization way and strategy analysis. *Journal of Management Informationization in China* 12(17), 81–83 (2009)
- [4] Du, X., Zhu, Q., Wen, H.: New rural informationization present situation and development countermeasures. *Rural Economy* (8), 95–98 (2009)

- [5] Huan, S.H., Sheoran, S.K., Wang, G.: A review and analysis of supply chain operations reference (SCOR) model. *Supply Chain Management* 9(1), 23–29 (2004)
- [6] Choi, T.Y., Dooley, K.J.: Supply networks and complex adaptive systems: control versus emergence. *Journal of Operations Management* 19(3), 351–366 (2001)
- [7] Zhang, A.: What time thinking about the construction of speed up agricultural informationization. *Journal of Agricultural Science and Technology* (1), 17–18 (2007)
- [8] Yang, X.: Thinking about China's rural informatization construction. *World Agriculture* (3), 19–21 (2008)
- [9] Jiang, X.: Strategy analysis of agricultural informatization development. *Journal of Agricultural Mechanization Research* (3), 32–35 (2005)
- [10] Liu, W., Ma, X.: Agricultural information technology development research in the construction of new socialist rural. *Agricultural Science of Anhui* (12), 2911–2912 (2006)

Developments on Informatization Technology in Agricultural Operations in China

Qiuping Zhou¹ and Guohua Fu^{2,*}

¹ College of Agriculture, Hainan University, 570228, Haikou, Hainan, China

² Hainan University, 570228, Haikou, Hainan, China

zqp5545@126.com, fgh328@163.com

Abstract. "Eleventh Five-Year" period of China's agricultural and rural information construction achieved important results in significant improvement in the information base. "Twelfth Five-year" period, agricultural and rural information environment for the development of more optimized, more urgent needs, some of the outstanding issues to be resolved, agricultural and rural information construction is about to enter a new historical stage of development, facing a major opportunity, the task is arduous.

Keywords: Summary, Informatization technology developments, Chinese agricultural operations.

1 Introduction

Under the leadership of the CPC Central Committee and the State Council, in close cooperation with community, the Ministry of Agriculture tightly around the development of modern agriculture and the goal of building a new socialist countryside, continue to implement projects; market and Economic Information Division set up at the information technology to promote, specifically responsible for promoting national agricultural informatization work in rural areas. China's agricultural and rural information construction progress is significant, the deepening of the field of application of information technology in agricultural production, the rapid development of information technology in agricultural operations, agricultural management information to further promote agricultural services information technology steadily improved, "Twelve Five" period of national agricultural the smooth development of the rural informatization work has laid a good foundation.

2 Agricultural Products Logistics Informatization

Comprehensive information technology to promote agricultural super-docking. Ministry of Agriculture, vigorously promote the information construction in agriculture super-docking process, the implementation of grading and packaging of agricultural

* Corresponding author.

products and logos, specification, acquisition, storage, transportation, sales and circulation, promote the use of modern circulation technology, information technology means to establish a quality traceability system, the development of online agriculture super-docking platform to encourage the supply and demand information through agriculture super-docking system, to carry out the contract online and trading pilot, and promote agriculture super-docking, modernization. As of the end of 2010, the country has 28 provinces (autonomous regions and municipalities) to carry out the agricultural super-docking, involving more than 10 categories of agricultural products, the Products held around the various forms of trade fairs, Fair more than 5,000 performances, there are more than 2,000 retail enterprises varying degrees, to carry out agricultural super-docking, Ministry of Agriculture directly helping more than 2,000 farmers 'professional cooperatives and supermarkets agriculture super-docking, driven 11,000 farmers' professional cooperatives and supermarkets and marketing relations, promote the circulation of agricultural products cost an average of 10% -15 % of farmers participating in the butt than undocked the farmers annual increase of 10% -15%.

Cold chain logistics information technology to accelerate the start. China is speeding up the establishment of the main varieties and key areas of agricultural products cold chain logistics system, information into safety traceability of the cold chain logistics, temperature control and shelf life, freshness and meticulous management to provide a guarantee, but also promoted the cold chain logistics resources the rational allocation. As of the end of 2010, there were cold storage nearly 20,000, the total cold storage capacity of 8.8 million tons, exports of fresh agricultural enterprises generally the whole low-temperature control, large-scale meat slaughtering enterprises began to use international advanced cold chain logistics technology, toward the full low temperature control the direction of rapid development. Sinotrans, COFCO social third-party logistics enterprises to establish international state-of-the-art cold chain facilities and management system, Shuanghui, public goods, Bright Dairy food production enterprises to actively improve the cold chain networks, large commercial enterprises chain terminal sale of part of the continuous improvement of cold chain management, cold chain logistics enterprises in the overall network, information technology development trend.

3 Agricultural E-commerce

Multi-level agricultural e-commerce network system has improved constantly. The end of 2010, the National Rural e-commerce site has more than 30,000, of which agriculture-related website 6000, led to profound changes in agricultural production, supply mode. The official website as the representative of Chinese agricultural marketing platform to further increase agricultural information dissemination efforts to close the production and sale of contact; dish housekeeper, I bought the network, as the representative of agricultural e-commerce website easy fresh fruit days with rich e-commerce business, full service online purchase, logistics and distribution, electronic payment; new Hope, love agricultural Inn as the representatives of agricultural production enterprises have self-built e-commerce platform, own agricultural

production, supply and electronic links formed a multi-level e-commerce network system of agricultural products, some good benefits, the information environment of national and regional markets, agricultural information dissemination and active zone of the transaction.

Regional staple agricultural products electronic trading market has developed rapidly. In 2010, China's agricultural trade and circulation mode continuous innovation, have established a number of bulk agricultural commodities online trading center, relying on the Internet organize all the members of the dealer directly online quote, matching, online ordering, electronic shopping bulk buyers and sellers face-to-face spot trading of agricultural products. For example, the Shanghai staple agricultural products market mainly oilseed commodity forward transactions in the standard contract bidding exchange and spot transactions special spot transactions, combined with the online trade of agricultural products, the improvement of standards of transactions, and settlement systems and ancillary storage and logistics delivery system. In addition, Shandong Shouguang Vegetable electronic trading market, Guangdong Shun Li bulk electronic trading market of agricultural products, bulk agricultural products in Hubei electronic trading market, Changsha Southern staple agricultural products market have set up and put into operation.

4 Agricultural Products Wholesale Market of Information Technology

Agricultural market system has improved constantly. Ministry of Agriculture in accordance with the requirements of the "Eleventh Five-Year" period of national agricultural market system planning "to guide an orderly way around the agricultural market system. According to statistics, China has agricultural products wholesale market over 4300, on the regional distribution to achieve full coverage of the producing areas and sales areas, to achieve a comprehensive and professional complement each other on the type of market, the business scope planting livestock, aquatic products and other agricultural products is all inclusive. At the same time, the number of farmers' markets stabilized at about 25,000, a steady increase in the proportion of supermarkets in the circulation of agricultural products, agricultural futures listed species 13. Information technology as an important support for the main channel to the wholesale market of agricultural products, farmers markets and other retail terminal-based, supermarket chains and other modern methods of distribution for the pilot, the futures market to complement the modern market system of agricultural products has been basically formed.

The information of the internal management of the wholesale market, to proceed with the transaction information. Group of economically strong agricultural product wholesale markets make full use of modern information technology, the implementation of a customer management, booth management, personnel management, financial management and administration of public security information technology. Some agricultural products wholesale market to abandon the cash transactions continue for many years "paid their dues, hand delivery, electronic unified settlement (including both

credit card transactions) way. A small number of wholesale markets of agricultural products such as Shenzhen Futian Market, Shandong Shouguang market attempts to implement electronic auction transactions; some markets also opened the e-commerce trading platform.

5 Agricultural Enterprise Information Technology

The agricultural enterprises starting to focus on information technology. With the popularity of the Internet, many agricultural enterprises began to realize the importance of the construction of enterprise information, the vast majority of companies have access to the Internet; agricultural companies recognize the importance of network publicity, have to build a corporate image display, publishing product information portal; construction of a number of leading agricultural enterprises of agricultural products e-commerce platform for the trading of agricultural products, greatly reduce the transaction costs and improve corporate earnings. There are some leading agricultural enterprises and enterprise management, improve the level of information of the enterprises in the procurement, production, sales, marketing, finance and human resources management and other aspects of the use of ERP systems.

The state-owned farm land management information pilot made significant progress. Beginning in 2004, the Ministry of Agriculture annual allocations of part of the central government funds used to explore state-owned farm land information management, and the construction of state-owned land resource management system pilot in Guangdong, Heilongjiang and Hainan Reclamation. Seven years, the pilot unit according to the requirements of the land use, management and protection of state-owned farms, push forward the construction of farm management subsystem, system sets land management, agricultural production, social security, the subsidy policy, staff management in one of the farm business farming precise management of the land and improve the level of comprehensive utilization of land resources and farm management level of information.

6 Professional Farmers Cooperatives Operating Information Technology

Around the farmers' cooperatives starting to focus on information technology. Around the farmers' professional cooperatives have established a website, cooperatives internal agricultural information can be released at any time through the website, you can achieve online trading, publishing agricultural news, and also the formation of the online Union to promote the standardization of the construction of farmers' professional cooperatives, standardized. Since 2009, Anhui Province, the implementation of farmers' professional cooperatives construction project, the province's 1500 professional farmers cooperatives "Anhui farmers' professional cooperatives network", to achieve a "production in the community, marketing network, service exchange, resource sharing". As of the end of 2010, Gansu Province, has more

than 6300 professional farmers cooperatives, in 2010, the Agriculture and Animal Husbandry Department of Gansu Province to help the province's 100 co-operatives to build a network information platform to achieve a cooperative digitization of information, management processes and product sales of electronic.

Professional farmer's cooperatives in the primary information services play an increasingly important role. "Eleventh Five-Year" period, China's development of farmer cooperatives momentum, the total amount of the rapid growth of farmers 'professional cooperatives, business areas continue to expand, is increasingly becoming an effective way to increase farmers' income. As of the end of 2010, the national farmers' professional cooperatives amounted to 379,100, there is entrance farmers 29 million, accounting for about 11% of the total number of households. These farmers' professional cooperatives are widely distributed in cultivation, animal husbandry, agricultural, fisheries, forestry and other industries, members of the cooperative jointly engaged in the purchase of agricultural production, agricultural marketing, storage, processing, entrance farmers income is generally higher interbank household income than non-members more than 20%.

7 Conclusion

In summary, the significant progress of China's agricultural and rural information construction, information technology applications in the field of agricultural production continued to deepen, the rapid development of information technology in agricultural operations, the agriculture management information to further promote agricultural services information technology steadily improved, as the "Twelfth Five-year "period of national agricultural and rural information work smoothly laid a good foundation.

References

1. Chen, X.: The evolution of agricultural informationization and countermeasures. *Science and Technology Management Research* (7), 437–03 (2009)
2. Yong, C.: To speed up the agricultural informationization construction to promote agricultural modernization development. *Journal of Inner Mongolia Science and Technology and Economy* (9), 63–64, 18 (2009)
3. Zhao, C.: Henan province rural informatization way and strategy analysis. *Journal of Management Informationization in China* 12(17), 81–83 (2009)
4. Du, X., Zhu, Q., Wen, H.: New rural informationization present situation and development countermeasures. *Rural Economy* (8), 95–98 (2009)
5. Huan, S.H., Sheoran, S.K., Wang, G.: A review and analysis of supply chain operations reference (SCOR) model. *Supply Chain Management* 9(1), 23–29 (2004)
6. Choi, T.Y., Dooley, K.J.: Supply networks and complex adaptive systems: control versus emergence. *Journal of Operations Management* 19(3), 351–366 (2001)

7. Zhang, A.: What time thinking about the construction of speed up agricultural informationization. *Journal of Agricultural Science and Technology* (1), 17–18 (2007)
8. Yang, X.: Thinking about China's rural informatization construction. *World Agriculture* (3), 19–21 (2008)
9. Jiang, X.: Strategy analysis of agricultural informatization development. *Journal of Agricultural Mechanization Research* (3), 32–35 (2005)
10. Liu, W., Ma, X.: Agricultural information technology development research in the construction of new socialist rural. *Agricultural Science of Anhui* (12), 2911–2912 (2006)

The Parameter Optimization and Performance Analysis of the Suspension System in the Cab of a Heavy Truck

Jihai Gu, Hui Wang, Chengwen Wang, Ming Pang, and Xiangyang Jin

Institute of Light Industry, Harbin University of Commerce, Harbin 150028, China
{Jihaigu,13796073912}@163.com, 499134464@qq.com,
chengwen_wang@yeah.net, jinxiangyang@126.com

Abstract. In this paper, we conduct a vibration simulation analysis of the suspension system in the cab of a heavy truck in ADAMS. Through establishing the parametric vibration mechanics model of suspension system and using the vibration signal as the excitation signal in the simulation, and regarding rms value of the weighted acceleration as the evaluation indicators, we optimize and match the parameters of the suspension system.

Keywords: cab suspension, vibration analysis, parameters optimization.

1 Introduction

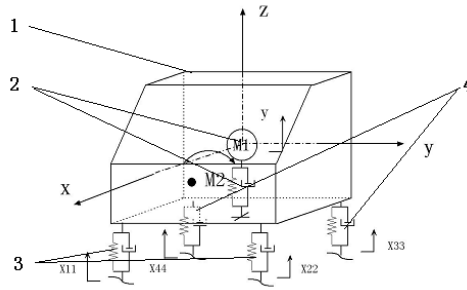
Heavy trucks need to work under bad conditions of the road, so in order to ensure the comfort of the cab, researchers should improve the vibration isolation performance of suspension system. Establishing accurate virtual prototype model combining with multi-body dynamics is the key to analyze the performance of avoiding vibration of the suspension system in the cab. The suspension system is a vibration system of many degrees of freedom by connecting the vehicle frame, the suspension elements with the cab. The main element of reducing vibration in the suspension of the cab is springs and dampers. Without changing the structure and position of the suspension system, the main parameters of influencing the elements of reducing vibration are the damping and stiffness of the vibration absorber. Therefore, the optimization and matching of the parameters of the stiffness and damping of the front and rear suspension systems is the main way to improve the vibration performance of the suspension system. In terms of the stiffness and damping of the suspension system in the cab of one heavy vehicle, we perform a parameter optimization and matching of the suspension system to reduce vibration with applying the theory of multi-body dynamics and the function of Design of Experiments, DOE in ADAMS.

2 Parametric Modeling of Virtual Prototype

2.1 The Establishment of Mechanical Model

Excitation, quality, elasticity and damping are main factors which influence the vibration of the mechanical system. Therefore, if we get the four elements accurately,

we can reflect the mechanical model of the physical process in a right way from the complex machine. For the scattering of the quality and elasticity of the actual vehicle system, we can't succeed in analyzing the continuous system in the analytic method, but change the scattering of the continuous system to several concentrated quality and then analyze with the springs and dampers connected[1]. This paper regards the suspension system in the cab as the research subject as a whole, the mechanical model of the spatial vibration equivalent system in the spatial coordinate is shown in Fig. 1.



1. Cab 2. People- seat system
3. The front suspension system 4. The rear suspension system
Fig. 1. The mechanic model of the suspension system in the cab

Before establishing the dynamics model of the suspension system in the cab, we should acquire the geometric model parameters, quality parameters, mechanic parameters to ensure the correctness of the model and the accuracy of the simulation. All the main parameters are provided by the manufacturers and furthered tested by the degree of freedom after establishing system model in ADAMS. The acquired 47 degrees of freedom of the system mainly include:

(1) The stabilizer bar freedom: with being changed into 8 flexible elements, connected by 2 fixed hinge with the lower bracket, 12 degrees of freedom constricted, the degree of freedom from the stabilizer bar is $8 \times 6 - 2 \times 6 = 36$.

(2) The degree of freedom of the cab and the suspension elements: 6 degrees of freedom.

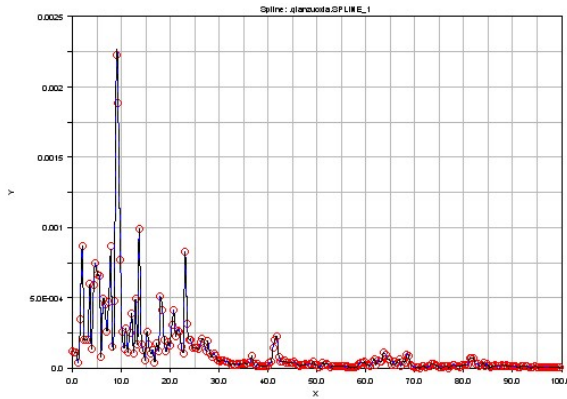
(3) The degree of freedom of the seat: with constricting the movement of the seats and the cab, only one degree of freedom of vertical movement according to the cab remains of the seats.

(4) 4 degrees of freedom of the vibration table: vertical direction

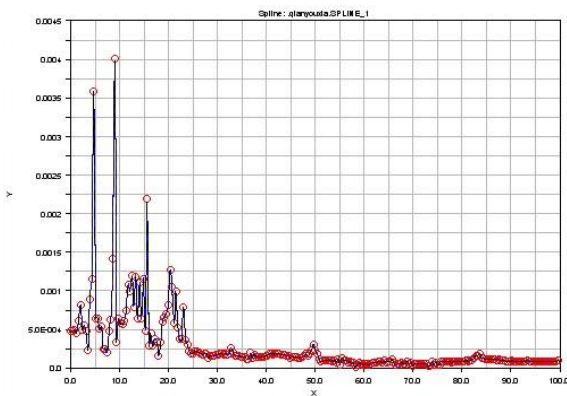
In ADAMS, we have to ensure the model is neither under under-constrained nor over-constrained. Under-constriction makes it hard for us to ensure the correctness of the simulation; a warning will be given in the simulation under over-constriction and the simulation cannot work normally. Through the verification of the degree of freedom and static equilibrium, the model is established accurately. Then we can conduct the following simulation.

2.2 The Establishment of Model Input Excitation

The excitation signal applies the vibration accelerating speed of the 4 test points under the suspension acquired from the road vibration test as the excitation input, as shown in Fig.2. For the actual test signals are combined from the road roughness incentives, engine vibration, frame bending vibration and torsional vibration transmission, so we apply the actual signals as the stimulation excitation sources, making the simulation closer to the actual situation. With establishing the multi-body dynamics model of the suspension system in the cab in the multi-body mechanic software ADAMS, regarding the weighted rms acceleration value of the cab’s seat as the assessment target output, selecting the actual signal of the vehicle at the speed of 60km/h as the excitation source in the simulation, and separately entering them into the lower excitation model of the front and rear suspension system of the model, we conduct a vibration simulation analysis of the suspension system.

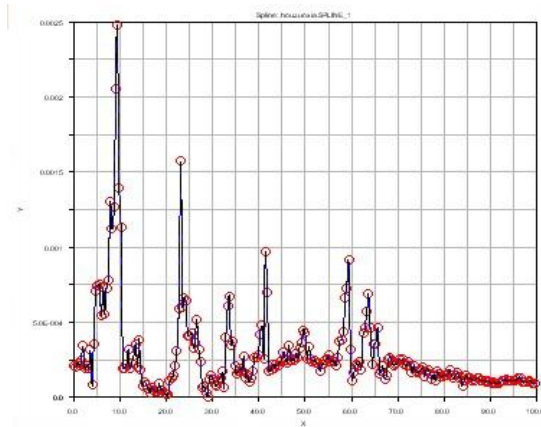


(a) Power spectrum of the lower left front suspension

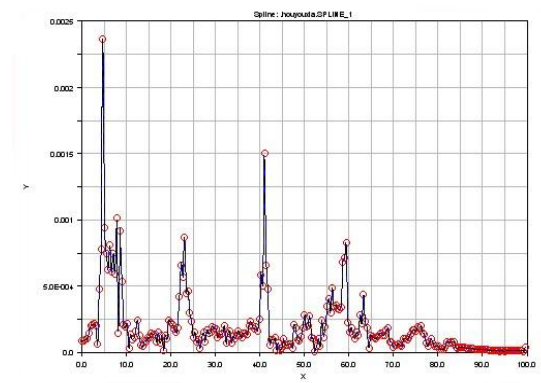


(b) Power spectrum of the lower right front suspension

Fig. 2. Model excitation signal



(c) Power spectrum of the lower left rear suspension



(d) Power spectrum of the lower right rear suspension

Fig. 2. (Continued.)

2.3 The Vibration Simulation Analysis

We confirm the excitation input of the suspension system model in the cab, conduct a vibration simulation of the model and then choose the forced damped vibration analysis. We get the power spectrum after the analysis, as shown in Figure 3. The measured signals in the same position are shown in Fig.4.

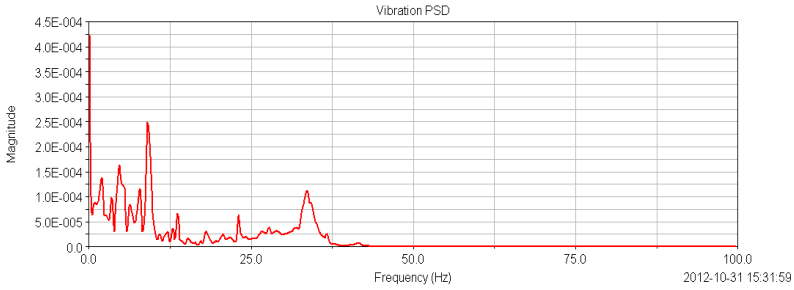


Fig. 3. The power spectrum of the simulation test

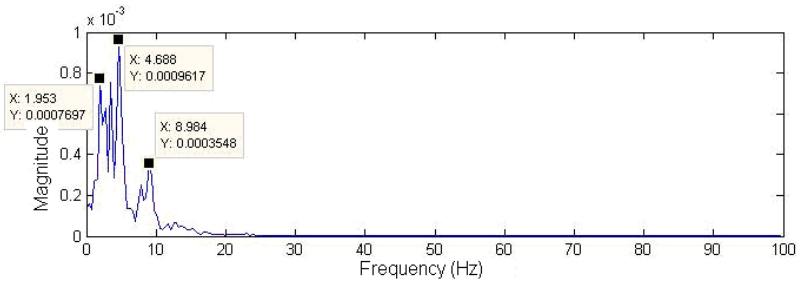


Fig. 4. The power spectrum of the measured signal

The vibration peak frequencies of the power spectrum curve of the cab’s seat acquired from the simulation are 0.1 Hz, 0.1995 Hz, 1.9907 Hz, 4.7769 Hz, 9.0558 Hz, 33.6347Hz in turn. After comparing with the actual vibration peak frequencies of the power spectral curve of the cab’s seat, as shown in table 1, we can know 1.953Hz, 4.688Hz and 8.984Hz are separately close to 1.9907Hz, 4.7769 Hz and 9.0558 Hz.

Table 1. The comparison of the main peak frequencies from simulation and the measured test

The main peak frequencies from simulation in ADAMS(Hz)	The main peak frequencies from measured test(Hz)
0.1995	—
1.9907	1.953
4.7769	4.688
9.0558	8.984
33.6347	—

Although the peak frequencies change a little in the result from the simulation, they are still the main peak frequencies of vibration. The corresponding frequencies are basically consistent with the peak frequencies of the actual signals, proving that the vibration state of the simulation model can simulate the vibration of the vehicle cab’s actual state.

3 The Parameter Optimization of Vibration Based on DOE

Design of Experiments, DOE mainly does research in the influence of every design variable to performance of the prototype when several design variables change at the same time. It is a method to optimize the prototype model through tests. The design of experiments mainly includes the establishment of design matrix and the statistical analysis of test results[2].

The experiment scheme in the process of DOE is described by the test design matrix. The size of the test design matrix is related to the number of factors, the level of each factor and their way of arrangement and combination. Good test design can get enough test data from relatively less number of trials. Therefore, The construction of the design matrix of DOE is the key to the test design[3]. The method of DOE combines orthogonal experiment design. To conduct the construction of the test design matrix with the tool of the orthogonal experiment design—the orthogonal table, thus reducing large amount of test work. Arrange for tests with orthogonal tables, that is, randomly arranging the test factors to various columns on the orthogonal table (blank columns allowed), and arrange the levels of factors to various lines on the orthogonal table. The provided DOE technical tools in ADAMS can efficiently fulfill the analysis process[4].

3.1 Determine the Experiment Scheme

(1) Select experiment factor

Suspension system's stiffness, damping are main factors of influencing the comfort and smoothness of the cab. Therefore, we separately select the stiffness and damping parameters of the air spring damper of the front and rear suspension system in the cab as the experiment factors, they are separately front suspension stiffness K_f , damping C_f , rear suspension stiffness K_r and damping C_r .

The air spring damper of the suspension system in the cab is nonlinear damping elements. In order to simplify the operation, in the process of establishing dynamic model, the damper is regarded as the linear element. According to the document provided by the manufacturer, we select the front and rear suspension stiffness as 30N/mm, the damping as 1.8Ns/mm, as the initial values of the simulation models.

(2) Determine the scope of factor levels

According to the test data of the air spring stiffness provided by the manufacturer, the stiffness in the DOE test ranges from 20 to 70 N/mm, and the damping ranges from 1.8~8Ns/mm.

(3) Construct experimental design matrix

The orthogonal table is used in experiment design, we divide the range scope of stiffness of damping 20~70N/mm and 1.8~8Ns/mm into 6 equal parts and get the medium date of every factor, as shown in the following table 2.

Table 2. The level factor values of test factors

Level	Factors			
	$A(K_f)$	$B(C_f)$	$C(K_r)$	$D(C_r)$
1	20	1.8	20	1.8
2	30	3.04	30	3.04
3	40	4.28	40	4.28
4	50	5.52	50	5.52
5	60	6.76	60	6.76
6	70	8	70	8

3.2 The Analysis of the Simulation and Optimization Results

With the minimum of the vibration power spectral peak of the seat as the optimized target, we conduct a DOE simulation calculation of the dynamics model in the suspension system. When the design variables are $K_f=30\text{N/mm}$, $C_f=5.52\text{Ns/mm}$, $K_r=60\text{N/mm}$, $C_r=8.0\text{Ns/mm}$, the optimized target value reaches the minimum. The group of optimized parameter is noted as scheme 1. Because the orthogonal test technology shrinks the test scale, so to avoid some schemes may be ignored, we conduct a range analysis of the data from the simulation[5]. The parameter data in the scheme 2 is shown in table 3.

Table 3. The comparison of the simulation optimization results

Scheme	$A(K_f)$	$B(C_f)$	$C(K_r)$	$D(C_r)$	Accelerated speed rms (m/s^2)	The reduced range of optimized results (%)
Original scheme	30	1.8	30	1.8	0.5477	—
Optimized scheme 1	30	5.52	60	8	0.4359	20.41
Optimized scheme 2	30	5.52	70	8	0.4358	20.43

Compared with the original scheme, the assessed target values in scheme 1 and scheme 2 reduce separately by 20.41% and 20.43%. The final scheme 2 is the best optimized parameter: the front suspension stiffness is 30N/mm ; the front suspension damping is 5.52Ns/mm ; the rear suspension stiffness is 70N/mm ; the rear suspension damping is 8Ns/mm .

We change the design variables to the optimized stiffness and damping values in the model and analyze the vibration simulation once again. Then we get the output power spectral density of the cab's seat and compare it with the original spectral. Fig. 5 is the curve before and after optimization, with the optimization fulfilling the target of avoiding vibration.

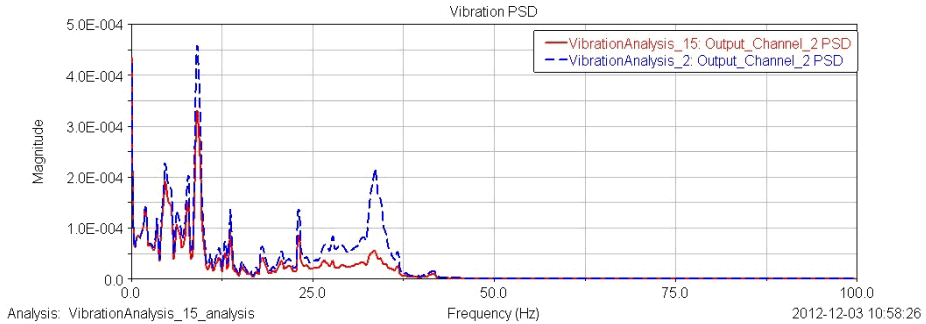


Fig. 5. The comparison of simulation results

4 Conclusions

With applying the parameter match optimization method of the suspension system based on the dynamics modeling and vibration simulation, we succeed in reducing the vibration of the cab. With applying multi-body dynamics theory, we establish the dynamics model. Through the vibration simulation and parameter optimization of the suspension system in the cab, we get a group of optimized stiffness and damping values of the performance of avoiding vibration: the front suspension stiffness value is 30N/mm; the front suspension damping value is 5.52Ns /mm; the rear suspension stiffness value is 70N /mm; the rear suspension damping value is 8Ns /mm. The simulation results show that with the group of suspension parameter, the weighted acceleration RMS of the cab's seat is reduced by 20.43% compared with the original vehicle index, which improves the stability of the model vehicle and reduces the vibration.

Acknowledgment. This research was supported by the Science and Technology Research Foundation from the Education Department of Heilongjiang Province (No. 12521130).

References

1. Zhang, C.: Simulation Research of the matching and Optimization on Vehicle Powertrain Mounting System. Dissertation. Chongqing University of Communication, Chongqing (2011)

2. Yu, C., Ma, L., Zhu, Z., Li, P.: Design of vibration isolating for commercial vehicle's cab suspension system based on DOE technology. *Tractor & Farm Transporter* 33(6), 15–17 (2006)
3. Zhang, J.: *ADAMS Introduction and Improvement of Virtual Prototype Technology*, pp. 154–155. China Machine Press, Beijing (2002)
4. Chen, L., Zhang, Y., Ren, W., Qin, G.: *Dynamic analysis of mechanical system and ADAMS Application Tutorial*. Tsinghua University Press, Beijing (2005)
5. Liu, W.: *Design of Experiments*. Tsinghua University Press, Beijing (2005)
6. Lee, D.-J., Robert, S., James, A., et al.: Development of A Machine Vision System for Automatic Date Grading Using Digital Reflective Near-Infrared Imaging. *Journal of Food Engineering* 10(021), 1–40 (2007)
7. Demigny, D.: On Optimal Linear Filtering for Edge Detection. *IEEE Trans. Image Processig* 11(7), 728–737 (2002)
8. Pizlo, Z., Rosenfeld, A.: Recognition of planar shapes from perspective image using contour-based invariants. *Imaging Understanding* 56(3), 330–350 (1992)
9. Huh, K., Choi, J., Yoo, H.: Development of a multi-body dynamics simulation tool for tracked vehicles. *JSME International Journal, Series C:Mechanical Systems, Machine Elements and Manufacturing* 46(2), 550–556 (2003)
10. Auston, D.H.: Picosecond Optoelectronic Switching and Grating in Sinlin. *Appl. Phy. Lett.* 26(1), 101–103 (1975)
11. Rubinstein, D., Hitron, R.: A detailed multi-body model for dynamic simulation of off-road tracked vehicles. *Journal of Terramechanics* 41, 2–3 (2004)

Evolution of Growing Season Precipitation Series in the West Region of Heilongjiang Province Based on Wavelet Analysis

Wensheng Zheng^{1,2}, Sijia Shi¹, and Zhenping Gong¹

¹ College of Agronomy, Northeast Agriculture University, Harbin 150030, China

² Heilongjiang Provincial Hydraulic Research Institute, Harbin 150080, China
zhengwensheng@126.com

Abstract. Global climate change is more and more serious for drought and affect for agricultural production in Semi-arid Area of the West region of Heilongjiang Province. So, steady progression of agricultural production impose challenge in this area. In order to solve above-mentioned problems, the authors took Gannan county as example, analyzed the multi-time scales variation characteristics and jump characteristics of actual growing seasons precipitation time series in Gannan county through using the wavelet theory, and the main periods of growing season precipitation change and variation trend of drought-flood in this area were revealed. The study can provide scientific gist for fully utilizing natural precipitation and exploiting maize water potential productivity in Gannan county so much as the entire Area of the West region of Heilongjiang Province.

Keywords: West region of Heilongjiang Province, growing season precipitation, wavelet transform, multi-time scales analysis.

It is belongs to warm temperate continental monsoon climate, characterized by significant winds, four seasons, rain hot during the same period in west region of Heilongjiang province, is China's important commodity grain production base. Agricultural production mode is rain-fed agriculture, therefore, it is important significance precipitation for agricultural production. Crop growth season is from May to September in west region of Heilongjiang province, so it is more conscious version to precipitation of crop growth season for effectively conducting agricultural production and guiding scientific agricultural development planning. Feature of growth season precipitation is researched, based on observed data of Gannan site, so this paper researched time variation trends of precipitation in growth season, and in order to provide the reference for local agricultural production.

1 Materials and Methods

This paper used crop growth season precipitation time series of Gannan site from 1956 to 2009. Gannan county is located in the western region of Heilongjiang

province, it belongs to the temperate zone continental monsoon climate, spring temperature picks up fast, strong wind more frequently, so the spring drought serious, it is a typical rain-fed agricultural region. Under the background of global climate change, so it is vital significance to analysis Gannan county crop growth season precipitation rule, and to understand precipitation rule of western half arid area in Heilongjiang province.

Wavelet analysis method used this article is based on the Fourier transform into window function, thus the time series is decomposed for contribution of time and frequency. It is very effective to obtain a complex sequence of time adjustment rules, to diagnosis internal level structure of climate change, to distinguish evolution feature of time series in the evolution of different scales. Through the wavelet analysis, we can get cycle structure and abnormal change rule of the research object series in different time scales, so we can provide scientific grounds for short-term climate prediction. For wavelet analysis principle and application, see the references [1~10].

2 Result and Analysis

2.1 Temporal Evolution Characteristics of Precipitation in the West Region of Heilongjiang Province

Anomaly variation curve of annual total precipitation and growing seasons precipitation are drawn on the basis of 54 years' annual precipitations in Gannan County, to see Figures 1 and 2.

The absolute value of the slope of anomaly trend line of growing seasons precipitation is larger than the slope's of anomaly trend line of annual total precipitation in Figures 1 and 2, which point out that a the falling range of growing seasons is larger than annual total precipitation's. Mean of growing seasons precipitation was 399.6mm, growing seasons precipitation varied between 148.5mm and 916mm, and coefficient of variation of growing seasons precipitation was 31.1% from 1956 to 2009. The coefficient of variation of growing seasons precipitation was greater than annual total precipitation's, so growing seasons precipitation had an more volatile variation than annual total precipitation.

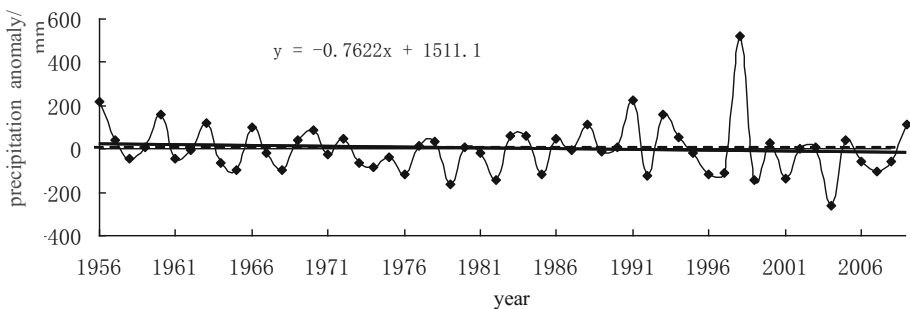


Fig. 1. Anomaly variation curve of annual total precipitation from 1956 to 2009

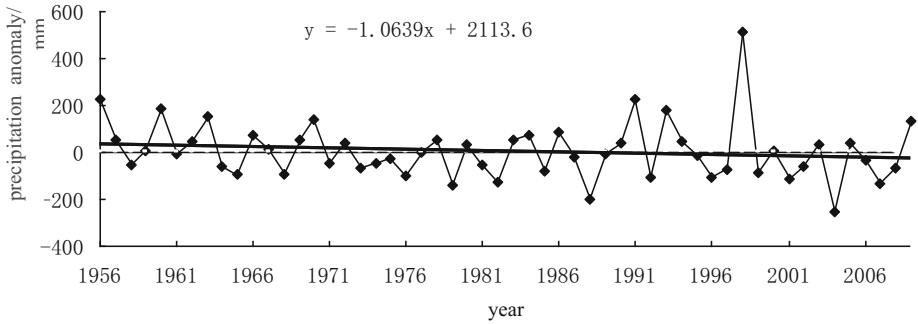


Fig. 2. Anomaly variation curve of growing seasons precipitation from 1956 to 2009

From the time (Figure 2), 54 years' growing seasons precipitation in Gannan County has a total decreasing trend, particular precipitation of growing seasons precipitation from 1999 to 2009 is obviously more decreasing than other years's. For those districts which has highly concentrated precipitation in growing seasons, precipitation is not enough for moisture of crop growth as precipitation less than 400~450mm, and it is bad for crop growth and development in where there is no irrigation condition. From the fluctuations of curve, although precipitation trended to decrease before 1982, but not too much, between 420mm and 580mm. And precipitation always had a large fluctuation from 1985 to 1999, between 430mm and 640mm. Growing seasons precipitation decreased obviously from 1999 to 2004, which was the minimum in 44 years, and it is fluctuant between 380mm and 480mm.

2.2 Analyze the Multi-time Scales Variation Characteristics of Growing Seasons Precipitation Time Series in the West Region of Heilongjiang Province

In order to know detailed structure characteristics and change tendency of growing seasons precipitation time series in different time scales, this article analyzed the multi-time scales variation of actual growing seasons precipitation time series in Gannan county on the basis of the wavelet analysis theory. Calculate the wavelet transform coefficients $Wf(a, b)$ of growing seasons precipitation anomaly series $f(k\Delta t)$ ($k=1, 2, \dots, 53; \Delta t=1$) in Gannan county.

2.2.1 Time-Frequency Analysis of Growing Seasons Precipitation Anomaly Series

Draw wavelet transform coefficients $Wf(a, b)$ modulus square isoline (see Figure 3) and real part time-frequency distribution isoline (see Figure 4) of growing seasons precipitation anomaly series in Gannan county on the basis of the wavelet transformation theory, so as to analyze time frequency transformation of growing seasons precipitation anomaly series.

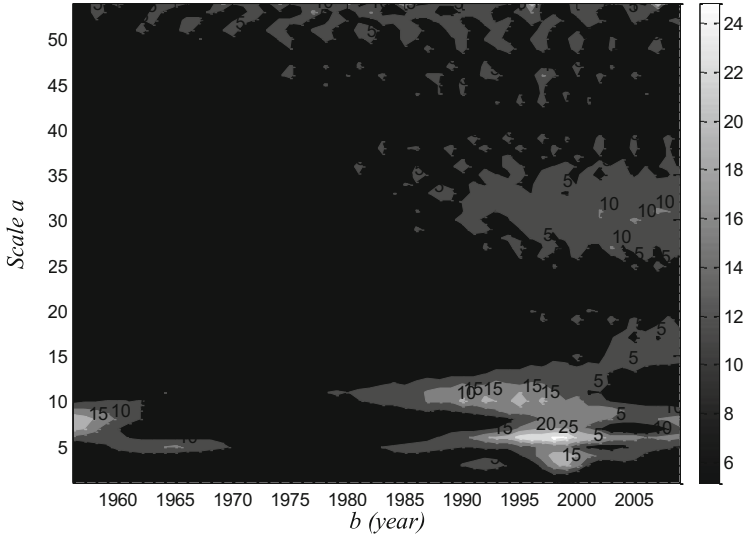


Fig. 3. Wavelet transform coefficients modulus square ($\times 10^3$) isoline of growing seasons precipitation anomaly series from 1956 to 2009

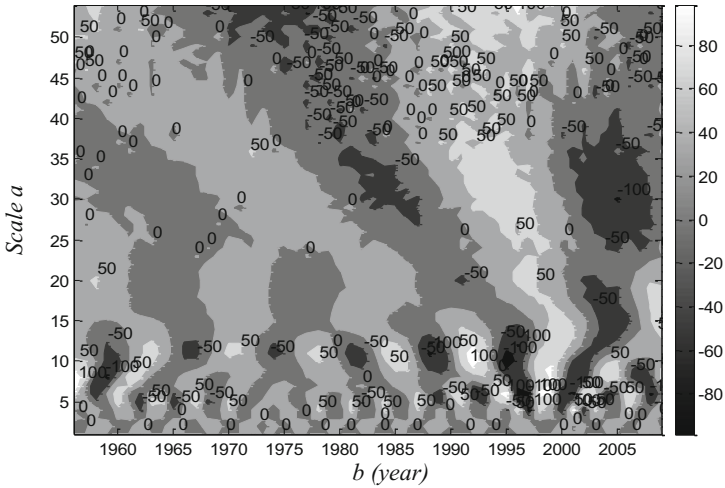


Fig. 4. Wavelet transform coefficients real part time-frequency distribution isoline of growing seasons precipitation anomaly series from 1956 to 2009

According to Figure 3, time frequency characteristic of wavelet transform coefficients modulus square is analyzed, and the strength of signal energy distribution of different time scale can be seen from Figure 3. Change of signal energy was the

strongest between three and eight years time scales, mainly it was between 1991 and 2003, oscillation center was in 1998. Change of signal energy was the stronger between 8 and 14 years time scale, mainly it was between 1980 and 2009, oscillation center is in 1959. Change of signal energy between 25 and 35 years time scale, mainly was between 1989 and 2009, oscillation center was about 2008. Change of signal energy of the others time scale was not strong.

According to Figure 4, time frequency characteristic of wavelet transform coefficients real part is analyzed. It can be seen from Figure 4 that change of Morlet wavelet transform coefficients real part of growing seasons temperature anomaly series of different time scale, distribution and phase structure of signal catastrophe point. In Figure 4, change of 3~8, 8~14 and 25~35 years time scale is most prominent, center of the time scale is about 6, 11, 31 years. In addition, between 15 and 25 years time scale also have a change, center of the time scale is about 19 years.

2.2.2 Analyze Main Period of Growing Seasons Precipitation Time Series

The main period of growing seasons precipitation time series in Gannan county was analyzed and studied by using wavelet variogram. Use wavelet transform coefficients of different time scale, calculate on the basis of computing method of wavelet variance, and draw wavelet variogram of growing seasons precipitation anomaly series in Gannan county, see Figure 5.

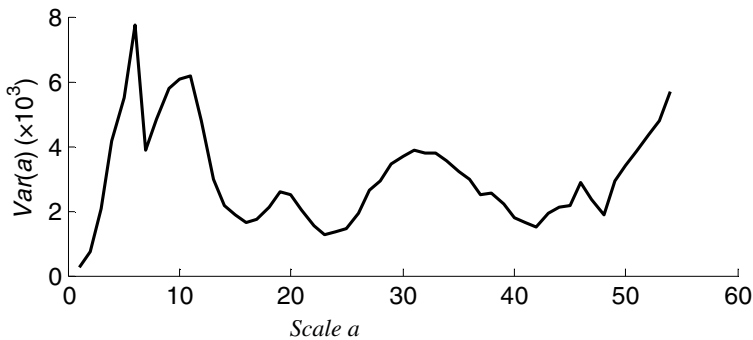


Fig. 5. Wavelet variance of growing seasons precipitation anomaly series

As you can see in Figure 5, the main crest value of wavelet variance appeared respectively in those point where the value of scale equal to 6, 11, 19 and 31, and the first crest value appeared in the point where the value of scale equal to 6, which illustrated that periodic oscillation was the strongest about 6 years and the period was the first main period, moreover, the second and the third main period was 11 and 31 years respectively.

3 Conclusion

Study of variation trend and the multi-time scales variation characteristics of growing seasons precipitation time series in the west region of Heilongjiang Province is thought as to be a foundation for researching how to fully utilize grain crop water potential productivity. It can provide important theoretic meaning for reasonably exploiting grain production in the west region of Heilongjiang Province. Growing seasons precipitation time series in Gannan county is analyzed by using regression analysis and wavelet transformation analysis, and the results show that:

(1) 54 years' growing seasons precipitation has a total decreasing trend from 1956 to 2009, obviously to the disadvantage of the stable development of agricultural production.

(2) Growing seasons precipitation time series in Gannan county is recognition that maybe have four main periods which is about 6, 11, 19 and 31 years by using wavelet analysis, and the future total variation trend of growing seasons precipitation in Gannan county is uncovered. According to the amount of precipitation, various technology measures is positively taken to make the most use of natural precipitation resources, and then achieve the goal of the sustainable use of local climate resources.

Acknowledgment. This work is supported by National Science-technology Support Plan Projects (2011BAD25B06), Ministry of water resources technology import project 948 (201121, 201222), Departments of scientific research project in heilongjiang province (201101), Heilongjiang Postdoctoral Fund(LBH-Z12038).

References

1. Xin Quan, G., Wen, Z.: Nonlinear evolution characteristics of the climate system on the interdecadal-centennial timescale. *Chinese Physics* 14(11), 2370–2378 (2005)
2. Deng, Z., You, W., Lin, Z.: Application of wavelet transformation to analysis of multiple time scale climate change. *Journal of Nanjing Institute of Meteorology* 20(4), 505–510 (1997)
3. Jiang, X.-Y., Liu, S.-H., Ma, M.-M., et al.: A wavelet analysis of the precipitation time series in Northeast China during the last 100 years. *Geographical Research* 28(2), 354–362 (2009)
4. Liu, D., Fu, Q.: Variation Trend Analysis of Annual Precipitation Series Based on Wavelet Transform in Well-Irrigation Area of Low-lying Wetland in Sanjiang Plain. *Scientia Geographica Sinica* 28(3), 380–384 (2008)
5. Liu, H., Shao, X., Huang, L., et al.: Statistical Characteristics of Annual Precipitation Variation During The Past 1000 Years in Delingha, Qinghai Province, China. *Quaternary Sciences* 25(2), 176–182 (2005)
6. Liu, J., Wang, A., Pei, T., et al.: Flow trend and periodic variation of Zaganao River using wavelet analysis. *Journal of Beijing Forestry University* 27(4), 49–55 (2005)
7. Liu, Z., Wang, Y., Ding, Y., et al.: Multiple Time-Scale Analysis of Precipitation Variation in Zhengzhou during Last 54 Years. *Scientia Meteorologica Sinica*. 33(suppl.), 123–126 (2005)

8. Wang, S., Ding, J., Li, Y.: Hydrology Wavelet Analysis, pp. 115–141. Chemical Industry Publishing House, Beijing (2005)
9. Wei, Z., Huang, R., Dong, W.: Interannual and Interdecadal Variations of Air Temperature and Precipitation over the Tibetan Plateau. *Chinese Journal of Atmospheric Sciences* 27(2), 157–170 (2003)
10. You, W., Duan, X., Deng, Z., et al.: The multihierarchical structure and the jumpfeatures of climate changes for the globe, China and Yunnan during the last one Hundred Years. *Journal of Tropical Meteorology* 14(2), 173–180 (1998)

The Matching Research of Strawberry Diseases Image Features Based on KD-Tree Search Method

Chen Jianshu, Wang Jianlun^{*}, Wang Shuting, and Liu Hao

College of Information and Electrical Engineering, China Agricultural University,
Beijing 100083, P.R. China
wangjianlun@cau.edu.cn

Abstract. According to the problem of the low matching accuracy rate and the low speed in the matching technology for image search, we choose the image of the strawberry diseases as the object of the research, to extract the feature of strawberry diseases image and then do cluster analysis using SPSS, and choose the feature combination according to the clustering effect. Do search matching experiments on the feature combination by KD-Tree matching algorithm respectively, and determine the characteristics combination which search matching accuracy is higher by comparing the results. This feature combination of strawberry powdery mildew matching accuracy reached 83.3%, the deformity of strawberry matching accuracy reached 60.0%, the aim is to provide the research basis for rapid disease diagnosis on strawberry.

Keywords: Feature extraction, SPSS, KD-Tree, Search matching, Feature combination.

1 Introduction

Corp diseases are easily happens and spreads quickly, and once the disaster occurs it will bring a great loss to farmers. Due to the traditional crop disease and pest database and diagnosis expert system using text description of shape, color, symptoms of crop diseases and insect pests, but the text description is inaccurate and subjective, and will lead to crop pests and diseases diagnosis result deviation and slowly.

With the popularity of hardware equipment and mature technology in image processing, automatic classification, growth monitoring in fruits and vegetables and plant diseases and insect pests prevention, agricultural engineering applications are using various methods based on computer vision technology.

Among them the search based on image feature point matching is one of the most important processes of image matching, and KD-Tree matching search is a commonly used method. For example, Du Zhenpeng image matching for feature detection and matching the search time is long, they do research on the image matching algorithm based on KD-Tree search method and SURF features. The algorithm firstly extracted from SURF image features and generate a feature vector, then the vector to construct

^{*} Corresponding author.

KD-Tree index for the feature description, finally calculated the distance of the nearest neighbor for each feature point of a plurality of KD-Tree and finish the work of feature matching[1].Wu Han et.al for miniature in the design of the database engine to achieve a nested query and multi-table join queries introduced KD - Tree, and on the basis of B + Tree is improved, thus to speed up the query speed[2]. J.J. Aguila et.al introduced a parallel implementation of fuzzy neural network method for distributed memory architecture based on the KD tree. This method has good precision and can better realize the fuzzy neural network method based on KD tree, the results of their implementation has good speed and efficiency, particularly in terms of speed, their method is 3~20 times faster than the sequential algorithm [3].

2 Material and Method

2.1 Material

The characteristic of image content mainly includes three types: color feature, shape feature and texture feature. In this paper we choose strawberry as the object of research, one reason is strawberry is a small berry with high economic value, it has a short growth period, high nutritional value and widely grown in the greenhouse. Another reason is strawberry both have clear characteristics of color and texture. The main object of study is normal strawberry, deformity strawberry and powdery mildew of strawberry. Due to the presence of powdery mildew of strawberry also covers abnormal and normal strawberry shape, therefore, in this study only do the color, texture features extracted and research.Fig.1 shows tree type of strawberry in the research.



(a) normal

(b) deformity

(c) powdery mildew

Fig. 1. Conventional and spectra after pretreatment

For color feature, it mainly contains the RGB and HSI color space[4], according to the analysis results, the mean and variance of the color components of RGB and HSI color space as a characteristic parameter under construction.

For texture feature, Haralick defined 14 gray co-occurrence matrix parameters for texture analysis. But Ulaby research found that Based on 14 texture features in CLCM, only 4 characteristic is not related[5]. These four characteristics is easy to calculate and can give a higher classification accuracy, so this paper uses the following four characteristics of the most commonly used to extract texture features of images: second moment, contrast, correlation, entropy.

2.2 SPSS

SPSS is a powerful data analysis software, it is the world's first statistical analysis software, its basic functions include data management, statistical analysis, chart analysis, clustering analysis and so on, in this paper we use the SPSS software of analysis functions.

Clustering is to get a collection of physical or abstract objects into a similar object composed of multiple classes of process, the clustering generated by the cluster is a collection of data objects, these objects with the same object in a cluster are similar to each other, and other objects in different clusters. Clustering of multi-dimensional image features in this paper, analysis that can make a normal and disease samples strawberry good clustering feature descriptor.

2.3 KD-Tree

KD-Tree (K-dimension tree functions) is a kind of data structure of data points in K dimensional space division, it was first proposed by Bentley [6], through by extended a binary search tree to high dimension space, realize retrieving multiple attribute data or multidimensional data, its purpose is to search the nearest data point and the query point the distance in the KD-tree, the most commonly used nearest node search algorithm is KNN nearest neighbor node search algorithm [7].

In this paper, characteristics of strawberry image is a set of multidimensional data, mainly through the combination of similarity matching between samples, that is to find the most adjacent nodes and feature point strawberry disease image to realize the rapid diagnosis of diseases of strawberry sample type, in this study using the KD-Tree search matching method. The structure of KD-Tree description as shown in table 1:

Table 1. Description of the KD-Tree data structure

Domain name	Data Type	Description of each domain name
Node-Data	Data vector	Data from a data point, is an n-dimensional vector
Range	Space vector	The space of the node represents
Split	Integer	The axis number perpendicular to the direction of super split plane
Left	KD-Tree	A KD-Tree Composed by all data points located in the super split plane of left sub-tree
Right	KD-Tree	A KD-Tree Composed by all data points located in the super split plane of right sub-tree
Parent	KD-Tree	Parent node

KD-Tree search in a small scale space has a very good performance, but when the number of nodes searches exponentially and will increase with dimension as space, especially the dimension is larger than 10 the KD-Tree search will become very slow. When carried out the KD-Tree nearest node searching and matching, the similarity evaluation of two feature vector can be adopted by a Euclidean distance of key point's characteristic as the evaluation standard [8].

3 Experiment and Results

In this paper we uses C1, C2, C3, C4, C5, C6 respectively represent the mean and variance of color components in RGB color space , C7, C8, C9, C10, C11, C12 respectively represent the mean and variance of color components in HSI color space for color feature. We uses T1, T2, T3, T4, T5, T6, T7, T8 to respectively represent the two order moment, contrast, correlation, entropy for texture feature.

3.1 SPSS Cluster Analysis

According to the color histogram and gray level co-occurrence matrix[9-10] and other methods of strawberry, powdery mildew of strawberry, deformity strawberry and normal strawberry image (for comparison) to extract color features and texture features, each feature clustering results(when the feature quantity of correct classification rate over 60 percent,we think it has a good performance in clustering) for each type of sample (in the divided into a kind of sample volume of the largest class definition for correct classification) statistical results as shown in Table 2, table 3, table 4:

Table 2. The clustering results of normal strawberry characteristic quantity

Feature quantity	Number of samples	Number of classification	Number of successful classification	Number of unsuccessful classification	Correct classification rate
C1	30	13	5	25	16.7%
C2	30	8	10	20	33.3%
C3	30	10	10	20	33.3%
C4	30	4	16	14	53.3%
C5	30	10	10	20	33.3%
C6	30	3	29	1	96.7%
C7	30	6	13	17	43.3%
C8	30	6	15	15	50.0%
C9	30	8	13	17	43.3%
C10	30	16	7	23	23.3%
C11	30	15	5	25	16.7%
C12	30	22	2	28	6.7%
T1	30	5	24	6	80.0%
T2	30	13	13	17	43.3%
T3	30	13	10	20	33.3%
T4	30	11	12	18	40.0%
T5	30	6	15	15	50.0%
T6	30	4	26	4	86.7%
T7	30	14	6	24	20.0%
T8	30	7	22	8	73.3%

From the table 2, it is clear that four feature quantities(Namely C6,T1,T6,T8) reach a good performance in clustering.

Table 3. The clustering results of deformity strawberry characteristic quantity

Feature quantity	Number of samples	Number of classification	Number of successful classification	Number of unsuccessful classification	Correct classification rate
C1	30	5	16	14	53.3%
C2	30	17	6	24	20.0%
C3	30	15	6	24	20.0%
C4	30	10	8	22	26.7%
C5	30	13	7	23	23.3%
C6	30	13	7	23	23.3%
C7	30	2	29	1	96.7%
C8	30	9	18	12	60.0%
C9	30	10	8	22	26.7%
C10	30	16	2	25	6.7%
C11	30	17	3	27	10.0%
C12	30	3	27	3	90.0%
T1	30	15	7	23	23.3%
T2	30	11	8	22	26.7%
T3	30	9	8	22	26.7%
T4	30	15	9	21	30.0%
T5	30	5	16	14	53.3%
T6	30	11	12	18	40.0%
T7	30	16	3	27	10.0%
T8	30	2	28	2	93.3%

Table 4. The clustering results of powdery mildew of strawberry characteristic quantity

Feature quantity	Number of samples	Number of classification	Number of successful classification	Number of unsuccessful classification	Correct classification rate
C1	30	10	6	24	20.0%
C2	30	6	12	18	40.0%
C3	30	7	11	19	36.7%
C4	30	7	15	15	50.0%
C5	30	8	8	22	26.7%
C6	30	4	19	11	63.3%
C7	30	8	17	13	56.7%
C8	30	12	6	24	20.0%
C9	30	6	10	20	33.3%
C10	30	7	15	15	50.0%
C11	30	5	12	18	40.0%
C12	30	7	19	11	63.3%
T1	30	15	4	26	13.3%
T2	30	16	3	27	10.0%
T3	30	17	5	25	16.7%
T4	30	12	5	25	16.7%
T5	30	10	9	21	30.0%
T6	30	8	18	12	60.0%
T7	30	14	5	15	16.7%
T8	30	2	29	1	96.7%

From the table 3, it is clear that four feature quantities(Namely C7,C8,C12,T8) reach a good performance in clustering.

From the table 4, it is clear that four feature quantities(Namely C6,C12,T6,T8) reach a good performance in clustering.

3.2 KD-Tree Search Matching

In this paper we uses 90 strawberry samples(including normal strawberry, strawberry of powdery mildew and deformity strawberry, each type samples includes 30 samples) selected three features to build 3D-Tree, three features to be matched samples of input KD-Tree search matching program. Here similarity evaluation for the two feature vector Euclidean distance metric is a key point features can be used as the evaluation standard. Because the feature vector consists of three parts, and can be set to the feature representing the two nodes. The Euclidean distance between them as follows:

Table 5. The matching results of deformity strawberry

Sample	Nearest neighbor node coordinates			Euclidean distance	The Search nodes and sample type	
	X-Axis	Y- Axis	Z- Axis			
sample1	0.151583	0.114053	0.487964	0.0498854	62	Normal
sample2	0.16766	0.137424	0.872836	0.0424372	70	Deformity
sample 3	0.146195	0.117112	0.367566	0.0249852	57	Deformity
sample 4	0.276683	0.212421	0.234173	0.0446088	37	Powdery
sample 5	0.214051	0.169284	0.594228	0.118599	69	Normal
sample 6	0.107811	0.102575	0.164185	0.016096	44	Deformity
sample 7	0.152462	0.106678	0.450741	0.0140581	59	Deformity
sample 8	0.169123	0.135545	0.502643	0.0278196	63	Deformity
sample 9	0.082651	0.0960127	0.101104	0.00424334	36	Deformity
sample 10	0.180979	0.151676	0.526856	0.0674990	69	Powdery
sample 11	0.132939	0.101810	0.349519	0.0580199	49	Deformity
sample 12	0.142896	0.142075	0.496051	0.0278196	60	Deformity
sample 13	0.130797	0.113844	0.327825	0.014884	50	Normal
sample 14	0.157395	0.130031	0.409041	0.0270746	59	Normal
sample 15	0.130551	0.0964061	0.160626	0.0118761	55	Normal
sample 16	0.102352	0.090021	0.172653	0.0160960	56	Deformity
sample 17	0.16314	0.132223	0.830962	0.0424372	70	Deformity
sample 18	0.13495	0.125852	0.335578	0.0275788	61	Deformity
sample 19	0.143318	0.107794	0.390569	0.0249852	57	Deformity
sample 20	0.122062	0.107776	0.0855459	0.0253014	41	Powdery
sample 21	0.130797	0.113844	0.327825	0.0249000	51	Normal
sample 22	0.162125	0.123367	0.0777855	0.0301397	65	Normal
sample 23	0.146915	0.113122	0.0545784	0.0322891	52	Normal
sample 24	0.116402	0.10256	0.325141	0.00541093	45	Normal
sample 25	0.163326	0.113567	0.456412	0.0140571	53	Deformity
sample 26	0.0846707	0.0992257	0.103003	0.00424334	35	Deformity
sample 27	0.160056	0.131389	0.325597	0.0307228	74	Deformity
sample 28	0.0846707	0.0992257	0.103003	0.0306622	45	Deformity
sample 29	0.160056	0.131389	0.325597	0.0175819	62	Deformity
sample 30	0.180978	0.172669	0.537890	0.0237166	53	Deformity

$$d(x_i + x_j) = \sqrt{(x_{i1} - x_{j1})^2 + (x_{i2} - x_{j2})^2 + (x_{i3} - x_{j3})^2} \quad (15)$$

Matching results can be obtained by calculating the Euclidean distance nearest neighbor search for matching nodes, and analysis of a representative sample of the node type, whether right or wrong type of samples (mainly through the sample to be matching matches consistent criteria for judging), deformity strawberry and powdery mildew of strawberry search for matching results are shown in table 5, table 6 below:

Table 6. The matching results of powdery mildew of strawberry

Sample	Nearest neighbor node coordinates			Euclidean distance	The Search nodes and sample type	
	X- Axis	Y- Axis	Z-Axis			
Sample1	0.150491	0.106692	0.0466092	0.00340927	42	Powdery
Sample 2	0.139989	0.109184	0.0182249	0.0186919	47	Powdery
Sample 3	0.133554	0.120663	0.246202	0.0125674	45	Powdery
Sample 4	0.203901	0.164683	0.381373	0.0211159	41	Normal
Sample 5	0.130551	0.0964061	0.160626	0.0189952	54	Normal
Sample 6	0.175663	0.166097	0.49239	0.0390932	60	Powdery
Sample 7	0.149334	0.109777	0.0474865	0.00820598	40	Powdery
Sample 8	0.121279	0.105738	0.0778598	0.00799019	37	Powdery
Sample 9	0.143153	0.119272	0.0277412	0.0106403	42	Powdery
Sample 10	0.153292	0.145267	0.282223	0.0284982	66	Normal
Sample 11	0.127353	0.112451	0.242179	0.0251362	58	Powdery
Sample 12	0.0584718	0.119704	0.0186351	0.0106403	46	Powdery
Sample 13	0.117785	0.095876	0.0486139	0.0069166	39	Powdery
Sample 14	0.170719	0.141748	0.0251527	0.0250481	43	Powdery
Sample 15	0.149337	0.109777	0.0474865	0.00340927	32	Powdery
Sample 16	0.20153	0.157729	0.492711	0.0271892	55	Normal
Sample 17	0.180979	0.151676	0.526856	0.0237166	55	Powdery
Sample 18	0.146915	0.113122	0.0545784	0.0115159	44	Powdery
Sample 19	0.171319	0.132066	0.0282659	0.0101883	42	Powdery
Sample 20	0.133554	0.120663	0.246202	0.0110485	41	Powdery
Sample 21	0.133554	0.120663	0.246202	0.0110485	41	Powdery
Sample 22	0.273167	0.201867	0.277682	0.0449088	36	Deformity
Sample 23	0.127353	0.112451	0.242179	0.0110485	32	Powdery
Sample 24	0.170719	0.141748	0.0251527	0.0101883	44	Powdery
Sample 25	0.120286	0.0922447	0.0432852	0.0069116	36	Powdery
Sample 26	0.14864	0.119704	0.0186351	0.0136266	47	Powdery
Sample 27	0.196121	0.169159	0.0556842	0.0141064	36	Powdery
Sample 28	0.122062	0.107776	0.0855459	0.00799019	38	Powdery
Sample 29	0.197011	0.15916	0.0457738	0.0141064	38	Powdery
Sample 30	0.121279	0.105738	0.0778598	0.0147406	54	Powdery

For the deformity strawberry image feature points to the adjacent node searching, the number of matching correct results is 18, incorrect is 12, the search matching accuracy is 60%; For each samples of powdery mildew of strawberry image feature points to the adjacent node searching, the number of matching the correct result is 25, incorrect is 5, the search matching accuracy is 83.3%.

4 Discussion and Conclusion

4.1 Discussion

In this paper we uses KD-Tree search algorithm to carry on the adjacent node search for each samples of deformity strawberry and powdery mildew of strawberry image feature points, as it can be seen from the search nodes of the method has excellent speed and better matching accuracy. For higher classification accuracy characteristics to a large extent on behalf of the samples in the characteristic quantities have similar common, so a comprehensive analysis of the classification accuracy of each characteristic quantity, the final choice C6, C12, T8 is carried out as a combination of characteristics Search Match study.

However, we found that when searching neighboring nodes for most powdery mildew of strawberry image feature points, Euclidean distance are focused on the range of 0.00340927 to 0.0147406 in the correct match result and the average search node is 43.2, but when searching neighboring nodes for deformity strawberry image feature points, the Euclidean distance range are more dispersed in the correct match result and the average search node is 55.8. Through by study the size of characteristics we know that the reason why the above conditions are mainly attributed to different types of strawberries manifested differences of amount between the each type of feature.

4.2 Conclusion

From the above matching results, select three characteristic quantities(C6, C12, T8) as the searching and matching feature combination of strawberry powdery mildew achieve a better search result for matching accuracy, and the search matching accuracy for strawberry powdery mildew is 83.3%, the deformity of strawberry matching accuracy reached 60.0%, the number of nodes of powdery mildew strawberry the adjacent nodes search to be less than deformity strawberry, and it can be seen from the search nodes of the method has excellent speed and better matching accuracy but search for deformity strawberry rate has yet to be matched by choosing some other combination of improved features.

The reason for searching and matching of three-dimensional data instead of higher dimensional in this paper is for various characteristic quantities manifested classification characteristics by the cluster analysis through SPSS, but in order to improve search matching accuracy rate we can manually add a dimensional data and by changing the size of the data to improve search matching accuracy rate and the expense is to search for matching speed will be slower than before.

References

1. Du, Z., Li, D., et al.: Research on image matching algorithm based on KD-Tree search and SURF. *Computer and Digital Engineering* 40(2), 296–298 (2012)
2. Wu, H., Yang, K., et al.: Based on KD tree multidimensional index in a database application. *Automation Technology and Application* 26(9), 37–39 (2007)

3. Aguilaa, J.J., Ariasb, E., Artigaoc, M.M., Mirallesc, J.J.: A distributed memory implementation of the False Nearest Neighbors method based on kd-tree applied to electrocardiography. *Procedia Computer Science* 1, 2579–2587 (2012)
4. Xi, Z.: Research and application of intelligent fault diagnosis system of wheat leaf disease. China University of science and technology, He Fei (2010)
5. Haralick: Statistical and Structural Approaches to Texture. *Proc. IEEE* 67, 786–804 (1979)
6. Bentley, J.L.: Multi dimensional binary search trees used for associative searching. *Communications of the ACM*, 509–217 (1975)
7. Ping, X., Xu, L.: Huge amounts of data K neighboring new algorithm based on space partition. *Journal of South China University of Technology* (35), 65–70 (2007)
8. Zhang, Y., Li, M., Zhang, X., et al.: The greenhouse cucumber leaf nutrition information detection based on computer vision technology. *Journal of Agricultural Engineering* 21(8), 102–105 (2005)
9. Wang, J., Kong, B., Jia, Q.: Image retrieval techniques based on color feature 20(7), 160–164 (2011)
10. Gao, C., Hui, X.: Texture feature extraction based on gray level co-occurrence matrix. *Computer System Application* (19), 195–198 (2010)
11. Xiong, Y., Mao, Y., et al.: Application of the ordered KD-Tree on the image features matching. *Chemical IndustryInstrument and Automation* 37(10), 84–87 (2010)
12. Liu, Z., Zhang, Y.: Comprehensive utilization of color and texture features for image retrieval. *Journal of Communication* 20(5), 36–40 (1999)
13. Xiao, P., Xu, J., Chen, S.: Texture feature extraction method. *Electronics Technology* (6), 49–52 (2010)
14. Wu, F., Yang, Z., Zhu, H., Zheng, L., et al.: Review of the application of crop image classification and recognition based on color features. *Review of China Agricultural Science and Technology* 5(2), 76–79 (2003)
15. Zou, X.: Crop diseases and insect pests recognition based on computer vision research status. *Computer Application* 20(6), 238–242 (2011)
16. Tan, F., Ma, X.: Identification method based on the leaves of plant pests and diseases. *Journal of Agricultural Mechanization Research* (6), 41–43 (2009)

Research on Automatic Irrigation Algorithm of Strawberry Greenhouse Based on PLC

Wang Jianlun^{*}, Wang Shuting, Chen Jianshu, Liu Hao, and Xu Dongbo

College of Information and Electrical Engineering, China Agricultural University,
Beijing 100083, P.R. China
wangjianlun@cau.edu.cn

Abstract. In order to realize efficient water-saving irrigation of strawberry greenhouse in precision agriculture, the paper proposed an automatic irrigation algorithm based on fuzzy comprehensive evaluation irrigation based on PLC and the configuration software, and build a remote control system. By measuring the greenhouse soil parameters and strawberry soil moisture data to determine the upper and lower limits of irrigation and set buried position of moisture sensors. Use fuzzy comprehensive evaluation method to handle multi-sensor data, and develop an automatic irrigation control algorithm that depends on the strawberry irrigation system. Set up a C / S mode of automatic irrigation control system through the 3G network and the remote computer. The experimental results show that the algorithm is reasonable and reliable, and can be well adapted to the strawberry greenhouse. The automatic irrigations meet the steady demands for real-time performance and high scalability. The irrigation automation of strawberry greenhouse provides a theoretical and practical basis for intelligent irrigation of strawberry greenhouse.

Keywords: Strawberry greenhouse, Irrigation Control, Fuzzy Comprehensive Evaluation, Programmable Logic Controller.

1 Introduction

Strawberry is a nutritious and high economic value crop, adaptability, with advantages of strong adaptability, precocity fruiting, short-term growth cycle, and considerable benefits. Since 1980s, the strawberry industry has expanded rapidly in China, and its cultivated area and output also expanded to a great extent, as the diversification of its cultivated form. Although the strawberry production in China ranks first in the world, the production management level is still very limited, especially the fertilization irrigation management, which restricts the economic value of the strawberry severely in its growing process. There is no doubt that it's effective to improve facility agriculture of strawberry greenhouse to promote strawberry water-saving irrigation.

^{*} Corresponding author.

Wang Jian[1] and others propose that the implementation of strawberries facilities development of drip fertilization can significantly increase the production of strawberries; Wang Lingxiang [2] hold the point that strawberry fertilizer management is effective and feasible under clay planting conditions by using drip irrigation and semi-matrix irrigation manner. As for the automated management of irrigation, Kuang Qiuming[3] and others design a set of water-saving irrigation automatic control system, which includes moisture content of the plant irrigation threshold to realize the automatic irrigation system. According to low levels of irrigation management in the present development of strawberry production, a suitable organic strawberry greenhouse irrigation algorithm is proposed based on the strawberry irrigation threshold, and it can be achieved by using Wi-Fi technology, 3G network and remote server. The automatic control system can monitor the real-time situation remotely, collect sensor data and even send irrigation demands, which provide theoretical and practical experience for the sustainable development of the organic strawberry greenhouse production.

2 Strawberry Greenhouse Environment

2.1 Greenhouse Environment

The experiment is conducted in organic strawberry greenhouse on Shangzhuang Town, Haidian District, Beijing, which located in north latitude $40^{\circ} 08'$, east longitude $116^{\circ} 22'$, and belongs to the temperate humid monsoon climate zone, with climates of cold and dry in winter, Spring and Autumn-arid, much rain in summer while the prevalence of the northwesterly wind is blowing. The strawberry variety in this study is called HongYan, with high yield and big fruits.

Drip irrigation is applied in strawberry greenhouse, and the cultured soil mainly consists of peat soil, vermiculite and clay. This kind of soil includes favorable permeability, water retention and rich multi-nutrient content, even the soil temperature change is slow. The culture ridge shape is trapezoidal, and its width are 30 and 50cm respectively, with ridge height 30cm. Irrigation in plastic film greenhouses is seldom affected. The length of strawberry greenhouse is 80m, and height 7m. Strawberry can be planted once every year in this greenhouse. The ridge distance in planting specifications is 80cm, spacing is 20cm, and the dripper spacing is 20 cm. Each ridge arranged a drip tape, with emitter flow rate at 1.1 L / h.

Use the cutting ring method to test the soil bulk density and field capacity, calculation formula as follows:

$$r = \frac{W}{V} \quad (1)$$

In the formula r —soil bulk density (g/cm^3);

W —the soil quality in circular knife after drying (g);

V —circular knife volume (cm^3).

Formula for calculating the of the field capacity as follows:

$$l = \frac{M_2 - M_1}{M_1} \times 100 \tag{2}$$

In the formula l —Soil field capacity (%);

M_1 —mass of dry soil in circular knife (g);

M_2 —mass of moist soil in circular knife (g).

Repeat the test at least three times and take an average of value as the final result. Because of the soil that consists of peat soil, vermiculite and clay is uniformly mixed before planting, the soil bulk density and field capacity are basically the same, with average value of 1.03 g/cm³ and 50.72% respectively.

2.2 The Irrigation Upper and Lower Limits

A. The soil profile and humidity data

The distribution of greenhouse strawberry roots is mainly in 0~25cm in the test, so this range of soil moisture can be used as control measures. Taking delay of the penetration of moisture into account, the mean value of parameters measured at different developmental stages before irrigation is needed to make the upper and lower control limits. According to the statistical data in the test, irrigation limit is developed depends on the mean of the whole soil profile from the experimental data.

Table 1. Statistics pre-irrigation soil moisture data / (m³ / m³)

depth	1	2	3	4	5	6	7	8	9	10	Mean Value
15cm	0.235	0.217	0.206	0.204	0.212	0.245	0.255	0.249	0.255	0.238	0.235
25cm	0.261	0.246	0.235	0.241	0.264	0.275	0.241	0.237	0.263	0.254	0.250

Average field capacity of the soil in the greenhouse is 50.72%, the soil moisture capacity is strong and uneasy to evaporate due to the covered film. In order to ensure the fruits growth rise superior to the plant growth, the humidity in the greenhouse must be reasonable. According to the results in Table 2-6, set the mean lower irrigation as 0.235m³/m³ and 0.250m³/m³ in the irrigation algorithm. The upper limit is 1 in theory, but during the actual irrigation process, the maximum is 80% field capacity at most, and it seldom happens, so set the upper limit as 0.330m³/m³, which takes 65% of the field capacity.

B. Sensors buried position

Since the cultivation formulation soil in greenhouse is mixed with different ingredients, organic matter mix uneven may occur in an individual case. So the test needs to collect much data of several irrigation processes and the saturated soil layers profile data

.Calculate the mean of each layer and its overall mean for comparison, reflecting the mean value of about 15cm is typical of the mean of the entire range of the closest. Though this position can reflect the overall soil moisture, it's treated as the best laying position for sensor. In addition, because of the greenhouse cultivation soil at about 25cm deep is the border of the formulation soil and clay; it is used to bury another humidity sensor. The two positions can determine irrigated conditions accurately.

3 Automatic Irrigation Fuzzy Control Algorithm

Because of major factors such as the temperature and humidity can't be defined entirely by mathematical model, the fuzzy control algorithm that combined qualitative analysis and quantitative analysis is proposed in this article to make the automatic irrigation control algorithm. Fuzzy comprehensive evaluation results are used as humidity sensor output, and ultimately decision making depends on membership results.

3.1 Fuzzy Comprehensive Evaluation

The fuzzy comprehensive evaluation is based on fuzzy mathematics, which provides integrated solutions to specific practical problems. Fuzzy comprehensive evaluation is based on fuzzy math actually, and according to fuzzy relation principles of synthesis of the corresponding, situations of the boundary is not clear and is not easy to quantitative determinants can be evaluated. Evaluation objects can be evaluated from several factors by using comprehensive evaluation. Comprehensive evaluation can get non-negative real numbers on each object according to the given conditions, judging indexes can also be sorted merit.

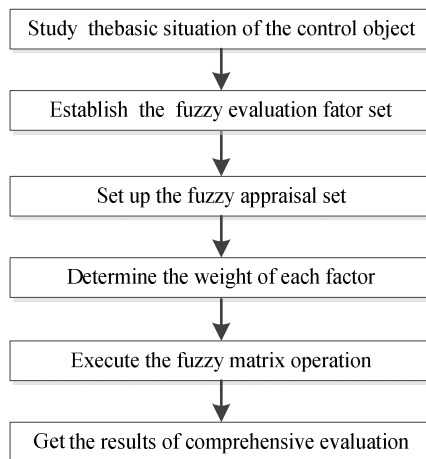


Fig. 1. Fuzzy comprehensive evaluation steps

In greenhouse irrigation control process, the need for irrigation is mainly decided by factors such as in-situ soil moisture and temperature in strawberry greenhouse. Temperature indoor is used to as precondition of whether it's suitable to start irrigation, but specifically when to start irrigation is required from analysis of soil moisture sensor data. For data fusion of multiple sensors, this paper used fuzzy comprehensive evaluation method for analysis.

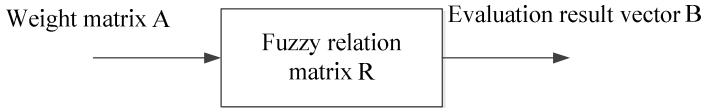


Fig. 2. Schematic basic model of fuzzy comprehensive evaluation

Fuzzy relation matrix element is set as a fuzzy converter, and each set of input and output weight vector correspond its evaluation results. The basic model is shown in Fig 2.

3.2 The Fuzzy Comprehensive Evaluation Calculation

First, establish evaluation factors. This evaluation factors set all of the humidity values, and distributed at different distances at different depths. Eight sensor value integrated decision-making has a very good representation. Factor set matrix as follows

$$U = \begin{bmatrix} u_{11} & u_{12} & u_{13} & u_{14} \\ u_{21} & u_{22} & u_{23} & u_{24} \end{bmatrix} \tag{3}$$

From u_{11} to u_{24} correspond to the sensors R 1 to 8, represents respectively four sensors at 15cm and four sensors at 25cm.

Secondly, establish fuzzy relationship matrix of 8 humidity sensors, the matrix as follows

$$R = \begin{bmatrix} r_{11} & r_{12} & r_{13} & r_{14} \\ r_{21} & r_{22} & r_{23} & r_{24} \end{bmatrix} \tag{4}$$

Where r_{11} to r_{24} respectively correspond to the ratio of the measured values and the threshold value. Based on analysis of the humidity data , set irrigation lower limit at 15cm, 25cm irrigation limit as l_{10} and l_{20} ,the measured values are $0.235 \text{ m}^3/\text{m}^3$ and $0.250 \text{ m}^3/\text{m}^3$, then

$$r_{1i} = \frac{\text{sensor values}}{\text{lower irrigation limit at 15cm}} \tag{5}$$

$$r_{2i} = \frac{\text{sensor values}}{\text{lower irrigation limit at 25cm}} \quad (6)$$

Next, establish the weight set. A reasonable weight value for the fuzzy comprehensive evaluation result has great influence on the finally results. In the evaluation system, because of functions of severity of different factors on the ultimate goals is different, the weight becomes the important information in evaluation process. It's necessary to consider its importance and identify its scale factor. Commonly there are many methods used to determine the weight, for example, the Delphi method with qualitative nature, principal component analysis with quantitative analysis method, and qualitative and quantitative analysis method. Based on practical irrigation experience, weight of the humidity sensor data is determined subjectively.

In actual greenhouse soil environment, the sensors at different depth locate in vertical position .Since the lower sensor is inserted in the junction of formulation soil and clay, and the humidity changes slowly under normal circumstances. According to the professional experience of planters and the actual measured data, weights of the upper and lower sensors are respectively 0.7 and 0.3. Expressed as

$$A = [a_{11} \quad a_{12}] = [0.7 \quad 0.3] \quad (7)$$

Finally, execute fuzzy comprehensive evaluation. Factor set to review set fuzzy transformation is realized by the fuzzy relation matrix, evaluation results can be get by the corresponding weight vector of input factor. The fuzzy operator used in this paper contains the most information, as follows

$$B = AR = [a_{11} \quad a_{12}] \begin{bmatrix} r_{11} & r_{12} & r_{13} & r_{14} \\ r_{21} & r_{22} & r_{23} & r_{24} \end{bmatrix} \quad (8)$$

$$= [b_{11} \quad b_{12} \quad b_{13} \quad b_{14}]$$

Select the maximum membership degree method to determinate the evaluation results. Accordingly, the lower limit is used to decide whether to begin irrigation.

Compare $\max(b_{1j})$ with 1.

If $\max(b_{1j}) > 1$, there is no need to irrigate;

If $\max(b_{1j}) \leq 1$, then need to begin irrigate immediately.

Similarly, based on the irrigation upper limit to decide whether to stop irrigation.

$$r_{1i} = \frac{\text{sensor values}}{\text{upper irrigation limit}} \quad (9)$$

$$r_{2i} = \frac{\text{sensor values}}{\text{upper irrigation limit}} \quad (10)$$

Compare $\max(b_{1_i})$ with 1 to decide whether to stop irrigation.

If $\max(b_{1_i}) > 1$, then stop irrigation;

If $\max(b_{1_i}) \leq 1$, then continue irrigation.

3.3 Automatic Irrigation Control Algorithm

The entire basic idea fuzzy of control algorithm is: PC machine collects humidity data for fuzzy comprehensive evaluation, and the output is sent to PLC; according to the irrigation experience, set a fixed irrigation cycle with PLC, which begin irrigation cycle after planting. Air temperature of the greenhouse is taken as the premise of irrigation. Only air temperature is within the allowable range, can irrigation operations can be executed. In the fixed irrigation period, execute irrigation operations regularly; outside the irrigation cycle, irrigation decision about whether to stop irrigation and irrigation mainly depends on the sensor data. Set the maximum irrigation time as 3h, which is prior to the humidity data to stop irrigation.

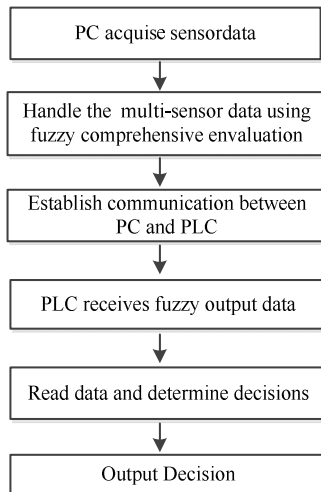


Fig. 3. Automatic irrigation algorithm flowchart

4 Realize Automatic Irrigation Control Algorithm

Based on study of greenhouse strawberry and soil profile data, this paper sums up an automatic irrigation algorithm that suits the greenhouse, which makes decisions by the feedback sensors data.

The algorithm is based on PLC and configuration software to implement. Field operations can be controlled by PLC program, and the remote control can rely on the configuration software. Computer sends instructions to operate the actuator, to adjust the soil moisture to keep it suitable for strawberry growth.

4.1 Fuzzy Control Algorithm Based on PLC

PLC mainly is used in the scene control and get data from PC to make judgments based on automatic irrigation algorithm to decide whether begin or stop irrigation.

Input port of the control system include such as solenoid valve A switch button (X10), the solenoid valve B switch button (X11), the pump switch button (X12), the system manual/automatic button (X13/X15); output device of the control system include such as solenoid valve A(Y14), solenoid valve B (Y15), and the total pump (Y16), system alarm display (Y17).Beside, data includes humidity sensor and temperature sensor data. PLC can also complete irrigation time setting. Fig.4 is the flow chart of a PLC-based automatic irrigation control algorithm.

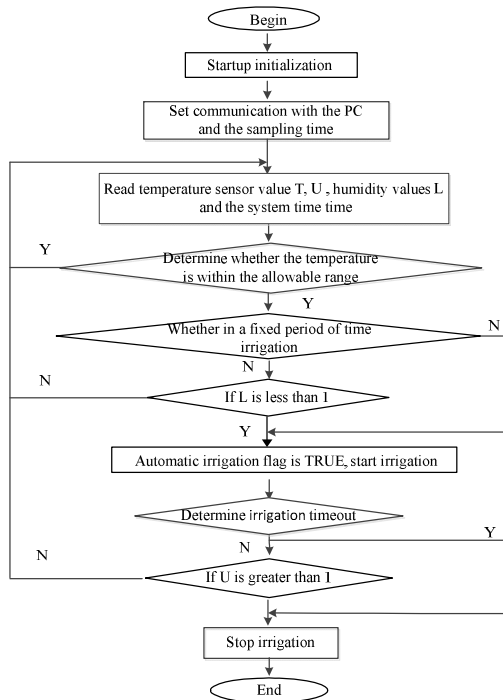


Fig. 4. Flow chart of automatic irrigation control algorithm based on PLC

4.2 Automatic Irrigation Control System Structure

The system configuration in control process is shown in Fig.5. System is composed with the central monitoring computer, a programmable logic controller, soil moisture sensors and solenoid valves.

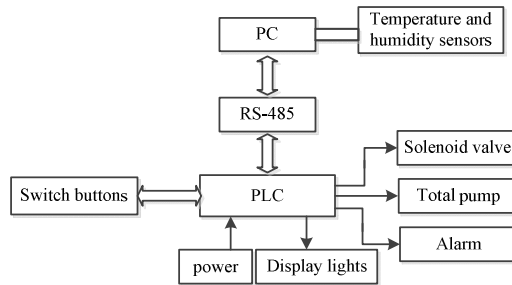


Fig. 5. Structure diagram of control system

In irrigation control system(Fig.5), the sensor uses Decagon ECH2O upgrade 5TE soil moisture sensor is used to measure soil moisture, three points need to be controlled, coupled with the temperature and humidity control, so the PLC selects Delta DVP series PLC, the experimental for other experiments vacated control communication channel and subsequent functional expansion choose to use DVP60ES200R Model. The whole solenoid valve actuator control circuit, optional 24 V AC drive form, to 2 W. PC as the control system of the host computer using the configuration software to communicate between the PLC to complete the exchange of data, that is controlled via a PC input parameters, data uploaded regularly monitored by the PLC and stored in the PC, provide data for later analysis and processing.

4.3 System Control Working Principle

The hardware part of the irrigation system PLC control solenoid valve start, enter start and stop switch for irrigation, output via solid state relays, control solenoid valve opening and power to control the opening of the drip off. The greenhouse irrigation can also be based on changes in soil moisture dynamic feedback control.

Changes in soil moisture, temperature data collected in accordance with the soil moisture sensor to pass information to the PLC control program, and continue to query fuzzy control rule table to determine each irrigation solenoid valve is open or not, to maintain a constant soil moisture. According to the fuzzy control rules, when the real-time acquisition of soil moisture than the set humidity value, the solenoid valve without opening; collected in real time soil moisture than the set humidity value hours, the solenoid valve to open a certain period of time, the irrigation time; when measured value equal to the set value, according to the trend of the measured values to decide whether or irrigation, soil moisture until the real-time acquisition is equal to the set humidity value or within the permissible error range, the end of the first irrigation. The important prerequisite irrigation indoor temperature must reach the irrigation permissible range. Irrigation has been guided by the principle: soil moisture is maintained under suitable for the growth of strawberry constant soil moisture environment.

5 Conclusions

In this paper, the statistical analysis of data on strawberry growth and development of irrigation, to determine the lower limit of the strawberry irrigation, developed a the strawberries irrigation fuzzy control strategy, the fuzzy control and PLC control system combined, while demonstrating the PLC reliable, flexible and adaptable strong features, and can better adapt to the strawberry growth cycle of water, greatly increased the level of intelligence of the irrigation and irrigation efficiency. Based on PLC fuzzy control system is suitable for many occasions, the control program can be easily modularity, standardization, also has some reference value of other crops, irrigation control or control of industrial applications.

References

1. Wang, J., Zhang, J.: Effect of strawberry in greenhouse fertigation research. *Chinese Soil and Fertilizer* (1), 78–79 (2008)
2. Wang, L.: The problem of the development and production of strawberry and corresponding countermeasure. *Journal of Anhui Agricultural Sciences* 38(33), 18707–18708 (2010)
3. Kuang, Q., Hao, Y., Bai, C.: Automatic monitor and control system of water saving irrigation. *Transaction of the CSAE* 26(6), 136–139 (2007) (in Chinese with English abstract)
4. Qian, X.: Effect of Irrigation Modes on Production, Quality and Water Metabolism of Strawberry. Anhui Agriculture University, Hefei (2009)
5. O'Shaughnessy, S.A., Evett, S.R., Colaizzi, P.D., Howell, et al.: A crop water stress index and time threshold for automatic irrigation scheduling of grain sorghum. *Agricultural Water Management* (107), 122–132 (2012)
6. Pfitscher, L.L., Bernardon, D.P., Kopp, L.M., et al.: Automatic Control of Irrigation Systems Aiming at High Energy Efficiency in Rice Crops. In: 8th International Caribbean Conference on Devices, Circuits and Systems, pp. 1–4 (2012)
7. He, W., Cai, M., Wang, Y., et al.: Automatic Water Supply Control System of Graded Constant Pressure by Variable Frequency Speed and Its Application to Pipeline Irrigation. In: 2010 Second WRI Global Congress on Intelligent Systems, pp. 385–388 (2010)
8. Yuan, B.Z., Sun, J., Nishiyama, S.: Effect of irrigation on strawberry growth and yield inside a plastic greenhouse. *Biosystems Engineering* 87(2), 237–245 (2004)
9. Zhang, Z., Huang, Y., Gao, E.: A Fuzzy and Comprehensive Evaluation Model for Developing Teaching Evaluation. In: 2nd International Conference on Consumer Electronics, Communications and Networks (CECNet), pp. 774–777 (2012)
10. Dai, J.: Fuzzy Comprehensive Evaluation on Water Resources Bearing Capacity of Boertala River Basin. *Desert and Oasis Meteorology* (4), 35–39 (2010)
11. Ren, X., Wang, S., Hu, H.: Index weight of evaluation of water-saving irrigation project with the contrary problem of fuzzy comprehensive evaluation method. *China Rural Water and Hydropower* 5, 40–42 (2005)
12. Chen, D., Lei, X., Cao, W., et al.: Research on Irrigation Decision Support System of Drip Irrigation Cotton. *China Rural Water and Hydropower* 11, 72–75 (2012) (in Chinese with English abstract)

13. He, H., Zhao, H., Han, S.: Experimental study on drip irrigation index for Greenhouse Tomato. *Water Saving Irrigation* 4, 22–25 (2005)
14. Lv, Y., Hu, T., Lei, L.: *Systems engineering*. Northern Jiaotong University press, Beijing (2003)
15. Xie, S., Li, X., Yang, S., He, B.: Design and implementation of fuzzy control for irrigating system with PLC. *Transaction of the CSAE* 23(6), 208–210 (2007)
16. Su, C., Sun, Y., Chen, Y.: Study on Application of Newly Water-Saving Irrigation Control. *Advances in Water Science* (2), 142–148 (1994) (in Chinese with English abstract)
17. Passino, K.M., Yurkovich, S.: *Fuzzy Control*. Tsinghua University press, Beijing (2001)
18. Sun, P., Li, D., Shi, X.: Research on fuzzy control irrigation system based on PLC. *China Rural Water and Hydropower* 12, 26–30 (2010)
19. Passino, K.M., Yurkovich, S.: *Fuzzy Control*. Tsinghua University press, Beijing (2001)
20. *Solar Greenhouse Strawberry Cultivation Technology*. Jindun publishing house, Beijing (2009)
21. *Strawberry standardized production overall fine solution*. China Agricultural Press, Beijing (2010)

A Dynamic Knowledge Models of Nitrogen Fertilizer and Computer System for Cotton

ChunJing Si

College of Information Engineering, Tarim University, Xinjiang 843300, China
smallx1002@sina.com

Abstract. Through analyzing the newest research results about nitrogen management of cotton and experimental results, and on the basis of the different effects of cotton yield, plant height and leaf area, a dynamic knowledge model for decision making on total nitrogen and their distribution among main growth stages of cotton under different environments and yield targets was developed with the principles of nitrogen balance and by integrating the factors of climate, soil, yield and so on. A comprehensive and intelligent computer system for cotton management was established using VC++6.0 and SQL Server 2003.

Keywords: nitrogen management, influence factors, dynamic knowledge models, decision support system.

1 Introduction

As nitrogen is one of the important components of protein, which is also the important element making up of cellular plasm, so to speak, life activities cannot be formed without nitrogen. The nutrition level of nitrogen fertilizer has a very essential influence on cottons' growth and development, which not only limits the height of cotton leaves, but also cotton yields. In the case of lacking the nitrogen fertilizer, cottons take on a slow and weak growth, with undersized and thin stems, cotton buds and bolls with a high expulsion rate and rare bolls; in the case of using too much or improperly fertilizing in different growth periods of cottons, sugars formed by organic nutrition consume too much with little accumulation, excessive vegetative growth and increasing expulsion. Fertilization of abundant nitrogen fertilizers will not only decrease the utilization rate of fertilizer and increase its cost, but also cause adverse effects to the environment. Different treatments of nitrogen fertilizer have certain influence on the growth of cotton organs and the yields. So, it will be of much importance for guiding the agricultural production to create accurate and effective nitrogen management models and design and develop them into systems.

2 Materials and Methods

2.1 Experiment Design

The experiment is conducted in agricultural experiment station (with latitude of 40°32' N and longitude of 81°18' E) of Tarim University in Xinjiang Province in April, 2011.

With a height above the sea level of 900-950 meters and of warm temperate desert climate, the experimental zone locates in the upper and middle reaches of Tarim River, graced with rich resources of water and soil, dry weather, abundant sunlight and four distinctive seasons. For nearly 30 years, the area has an average annual precipitation of 40.1-82.5 mm, with little rain in summer and little snow in winter, an average annual temperature of 10.7°C and a total annual sunshine duration of 2900 hours, suitable for the growth of long-staple cotton. The cottons are planted by means of plot, with a planting density of 12200 plants per mu. The experimental soil is loam, with 14g/kg organic content, 0.5g/kg total nitrogen, 85mg/kg effective nitrogen, 14mg/kg available phosphorus and 75mg/kg rapidly available potassium. The experimental variety is the New Sea 21 of long-staple cotton, with a plot area of 132m².

This experiment designs five nitrogen fertilization treatments, namely, 0, 180, 240, 300, 360kg/hm², with the amount of base fertilizer holding 45% of the total fertilization amount, and the remainder being top dressing/nitrogen application, respectively in the periods from the bud period to the flower and boll stage and 3 fertilization proportions with water of 15%, 25% and 15%. Besides, the phosphorus and potassium fertilizers in the base fertilizer separately are P₂O₅ 138 kg/hm² and K₂O 72 kg/hm². The experiment is arranged in random groups, with 3 repeated treatments in each group. The samples make up of the following table 1:

Table 1. Schemes of every fertilization treatment in the experiment

Treatment	Total amount			Base fertilizer			Topdressing nitrogen fertilizer		
	N	P ₂ O ₅	K ₂ O	N	P ₂ O ₅	K ₂ O	1 st (6.10)	2 nd (7.15)	3 rd (8.20)
N0	0	138	72	0	138	72	0	0	0
N1	180	138	72	81	138	72	27	45	27
N2	240	138	72	108	138	72	36	60	36
N3	300	138	72	135	138	72	45	75	45
N4	360	138	72	162	138	72	54	90	54

2.2 Experimental Method

In the main growth period, seedling stage, bud stage, flower and boll stage and boll period, samples are respectively taken in the time between 10:00-12:00 am on the corresponding dates. Each nitrogen fertilizer treatment area randomly selects 3 representative cotton plants (5 plants in the bud period), and measures related data from the selected plant samples.

The plant height of cotton: the plant heights of cotton are measured with rulers on June 9th, June 17th, July 2nd, July 17th and September 15th.

The length and width of cotton leaves: the length and width of the largest leaves in representative plants are measured with rulers on June 9th, June 17th, July 2nd, July 17th and September 15th.

The leaf area: according to the quantitative functional relationship between pulse length and leaf area in cotton leaves applied in Literature [2], the leaf area is solved. With the pulse length x as the independent variable and the leaf area y as the dependent variable, the quadratic regression equation of one variable $=2.4337-0.4328x+0.8265x^2$ is established.

3 The Influence of Nitrogen Fertilizer on the Growth of Long-Staple Cotton

3.1 The Influence of Nitrogen Fertilizer on the Yield of Long-Staple Cotton

The research literature [3-5] show there is certain quantitative relationship existing between nitrogen fertilizer NR and the target of yield TY (kg/ha), which can be expressed in the following linear function:

$$NR = 0.1062 \times TY + 17.181 \quad R = 0.8313^{**} \quad (1)$$

The literature [6] proves that under the condition of border irrigation in southern Xinjiang area, different amounts of nitrogen fertilization have influences on the boll number of each cotton plant, the weight of each boll and the yield of seed cottons. This research suggests that under different nitrogen treatments, there is certain difference in the boll number of each cotton plant, the weight of each boll and the yield of seed cotton. Thereinto, the relationship of the boll number of each cotton plant and nitrogen treatments accords with quadratic curve equation. At first, the yield of seed cotton increases with the increasing amount of nitrogen fertilization, but when the nitrogen level reaches N3, the yield takes on downtrend. By simulating and matching the nitrogen fertilizer effect of cottons with quadratic equation of one variable, the experimenter concludes the correlation between the amount of nitrogen fertilization and the cotton yield as follows:

$$y = -0.0039x^2 + 2.6895x + 1962.9 \quad R^2 = 0.9576^{**} \quad (2)$$

In the equation, y refers to the yield and x the amount of nitrogen fertilization.

Table 2. The influence of different amounts of nitrogen fertilizer on cotton yields

Treatment	Boll numbers of each plant(No./plant)	Weight of each plant(g)	Yield of seed cotton(kg./hm ²)
N0	7.6	2.9	4562.2
N1	8.3	2.8	4810.7
N2	8.4	2.9	5042.5
N3	8.5	3.1	5454.5
N4	8.4	3.0	5216.4

3.2 The Influence of Nitrogen Fertilizer on Plant Height and Leaf Area of the Long-Staple Cotton

The experimental result (seen in Chart 3) shows that with the advancement of long-staple cotton's growth process, there is no difference in different nitrogen fertilizer treatments in periods of seedling and bud, that the growth processes of cotton in the beginning of flowering and at full-blossom stage are both a little delayed and that in the full-blossom stage, the heights of front plants rapidly increase and after that, the difference in plant height with different nitrogen treatments gradually increases with the growth process.

Table 3. The influence of different nitrogen levels on plant height, leaf number and leaf area

Treatment	Plant height(cm)	True leaf number(leaf number/plant)	Leaf area (cm ² /plant)	Plant height(cm)	True leaf number(leaf number/plant)	Leaf area (cm ² /plant)
	(Stage of 4 leaves) May 21th			(Stage of 5 leaves) May 21th		
N0	4.0	3.5	61.2	5.1	4.8	109.8
N1	4.1	3.6	64.3	5.6	5.0	118.5
N2	4.3	3.8	84.5	6.1	5.0	133.0
N3	3.1	3.5	59.8	5.7	5.1	122.3
N4	3.6	3.5	55.7	5.4	5.0	114.5

4 The Dynamic Knowledge Model of Nitrogen Management

4.1 The Establishment of the Model/the Modeling

Based on the widely collecting and consulting the latest literatures about the cultivation, the soil science and plant nutrition of the long-staple cotton, by means of the principle of system analysis and mathematical modeling method, the experiment builds the relevant quantitative mathematical model of nitrogen management and develops the cotton nitrogen management system based on dynamic knowledge model, and finally tests the correctness of this model with practical applications and optimizes the model with understanding and analyzing the feedback information from the system.

4.2 Descriptions of Model Algorithm

4.2.1 The Amount of Soil Nitrogen Supply in Season

The amount of soil nitrogen supply in season: $SN = ON + ION$

In the equation, ON refers to the supply amount of reducible N element in season and ION the supply amount of irreducible N element in season.

(1). the supply amount of reducible N element in season

$$ON = \frac{0.08 \times TSN \times SPD \times SBW \times N(t) \times SNUE}{365} \times 1000 \tag{3}$$

In the equation, TSN refers to the real total amount of N element in the soil (g·kg⁻¹); SPD the thickness of the top layer (cm); SBW the volume (g·kg⁻¹). The utilization rate of the fertilizer in season is affected by the fertilizer variety, fertilizing method, weather conditions and soil environment and so on. Under the conventional fertilizing technique, the utilization rate of fertilizer in season is generally 32.5%±2.5%. Recently, as a new fertilizing technique, drip fertigation has obtained/achieved much development. Because the fertilizer is quantitatively applied with water, the solubleness of the fertilizer and the close fertilization are increased, thus improving the fertilizer efficiency and the utilization rate of nitrogen fertilizer reaches 50.5%±3.5%. According to the fertilization pattern and past experience, users can determine the utilization rate of corresponding fertilizers in season.

$N(t)$ refers to the total number of standardized days under water temperature effect:

$$N(t) = N(t)'_1 + N(t)'_2 + \dots + N(t)'_{365}$$

$N(t)_i$ refers to the number of standardized days under the effect of water and the temperature of Number i , whose value is:

If the value of PDT_i (psychological development time the variety accumulates gradually under actual sowing dates) is taken and fixed from 0 to 144, then

$$N(t)'_i = F_T(t) \times F_w(t) \tag{4}$$

Otherwise, its value is 0.

$F_T(t)$ is the influence function of temperature to nitrogen fertilization, whose value is $F_T(t) = \left(8 \times e^{-0.058 \times STA_{20}}\right)^{\frac{STA_{20}-30}{10}}$. Thereinto, STA_{20} is the soil temperature when the plough layer is 20 cm thick.

$F_w(t)$ is the influence function of moisture to nitrogen fertilization.

$$F_w(t) = \begin{cases} 0.2 & W(t) \leq W_D \\ 0.2 + 0.8 \times \frac{W(t) - W_D}{W_o - W_D} & W(t) \leq W_o \\ 1 - 0.6 \times \frac{W(t) - W_o}{W_s - W_o} & W(t) \leq W_s \\ 0 & W(t) > W_s \end{cases} \tag{5}$$

W_D is the wilting moisture content; W_o the optimum soil moisture content under mineralization; W_s saturated moisture content of soil; $W(t)$ the actual moisture content of soil.

(2). The supply amount of irreducible N element in season

$$ION = AOVN \times SPD \times SBW \times 10$$

In the equation, $AOVN$ is the content of irreducible N element and effective nitrogen in the top layer of soil; SPD the thickness of the topsoil (cm); SBW soil capacity ($g \cdot kg^{-1}$).

4.2.2 The Necessary/Needed Amount of N under Specific Yields

The necessary amount of N under specific yields URN ($kg \cdot hm^{-2}$)

$$UR_N = \frac{418.5966}{1 + e^{-0.0004 \times (TY - 4151.962)}} \tag{6}$$

In the equation, TY (kg/hm^2) is used to calculate the realizable yield potential of users.

$$TY = \begin{cases} TY_{max} & YM \times \left(1 + \frac{YLPP - YM}{4 \times YLPP}\right) \geq TY_{max} \\ YM \times \left(1 + \frac{YLPP - YM}{4 \times YLPP}\right) & YM \times \left(1 + \frac{YLPP - YM}{4 \times YLPP}\right) < TY_{max} \end{cases} \tag{7}$$

In the equation, TY_{max} is the yield potential under the earliest time of suitable sowing period; YM the average yield in the first three years; $YLPP$ the production potential of production technology.

4.2.3 The Fertilizing Ratio of Organic N to Inorganic N $OINR_1$: $OINR_2$

(1) The fertilization amount of organic N

$$OINR_1 = \begin{cases} 5 - (1 - 2.5/LA') - (1 - 1.5 \times TY/TY_{max}) & OMC < 8 \\ 4 - (1 - 2.5/LA') - (1 - 1.5 \times TY/TY_{max}) & 8 \leq OMC < 14 \\ 3 - (1 - 2.5/LA') - (1 - 1.5 \times TY/TY_{max}) & OMC \geq 14 \end{cases} \quad (8)$$

In the equation, TY (kg/hm^2) is used to calculate the realizable yield potential of users; TY_{max} is the yield potential under the earliest time of suitable sowing period; OMC the organic material content in the soil (g/kg).

LA is the age of transplanted leaves after PS correcting the seeding method, whose value is:

$$LA' = \begin{cases} 2.5 & \text{direct seeding} \\ LA & \text{Otherwise} \end{cases}, \quad LA \text{ refers to the age of transplanted leaves} \quad (9)$$

(2) The fertilization amount of inorganic N $OINR_2$

$$OINR_2 = 10 - OINR_1 \quad (10)$$

4.2.4 The Drip Fertigation

In different growth stages of cotton, the ratio of base fertilizer to top-dressing; the drip fertigation ratio in base fertilizer, bud stage, the beginning of flowering, the full-blossom stage, boll stage and early flocculant stage, namely, $BTRND1$: $BTRND2$: $BTRND3$: $BTRND4$: $BTRND5$: $BTRND6$.

(1) The base fertilizer

$$BTRN_{D1} = \begin{cases} 4.5 - (1 - 2.5/LA') + CLAYC/100 + (1 - 1.5 \times TY/TY_{max}) & TY \leq 0.4 \times TY_{max} \\ 3.5 - (1 - 2.5/LA') + CLAYC/100 + (1 - 1.5 \times TY/TY_{max}) & 0.4 \times TY_{max} < TY \leq 0.7 \times TY_{max} \\ 2.5 - (1 - 2.5/LA') + CLAYC/100 + (1 - 1.5 \times TY/TY_{max}) & TY > 0.7 \times TY_{max} \end{cases} \quad (11)$$

In the equation, LA is the age of transplanted leaves after PS correcting the seeding method; TY (kg/hm^2) is used to calculate the realizable yield potential of users; TY_{max} is the yield potential under the earliest time of suitable sowing period.

$CLAYC$ is the content of the physical clay (%), whose value is listed in Chart 4 as follows:

Table 4. The soil texture and the corresponding values of CLAYC

Soil texture	CLAYC value
Sandy soil	7.5
Sandy loam	15
Light loam	25
Middle loam	37.5
Heavy loam	52.5
Clay	65

(2) The bud stage

$$BTRN_{D2} = \begin{cases} 1 & TY \leq 0.4 \times TY_{\max} \\ 0.9 & TY > 0.4 \times TY_{\max} \end{cases} \quad (12)$$

TY (kg/hm²) is used to calculate the realizable yield potential of users; TY max is the yield potential under the earliest time of suitable sowing period.

(3) The beginning of flowering stage

$$BTRN_{D3} = \begin{cases} 2.2 + (1 - 2.5/LA') - CLAYC/100 - (1 - 1.5 \times TY/TY_{\max}) & TY \leq 0.4 \times TY_{\max} \\ 2 + (1 - 2.5/LA') - CLAYC/100 - (1 - 1.5 \times TY/TY_{\max}) & 0.4 \times TY_{\max} < TY \leq 0.7 \times TY_{\max} \\ 1.8 + (1 - 2.5/LA') - CLAYC/100 - (1 - 1.5 \times TY/TY_{\max}) & TY > 0.7 \times TY_{\max} \end{cases} \quad (13)$$

(4) The full-blossom stage

$$BTRN_{D4} = \begin{cases} 2 - (1 - 2.5/LA') + CLAYC/100 - (1 - 1.5 \times TY/TY_{\max}) & TY \leq 0.4 \times TY_{\max} \\ 2.5 - (1 - 2.5/LA') + CLAYC/100 - (1 - 1.5 \times TY/TY_{\max}) & 0.4 \times TY_{\max} < TY \leq 0.7 \times TY_{\max} \\ 3 - (1 - 2.5/LA') + CLAYC/100 - (1 - 1.5 \times TY/TY_{\max}) & TY > 0.7 \times TY_{\max} \end{cases} \quad (14)$$

(5) The boll stage

$$BTRN_{D5} = \begin{cases} 0.3 + (1 - 2.5/LA') - CLAYC/100 + (1 - 1.5 \times TY/TY_{\max}) & TY \leq 0.4 \times TY_{\max} \\ 0.8 + (1 - 2.5/LA') - CLAYC/100 + (1 - 1.5 \times TY/TY_{\max}) & 0.4 \times TY_{\max} < TY \leq 0.7 \times TY_{\max} \\ 1.4 + (1 - 2.5/LA') - CLAYC/100 + (1 - 1.5 \times TY/TY_{\max}) & TY > 0.7 \times TY_{\max} \end{cases} \quad (15)$$

(6) The early flocculant stage

$$BTRN_{D6} = \begin{cases} 0 & TY \leq 0.4 \times TY_{\max} \\ 0.3 & 0.4 \times TY_{\max} < TY \leq 0.7 \times TY_{\max} \\ 0.4 & TY > 0.7 \times TY_{\max} \end{cases} \quad (16)$$

4.3 Verification of the Model

By systemically using the meteorological data, soil bank, commercial variety, perennial production data of 5 areas with different latitudes like Alear City, Bachu, Bytown, and Shihezi, the experimenter designs management schemes of cotton nitrogen in normal

years for these areas and then compares with the cotton cultivation mode in local use to find that they are basically consistent, which suggests this system is of good practicality and accuracy.

5 The Design and Development of Nitrogen Management System

By understanding and refining document literatures and expert knowledge, combining with field trials and dynamic knowledge model of nitrogen management, with the help of programming language VC++6.0 and data platform SQL 2000, the experiment designs and develops nitrogen management system based on dynamic knowledge model, which mainly covers 4 modules.

The first three modules simulate the influences of different nitrogen treatments on such parameters as the yield of long-staple cotton, the plant height and leaves. Thereinto, the module of production estimation realizes the influences of 5 nitrogen treatments on the number of bolls in each cotton plant, the weight of each boll and the seed cotton yield, further realizing the estimation of long-staple cotton yield; by analyzing the influences of 5 nitrogen treatments on long-staple plants, the module of plant height prediction concludes to predict the plant height by the fertilization amount of nitrogen fertilizer; by the influences of 5 nitrogen treatments on leaf number and leaf area, the leaf parameter estimation module concludes to estimate related parameters of leaves according to the fertilization amount of nitrogen fertilizer.

According to input parameters by users, nitrogen management module can help users calculate the amount of soil nitrogen supply in season, the necessary amount of nitrogen under specific yields, and the fertilization proportion of long-staple cotton in different growth stages under drip fertigation.

6 Conclusion

By understanding and refining document literatures and expert knowledge, combining with field trials, the study analyzes the influences of nitrogen fertilizer on relevant parameters such as the cotton yield, plant height and leaves, further giving out the dynamic knowledge model of nitrogen management and designs and develops the cotton nitrogen management system based on dynamic knowledge model. Proved by practical applications, dynamic knowledge model is of good practicality and accuracy, and the system is characterized by fast and convenient uses, practicality and universality. In the future studies, the system will strengthen the study on the influence of nitrogen fertilizer on other cotton organs and be able to make better service for production.

References

1. Xue, X., Chen, B., Zhou, Z.: The Influence of Cultivation Pattern on Cottons' Growth. *Cotton Science* 19(6), 440–445 (2009)
2. Li, X., Chen, Y.: The Quick Calculation of the Long-staple Cotton Leaf Area by Look-up Table. *Xinjiang Agricultural Sciences* (4), 154–155 (1993)

3. Research Institute of Chinese Academy of Agricultural Sciences. Chinese Cotton Cultivation, pp. 449–501. Shanghai Science and Technology Press, Shanghai (1983)
4. Li, J., Liu, R.: Cotton Nutrition Fertilization and Diagnosis, pp. 64–97. China's Agricultural Science and Technology Press, Beijing (1992)
5. Mao, S.: Cotton Nutrition and Fertilization, pp. 13–44. China's Agricultural Science and Technology Press, Beijing (1993)
6. Wang, X., Zhang, Y.: Diagnostic Study on Nitrogen Nutrition Status in Cottons. *Plant Nutrition and Fertilizer Science* 12(5), 656–661 (2006)
7. Wang, J., Gao, S., Chen, L., Ma, F.: The Dynamic Knowledge Model of the Management of Processing Tomato Fertilizer. *Chinese Journal of Eco-agriculture* 19(2), 285–292 (2011)
8. Mao, D., Chen, L., Zhang, C., Luo, M.: The Study on Crop Fertilization Model and System in Quzhou. *Journal of Chinese Agricultural University* 8, 53–56 (2003)

Research and Design of One Webpage System for Each Village in Shandong Province

Wenjie Feng, Huaijun Ruan, Yan Tang, Wenxiang Zhao,
Qingfu Kong, and Fengyun Wang*

S&T Information Engineering Research Center, Shandong Academy of Agricultural Sciences,
Jinan 250100, Shandong Province, P.R. China

fengwjcn@qq.com, {rhj64,tangyan8000,zhaowx0502,
kongqf1122,wfy1lily}@163.com

Abstract. With the development of informationization in village in Shandong Province, it needs a system to create a webpage for each village on which the villager can look for their interested information and post message. The article puts forward the frame design of the system from its function, hardware, performance and items etc aspects. The system provides the platform for “information to countryside” so as to make the rural government affairs public, reduce the contradiction between the party and the masses and between the cadres and masses and construct the harmonious new village.

Keywords: Webpage for each village, Frame, Function, Column.

1 Introduction

With the development of information technology, the agricultural informationization develops rapidly. Many websites, databases, expert systems and information integrated service platforms related to the agriculture have been built at home and abroad. But there is no one webpage system for each village at home [1][2]. In some developed countries, some systems were used in special farm. For example, many advanced monitoring systems were used in modern greenhouses in Holland. Because of different national conditions, some country needn't a webpage for one village [3].

As of the end of 2010, there are 78015 village committees in Shandong Province [4] which quantity is among the top of the nation. In 2009, there were about 10.8 sets of home computer among 100 rural residents in Shandong Province. At the end of 2010, Shandong realized that the optical cable covered all the areas to towns and 90% areas of villages [5]. During the 12th-five-year plan, Shandong will further prolong optical cable network to make the rural optical cable coverage up to 100%. Shandong

* Corresponding author. Supported by: National science and technology support plan of P. R. China (2011BAD21B06), Key Applied Technological Innovation Project in Agriculture of Shandong Province: Key Technology Study and Application of Regulation and Control between Fertilizer and Water of Tea with Good Quality and High Yield.

is the first pilot province of computer-to-village project which solves the last-one-kilometer question in rural informationization [6].

The infrastructure of rural information in Shandong has been more perfect. But if there is only computer and no information for villagers, the villager only can use the computer to play games or the computer is only for show [7]. It is the focus of rural informationization how to use the modern computer technology to service the new village construction, promote the agricultural development, increase farmer's income and exploit the rural market [8]. Therefore, we designed the system so as to promote rural government affairs public, reduce the contradiction of society and construct the harmonious new village. Some departments of government can also know about some information related to rural affairs, social insurance and so on in time and accurately and then speed up the progress of agricultural and rural informationization in Shandong Province [9][10].

2 System Composition and Function

The system is mainly composed of register system, publishing system and management system. The management system is the core which manages the register system and publishing system to delete the unreasonable website that register system creates and bad information that the publishing system releases. The system composition and function frame are shown in Fig. 1.

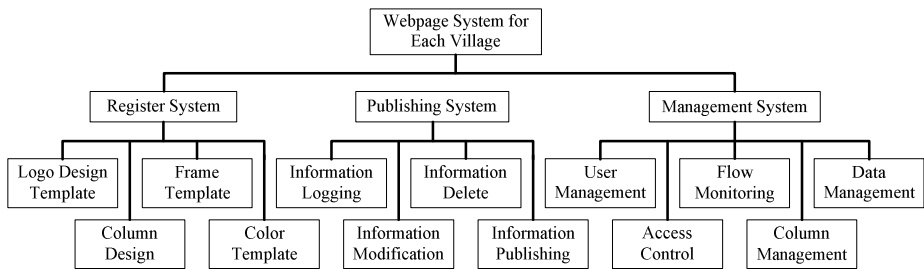


Fig. 1. System composition and function frame diagram

2.1 Register System

There are about 80000 administrative villages in Shandong and the register system provides the unique webpage navigation for each village. In order to avoid the same name of village, the village is registered in according to the regional, urban and rural codes for statistic in 2012 (refer to <http://www.stats.gov.cn/tjbz/cxfldm/2012/37.html>) released by State Statistics Bureau. The code is as the unique identification. When you look for some village, you can as per the order of province, city, county, town and village to seek. The system provides the visual template and has the following functions:

- (1) Logo design template, including the village name and photo etc.
- (2) Column customization, when registered, the column is created automatically and can be modified as per requirement.

- (3) Frame design template through which you can select proper frame suitable to your design.
- (4) Color template to make the webpage with different color.

2.2 Publishing System

The publishing system manages the updating information that need some modification, classifies them with some common characteristic and releases them onto the webpage. The information is loaded into a database by a simple interface and then released onto the webpage through the template format after verified by the administrator.

The publishing system can make the rural messenger conveniently and efficiently classify, add, modify, delete and edit the information etc. The category, title, introduction and photo of products etc can automatically create a page and be saved on the database to make the user inquire conveniently. The main part of the system is the on-line compiler which can carry out many types of word processing by the WYSIWYG edit mode e.g. editing the article, news and notice etc.

2.3 Management System

The management system provides the uniform management and control for the user, access right, page views, column, content and data etc and related auxiliary functions. It is mainly managed by the administrator.

2.3.1 User and Access Right Management

The user is divided into administrator, messenger and ordinary user with different access right. The system certifies the user by login and password. The administrator has all rights of the system including the addition, modification and deletion of basic data. The messenger can only have the rights to register and publish and he can't add, modify and delete any important data. The ordinary user can publish the supply and demand, job wanted and job application etc information. The safety of information publishing system is insured by user management and rights management.

2.3.2 Page Views Management

The system monitors various information on the website, including page views, data updating etc. The administrator can record and monitor the website through the page views management. The record and statistic analysis of various visitors can provide the basis to regulate the contents and functions of website.

2.3.3 Column Management

The column management dynamically configures the column of website and automatically creates the website map. The background program manages column in according to the created tree structure. The tree levels haven't limitation. The frame of column is flexibly customized by XSLT (Page extension) + XML (Data extension) design which realizes the flexible configuration between page and column and

between column and data. It includes the column customization, page model management and data model management etc functions.

2.3.4 Data Management

The data management mainly realizes the management and maintenance of data resource within the website. The system can automatically back up the related configuration data. When a fault occurs, the system can automatically restore the data. The system provides the data backup interface through which the administrator can periodically or aperiodically export the backup data to store in other place so as to ensure the safety and completeness of the whole system and ensure the normal and stable working of system.

2.4 Other Functions

2.4.1 Information Retrieval (Search Engine) Function within the Website

The information retrieval system within the website runs through the whole website which makes the user conveniently find the needed information more efficiently. The system provides many finding modes, e.g. as per column, title, content, content and date etc, for the browsers who can find his wanted information among the huge information database as per his favor. The function supports the complicated combination search for random field, combined search of Chinese and English and intelligent fuzzy search.

2.4.2 Statistical form Print Function

It mainly realizes the statistics, report form and print functions etc.

2.4.3 Log Management

It records various running log to realize the analysis and statistics etc functions of them. It manages various user login, operation and accessing for the resource on the website etc logs. And at the same time, it monitors the operation of user to prevent the user from illegal operation. When the system has fault, it can restore some operation in according to the related log information to make the loss of system minimum. The accessing and application degree of different users on the related resource can be traced and counted through the log management.

2.4.4 Database Backup and Restore

It provides the function of database backup and restore to ensure the safety of database on the website.

3 Performance Design

The running and normal visiting of website system can be ensured by configuring Web server, application server and data server etc special servers with high performance and hardware firewall, invading testing equipments and stable network

transmission conditions with high speed. The design should consider the following performance index.

3.1 Website Stability

The mean free error time of website can be up to 10000 hours (i.e. there is about one time of server fault with one year except for the server fault that occurred by normal maintenance of computer room or natural conditions).

3.2 Concurrent Processing Capacity of Website

The system can undertake the concurrent access with 100,000 levels and the daily accessing quantity can be 50,000,000 levels. The processing capability can be improved double by adding Web server.

3.3 Response Speed of Webpage

The average response speed of webpage should be controlled with 3s by adopting multilayer cache mechanism and dual-network duplet accessing strategy between China Netcom and Telecom users.

3.4 SEO Optimization

All the pages adopt DIV+CSS to optimize the keywords, content, picture, link, page description, page title and content title etc strictly as per the SEO standard.

4 Detailed Design

The system provides uniform user login interface to realize the level-to-level administration of access user and administrative user. The system displays by different level and category which structure is distinct and concise.

The design includes two version i.e. village version and comprehensive version. The village version mainly aims at the villager and releases the news, related policies and information of the village. The objective of comprehensive version is wide and its information comes from the village version and includes some information that the village version hasn't e.g. Charming villages (characteristic village, folk customs village and tourism village) etc.

4.1 Column on the Home Page

4.1.1 Search

The home page displays by the village version which is directed to some village by hierarchy index and map index.

- (1) Area search: It is searched by the order of city, county, town and village.
- (2) Hierarchy search: It is searched as per the administrative division published by State Statistics Bureau in 2012, sourced by <http://www.stats.gov.cn/tjbz/>.
- (3) Map search: It is searched by the map in according to the order of 17 cities, counties, towns and villages in Shandong Province.

4.1.2 Content

The column on the homepage includes village trends, village official, characteristic product, invite investment, supply and demand, job wanted and application, charming village (rural home inns, leisure tourism etc), township enterprise, cooperative association and service etc.

- (1) Village trends: It releases the news information of the village.
- (2) Village official: It reports the moving deeds of college-grade village officials and introduces their working experience.
- (3) Characteristic product: There is a saying of different manners in five miles and different customs in ten miles. The agricultural products have strong regionalism. The column mainly reports the product that is with special characteristic in the village or in the town.
- (4) Invite investment: The column provides the information of finance investing and demanding requirements, investment project resources and business opportunity etc to promote the docking of project, capital and attractive investment requirements.
- (5) Supply and demand: It includes the information of supply, purchase, popular product, agricultural business opportunity, rural broker and consumption guide etc.
- (6) Job wanted and application: It includes the information of job wanted, recruitment, company homepage, resume center, industry trends, vocational guidance and strategy of job wanted etc.
- (7) Charming village: It introduces the information of rural home inns, leisure tourism and folk custom village etc.
- (8) Township enterprise: It provides a show window for the township enterprise to promote the development of the township enterprise.
- (9) Cooperative association: It introduces various cooperative associations to realize the cooperation of funds, technology, purchase, production, machining and marketing etc.
- (10) Service: It includes the weather and train etc information related to rural life and trip.

4.2 Column on the Village Webpage

It includes fixed column and user-defined column. The fixed column includes village introduction, village leader, news, village affairs, medical treatment and public health, characteristic product and notification that cover the basic information in the village. The user-defined column includes invite investment, business, charming village etc which is added by the messenger. In addition, there can be some service information.

4.2.1 Fixed Column

The fixed column includes:

(1) Village introduction: It introduces the geographic position, population, resource and social production status etc.

(2) Village leader: It mainly introduces the members, duties and office contact etc of village party branch, village committee, villagers group and ladies' committee etc organizations.

(3) News: It releases the news and great event etc.

(4) Village affairs: It makes the village affairs more transparent.

(5) Medical treatment and public health: It releases the information of doctor and new rural cooperative medical system.

(6) Characteristic product: It introduces the agricultural products with regional characteristic in the village or adjacent area.

(7) Notification: It releases the important notification in the village and provides the short message notice.

4.2.2 User-Defined Column

The user-defined column includes:

(1) Invite investment: It introduces the investment environment, strategic study, planned layout, investment guide and policies and laws related to the inviting investment etc.

(2) Business: It introduces the business information in the village.

(3) Charming village: It includes beautiful village, new village new look and village tourism etc.

(4) Service information: It includes the common contact telephone and contact person in the village etc that provides the convenience for the villagers.

5 Conclusion

The paper designs the frame and function of one webpage system for each village in Shandong Province which realizes the realtime updating and maintenance of the basic date of the village. It is the part study of national science and technology support plan i.e. key technology integration and demonstration of agricultural and rural informationization which will provide the reference for the village information system in other province.

References

1. Li, X.X.: Brief Talk about the Construction of Agricultural Informationization. Rural Economy of Shanghai (02), 38–40 (2010)
2. Zhou, J., Guan, S.H., Fu, Y., Zeng, X.J.: Thought about the Construction and Development of Rural Informationization in Jiangxi Province. Acta Agriculturae Jiangxi (06), 171–174 (2010)

3. Shi, S.T., Zeng, S.X.: Macroscopic Definition of Development Stage of Rural Informationization. *Gansu Technology* (02), 9–11 (2010)
4. Statistics Bureau of Shandong Province. *Statistical Yearbook of Shandong*. China Statistics Press, Beijing (2011)
5. The Twelve-five Year Development Plan of Broadband Network in Shandong Province [EB/OL],
<http://www.50cnet.com/html/zhengcejiedu/20110609/16992.html>
6. Li, J.: Promote the Construction of Rural Informationization by Integrating the Sky and Ground. *Telecommunications Technology* (04), 60–62 (2010)
7. Wen, X.: Wushan Mode during the Construction of Rural Informationization. *Gansu Agriculture* (04), 98 (2010)
8. Shi, W., Ma, C.H., Yang, J., Wang, J.M., Zheng, X.: Development Status Survey of Rural Informationization in Fifty Counties and Cities. *World Telecommunications* (10), 31–36, 6 (2010)
9. Jin, T.C., Li, G.S., Pei, D.F.: Practically Promote the Infrastructure Construction of Agricultural Informationization. *Masses* (07), 62–63 (2010)
10. Zhang, Z.Z.: Resource Integration Service Optimization Pull New Development of the Construction of Agricultural and Rural Informationization – Address on Job Meetings about Agricultural and Rural Informationization in the Whole Province. *Yun Nan Agriculture* (04), 55–56 (2010)

Simulation Study of Winter Wheat Photosynthate Distribution Effect on Controlled Water and Fertilizer Measure

Yan Li, Yang-ren Wang, and Shuhong Sun

Hydraulic Engineering Department,
Tianjin Agricultural University, Tianjin 300384, China
{bfsqz0922,wyrf}@163.com, hongss63@126.com

Abstract. From the morphological characteristics of crop growth, the mechanism model of photosynthate distribution based on the dynamic relationship between root, shoot, leaf and grain is proposed in this paper. And the method of the determining model parameters with the field experiment data is proposed. The root-cap growth equilibrium coefficient, the shoot-leaf growth equilibrium coefficient, the grain-shoot growth equilibrium coefficient, the water stressed coefficient and the nutrient stressed coefficient are obtained by the nonlinear program according to the measured dry matter of the winter wheat root, shoot, leaf and grain in 2008 in the irrigation experiment station of Tianjin agricultural university and the objective function of the minimum absolute error sum on the simulated and measured dry weight. And they are verified by the winter wheat measured data in the irrigation experiment station of Tianjin agricultural university in 2009. The results show that the simulated value and observed data of the dry weight of root, stem, leaf and grain are consistent. The correlation coefficients (R^2) of the comparison between simulated and measured value of the root, shoot, leaf and grain dry weight on every treatments were all over 0.81. It shows that the model on the simulation of the root, shoot, leaf and grain in this paper is reasonable. It provides a theoretical basis on reasonable farmland irrigation and fertilization.

Keywords: photosynthate, mechanism model, winter wheat, dry weight.

1 Introduction

The Chinese and foreign scholars have done a lot of work on the tendency of the wheat growth for forties years and proposed many crop growth models. But, the existing wheat growth simulation models also have some shortcomings. Especially, the photosynthate allocation in the existing crop growth models is a empirical model. This has affected the development and application of the crop growth models to a certain extent. It is further studied and developed a mechanistic model. It need to be improved its explanatoriness [1-5].

2 Creation of the Model

2.1 Hypothesis of the Model

According to the same stretch law of the crop growth, there are several following hypotheses in the establishment of the distribution coefficient model on the winter wheat photosynthate.

(1) Balance hypothesis of the stem-leaf growth

$$Q^{x_1} C^{y_1} W_s = K_{sl} \cdot W_l \quad (1)$$

Where W_l is the dry matter weight of the leaves, kg/hm^2 ; W_s is the dry matter weight of the stems, kg/hm^2 ; Q, C are the Nitrate average concentration (g/kg) and the average volumetric moisture content (cm^3/cm^3) in the soil of 0-100cm depth, respectively. x_1 and y_1 are the index. K_{sl} is a proportionate coefficient related to the crop species and the growing period. In this paper, the coefficient of the stem-leave growth balance was defined. It is one of the crop hereditary parameters related to the crop species and the environmental factors.

(2) Balance hypothesis of the seed-stem growth

$$Q^{x_2} C^{y_2} W_e = K_{se} \cdot W_s \quad (2)$$

Where W_e is the dry matter weight of the seed, kg/hm^2 ; x_2 and y_2 are the index. The remaining symbols are the same meaning as the former. K_{se} is a proportionate coefficient related to the crop species, the growing period and the environmental factors. In this paper, the coefficient of the seed-stem growth balance was defined. It is one of the crop hereditary parameters.

(3) Balance hypothesis of the root-shoot functions

$$Q^{x_3} C^{y_3} W_r \times S = A \times (W_l + W_s + W_e) \times P_d \quad (3)$$

Where W_r is the dry matter weight of the roots, S is the absorbing water velocity of the roots, P_d is the canopy photosynthetic rate. x_3 and y_3 are the index. Because the whole crop growth was analysed, the absorbing water velocity of the roots (S) was equal to the actual transpiration rate of the crop (T_d). In this paper, A related to the species, the variety characteristics of the crops and the environmental factors was defined as the coefficient of the root-shoot growth balance. It is one of the genetic parameters of the crops.

(4) The composition of the roots, stems leaves and seeds was not significant difference. The substrate of the growth was transformed the dry matter with the conversion efficiency Y_g . The rest ($1-Y_g$) was consumed by the respiration [6-9].

Through the one day's accumulation of the photosynthate, the dry matter weight increment of the roots, stems, leaves and seeds(dW_r , dW_s , dW_l , dW_e) were as following

$$dW_r = f_r \cdot P_d \cdot Y_g$$

$$dW_s = f_s \cdot P_d \cdot Y_g$$

$$dW_l = f_l \cdot P_d \cdot Y_g$$

$$dW_e = f_e \cdot P_d \cdot Y_g$$

The dry matter increment of the plant (dW) can be described as

$$dW = dW_r + dW_s + dW_l + dW_e = Y_g \cdot P_d \quad (4)$$

Where P_d is the total amount of one day photosynthate, Y_g is the conversion efficiency of the photosynthate.

2.2 Deduction of the Model

It is supposed that the dry matter weight of the various parts of the plants is W_l , W_s , W_r , W_e in the t time. The canopy photosynthetic rate is P_d , the absorbing water velocity of the roots is S , the plant is in a growth equilibrium state in the t time. It can be described as equation (1), (2) and (3).

In the $t+\Delta t$ time, the various parts of the plant is W_l+dW_l , W_s+dW_s , W_r+dW_r , W_e+dW_e and still in a function equilibrium state. It is described as,

$$Q^{x_1} C^{y_1} (W_s + dW_s) = (K_{sl} + dK_{sl}) \cdot (W_l + dW_l)$$

$$Q^{x_2} C^{y_2} (W_e + dW_e) = (K_{se} + dK_{se}) \cdot (W_s + dW_s)$$

$$Q^{x_3} C^{y_3} (W_r + dW_r) \cdot S = (A + dA) \cdot (W_l + dW_l + W_s + dW_s + W_e + dW_e) \cdot P_d$$

The before-mentioned 3 formulas were arranged and the high-level infinitesimal($dK_{se} \cdot dW_s$, $dK_{sl} \cdot dW_l$, $dA \cdot dW_s$, $dA \cdot dW_l$ and $dA \cdot dW_e$) was omitted. That is obtained,

$$dW_e = [W_s \cdot dK_{se} \cdot Q^{x_1} C^{y_1} + K_{se} \cdot (W_l \cdot dK_{sl} + K_{sl} \cdot dW_l)] / Q^{x_1+x_2} C^{y_1+y_2} \quad (5)$$

$$dW_s = (W_l \cdot dK_{sl} + K_{sl} \cdot dW_l) / Q^{x_1} C^{y_1} \quad (6)$$

$$dW_r = \frac{A \cdot P_d}{S \cdot Q^{x_1+x_2+x_3} C^{y_1+y_2+y_3}} [W_l \cdot dK_{sl} \cdot Q^{x_2} C^{y_2} + K_{sl} \cdot dW_l \cdot Q^{x_2} C^{y_2} + W_s \cdot dK_{se} + K_{se} (W_l \cdot dK_{sl} + K_{sl} \cdot dW_l)] + \frac{(W_e + W_s + W_l) \cdot P_d \cdot dA}{SQ^{x_3} C^{y_3}} \quad (7)$$

Substituted equation (5), (6) and (7) into equation (4), the distributive mechanism model of the crop photosynthate will be obtained.

The distributive coefficient of the roots was calculated as

$$f_r = \frac{A}{S \cdot Q^{x_1+x_2+x_3} C^{y_1+y_2+y_3} \cdot Y_g} [W_l \cdot dK_{sl} \cdot Q^{x_2} C^{y_2} + K_{sl} \cdot dW_l \cdot Q^{x_2} C^{y_2} + W_s \cdot dK_{se} + K_{se} \left(W_l \cdot dK_{sl} + K_{sl} \cdot \frac{Q^{x_1} C^{y_1} W_s - K_{sl} W_l}{dK_{sl}} \right)] + \frac{(W_e + W_s + W_l) \cdot dA}{SQ^{x_3} C^{y_3} \cdot Y_g} \quad (8-1)$$

The distributive coefficient of the stems was calculated as,

$$f_s = \frac{W_l \cdot dK_{sl} + K_{sl} \cdot \frac{Q^{x_1} C^{y_1} W_s - K_{sl} W_l}{dK_{sl}}}{Q^{x_1} C \cdot P_d \cdot Y_g} \quad (8-2)$$

The distributive coefficient of the leaves was calculated as,

$$f_l = \frac{Q^{x_1} C^{y_1} W_s - K_{sl} W_l}{dK_{sl} \cdot P_d \cdot Y_g} \quad (8-3)$$

The distributive coefficient of the seeds was calculated as,

$$f_e = \frac{W_s \cdot dK_{se} \cdot Q^{x_1} C^{y_1} + K_{se} \cdot (W_l \cdot dK_{sl} + K_{sl} \cdot \frac{Q^{x_1} C^{y_1} W_s - K_{sl} W_l}{dK_{sl}})}{Q^{x_1+x_2} C^{y_1+y_2} P_d \cdot Y_g} \quad (8-4)$$

2.3 Determine of the Organ Quality and Economic Yield

According to the before-mentioned concept of the photosynthate distributive coefficient, the dry matter of the roots, stems, leaves and seeds are calculated as follows,

$$W_{r,i} = W_{r,i-1} + f_{r,i} \cdot P_{d,i} \cdot Y_{g,i} \quad (9-1)$$

$$W_{s,i} = W_{s,i-1} + f_{s,i} \cdot P_{d,i} \cdot Y_{g,i} \quad (9-2)$$

$$W_{l,i} = W_{l,i-1} + f_{l,i} \cdot P_{d,i} \cdot Y_{g,i} \quad (9-3)$$

$$W_{e,i} = W_{e,i-1} + f_{e,i} \cdot P_{d,i} \cdot Y_{g,i} \quad (9-4)$$

Where $W_{r,i}$, $W_{s,i}$, $W_{l,i}$ and $W_{e,i}$ are the dry matter weight of the roots, stems, leaves and seeds on the i day, kg/hm^2 . $P_{d,i}$ and $Y_{g,i}$ are the amount of the photosynthate (kg/hm^2) and the transformation efficiency of the photosynthate. $W_{r,i-1}$, $W_{s,i-1}$, $W_{l,i-1}$ and $W_{e,i-1}$ are the dry matters of the roots, stems, leaves and seeds on the $i-1$ day (kg/hm^2). $f_{r,i}$, $f_{s,i}$, $f_{l,i}$ and $f_{e,i}$ are the photosynthate distributive coefficients of the roots, stems, leaves and seeds on the i day.

2.4 Calculation of the Water and Nutrient Stressed Coefficients

(1) the water stressed coefficient. Where it is calculated with the power function.

$$FW_i = \left(\frac{T_{ai}}{T_{pi}} \right)^\sigma \quad 0 < FW_i \leq 1 \quad (10)$$

Where T_{ai} is the crop transpiration on the i day in the water stressed condition(mm/d). T_{pi} is the potential crop transpiration(mm/d). σ is the sensitivity index of the crop growth and yield in the water shortage condition, it also is called the water shortage sensitivity index. The crop transpiration T_{ai} is equal to the water amount of the crop root absorption.

(2) the nutrient stressed coefficient. Where it is also calculated with the power function.

$$FN = \left(R_{pyN}(t) \right)^\lambda \quad (11)$$

Where λ is the sensitivity index of the crop growth and yield in the nutrient shortage condition, it also is called the nutrient shortage sensitivity index.

$$R_{pyN}(t) = \min[1, P_N(t) / P_{critN}(W)] \quad (12)$$

Where $P_N(t)$ is the crop Nitrogen content on the t time (%). $P_{critN}(W)$ is the critical crop Nitrogen content, it is also the Nitrogen minimum amount of the crop growth in the no Nitrogen stressed condition (%), it is calculated as follows[10],

$$P_{critN}(W) = 1.35 \left(1 + 3e^{-0.26W^*} \right) \quad (13)$$

Where $W^* = \max[1, W]$, W is the dry matter accumulation on the computed time (t/hm^2).

2.5 Accumulate of the Organ Dry Matter

The crop photosynthate simulation in the water and nutrient stressed condition is calculated as follows. First of all, the potential crop photosynthate is calculated in the no water and nutrient stressed condition, it multiplied by the water and nutrient stressed coefficients then, the crop photosynthate on the *one* day is calculated as follows,

$$P_{di} = P_{dmi} \cdot FW_i \cdot FN_i \quad (14)$$

Where P_{dmi} is the amount of the photosynthate in the no water and nutrient stressed condition on the i day (kg/hm^2). P_{di} is the amount of the photosynthate in the water and nutrient stressed condition on the i day (kg/hm^2). FW_i and FN_i is the water and nutrient stressed coefficient, respectively.

Formulate (14) is calculated the amount of the crop photosynthate on the i day, and then it is multiplied by the distribution coefficients of the photosynthate for the organs (the roots, stems, leaves and seeds), the dry weight of the organs are acquired on the i day, and then it is added to the the amount of the photosynthate on the previous day, the sum accumulated every day is the final photosynthate cumulative value. The dry weight of the roots, stems, leaves and seeds is calculated as formulate (9).

3 Model Examination

3.1 Experimental Execution

Winter wheat phased draught experiment is performed in the irrigation experiment station of Tianjin Agricultural University. The experiment station is located at Lat.39°08', Long. 116°57', sea-level elevation is 5.49m and groundwater level is 3.70-1.06 m. The experimental field covers an area of approximately 1 hm². Water for irrigation is groundwater transmitted by plastic hose and is metered. Winter wheat variety 6001 is selected for experiment. Based on local rainfall of the experiment station and water demand of the crop and by referring to previous experimental and research results, it is determined to carry out treatment as per winter wheat water-fertilizer double factorial experiment. Irrigation is divided into 5 levels (240mm, 180mm, 120mm, 60mm and non-irrigation) and is made at wintering, jointing, earing and filling stages. Fertilizer is applied at 4 levels (750kg/hm², 450 kg/hm², 150 kg/hm² and non-fertilizing). Compound fertilizer with total primary nutrient of no less than 54% is used as base fertilizer and is applied to soil with seeding; carbamide with 46% nitrogen content is used as top dressing and is applied along with jointing irrigation, i.e. fertilizer application is immediately followed by irrigation. Considering partial combination of base fertilizer and top dressing, 8 treatments are designed in 2008. A part of treatments are adjusted in 2009 on the basis of experiment in 2008 and number of treatment is increased to 10.

For experiment made in 2008, it is seeded on Sep. 25, 2007 and harvested on Jun. 14, 2008. Precipitation during the experiment is 187.4mm. For experiment made in 2008, it is seeded on Oct. 7, 2008 and harvested on Jun. 15, 2009. Precipitation during the experiment is 84.6mm. Seeding rate is 187.4kg/hm² in 2008 and 2009. Seeding is made mechanically with 25cm row spacing and approximately 5cm depth. Neutron survey meter is used to observe soil moisture content at depth 0-180cm by layers, 20cm per layer. Measurement is made at seeding, wintering, regreening, jointing and harvesting stages against each treatment. Generally, measurement is made once every 10 days before jointing and is conducted at the same time with dry weight measurement after jointing. Additional measurement is made before irrigation and after rainfall (daily precipitation more than 30mm).

3.2 Model Examination

Minimizing sum of absolute value of the error between simulated and measured values of dry weight is used as the the objective function. For programming solution to solve indexes of shoot-leaf growth equilibrium coefficient K_{sl} , root-cap growth equilibrium coefficient A and grain-shoot growth equilibrium coefficient K_{se} $x_1=0.3265$, $y_1=0.1858$, $x_2=0.0499$, $y_2=0.01731$, $x_3=-0.3675$, $y_3=-0.5639$ and solve water and nutrient stressed coefficients $\lambda=0.5695$, $\sigma=0.5026$ with dry weight of root, shoot, leaf and seed measured by experiment made in winter wheat experimental field at the west campus of Tianjin Agricultural University in 2008. Scatter plot of simulated and measured values is drawn with 126 series data of 21 winter wheat zones in 2009. Compared between simulated and measured values of dry weight of root, shoot, leaf and seed in whole growth period of winter wheat is shown in figure 1~4 as medium water medium nutrient. Related coefficients are 0.9998, 0.8142, 0.898 and 0.8726 respectively. It is shown that simulation of organs of winter wheat is reasonable.

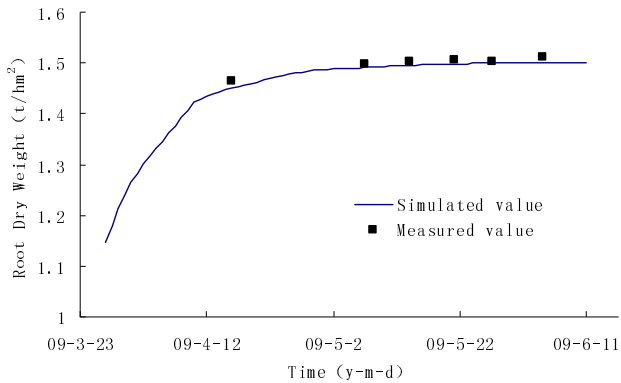


Fig. 1. Comparison between simulated and measured value of root dry weight

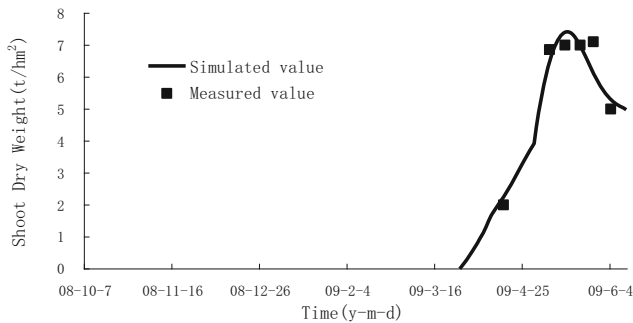


Fig. 2. Comparison between simulated and measured value of shoot dry weight

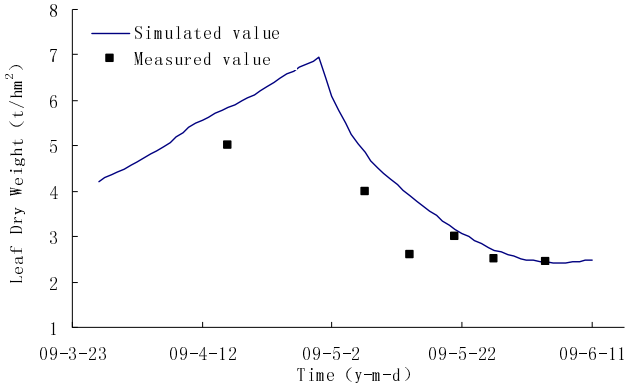


Fig. 3. Comparison between simulated and measured value of leaf dry weight

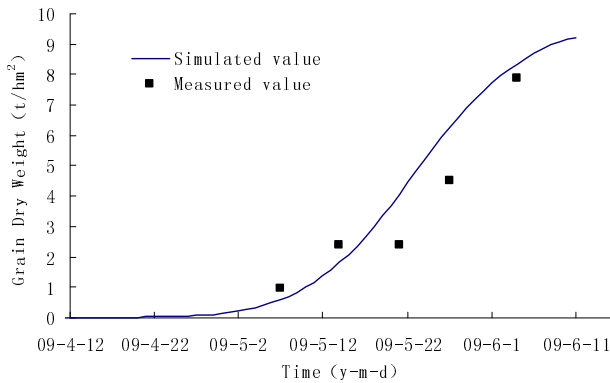


Fig. 4. Comparison between simulated and measured value of grain dry weight

4 Conclusion

1. Where the time, amount of irrigation and fertilization, influence of photosynthate distribution for the time and amount of irrigation and fertilization in the model of photosynthate distribution are important for formulating controlled measures of the irrigation and fertilization of the winter wheat. This improves the mechanism of the crop growth model.

2. Where the calculation of the water and nutrient stressed coefficients with the power function is simple and beneficial to analysis and calculation of the data of the field experiment. It provides a theoretical basis on the reasonable farmland irrigation and fertilization.

Acknowledgment. Funds for this research was provided by the Scientific Research Development Foundation of Tianjin Agricultural University No.2012N06 and the National Science and Technology Support Program No. 2012BAD08B01.

References

1. Tu, X.-L., Hu, B.-M.: Study on Simulation of Wheat Phenological Development. *Hubei Agricultural Sciences* 3, 13–14 (1999)
2. Yan, M.-C., Cao, W.-X., Luo, W.-H.: Study on Simulation Model of Wheat Stem Top Primordia Development. *Crops Journal* 27(3), 356–362 (2001)
3. Li, Y.: Simulation Study of Winter Wheat Photosynthate Distribution Effect on Controlled Water and Fertilizer Measure. Shenyang: Shenyang Agricultural University Doctoral Thesis, 7–9 (2011)
4. Xie, Y., Jmaes, R.K.: Review on Development of Foreign Crop Growth Models. *Crops Journal* 28(2), 190–195 (2002)
5. Payne, R.W.: New and Traditional Methods for the Analysis of Unreplicated Experiments. *Crop Science* 46(6), 2476–2481 (2006)
6. Shi, J.-Z., Wang, T.-D.: Mechanism Model on Assimilate Distribution of Plant Vegetative Stage. *Plant Journal* 6(3), 181–189 (1994)
7. Liu, T.-M., Cao, W.-X., Luo, W.-H., et al.: Quantitative Simulation on Dry Matter Partitioning Dynamic in Wheat Organs. *Journal of Triticeae Crops* 21(1), 25–31 (2001)
8. Duan, A.-W., Cao, W.-X., Luo, W.-H., et al.: Irrigation quota of the main crops in the northern region, pp. 52–80. *Agricultural Science and Technology Press of China, Beijing* (2004)
9. Cao, W.-X., Luo, W.-H.: System simulation and intelligent management of crop, pp. 15–25. *Higher Education Press, Beijing* (2000)
10. Wang, K., Shen, R.-K., Wang, F.-Q.: Simulation of Biomass Formation and Nitrogen Uptake in Winter Wheat under Different Water and Nitrogen Supply. *Irrigation and Drainage* 21(1), 6–11 (2002)

Secure Gateway of Internet of Things Based on AppWeb and Secure Sockets Layer for Intelligent Granary Management System

Rong Tao¹, Senbin Yang², Wei Tan¹, and Changqing Zhang¹

¹ Xi'an Communications Institute, Xi'an 710106, China

² Special Operations University

firstttaorong@sohu.com, {ysb-007,dzxxlab,zhangcq1108}@163.com

Abstract. To develop an intelligent granary management system (IGMS) based on Internet of Things (IOT), secure gateway of IOT (IOTGW), the key component in the system, is designed and achieved. According to the functional requirements of IOTGW in IGMS, embedded Web server is adopted as a lightweight approach for accessing perception devices and interacting with heterogeneous networks. The design scheme based on ARM chip and embedded Web server is given and the hardware and software architectures of IOTGW are investigated in detail. By comparing the major performances, AM3352, Linux, AppWeb, SQLite and C language are chosen for IOTGW implementation. In order to protect the sensitive information transmitted between the client and server, the secure sockets layer (SSL) protocol is added in AppWeb, and the compilation and transplantation of AppWeb with SSL are given detailedly. Experiment shows that the IOTGW can access different types of perception devices and actuators widely, exchange information between the perception layer and network layer safely, and control the perception nodes remotely, so the management of granary becomes convenient, efficient and intelligent.

Keywords: gateway, internet of things, intelligent granary management system, AppWeb, secure sockets layer.

1 Introduction

Granary is a storehouse or room in a barn for threshed grain, and grain reserve has become a key issue concerning about people's livelihood and national defense. In order to reduce unnecessary losses caused by animals, floods, fires, etc in the process of grain storage, granary monitoring system is applied subsequently. The original method is manual inspection by sampling, which is time-consuming, inaccurate and inefficient. The second generation technique is electronic detection using computer and bus standard, that is, electronic monitoring equipments such as temperature and humidity sensors are installed to collect the temperature and humidity data of granary, and bus standard, take RS485, RS422 or fieldbus for example, is adopted to transmit these data to the monitoring computer [1]. This technique improves the accuracy of monitoring data and reduce the costs of granary management, however, there are

some disadvantages including low transmission rate, weak system reliability, difficult for remote communication and big workload of wiring. With the rapid development of communication and network technology, the third generation monitoring system is featured by networking, in other words, short-range wireless communication technologies such as Wireless Sensor Network (WSN) are employed to connect monitoring equipments and collect data, meanwhile, long-range wired and wireless communication technologies such as Internet and mobile communication system are used to convey sensor data and control commands remotely [2]. In this way, the management level of automation and information is improved greatly. Nevertheless, the system's scalability and intelligence are not good enough for it's not easy to increase the number or type of monitoring nodes, or to obtain, fuse and process monitoring information in real time and actively. To address these issues, Internet of Things (IOT) is introduced to granary monitoring as a new technique [3].

Internet of Things is a dynamic global network infrastructure with self configuring capabilities based on standard and interoperable communication protocols where physical and virtual "things" have identities, physical attributes, virtual personalities and use intelligent interfaces, and are seamlessly integrated into the information network. IOT is characterized by more thorough sense and measure, more comprehensive interoperability and intelligence, whose application areas cover modern agriculture, infrastructure construction, public security, environment protection, intelligent industry, urban management and other fields [4].

Restricts of time, space, region and human to real-time monitoring of granary can be broken through by using the technology of IOT, and the IOT-based granary monitoring system can collect, memorize and transmit the parameters including food temperature, humidity, gas concentration, insect and water content to the control center as well as execute the orders from the control center [5]. Baisen Xu et al. analyzed the information function model and architecture reference model of IOT-based grain monitoring system, which is composed of four layers: perception layer, transport layer, processing layer and application layer [3]. However, they only discussed the related key technical problems theoretically, the methods and steps of system implementation were not given. [6] proposed a wireless LAN monitoring system adopting intelligent granary monitoring, which is consisted of a central monitoring station, a wireless relay station and wireless collection points. The multi-function real time data is collected by collection points made by ARM11 embedded processor, and then they were sent to the wireless relay station by ZigBee wireless module. The wireless relay station was responsible for monitoring and preserving the information from the collection points, and sending the comprehensive information to the central monitoring station by WiFi module. The received data was processed by the central monitoring station to realize the monitoring of the real-time information of granary working status. However, the wireless relay station has many deficiencies. Firstly, it can only access these collection points supporting ZigBee protocol, and the collecting information is confined to temperature, humidity, oxygen and pest pictures; Secondly, it can't manage or control the collection equipments; Thirdly, it communicates with the central monitoring station only by WiFi, which has small network coverage, high cost and susceptible radio channel; Finally, its security is poor, for it lacks authentication, encryption and other information security measures.

Furthermore, many granary monitoring systems based on IOT given in other literatures exist above defects more or less.

In order to maximize the advantages of IOT, achieve broad access and management of perception devices and secure information transmission, gateway of Internet of Things (IOTGW) should be exploited to replace the wireless relay station. Therefore, this paper focuses on the design and implementation of secure IOTGW for the Intelligent Granary Management System (IGMS).

2 Intelligent Granary Management System Based on Internet of Things

2.1 IOT Architecture of Intelligent Granary Management System

The requirements of intelligent granary management system are as follows: First of all, the environment of grain storage should be monitored dynamically and adjusted automatically, i.e. temperature, humidity, gas conditions of granary and the extent of food mildew can be sensed in real time and storage conditions will be adjusted by automatic adjustment system accordingly; In the next place, dynamic perception of quantity and location of grain can be achieved for efficient inventory management; Last but not least, personnel access and pest invasions should also be apperceived to ensure the security of granary.

According to the above requirements, the IOT-based architecture of IGMS is shown in Fig. 1, which can be divided into three layers: perception layer, network layer and application layer.

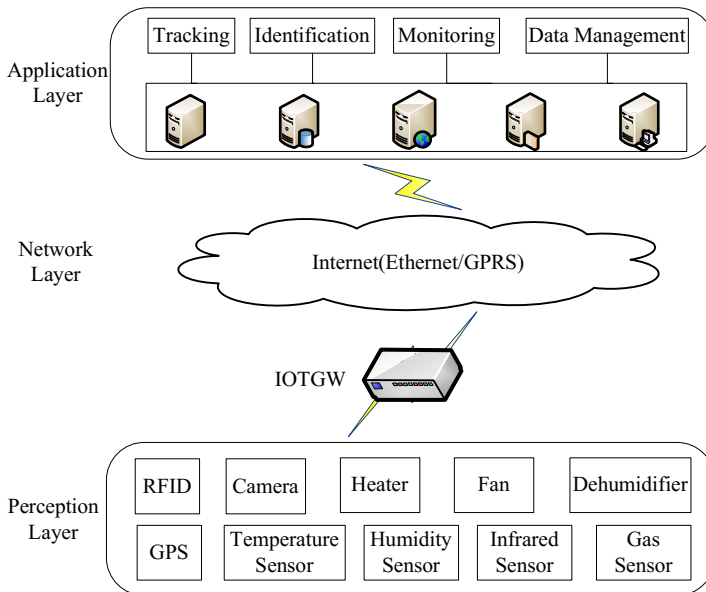


Fig. 1. IOT architecture of IGMS

The perception layer aims to acquire, collect and process the data from perception devices including RFID label, GPS, camera, temperature sensor, humidity sensor, infrared sensor and gas sensor, and control the actuators such as heater, fan and dehumidifier. The major communication protocols between these equipment and IOTGW are ZigBee, Bluetooth, WiFi and USB. The network layer aims to transfer the data collected from perception layer and commands issued by application layer in a large area or long distance, which is constructed based on the Internet (via Ethernet and GPRS). Data processing and services providing are two major purposes of the application layer. The data from network layer is handled by corresponding management systems and then various services including tracking, identification, monitoring and data management will be provided to granary manager.

2.2 Analysis of IOTGW in Intelligent Granary Management System

As shown in Fig. 1, it's difficult to connect different devices in perception layer and communicate with Internet, for it lacks of uniform standardization in communication protocols and sensing technologies [7]. Therefore, IOTGW is introduced to carry out data communication between the two kinds of networks by coping with both the protocol transformation and the device heterogeneity throughout IOT network. In other words, IOTGW is the bridge to connect the perception layer with network layer, which has the following functional requirements: 1) Broad access. The perception devices and actuators should be integrated through IOTGW, namely, the IOTGW can access devices with different protocols including ZigBee, Bluetooth, WiFi and USB. 2) Protocol conversion. The core protocol of Internet is HTTP/IP, which is different from the protocols of perception layer in many aspects such as data formats, data rate and data meaning. In order to exchange information between these two layers, the IOTGW should fuse heterogeneous networks and support protocol interworking seamlessly including conversion of data messages, events, commands and time synchronization. 3) Manageable capability. The management of IOTGW contains perception nodes management and gateway device management. The former aims to acquire the node's identification, status and properties, and to realize remote startup, shutdown, control and diagnosis, the latter aims to realize the gateway device's configuration, supervision, upgrade and maintenance. 4) Information security. The information transmitted in the network may affect the granary security, and they are transmitted by wireless channel, therefore, safety precautions should be taken to ensure information security.

3 Design of IOTGW Based on ARM and Embedded Web Server

3.1 Design Elements and Principles

There are already some researches on the design and implementation of IOTGW system. Qian Zhu et al. proposed an IOTGW system based on Zigbee and GPRS protocols according to the typical IOT application scenarios and requirements from

telecom operators, and the implementation of prototyping system based on ARM9 and Python were given [8]. Till Riedel et al. used Web service based interface descriptions paired with a model driven approach to achieve a high flexibility at a low runtime overhead when designing message based communication within an Internet of Things. The experiments with an industrial servicing use case showed that Web Services and standard HTTP communication based gateways for sensor nodes can integrate multiple concurrent IOT systems [9]. In a word, IOTGW plays a leading role in the IOT systems, and the technologies of ARM and Web service are helpful for its development.

An embedded Web server is a component of a software system that implements the HTTP protocol. The embedded Web server technology is the combination of embedded device and Internet technology, which provides a flexible remote device monitoring and management function based on Internet browser and it has become an advanced development trend of embedded technology. Through this embedded Web server user can access their equipments remotely [10]. There are some advantages to using embedded Web server to design IOTGW: 1) HTTP is a well studied cross-platform protocol and there are mature implementations freely available; 2) Web browsers are readily available with all computers and mobile phones, and other utility software are needless in the application layer; 3) With the usage of Web service, interacting with a perception device becomes as easy as typing a URI in a Web browser. Consequently, embedded Web server can be adopted as a lightweight approach for accessing perception devices and interacting with heterogeneous networks. Moreover, the general problem of using embedded Web services is that even light-weight implementations are too resource heavy for many IOT systems.

The IOTGW is designed with three main principles in mind: simplicity, extensibility and modularity. Simplicity and extensibility refer to users can extend and customize the IOTGW to their needs. Modularity means that internal components of the IOTGW can interact only through small interfaces, thus allowing the evolution and exchange of individual parts of the system.

3.2 Architecture of Hardware and Software

According to above elements and principles, hardware architecture of IOTGW system is shown in Fig. 2.

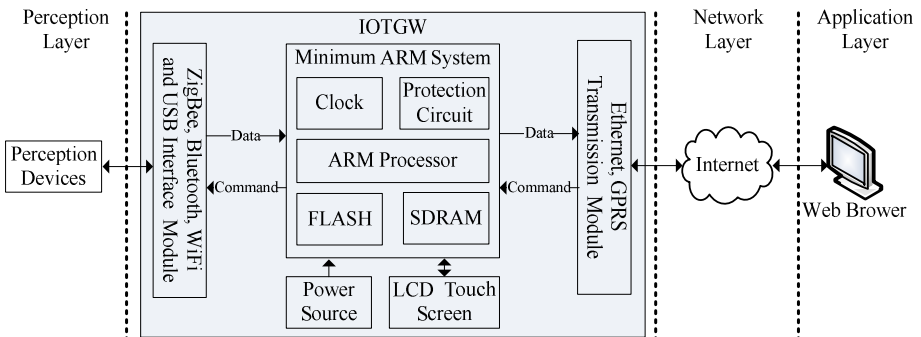


Fig. 2. Hardware architecture of IOTGW system

As shown in Fig. 2, the hardware architecture is composed of five major modules: minimum ARM system, interface module, transmission module, LCD touch screen and power source, each responsible for a well defined set of tasks. Minimum ARM system is the kernel of the IOTGW, which provides the utilities of processing, control and storage. Embedded Web server with TCP/IP protocol suite is built in the ARM processor, and some web application programs, take protocol conversion, message parsing and device management for example, are written in ARM. The interface module makes the IOTGW accessible to different perception devices. With the help of software, these devices can be controlled and managed by appointing unique IP address, and their heterogeneity is shielded. The Ethernet and GPRS transmission module realizes the data transmission based on Internet by the means of wired and wireless respectively. The heterogeneity between these two protocols and perception devices is shielded too, so data and command can be exchanged and understood between perception layer and network layer. The LCD touch screen is used for output and input of data, command and status, which are useful during equipment debugging and testing. After the IOTGW is in proper working order, the LCD touch screen can be removed. The power source supplies direct current (DC) for all IOTGW components, such as 3.3V, ± 5 V, and the source type contains electric supply and battery.

In order to implement the IOTGW's functionalities, the software is designed as Fig. 3.

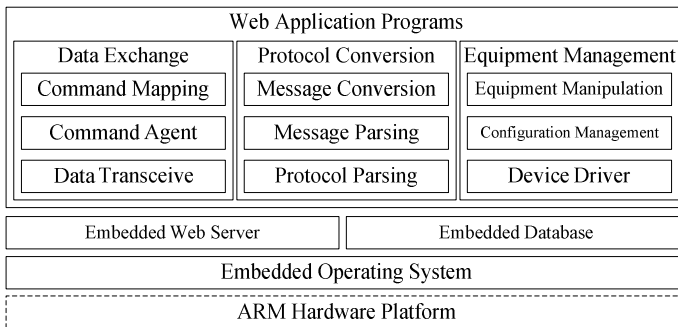


Fig. 3. Software architecture of IOTGW system

As shown in Fig. 3, Embedded Operating System (EOS) is installed on the hardware platform firstly, and then three functional blocks including data exchange, protocol conversion and equipment management are programming under the EOS.

4 Implementation of Secure IOTGW Based on AppWeb with Secure Sockets Layer

4.1 Selection of System Platform and Tools

Selection of ARM Chip. The AM3352 microprocessor, based on the ARM Cortex-A8, is the product of Texas Instruments. The device supports Linux and Android

operating systems and has excellent features including enhanced microprocessor unit, additional peripheral interfaces and real-time clock [11]. Consequently, we choose AM3352 as the hardware platform, corresponding, Linux, which is leading, free and open source EOS, is adopted for hardware resources management and program running control.

Selection of Embedded Web Server. The common open source embedded Web servers which support Linux EOS are AppWeb, Goahead, Boa, Thttpd, Lighttpd, Shttpd and Mini_htttd. The comparisons of their major performances are shown in table 1.

Table 1. Performances comparisons of common embedded Web servers

Server	Benefits and features	Memory usage	Security and reliability
AppWeb	Over 4500 requests per second (r/s); Supports HTTP/1.0, HTTP/1.1, CGI/1.1, SSL RFC 2246, HTTP RFC 2617; Easy to configure and manage; Apache compatible configuration; Called as mini-Apache.	110 KB	Secure Socket Layer (SSL/TLS); Digest and basic authentication; Directory and URL location based authorization; Sandbox resource limits.
Goahead	Over 50 r/s; Supports HTTP/1.0, HTTP/1.1; Minimal security features.	60 KB	SSL/TLS; Basic, digest and form authentication; Security sandbox with DOS protection.
Boa	Over 726 r/s; Single-tasking HTTP server; Supports HTTP/1.0; No server side includes (SSI), access control lists (ACL) and chroot option.	95 KB	No SSL support.
Thttpd	Over 800 r/s; Supports HTTP/1.0, HTTP/1.1, IPv6; URL-traffic-based throttling; Suited to service high volume requests for static data.	150 KB	Basic authentication; Syslog is vulnerable to a buffer- overrun attack.
Lighttpd	Over 1000 r/s; Single-process design with only several threads; Doesn't support sending large files.	200 KB	SSL/TLS; Digest and basic authentication.
Shttpd	No configuration files and external dependencies; No SSI and ACL.	160 KB	SSL/TLS; Digest (MD5) authorization
Mini_htttd	Supports HTTP/1.0, HTTP/1.1, IPv6, CGI; Custom error pages; Suitable for low or medium traffic sites.	90 KB	SSL/TLS; Basic authentication.

In view of the requirements of IOTGW in the IGMS, such as high security, large requests, multi-business types and easy maintenance, the AppWeb is selected as the embedded Web server because of its extended security and higher performance [12].

Selection of Embedded Database. SQLite, which is contained in a small (about 350 KB) C programming library, is a software library that implements a self-contained, serverless, zero-configuration, cross-platform, transactional SQL database engine. It has some outstanding features, such as 1) Transactions are atomic, consistent, isolated, and durable (ACID) even after system crashes and power failures; 2) Faster than popular client/server database engines for most common operations; 3) Implements most of SQL92; 4) Several processes or threads may access the same database concurrently. So SQLite is employed accordingly.

Selection of Development Language. Common Gateway Interface (CGI) applications can be written in a number of different languages, such as C, C++, Java, PHP, Python and PERL. C is a structured, procedural programming language that has been widely used both for operating systems and applications and that has been standardized as part of the Portable Operating System Interface (POSIX). C is employed to write the CGI scripts for the following reasons: 1) CGI programs written in C are stable and secure for the program is compiled and unmodifiable; 2) Linux is written in C with built-in C compiler, and it's a waste of resource to install other languages' compiler; 3) The scripts generated by C are relatively small and have faster execution speed; 4) The logic interactions of the hardware must use the C language.

In a word, the system platform and tools for IOTGW implementation are AM3352 + Linux + AppWeb + SQLite + C language.

The development of IOTGW system includes the realization of hardware and software, and the specific contents are as shown in Fig. 2 and Fig. 3 respectively. Due to space constraints, the following focuses on the core part of the secure IOTGW development—compilation and transplantation of AppWeb with Secure Sockets Layer (SSL).

4.2 Compilation and Transplantation of AppWeb with SSL

In the IGMS, the communication between the server and the client contains the device status, user data, control commands and other sensitive information, so it's necessary to configure the secure transmission system in the AppWeb. The Secure Sockets Layer is a commonly-used protocol for managing the security of a message transmission on the Internet. SSL uses the public-and-private key encryption system from RSA, which also includes the use of a digital certificate, to establish the security of connection between the client and server and to prevent eavesdropping and tampering. Therefore, the SSL protocol is added in AppWeb to establish an encrypted data connection, and the main steps are as follows.

Building the Cross Compile Environment. The host computer is a general-purpose PC running the Linux operating system, which communicates with the target, AM3352, via a serial port and network connection. The prepared cross compilation tool chain (cross-3.2.tar.bz2) can be downloaded from "ftp://ftp.arm.linux.org.uk". In order to make the arm-linux cross compiler ready to use, the toolchain is decompressed and environment variable PATH is modified by following codes.

```
tar xvzf cross-3.2.tar.bz2
export PATH=/usr/local/arm/3.2/bin:$PATH
```

After the cross compilation tool chain is installed, the Configure file is modified by following commands.

```
export CC="/usr/local/arm/bin/arm-linux-gcc"
export AR="/usr/local/arm/bin/arm-linux-ar"
export LD="/usr/local/arm/bin/arm-linux-ld"
export RANLIB="/usr/local/arm/bin/arm-linux-ranlib"
export STRIP="/usr/local/arm/arm-linux-strip"
export CC_FOR_BUILD="gcc"
```

The IP addresses of host computer and target board are in the same segment, for example, the former is 192.168.1.6 and the latter is 192.168.1.15. The TFTP service is enabled to download the kernel image and file system mirroring to the target board. Using the NFS, the file directory of host computer is mounted to the target board via “sudo mount 192.168.1.15:/tftpboot/mnt/nfs”, consequently, host files can be directly read and written on the target board and application programs can be debugged expediently.

Download and Decompression of Source. The AppWeb source package and MatrixSSL open source are downloaded from “http://appwebserver.org/” and “http://www.matrixssl.org/” respectively, and then the following commands are executed to decompress them.

```
tar -xvzf appweb-4.3.0-1-src.tgz-C/usr/local/src
tar -xvzf matrixssl-3-4-2-open.tgz-C/usr/local
```

Cross Compilation of AppWeb with MatrixSSL. The CPU types of host computer and target board are i686 and ARM Cortex-A8, so the Configure commands are as follows.

```
./configure --host=arm-Cortex-A8-linux --build=i686-pc-linux
--port=80 --type=RELEASE --enable-log --disable-shared-libc
--disable-access-log --disable-shared --enable-static
-- enable-multi-thread --disable-test --disable-samples
--prefix=/usr/appweb --webDir=/var/www
--with-cgi=builtin --with-copy=builtin --with-auth=builtin
--with-esp=builtin --with-upload=builtin --with-matrixssl=builtin
--with-ssl=builtin --with-matrixssl-dir=/usr/local/matrixssl/src
--with-matrixssl-libpath=/usr/local/matrixssl/src
--with-matrixssl-iflags="-I/usr/local/matrixssl/src"
--with-matrixssl-libs=libmatrixsslstatic
make
```

The cross compilation result is shown in Fig. 4.

```
cp conf/standard.conf install.conf
chmod +w install.conf
BLD_PREFIX="/etc/appweb" BLD_WEB_PREFIX="/var/www/appweb-default" \
    BLD_DOC_PREFIX="/usr/share/doc/appweb" BLD_LIB_PREFIX="/usr/lib/appweb" \
    BLD_SERVER='hostname' BLD_LOG_PREFIX="/var/log/appweb" \
    BLD_HTTP_PORT=80 BLD_SSL_PORT=4443 \
    patchAppwebConf install.conf
# Return from make -C ./appweb

make -C ./samples compile
# Return from make -C ./samples

make -C ./package compile

make -C ./package/LINUX compile
# Return from make -C ./package/LINUX
# Return from make -C ./package
tequila@tequila-laptop:~/tequila_paper/appweb+matrixssl/appweb-src-2.4.1$ ls
appweb  buildConfig.h  configure  esp  http  make.dep  obj  releases
bin  buildConfig.make  doc  fileList.txt  INSTALL.TXT  Makefile  package  samples
build  buildConfig.sh  ejs  FILES.TXT  lib  mpr  README_SRC.TXT  tools
```

Fig. 4. Cross compilation result of AppWeb with MatrixSSL

Then, the executable and configuration files of AppWeb and dynamic and static linking libraries of MatrixSSL will be generated.

Transplantation of AppWeb with MatrixSSL. The files in /etc/appweb, such as appweb.conf, conf/, groups.db, users.db, mime.types, are moved to working directory firstly, then the appweb.conf is modified as follows.

Open the Web Service. Finally, the Web service is enabled via “./appweb -f appweb.conf &”, and the AppWeb server can be visited in PC browser by “httpS://192.168.1.15:4443”, as shown in Fig. 5.

```
ServerRoot "."
ErrorLog "logs/error.log"
DocumentRoot "/var/www"
LoadModulePath "/usr/appweb/modules"
Listen 80
<if SSL_MODULE>
Listen 4443
</if>
<if SSL_MODULE>
LoadModule ssl libsslModule
<if MATRIXSSL_MODULE>
LoadModule matrixSsl libmatrixSslModule
</if>
</if>
LoadModule cgi libcgiModule
AddHandler cgiHandler .cgi .cgi-nph .bat .cmd .pl .py
ScriptAlias /cgi-bin/ "$DOCUMENT_ROOT/cgi-bin"
SSLCertificateFile "$SERVER_ROOT/server.crt"
SSLCertificateKeyFile "$SERVER_ROOT/server.key.pem"
```

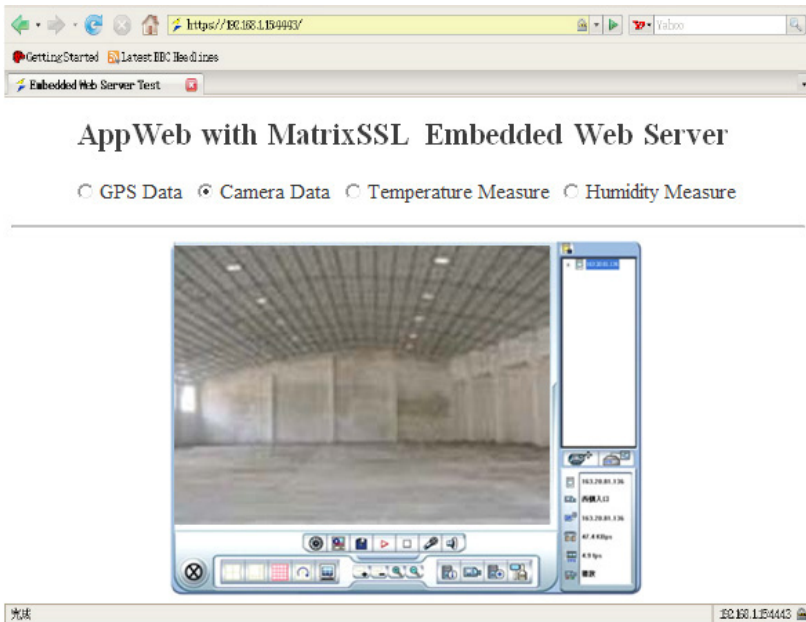


Fig. 5. Interface of video surveillance in the browser

5 Conclusions and Future Work

Internet of Things is a huge global information system composed of hundreds of millions of objects that can be identified, sensed and processed based on standardized and interoperable communication protocols. The IOT based granary management can intelligently process the perception devices' state, provide management and control for decision-making, and even make them cooperate with each other autonomously without manager's intervention. IOTGW plays an important role in IGMS, which facilitates the seamless integration of perception objects and Internet, and the management and control with perception devices. This paper presents a secure IOTGW based on AppWeb and MatrixSSL, which has guarantee of information security in addition to achievement of data forwarding, protocol transformation and device control. Furthermore, the IOTGW framework is flexible, making it usable for many applications, such as smart home, industrial monitoring, smart grid, environment monitoring and so on. In future works, the IOTGW will be put into practice to build a county intelligent granary management system, then improvement and production will be considered.

Acknowledgment. This work has been funded by Advance Research Project of Xi'an Communications Institute under grant No.XATYB013. The authors would like to thank Prof. Yanpu Chen for his help and valuable comments.

References

1. Xiao, K.: Design of a Wireless Granary Temperature Monitoring System, pp. 5–12. Hefei Industrial University, Hefei (2008) (in Chinese)
2. Zhang, Z.: Research of Granary Monitoring System Based on Wireless Sensor Network, pp. 6–16. Zhengzhou University, Zhengzhou (2010) (in Chinese)
3. Xu, B., Zhang, D., Yang, W.: Research on architecture of the Internet of Things for grain monitoring in storage. In: Wang, Y., Zhang, X. (eds.) IOT Workshop 2012. CCIS, vol. 312, pp. 431–438. Springer, Heidelberg (2012)
4. Atzori, L., Iera, A., Morabito, G.: The Internet of Things: a survey. *Science Direct Journal of Computer Networks* 54(15), 2787–2805 (2010)
5. Xie, Y., Cheng, H., Pan, Y.: Application of network of things technologies on granary monitoring system. *Hubei Agricultural Science* 51(20), 4645–4650 (2012)
6. Xu, P., Yao, Y.: Design of a granary monitoring system based on Internet of Things. *Journal of Xi'an University of Post and Telecom* 18(3), 122–124 (2013)
7. Chen, H., Jia, X., Li, H.: A brief introduction to IoT gateway. In: IET International Conference on Communication Technology and Application, pp. 610–613 (2011)
8. Zhu, Q., Wang, R., Chen, Q., et al.: IOT gateway: bridging wireless sensor networks into Internet of Things. In: Proceedings of 2010 IEEE/IFIP International Conference on Embedded and Ubiquitous Computing, pp. 347–352 (2010)

9. Riedel, T., Fantana, N., Genaid, A., et al.: Using Web service gateways and code generation for sustainable IoT system development. In: Internet of Things 2010-Second International Conference for Academia and Industry, pp. 1–8 (2010)
10. Chhatwani, S., Khanchandani, K.B.: Embedded Web server. *International Journal of Engineering Science and Technology* 3(2), 1233–1238 (2011)
11. Texas Instruments Incorporated. AM335x ARM Cortex-A8 Microprocessors (EB/OL) (May 11, 2013), <http://www.ti.com>
12. Embedthis Software. Appweb for Dynamic Applications (EB/OL) (April 13, 2013), <http://appwebserver.org>

Feature Based Hole Filling Algorithm on Triangular Mesh

Bin Xu¹, Zhongke Li², and Ying Tan³

¹ Teaching and Research Section of Computer, The Second Artillery Engineering University,
Xi'an, 710025, China
xubinliuxia@sina.com

Abstract. Aiming at the problem of triangular mesh hole repairing, a new geometric feature based hole filling algorithm was presented. The holes boundary were extracted and pretreated, and the advancing front mesh technique is used to cover the hole with newly created triangles; The Euclidean-coordinate and lapacian of mesh points near the hole boundary were chosen as training sample for support vector machines and deduced lapacian of filling points;calculated coordinate of filling point throw possion equations based on deduced lapacian of filling points to file the hole precisely. Examples proved that this algorithm furbished geometric details to missing area of triangular mesh surface very good.

Keywords: Triangular mesh model, hole repairing, Laplacian, least-squares support vector machines, possion equation.

1 Introduction

Polygonal representations of 3D objects, and particular triangular meshes, have become prevalent in numerous application domains. As 3D optical scanners become widespread, triangle meshes can be easier created and widely applied in the fields of CAD and reverse engineering. Even with high-fidelity scanners, the data obtained is often incomplete. The existence of holes makes it difficult for many operations based on meshes, such as model rebuilding, rapid prototyping and finite element analysis. Therefore, certain repairs must be done before taking incomplete mesh models into actual applications, and hole-filling is the most important one among them. In many computer-aided engineering applications, detailed geometric features are very important, so how to make patched surface to match the missing geometry well is an core problem. Surround this center various mesh hole-filling approaches have been proposed in recent years.

Davis [1] apply a volumetric diffusion process to extend a signed distance function through this volumetric representation until its zero set bridges whatever holes may be present. Guo[2] employed space carving and iso-surface extraction to fill holes. Ju [3] constructed an inside or outside volume using an octree grid and re-constructed the surface by contouring. Joshua and Szymon [4] used a min-cut algorithm to split space into inside and outside portions, and patched the holes simultaneously in a globally

sensitive manner. Holes with regular boundary over a relatively planar region can be easily patched via planar triangulation, which has been described in detail by a number of textbooks and papers [5, 6, 7]. However, filling a complex hole over an irregular region is much more difficult. To solve this problem, Carr [8] used radial basis function to construct an implicit surface to cover the hole. This method works well for convex surfaces and can handle irregular holes. But difficulties arise when the underlying surface is too complex to be described by a single-value function. Liepa [9] presented an umbrella operator to fair the triangulation over the hole to estimate the underlying geometry. However, the $O(n^3)$ performance of the triangulation method limits this method from being used widely. Jun [10] proposed a hole-filling method based on a piecewise scheme. His method divides a complex hole into several simple holes and all sub-holes are sequentially filled with planar triangulation; sub-division and refinement are then employed to smooth the new triangles. Chen [11] proposed a hole-filling method which can fill the hole and recover its sharp feature involved in the hole area. With this method, holes are filled using a radial basis function; a feature enhancement process based on Bayesian classification [12] and sharpness dependent filter [13] is then applied if there exists any sharp feature on the hole boundary. Some hole-filling algorithms for parametric surfaces have been presented [14, 15, 16]. Since the boundaries of the holes handled are usually made up of a B-spline curve, conserving continuity is more important for these holefilling algorithms. Ideally, hole-filling algorithm should possess the following properties: (1) able to cover an arbitrary hole for any model (robustness), (2) capable of filling large holes in a reasonable amount of time (efficiency), (3) enable the patched surface to match the missing geometry well (precision). Unfortunately, due to the complexity and diversity of the holes, no existing hole-filling methods satisfy all the above desirable properties. In this thesis, we present a novel hole-filling algorithm for mesh models. The advancing front mesh technique is employed first to generate a new triangular mesh to cover the existing hole. Then we utilize the Poisson equation to optimize the new mesh. The algorithm is intended to be simple, fast and robust. The main advantage of algorithm in this thesis is can preserve geometric features to certain extent. Moreover, the hole-filling mesh models are of excellent quality for engineering.

2 Main Mathematical Tool

There are three important mathematical tools in this thesis, one is least-squares support vector machines, another is Laplacian on triangular mesh surface and the last one is discrete Poisson equation. As mentioned above, keeping geometric features is very important to hole filling algorithm in many applications. Therefore, how to enable the patched surface to match the missing geometry well (precision) is a core problem in this thesis.

2.1 Laplacian on Triangular Mesh Surface

Laplacian is the most popular mathematical tool to describe geometric features on triangular mesh surface. A local film of one vertex on triangular mesh model surface comprised by vertex V_i and vertices on one edge. Fig. 1 is a local film of vertex V_i .

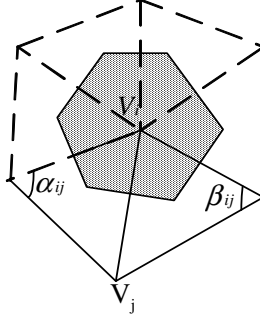


Fig. 1. Local flim of V_i

Eq (1) is Laplacian of vertex V_i , w_{ij} is weight coefficient. Eq (2) and Eq (3) is calculating formulas for weight coefficient.

$$\delta_i = \sum_{v_j \in N(i)} w_{ij}(v_j - v_i) \quad (1)$$

$$w_{ij} = \frac{\omega_{ij}}{\sum_{v_j \in N(i)} \omega_{ij}} \quad (2)$$

$$\omega_{ij} = \cot \alpha_{ij} + \cot \beta_{ij} \quad (3)$$

δ_i is cotangent laplacian of V_i calculating by Eq (1), Eq (2) and Eq (3).

$$\bar{k}ini = \delta_{ci} = \frac{1}{4A(v_i)} \sum_{v_j \in N(i)} (\cot \alpha_{ij} + \cot \beta_{ij})(v_i - v_j) \quad (4)$$

As Eq (4), cotangent laplacian linear approximate mean curvature in value and approximate principal curvature in direction, therefore cotangent laplacian is perfect mathematic tools to describe geometrical details of triangular mesh. $A(v_i)$ in Eq (4) is Voronoi graph (Shaded area in Fig1).

$$L = \begin{vmatrix} L_{11} & \cdots & L_{1n} \\ \vdots & L_{ij} & \vdots \\ L_{n1} & \cdots & L_{nn} \end{vmatrix} \quad (5)$$

$$L_{ij} = \begin{cases} -1 & i = j \\ w_{ij} & v_j \in N(i) \\ 0 & otherwise \end{cases} \quad (6)$$

$$\Delta_d = LV_d = [\delta_{1d}, \delta_{2d}, \delta_{3d}, \cdots, \delta_{nd}]^T, \quad d \in \{x, y, z\} \quad (7)$$

$$V_d = [v_{d1}, v_{d2}, v_{d3}, \cdots, v_{dn}]^T, \quad d \in \{x, y, z\} \quad (8)$$

For the purpose to calculate lapacian on vertex, lapacian matrix (as Eq (5)) has been introduced in this thesis. As Eq (5), L is lapacian matrix of order $n \times n$, n is the number of vertexes in computational domain.

Form of L_{ij} in Eq (5) such as Eq (6), and V_d is component of the vertex coordinates in a coordinate axis, Δ_d is component of the lapacian in a coordinate axis.

2.2 Least-Squares Support Vector Machines

least-squares support vector machines is introduced by Suykens first, in this method the least square linear system be used as loss function, thus outstanding advantages of this method is high speed and robustness. The application of least-squares support vector in this thesis is a typical regression problem, regression purpose is optimize fuction $f(x)$. The training sample set in this thesis is components of spatial coordinate around the hole area mesh vertices in the same coordinate axis.

$$S = \{(V_{id}, \delta_{id}), V_{id} \in R, \delta_{id} \in R\}_{i=1}^l \quad (9)$$

As in Eq (9), $d \in \{x, y, z\}$, l is the of samples in training sample set. Based on the structural risk minimization principle, and considering the complexity and the fitting error fuction, the regression problem can be described as the following optimization problem (as Eq (10) and Eq (11)).

$$\delta_{id} = w^T \phi(V_{id}) + b + e_i \quad (10)$$

$$\min Q(w, b, e) = \frac{1}{2} \|w\|^2 + \frac{\gamma}{2} \sum_{i=1}^l e_i^2 \quad (11)$$

As in Eq (11), w is weighting vector, e_i is slack variable, γ is regularization parameter, deviation variable, in the purpose to solve above optimizatoin problem, Lagrange fuction need to be established. (As Eq (12))

$$L(w, b, e, a) = Q(w, b, e) - \sum_{i=1}^l a_i [w^T \phi(x_i) + b + e_i - y_i] \quad (12)$$

$$\begin{cases} \frac{\partial L}{\partial w} = 0 \Rightarrow w - \sum_{i=1}^l a_i \phi(x_i) = 0 \\ \frac{\partial L}{\partial b} = 0 \Rightarrow \sum_{i=1}^l a_i = 0 \\ \frac{\partial L}{\partial e_i} = 0 \Rightarrow C e_i - a_i = 0 \\ \frac{\partial L}{\partial a_i} = 0 \Rightarrow w^T \phi(x_i) + b + e_i - y_i = 0 \end{cases} \quad (13)$$

Write Eq (13) into matrix form, and expunction w and e can get Eq (12).

$$\begin{bmatrix} 0 & \bar{I}^T \\ \bar{I} & \Omega + \gamma^{-1}I \end{bmatrix} \begin{bmatrix} b \\ a \end{bmatrix} = \begin{bmatrix} 0 \\ y \end{bmatrix} \tag{14}$$

In Eq (14) $\Omega_{ij} = K(x_i, x_j)$, and Solve formula (12) to get regression function as Eq (15).

$$f(x) = \sum_{i=1}^l a_i K(x, x_i) + b \tag{15}$$

2.3 Discrete Possion Equation

In our implementation, we choose the Poisson equation with Dirichlet boundary conditions to refine the patch mesh. The Poisson equation with the Dirichlet boundary is formulated as $\Delta f = \text{div } h$, $f|_{\partial\Omega} = f^*|_{\partial\Omega}$, where f is unknown scalar fuction h is the guidance vector filed, $\text{div } h$ is the divergence of h , and f^* is a known scalar function providing the boundary condition. It can be verified that the Poisson equation is the equivalent to the minimization problem as Eq (16).

$$\min_f \int |\nabla f - h|^2, \text{ with } f|_{\partial\Omega} = f^*|_{\partial\Omega} \tag{16}$$

The discrete Poisson equation is actually a sparse linear system $Ax = b$, where the unknown vector x represents special coordinates of all vertices on the reconstructed patch mesh, the coefficient matrix A is determined by Eq (5), and the vector b is a known vector field obtained from the collection of divergence values at all boundary vertices formulated by Eq (1), which is taken as the boundary condition. The Poisson equation implies that in order to reconstruct the patch mesh we need a guidance vector field defined on the triangles of the patch mesh.

3 Hole-Filling Algorithm

Algorithm in this thesis can be divided into three following parts. (1) The hole boundary pre-treatment: Include a hole boundary indentification and boundary edge pre-trement. (2) Initial patch mesh generation : Include initialize the front using the boundary vertices of the hole; Calculate the angle between two adjacent boundary edges; Starting create new triangles on the plane determined by two adjacent edge until the whole hole has been patched by all newly created triangles. (3) Filling patch refinement based on Poisson equation: Include gather train sample and regression function's solving of least-squares support vector machine; re-positioned vertices of filling patch by solving poisson equation in order to make the patch mesh connect the boundary vertices smoothly and approximate the missing geometry more accurately is employed to refine the patch mesh.

3.1 Hole Boundary Pretreatment

There is two steps in this section: hole boundary identification and boundary edge pretreatment. Since a vertex-based topological structure is used in this work, all boundary vertices can be easily identified by checking the numbers of their 1-ring triangles and 1-ring edges, in this thesis octree be used in this to increase identification speed. The concrete step of boundary identification as follows:

Step1: Compute center of each triangle patch and contaction between the center and its vertices;

Step2: Generate octree based on triangle patch centers;

Step3: Searching octree, and detecting topology connection between its edges, if one edge belong to one triangle patch, the edge is boundary edge;

Step4: Distinguishing different boundary loop by vertex geometric connectivity, showing different holes.

The second step in this section is boundray edge pretreatment. Because data information of hole area in not complete, shape of reconstructed triangle patch is not always good, some patch is long and narrow triangle. In propose to reduce influence of bad shape triangle patch, edge pre-treatment must do before filling the mesh hole. The concrete step as follows:

$v_i (i = 1, 2, \dots, n)$ is n vertices on hole boundary, \mathcal{E} is edges on hole boundary.

Step1: Compute average length of edges on hole boundary L_{ave} .

Step2: Traversal all edge on hole boundary, if length of one edge ($\mathcal{E}_{ij} = (v_i, v_j)$) $L_{\mathcal{E}_{ij}} > k \cdot L_{ave}$, compute middle point v_{new} of \mathcal{E}_{ij} .

Step3 : Take v_{new} as new boundary point, and delete \mathcal{E}_{ij} and triangle patch $v_i v_j$, add edge $v_i v_{new}$ 、 $v_j v_{new}$ and triangle patch $v_i v_{new} v_j$ 、 $v_{new} v_j v_i$, as shown in Fig 2.

At last iterate step3, until boundary edge didn't change.

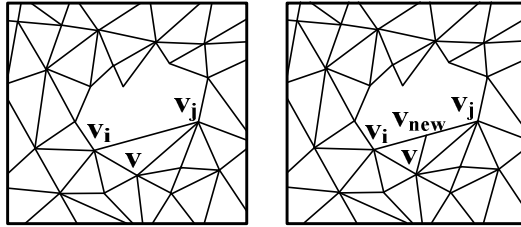


Fig. 2. Hole boundary Pretreatment

3.2 Initial Patch Mesh Generation

In this thesis, we adopt the advancing front mesh (AFM) technique to generate an initial patch mesh over the hole. The method consists of the following six steps:

Step 1: Initialize the front using the boundary vertices of the hole.

Step 2: Calculate the angle θ_i between two adjacent boundary edges (e_i and e_{i+1}) at each vertex V_i on the front.

Step 3 : Starting from the vertex V_i with the smallest angle θ_i , create new triangles on the plane determined by e_i and e_{i+1} with the three rules shown in Fig. 3.

Step 4 : Compute the distance between each newly created vertex and every related boundary vertex; if the distance between them is less than the given threshold, they are merged.

Step 5 : Update the front.

Step 6 : Repeat Steps 2 through 5 until the whole region has been patched by all newly created triangles.

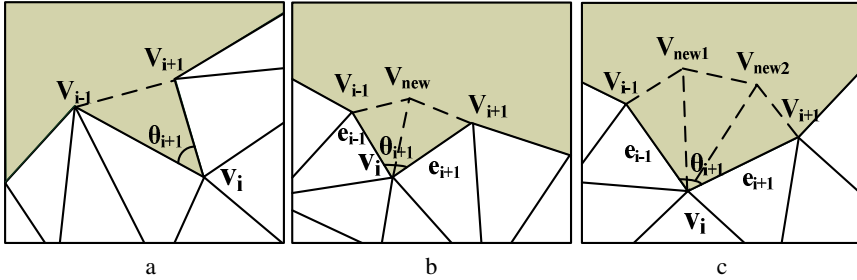


Fig. 3. Rules for creating triangles: A $\theta_i \leq 75^\circ$; b $75 < \theta_i \leq 135^\circ$; c $\theta_i > 135^\circ$

3.3 Establish the Training Sample Set

Up to the present all mesh hole filling algorithm deduce geometric characteristic of filling patch depend on geometric characteristic on initial mesh surface surrounding the hole. In this thesis we take lapacian and euclidean coordinate on vertices surrounding the hole boundary as training sample set to least-squares support vector machines.

In case of V_e is vertex set on hole boundary B , $SV_j (j = 0, 1, \dots, k)$ is j layer of vertex around hole boundary, in practice there is four step in the traning sample collection method.

Step1 : Take vertex V_i on hole boundary, search vertex in same traingle patch with V_i , if that vertex does not in V_e , put it in SV_1 .

Step2 : Traversing every vertex in arrays V_e , repet step1, than gathered vertices on the first layer from hole boundary and put these vertices in SV_1 .

Step3 : To vertices in $SV_j (j = 1, 2 \dots k - 1)$ search vertex in same traingle patch with them, than put vertices not in SV_j and SV_{j-1} into SV_{j+1} .

Step4 : Iterate step3, until the setted up layer number of $SV_j (j = 0, 1, \dots, k)$ attained.

Under this circumstances all vertices and its lapacian consist training samples set, the set of sample points as Fig 4.

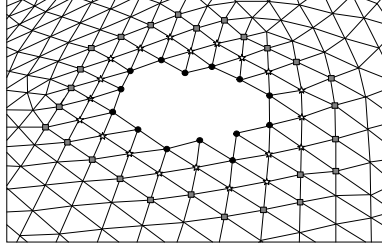


Fig. 4. Training sample set for least-squares support vector machines

3.4 Filling Patch Refinement Based on Poisson Equation

According to method mentioned in section 2.2, Put training sample set in least-squares support vector machines, get three regression function : $f_x(x)$, $f_y(x)$, $f_z(x)$. By three regression function we can get new lapacian field that the poisson equation requires. Once a discrete lapacian fields is given, we consider the new lapacian field as the lapacian field in the Poisson equation, a piecewise continuous scalar function, a connected mesh, can be reconstructed, which computes euclidean coordinate of vertices on filling patch in the least squares sense.

In this thesis, process of computing new coordinates of vertices on filling patch is solution of $n \times n$ linear equations as (18).

$$V'_d = [v'_{d1}, v'_{d2}, v'_{d3}, \dots, v'_{dn}]^T, \quad d \in \{x, y, z\} \quad (17)$$

$$L_{Vn} V'_{nd} = \Delta'_{dn} \quad (18)$$

$$\Delta'_{dn} = L_{Vn} V_d = [f_d(v'_{1d}), f_d(v'_{2d}), \dots, f_d(v'_{nd})]^T, \quad d \in \{x, y, z\} \quad (19)$$

L_{Vn} in (18) is contangent lapacian matrix established by method mentioned in section 2.1 of filling patch, Δ'_{dn} in (19) is one component of lapacian of vertices on reconstructed filling patch. $f_d(v'_{nd})$ in (19) is one regression function.

4 Implementation and Analysis

The proposed hole-filling algorithm has been implemented with VisualC++2010 and OpenGL. All experimental results in this paper were obtained on a $\tilde{20}$ GHz Pentium IV personal computer with 1024MB memory. Many examples have been used to test the robustness, efficiency and accuracy of the method.

Figure 5a shows head model, there are a large number of geometric details on this mesh model. Figure 5b shows head model with hole in the part of hair. In this section the hole-filling result on head model by direct filling algorithm, algorithm in reference[17] and algorithm in this thesis. The reason of taking algorithm in

reference[17] compare to algorithm in this thesis is the algorithm in reference[17] is based on solution of poisson equation same to algorithm in this thesis, the difference between them is least-squares support vector machine has been used in algorithm in this thesis to estimate geometric details of filling patch, so the comparison of two algorithms show the advantage of algorithm in this thesis at keeping geometric style between filling patch and other part of mesh model.

Figure 6 depicts filling result by direct filling algorithm, obviously very rough. Figure 7 depicts filling result by filling algorithm in reference[17], as shown in figure 7, filling result is very good, mesh quality of filling patch is well two, the only disfigurement is filling patch and other part of model is not coincident in geometric style at all. Figure 8 depicts filling result by algorithm in this thesis, from the picture we can see that mesh quality is as good as in Figure 7, and keeping geometric style between filling patch and other part of mesh very well.

Table 1 is error evaluation for algorithm in reference[17] and in this thesis. Table 2 is running time of two algorithms states above.

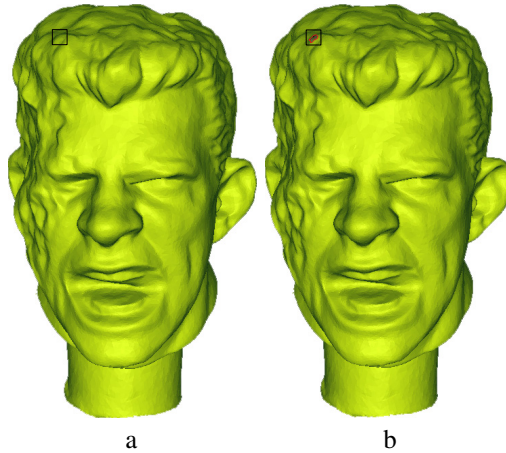


Fig. 5. Preliminary head model and head model with hole

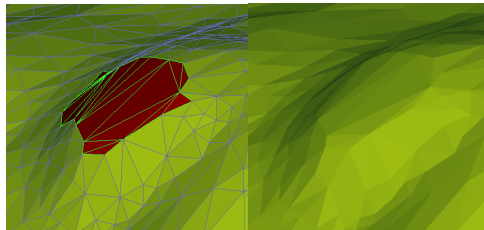


Fig. 6. Filling result by direct filling algorithm

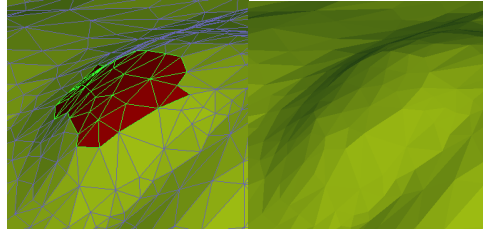


Fig. 7. Filling result by filling algorithm in reference 17

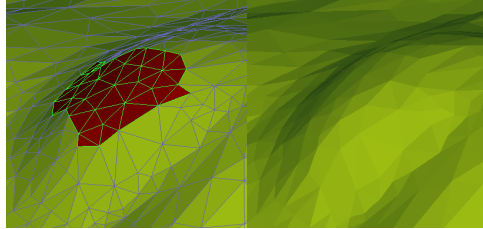


Fig. 8. Filling result by filling algorithm in this thesis

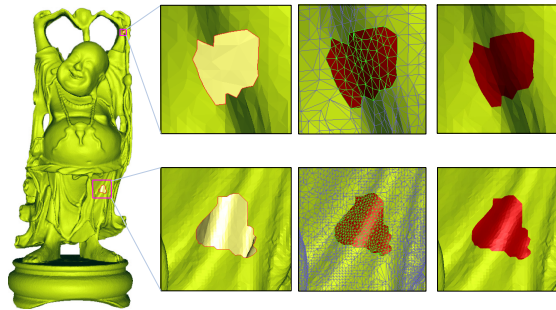


Fig. 9. Filling result on happyvrip model by filling algorithm in this thesis

Table 1. Error evaluation

Algorithm	Vertices num on filling patch	Triangle num on filling patch	Average distance	Average error
In reference 17	28	69	0.05(mm)	0.0015
In this thesis	31	75	0.042(mm)	0.00142

Table 2. Computing time

Algorithm	Vertices num on filling patch	Triangle num on filling patch	Time of Initial patch mesh generation	Time of solving position equation
In reference 17	28	69	10.6ms	15.7ms
In this thesis	31	75	10.4ms	15.9ms

In this thesis the distances between the vertices on the patch mesh and the original analytic surface are used to evaluate the precision of our algorithm. The quotient of the average distance and the square root of analytic surface area is considered as the

error of our algorithm. From table 1 and table 2 we can see that by algorithm in this thesis we can get higher precision while spending similar time.

Fig 9 depicts the filling result by the algorithm in this thesis on a big hole. From the picture we can see that the algorithm works very well in keeping geometric style between the filling patch and other parts when the hole to be filled is compared to a bigger one.

5 Conclusion

The innovation point of this thesis is taking the Laplacian of vertices on the filling patch as the output of the regression function and reconstructing the filling patch by solving the Poisson equation. The advantage of this algorithm is that it uses the Laplacian to depict geometric details of the mesh surface model, therefore making the filling mesh patch and the original mesh surface more naturally integrated.

A limitation of the algorithm in this thesis is that the filling result may lose some geometric details when the hole is too big. This limitation exists in all popular mesh surface filling algorithms. The method dealing with this problem is taking the whole geometric characteristic of the mesh model as a reference while filling the mesh surface hole. This is also a research area of this thesis.

References

1. Davis, J., Marschner, S.R., Garr, M., Levoy, M.: Filling holes in complex surfaces using volumetric diffusion. In: First International Symposium on 3D Data Processing Visualization and Transmission, Padova, pp. 428–438 (2002)
2. Guo, T.-Q., Li, J.-J., Weng, J.-G., Zhuang, Y.-T.: Filling holes in complex surfaces using oriented voxel diffusion. In: 2006 International Conference on Machine Learning and Cybernetics, pp. 4370–4375. IEEE, Los Alamitos (2006)
3. Ju, T.: Robust repair of polygonal models. In: Processing of SIGGRAPH, Los Angeles, CA, USA, August 8–12, pp. 888–895. ACM Press, New York (2004)
4. Joshua, P., Szymon, R.: Atomic volumes for mesh completion. In: Proceedings Eurographics Symposium on Geometry Processing, Dublin, Ireland, August 29–September 2, pp. 33–41. Blackwell Press (2005)
5. Brunton, A., Wuhler, S., Shu, C., Bose, P., Demaine, E.D.: Filling holes in triangular meshes by curve unfolding. In: IEEE International Conference on Shape Modeling and Applications, pp. 66–72 (2009)
6. Li, B.J., Zhang, X.K., Zhou, P., Hu, P.: Mesh parameterization based on one-step inverse forming. *Comput. Aided Des.* 42(7), 633–640 (2010)
7. Gao, S., Zhao, W., Lin, H., Yang, F., Chen, X.: Feature suppression based CAD mesh model simplification. *Computer-Aided Design* 42(12), 1178–1188 (2010)
8. Carr, J., Beatson, R., Cherrie, J., Mitchell, T., Fright, W., McCallum, B.: Reconstruction and representation of 3D objects with radial basis functions. In: Processing of SIGGRAPH, Los Angeles, CA, August 12–17, pp. 67–76. ACM Press, New York (2001)
9. Liepa, P.: Filling hole in meshes. In: Proceedings Eurographics Symposium on Geometric Processing, Granada, Spain, September 1–6, pp. 200–207. Blackwell Press (2003)
10. Jun, Y.: A piecewise hole-filling algorithm in reverse engineering. *Comput. Aided Des.* 22(8), 263–270 (2005)

11. Chen, C.Y., Cheng, K.Y., Liao, H.Y.M.: A sharpness dependent approach to 3D polygon mesh hole filling. In: Proceedings of Eurographic, Trinity College, Dublin, Ireland, August 29-September 2, pp. 13–16. Blackwell Press (2005)
12. Chen, C.Y., Cheng, K.Y.: A sharpness dependent filter for mesh smoothing. *Comput. Aided Geom. Des.* 22(5), 376–391 (2005)
13. Chen, C.Y., Cheng, K.Y., Liao, H.Y.M.: Fairing of polygon meshes via Bayesian discriminate analysis. In: The 12th International Conference in Central Europe on Computer Graphics, Visualization and Computer Vision, Plzen-Bory, Czech Republic, pp. 175–182. UNION Agency-Science Press (2004)
14. Lou, R., Pernot, J.-P., Mikchevitch, A., Véron, P.: Merging enriched finite element triangle meshes for fast prototyping of alternate solutions in the context of industrial maintenance. *Comput. Aided Des.* 42(8), 670–681 (2010)
15. Ju, T.: Fixing geometric errors on polygonal models: a survey. *Journal of Computer Science and Technology* 24(1), 19–29 (2009)
16. Li, Z., Meek, D.S., Walton, D.J.: Polynomial blending in a mesh hole-filling application. *Computer-Aided Design* 42, 340–349 (2010)
17. Zhao, W., Gao, S.M., Lin, H.W.: A robust hole-filling algorithm for triangular mesh. *The Visual Computer: International Journal of Computer Graphics* 23(12), 987–997 (2007)

Design and Implementation of Aquarium Remote Automation Monitoring and Control System

Yinchi Ma^{1,2,*} and Wen Ding^{1,2}

¹ Beijing Fisheries Research Institute, Beijing, 100068, China

² National Engineering Research Center of Freshwater Fisheries, Beijing, 100068, China

Abstract. In recent years, with the rapid development of ornamental fisheries and recreational fisheries, different varieties of ornamental fish have come into many office business palaces and people's house. The Aquarium and many other aquarium equipment are developing from functionality to intelligentize. Through the industry research, a set of remote automation monitoring and control equipment for the aquarium will have important significance and development prospect. The system stores and transmits the video of the aquarium gathered by camera through the IImagineWorld center platform software. The Internet user accesses the center platform to monitor the aquarium by IE or mobile terminal software. The user can get the temperature data of the aquarium through RS485 transparent protocol. And the user can also control the oxygen adding, warmer and filtering equipment remotely by the I/O alarm output of the video server. Through the user testing, the system plays a good effect and has wide application and popularization value.

Keywords: aquarium, remote, automation, monitoring and control.

1 Introduction

At present, there is a wide variety of aquarium in the market. And some multifunction aquariums such as controlling water temperature, increasing oxygen, and filtering, feeding, and other functions have appeared. But most functions need to be operated manually in site. With the progress of modern electronic information and automation technology, in some fields such as intelligent manufacturing, precision agriculture, and household, have been able to realize the remote video monitoring, environmental parameters monitoring, equipment condition monitoring and controlling [1]. These technologies have had some simple application on the aquarium equipment, but the multi-functional integration application is still a blank in this area. Tu used the on-line video to monitor the oil contamination level [2]. Peng, Yao, Zhang and Yu monitored and controlled the aquarium equipments based single-chip computer technology, but

* Ma Yinchi (1982 -), Beijing Fisheries Research Institute, Engineer, Master, graduated from Beijing Normal University, State Key Laboratory of Remote Sensing Science, mainly engaged in research of agriculture remote sensing and fisheries information technology.

not realized the remote control and the on-line remote video monitoring [3] – [6]. Ge realized the remote control of the aquarium equipments based RS-485 bus. But the dynamic IP problem was not solved [7]. Yang realized to control the oxygen adding equipment of the fish pond based GSM and WIFI technology [8]. Through analysis and study of the most aquarium controlling equipment application status at present, people can't stand work of the aquarium, and also cannot monitor or control the electrical equipment of the aquarium in real-time. These problems cause a lot of trouble for daily maintenance, and even cause some economic losses [9]. In this article, we propose a system solution method that can realize remote automation monitoring and controlling of the aquarium. By applying IImagineWorld center platform, RS485 protocol software and I/O alarm output control technology, the system can realize to view video of the aquarium, to monitor temperature of the water, to add oxygen, and to warm or filter the water based through the Internet. At the same time, The dynamic IP problem is also solved which makes the system convenient for simple household application. The design and implementation of this system will have an important innovation meaning for the design and manufacture area of the aquarium.

2 System Composition

The System is composed of the monitoring module, the control module, the video server, the center server platform and the client.

The monitoring module monitors the real-time video and the water temperature of the aquarium.

The control module is designed to control the light equipment, the heating equipment, the oxygen adding equipment and the filtering equipment.

The video server is the core part of the system, and we have improved and expanded its function. The I/O alarm output function of the video server is encapsulated into the system I/O control unit. The Unit receives all kinds of orders sent from the center server platform, and controls the equipment belonging to the control module in the aquarium. At the same, the unit encodes the data from the temperature sensor and uploads the data to the center sever platform through the RS485 transparent protocol. The real-time video data of the aquarium gathered by CCD sensor is compressed and coded, and then is also uploaded to the center server platform automatically. These functions are encapsulated into the data service unit.

The IImagineWorld management software is installed on the center server platform. The software can deal with the temperature and video data sent from the video server, and put forward these data to the request client. At the same time, all the monitoring and controlling orders by user are also sent to the control unit of the remote video server through the platform.

The system client is divided to two kinds. For normal PC users, we design an internet server based on the ASP technology on the center server platform. The users can visit the system and use all functions through internet by IE explorer. For other mobile users,

we design client software running on the Android mobile operation system platform. The users can use the system through GPRS network or WIFI network by the client. Considering the safety and privacy of users, the system has a strict user authentication mechanism. All the monitoring and controlling operations from IE or the client must base on the legitimate login.

The structure design of the system is shown as follow (Fig.1).

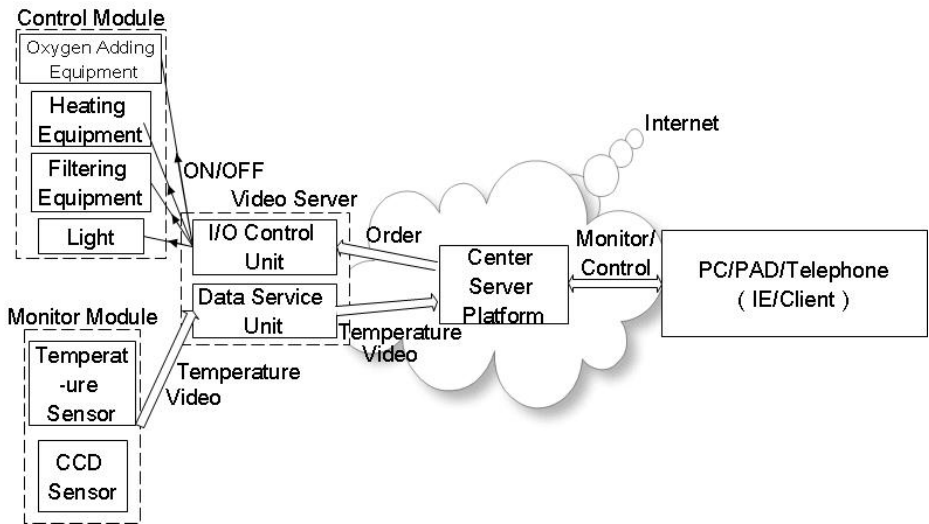


Fig. 1. System Structure Design

2.1 Hardware

The system hardware consists of the control module, the monitoring module, the video server and the web server.

Based on the current popular aquarium equipment, the control module consists of the light, the heating equipment, the filtering equipment and the oxygen adding equipment. These equipments are controlled by an independent circuit. There are control buttons on the control panel of the aquarium. And every control circuit is connected to the I/O control unit of the video server. This design realized the local control and the remote control at the same time.

At present, the monitoring module is composed by the water temperature sensor and the real-time video CCD sensor. The tiny custom water temperature sensor is applicable to the household aquarium. The DS18B20 component uses the waterproof packaging technology. The sensor is connected to the video server by leading wire. Its testing range is between -55°C~125°C. And the accuracy of the sensor is $\pm 0.5^\circ\text{C}$ working

under the $-10^{\circ}\text{C}\sim 85^{\circ}\text{C}$ condition. The Temperature data is converted to RS485 signal through the video server. And then the video server sends these data to the remote center service platform by internet or GPRS network. User can set up the time interval of the water temperature refreshment in the system, and the temperature data can be refreshed on the client or IE automatically. The video acquisition device encapsulates a color CCD sensor with 420 line horizontal resolution. It uses PAL or NTSC signal mode. The camera has wide-angle function and can eliminate spherical deformation of the video. The camera base uses the sucker structure, and the reinforced sucker can fix the camera on the outer wall of the aquarium hardly. User can change the location and angle of the camera due to requirement. The camera is connected to the video server by 1.0Vp-p/75 Ω /BNC interface.

In recent years, the video server has been widely used in remote monitoring and security area. It is a kind of embedded device to compress and deal with the audio and the video data. It is composed of AV compression and encoder device, input and output channel, network interface, AV interface, RS485/RS232 serial interface, protocol interface and software interface, etc.

This system is equipped with a high quality video server with high quality SOC computing chip which is stable and reliable, and has low power consumption. The video server uses the H.264 video coding technology with a high compression ratio and high image quality. The video server supports NTSC or PAL video formats and its image resolution can reach 704*576 pixels, and the video compression rate is 32kbps~4Mbps, the most high frame rate can be up to 30 frames per second. The video server can support 4 alarm input signal and 4 alarm output switch signal. It has the RJ45 adaptive 10M/100M Ethernet port, and supports transparent RS485 reading and writing protocol. The video server has a dynamic DNS client inside, and can be configured as the secondary domain name. This makes it particular convenient to the family dynamic IP users. The video server uses the DC12V/2A ballast for power supply.

We design an I/O power controller for the video server, so as to control the switch of the aquarium equipment in remote way. The main structure components are composed of a transparent cover, an upper cover body, a fixing rail and a terminal block, etc. All the built-in electric switch components adopt with 9mm module electric equipment, and are fixed on the fixing rail. The Grounding is firm and reliable, and can be convenient to use. The controller is equipped with 4 groups of 10A socket, 12V/5A switch power and 4 12V relays. The 4 groups of I/O switch control the 4 relays, and the 12V switch power supplies power to the RS485 water temperature sensor and the 4 relays. The inside circuit structure of the I/O power controller is shown as follow (Fig.2).

2.2 Software

The network system service is setup on the center server platform, and the IImagineWorld software is also setup on it. IImagineWorld is the core software of the center server platform, and is responsible for storing and forwarding of the real-time

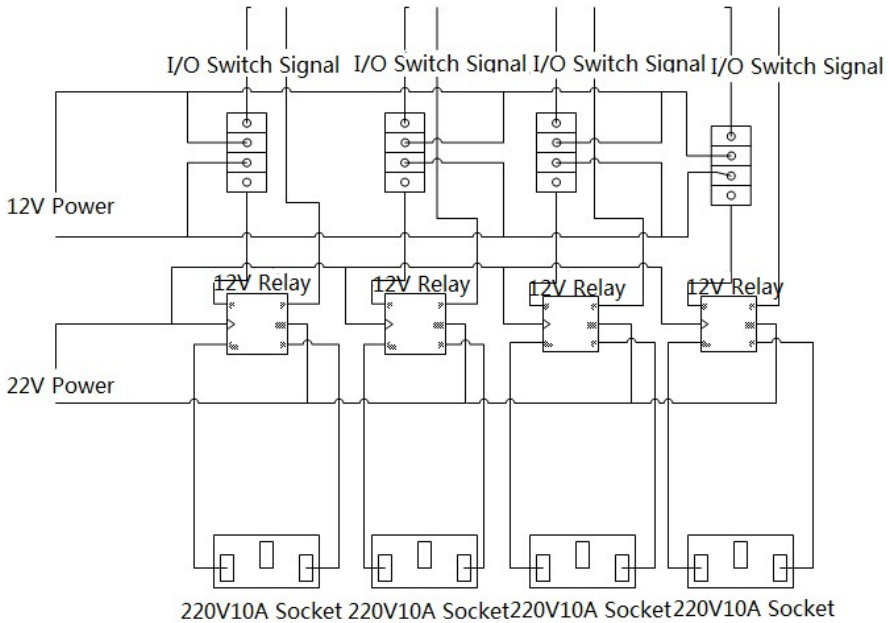


Fig. 2. Inside Circuit Structure of I/O Power Controller

video. After the system administrator checks the count of the user who owns the system equipment, he will add the device ID into the system service list. The device ID is the only identifier of the system equipment. Only the system equipment whose device ID recorded in the system service list can upload the real-time video to the center server platform, then store and forward the video to the remote client through the center server platform.

The network users can visit the system through internet by IE, and they can monitor and control the aquarium by the IE widgets. We setup a set of rules for the user management. User must register a count on the network system first, and then the system administrator will check it. The center server platform can bind one or more sets of the system equipment for every user, and the user can switch among these equipments through the client or IE interface.

Aiming at the development of smart mobile terminals, for the convenience to monitor and control the remote aquarium anytime and anywhere, we develop a client for this system based on Android smart mobile operating system platform. For the legal users who have registered successfully, they can download and installed the client on their phone or pad running the Android system. And then they can login and use the system freely. The mobile client not only provides all the functions of the web system, but also provides image snapshot and video record function. The center server compresses the transfer data, and optimizes the network resource occupancy and data traffic. So users can operate the system through GPRS or WIFI network smoothly.

3 Conclusions

In this paper, we make detail design and implementation for remote automation monitoring and controlling of the aquarium. The structure of the system is simple and the performance is reliable. After strict system test, the system has obtained good effect. The aquarium water temperature data can be sent to the user client in real-time through the internet. Users can remote control the heating device due to the temperature data initiatively. And at the same time, users can remote control the oxygen adding device and the filtering device due to the video data from the CCD sensor initiatively.

Monitoring and controlling the aquarium in real-time can ensure the breeding security and reduce the breeding risk and loss. The application of this system can eliminate the influence of human factors during the breeding process, and increase efficiency significantly. For home and commercial places aquarium users, the beautiful and lightweight hardware structure design is important. And the software interface is also required to be friendly and operable. We will optimize and improve the system for these requirements. Industrial hardware structure design of the system can make it product and apply at scale. And the system will have a more practical usage. To expand the control circuit and do modular design will allow users to easily customize their own remote monitoring and controlling module in this system. And to expand the operating system platform of the mobile client will strengthen the portability of the system software. At the same time, we also design a particular system that can be used in large breeding sink to expand the system application.

References

1. Zhou, G., Zhou, J., Miao, Y., et al.: Development and application on GSM-based monitoring system for digital agriculture. *Transactions of the CSAE* 21(6), 87–91 (2005) (in Chinese with English abstract)
2. Tu, Q., Zuo, H.: Study on a New Technique of On-line Monitoring of Oil Contamination Level Using Computer Vision Technology. *International Journal of Plant Engineering and Management* (02), 103–109 (2004)
3. Peng, G., Deng, H., Liang, Z.: The Design of Automatic-Control Instrument for the Aquarium. *Guangdong Automation & Information Engineering* Z1, 44–46 (1998) (in Chinese with English abstract)
4. Yao, L., Yang, Y.: The design of aquatic animal case/s auto adding oxygen system. *Journal of Shenyang Institute of Aeronautical Engineering* 25(1), 64–66 (2008) (in Chinese with English abstract)
5. Zhang, J.: Making the oxygen pump control switch of aquarium with single chip microcomputer. *Electronics World* (10), 28–29 (2004) (Chinese reverse to English)
6. Yu, H., Shan, H., Jiang, L.: Design of the automation oxygen controller based single chip microcomputer. *Fishery Modernization* (6), 42–44 (2006) (Chinese reverse to English)

7. Ge, H.: The Realization of the Remote Communication between PC and the Controller in Aquarium Based on RS-485 Bus. *Journal of Shazhou Professional Institute of Technology* 12(3), 8–11 (2009) (in Chinese with English abstract)
8. Yang, S., Qi, J., Li, Y., et al.: Wireless system for monitoring and control of dissolved oxygen in fish pond water. *Fishery Modernization* 37(6), 11–14 (2010) (in Chinese with English abstract)
9. Zheng, W.: Technology of Breeding Seawater Fancy Fishes in Household Aquarium. *Fisheries Economy Research* (1), 45–48 (2009)

Study on Conditional Autoregressive Model of Per Capita Grain Possession in Yellow River Delta

Yujian Yang^{*}, Huaijun Ruan, Yan Tang, Wenxiang Zhao, and Xueqin Tong

S & T Information Institute of Shandong Academy of Agricultural Science
Number 202 Gongye North Road, Licheng District of Jinan, 250100,
Shandong Province, P.R. China
yyjtshkh@126.com

Abstract. In the paper, we reviewed hierarchical statistical modeling about conditional autoregressive models method for spatial data located in Yellow River Delta. Moreover, we also proposed a new method about the evaluation and prediction of per capita grain possession on county-level in the high-efficiency ecological zone. With the support of MCMC approaches and conditional auto-regressive (CAR) Model, we estimated the posterior distribution through iterative sampling among per capita grain possession and the correlated factors. As a useful tool, the spatial bayesian model appeared to gain insights into per capita grain possession on spatio-temporal variability related to the grain sowing area, efficient irrigation area, agriculture machinery conditions. The study results showed that auto correlation characteristics and the posterior density distribution were described by the quantity method with CAR model, correspondingly the posterior mean of observed value and the posterior mean of predicted value of per capita grain possession were developed in Yellow River Delta. The posterior probability was more evident statistical significance on basis of prior information and sample characteristics in credible interval. Apparently, three factors of the grain sowing area, efficient irrigation area and agriculture machinery resulted in complex random effects on per capita grain possession. The results also indicated that bayesian method was not only the more quantitative evaluation, but also the more estimated accuracy for the per capita grain possession on country level in Yellow River Delta.

Keywords: Yellow River Delta, Per capita grain possession, CAR model, Bayesian.

1 Introduction

In the recent decades, hierarchical models had drawn the attention of scientists in many fields and were especially suited to studying the spatial variables. The approach to spatial modeling was fairly effective to evaluate the variables, and the merits of solving the flexibility and stability for high-dimensional spatial model or spatio-temporal model were very evident with bayesian hierarchical model. The bayesian estimation indicated significance for this variable whereas maximum likelihood estimates did not, and the bayesian considered the prior information regarded as the

^{*} Corresponding author.

prior distribution for the variables, had the highest posterior density. So the posterior distribution was given the better precision. Recent development of the spatial bayesian hierarchical framework had gained increasing popularity in many domains. The spatial effects can be explicitly expressed in the model by assuming a prior distribution with its parameters specified from the information of spatial neighbors from spatial bayesian models. Based on a statistical point of view, however, the observations were not independent since proximity in space playing a key role in complicated spatio-temporal model. The importance of space and the problem of parameter heterogeneity were emphasized by Martin Feldkirche(2007), Doppelhofer et al. (2004) and Fernandez et al. (2001), In particular, hierarchical bayesian modeling allowed borrowing of strength across similar (say, geographically adjacent) countries, hence improved estimation prediction and mapping of underlying model features driving the data[1,2,3]. CAR model is more suitable for scientific research. Anselin(2002), Haining(2003) on one hand. From the model perspective, on the other hand, the computerization of Spatial weight matrix was emphasized in CAR model, undoubtedly, the quantitative degree was improved in variable computerization process. Moreover, distance range attenuation function was used in spatial weight matrix, which was determined by the correlated prior knowledge, and estimation of semi-variogram plot or correlated plots. Apparently, considering of prior knowledge improved the predication accuracy of model variables [4, 5].

The Yellow River Delta was formed on basis of the yellow river alluvial plain and the adjacent coastal regions in Shandong province, including Dongying city, Binzhou city, Hanting district, Shouguang city, Changyi city in Weifang city, Laoling and Qingyun in Dezhou city, Gaoqing country in Zibo city and Laizhou city in Yantai city. The total area is 26500Km². In 2009, the construction of high-efficiency ecological zone has been officially christened, in 2011, national science and technology demonstration of modern agriculture in Yellow River Delta was established to enforce the total development of agriculture. Due to the bayesian model provided the flexibility to accommodate that possibility, and the flexible nature of the model also made it possible to consider the inclusion of additional spatial (e.g., grain production) variables when appropriate. The study was carried out to analyze the location and interaction of taking the case of per capita grain possession, conditional autoregressive models of per capita grain possession considering of the typical variable heterogeneity and the better prediction were achieved by the bayesian method.

2 Material and Methodology

2.1 Data Acquisition and Preprocessing

It was necessary to preprocess the spatial data before Bayesian inference Using Gibbs Sampling (GeoBUGS) analysis, which attributed the model of WINBUGS software. log transformation on per capita grain possession was used to ensure a constant variance. The map was comprised of 19 country units. The data came from Shandong Statistical Year Book-2008, Chinese county (city) social economic statistical yearbook-2008[6].

Considered of the special data format for GeoBUGS, firstly the transformation from *.shp format was carried out to ensure the following steps in the study. In general, 4 steps were carried out to data transformation and correlated computerization. The first step, the first line contains the key word “map” followed by a colon and an integer, N, where N was the number of distinct areas in the map. The second steps, the import file is a 2 column list giving: (column 1) the numeric ID of the area, this must be a unique integer between 1 and N; the areas should be labelled in the same order as the corresponding data for that area appears in the model. The third step, it begins with a line containing the key word “regions”. The fourth step, the final part of the import file gives the co-ordinates of the polygons. However, they are not used by GeoBUGS, so can be arbitrary. Subsequent rows contain a 2-column list of numbers giving the x- and y-coordinates of the poly. The polygon coordinates can be listed either clockwise or anticlockwise. In the process, polygons should be separated by a line containing the key word END[7].

2.2 Spatial Model Framework of Conditional Autoregressive Model

In CAR model, the expected value of the response variable was regarded as being conditional on the recorded values at all other locations, we may smooth the observed value of per capita grain possession by fitting a random effect on poisson model allowing for spatial correlation, using the intrinsic CAR prior proposed by Besag(1974), York and Mollie (1991) [8]. For the risk evaluation of per capita grain possession, the expected value of the response variable in this model was regarded as being conditional on the recorded values at all other locations. CAR was also a popular hierachical spatial model for use with areal data, or popular auto-gaussian model, the implementation of the CAR model was convenient in hierarchical bayesian settings because of the explicit conditional structure. The model may be written as:

$$O_i \sim \text{Poisson}(\mu_i) \quad (1)$$

$$\log \mu_i = \log p_i + \alpha_0 + \alpha_1 x_i / 10 + b_i \quad (2)$$

where α_0 is an intercept term representing the baseline (log) relative risk of per capita grain possession across the study region, x_i is the covariate in district i , with associated regression coefficient α_1 and b_i is an area-specific random effect capturing the residual or unexplained (log) relative risk of per capita grain possession in area i . We often think of b_i as representing the effect of latent (unobserved) risk factors. The distribution sets the value of b_i equal to zero for areas i that are islands, hence the posterior relative risks depend on the overall baseline rate 0 and the covariate x_i . To allow for spatial dependence between the random effects b_i in nearby areas [9], we may assume a CAR prior for these terms. Intrinsic CAR model given referred to the following description:

$$\phi_i | \phi_{-i} \sim N(\bar{\phi}_i, 1/(\lambda m_i)) \quad (3)$$

Where, $\phi_{-i} \equiv (\phi_1, \dots, \phi_{i-1}, \phi_{i+1}, \dots, \phi_p)^T$, m_i is the number of adjacent regions of region i , and $\bar{\phi}_i = m_i^{-1} \sum_{j \text{ adj } \phi_j}$ the average of the adjacent regions values. This model corresponded to a multivariate normal distribution for $\phi \equiv (\phi_1, \dots, \phi_p)^T$ with a less than full rank covariance matrix. This arose due to the translation invariance clearly visible in formular (3), the prior was a pairwise difference prior, identified only up to an additive constant. This impropriety was typically ignored, since the posterior for ϕ will typically emerge as proper even though this prior is not. In order to clarify the parameterisation and the suitable hyperpriors for the parameters of this model, application of proper CAR model required the user to specify unnormalized weights, must always be used, so the new description was chosen an alternative parameterisation from Stern and Cressie (1999), as the following illustrated. $M_{ii} = 1/E_i$ (the inverse of the expected count in area i , $C_{ij} = (E_j/E_i)^{1/2}$ for neighboring areas i, j and 0 otherwise. So we used the dflat() distribution in WINBUGS developed the prior information for the intercept term in a model including CAR random effects[10].

MCMC procedure was now automated within WinBUGS, its spatial package GeoBUGS can be used to carry out bayesian computations, this software packages now routinely used by practicing biostatisticians and spatial workers. The adjacency matrices were edged from the GeoBUGS module including an option to produce a data file containing the adjacency matrix for any map loaded on the system. We edit ed the adjacency map of Yellow River Delta to include these areas as neighbors. In the article, the sum of 80 neighboring areas was given by spatial CAR models to the risk evaluation of per capita grain possession on country-level in Yellow River Delta.

3 Results and Analysis

3.1 Bayesian Posterior Analysis of CAR Model Parameters

There was a large and growing literatures on bayesian analysis and Markov chain Monte Carlo (MCMC) method. MCMC method offered an iterative computational method suitable for solving this problem. We obtained posterior estimation of key fixed effects, smoothed maps of both frailties and spatially varying coefficients. MCMC also provided a mechanism for taking spatially dependent samples from probability distributions in situations, where the usual sampling was difficult, if not impossible. Many auto-models fall into this category, particularly because the normalizing constants for their joint or posterior probability distributions were either too difficult to calculate or analytically intractable. MCMC approaches can be utilized to estimate the posterior distribution through iterative sampling. The series of results were detailed given in the contexts.

There was no evidence of drift in the study, the mixing was quite good with the full range of each parameter covered in relatively few simulations. The plot also showed the median and 95% credible interval for each parameter. Trace plots can be usefully displayed individually, as shown here. Well-behaved MCMC output was characterized by parallel-chain trace plots showing that each sampler in a set of parallel simulations (started at over-dispersed points in parameter space) has moved freely around a common parameter space, with no sign of being stuck within a localized region, and with no systematic trends. The iteration trace of alpha0, alpha1, tau and the trace plots about sigma parameter were analyzed in the article. The iteration results indicated that the markov chain based gibbs sampler of model parameters presented the convergence, including the two groups of initial values of sigma parameter according to the trace plot after 10000 iterations [11,12]. After that the gibbs sampler, we also developed the correlogram plots the autocorrelations of the chain for each parameters of interests (alpha0, alpha1, sigma and tau) to understand the convergence of the parameters in detail.

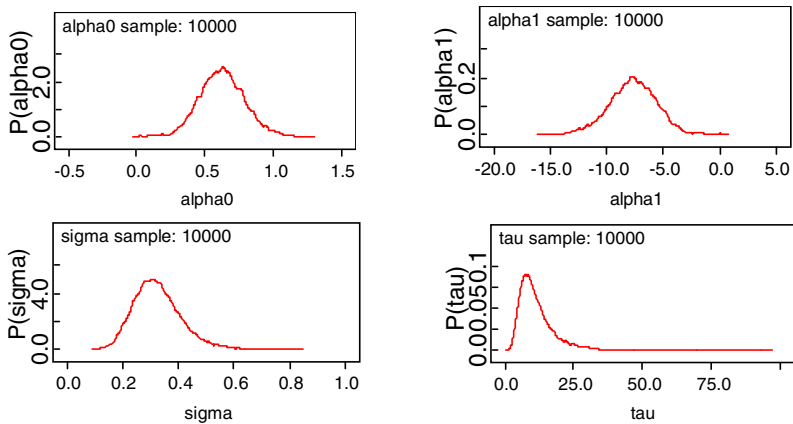


Fig. 1. Parameters posterior kernel density of CAR Model

Figure1 was produced by computerization and was showed by the densities of sections of the chains for the parameters alpha0, alpha1, sigma and tau, and was produced an approximate visual kernel estimate of the posterior density or probability function. The posterior summary was estimated by the MCMC output: mean, standard deviation, MC (Monte Carlo) error, and selected percentiles (default values are 2.5%, 50%, and 97.5%). It also provided iterations finally kept for estimation. MC error was estimated using the batch mean method, the posterior mean table of variables was showed in Table1.

Table 1. Posterior mean table of variables

	sd	MC_error	val2.5pc	median	val97.5pc	start	sample	mean
sigma	0.08675	0.0021	0.1828	0.3174	0.5231	1	10000	0.3259
alpha0	0.1725	0.0072	0.2977	0.624	0.9819	1	10000	0.625
alpha1	2.181	0.0919	-12.15	-7.633	-3.518	1	10000	-7.651
tau	7.334	0.1717	3.662	9.925	29.93	1	10000	11.71

Table 1 summarized the results for the key variables. The density estimated of the posterior distributions for the prior, the bayesian estimation of 4 parameters(alpha0, alpha1, sigma and tau) was 0.625, -7.651, 0.3259 and 11.71, the confidence intervals of the parameters were (0.2977, 0.9819),(-12.15, -3.518),(0.1828, 0.5231), respectively[12].The literature reviews showed that MCMC was an effective method for bayesian computerization on the premise of the Markov convergence, so it was significant for estimation of simulation sampler, the iterations times to reject the influence of the initial values, it was suitable for 10000 iterations to estimate the parameters of bayesian model in the study considering of these factors, correspondingly, the posterior mean plots were given, the high sustainable status of model were resulted from the data transformation, or policy and the micro-structure of market usually caused the results[13].

3.2 The Posterior Mean of Per Capita Grain Possession

Posterior density plots of parameters were estimated from posterior sample using gibbs sampler, the results generally confirmed our previous conclusion, the bayesian analysis of the coefficient alpha0, alpha1, sigma and tau was given independent non informative normal priors while the standard deviation of the random effect, a spatial bayesian hierarchical approach was employed to simulate the relationships of 3 factors to per capita grain possession. In the study, according to the series of random numbers relevant to the uncertainty of per capita grain possession, the results was expressed to estimate the risk, maps of posterior mean of observed value and predicted value for the models in the paper.

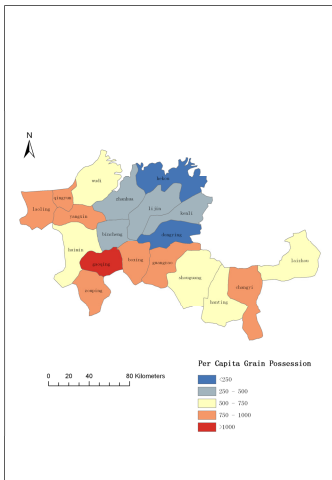


Fig. 2. The posterior mean of observed value per capita grain possession on country level in Yellow River Delta

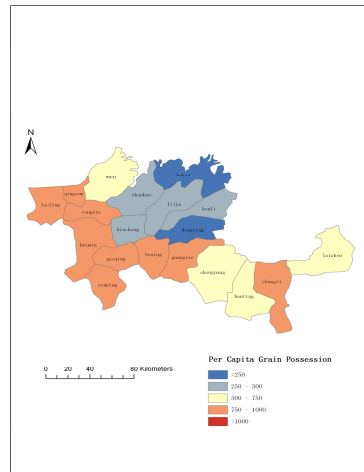


Fig. 3. The posterior mean of predicted value of per capita grain possession on country level in Yellow River Delta

The posterior mean of observed value per capita grain possession observation in Yellow River Delta, respectively. Hekou district and Dongying district (<250 kg per capita grain possession), Zhanhua country, Lijin country, Kenli country and Bincheng district(250 kg -500 kg per capita grain possession), Huimin country, Wudi country, Shouguang city, Hanting district and Laizhou city (500 kg -750 kg per capita grain possession),Qingyun country, Laoling city, Yangxin country, Zouping city, Boxing country, Guangrao country Changyi city (750kg -1000kg per capita grain possession), Gaoqing country(>1000 kg per capita grain possession), as illustrated in Figure2.

The posterior mean of predicted value about per capita grain possession was computerized on country level in Yellow River Delta, respectively. Hekou district and Dongying district (<250kg per capita grain possession), Zhanhua country, Lijin country, Kenli country and Bincheng district(250kg-500kg per capita grain possession), Wudi country, Shouguang city, Hanting district and Laizhou city (500kg -750kg per capita grain possession), Huimin country, Qingyun country, Laoling city, Yangxin country, Zouping city, Boxing country, Guangrao country, Changyi city and Gaoqing country (750kg -1000kg per capita grain possession), as shown in Figure 3.

These results indicated that the observed values were consistent with the predicted values from the posterior predictive distribution and the spatial maps of CAR model, and the parameters responded to the characteristics of model computerization. three types of the grain sowing area, efficient irrigation area and agriculture machinery resulted in complex random effects on per capita grain possession was given to estimate the CAR model, the proposed model gave a quantitative result. Our results generally agreed with previous research findings in the literature, referred to GWR results in another paper[14].

4 Conclusions and Discussion

As mentioned above, we had shown the application of spatial conditionally autoregressive model to examine the random effects on per grain possession, and we had also estimated per capita grain possession a set of 19 heterogeneous countries in Yellow River Delta. The Bayesian hierarchical approach distinguished itself by being able to explicitly model the spatial association of grain production data, the bayesian results showed the observed value and predicted value of per capita grain possession can be fitted using MCMC based on CAR model, the flexibility and stability estimation offered by model established were improved. 4 parameters in the model (including α_0 , α_1 , σ and τ) showed that the posterior probability was more evident statistical significance on basis of prior information and sample characteristics in confidence interval. So CAR of per capita grain possession on country-level in Yellow River Delta was not only the more estimated accuracy, but also the more quantitative evaluation depending on bayesian method. The Bayesian model provided the flexibility to accommodate that possibility. The flexible nature of the model also made it possible to consider the inclusion of additional spatial (e.g., soil or topographic) variables when appropriate.

References

1. Feldkircher, M.: A Spatial CAR Model applied to a Cross-Country Growth Regression. Institute for Advanced Studies Applied Empirical Homework (2007)
2. Doppelhofer, G., Miller, R.I., Sala-i Martin, X.: Determinants of long-term growth: A bayesian averaging of classical estimates (bace) approach. *American Economic Review* 94, 813–835 (2004)
3. Fernandez, C., Ley, E., Steel, M.F.: Model uncertainty in cross-country growth regressions. *Journal of Applied Econometrics* 16, 563–576 (2001)
4. Anselin, L.: Under the hood: issues in the specification and interpretation of spatial regression models. *Agricultural Economics* 17(3), 247–267 (2002)
5. Haining, R.: *Spatial data analysis theory and practice*, pp. 328–350. Cambridge University Press (1993)
6. Statistical Bureau of Shandong Province, *Shandong Statistical Yearbook*. China Statistics Press, Beijing (2008) (in Chinese)
7. GeoBUGS User Manual, Version 3.2.1 (March 2011)
8. Horabik, J., Nahorski, Z.: Statistical Spatial Modeling of Gridded Air Pollution Data. In: 2nd International Workshop on Uncertainty in Greenhouse Gas Inventories, September 27–28, pp. 101–105. International Institute for Applied Systems Analysis A-2361, Laxenburg (2007)
9. Arab, A., Hooten, M.B., Wikle, C.K.: *Hierarchical Spatial Models*, Department of Statistics, University of Missouri-Columbia (June 2006)
10. Pingping, J.Æ., Zhuoqiong, H.Æ., Kitchen, N.R.Æ., Sudduth, K.A.: Bayesian analysis of within-field variability of corn yield using a spatial hierarchical model. *Precision Agric.* 10, 111–127 (2009)
11. King, M.D., Calamante, F., Clark, C.A., Gadian, D.G.: Markov Chain Monte Carlo Random Effects Modeling in Magnetic Resonance Image Processing Using the BRugs Interface to WinBUGS. *Journal of Statistical Software* 14(2), 1–20 (2011)
12. Zhu, H., Lin, J.: *The economical model of Bayesian computation*. Science Press, Beijing (2009) (in Chinese)
13. Haijun, M., Virinig, B.A., Crain, B.P.: *Spatial Methods in Geographic Administrative Data Analysis* (August 16, 2005)
14. Yujian, Y., Xueqin, T., Jianhua, Z.: A geographically weighted model of the regression between grain production and typical factors for the Yellow River Delta. *Mathematical and Computer Modelling* 58, 582–587 (2013)

Agent-Based Simulation of Rural Areas and Agriculture Information of 11 Country Units in Shandong Province

Yujian Yang, Lili Wang, Qingyu Chen, and Jingling Li*

Science & Technology Information Institute of Shandong Agricultural Science Academy
Number 202 Gongye North Road, Licheng District of Jinan,
250100, Shandong Province, P.R. China
tshkhyyj@gmail.com

Abstract. This paper constructed the agent-based modeling framework and discussed the mechanism and implementation of agent-based rural areas and agriculture information by open-source program on country scale. In the paper, 13 indices were proposed to measure the rural areas and agriculture information level in the overlay 11 country regions located in Yellow River Delta and the Blue Economic Zone of Peninsula. The energy node agents represented for informatization involved in agent context were also constructed, network and grid of rural areas and agriculture information. In the study, 11 informatization node agents were given as the energy for the comprehensive evaluation of rural areas and agriculture information, which indicated the strength changes of rural areas and agriculture information. Correspondingly, the node process simulation of rural areas and agriculture information was explored from dual strategy mechanism driving. Then the agent energy transmission mode was put forward for 11 informatization node agent, after that three grades change status of energy transmission was displayed in the study, which responded to the gradient changes of rural areas and agriculture information. Moreover, the spatial process of 11 informatization nodes was obviously described by the agent simulation with the Repast-S IDE, and the unsealed link among node agents was also analyzed in the paper.

Keywords: Rural areas and agriculture information, Agent-based modeling and simulation.

1 Introduction

The emergence of new technologies has evolved in rural areas and agriculture information domain. Agent-based modeling and simulation (ABMS), as a part of distributed artificial intelligence, has developed rapidly since it arose from 1970s, and it was a popular direction of artificial intelligence now. Agent-based modeling and simulation currently provided methods and tools for solving complicated problems decision, and for setting up distributed, intelligent, integrated, and man-machine harmony decision making supporting system. In conclusion, ABMS has given us a new way to look at distributed systems and provided a path to more robust intelligent applications [1,2,3].

* Corresponding author.

In recent years, ABMS theory and technology have rapidly developed. Olfati-Saber presented a theoretical framework for design and analysis of distributed flocking algorithms and provided a theoretical framework for analysis of consensus algorithms for agent network system. Badjovski and Bentham had developed agent expert system for genetic breeding and management of crop production [4,5]. Agent-based modeling is intended to explore the relationship between observed spatial patterns and the process creating them (Parker et al. 2003) [6,7].

2 Material and Methodology

2.1 Indicator System of Rural Areas and Agriculture Information

11 country units from the overlay regions of Yellow River Delta high-efficiency ecological zone and blue economic zone of peninsula, including Dongying District, Shouguang City, Hanting District, Guangrao Country, Hekou District, Changyi City, Laizhou City, Kenli Country, Lijin Country, Wudi Country and Zhanhua Country in Shandong province. The comprehensive development of rural areas and agriculture information level in overlay country level is a crucial part of the National Demonstration Province of rural areas and agriculture information in the 11th and 12th Five-Year Plan of China. So agent simulation based on rural areas and agriculture information was obviously significant from the case study.

The system establishment of indicators was the premise of energy transmission mode of rural areas and agriculture information nodes, so we constructed the indicator system referred to the new countryside planning of socialism construction from the following principles of Development and Reform Commission of Shandong Province "developed production, affluent life, civilized rural atmosphere, clean and tidy village and democratic administration." Combined with the well-off indices from Wu Dianting (2006), the data were effectively collected and the selected 13 indices were applied in the study [6]. Six indices (Enger's coefficient, per house area of household, tap water countryside, household car, hospital numbers, urbanization) responded to the material life. Three indices reflected spiritual life (telephone communication countryside, cable television countryside, patents per year). Two indices were about income and distribution aspect, including per capita net income and per capita GDP. Population quality was reflected by 2 indices (students in middle school and per capita expenditure of education, science-technology and culture). As mentioned, the system of measurement indices was used to define the energy of rural areas and agriculture information nodes and explore the agent energy simulation process of rural areas and agriculture information level. Key steps were carried out to deal with the correlation data, including data acquisition, elimination dimension, determination of index weight, model establishment, comprehensive index computerization and comparison analysis, the results showed the weight values of 11 Informatization Nodes was 13.642(Dongying District), 4.592(Shouguang City), 2.456(Hanting District), 1.947(Guangrao Country), 1.678(Hekou District), 1.354(Changyi City), 0.707(Laizhou City), -0.576(Kenli Country), -2.249(Lijin Country), -2.358(Wudi Country), -2.879(Zhanhua Country), respectively.

2.2 Agent-Based Modeling

2.2.1 Construction of Agent Simulation Project

The Repast-Simphony framework provided many other tools for assisting the model developer to create a model, but the standard model structure was based on these contexts and projections. Repast-Simphony was also a free and open source agent-based modeling toolkit that offers users a rich variety of features including the following content: an optional point-and-click model development environment, a pure Java point-and-click model execution environment, etc. The Repast S framework provided many other tools for assisting the model developer to create a model, but the standard model structure was based on these contexts and projections, so we selected Repast-Simphony program to clarify the agent simulation process [5,9-12].

InformationNode simulation in the paper responded to the development situation of rural areas and agriculture information. In this study, these nodes resources given as Informatization energy indicated the strength changes of rural areas and agriculture information. A large number of agents walked in the space, and constantly increased the energy by the method of learning from their around agents. Energy nodes of rural areas and agriculture information would be consumed in one cycle, so the energy from rural area and agriculture information node was consumed when it died. During the energy transmission, Informatization node agents transmitted in accordance with the established rules. The node process simulation of rural areas and agriculture information was explored from the dual policy in the study, the unsealed link and analysis was developed by agent simulation. Finally, we constructed the agent behavior model.

InformationNode model was now fully defined by Repast-Simphony IDE. It contained a definition for a single agent type, a network projection, and a grid projection. We created agent elements of "InformationNode", the most often (and only) property and style are changed and the label property and enter "InformationNode" property was selected. 11 Informatization nodes, respectively, the energy of Informatization node had a certain change. Especially, in the case study, repast Symphony agent, the Math Operation for assigning a random number was selected as an important step, "Grid" and the dimensionality property is "2", and we defined the agent behavior according to the fundamental simulation steps, which included creating a "Deltademo" Model, creating a simple Repast model, running the simple Model, custom display properties, data sets and charts. Finally, the "delta_class" project was created, which included InformationNode agent, InformationNode groovy, etc.

2.2.2 Data Processing and Data Analysis

To initialize the agent model was the first step of agent simulation process. When the model was initialized, agent parameter displays will be created and shown in the runtime window. Note that since no agent instances have been created yet, the

simulation time would not run forward if the play button was pressed, as there were no scheduled actions. Agent instances may be created in the runtime window using the agent editor tool to connect the correlation nodes.

The agent behavior specified in this “Deltademo” was only reactive in nature, meaning that the agents would only do something based on a specific event occurring, in this case a reaction to a change in energy from an agent connected to it. The agents in the display can be probed by double clicking on them, and mainly the external response was inspected by the double-clicking mouse_event, implement of agent listen event, responded to the auto adapting.

3 Results and Analysis

The agent behavior that was defined should cause agents to connect to the first agent, and to change their energy property after 11 simulation ticks. Initialized program was carried out and the model run. Now the model can be run without first needing to make a change to an agent energy since the measured energy property was scheduled to be calculated every tick. Open the 2D Display, change the first Informatization Node’s energy property to 100 and continue running the model. If the step simulation button was clicked until the tick count reaches 11, the next agent in the chain should change its energy from 300 to 200, to 100. Double click on the second agent to display its properties in the probe panel to verify this. Finally, run the model to observe the propagation of the change in energy to the downstream nodes. To test the chart, switch back to the 2D Display, probe an agent and change its energy from 300 to 200, to 100. Now run the simulation and observer, the energy changes were recorded on the chart.

The transmission mode was presented in Fig. 1 from the small value (from 100 to 200) to the high value, The transmission mode was presented in Fig. 2 from the middle value to high value(from 200 to 300), the kind of energy transmission mode was extracted from 11 country levels referred to Fig. 3.

The results from Fig. 5 showed that the energy of rural areas and agriculture information had an obvious gradient characteristics, which presented the dynamic changes of 11 Informatization Nodes located in the Yellow River Delta “and” the Blue Economic Zone of Peninsula”. Each Informatization Node had changed characteristics itself, and the scope of Informatization energy had the certain rule from 100 to 300 on the whole, but there is the fluctuation characteristics round the threshold, such as 300,200,100 in the study case, respectively.

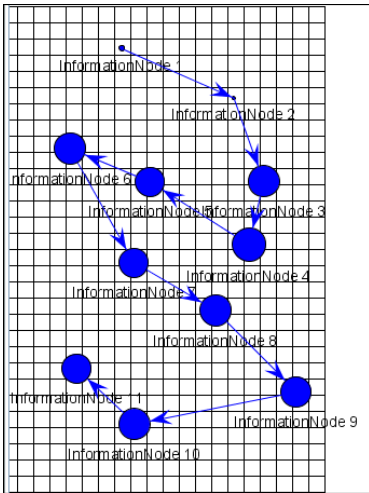


Fig. 1. Energy transmission mode of rural area and agriculture information (from 100 to 300) (left)

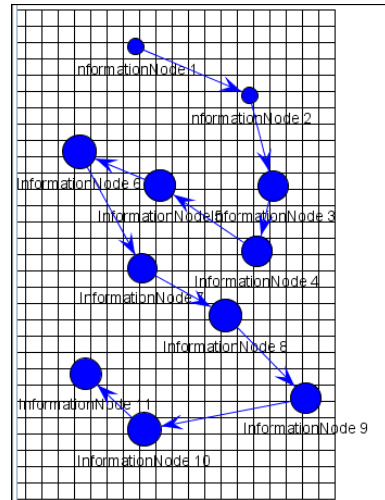


Fig. 2. Energy transmission mode of rural area and agriculture information (from 200 to 300) (right)

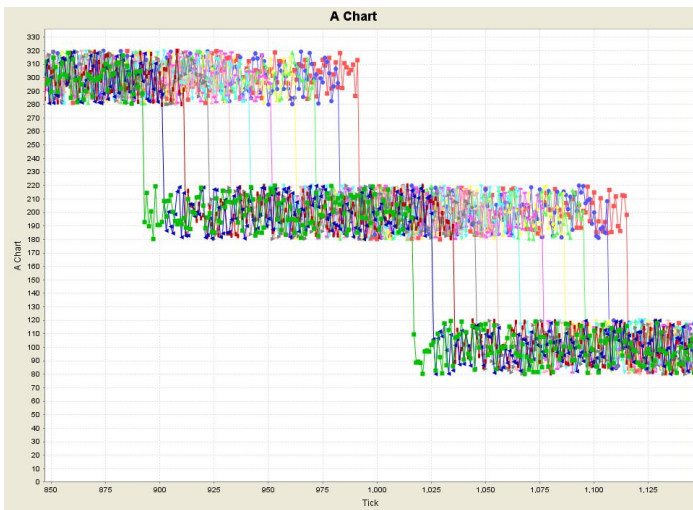


Fig. 3. The agent simulation based on Informatization energy transmission

4 Conclusions and Discussion

Agent-based simulation of rural areas and agriculture informatization was explored in the study, and some conclusions could be drawn as follows.

The paper proposed that the rural area and agriculture information level was measured by 13 indicators in the overlay 11 country levels located in case regions. The study

constructed the energy nodes agents involved in agent context, network and grid of rural area and agriculture information. Furthermore, in dual policy mechanism driving of “high-efficient ecological zone in Yellow River delta “and” the Blue Economic Zone of Peninsula”, we also developed that the spatial process of dissipation of energy of located in 11 informatization Nodes was obvious described by the agent simulation with Repast-S IDE, and analyzed the unsealed link among nodes. The article put forward the agent energy transmission mode from 11 informatization Nodes, the energy of rural areas and agriculture information has an obvious gradient characteristics, which presented the dynamic changes of 11 informatization Nodes; each informatization Node had change characteristics itself, but there was the fluctuation characteristics round the threshold, such as 300,200,100, respectively, which responded to the gradient changes of informatization energy transmission.

References

1. Bordini, R.H., Wooldridge, M., Hübner, J.F.: Programming multi-agent systems in agents peak using Jason. Wiley Series in Agent Technology. John Wiley & Sons (2007)
2. Bordini, R.H., Fisher, M., Visser, W., Wooldridge, M.: Verifying Multi-Agent Programs by Model Checking. *J. Autonomous Agents and Multi-Agent Systems* 12(2), 239–256 (2006)
3. Zhu, Y., Feng, Z.: Application of Agent in Agricultural & Forestry Economy Decision Support System. *Journal of Beijing Forestry University*, 218–221 (2005)
4. Olfati-Saber, R.: Flocking for multi-agent dynamic systems: algorithms and theory. *IEEE Transactions on Automatic Control* 51(3), 401–420 (2006)
5. Recursive Porous Agent Simulation Toolkit guide (2012)
6. Parker, D.C., Manson, S.M., Janssen, M.A., Hoffmann, M.J., Deadman, P.: Multi-agent system for the simulation of land-use and land-cover change: a review. *Annals of the Association of American Geographers* 93(2), 314–317 (2003)
7. Johnston, K.M.: Agent Analysis Agent-Based Modeling in ARCGIS. ESRI Press, Redlands (2013)
8. Liu, S.: Study on the indicator system for measuring the rural area information level in China. *Library And Information Service* 51(9), 33–35 (2007)
9. Howe, T.R., Collier, N.T., North, M.J., Parker, M.T., Vos, J.R.: Containing Agents: Contexts, Projections, and Agents. In: Proceedings of the Agent 2006 Conference on Social Agents: Results and Prospects, Argonne National Laboratory, Argonne, IL USA (September 2006)
10. North, M.J., Sydelko, P., Vos, J.R., Howe, T.R., Collier, N.T.: Legacy Model Integration with Repast Symphony. In: Proceedings of the Agent 2006 Conference on Social Agents: Results and Prospects, Argonne National Laboratory, Argonne, IL USA (September 2006)
11. Parker, M.T., Howe, T.R., North, M.J., Collier, N.T., Vos, J.R.: Agent-Based Meta-Models. In: Proceedings of the Agent 2006 Conference on Social Agents: Results and Prospects, Argonne National Laboratory, Argonne, IL USA (September 2006)
12. Tatara, E., North, M.J., Howe, T.R., Collier, N.T., Vos, J.R.: An Introduction to Repast Modeling by Using a Simple Predator-Prey Example. In: Proceedings of the Agent 2006 Conference on Social Agents: Results and Prospects, Argonne National Laboratory, Argonne, IL USA (September 2006)

Influence of Digital Computer Technology on Architectural Design Teaching Mode

Huang Ting¹ and Jiang Sicheng²

¹ Department of Architecture, College of Civil Engineering, Yancheng Institute of Technology, Yancheng, 224000

² Yancheng Architectural Design Research Institute Co., Ltd., Yancheng, 224000

Abstract. This paper starts from the influence of CAAD system on different stages of architectural design and describes the application of digital technology in architectural design based on the development status of architectural design; meanwhile analyzes the teaching status of domestic computer aided architectural design curriculum and existing problems; and discusses its influence on architectural design field and even the educational pattern of architectural design major in combination with new features of the development of the current construction industry and computer aided architectural design technology. The emphasis lies in proposing constructive instructions for the reform of educational pattern of architectural design major in China.

Keywords: digital technology, computer aided architectural design, architectural design, teaching mode.

1 Introduction

No digital computer technology in any era has such strong impact on architectural design, architectural teaching and practice. “Image architecture, digital simulation and virtual scene” etc. have gradually become “progressive” architectural design nouns. Ranging from computer aided drawing (CAD) to computer aided architectural design (CAAD), architecture has changed in the reform of design means, tools and medium. We can be more clear about how architectural design teaching mode should adapt to such reform by analyzing the influence of digital computer technology on architectural design. The change of design object results in the change of the role of architect and the teaching orientation of architecture major. New architecture and even new architect emerge at the right moment.

2 Application of Digital Technology in Architectural Design and Its Influence on Design Thinking

2.1 Application of Digital Technology in Architectural Design

The application of digital computer technology in architectural design not only involves drawing, model, animation, network and free form, but also reaches various

fields in the process of architectural construction such as building construction, structural design and environmental index design.

Architect Frank Gehry used French aviation industrial manufacturing aircraft computer software “CATIA” system to construct architecture work. Digital means make architecture work with irregular shape a reality. In the past, Gehry always thought that model and drawing were easier to express architecture visually than computer. However, with the deepening of inspiration degree of his work, traditional design methods can hardly bear the great pressure brought by fantastical notion about shape, causing Gehry to gradually practice and finally completely accept computer. In his work Disney Concert Hall, the external form of the main part of the whole building develops completely according to acoustic design result; the internal spatial scale of the room is adjusted according to the sound vibration time evaluated by digital technology, including the measurement of air duct curvature, change of luminous environment in one day and wind load analysis etc. However, Eisenman applied computer in a different way. He no longer gave the concept of “computer aided”, but conducted architectural design directly on computer. They represent two different trends of using computer for design.

Digital virtual reality technology is a computer system that can create and manifest virtual world. The application of VR technology in the process of architectural design allows the design process to be visual and architects to fully experience advantages and disadvantages of the internal functional layout and external environmental design of buildings as if they are staying in the place to be constructed and helps architects to better verify the correctness and feasibility of design.

2.2 Influence of Digital Technology on Architectural Design Thinking Model

For a long time, graphical information is the main medium of design and expression of architectural space. It plays an irreplaceable role in the process of formation, analysis and professional expression of conception of building scheme. Professional technological means and tools of graphical information often influence design thinking. As a professional thinking model, the traditional graphical thinking mode makes the content object and professional design information of architectural design closely connected through a series of links such as drafting, model making and drawing formation and modification. Digital technology represented by computer aided design can transfer this process to virtual 3D digital world. This situation is called as “digital thinking”. In the early stage of technological development, design thinking under digital technology does not support the rapid development of concept directly in the thinking process of designers. Therefore, they used to only accurately describe, refine and file concepts with complete development. Currently, digital technology has made substantive progress. Besides allowing architects to have more visual abstract thinking closer to the reality, more importantly, it can break through regular design rules and allow architects to get breakthrough and innovation in technology and find poetic shape pursuit. The conception of architectural space can

have freedom and randomness like sculpture. Moreover, it may update design thinking and method and form architectural digital information model with overall integration, more dynamic participation and wide horizontal cooperation etc.

3 Teaching Situation of Traditional Computer Aided Architectural Design Curriculum

Currently, the teaching of computer aided architectural design curriculum is led mainly according to two different clues domestically. One is design expression, including 2D architectural drawing and 3D modeling, 3D architectural rendering and image processing, multi-media architectural expression and demonstration[1]. For example, architecture major of the College of Architecture and Urban Planning, Guangzhou University currently provides architectural CAD teaching mainly in two parts - basic theories of architectural CAD and CAD aided drawing and making of computer aided architectural design sketch. The other is design concept. For example, Southeast University attempted to establish architectural design model by using computer as the design tool, simulate the whole process of program conception in three steps - volumetric model, structural model and architectural model and realize collaborative design with internet as the communication platform. Through the analysis on the application of computer in architectural design by two avant-garde American architects Gehry and Eisenman, we clearly realize that the influence of computer on architectural design not only involves expression. University academic advisory committee also advocates that architectural CAD should take the clue of design concept. However, it is restricted by many factors in actual operation, such as the lack of easy-to-learn, easy-to-use and effective computer software technology and guidance of architectural CAD experts. Moreover, it is better to synchronize computer aided architectural design and architectural design curriculum. Such operation has a high difficulty of coordination. Therefore, teaching with design expression as the clue is more often used currently.

4 How to Reform Architectural Design Teaching Mode So as to Give Full Play to Advantages of Architecture Major in Digital Times

The author thinks that CAD teaching throughout architecture major should not stand on expression clue or conception clue because expression and conception should be basic qualities of architectural designers. Our teaching of architecture should be led by requirements of the market for architects with the clue of the process in which students accept and learn architectural design. Complete CAD teaching should contain three parts: part 1 includes brief introduction to the development history of architectural CAD technology, application situation, software and hardware system and main technologies; part 2 includes computer aided analysis in terms of architectural environment, shape, space and physical characteristics; part 3 is 2D, 3D

and multi-media computer performance of design achievements. Currently, in terms of architectural CAD course arrangement in many universities, computer aided architectural design expression occupies the majority of class hours. Some universities even incorporate architectural CAD into design expression courses in teaching curriculum system planning. This obviously neglects the important role of basic theories of computer aided architectural design and computer aided architectural design concept in architecture major.

As a professional teacher of architectural graphing and architectural design curriculum, the author brings forward his own opinions on CAD course teaching of architecture according to his years of teaching experience. As the first part of architectural CAD, basic theories of architectural CAD and contents of drawing part can be explained in combination with descriptive geometry and computer part of shadow and perspective in freshman year so as to help students establish the elementary contour of this technology. In this part, we can be oriented at practicality and teach in combination with small architectural design in basic courses of architectural design in freshman year so as to arouse students' learning interest and improve the operability of architectural CAD technology. Previously, most of us thought that students majoring in architecture should not touch computer too early, which is adverse to the cultivation of students' early architectural accomplishment. The author thinks that, with the increasing development of computer today, if computer aided teaching is beneficial to the study of professional knowledge and training of professional skills and good for arousing students' learning enthusiasm and cultivating students' innovation ability, we should spare no effort to apply it. For the second part computer aided architectural design concept, we can gradually teach in stages and grades. For example, we can start from architectural design curriculum in sophomore year, conduct environmental simulation, spatial analysis, form conception and achievement expression in the conception process of program design with SketchUp software, use it as the computer tool of aided architectural design concept and teach ideological contents of computer architectural design concept. Architectural design curriculum in junior year can further involve "VR" technology, architectural environment and architectural program modification with software "Ecotect". Less class hours are provided for the last part - computer design sketch making course. Students should mainly study on their own and teachers explain key points and difficult points of this technology in class and guide students to complete course work. Through such series of course learning, students can comprehensively understand architectural CAD technology. This technology is no longer only a drawing tool, but it actually applied in each stage of design.

Architecture is an integrated discipline. The education of architecture major shows the superiority of systematic cultivation of students majoring in architecture in multiple aspects such as color sense, relationship of composition of proportions, streamline functional space organization design, style design, structural form selection, building construction, building materials and architectural history. Digital technology is only a tool used in architectural design, which is conducive to producing more excellent architectural design works, accelerating architectural design mapping and improving architects' sense of 3D space. However, it cannot replace

architectural design of architecture major based on system theory. Today, with increasingly wider computer aided architectural design, some students think that free basic skill training is not indispensable. It seems that computer can accomplish all work completed by manpower previously, resulting in sharp decrease of students' on-hand expression ability. This becomes a universal phenomenon in the department of architecture of various universities. In fact, when technologies become more advanced, people should attach more importance to the improvement of their own quality and ability. Basic skills contain double meanings - graphic capability (ability of expression) and design ability. The cultivation of design ability mostly originates from the training process of the ability of expression. Therefore, proper use and correct understanding of computer technology will help students to learn architecture well more smoothly.

5 Conclusion

Though digital technology has been applied in architectural design for a short time, the change brought by it is very striking and it gradually becomes mature. Ranging from program design drawing and working drawing in the early stage to 3D modeling and image processing to animation and virtual reality and the establishment of architectural information model, its major function is not impairing architects' creative activity but freeing architects with creative talent from a lot of tedious and repetitive work through the superiority of digital technology and allowing them to have more energy to be engaged in architectural creation.

References

- [1] Wang, G.: Digital Means and Virtual Reality Technology in Architectural Design - Application and How to Promote Innovation and Development of Architectural Design. School of Architecture, Central Academy of Fine Arts, Beijing (2007)
- [2] Yang, L.: Research on Digital Technology and Architectural Design Methods. Master's Thesis. Tongji University, Shanghai
- [3] Yang, H.: Research on Non-linear Form Design Methods of Architecture. Master's Thesis. Tongji University, Shanghai
- [4] Guo, L.: Analysis and Research on Digital Architectural Expression Art Based on 3D Computer Technology. Master's Thesis. Nanchang University, Jiangxi
- [5] Zhang, L.: Architecture and Architectural Design in Information Era. Tsinghua University Press, Beijing (2000)

Optimization Design on Deep-Fertilization Fertilizer Amount Adjusting Mechanism for Paddy Field

Jinfeng Wang¹, Detang Zou², Jinwu Wang¹, and Xinlun Yang¹

¹ College of Engineering, Northeast Agricultural University, Harbin 150030, China

² College of Agriculture, Northeast Agricultural University, Harbin 150030, China
{ju_jinyan, zoudt, jinwu}@163.com, yang_xin_lun@126.com

Abstract. In order to solve the deliquesced fertilizer adheres to fertilizer conveying pipe, and leads to fertilizer conveying pipe blocked, a kind of fertilizer amount adjusting mechanism of deep-fertilization machinery for paddy field was designed. This adjusting mechanism was taken as research object, the distance between hinge axis and the center of blade connection seat, the distance between hinge axis and sliding limited post axis, the rotation angular velocity of cam ring and the angular velocity of blade rotating around hinge axis were taken as objective function, the diameter of fertilizer through-hole, the number of blades and the changing range of curvature radius of guide chute were taken as constraint conditions, the aided design and analysis software for fertilizer amount adjusting mechanism was programmed by VB software, through which kinematics optimization was carried out for fertilizer amount adjusting mechanism. The obtained optimal parameter ranges are: the radius of inner ring of cam is 30mm, the number of blade is 6, the distance between the hinge axis and the center of blade connection seat is 47.5mm, the distance between hinge axis and sliding limited post axis is 12.5mm, the rotation angular velocity of cam ring is 25-35r/min, the angular velocity of blade rotating around hinge axis is 30-35r/min. According to optimization results, the fertilizer amount adjusting mechanism was simulated by Pro/E software, the simulation results were validated by experiment. The results show that the adjustable range of diameter of fertilizer through-hole for fertilizer amount adjusting mechanism is 9-56mm, the sliding limited post of blade and the guiding chute of cam ring have good sliding performance, and the designed fertilizer amount adjusting mechanism can satisfy the expected design requirements.

Keywords: fertilizer applicator, fertilizer amount, adjustment, simulation, mechanism, optimization.

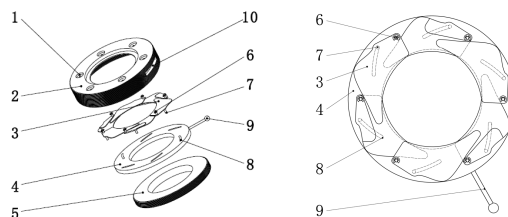
1 Introduction

Fertilizer is easily deliquescent chemical product, after moisture absorption, fertilizer has low flow ability, high adhesive ability, often adheres to fertilizer box and conveying fertilizer pipe, which results in technical issues, such as fertilization amount reduce, fertilization quality decline, or even conveying fertilizer pipe blockage, and cannot continue to operate, which reduce the operation efficiency of the equipment [1].

In order to solve the above problems, in recent years, the structure of configuration helical screw blades in fertilizer box and conveying fertilizer pipe emerges, but when operating, a large amount of deliquescent fertilizer still adheres to helical screw blades, the dredge effect is not ideal. Aiming at the existing technical problems, deep-fertilization mechanism for paddy fields was developed, which uses spiral wire instead of the helical screw blade, in this mechanism the traditional outer-fluted roller fertilizer distributor has been unable to matching, therefore, it is imminent to design a new fertilizer amount adjusting mechanism. In order to facilitate the adjustment of the amount of fertilizer, and the installment of spiral wire for deep-fertilization mechanism, a kind of fertilizer amount adjusting mechanism was designed, and its main parameters were optimized. Fertilizer amount adjusting mechanism was analyzed using kinematics theory, its mathematical model was developed, human-computer interaction simulation software was developed by VB software, which was used to obtain optimization parameters, structure design and simulation for fertilizer amount adjusting mechanism were carried out by Pro/E software, thus the movement of fertilizer amount adjusting mechanism was simulated [2-3], the simulation results were validated by experiment.

2 Structure and Operation Principle

The structure of fertilizer amount adjusting mechanism is shown in figure 1. The hole 1 of hinge axis is set on the upper surface of blade connection seat 2, the lower side portion of the hinge axis 6 is plugged in the adjacent blade 3, annular assembly is composed by blade 3, the upper side portion of hinged axis 6 is plugged in hole 1 of hinge axis of the blade connection seat 2, annular assembly composed by blade 3 is mounted on the inner of blade connection seat 2, sliding limited post 7 is fixed on the lower side of blade 3, the cam ring 4, which has a guide chute 8, is fixed on the lower part of blade 3, sliding limited post 7 is plugged in the guide chute 8, the locked ring 5 is assembled in the lower side of blade connection seat 2 by thread, which is located in the lower part of cam ring 4. The handle 9 is inserted in slots 10 of blade connection seat, the inner part of handle 9 is connected to cam ring 4.



1. hole of hinge axis 2. blade connection seat 3. blade 4. cam ring 5. locked ring 6. hinge axis 7. sliding limited post 8. guiding chute 9. Handle 10. Notch of the connection seat

Fig. 1. Structure drawing of fertilizer amount adjusting mechanism

When operating, the upper side of fertilizer amount adjusting mechanism was connected to fertilizer box; the lower side was connected to fertilization pipe, non-helical part of the longitudinal spiral wire passed through the center of fertilizer through-hole of fertilizer amount adjusting mechanism. When adjusting the amount of fertilizer, the handle 9 was moved in the slots 10 of blade connection seat, which drove cam ring 4 to rotate, under the control of guide chute 8, sliding limited post 7 made radial arc movement in the guide chute 8, the blade 3 moved around the hinge axis 6, the opening size of center hole was adjusted, which was composed by blade 3, the amount of fertilizer application was adjusted.

3 Mathematical Models

When fertilizer amount adjusting mechanism operating, the blade connection seat was fixed, cam ring was drove by adjusting handle, which realized the adjustment of the amount of fertilizer application. Handle and cam ring were fixed, the adjustment of the amount of fertilizer application can also be realized by rotating the blade connection seat, the latter method was used to develop mathematical model, as shown in figure 2. xoy is fixed reference system, $x'oy'$ is moving reference system, and the origin of coordinate system is coincide. M is the pivot point of sliding limited post, the relative motion is fixed axis rotating around hinge axis hole of blade connection seat, translational motion is the blade connection seat rotating around cam ring. The relationship of absolute, relative and translational motion was established by coordinate transformation relation (1) [4-5].

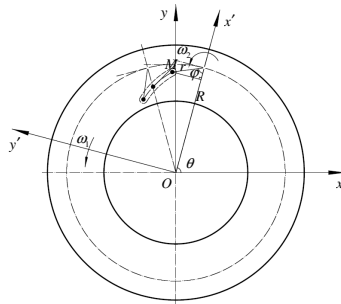


Fig. 2. Movement analysis diagram of fertilizer amount adjusting mechanism

$$\begin{cases} x = x_{O'} + x' \cos \theta - y' \sin \theta \\ y = y_{O'} + x' \sin \theta - y' \cos \theta \end{cases} \quad (1)$$

Where x and y are absolute motion coordinates of points, $x_{O'}$ and $y_{O'}$ are coordinate origin of moving reference system, x' and y' are relative motion coordinates of points, θ is rotation angle from x axis to x' axis, taking the counterclockwise direction as positive, relative movement equation of point M is shown as follow:

$$\begin{cases} x' = R - r \cos \omega_2 t \\ y' = r \sin \omega_2 t \end{cases} \quad (2)$$

R is the distance between hinge axis and the center of blade connection seat, unit: mm; ω_2 is the angular speed of blade rotating around hinge axis, unit: r / s; r is the distance between hinge axis and the axis of sliding limited post, unit: mm; t is time, unit: s. The equation of transport motion is shown as follow:

$$x_{O'} = x_O = 0, \quad y_{O'} = y_O = 0, \quad \theta = \omega_1 t$$

The equation of absolute motion of point M was obtained by equation (1) and (2), which is shown as follow. ω_1 is the rotation angular velocity of cam ring, unit: r / s.

$$\begin{cases} x = (R - r \cos \omega_2 t) \cos \omega_1 t - r \sin \omega_2 t \sin \omega_1 t \\ y = (R - r \cos \omega_2 t) \sin \omega_1 t - r \sin \omega_2 t \cos \omega_1 t \end{cases} \quad (3)$$

4 Parameters Optimization

4.1 Objective Function and Constraint Conditions

In order to satisfy the fertilizer requirement of rice in different periods, the structure of fertilizer amount adjusting mechanism has the following requirements: (1) $30\text{mm} \leq$ the diameter of the fertilizer through-hole $\leq 80\text{mm}$; (2) the number of blade is greater than or equal to 6; (3) the guide chute of cam ring is smooth, curvature radius is greater than or equal to 15mm ; (4) the distance between hinge axis and the center of blade connection seat is greater than the diameter of fertilizer through-hole. In this case, taking lightweight of the fertilizer amount adjusting mechanism as target, thus the flexibility of adjustment was improved. The objective functions of fertilizer amount adjusting mechanism are the distance between hinge axis and the center of blade connection seat (R), the distance between hinge axis and the sliding limited post axis (r), the rotation angular velocity of cam ring (ω_1) and the angular velocity of blade rotating around hinge axis (ω_2).

The constraint conditions and objective functions are multi-variable nonlinear function, it is difficult to solve global optimal solution using traditional optimization methods, therefore, based on mathematical models and objective functions, on the premise of satisfy the constraint conditions, human-computer interaction simulation software was developed to optimize parameters by VB software [6].

4.2 Human-Computer Interaction Simulation Software

The input parameters of software include a, h, n, R, r, ω_1 and ω_2 , a is the radius of inner ring of cam ring, h is the width of cam ring, n is the number of blades. According to the variation of system parameters, software can output calculation

parameters in real-time, and display the trajectory, meanwhile the absolute motion of the blade sliding limited post can also be simulated, as shown in figure 3.

When using this software, firstly enter a set of parameters based on experience, the computer calculates results, displays trajectory and simulates moving trajectory in real-time. Then based on these results, with people's experience and logical thinking to determine whether this set of parameters are good or not [7-14].

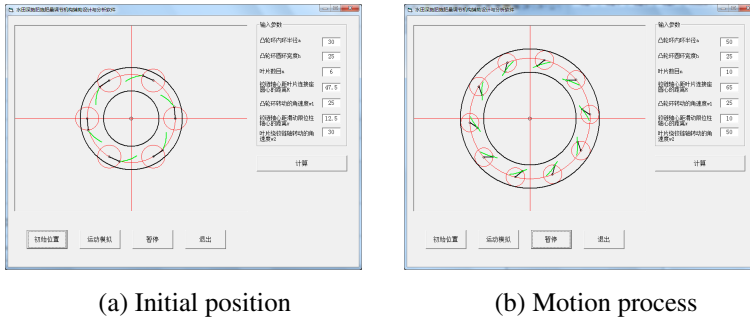


Fig. 3. Optimization interface of visible human-computer interaction

4.3 Analysis of the Influence of Variables on Results

As shown in simulation software:

(1) The rotation angular velocity of cam ring (ω_1) affects the length of guide chute, which increases with the increase of ω_1 .

(2) The angular velocity of blades rotating around hinge axis (ω_2) affects the changing rate of the area of adjusting fertilizer through-hole, which increases with the increase of ω_2 .

(3) k is the ratio of ω_1 and ω_2 , which influences curvature radius of the guide chute, curvature radius of the guide chute increase with the increase of k .

(4) The distance between hinge axis and the center of the blade connection seat (R) affects the mounting position of blade, the mounting position increases with the increase of R .

(5) The distance between hinge axis and the center of the blade connection seat (R), the distance between hinge axis and the sliding limited post axis (r) and the number of blades (n) can determine parts of blade size, the profile of blade can be determined in three-dimensional software.

4.4 Optimization Results

The optimization results which satisfy the movement requirements were obtained by software, as shown in table 1.

Table 1. Optimization results

a /mm	h /mm	n	R /mm	ω_1 /r min ⁻¹	r /mm	ω_2 /r min ⁻¹
30	25	6	47.5	25~35	12.5	30~35

5 Structure Design and Simulation

Parameters optimization, trajectory simulation and structure schematic of the fertilizer amount adjusting mechanism were realized by human-computer interaction simulation software, which was developed by VB software, but the blade, the movement of cam ring and the inspection of interference problems for fertilizer amount adjusting mechanism need to be realized by three-dimensional solid modeling and simulation software. A set of optimized parameters were selected, which were $a = 30\text{mm}$, $h = 25\text{mm}$, $n = 6$, $\omega_1 = 25\text{r/min}$, $\omega_2 = 30\text{r/min}$, $R = 47.5$ and $r = 12.5$ mm, fertilizer amount adjusting mechanism was designed by Pro / E, its structure simulation diagram is shown in figure 4.

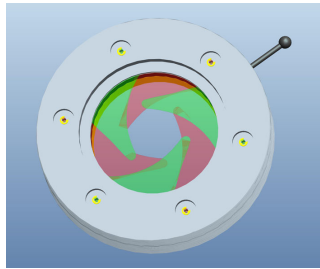


Fig. 4. Structure simulation diagram of fertilizer amount adjusting mechanism

Kinematics simulation was carried out for fertilizer amount adjusting mechanism by Pro / E, the profile of blade was modified, the blade assembly had no gap in the rotation process. The range of the diameter of fertilizer through-hole was adjusted from 7 mm to 56mm, as shown in figure 5. Interference test was carried out by Pro / E, the test results show that the moving process of the designed fertilizer amount adjustable mechanism has no interference, the sliding performance of the blade sliding limited post and the guide chute of cam ring is good, the designed fertilizer amount adjustable mechanism can meet the design requirements.

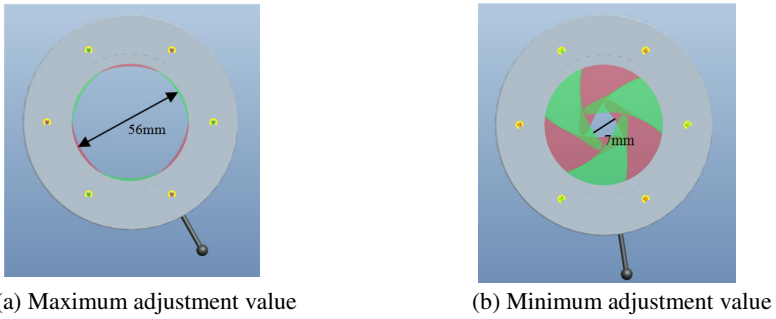


Fig. 5. Adjustable range of fertilizer amount adjusting mechanism in simulation

6 Experimental Results and Analysis

Fertilizer amount adjusting mechanism was processed, and then the experiment was carried out. To turn the adjustment handle, the size of the diameter of fertilizer through-hole can be adjusted. The maximum diameter of fertilizer through-hole was 56mm, as shown in figure 6a. The minimum diameter of fertilizer through-hole was 9mm, as shown in figure 6b. The maximum value of the diameter of fertilizer through-hole was the same as the simulation results. The minimum value of the diameter of fertilizer through-hole was 2mm greater than the simulation results. A gap of 1mm in width between the two blades emerged in the process of adjusting the diameter of fertilizer through-hole smaller, which mainly due to the processing accuracy of the blade hinge axis and the position and verticality of the sliding limited post with the blade didn't satisfy the design accuracy requirements. In order to ensure that no gap appears between blades in the process of through-hole diameter changing, on the premise of without changing any other design parameters and improving the design accuracy, the number of blades can be increased by one.



(a) Maximum adjustment value (b) Minimum adjustment value

Fig. 6. Adjustable range of fertilizer amount adjusting mechanism in experiment

7 Conclusions

(1) Aided design and analysis software for fertilizer amount adjusting mechanism was programmed by VB software, kinematics optimization was carried out using this software, the optimization results show that the radius of inner ring of cam is 30 mm, the number of blades is 6, the distance between hinge axis and the center of blade connection seat is 47.5mm, the distance between hinge axis and the axis of sliding limited post is 12.5mm, the angular velocity of cam ring is 25-35r/min, the angular velocity of blade rotating around hinge axis is 30-35r/min.

(2) According to kinematic optimization results, fertilizer amount adjusting mechanism was designed by Pro/E software, kinematics simulation was carried out for fertilizer amount adjusting mechanism. The simulation results show that the adjustable range of diameter of fertilizer through-hole is 7-56mm for fertilizer amount adjusting mechanism, the sliding performance of the blade sliding limited post and the guide chute of cam ring is good, the designed fertilizer amount adjusting mechanism can meet the design requirements.

(3) Experimental results show that the adjustable range of diameter of fertilizer through-hole is 9-56mm for fertilizer amount adjusting mechanism, which satisfies the design requirements, a gap of 1mm in width between the two blades emerged in the process of adjusting the diameter of fertilizer through-hole smaller, which mainly due to the processing accuracy didn't satisfy the design accuracy requirements. In order to ensure that no gap appears between the blades in the process of adjusting the diameter of fertilizer through-hole, the processing accuracy can be improved or the number of blades can be increased by one.

Acknowledgment. This research was supported by National Natural Science Foundation of China (51205056), Youth Science Foundation of Heilongjiang Province (QC2011C007), Special Funds of Science and Technology Innovative Talents of Harbin (2012RFQXN004), Postdoctoral Fund Project of Heilongjiang Province (LBH-Z11222).

References

1. Yuan, Z.: Research on Fertilizer Deep Application Technology for Paddy Field. *Chinese Agricultural Mechanization* (12), 38–39 (1996)
2. Wang, J., Ji, W., Feng, J., et al.: Design and Experimental Investigation of the Liquid Fertilizer Applicator. *Transactions of the CSAE* 24(6), 157–159 (2008)
3. Wang, J., Wang, J., Ge, Y.: Design and Experiment on Liquid Fertilizer Device of Deep-fertilization. *Transactions of the Chinese Society for Agricultural Machinery* 40(4), 58–63 (2009)
4. Feng, L., Guo, S., Li, Y.: Composition Motion of a Point and the Method for Full- Process Analysis. *Journal of Air Force Engineering University* 3(5), 86–87 (2002)
5. Tang, H., Wang, L., Shi, Y.: On the Establishment of System Info of Composite Movement of a Point. *Journal of Xi'an University of Arts & Science* 13(4), 44–46 (2010)

6. Wang, J., Wang, J., Ge, Y., et al.: Optimization Design on Pricking Hole Mechanism of Deep-fertilization Liquid Fertilizer Applicator. *Transactions of the Chinese Society for Agricultural Machinery* 41(4), 52–55 (2010)
7. Wang, J., Wang, J., Ju, J.: Dynamics Optimization for Pricking Hole Mechanism of Deep-Fertilization Liquid Fertilizer Applicator. *Transactions of the CSAE* 27(1), 165–169 (2011)
8. Yu, G., He, Y., Chen, J., et al.: Automatic Search of Pareto Solutions of Multi-objective for Rotary Transplanting Mechanism Kinematic. *Transactions of the Chinese Society for Agricultural Machinery* 40(6), 47–52 (2009)
9. Wu, C., Zhao, Y., Chen, J.: Optimization Design of Rice Trans Planter Separating-planting Mechanism with Visualization Human-computer Interaction Method. *Transactions of the Chinese Society for Agricultural Machinery* 39(1), 73–74 (2008)
10. Xi, X., Wang, J., Lang, C., et al.: Optimal Design and Simulation on Pricking Hole Mechanism of Liquid Fertilizer Applicator. *Transactions of the Chinese Society for Agricultural Machinery* 42(2), 80–83 (2011)
11. Yin, J., Wu, C., Liu, Y.: Optimization Design of Birotary Arm Type of Separating-transplanting Mechanism with Differential Eccentric Gear Train. *China Mechanical Engineering* 23(24), 2930–2935 (2012)
12. Feng, J., Jiang, Y.: Mechanism and Performance Test of Pivot Turning System with Single Driving for Rice Combineharvester. *Transactions of the Chinese Society of Agricultural Engineering* 29(4), 30–35 (2013)
13. Chen, J., Zhao, Y.: Parameters Optimization of Transplanting Mechanism with Planetary Elliptic Gears for High-speed Transplanter. *Transactions of the Chinese Society for Agricultural Machinery* 34(5), 46–49 (2003)
14. Wang, J., Ju, J., Wang, J.: Experimental Study on Pricking Hole Performances of Deep Application Liquid Fertilizer Device. In: 2011 Fourth International Conference on Intelligent Computation Technology and Automation, vol. 1(2), pp. 71–76 (2011)

Testing and Analysis of the Shear Modulus of Urea Granules

Jinfeng Wang¹, Detang Zou², Jinwu Wang¹, and Wei Zhou¹

¹ College of Engineering, Northeast Agricultural University, Harbin 150030, China

² College of Agriculture, Northeast Agricultural University, Harbin 150030, China
{ju_jinyan, zoudt, jinwuw}@163.com, 592091975@qq.com

Abstract. In order to study the interaction between urea and mechanical structure, using direct shear test method, the shear modulus of urea was tested by C-LM4 computer measurement and control shear force measuring instrument. The obtained test curves show that: extrusion makes the binding strength between urea molecules reduce, shear force peak emerge, then decline rapidly; as rolling granules and surrounding granules formed compression and friction resistance in contact surface along the direction of shear, shear force emerges rise again. At the test temperature 22°C, ambient humidity 45%, the density of urea granules $1.33 \times 10^3 \text{kg/m}^3$, the values range of shear modulus of urea granules was measured, which was 0.23- 0.3GPa.

Keywords: urea, shear force, shear modulus, test.

1 Introduction

China is a big agricultural country, which is also a big fertilizer production and consumption country. Fertilizers play an important role in the development of agricultural production, especially in grain production. China uses less than 10% of the world's arable land to feed 22% of the world's population, which is inseparable with the contribution of fertilizer. For quite a long time, fertilizer is still an essential part to realizing agricultural sustainable development.

Rice is one of China's most important grain crops. Urea is widely applied in rice farming process, which is directly synthesized by raw materials of liquid ammonia and carbon dioxide under high temperature. The researches of urea are mainly concentrated in the application of urea in agriculture, the fertilizer proportion of urea and other fertilizers, the fertilizer utilization of urea, the synthesis of urea, and the chemical composition and so on, but the physical characteristics of urea are rarely researched[1-2]. Urea plays an important role in the process of rice farming, when applying fertilizer using paddy field fertilization machinery, urea often absorbs moisture, which results in urea has low flowability, adheres to fertilizer box and the conveying pipe, and leads to technical problems of fertilization rate reduced, fertilization quality decline, therefore, when researching the interaction of urea and mechanical structure, the physical characteristics of urea must be studied, such as

density, elastic modulus, shear modulus and Poisson's ratio, etc. [3-5]. The shear modulus of urea was measured using direct shear test method, the shear modulus of urea was obtained, which provides related research methods and data reference for the research of physical characteristics of urea [6-9].

2 Materials and Methods

2.1 Structure and Working Principle of Test Equipment

Shear modulus test equipment includes shear force measuring instrument, data lines, measurement and control program, as shown in figure 1. The fixed shear-slice of the shear force measuring instrument was replaced by shear-slice of urea granules, shear force measuring instrument was connected with computer using dedicated data line, one end of data line was inserted into the computer USB port, the other end was connected to the rear 9-hole D-type data communication interface of the shear force measuring instrument. To open the power switch of shear force measuring instrument, and start the measuring and control program on the computer.

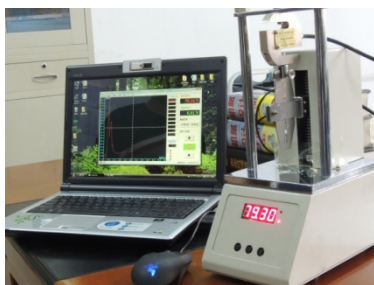


Fig. 1. Test equipment and test process of shear modulus

Click the “up” button of the measurement and control program of the computer, the activity shear frame of shear force measuring instrument was raised, which made the distance between the underneath of activity shear frame and the square hole of fixed shear-slice was more than 40mm. Urea granules, which will be measured, were fixed on shear-slice, click the “down” button, the instrument started to shear urea granules, when urea granules were shear off, the test was over. Measurement and control program of computer can record experiment data, and display curves.

2.2 Experimental Equipment

Shear modulus test equipment was mainly composed by shear force measuring instrument, data lines, measurement and control program.

Shear Force Measuring Instrument. C-LM4 computer measurement and control shear force measuring instrument was used, which was developed by northeast agricultural

university, this instrument can measure seed, fertilizer and food from 0.05 N to 250N, the measurement accuracy was $\leq \pm 1\%$, the shear speed was 5 mm / s, the voltage was 220V, frequency was 50Hz, the input power of electric machine was 20W.

Measurement and Control Program. Measurement and control program has operation control, test curve display, peak force maintain, test data management and other functions. The display window of test curve shows the time - shear force curve, which can display multiple samples test curve simultaneously, and has coordinate zoom function. Sampling rate of the measurement and control program is 100 test points / s, sampling interval is 0.01 s, and recorded data are stored into computer with Excel file format.

2.3 Experimental Materials

Experimental material is urea granules, which has bigger structure size. Circular urea fertilizer was grounded into cube by file and sandpaper, the length of cube was 2mm, 2.5mm, 3mm, 3.5mm, 4mm and 4.5mm, which were taken as test samples, the test temperature was 22°C, ambient humidity was 45%, the density of urea particle was $1.33 \times 10^3 \text{kg/m}^3$.

2.4 Experimental Methods

Experimental method of shear modulus of urea was direct shear, the obtained data were the changing curves of the time and shear force by shear force measuring instrument, the line segment of linear elastic deformation was identified on the time - shear force curve [10-11], according to equation (1), shear modulus G was obtained as follow:

$$G = \frac{\tau}{\gamma} = \frac{\Delta Q/A}{v \cdot \Delta t/d} = \frac{d}{vA} \cdot \frac{\Delta Q}{\Delta t} = \frac{kd}{vA} \quad (1)$$

Where ΔQ is the increment of shear force when urea granules linear elastic deformation, unit: N; A is the area of shear surface of urea granules, unit: mm^2 ; Δt is the increment of time when urea granules linear elastic deformation, unit: s; v is the moving velocity of activity shear frame, unit: mm/s; $v \cdot \Delta t$ is the increment of displacement when urea granules linear elastic deformation, unit: mm; d is the size of urea granules sample, unit: mm; k is the ratio of the shear force increment and the time increment when urea granules linear elastic deformation, namely the slope of the linear elastic deformation on the time - shear force curve.

3 Results and Analysis

Different size of urea granules were selected to make shear test, the shear modulus of urea granules were measured, but due to the limited length of paper, only urea granules with side length 3.5mm and 3mm were analyzed in this paper. Three urea granules with side length 3.5mm were selected to do shear test, the test curves were obtained by measurement and control program, as shown in figure 2.

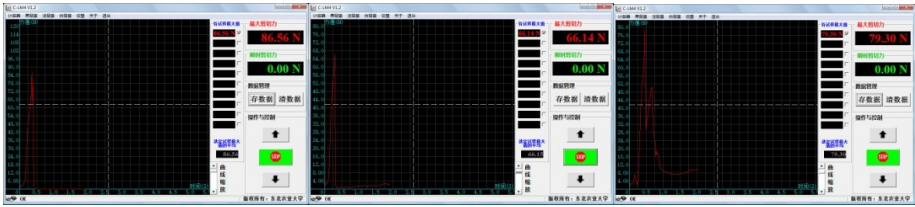


Fig. 2. The course of shear force - time of urea granules with side length 3.5mm

Three urea granules with side length 3mm were selected to do shear test, the test curves were obtained by measurement and control program, as shown in figure 3.

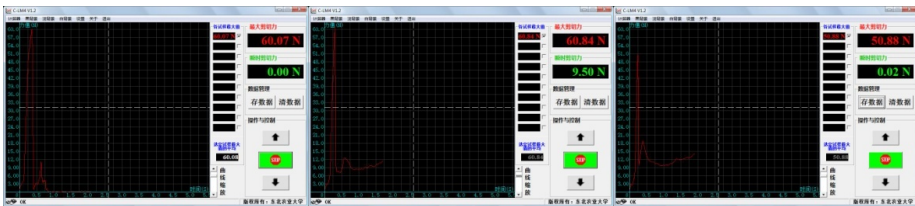


Fig. 3. The course of shear force - time of urea granules with side length 3mm

As shown in figure 2 and figures 3, With the moving of activity shear frame of shear force measuring instrument, firstly shear force increased rapidly, and reached a maximum, and then reduced rapidly, which had the same curve changing rule with the existing shear physical test. When activity shear frame contacted with urea granules, activity shear frame and fixed shear-slice surface had compression force to urea granules, but the action force between them was small, stress distribution of urea granules was uniform. With the moving of activity shear frame, sheared part formed shear zone with longitudinal width about 1mm, the extrusion force of activity shear frame to urea granules was enhanced, which made urea molecules in central part of the shear zone lost link, and appeared crack, shear force continued to increase, the peak of shear force appeared, and then decreased rapidly. With the increase of movement amount of activity shear frame, shear force of activity shear frame to urea granules further strengthened, shear zone was further squeezed, parts of granules, which lost connection force, rolled along the shear direction, and contacted with surrounding granules to form compression and friction resistance, shear force increased again. Finally, under the action of activity shear frame, the rest urea granules were further cracked to overcome frictional force between urea granules, which made urea granules between activity shear frames and fixed shear-slice staggered, shear force decreased to zero, urea granules were sheared off.

The obtained test data from the measurement and control program were fitted by Excel software, the curves of test points – shear force were obtained. The curve of test points – shear force of urea granules with side length 3.5mm was obtained, as shown in figure 4, The curve of test points – shear force of urea granules with side length 3mm was obtained, as shown in figure 5.

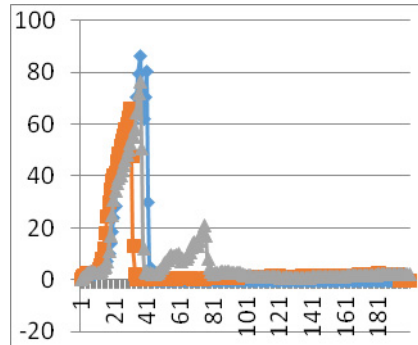


Fig. 4. Changing curves of test points – shear force of urea granules with side length 3.5mm

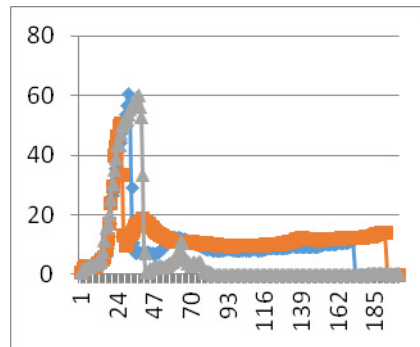


Fig. 5. Changing curves of test points – shear force of urea granules with side length 3mm

In figure 4 and figure 5, the horizontal axis indicated test points, there were 200 test points, the vertical axis indicated shear force. As the measurement and control program recorded a test point data every 0.01s, while the moving speed of activity shear frame of the shear force measuring instrument was 0.5mm / s, so the horizontal axis can be converted into time, and also can be converted into displacement.

As shown in figure 5, the changing rule of the curve of test points - shear force was very similar to figure 4, but different shear force peaks. In order to obtain the shear modulus of urea granules, a straight line should be identified on the test points - shear force curve before the first peak appeared. As shown in equation (1), the slope of this straight line can reflect the shear modulus of urea granules. Test points from 0 to 20 can't be selected as straight-line segment, because generally instrument exist error in the measurement range of 10% or urea granules specimen was not standard.

In order to find a segment of straight line on the test points - shear force curve, the experimental data of shear force, which present linear changing rule, were obtained from 6 groups test results of urea granules with side length of 3.5mm and 3mm by the measurement and control program, the test data were analyzed by Design-Expert6.0.1 software.

Taking shear force as performance index, test time as factor, 25-30 data of test points of shear force were selected to fit curve, the function relationship between shear force and time was obtained, test data are shown in table 1.

Table 1. Test data of shear force

test points	time/s	shear force/N					
		3.5×3.5/mm ²			3×3/mm ²		
		1	2	3	1	2	3
25	0.115	40.2504	40.3289	39.4166	32.8009	29.9266	33.3914
26	0.12	43.0561	41.6140	40.6919	33.5293	31.5293	36.3552
27	0.125	46.1462	45.7735	42.5950	35.9144	35.8581	39.0242
28	0.13	49.4620	49.1187	44.5570	39.1125	39.0168	41.4485
29	0.135	51.8066	51.6889	46.4307	41.6435	39.3326	42.4581
30	0.14	53.2094	54.0727	48.3339	44.4099	41.7269	44.2253

The fitting regression curve of the influence of the test time to shear force was obtained for urea granules with side length 3.5mm by Design-Expert 6.0.1 software, as shown in figure 6.

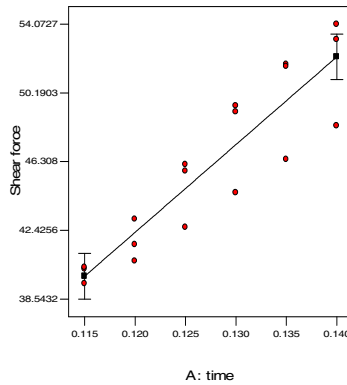


Fig. 6. The fitting regression curve of the influence of the test time to shear force for urea granules with side length 3.5mm

Variance analysis showed that model was significant, the time *t* was a valid model items. The obtained regression equations is shown as follow:

$$Q=496.03t-17.21 \tag{2}$$

The slope of curve was 496.03 in equation (2), which was substituted into equation (1), the value of shear modulus *G* was obtained, which was 2.83×10^7 Pa.

The fitting regression curve of the influence of the test time to shear force was obtained for urea granules with side length 3mm by Design-Expert 6.0.1 software, as shown in figure 7.

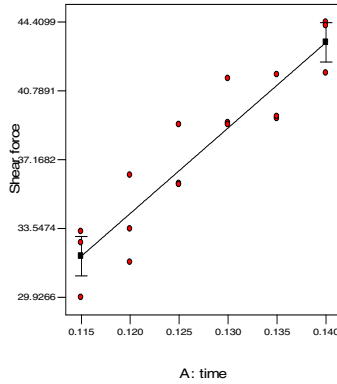


Fig. 7. The fitting regression curve of the influence of the test time to shear force for urea granules with side length 3mm

Variance analysis showed that model was significant, the time t was a valid model items. The obtained regression equations is shown as follow

$$Q=450.09t-19.67 \tag{3}$$

The slope of curve was 450.09 in equation (3), which was substituted into equation (1), the value of shear modulus G was obtained, which is 3×10^7 Pa. Urea granules with side length 2-4.5mm were selected to do experiment, the obtained values range of the shear modulus G is 2.3×10^7 Pa - 3×10^7 Pa.

4 Conclusions

(1) Urea granules was sheared off by C-LM4 computer measurement and control shear force measuring instrument, which was developed by northeast agricultural university, test data were obtained and test curves were displayed by measurement and control program of equipment. The obtained test curves show that: the compression between shear frame and urea granules makes the binding strength between urea molecules reduce, the peak of shear force emerge, then decline rapidly; as the rolling granules and surrounding granules formed compression and frictional shear force in contact surface along the shear direction, shear force emerges rise again.

(2) The obtained test data from the measurement and control program were fitted by Excel software, the test points – shear force curves were obtained. The regression equation of urea granules in the elastic deformation was fitted by Design-Expert software, the shear modulus of urea granules with side length 3.5mm and 3mm are respectively 2.83×10^7 Pa and 3×10^7 Pa.

(3) At the test temperature 22°C , ambient humidity 45%, the density of urea particle $1.33 \times 10^3 \text{kg/m}^3$, the values range of shear modulus of urea granules was measured by shear force measuring instrument, which is from 2.3×10^7 Pa to 3×10^7 Pa.

Acknowledgment. This research was supported by National Natural Science Foundation of China (51205056), Youth Science Foundation of Heilongjiang Province (QC2011C007), Special Funds of Science and Technology Innovative Talents of Harbin (2012RFQXN004), Postdoctoral Fund Project of Heilongjiang Province (LBH-Z11222).

References

1. Li, Q., Jiang, X., Dai, H., et al.: Study on Properties of PVA Plasticized Urea /Formamide. *China Plastics Industry* 40(2), 24–26 (2012)
2. Cheng, Z., Yu, Z., Sun, X., et al.: Performance Analysis and Comparison for Radial with Axial Flow Urea Reactors. *Chemical Fertilizer Design* 49(6), 36–39 (2011)
3. Ding, J., Jin, X., Guo, Y., et al.: Study on 3-D Numerical Simulation for Soil Cutting with Large Deformation. *Transactions of the Chinese Society for Agricultural Machinery* 38(4), 118–121 (2007)
4. Ding, Y., Zhang, X., Wang, S.: Preparation and Properties of Porous Bioceramics Made of Bovine Bone. *China Ceramics* 45(11), 28–31 (2009)
5. Yu, H.: Synthesis and Properties of Carbon Microtubes. Harbin Institute of Technology (2011)
6. Blunden, B.G., McLachlan, C.B., Kirby, J.M.: A High-Speed Shear Box Machine. *Journal of Agricultural Engineering Research* 56(1), 81–87 (1993)
7. Wheeler, P.N., Godwin, R.J.: Soil Dynamics of Single and Multiple Tines at Speeds Up to 20 km/h. *Journal of Agricultural Engineering Research* 63(3), 243–250 (1996)
8. Onwualu, A.P., Watts, K.C.: Draught and Vertical Forces Obtained from Dynamic Soil Cutting by Plane Tillage Tools. *Soil & Tillage Research* 48(4), 239–253 (1998)
9. Mootaz, A.-E., Hamilton, R., et al.: 3D Dynamic Analysis of Soil-Tool Interaction Using the Finite Element Method. *Journal of Terramechanics* 40(1), 51–62 (2003)
10. Karmakar, S., Ashrafizadeh, S.R., Kushwaha, R.L.: Experimental Validation of Computational Fluid Dynamics Modeling for Narrow Tillage Tool Draft. *Journal of Terramechanics* 46(5), 277–283 (2009)
11. Yang, W., Cai, G., Yang, J.: Dynamics Simulation of Direct Shear Test. *Transactions of the Chinese Society for Agricultural Machinery* 42(7), 96–101 (2011)

Analysis and Evaluation the Websites of Agridata Base on Link Analysis

Wang Jian and Wu Ding-feng

Agricultural Information Institute of CAAS, Beijing 100081, China
{wangjian02,wudingfeng}@caas.cn

Abstract. Through data collection tools, the Pagerank, inlink and the total number of retrieved pages of Agridata are computed. By considering website traffic as the flag of network influence levels, the paper analyze correlations between website traffic and Pagerank, inlink and the number of retrieved pages. Finally, the feasibility to regard the web link analysis as a factor to measure network influence of agricultural websites is discussed.

Keywords: Inlink, Pagerank, Link analysis, Agridata.

1 Background of the Research

With the information technology sweeping the globe, agricultural information has been attached great importance to government around the world and the level of agricultural information has become one of the key factors that have passed the agricultural sector competitiveness. As the main symbol of the agricultural basis of the information and level of development, agricultural sites not only are a window of agricultural information, but also become the main channel of agricultural research service for the agriculture-rural areas-farmers. Actually, agricultural sites have also become one of major route for traditional agriculture to modern agriculture.

In recent years, Chinese government attaches great importance to the construction of agricultural websites, which makes agricultural information website in China has made rapid development. According to the Ministry of Agriculture Information Center in China, the number of China's agricultural information site is increased from 2200 to 29738. In addition, among the first eight months of 2009, agricultural information sites' number is increasing 8183, which the growth rate is 38 percent, far higher than the average growth rate of Internet sites. However, although the current agricultural information website in China developing rapidly, it is worth noting that there are still many defects, the most prominent of which is the site of construction quality and service levels are not high. Actually, many agricultural sites are focus on building and light management, which results in low traffic of sites and constrains the long-term development of sites. Therefore, the establishment of a scientific and rational agricultural site evaluation system is important for promoting the agricultural site standardize operations and long-term development, which is also one of the focuses of the research areas of agricultural information.

The agricultural scientific data center (Agridata) is one of the experimental data centers supported by National Facilities and Information (NFII) of Ministry of Science and Technology. Based on agricultural scientific data sharing Standard, Agridata Integrated 12 types of agricultural scientific data which included crop science, animal science & veterinary medicine, agricultural resource and environment, grassland science, food science and standards, etc. these data resources could support the agricultural technology innovation and management decision greatly. The website group of Agridata has eight sub-sites, which is shown in table 1. Up to 2009, Agridata Formed a stable user group including more than 150 group users and 8,000 individual registered users. The total visit count of Agridata was 1.8 million. It showed that Agridata was an important information source of network users in rural areas.

Table 1. Sites in the website group of Agridata

Name of websites	URL
The main Center	http://www.agridata.cn
Crop sub-center	http://crop.agridata.cn/
Animal sub-center	http://animal.agridata.cn/
Tropical crops sub-centers	http://trop.agridata.cn/
Fisheries and aquatic sub-centers	http://fishery.agridata.cn/
Grass sub-center	http://grassland.agridata.cn/
Zoning sub-center	http://region.agridata.cn/
Agricultural scientific and technological sub-center	http://stb.agridata.cn/

In this passage, a set of evaluation system is proposed for agricultural information website based on the method of link analysis, which make the website group of Agridata as study object. On the other hand, the way of the log analysis is used for verifying the science and rationality of the evaluation system. Thus it will provide a reference for evaluation system of agricultural sites.

2 Indicators of Link Analysis

From the general sense, Link relationship among sites in Internet is very similar to citation relations between traditional literatures. This means that links in the sites like citations in publications can be used as quantitative indicators to measure the relative quality of the site. This method using link analysis can improve existing technologies of information science for evaluating websites. Therefore using link different among the number, distribution, aging and functions can be more accurate estimate websites' characters, the amount of information and information organization. Eventually a more scientific and reliable site evaluation results will be obtained.

In general, indicators of website evaluation include reverse links, outbound links, link, link density, the network impact factor, and so on. In these indicators, "reverse link" is also called inlink which is means that when there is a link in page A to page B,

the page A can be view as reverse link for Page B. in this way, during the process of website evaluation, we can make the following assumptions on the link analysis: page A supports page B if page A has reverse link for page B. Thus, the reverse link is an important symbol for the influence and information carried by a website. The greater of the number of reverse links for a website, the higher attention and utilization degree for the resources of the site's information are made, which can prove that the website has the better the quality.

PageRank that is developed from principle of link analysis is an indicator for measuring the importance of websites used by Google. The level of PageRank covers from 0 to 10. The higher PR value of a website, the more attention for the site is made. From the essence of algorithm, PageRank is based on the principle of the democratic nature of the network and reverse links which means that the value of a page is represented by link structure. In other word, a link is viewed as a vote, when page A has a link to page B, we can conclude that the page A voted for page B.

Of course, PageRank is not solely consider the number of voting, but also to analyze the voting website, which means that a vote for a page made by an important website will be strengthen its significance. Since PageRank is a quantifiable number, the quality of the theme site can be evaluated by calculating the average PageRank for all the pages of the website.

When using the method of link analysis evaluating agricultural sites such as Agridata, targets of the method must be based on the characteristics and main problem of agricultural sites. In this passage, we collect google search results, the reverse link and PageRank values for 8 websites of Agridata to evaluate the quality of Agridata website group. Through the result gotten above and consequent from network access log analysis, the relationship between the site score and site traffic patterns and trends will be found for further research.

3 Evaluation the Websites of Agridata Base on Link Analysis

3.1 Problem Proposing

The purpose of this passage is to find the trend or pattern of the relationship between PageRank, reverse link and site visits. On the other hand, whether the method using PageRank and reverse link can assess the influence of agricultural site and then analyzing the influencing factors traffic and the overall evaluation of websites is also the aim of this passage.

3.2 Research Methods

When using link analysis methods for site evaluation, data can be collected by Internet measurement and data mining. In general sense, these two methods for data collection may be used with some tools which include gathering, processing and statistics during the process of link analysis.

In the actual process, the Google search engine and Google toolbar will be used for data collection tools which gather the number of Google engine search results, value of PageRank and the number of reverse link for 8 sub-centers' homepage of Agridata. The specific collection strategy is as follows: for example, when collection data for the main center of Agridata, we get information such as the number of Google search results, the time consuming of search and so on through the result page as inputting "www.agridata.cn", the URL of the main center of Agridata in Google search engine. At the same time, when inputting "inlink www.agridata.cn", we can get the value of reverse link for the main center of Agridata. Furthermore, we can obtain the value of PageRank for main center using the function of Google Toolbar while opening the page which URL is "www.agridata.cn" by the browser with Google Toolbar. On the other hand, as the search engine uses regular collection and updating for maintenance, statistics in different stages of Google will be changed which leads to the value of PageRank and reverse links can be less than actual values. This condition will affect results of site evaluation and data analysis. So while data acquainting, we collect the appropriate data repeatedly in the period of time (three days) and choose maximum values as samples for site evaluation criteria and data analysis.

On the other side, we can use the website access log as reference for site evaluation system. These log files will be obtain from the sever of website and their format is W3C(W3C Extended Log File Format). At first, the data of access log is stored in a text format and then is converted to other format such as SAV format (the format file for SPASS) for the convenience of data processing.

During the process of the site evaluation, in this passage, the rate of a website is according to PageRank value of the website, which means that if a site's PageRank value is higher than the other, then we regards that its rate is higher. When some sites have the same PageRank, their rates is according to the number of reverse link or search results in Google. The site with higher number of reverse link or search results in Google has higher score.

In the area of data analysis, we apply the software of Weblog Expert to process web log files and use Eviews software as data analysis tools for finding the relationship between traffic and score of a web.

3.3 Result of Data Analysis

According to the above method, the experiment was collected all kind of data of Agridata website group from 7 to 9 March 2012. With these data, we scored for 8 sites of Agridata website group using the methods described above. Results of this experiment are shown in table 2.

Using the software of WebLog and Eviews to analyze the relationship between score results and site traffic, we can find that the site's ranking has reflected the level of site traffic in a certain extent. In other word, it has a high linear correlation between the

site's ranking and site traffic through regression analysis with Eviews. As shown in figure 1, Location of the point is mostly close to the line, which means that the score for a web using the method based on reverse link mentioned in this passage reflects the level of the site traffic and thereby embodies popularity of the site.

Table 2. Network data and site evaluation

Ranking	Name of website	Page Rank	Reverse link	Number of search results
1	The main Center	5	6220	59,700
2	Crop sub-center	5	139	34,400
3	Zoning sub-center	5	93	41,000
4	Animal sub-center	4	1190	11,900
5	Fisheries and aquatic sub-centers	4	165	29,600
6	Tropical crops sub-centers	3	295	20,500
7	Grass sub-center	3	85	15,000
8	Agricultural scientific and technological sub-center	3	35	13,200

With bivariate correlation to analysis the relation the sites ranking which is gotten by the method based on Reverse link and PageRank and site traffic, we can find that pearson correlation coefficient R^2 between these two values is 0.683, correlation close to 0.7, while the explanatory power of the score value on site traffic to 0.596 which shows that there are large correlation between the site score and site traffic. Thus, we can conclude that site score can largely reflected the level of site traffic and has as a high statistical significance. It can be used as indicators to measure site traffic or influence.

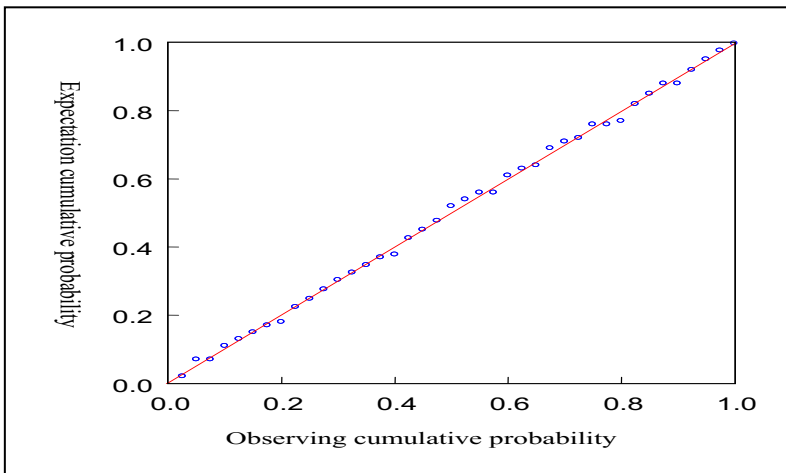


Fig. 1. Distribution map of normal regression

4 Consideration and Enlightenment for Promoting the Site of Agridata Construction

The evaluation method for Agricultural sites based on link analysis is able to correctly reflect the site's traffic, and thus reflects the influence level of the agricultural site. According the evaluation result for Agridata website group and log analysis combining with development requirements of Agridata website, we think that there are several aspects for promoting the site of Agridata construction.

(1) The member of Agridata website group should strengthen the work of maintaining its content to improve the quality of content. When they lined to each other, the link method should be standardize and link points could be clear, which might increase website reverse the number of links, improve the PageRank value and enhance impact factor of websites in a certain extent. At the same time the influence of Agridata is promoted.

(2) Agricultural data resources Agridata provided should be standardized. It means that Agridata website group should provide professional, personalized information services to meet the the data needs of agricultural scientists producers and manager. On the other side, the web group of Agridata can integrate the system of business, optimize column content and rational plan and organize data resources of Agridata to enhance sites functions. Through this way, website application system of resources standardization, section vivid, sever personalized is built for upgrading the overall image of Agridata.

(3) Agridata must allocate the professional category within group members and optimize the organizational structure of the individual site according professional characteristics. Through these methods, the reciprocity between the sites will be enhanced and internal link frequency of sites in the website group is promoted. So the core member of the group which has a top-ranking will play the leading role to increase network influence of Agridata.

5 Conclusion

Link analysis can be detailed and comprehensive analysis of resource utilization, special characteristics, influence and the degree of openness of the agricultural site. With this method coordinating with manual score, we can get more comprehensive results which the objectivity and effectiveness will be increased. These results can be used to assess influence and research productivity of the site. On the other hand, the link analysis used in the agricultural site evaluation is still in the initial stage and this method has not fixed pattern and means. Since the influence and resource utilization of the website depends not only on the site's traffic, but also by many other factors, thus the study for the evaluation method for agricultural websites based on link analysis is only an exploratory stage. This means that method is only an auxiliary evaluation methods and its result of the method is an indicator that partly reflects the site influence. We will carry further research and exploration for building comprehensive and deep system for website evaluation.

References

1. Du, J., Li, D., Li, H.: The study on the system of China's agricultural information website evaluation. *Acta Agriculturae Jiangxi* 23(3), 191–193 (2010)
2. Zhou, T., Chen, X.: The evaluation method for website based on link analysis. *Journal of Guangxi College of Education* 96(4), 138–141 (2008)
3. An, X., Lv, N.: Research on University Academic Level Based on Web Link Analysis. *Journal of Medical Informatics* 30(10), 38–41 (2009)
4. Yi, W., Zhu, W.: A Synthetic Approach to E-government Website Evaluation Based on Web Log. *Information Science* 25(10), 1495–1499 (2007)
5. Zhang, Y., Leng, F.: S&T Websites Influence Evaluation Based on Social Network Analysis. *Library and Information Service* (12), 56–60 (2011)
6. Fang, H., Sun, J.: Study on Website Evaluation based on Link Analysis: A Case Study of the Four Portal. *Journal of Intelligence* 30(1), 74–76 (2011)
7. Lili, S.: Study and Application of Hyperlink Analysis Method in Website Evaluation. *Journal of Library and Information Sciences in Agriculture* 21(6), 15–18 (2009)
8. Juping, Q.: Study on HyperLink Analysis and Website Evaluation. Wuhan University, WuHan (2004)
9. Li, J.: Analysis on the Defects of Link Indicators Applied to Web Site Evaluation. *Library Journal* 27(5), 40–44 (2008)
10. Maryellen, M.: Six degrees of affiliation: the small world of search tools. *Online* 24(5), 49–51 (2000)

Discussion on Fruiter Professional Information Service Mode of Shandong Province

Wang Zhi-jun^{1,2,*}, Jiang Meng², and Cheng Shu-han^{2,**}

¹ College of Horticulture Science and Engineering, Shandong Agricultural University,
Taian 271018 China

² College of Information Science and Engineering, Shandong Agricultural University,
Taian 271018 China

{wzj, shcheng}@sdau.edu.cn, jiangmengbz@163.com

Abstract. In order to grasp the real status of rural agricultural information services, relying on Fruiter Professional Information Service Mode of Shandong Province, professional information data collection and integration, information service mode, the construction of base and information site, building of expert team and training system are discussed in this paper. The research results have theoretical significance and practical value on the construction of rural informatization demonstration province. It will promote the country to explore the experience of rural agricultural information and patterns.

Keywords: professional information, service mode, agricultural informatization.

Shandong province is famous for its apple. The planting area is more than 5 million mu and the production is more than 7.988 million tons[1], accounted for 19.4% and 26.2% of the total respectively. The production stands first in China. But the production of apple in Shandong province is at the stage of decentralized management based on farmers whose comprehensive quality is not high. Therefore the information level of apple industrial technology is kept at a low level and the scale of apple processing enterprises other than concentration juice production is limited. Compared with standardized production, Standardization of processing and information management, there is still a long way to go. It's necessary to construct fruiter professional information service system, lengthen the Apple industrial chain in order to breaking through the Production bottleneck, innovating techniques of cultivation management and improving the fruit quality of apple.

In this paper, a bridge is built among farmers, production and marketing enterprises, buying and selling fruit and processing units, government authorities and scientific and technical personnel to provide integrated service for apple production, management and decision-making. It helps employees adapt to the complex and fast-changing market discipline, improve their scientific management and decision-making level in preproduction, production and post-production. It can also promote specialization,

* The main interesting research topics are computer networks and agriculture informationization.

** Corresponding author.

standardization and informatization of the apple industry and achieve the goals of increasing farmers' income, enhancing benefits of enterprises and promoting the new rural construction.

1 Professional Information Data Collection and Integration

1.1 Data Collection

(1) Achieving the information of orchard through the sensor network

We set up all kinds of sensors in orchard. According to different needs we can choose different data collection methods, such as real-time information collection, manual information collection and timing information collection. In order to provide basis to apple precision management decision-making consultation systems such as apple disease-carrying insect harms management decision-making consultation system precisely, the tree structure evaluation and regulation decision support system, orchard ecological environment dynamic assessment system meteorological information, growth dynamic information, plant diseases and insect pests occurrence information, and soil nutrient and water stress information will also be gathered timely and automatically from various sources of information.

(2) Through the science and technology literature query system

With the help of domestic and foreign large-scale agricultural science and technology literature database introduced by Shandong Agricultural University and other colleges and universities, such as Wanfang Data Service Platform, Zhonghong Database, PQDT, Tsinghua Tongfang Chinese periodical database and CABI Database, we can provide updated knowledge domain for agricultural management and agricultural science and technology personnel.

(3) Obtaining information timely through intelligent search engine

Developing stronger intelligent search engine, searching information resources on the internet timely and loading into the local database, we will complete to update information in time.

1.2 Data Integration

During the application of the developed program, we could select, review, edit and transport the collected information automatically to the content management module through the data provider, and finally realize the automatic storage operation of the data collection.

Considering the variability of the information selected—it covered diversified messages such as information on agricultural production, agricultural research, business management, cultural life, vocational education and so on, and it also included multiple media types like the text, audio, video, images, animation, ppt, etc—we unified the scientificity, popularity, consistency and timeliness of the integrated resources to make it flexible and accessible for the farmers, fulfilling the actual demand

of them[2]. In the functional design, simple, cross-database information retrieval make it easy for farmers to quickly and easily find relative information of all kinds to solve the practical problems. Navigation systems, decision support and other functions can effectively help increase the production of a farmer, corresponding with the farmer's cognition and habit.

2 Diversified Services

In the production of rural information service in the past, we mainly use the traditional media during the information transmission as the supporting platform, aided by the telecommunications network and the CATV network. But in the new service model, we are applying the triple play as an important supporting platform, taking apple professional information service system of the Shandong province as the basis, carrying out the integrated and professional services for the apple industry, providing technical support for the different types of the existing grassroots information services organization, extending their platform to the top of the industry chain, their services to the end of the industry chain. Professional information service apple supplied contains the following services:

2.1 Information Dissemination Online

According to data of The Statistics Report Of China Internet Development [3], until the end of December 2012, the scale of China's Internet users reached 564 million, Internet penetration rate reached 42.1%, rural population reached 156 million, accounted for 27.6% of the China's Internet users, making an increase of approximately 1960 people than the number by the end of the last year. Apple's professional information service platform of Shandong Province makes full use of the Internet platform for all types of users and published a variety of preproduction, production and post-production information for the whole industry chain. Fig.1.

2.2 12396 Service Hotline of the Spark Science and Technology

12396 is the public service number promoted by the Ministry of Science and Technology and the Ministry of Industry to the unify of the country's rural science and technology information. It's a platform aims to provide farmers hotline counseling, interactive messaging, remote video and technical training services. Shandong Province is one of the nation's first rural information pilot provinces, and had officially opened 12396 service hotline on December 25, 2008. At present, it has built a provincial information service center as the core, setting Ji'nan, Tai'an, Yantai 11 municipal information service center as the backbone, making 285 basic information service station as the main body, establishing a massively interacting, convenient and efficient 12396 Grass-roots Service system of the spark science and Technology.

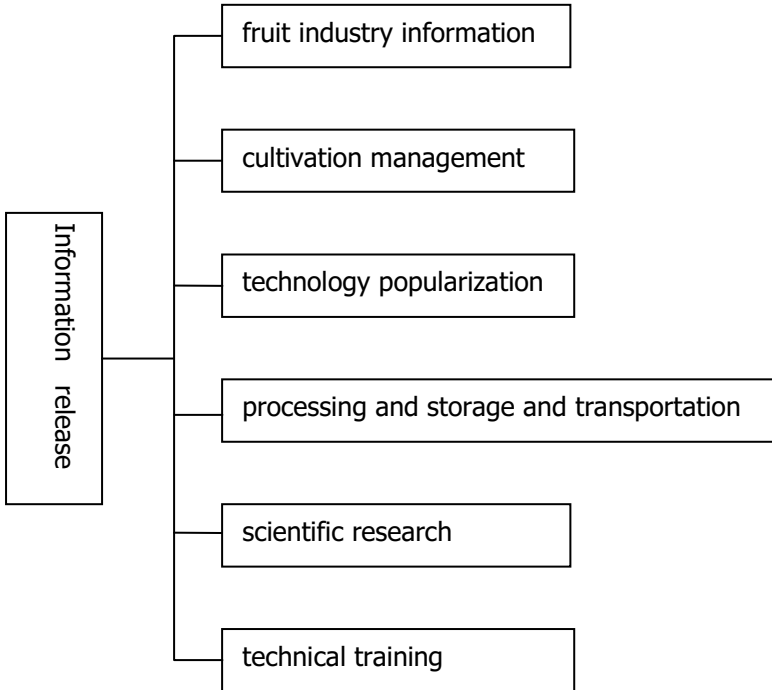


Fig. 1. Information delivery of Industry chain

At present, 12396 call platform is located in the provincial information service center. You can enjoy the automated voice, artificial agents, and three-way calling and other services[4-5], and effective docking with the rural Shandong Radio channels live broadcasts.12396 has become Radio telephone expert image and has turn to 1 to more service from the 1 to 1 service, and effectively expanded the scope of services and the influence of the platform.

2.3 Video System

According to the demand of farmers, we can install video system client in the information service stations, open the remote video system, and organize experts to teach. Also we can provide apple production technology, technical guidance, pest diagnosis of fruit tree, technical training, live video technology, expert lectures and other services online. [6]In order to avoid the high cost, low efficiency and so on by looking for experts solving problem and accepting technical guidance, we provide video&audio bidirectional answer, network interaction and remote dialogue with them. When communicating with them, specialists could provide the farmers timely and accurate production safety measures and timely technical service, give a guide to the farmers on the scientific management. We could also employ various experts regularly,

in an irregular or special way to do speeches, online teaching. The mode that direct dialogue between experts and farmers is established to enhance the pertinence and effectiveness of the farmers' work.

2.4 Short Message Service

SMS platform developed by Fruiter Professional Information Service platform of Shandong province send the farmers information about cultivation management, technology popularization, policy, market, science and technology, agricultural materials, weather, and product [7]. The information are divided into two categories: public good and value-added services. Some content can be sent to customers free of charge via a push such as government announcements, popularization of policy, agriculture news, outbreak epidemic, severe weather warning, market conditions, agricultural science and technology, rich information, labor supply and demand, health control, etc. Others can be sent by charging such as market analysis, professional and technical guidance, exporting statistical information. This kind of SMS platform not only widens the channel of the circulation of the rural information, close communication and interaction between the government and farmers but also motivates the farmers to learn information technology and promote the countryside informatization construction. Satisfying the personalized needs of farmers, growers can gain information anytime and anywhere, enjoy the fast, accurate, economical information service.

2.5 Expert System

Agricultural expert system summarizes and collects knowledge and technology in the field of agriculture, large amount of valuable experience of agriculture accumulated by agricultural experts, various information and data and mathematical model obtained from the experiments by using artificial intelligence, knowledge engineering knowledge representation, reasoning, knowledge acquisition technology. Based on the above, a variety of agricultural "computer expert" computer software system with intelligent analysis and reasoning, independent knowledge base which is very convenient to increase and modify the knowledge was established. Development tools have explanation function and make users do not have to understand the computer programming language. Usual computer program systems cannot come up to it.

At present, the developed expert systems based on apple's professional information service have apple precision management expert system, prevention and control of plant diseases and insect pests' expert system and nutrition diagnosis and recommended fertilization expert system. These systems provide users with decision-making and analysis of the predictive information that have processed and individualized information service and knowledge service. These also provide strong support for the auxiliary production, improving production efficiency, cultivating new type farmers and guiding the agriculture industrial structure adjustment.

2.6 Internet Protocol Television Service

IPTV, Internet protocol television is a manageable multimedia business of Security, interactivity, and the reliability. It contains the Internet, multimedia, communication technologies and delivers TV, video, graphics, and data, etc [8]. IPTV is different from the traditional analog cable TV, also different from classical digital TV. Traditional and classical digital television is unidirectional broadcast , frequency-divided, timing and so on. Although classical digital television has a lot of technical innovation, its signal form is changed. But the transmission mode of media content is not changed.

In this project, the IPTV service platform is built relying on the Shandong unicom company. Farmers can browse Qilu three agriculture information and watch live television program at home using TV by receiving a dedicated set-top box.

2.7 Mobile Internet

In recent years, rural informatization construction in China has made great achievements. But effected by computer penetration rate, the network cost and other factors, the implementation of information technology in rural areas has a certain difficulty [9]. Mobile Internet device, characterized by numerous in variety, low cost and convenient access, become the main Internet terminal for rural netizens. It has provided an opportunity for the popularization of the Internet in unenlightened rural areas[10]. (The Internet development report in rural China,2011). The report shows that up to the end of December 2012, the portion of mobile Internet users is increasing, from 69.3% to 74.5%. And using mobile phones to access the Internet is becoming the main method for rural information service. By the end of 2010,the number of mobile phone users in Shandong has reached 61.9 million (Shandong statistical yearbook in 2011) and there are an average of 2.3 mobile phones in each household. The use of 3G smart phones is rapidly growing with an annual growth rate of 45%. Therefore, we developed the specialized mobile version of apple professional information service system, in order to provide convenience for apple growers to get relevant information by mobile phones.

3 Apple's Professional Information Base and Site Construction

Rural information service station is an important content and carrier of the construction and promotion of rural informatization, and it's also the main guiding force and a kind of intermediate link. Rural information service stations are in a key position in the construction of rural information.

By setting up some agricultural informatization demonstration base and choosing growers with representative, stronger driving force, higher character of culture, innovative ideas and enthusiasm as applications demonstration households, we can gradually influence and improve the Information Consciousness of surrounding farmers, expand the radiation area, and promote agricultural informatization from point to area [11].

Take different varieties, different regions, different kinds of soil and orchard, tree-age, different technology and other factors into consideration during the process of project implementation. Now we have already built base stations and pilot sites in many places, such as Qixia, Penglai, Rizhao, Mengyin, Yiyuan, Feicheng and Xintai, and received a good demonstration effect.

Through the construction of service stations, we have directly integrated the provincial rural information service platform with rural areas, and reached a flattening goal. During the construction of the sites, we ensured the quality of service by completing the management system and unifying service standards. We also kept exploring the long-term development mechanism by innovating service mode and summarizing experiences.[12]

4 The Establishment of the Expert Team

Build a professional service team including technical staffs coming from higher education institutions, scientific research institutions and different government competent departments and growers who has rich planting experiences. They should work and serve all together. The system also cooperates with the Centre for National Apple and Industry Technology Innovation Strategic for Alliance, aiming to guide industrial development and promote technological innovation. We must make full use of interactive video, interactive messaging, telephone communication, remote online messages and all other informational means to answer farmers' production problems accurately and effectively.

5 Full Equipped Training System

We need to create a training pattern mainly focus on agricultural information training, build some informationalized training bases orienting to "three dimensional rural" and also exploit distinctive training course materials concerning fruit tree planting technique and workforce training skills. We must create a database for planting technique videos, supported by fruit professional information service platform, the rural modern Remote Education System and different kinds of agricultural information sites. With the help of these videos we can provide rich video content and improve farming skills. As to the issues of common concern and new technologies and problems resulting from development of times, we will let farmers take concentrated training, or invite experts to make technical sessions, in order to answer their questions and improve service performance. Carry out training for farmers aiming at rural labor transfer employment and agricultural practical technology application and promotion. We must meet the needs of skills and information service, promote the spiritual and cultural construction in rural areas, and then help farmers to improve ideological and moral standards and also to increase their cultural knowledge and production technology. Speeding up the transformation process from traditional farmers to modern farmers, we will eventually promote the economic development in rural areas.

6 Conclusions

Information Technology is the trend of economic and social development in the world, the rapid development of information technology and full penetration of China's agricultural and rural economic development provides a new opportunity[13,14]. This study aims to build a new type of rural agricultural information service system, to establish a long-term mechanism of agricultural information service in rural area, promote the combination of technology and industrial advantages, improve the level of rural information service, promote the development of modern agriculture and urban and rural areas as a whole and to promote rural agricultural informationization to explore the experience and mode.

References

1. Statistical Yearbook of Shandong (2011)
2. Zheng, G.H.-I., et al.: Study on the Agricultural Information Service Innovation and its Practice Exploration. *Journal of Anhui Agri. Sci.* 35(36), 12128–12129 (2007)
3. Statistical report on Internet development in China
4. Wang, Z.-L., Zhang, G.-Q.: The present situation and countermeasure research of rural informatization in Shandong Province. *Anhui Science & Technology* (2012)
5. Jing, D.-D., Duan, L.-J.: Discussion on the operation mode of Agricultural Science and Technology Information Service Platform——takeing Hunan Spark Science and Technology 12396 Information Service Platform as an example. *Technological Development of Enterprise* 7, 9–11 (2010)
6. Cai, S.-H., Xu, N.: The Implementation of Quaternity Information Model of Rural Area in Hebei Province. *Journal of Hebei Agricultural Sciences* 5, 103–105 (2011)
7. Chi, X.-Q.: Discussion on mobile phone SMS platform and promotion of agricultural information in China. *Journal of Anhui. Agri. Sci.* 18, 310–313 (2006)
8. Yang, W.-N., Zhao, J.: Analysis and design of IPTV technology based on P2P network television. *Information Systems Engineering* 11, 45 (2012)
9. Xue, F., Zhang, L.-Y.: Discussion on the rural information technology brace model based on cheap mobile phone. *Science & Technology Progress and Policy* 24, 89–91 (2010)
10. Rural China Internet Development Report of 2011 (2011)
11. Zhang, J.-P.: Discusses the development pattern of China's rural agricultural information service. *China Agricultural Information* 5, 14–17 (2011)
12. Li, X.-F., Lu, W.-L.: National progress and analysis of rural informationization demonstration province construction. *China Science and Technology Achievements* 13 (2012)
13. Fang, G.-Z.: Constructing the New Mode about Agriculture Information Service of Supply and the Demand——Based on Apart Areas of Shandong. *Chinese Agricultural Science Bulletin* 28(26), 291–297 (2012)
14. Zhao, J.: Research on Agricultural Informatization in and Abroad. *Document; Information & Knowledge* 6, 82–87 (2007)

The Application of Image Retrieval Technology in the Prevention of Diseases and Pests in Fruit Trees

Wang Zhi-jun^{1,2,*}, Liu Xin², Jiang Meng², and Cheng Shu-han^{2,**}

¹ College of Horticulture Science and Engineering, Shandong Agricultural University,
Taian 271018 China

² College of Information Science and Engineering, Shandong Agricultural University,
Taian 271018 China

{wzj,shcheng}@sdau.edu.cn, liuxinmails@sina.com,

jiangmengbz@163.com

Abstract. Diseases and pests in fruit trees is a key factor influencing the quality and quantity of fruit. Image retrieval technology into diseases and pests detection is an important way to improve the fruit tree management level and the quality and quantity of the fruit. This paper reviews the content-based image retrieval technology and the application of technology in the aspect of plant diseases and insect pests and proposed pest detection methods, steps and future research directions.

Keywords: image retrieval technology, pests and diseases of fruit trees, Preventive and treatment.

1 Introduction

China is a huge producer of fruit. Total harvested area and yield as well as a variety of fruit production are the highest in the world. In the year of 2010, the fruit production of our country is 214.014 million tons[1]. Fruit industry becomes the third largest industry in planting after grain and vegetable in our country. It has already been a pillar industry of China's rural economies and an important way of promoting the employment and income for farmers. China's fruit industry has the advantage of scale but the problems of low total yield and poor quality are becoming more pronounced in which diseases and pests in fruit trees is a key factor influencing the quality and quantity of fruit. In practical production, most orchard workers make diagnosis of fruit diseases and pests by experience and feeling. Although they have obtained some results, they caused harm to the growth of fruit trees. Unable to accurately detect diseases and peats in fruit trees, fruit producers blindly apply lots of fertilizer and pesticide in order to prevent the occurrence of diseases and pests in fruit trees which is not only a waste of financial resources, material resources and manpower but also of no use. And it also affects the fruit quality and yield and destroys the ecological environment. So building an effective

* The main interesting research topics are computer networks and agriculture informationization.

** Corresponding author.

disease and pests monitoring and system, introducing image retrieval technology into diseases and pests detection and realizing digitized, intellectualized, informative and networked fruit production management is an important way to improve the fruit tree management level and the quality and quantity of the fruit.

2 Review of Image Retrieval Technology

Image Retrieval Technology originated in the 1970s. Text-based Image Retrieval (TBIR) describes image content via text messages. Text information is often called keyword comments and annotation statements and this method is actually transforming the image retrieval into corresponding text retrieval. But TBIR has shortcomings such as subjectivity in understanding images, hefty workload and inefficiency [2]. Therefore TBIR already can't satisfy the people's needs. In the 1990s, there appears Content-Based Image Retrieval, a technology that combines color, texture, shape, layout, and other characteristics of the picture and then analyses them.

2.1 Original Data-Based Query

According to Neal Krawetz[3], the key technology of Original Data-based Query is called 'Perceptual hash algorithm'. It is used to generate a 64 - bit integer for each image, called 'fingerprint' character string and then compare the different fingerprints of these images.

Determine how many bits are not the same in this 64-bit integer. In theory this is equivalent to computing the 'hamming distance'. If the number of different bits is less than 5, then we can say that these two pictures are the same but if the number is greater than 10, they are different. This comparison is very specific and it is only helpful when using relatively exact matches. It demands high levels of image and is always used to search thumbnails and similar pictures. But it is unable to distinguish transmutative images. It has obvious advantages: speed and high accuracy.

2.2 Color-Based Retrieval

Color Histogram is the most common methods of color specification [4]. The thought is color space histogram matching. It will first divide color space into several fixed subspaces and then add up the number of pixels in these subspaces of each image and in the end use the histogram to measure the similarity between images. This algorithm has advantage of simple calculation and insensitivity of translation and rotation and so on [5]. Commonly used methods of color specification also include Color Moments, Color Sets color aggregation vector and so on.

Now the method based on global color feature which is brought up by Swain and Ballard[6-7] mainly use color histogram. This method counts the statistical probability of the appearance of each color based on the color histogram. Then it uses the

intersection of the color histograms to judge the similarity of the two images. Later Pass and Zabih[8] improved the algorithm and proposed to use color aggregation vector as the index of the image. To some extent, aggregate information in the aggregation vector still retains the color space information of the image [9]. Sangoh Jeong[10] et al. came up with the idea of extracting color histogram by GMVQ. K.Konstantinidis et al [11]. Put forward a kind of connected fuzzy color histogram retrieval algorithm based on $L^*a^*b^*$ space. [12]

Image retrieval is mostly based on color histogram which has the advantages of high operation speed, low storage requirement and insensitivity of size scale and rotation changes of the image. The drawback of color histogram is that query results based on different color space retrieval systems may vary. In addition, it contains the frequency of only one color and loses the pixel's location information. Also the accuracy is not very high [2]. Therefore we usually combine other retrieval methods to retrieve plant diseases and pests of fruit trees. For instance on the basis of detecting the disease spot area, we can use color-based retrieval technology [13] to identify diseases while shape and other characteristics are almost the same.

2.3 Shape-Based Retrieval

Such methods to describe shape feature currently include two major classes: edge-based and region-based shape methods. By the former, the description mainly includes straight line description, spline curve fitting, Fourier descriptors, Gaussian parameter curve and invariant moment description. As for the later one, it mainly includes irrelevant torque of the shape, area of the region, aspect ratio of the shape, eccentricity and so on[14]. In the shape- based retrieval, edge detection research is extensively used. At present there exist many image edge extraction algorithms such as Canny operator, Robert operator, Prewitt operator, Sobel operator and wavelet operator [15]. The edge detection algorithm has the advantages of simpleness and speed. But it is a bit more demanding. The algorithm directly processes on the original image, so the detection effect is poorer when the original image is disturbed by noise. If the color mutation of the image is not particularly evident, the original edge may also be smoothed while filtering out the noise. Fourier descriptor is also too complex. Invariant moment can't guarantee the invariance while the object is greatly rotated. In real production images may be greatly influenced by the weather conditions, so the effect is not stable.

Wavelet analysis with excellent time-frequency localization characteristics is widely used in the field of image processing and pattern recognition. Wavelet-based edge detection algorithm [16] can perfectly guarantee the accuracy of the edge and overcome the quality troubles came from traditional algorithm.

Shape-based image retrieval can pre-match diseases and pests of plants in order to narrow the matching region. It can narrow the scope of diseases according to the shape of diseased area and it also can reduce the disease types though retrieving the shape of the pests. Combine with other retrieval methods, it will be more accurate.

2.4 Texture-Based Image Retrieval

Texture feature which can quantitatively describe spatial information of image to some extent refers to varying patterns composed of gray scale and color in two-dimensional space. It is image features related with the surface material. The texture analysis methods can be basically divided into four classes: statistics method, structure method, model method and space method/frequency domain analysis method. There are mainly two kinds of texture image feature descriptions. One is concurrence matrix, raised by Haralick and Shanmugam. It highlights the spatial dependencies of the texture. The other is visual characteristics method, raised by Tamura. It analyses the texture from six visual features: thickness, contrast, orientation, degree of linearity, rules and roughness. And this method mainly emphasizes visual effect [17]. Owing to the relationship between texture characteristics and surface material we can use this to retrieve the diseases. The material of the diseased area will change, which is more convenient for retrieving diseases. Likewise, it can also retrieve diseases according to the different physical features of pests.

This image retrieval has rotation invariance and stronger resistance to noise. Its disadvantages is that when the resolution of the image changes the calculated texture may be greatly biased. Besides, due to the possible affection of illumination and reflection, texture reflected from two-dimensional image is not always the real texture form 3D object surface. In diseases and pests retrieval, images may be greatly influenced by environmental factors, so the stability and accuracy is poor, but it can be used as auxiliary retrieval combined with other retrieval methods.

2.5 Content-Based Multi-feature Image Retrieval

Texture, color and shape are the most commonly used and easily extracted features in image retrieval. Extraction is not only based on one character, but based on multiple characteristics. The effect of the image retrieval system is assessed from three aspects such as precision, recall ratio and query speed. Experiments have shown that the image retrieval system based on multi-feature is superior to the image retrieval system based on single vision feature in every aspect [2]. Different representation reflects the characteristics of the media from different angle. Integrate multiple features in accordance with users' actual demand in order to improve the efficiency of image retrieval [5]. One important problem needs to be solved in multi-feature retrieval is the normalization in algorithm matches. Their expectation and variance may be quite different, so they must be normalized so that different algorithm is equal in weight [18].

The most commonly used algorithm in content-based multi-feature image retrieval is SIFT algorithm. This algorithm was put forward in 1999 by David Lowe and completed in 2004[19-20]. Multi-feature retrieval is mainly used in diseases and pests retrieval, combined with other retrieval methods, in order to improve the accuracy and speed. SIFT algorithm mainly includes five steps: scale-space maximum detection, key point positioning, direction and size determining, key point description and feature vector matching. The algorithm has the advantage of basing on multi-characteristic content and

it can accurately extract the image features and improve the image recognition and matching rate. But the process is too complex time-consuming and lack of a general optimal algorithm and the computational cost is huge.

3 The Application Status of Image Retrieval Techniques in the Prevention of Diseases and Pests

Machine vision and image processing technology have been applied in the field of agriculture and plant protection in the US and other developed countries. The application of image processing has made a certain process and development in fruit tree industry. But at home, the application of image processing technology in industry and agriculture is just beginning and still in an infancy. However, many colleges and universities began to study with image detection technique applied to agroforestry and achieved some results. But there is still a long way to go to practice. We should speed up the research process of the application of image detection technology in fruits industry in order to achieve the aim of improving production efficiency so that we can finally realize intelligentizing and automation on production and management.

In foreign countries, YutakaSasaki et al.(1999) contraposed the impact the different spectral reflectance characteristics and optical filtering have on disease, studied automatic diagnosis technology of cucumber anthracnose using genetic algorithm to identify diseases[21].

Insect identification system, studied by Dr. Jeffrey and T. Drake et al. is used for rapid identification and classification in massive samples. Image segmentation algorithm can extract single segmentation in a large number of samples and it can segment most insect samples in order to obtain better effect [22].

Huang (2007) proposed a method of detection and classification of three kinds of diseases in phalaenopsis though image analysis technology and neural network and used adaptive index transformation method to segment diseased area. Extract color and texture features and use BP neural network to classify normal and diseased plants with an accuracy of 97.2% [21].

In recent years, domestic scholars also made certain research in this field. The expert system of plant diseases and pests forecast and control technology raised by Wang Qinglei et al.(2005) has forecast and prevention function such as automatic identification of pests, assistant identification of pests, diseases and pests prevention and control strategy of plant diseases and pests[22].

Song Kai et al. (2007) applied multiple classifier of SVM to identify various diseases and a pest of corn leaves [21].

Huang Xiaoyan et al. discussed the color digital image segmentation algorithm based on mathematical morphology and proposed the method of filtration colorized digital image with morphology template which can be used in the segmentation of colorized digital images of stored-grain peats[22].

Zhang Gongtao et al. completed image matching of stored-grain pests in 2009[23].

4 Steps of Diseases and Pests Image Testing in Fruit Trees

Presently, No image retrieval method is applicable to any situation. Different use needs different analysis. Aiming at diseases and pests image testing in fruit trees, we can use the following steps to complete.

First of all, all the tree pest species should be collected as much as possible. Inviting relevant experts to classify the pests according to the structure characteristics and color characteristics of pests, such as wings, head size, shard shape, and the number of feet, color, etc. Pest characteristics are extracted and it's convenient for matching testing. Diseases also should be classified comprehensively and systematically and the feature set is planned out. Then according to the different characteristics of diseases and pests in fruit trees, Designing image processing algorithm of feature extraction which is appropriate, efficient and accurate. On this basis:

(1) Preprocessing the image. Because the weather, light and other environment have deep impact on image acquisition, using edge detection, filtering and other algorithms for image to processing in advance. Cutting the edge of the useless background part and improving image recognition rate, the detection accuracy is improved. For disease, we can use edge detection and detection method based on color to extract the shape of the disease parts in advance; for pests, we need to remove background and extract the pest images. This narrows the matching space, reduces the amount of calculation, improves the matching speed and reduces the storage space.

(2) Normalization of characteristic value. The dimensions of the various features are not the same. There is also a great difference in magnitude. Subsequent processing will have a bad influence on the performance of the system. Before using a particular algorithm, we need to normalize the raw data for eliminating the influence of magnitude and making the indicators comparable. It is convenient for subsequent processing and it can improve the calculation speed and efficiency.

(3) Feature extraction. According to the pest's classification and characteristics of the analysis, we select the appropriate algorithm and extract characteristic values. Extractions based on color, shape and combining feature can be used to find the correct method of high speed. For disease, retrieval method based on color and shape can be used. According to the characters of disease, it basically can be achieved. Compared with the pest, Disease characteristics is much simpler. Considering lookup speed, accuracy and recall ratio three factors, appropriate algorithms can be chose by Comprehensive comparison.

(4) Similarity computation, match the similar images, so match the types of diseases and pests. Appropriate calculation method can be chose according to different algorithms. Combined with database data, we can provide professional prevention measures and right guidance to the farmers.

Based on the above steps, research directions that image processing can be applied to fruit industry can be analyzed:

(1) Study new algorithm that quicker and more efficient. Not only to study the image feature extraction algorithm, must we study the image similarity matching algorithm. Dealing with the matching image fast and accurately and reducing the requirements and dependencies of the image quality.

(2) Reduce costs. Based on the function realization, we can reduce equipment costs and costs of achieving functional operation.

(3) Real time and networking. Realize perfect combination of orchard and the Internet and achieve the real-time detection of diseases and pests.

(4) Intelligence and digital. Combined with the plant diseases and pests' image detection and expert answers and diagnosis online, we can accurately distinguish diseases and pests and provide solution, prevention and control measures.

5 Conclusion

Image retrieval, of course, can't be only limited to the above methods. It is still an imperfect field now, waiting to explore in various aspects and make progress every day. Image retrieval method is also springing out endlessly, varying from situation to situation. Yet there also have lots of improvements on the existing image retrieval algorithms. The future development in fruit tree production is informatization, unification and digitization. For now, the image detection part of fruit tree management platform based on digital and information is still in an embryonic stage, the potential development and application prospect is huge. In consideration of the rapid development of the Internet and the Internet of Things, combined with the existing image detection technology match detection of diseases and pests in fruit trees can be basically realized. The present situation of low yield and poor quality can be gradually improved in our country. It is widely believed that with the continuous development of technology and the unremitting efforts of researchers' image detection on diseases and pests in fruit trees will become more mature. This will promote further development of China's fruit industry and motivate the process of digitalization, informatization and intelligentization.

References

1. Regional Economic Yearbook of China (2011)
2. Feng, G.-G., Qi, Y.-H., Xiao, Y.-B.: Review on Technology of Text-based Image Retrieval. China Academic Journal Electronic Publishing House (2007)
3. Neal Krawetz, Looks Like It
4. Jain, A.K., Vailaya, A.: Image retrieval using color and shape. *Pattern Recognition* 29(8), 1233–1244 (1997)
5. Lou, B.-F., Shao, L.-Q.: Content-Based static Image Retrieval. *Study of Library Science* 3, 84–86 (2006)
6. Swain, M.J., Ballard, D.H.: Indexing via color histograms. In: *Proc. ICCV*, pp. 390–393 (1990)
7. Swain, M.J., Ballard, D.H.: Color indexing. *IJCV* 7(1), 11–32 (1991)
8. Zabih, G.R., Miller, J.: Comparing images using color coherence vectors. In: *Proc. of ACM Intern. Conf. Multimedia*, Boston, MA (1996)
9. Wei, L.-M.: Review on Technology of Text-based Image Retrieval (2012)

10. Jeong, S., Won, C.S., Gray, R.M.: Image retrieval using color histograms generated by Gauss mixture vector quantization. *Computer Vision and Image Understanding* 94(1/3), 44–66 (2004)
11. Konstantinidis, K., Gasteratos, A., Andreadis, I.: Image retrieval based on
12. Zhang, S.-L., Ren, S.-P., Wang, X.-F.: Research status and development trend of Content-based image retrieval technology (2007)
13. Shi, B.-X., Zhang, M.-X., Qiao, X.-N., Hao, R.-Z.: Retrieval Technique of Image Based on Color Features. *Microelectronics & Computer* (4), 164–167 (2010)
14. Liu, Q.-Y.: Retrieval Technique of Image Based on shape features. *Journal of Information* 4 (2004)
15. Gu, J., Xie, J.: A Fast Image Matching Retrieval Method Using Sobel. Operator. *Computer Programming Skills and Maintenance* (2010)
16. Dong, W.-J., Zhou, M.-Q., Li, X., Geng, G.-H.: Research of the Edge Detection Technique Based on Wavelet Analysis. *Computer Engineering and Applications* (2004)
17. Sun, J.-D., Cui, J.-T., Wu, X.-S., Zhou, L.-H.: Color Image Retrieval Based on Color and Shape Features. *Journal of Image and Graphics* (2004)
18. Deng, C.-Q., Feng, G.: Content-based Image Retrieval Using Combination Features. *Computer Applications* 7 (2003)
19. Lowe, D.G.: Object Recognition from Local Scale-Invariant Features (1999)
20. Lowe, D.G.: Distinctive Image Features from Scale-Invariant Keypoints (2004)
21. Li, Z.-R.: Reserach On Identify Technologies Of Apple's Disease Based on Image Analysis. Northwest A & F University (2010)
22. Cai, Q.: Reserach of Vegetable Leaf-Eating Pests Based on Image Analysis. Northwest A & F University (2010)
23. Zhang, H., Mao, H., Qiu, D.: Feature extraction for the stored-grain insect detection system based on imagerecognition technology. *Transactions of the CSAE* 2, 134–138 (2009)

Advances in the Application of Image Processing Fruit Grading

Chengjun Fang and Chunjian Hua

Institute of Mechanical Engineering, Jiangnan University, Wuxi 214122, China
{525890065, 277795559}@qq.com

Abstract. In the perspective of actual production, the paper presents the advances in the application of image processing fruit grading from several aspects, such as processing precision and processing speed of image processing technology. Furthermore, the different algorithms about detecting size, shape, color and defects are combined effectively to reduce the complexity of each algorithm and achieve a balance between the processing precision and processing speed are keys to automatic apple grading.

Keywords: Image-processing, Computer-vision, Fruit Grading.

1 Introduction

In the recent decade, most of the worldwide apple products are made in China. China produced 3598 million tons of apples every year, while the second-placed U.S.A has the production of 427 million tons. However, China still has a low export volume of apples, 103.47 million tons in 2011, accounts, only 2.87% of the yearly production. And it also is reduced by 7.86% year-on-year. By the investigation of the consequence, the first reason is the high quantity but low quality of products. Secondly, there is no any application which is efficient and high precision in grading apples, so the graded good quality apples are difficult to find in markets. At the last, the agricultural labor force is transferring to other industries in great quantities, the intelligent machine is needed to liberate human from heavy and monotonous work. The existing method of fruit grading can be divided into two categories, one is the mechanical classification and the other one is based on optical measurement device. The former one is mainly judged by hole or lever, the latter judge the diameter and size of fruit by photoelectric detector or test the surface color to judge the maturity. However, the fruit grading method based on machine vision has advances in the application. According to analyzing images by cameras, it is easily to calculate a lot of parameters such as area, diameter and so on. It can test size, color, defects and bruise in one time. In addition, the biggest advantage of machine vision grading is the high efficiency regardless of the influence of subject factor. Therefore, it is urgent to improve the technology of apple grading, especially the technology which can be applied to the actual production. For these, the paper reviews the apple grading technology in the world based on the image processing.

2 Research Situation

It is widely acknowledged that apples' size, shape, color and defects are concerned separately in the existing technology of grading apples. Under experimental conditions, the ideal accuracy and processing speed can be achieved. Consequently, the paper summarized the current technology inspecting the processing precision and speed.

2.1 Processing Precision

Miller developed a color computer vision system to inspect and grade peaches' surface. Digital color images of peaches were acquired as the fruit moved on a belt conveyor. Image analysis algorithms were developed to compare peach ground color to reference peach maturity colors estimating the amount of blushed surface area. Ground color maturity classification with the computer vision system agreed with manual maturity classification in 54% of the test samples, and was within one color standard in 88% of the samples. Correlation coefficient between machine and manual estimates of blush surface area was 0.92[1]. Leemans V. etc. presented a hierarchical grading method applied to Jonagold apples. Several images covering the whole surface of the fruits were acquired thanks to a prototype grading machine. These images were then segmented and the features of the defects were extracted. During a learning procedure, the objects were classified into clusters by k-mean clustering. The classification probabilities of the objects were summarized and on this basis the fruits were graded using quadratic discriminant analysis. The fruits were correctly graded with a rate of 73%. The errors were found in the segmentation of the defects or for a particular wound, in a confusion with the calyx end [2]. Devrim Unay etc. presented a novel application work for grading of apple fruits by machine vision. Following precise segmentation of defects by minimal confusion with stem/calyx areas on multispectral images, statistical, textural and geometric features are extracted from the segmented area. Using these features, statistical and syntactical classifiers are trained for two- and multi-category grading of the fruits. Results showed that feature selection provided improved performance by retaining only the important features, and statistical classifiers outperformed their syntactical counterparts. Compared to the state-of-the-art, their two-category grading solution achieved better recognition rates (93.5% overall accuracy). In this work, they further provided a more realistic multi-category grading solution, where different classification architectures are evaluated. Their observations show that the single-classifier architecture is computationally less demanding, while the cascaded one is more accurate [3].

Zhao Jing took the advantage of reference shape analysis and artificial neural network to identify and classify apples' shape, which improved the accuracy rate to 93%. On the basis of analysis of fruit shapes, 6 characteristic parameter is proposed to describe fruit shape, which include diameter, continuity, curvature and the symmetry of the former three-parameter[4]. Wang Jian etc. took different quality level apple color pictures by digital camera. Using R color branch to determine threshold value after image smoothing, they carried through image segment and erosion, then

transferred RGB to HSL. At last, the true apple area was obtained by means of pixel points transform method taking count of the number of pixels on the projection. The results showed that the method was proper for the apple sorting based on computer vision, and it had a result with a veracity of 89.8% compared with manual judgment[5]. Rao Xiuqin etc. put forward a grading method to improve the quality of fruits. They made use of HIS color model to analyze the fruit image after segmentation and calculated the principal component (PC) of the H component histogram weighted by the fruit surface area. And then the average values of the most significant MPCs of the red and yellow sample groups were calculated respectively, which were used as the centers of the two sample groups to setup a grade model. A fruit was graded to the red group if the Mahalanobis distance between the fruit and the center of the red sample group was less than that between the fruit and the center of the yellow group, or it was graded to the yellow group. The test results of 800 navel orange images showed that the first and the second PCs of the H component histogram weighted by the fruit surface area were enough to grade a fruit, and the total error was only 1.75% [6]. Liu Yanglong studied the fruit shape classification. Wavelet descriptor is extracted to describe the fruit shape from wavelet transform of the normalized fruit radius sequence. Matching rates of different wavelet and different number of coefficients are analyzed on the reconstruction of the fruit border. The dimensions of shape feature are reduced using kernel principal component analysis (KPCA). The research shows that fruit shapes can be describe well by 36 points of Biorthogonal wavelet transform. Matching ratio between the shape and the reality is 98.64%. Finally, dynamic nearest neighbor-clustering algorithm is used to make the radial basis function (RBF) neural network as fruit shape classifier. The results show that the classification accuracy is 90% while the superior fruit recognition rate is 93.75% among the experiment. Experiments between wavelet descriptor and Fourier descriptor are compared [7]. Further, Li Junliang researches the relationship between the external features such as size color shape texture and internal quality of sugar. BP neural network and SVM (Support Vector Machine) are adopted to establish sugar classification model according to external features. The result shows that external features and internal quality of sugar have complicate non-linear relation. The accuracy rate of SVM is 82% which is higher than 64% of BP neural network classification model. At last, principal component features were extracted out from the NIR (Near Infrared Reflection) spectrophotometer as apples' internal features. Then outward features and internal features were fused with SVM to constructed sorting model of apples' sugar. The result shows that the sorting model with fusion technology is 91% better than the model with single sensor [8].

In the process of apple image detection, the largest factor which affects the precision is miscalculation of fruit stalk and calyx. Because of similarity of the fruit stalk, calyx and defects in the image, it is easily judge for defects. P.Jancsok proposed a new method to identify stem-end/calyx from bruises. According their method, a hyper spectral imaging system was used for separating stem-end/calyx regions from true bruises. Based on principal component analysis (PCA) of the hyper spectral images, multiple effective wave bands were selected. Afterwards, PCA and image-processing techniques were applied to the multispectral images. The stem-end/calyx

regions were identified and distinguished from the cheek surfaces by analyzing the contour features of the first principal component score images. None of the sound tissue was misclassified as a stem-end or calyx region for both cultivars apples. In the investigated samples, all of the stem-end/calyx presented in the images were correctly recognized for the 'Golden Delicious' apples and 98.33% for 'Jonagold' apples. Less than 3% of bruises were misclassified as stem-end/calyx regions for both cultivars apples [9]. Zhang Wenying etc. did something similar. According to the characteristics of apple stem, they used block scanning to judge stem. In addition, they found out the damaged area as well as stem and fruit calyx by analyzing the different reflection characteristics of the damaged surface and healthy surface, and the statistical properties of different gray level value of pixel points. It was 100% accuracy rate on 15 fruit stalk pictures, while the accuracy of 90 stem picture was 88%. Experiment results proved that the method for detecting detected surface is efficient [10]. Song Yihuan etc. proposed a method to distinguish the apple stem/calyx and defect based on DT-CWT (Dual Tree Complex Wavelet Transform) and LS-SVM (Least Squares Support Vector Machine). They took apple image decomposition with DT-CWT and constructed feature vectors with the mean and variance of the transformed high frequency subband coefficients, then classified with LS-SVM. After the experiment on 180 apple images, the result showed that it had the best effect of extracting texture features with wavelet decomposition classifying by means of 3 layers DT-CWT to 64*64 image. The accuracy rate was 95.6% [11]. The hyper spectral imaging technology was proposed to detect the subtle bruises on fruits by Zhao Jiewen. Apples were adopted as the experimental object. The apples hyper spectral images between 500 nm and 900nm wavelength were analyzed via the principal components analysis, and the feature images under 547nm wavelength were selected to detect the bruises on apples. The asymmetric brightness of the images was eliminated with asymmetric second difference subsequently. Finally, the feature of bruise was extracted through appropriate image processing. The experimental results show that detecting subtle bruises on fruits online with hyper spectral imaging technology is realized and the accuracy is 88.57% [12].

2.2 Processing Speed

Li Qingzhong etc. proposed a fast approach for box-dimension estimation based on a dual-pyramid data structure. For the suspicious defect area in fruit images, they utilized traditional fractal dimension and 4 oriented fractal dimensions as input values. They calculated with the proposed fast calculation method, and then a BP neural network was designed for identifying fruit defect area and stem, calyx concave area. Test results proved that the rate of correct classification is 93% and the executing time of microcomputer for recognition of one undefined blob on the surface of apple is 4~7ms [13]. Shen Mingxia etc. adopted fuzzy threshold segmentation to process the original image. The process time of this method is 68 s, while the Ostu method uses 123 s. Obviously, the speed of this method had its advantage [14]. In the light of the characteristics and requirement of real-time inspection and grading, the continuous area-scans approach was put forward to acquire the image of fruits from

time to time in a time-series manner by Huang Yonglin etc. The test results verified that this system could grab 12 frames per second with the triggering from the proximity sensors[15]. Zhang Feng etc. selected roundness, volume and the gray-level histogram of R G B component as apple quality evaluation index. They calculated roundness and volume by apple binarization image. Compared the index of images' each R G B grayscale histogram with the standard apple, it can automatically detect appearance and quality of apples. It costs 0.9s to detect an apple which satisfied the requirement of the real-time detection. This technique can be used for the apple packaging product line, and also can be used for appearance quality detection of agricultural products similarly [16].

2.3 Combined with Processing Accuracy and Speed

Feng Bin etc. set up a standard sphere gray model, which can realize fruit defect segmentation. In addition, they used the single threshold while the threshold boundaries don't need to be considered. For recognition of stem, calyx and defect, they made full use of the influence of its space shape to gray feature, using Fourier transform to determine shape of gray line, which become a satisfied result. After identified 50 stems and 50 calyxes, the accuracy was higher than 90%. This method had a small amount of calculation and fast speed, which can meet the requirement of the computer vision on-line detection of fruit [17]. Zhang Yajing etc. proposed a method using intensity and color information for separating adjoined apples. Firstly, they used Lab model to segment apple image, followed by each segmented area was calculated to judge whether they were adjoined area or not. After calculating the light information within adjoined area, the segment adjoined area according light spot produced by brightness, which can shield the noise outside the area. However, the unique brightness information in the area can be utilized to segment adjoined apples effectively. Experimental results showed that the recognition rate was more than 92.89%, and it was simple and rapid. Furthermore, the average image recognition time was less than 0.5 s [18].

3 Conclusions and Prospect

In conclusion, since scholars have done a number of researches on apples during a long time, which comes various new algorithms and application methods. However, in practice, there is still a lot details to be improved. Therefore, the mainly problems of existing technology and the future direction of development can be summarized as the following points:

(1) Single detection feature. The existing technology always aims at detecting one single feature such as shape, weight, color or defects. However, we prospect to grade in the minimum times of detection that we can improve production efficiency in the work site. Therefore, we would like to obtain enough information at one time.

(2) Balance between speed and accuracy. It is able to reach the ideal detection speed and accuracy under laboratory conditions, but either can meet the actual

production requirement. Therefore, we need to reduce the complexity of the existing algorithm, yet we should not have much influence on the accuracy, which we must find a balance between speed and accuracy.

(3) We can consider using color image processing techniques because of the diversity of apples' surface color. Under these color images, it will be easier to judge stalk and calyx, avoiding mistaken for surface defects, as well as the apparent color and defects. Above all, the speed is still the problem to be solved yet.

(4) The lack of suitable mechanical structure for mass processing. Since most of the existing technologies are basically carried out under laboratory conditions, yet there are many uncertain factors in the process of production, thus we need to work out the suitable mechanical structure for image processing which makes the produce conditions as close as possible to the laboratory conditions.

In conclusion, simplifying the existing algorithms and fusing different detection algorithm to form higher speed and higher precision detection algorithm is the development direction in future image processing technology in practical production, which is supported by appropriate mechanical structure.

Acknowledgment. This work was supported by the National Natural Science Foundation of China (No. 61104213) and the Program for Innovative Research Team of Jiangnan University (No. 2009CXTD01).

References

- [1] Miller, B.K., Delwiche, M.J.: A color vision system for peach grading. *Transactions of the American Society of Agricultural Engineers* 32(4), 1484–1490 (1989)
- [2] Leemans, V., Destain, M.: A real-time grading method of apple base on features extracted from defects. *Journal of Food Engineering* 61, 83–89 (2004)
- [3] Devrim, U., Bernard, G., Olivier, K., Leemans, V.: Automatic grading of Bi-colored apples by multispectral machine vision. *Computers and Electronics in Agriculture* 75, 204–212 (2011)
- [4] Zhao, J., He, D.: Research on method of Fruit Shape Recognition. *Nuclear Science and Techniques* 17(2), 165–167 (2001)
- [5] Wang, J., Li, S.: Study on Computer Vision Grading Based on Apple Coloration Area. *Computer Engineering and Design* 29(2), 3813–3817 (2008)
- [6] Rao, X., Ying, Y.: Grading a fruit by its' surface color. *Journal of Zhejiang University* 43(5), 869–871 (2009)
- [7] Liu, Y.: Research on the shape grading of fruit based on the DSP machine vision, *Nanjing University of Aeronautics and Astronautics* (2010)
- [8] Li, J.: Research on the shape grading of fruit based on the machine vision and NIRS, *Nanjing University of Aeronautics and Astronautics* (2011)
- [9] Xing, J., Jancsok, P., De Baerdemaeker, J.: Stem-end/Calyx Identification on Apples using Contour Analysis in Multi-spectral Images. *Biosystems Engineering* 96(2), 231–237 (2007)
- [10] Zhang, W., Ying, Y.: Study on Detecting Methods for Apple Stem and Defected Surface with Computer Vision. *Journal of Zhejiang University* 27(5), 583–586 (2001)

- [11] Song, Y., Rao, X., Ying, Y.: Apple stem/calyx and defect discrimination using DT-CWT and LS-SVM. *Transactions of the Chinese Society of Agricultural Engineering* 28(9), 114–118 (2012)
- [12] Zhao, J., Liu, J., Chen, Q.: Detecting Subtle Bruises on Fruits with Hyper-spectral Imaging. *Journal of Agricultural Machinery* 39(1), 106–109 (2008)
- [13] Li, Q., Wang, M.: A Fast Identification Method for Fruit Surface Defect Based on Fractal Characters. *Journal of Image and Graphics* 5(2), 144–148 (2000)
- [14] Shen, M., Li, X., Ji, C.: Fuzzy Threshold Segmentation Method in Quality Detection of Fruit. *Journal of Agricultural Machinery* 34(5), 113–115 (2003)
- [15] Ying, Y., Rao, X., Huang, Y.: Methodology for images grabbing of massive numbers of moving fruits. *Journal of Zhejiang University (Agric. & Life Sci.)* 30(2), 147–152 (2004)
- [16] Zhang, F., Zhang, X.: External quality detection of apples using image processing technology. *Journal of Chinese Agricultural Engineering University* 11(6), 96–99 (2006)
- [17] Feng, B., Wang, M.: Study on Identifying Measurement About Defect of Fruit in Computer Vision. *Journal of Chinese Agricultural Engineering University* 7(4), 73–76 (2002)
- [18] Zhang, Y., Li, M.: Separating Adjoined Apples Based on Machine Vision And Information Fusion. *Journal of Agricultural Machinery* 40(11), 180–183 (2009)

Using Memcached to Promote Unified User Management System

Zuliang Zhao, Xiaodong Zhang, Lin Li, Zhe Liu, De-Hai Zhu, and Shao-Ming Li

College of Information and Electrical Engineering, China Agricultural University,
Beijing, China
mrzzl1987@gmail.com, zhangxd@cau.edu.cn, lilincau@126.com,
liuzhe23@vip.qq.com, zhudehai@263.net, lshaoming@sina.com

Abstract. In modern society, more and more companies have introduced different systems in corporate business sectors, furthermore, an employee may work in various systems. As a result, the employees need to record multiple usernames and passwords, which brings discomfort and lots of likelihood of errors, and posts security risks for the different systems that have their own security user authentications. Meanwhile, most of management systems are based on B/S model, where one of the foremost requirements is to provide low-latency access to frequent and large amounts of requests. To address this needs, in this paper, we firstly demonstrate the design of a web unified user management system which based on the Role-based access control (RBAC) model and Memcached. Secondly we conducted an experiment on two groups of integrated prototype systems to validate our results. Finally we draw a conclusion that it can not only monitor users in real time and configure the permissions safely and flexibly, but also reduce the response time significantly and improve the system performance.

Keywords: Memcached, caching technology, unified user management.

1 Introduction

Nowadays, with the development of the internet and the popularization of computers, more and more staff accomplish their daily tasks in computer. Here is problem: on the one hand, the employee and corporate structures have become more and more complicated. For instance, the jobs change frequently and a plenty of High multi-tasters exist in different departments in a small business. These factors require that the user management need to be more flexible. Furthermore, it should not only be customized different permission to different users, but also achieve the goal that different staff members use different functions in the integrated enterprise management system. On the other hand, the concurrency and PV (page view) have increased dramatically in the Web-based enterprise management system. With the purpose of improving system response, in this paper [6], we have optimized the design of the traditional unified user management platform: by using the Memcached caching technology. In our architecture, the user management data which doesn't

change but needs to access frequently will be stored in the memory. While the web applications exchange data with memory directly. Therefore, the read rate increases by several orders of magnitude and the user experience (UE) will be enhanced.

1.1 Unified User Management Platform [9]

The traditional unified user management platform, which is based the Lightweight Directory Access Protocol (LDAP) or database [2], manages the storage, authentications and permissions of user information uniformly among the applications in the enterprise organization. Users will be able to use the resources and services which have been authorized simply with Single sign on (SSO) [7].

1.2 Memcached and .net Cache [10]

Memcached is a general-purpose distributed memory caching system that was originally developed by Danga Interactive for LiveJournal. It is often used to speed up dynamic database-driven websites by caching data and objects in RAM to reduce the number of reading times from an external data source (such as a database or API). Therefore, it can be used to improve the speed of dynamic Web applications and the system scalability.

In the development of Unified user management platform based on asp.net, it is found that these functions can be implemented by exploiting a cache class in .net. In most cases we can improve the performance by using the Cache class, but some bottlenecks may also be introduced: One thing is that it is difficult to specify the occupied memory according to cache classes. The other thing is that it is impossible to exchange the data in the cache of one computer with that of another computer. In some cases, the system managers need to do some security control in real time, e.g., making the login users log out the system, changing the user permissions in real-time and so on. However, these functions cannot be realized by using the Cache class. Therefore, we import the distributed cache in this paper, which can be regarded as an extension of the traditional concept of cache used in a single locale. A distributed cache may span multiple servers so that it can grow in size and in transactional capacity. As a consequence, it will significantly enhance the reusability and real-time control of cached data.

1.3 Role-Based Access Control (RBAC) System Model

In most of enterprises, roles are created for various job functions. [3]The permissions to perform certain operations are assigned to specific roles. Members of staff (or other system users) are assigned particular roles, and through those role assignments acquire the computer permissions to perform particular computer-system functions. Since users are not assigned permissions directly, but only acquire them through their role (or roles), management of individual user rights becomes a matter of simply assigning appropriate roles to the user's account; this simplifies common operations, such as adding a user, or changing a user's department.

2 System Design and Implementation

2.1 System Architecture

The system architecture is object-oriented, which is consistent with the core idea of MVC. The details of this architecture are described in the following:

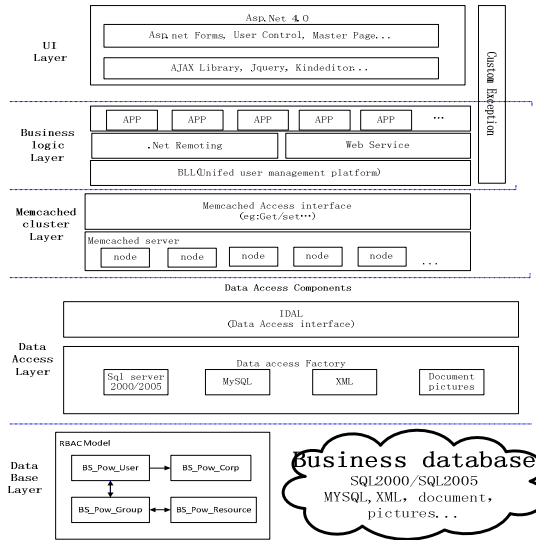


Fig. 1. System Framework

UI Layer: as illustrated in Fig. 1, it can be any output representation of data, such as a chart or a diagram. Note that some data can be represented by different views, such as a pie chart for management and a tabular view for accountants.

Controller Layer: mediates input, converting it to commands for the Memcached.

Memcached Layer: data input and request, converting it to commands for the controller or database access, Storage of the user manager data.

Database Access Layer: data input and request, converting it to commands for Memcached or data base.

Data Base Layer: storage of data.

2.2 Database Design

The database is explained in detail as follows:

BS_Pow_User table: user information, including users' personal information, username and password.

BS_Pow_Corp table: enterprise organization information by tree structure. We use department's bits (field: CorpNum) to confirm the department affiliation. This

structure is able to cope with most kinds of substantially requirements in different departments of enterprises.

BS_Pow_UserWithCorp table: user’s department. In some cases, one user may belong to different departments at the same time. To solve this problem, we create a main department mark (field: Main, value: “1” means main department; “null” means: subsidiary departments).

BS_Pow_Group table: role’s information. System managers can define different roles by themselves.

BS_Pow_Resource table: we store data by tree structure. We define menus and operations as resources in platform. Menus include access paths to different systems, while operations include what users can do in different systems just as adding, deleting, changing, searching, input, output, printing and etc. They are distinguished with each other by the field “ResUrl” (“null” means it is operation and the other is resources).

BS_Pow_UserWithGroup table: relationships between users and roles.

BS_Pow_GroupWithResource table: relationships between roles and resources.

BS_Pow_LoginLog table: User’s login information. System managers can check the users’ login information such as IP, permissions from this table.

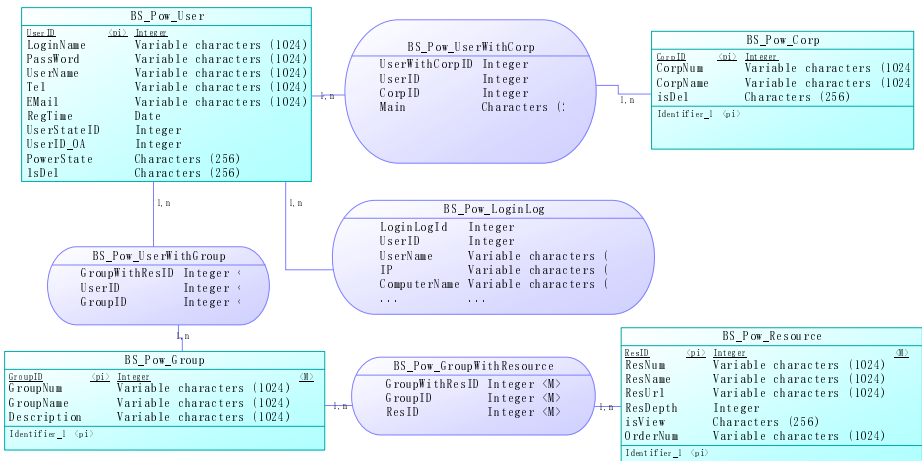


Fig. 2. Database Design [8]

2.3 Data Initialization in Memcached [13]

After Memcached configuration is completed, we need to copy a mirror file of the user-role-resource information from the database. First, we should make a serialization for the permission configuration data in the database. Serialization, represents the process of converting a data structure or object state into a format that can be stored and "resurrected" later in the same or another computer environment. When the resulting series of bits are reread according to the serialization format, it can be used to create a semantically identical clone of the original object.

Memcached supports custom data types which only require a [Serializable] mark when a new data type is defined. We create a user class; includes user information, departments, roles and role-resources. Memcached uses a key-value associative array. In this paper, we use user-id as the key and the user class instance as the value.

2.4 The Basic Process [5]

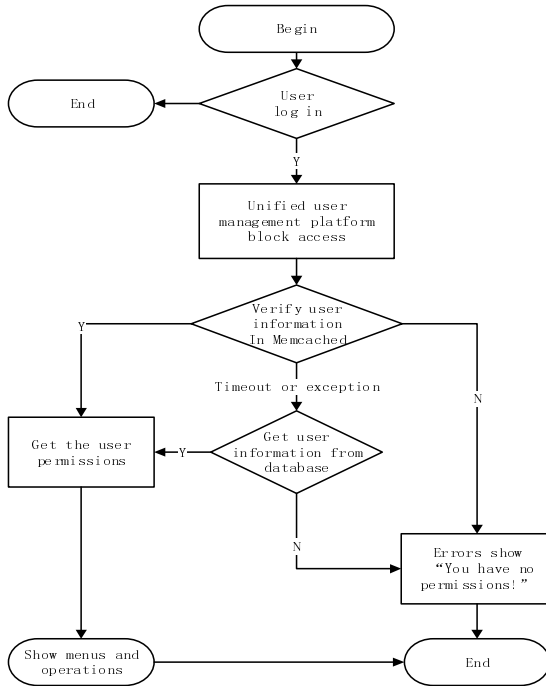


Fig. 3. The basic Process

2.5 Permission Data Read

When Memcached receives a get (incr/decr/...) request, it queries its own cache, or tries to access the database in case that the first query is missed. The algorithm runs as follows: Firstly get the data from database and post it to the user, secondly store it to Memcached's cache. If there is another post for the same key, then send this key-value back to the host. In order to prevent the system from the "Dos attacks" which works in exhaustive manner and may would result to database crash, we only try to connect the database until the Memcached is unable to connect or throw an exception.

2.6 Permission Date Modification

When Memcached receives a set (add/replace/...) request and has stored the new value to Memcached key-value successfully, it would be triggered to access the database, and then do an operation of deserialization to the changed key-values, finally store them to the database.

2.7 Memcached Persistence

Memcached runs as the Daemon model in one or more servers and accepts the connection operation of a client at any time. Since the whole data is stored in the memory, it would be lost whenever the servers rebooted. Therefore, a timer is needed to synchronous the data between the database and Memcached. The data would be lost anywhere from this. In this case, the data would not be lost even when the servers are crashed.

3 Performance Testing

Microsoft's Web Application Stress Tool, which is developed by Microsoft's website testers, provides an easy way to simulate large number of users against Web application. This tool makes it possible to make intelligent decisions about hardware and software load incurred by application and how much traffic a given machine or group of machines can handle.

3.1 Test Environment

Table 1. Test environment

Hardware environment	Software environment
Server1 CPU:XEON MP 7300, RAM 2GB	Sql2005 + iis6.0
Server2 CPU:XEON MP 7300, RAM 2GB	Sql2005 + iis6.0
Client Dual-Core 3.2*2, RAM 4GB	Microsoft Web Application Stress Tool

3.2 Test Plan

In this simulation, we consider the case when respectively 50,100 and 300 users concurrently log in, for the purpose of testing Memcached performance.

Data and server configuration instructions are described in the following: A Group Company is considered which is consisted of 6 subsidiaries, 627 departments and more than 2000 staff, including formals and temporaries. There is almost 10 MB user management data. The time that Memcached services take to start after the server reboots is Microsecond, as same as the time that Memcached completed a comparison with database.

Table 2. No Memcached (Unit: Ms)

users	average	median	90%line	min	max
50	1620	1754	1812	125	6412
100	6680	6789	7054	250	10121
300	12560	14576	15746	328	17123

Table 3. Using Memcached (Unit: Ms)

users	average	median	90%line	min	max
50	1220	1254	1312	64	3412
100	3680	3789	4054	201	6121
300	5960	6576	6746	300	9123

Illustrating:

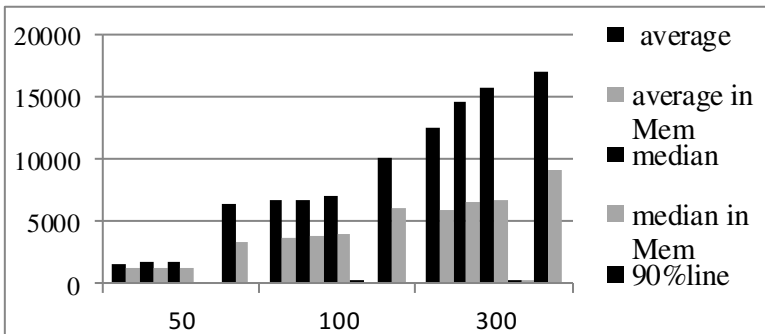
average: Average response time: in default, is the average response time for a single request

median: Median, 50% of the user's response time

90% line: 90% of the user's response time

min: The minimum response time

max: The maximum response time

**Fig. 4.** Contrast Chart**Table 4.** Response time and UE

Response time	UE
Within 2s	Speedy
2-5s	Accepted
5-10s	Anxiety, some users try to re-click
More than 10s	Believe system had crashed

4 Conclusions

In this paper, we optimize the traditional Unified User Management Model by using the Memcached cache technology. The results of performance test show that our proposed approach can significantly speed up the system operation and improve the performance, while the load of servers are substantially released. Moreover, our approach makes it possible to control and adjust the user permissions in real-time, which guarantees the security of the system.

Acknowledgment. This paper is supported by the “National Key Technology R&D Program under the Twelfth Five-Year plan of P.R. China” (Grant No. 2012BAK19B04-03).

References

1. Jose, J., Subramoni, H., Luo, M., Zhang, M., Huang, J., Wasiur-Rahman, M., Islam, N., Ouyang, X., Wang, H., Sur, S., Panda, D.K.: Memcached Design on High Performance RDMA Capable Interconnects. In: Proceedings of the 2011 International Conference on Parallel Processing, pp. 743–752. IEEE Computer Society, Washington, DC (2011)
2. Memcached Command Binary Protocol, <http://code.google.com/p/memcached/wiki/BinaryProtocolRevamped>
3. http://en.wikipedia.org/wiki/Role-based_access_control
4. Sobel, J.: Keeping Up (The Facebook Blog) (2011), <http://blog.facebook.com/blog.php?post=7899307130>
5. Memcached Commands, <http://code.google.com/p/memcached/wiki/NewCommands>
6. Memcached: High-Performance, Distributed Memory Object Caching System, <http://memcached.org/>
7. Appavoo, J., Waterland, A., Da Silva, E.A.: Providing a cloud network infrastructure on a supercomputer. In: Proceedings of the 19th ACM Int'l Symposium on High Performance Distributed Computing, HPDC 2010, pp. 385–394. ACM, New York (2010)
8. Vaidyanathan, K., Narravula, S., Balaji, P., Panda, D.K.: Designing Efficient Systems Services and Primitives for Next-Generation Data-Centers. In: Workshop on NSF Next Generation Software(NGS) Program; Held in conjunction with IPDPS (2007)
9. IBM, Message Passing Interface and Low-Level Application Programming Interface (LAPI), <http://www-03.ibm.com/systems/software/parallel/index.html>
10. Chalamalasetti, S.R., Lim, K., Wright, M., AuYoung, A., Ranganathan, P., Margala, M.: An FPGA memcached appliance. In: FPGA 2013 Proceedings of the ACM/SIGDA International Symposium on Field Programmable Gate Arrays, pp. 245–254 (2013)
11. Jose, J., Subramoni, H., Kandalla, K., Wasi-ur-Rahman, M., Wang, H., Narravula, S., Panda, D.K.: Scalable Memcached Design for InfiniBand Clusters Using Hybrid Transports. In: 2012 12th IEEE/ACM International Symposium on Cluster, Cloud and Grid Computing (CCGrid), pp. 236–243 (2012)
12. Li, F., Zhan, S., Li, L.: Research on using memcached in call center. In: 2011 International Conference on Computer Science and Network Technology (ICCSNT), December 24–26, vol. 3, pp. 1721–1723 (2011)
13. Xu, J., Zou, W.: Application Research of Memcached. Science Mosaic 7, 95–97 (2012) ISSN: 1671-4792

A Growth Measuring Approach for Maize Based on Computer Vision

Chuanyu Wang^{1,2}, Boxiang Xiao^{1,2,*}, Xinyu Guo^{1,2}, and Sheng Wu^{1,2}

¹ Beijing Research Center for Information Technology in Agriculture, Beijing 100097, China

² National Engineering Research Center for Information Technology in Agriculture,
Beijing 100097, China

{wangcy, xiaobx, guoxy, wus}@nercita.org.cn

Abstract. Growth measuring for plant is an important work both in agriculture and botany. Computer vision provides a convenient non-contact way for measurements in many fields. In this paper, a growth measuring approach for maize based on computer vision is presented. Firstly, a computer vision system for maize in field consisting of binocular camera on a path beam is constructed, and doubles of maize images are captured. Under the definition of average growth velocity of maize, we measure the growth of given maize plant by image processing and relevant calculations. Part of experimental results are given and discussed. Results and analysis show that the presented method is practicable for maize growth measuring in assigned time period. Finally, some limitations are pointed and more future works are addressed in computer vision-based measurement for plants.

Keywords: growth measuring, maize, computer vision.

1 Introduction

In past decades, information technology was deeply used in agriculture, and it provided various tools and devices for promotion modern agricultural productions [1]. Crop growth status is an important target and parameter in many agricultural applications [2-4] such as precision management, crops breeding, production estimation and breed evaluation. Crop growth monitoring became a rising research hot issue in past years, and many researchers proposed various methods for different plants and targets. To detect the growth status and predict the yield of the crop, Cui and coworkers [5] developed a crop growth monitor measuring system about nitrogen content in the plant based on optical principle. Cheng and colleagues [6] presented a plant growth status analyzer based on photoelectric technology by analyzing the variation of chlorophyll content in leaves.

Computer vision-based method is an effective way for non-destructive measurement [7-9], and it has peculiar advantages comparing to traditional approaches. Brosnan and Sun [8] presented a review on inspection and grading of agricultural and food products by computer vision systems. Yang and Tang [9] carried

* Corresponding author.

out research work on target visibility and measure precision analysis of stereo vision systems. Camera calibration is the most important task in computer vision systems, and Tian et al [10] provided a camera calibration method based on OpenCV. Because of the prominent advantages, computer vision-based methods were widely used in many fields including agricultural applications.

In this paper, the authors presented a maize growth measuring approach for monitoring based on computer vision. By use of binocular stereo camera system, the flowchart of this work is shown in Fig. 1. The main operations include images capture based on computer vision and feature extraction under the definition of maize growth. Finally, the maize growth velocity is calculated by a series of translations and the growth was measured. The paper is organized as follow: Section 2 introduces the computer vision system and images acquisition; Main growth measuring algorithm including growth definition, image processing and growth calculation was described in Section 3; Part of experimental results and discussions are given in Section 4; Finally, we summarize the whole work and address the future work in Section 5.

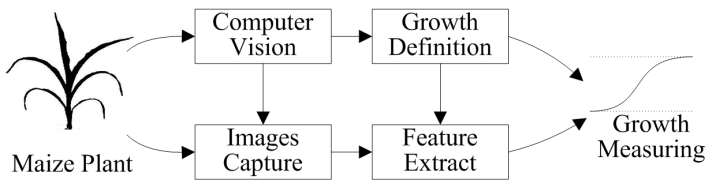


Fig. 1. The flowchart of this method

2 Computer Vision System and Images Capture

To capture images for given maize plants in field, a computer vision system is constructed by use of binocular stereo camera. The frame work and components of the system is shown in Fig. 2. A path beam is supported by two trestles to form a frame, and the frame is placed on the planting line of maize. The length of the path beam in our device is 4m, and the height is 1.8m. The binocular stereo camera is fixed on a platform downwards which can glide along with the path beam. The camera is also linked to a portable computer, and it can be control by the computer to collect images.

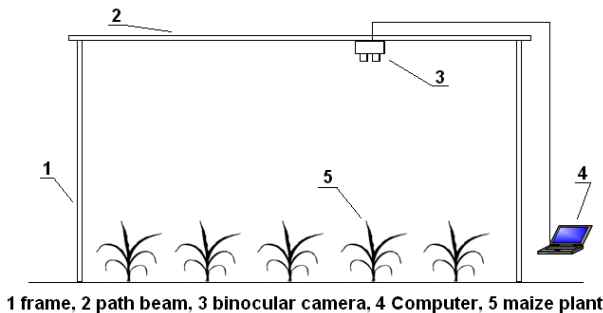


Fig. 2. The computer vision system of this work

In images acquisition, the device was placed upwards the maize objects. Firstly, the binocular stereo camera was calibrated by a black and white checkerboard mark, and the calibrations were respectively implemented on several prearranged positions which sited at the upper range of aiming maize plants. The experimental maize was planted in farm of Beijing Academy of Agriculture and Forest Science. We selected a maize colony including 4 lines and 8 rows as the images source. For a selected maize plant, two images with different positions were captured by the binocular stereo camera, and Fig. 3 shows an example of images relevant a same maize plant.



Fig. 3. Captured images of maize plant

3 Growth Measuring for Maize

In this work, maize is selected as the example plant, and we plant the experimental maize in farm. Firstly, we define the measurement of maize growth according to several relevant works. Secondly, the measuring process is implemented by steps of image processing and calculations. The details of the method are illustrated as follow.

3.1 Definition of Maize Growth

Measurement of plant growth is a public topic both in botany and agriculture, and there are many methods that how to measure growth rate of plants. For a typical plant, measuring parameters include fresh weight, dry weight, leaf surface area, and so on [11]. Furthermore, for a crop, calculable parameters include AGR (Absolute Growth Rate), RGR (Relative Growth Rate), LAR (Leaf Area Ratio), NAR (Net Assimilation Ratio), CGR (Crop Growth Rate) [12]. Here, we focus the measure method and system tool, thus we selected a simple definition of maize growth. We selected the same point in a same maize leaf with relevant static locations as reference for growth. The marks are set on selected maize leaf, as shown in Fig. 3. We consider the absolute displacement of marked points as the growth value.

3.2 Image Processing

Original images of plant are not directly available for feature extraction because they include lots of noise points. Several image processing operations are implemented in this step including median filter, plant division, binarization and feature points extraction. They are introduction in detail as follow.

Firstly, a median filter algorithm is used for noise data reducing. Most of noise data exist as isolated points which are sensitive to median filter. In operation, we select a 7×7 pixel rectangle centered at the processing pixel, and calculate the middle value of all pixels as the new value of the processing pixel. Circulating operation is implemented for all pixel of image, and the noise data is filtered.

Secondly, we extract the maize plant in the images by division algorithm which can distinguish green plant and soil background. Because of the difficulty of light control in field, the image quality is influenced by many reasons, and simple division approach is not suitable for this task. Here, we propose a decision surface algorithm to divide the plant object in image with complex background. The algorithm can be expressed by Eq. (1)

$$C = \frac{R^2}{V^2} + \frac{(1-G)^2}{(Y \times B + U)^2} \quad (1)$$

Where R, G, B are respectively the normalized value of component of Red, Green and Blue in the image. V, Y, U are parameters which can describe the surface shape. Here we appoint $V = 0.85$, $Y = -0.37$, $U = 0.74$, and relevant C can be calculated. If $C < 1$, we consider the pixel as the background, otherwise the plant.

Thirdly, binarization is implemented for images which are processed as gray mode. In experiments, we assigned a threshold value $\mu=25$ for gray mode pixels. All pixels upper 25 are set 255, the others are set 0. Fig. 4 shows an example of a couple of maize images.



Fig. 4. Processed images by Binarization algorithm

Finally, we extract the marks on maize leaf in binary images. We employ a rectangle 16×16 pixel for mark detection. For a rectangle, if all its border pixels are white with value 255 and there are both black with value 0 and white with value 255 in its inter area, the rectangle is considered including a mark. If a rectangle includes a mark, its border is reduced. The algorithm recalculates the border pixel value, until all sides of the border include both black pixel and white pixel. The center of the rectangle is the center of the mark. By circulating operation on all pixels, all marks are collected and calculated.

3.3 Growth Calculations for Measuring

According to the mark positions in two images, we can calculate the three dimensional coordinate values x, y, z. The projection matrix P expressed in Eq. (2) can be constructed by use of plane calibrating algorithm. The matrix respectively defined for left camera and right camera when i = 1 or 2.

$$P_i = \begin{bmatrix} a_{11}^i & a_{12}^i & a_{13}^i & a_{14}^i \\ a_{21}^i & a_{22}^i & a_{23}^i & a_{24}^i \\ a_{31}^i & a_{32}^i & a_{33}^i & a_{34}^i \end{bmatrix} \quad i=1,2 \tag{2}$$

We define the 3D value of the mark as M[x, y, z], m1(x1,y1) and m2(x2,y2) respectively the projected point of the mark on left and right images. The equation (3) is established as follow which can get the value M[x, y, z].

$$\begin{bmatrix} (a_{11}^i - a_{31}^i x_i) & (a_{12}^i - a_{32}^i x_i) & (a_{13}^i - a_{33}^i x_i) \\ (a_{21}^i - a_{31}^i y_i) & (a_{22}^i - a_{32}^i y_i) & (a_{23}^i - a_{33}^i y_i) \end{bmatrix} \begin{bmatrix} X \\ Y \\ Z \end{bmatrix} = \begin{bmatrix} (x_i a_{14}^i) \\ (y_i a_{24}^i) \end{bmatrix} \tag{3}$$

4 Results and Discussion

4.1 Experiments and Part of Results

To implement the measuring system, we carried out agricultural experiments in farm of Beijing Academy of Agriculture and Forest Science. A set of original images are collected by the system. To achieve image-based calculation and measurement, we developed a software system for the tool by use of C++ program language and OpenCV library.

In experiments, we measure the average growth velocity of selected maize leaf in different time periods. Table 1 gives part of measuring results of an example leaf in three time periods. The value of growth velocity is calculated by algorithm introduced in upper sections. Finally, the growth curve of maize leaf is generated by calculated parameters.

Table 1. Part of experimental results of measured maize growth

Order	Measuring Time	Average Growth Velocity (cm/h)
1	8:00	0.27
2	14:00	0.25
3	20:00	0.32

4.2 Discussions

Experimental results show that the presented method and system is effective for maize growth measuring. Compare with traditional measuring methods, computer-vision-based way is non-destructive, and the plant organs are protected in measuring. The process is fast and the efficient in experiments. The precision of measurement is satisfied for applications of agriculture such as plant form analysis, growth evaluations.

One of limitation of the method is that the binocular stereo camera device must be fixed on top of measuring maize plant. The limitation of position of measuring is an obvious problem. On the other hand, the device is also difficult for large range maize canopy measurement, and some necessary promotion should be made in future work.

Furthermore, a phenomenon was also discovered that the average growth velocity of maize leaf is larger in night than in daytime. It may be caused by photosynthesis restraint which should be studied deeply in ecophysiology.

5 Conclusions

To sum up, a growth measuring approach for maize based on computer vision was proposed in this paper. To achieve the measuring aim for maize growth, we design and install a computer vision-based system including binocular stereo camera. By definition of maize growth, the images were processed and growth velocity was calculated by a serious of transforms. Part of experimental results was given in sections and the approach was discussed subsequently. As a non-destructive measurement way, the presented method provided a technological way for dynamic maize growth measurement. It was also a technological reference for relevant applications in agriculture. In future, we focus on more automatic and robust monitor technology and systems for maize as well as other plants.

Acknowledgment. This work is supported by National Natural Science Foundation of China (Grant No. 31171454); by Beijing Natural Science Foundation (Grant No. 4132028); by National Science & Technology Pillar Program (Grant No. 2012BAD35B01); by Special Fund for S&T Innovation of Beijing Academy of Agriculture and Forestry Sciences (Grant No. KJCX201204007).

References

1. Cox, S.: Information technology: the global key to precision agriculture and sustainability. *Computers and Electronics in Agriculture* 36(2-3), 93–111 (2002)
2. Zhang, N., Wang, M., Wang, N.: Precision agriculture-a worldwide overview. *Computers and Electronics in Agriculture* 36(1), 113–132 (2002)
3. Ortiz-Monasterio, J.I., Palacios-Rojas, N., Meng, E., Pixley, K., Trethowan, R., Peña, R.J.: Enhancing the mineral and vitamin content of wheat and maize through plant breeding. *Journal of Cereal Science* 46(3), 293–307 (2007)
4. Guo, Y., Ma, Y., Zhan, Z., et al.: Parameter Optimization and Field Validation of the Functional-Structural Model GREENLAB for Maize. *Annals of Botany* 97, 217–230 (2006)
5. Cui, D., Li, M., Zhu, Y., et al.: Monitoring Crop Growth Status Based on Optical Sensor. In: Li, D. (ed.) CCTA 2007. IFIP, vol. 259, pp. 1397–1401. Springer, Boston (2007)
6. Cheng, X., Shang, X., Teng, S.: Design of Plant Growth Status Analyzer Based on Photoelectric Technology. In: Proc. of International Conference on Electronics and Optoelectronics (ICEOE), pp. 426–429 (2011)
7. Noble, J.: From inspection to process understanding and monitoring: a view on computer vision in manufacturing. *Image and Vision Computing* 13(3), 197–214 (1995)
8. Brosnan, T., Sun, D.: Inspection and grading of agricultural and food products by computer vision systems-a review. *Computers and Electronics in Agriculture* 36(2-3), 193–213 (2002)
9. Yang, H., Tang, G.: Target Visibility and Measure Precision Analysis of Stereo Vision Systems. *Systems Engineering and Electronics* 34(9), 1889–1894 (2012)
10. Tian, K., Zhang, A., Wang, S.: A Camera Calibration Method Based on OpenCV. *Journal of Capital Normal University (Natural Science Edition)* 29(2), 14–17 (2008)
11. Judithavory, B.R.: TheBev, Kalyx. How to Measure Growth Rate of Plants (June 18, 2013), <http://www.wikihow.com/Measure-Growth-Rate-of-Plants>
12. Turner, P.: eHow Contributor. How to Calculate Crop Growth (June 18, 2013), http://www.ehow.com/how_7459815_calculate-crop-growth.html

The Comprehensive Assessment of Planting Elements Based on Analytic Hierarchy Process

Yujian Yang, Huaijun Ruan^{*}, Jingling Li, and Lei Wang

Science & Technology Information Institute of Shandong Academy of Agricultural Science,
Number 202 Gongye North Road, Licheng District of Jinan,
250100, Shandong Province, P.R. China
yyjtskhk@gmail.com

Abstract. There were many factors having an effect on planting development, this paper designed an indicator system for planting assessment, mainly including three kinds of essential sub-system elements, they were resource sub-system, information and energy sub-system and social-economic sub-system, the detailed indicator system involved in 8 concrete indicators from the three sub-systems. In the way, a set of reasonable indicator system of planting assessment was proposed on township/town scale, there was the characteristics involved in rural areas and agriculture information introduced in the case of indicator system. Based on it, the paper constructed the hierarchical structure model of the planting elements assessment, the weight of each indicator was calculated through AHP method. The study results showed that the planting elements development level from the comprehensive assessment was Juzhen township, Fangsi town, Shizhong subdistrict office, Xinzhai town, Xindian town, Zhangzhuang town, Liangjia town, Anren town, Lunzhen town, Shiliwang township and Litun township. Obviously, the comprehensive assessment model had preferable operability and practicability, it not only combined subjective evaluation with objective appraisal, but also qualitative with quantitative study, and fully considered of each assessment factor. Therefore, AHP method is scientific and reasonable and suit to be used to evaluate the level of planting elements assessment.

Keywords: Indicator system, planting elements assessment, the analytic hierarchy process.

1 Introduction

Planting was the foundation of agriculture and a special place in agriculture, which only related to the overall situation of national food security. It was also an important income source of the farmers, its value was more than 50% of the total agricultural value. A total of 66 articles were retrieved in the Chinese journal of literature since 2011 as a summary of the key word “planting evaluation”. Retrieval results showed that Gaojun “the high military cropping systems in the suburbs of Beijing ecological security assessment and technical countermeasures – take the case of Shunyi District,

^{*} Corresponding author.

Beijing”, Shi Chenyang, etc. “The Study of the Technology Path of the Efficient Using Water of the Piedmont of Mt. Taihang Mountain in Hebei Province”, Zheng Yalian “Cultivated Land Fertility Evaluation and Planting Industry Layout in Tongzhou District of Beijing” and Liu Tian-sen “research on the application of comparative advantage theory in Chinese regional farming” were retrieved in database. The less literature study and the weak quantitative study related to planting evaluation were presented in the retrieval contents. It was necessary to establish a set of scientific indicator system on township/town scale for the comprehensive assessment of planting elements. Among evaluation methods, the analytic hierarchy process (AHP) can use opinions of experts to construct the judgment matrix, so it was meaningful. So the objective of the study was develop the quantitative evaluation of planting elements on town/township scale in Yucheng city, and the article regarded the rural areas and agriculture information as the evaluation indicator, a set of reasonable indicator system of planting assessment was proposed on township/town scale, and the system provides a visual way for users to do all the works of AHP, so the study presented academic significance[1,2,3,4]. In some correlated research, the quantitative studies were developed by fuzzy method and other methods as the above research, but the planting elements assessment had the less study from the correlation literatures and the study did not involve in the country level, and AHP method was scientific and reasonable and suit to be used to evaluate the level of planting elements assessment, so the method was selected in the article.

2 Material and Methodology

2.1 Analytical Hierarchy Process

Analytical Hierarchy Process (AHP) was developed by A.L.Saaty. AHP method was a multi-objective decision analytical method that combines qualitative with quantitative analysis and also a kind of optimization techniques, so it could be used to calculate the weight of each indicator. The essence of the process was decomposition of a complex problem into a hierarchy with goal (objective) at the top of the hierarchy, criteria and sub-criteria at levels and sub-levels of the hierarchy, decision alternatives at the bottom of the hierarchy. Elements at given hierarchy level were compared in pairs to assess their relative preference with respect to each of the elements at the next higher level. The verbal terms of the Saaty’s fundamental scale of 1–9 was used to assess the intensity of preference between two elements. The number of 1 indicates equal importance, 3 moderately more, 5 strongly more, 7 very strongly and 9 extremely more importance. The numbers of 2, 4, 6, and 8 were allotted to indicate compromise values of importance. The method computed and aggregated their eigenvectors until the composite final vector of weight coefficients for alternatives was obtained. The entries of final weight coefficients vector reflected the relative importance (value) of each alternative with respect to the goal stated at the top of hierarchy. During the AHP process, the steps were as follows: Form assessment indicator set. Establish stepped hierarchical construction. Ascertain the weight of the indices. Construct comparison judgment matrix and monolayer weights order. Consistency test and comprehensive assessment of AHP[4].

2.2 Construction of Indicator System of Planting Elements Assessment

Construction of indicator system was the premise of planting elements evaluation, so we constructed the indicator system according to the following principles: (1) Comprehension: The factor must reflect each side of the appraised object, study its connotation and extension deeply in the process of construction, making every effort to fully and actually manifest it. (2) Operability: Weight of each indicator should be determined and the evaluation method stresses on availability of indicator data. (3) Guidance : Prospective and tendency factors should be introduced to guide the direction of planting development. (4) Connection: The indicator system should link up with regional planting index system and reflect the development characteristic of planting itself. (5) Comparability: The general targets should be introduce in the system indicator[5].

We selected 8 indicators from the above principles to develop the comprehensive assessment of planting elements, the detailed contents referred to Table 1. In the indicator system, agriculture information indicator was introduced firstly in information and energy sub-system in the AHP model. The core content of planting elements assessment included 3 mutually and closely contacted planes: resource sub-system, information and energy sub-system and social-economic sub-system.

Table 1. Contents of Indicator System based on AHP

	Indicator name	Indicator content and significance
B ₁ :Resource sub-system	C ₁ :Fertilizer consumption per sown area	Fertilizer consumption/crop sown area
	C ₂ :Pesticide consumption per sown area	Pesticide consumption/ crop sown area
	C ₃ :Farmland plastic Film consumption per sown area	Farmland plastic film consumption/ crop sown area
B ₂ :Information and energy sub-system	C ₄ :Agriculture information status	Synthesis weight for infrastructure information of agriculture and production information of agriculture
	C ₅ :Total agricultural machinery power and energy information	The weight included the total agricultural machinery power, main energy and power consumption information
B ₃ :Social-economic sub-system	C ₆ :Agricultural scale management	Arable land/ The number of rural labor force
	C ₇ : effective irrigation capacity	Mechanical and electrical drainage and irrigation area/ crop sown area
	C ₈ :output ratio of planting industry	Output value of the planting industry/ agricultural output value

Selection principle of indicator AHP model, combined with the indicator system of planting elements Assessment in Yucheng city, hierarchy construction schematic diagram was shown in Fig.1. The graded hierarchical construction model of planting elements assessment included four layers on regional scale, target layer, rule layer, measure layer and object layer.

Where, the parameter meaning of B1,B2,B3 C1,C2,C3,C4,C5,C6,C7,C8 referred to Table.1, S1, S2, S3, S4, S 5, S 6, S 7, S 8, S 9, S10 and S11 respond to the Shiliwang township, Anren town, Lunzhen town, Juzhen township, Litun township, Fangsi town, Xinzhai town, Xindian town, Zhangzhuang town, Liangjia town and Shizhong subdistrict office in Yucheng city.

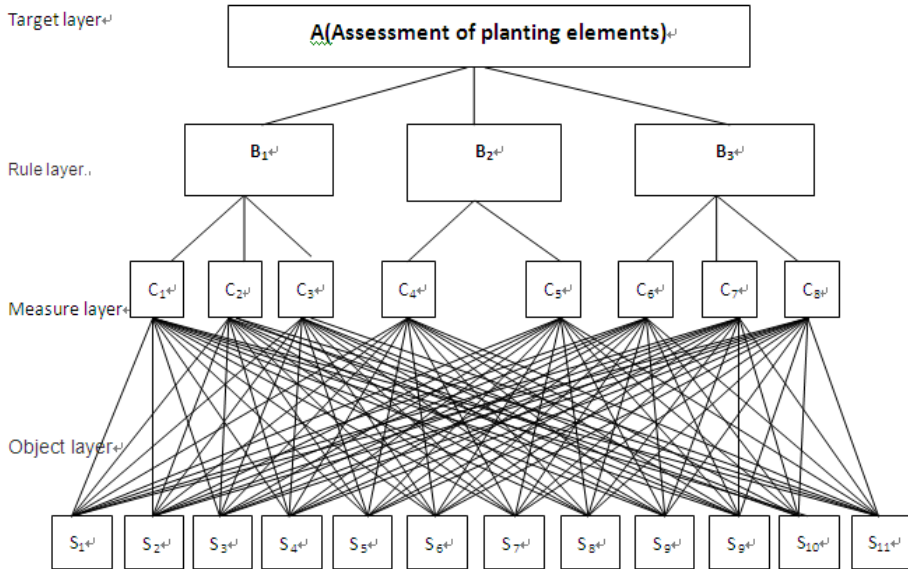


Fig. 1. Hierarchy Construction of planting elements assessment in Yucheng city

3 Results and Analysis

By pairwise comparing elements of the same layer in accordance with certain upper factor, each element of the judgment matrix was able to be defined. The relative importance of each element followed 1-9 proportion evaluation scale. Several judgment matrixes can be established based on the scores that experts provided. The importance that each element of No.(k+1) layer relative to No.k layer was ordered according to the judgment matrix. The weights of judgment matrix of AHP model were shown in Table 2. and Table 3.

Table 2. Comparison Judgment Matrix of Eigen Vector

Eigen Vector of A-B matrix	Eigen Vector of B ₁ -C matrix	Eigen Vector of B ₂ -C matrix	Eigen Vector of B ₃ -C matrix
0.694	0.458	0.500	0.429
0.132	0.126	0.500	0.143
0.174	0.416		0.429

Table 3. Comparison Judgment Matrix of Eigen Vector

$C_1 \rightarrow 1$ matrix	$C_2 \rightarrow 1$ matrix	$C_3 \rightarrow 1$ matrix	$C_4 \rightarrow 1$ matrix	$C_5 \rightarrow 1$ matrix	$C_6 \rightarrow 1$ matrix	$C_7 \rightarrow 1$ matrix	$C_8 \rightarrow 1$ matrix
0.037	0.029	0.076	0.123	0.121	0.042	0.070	0.032
0.020	0.080	0.113	0.076	0.123	0.032	0.181	0.026
0.056	0.068	0.019	0.102	0.023	0.050	0.062	0.257
0.270	0.049	0.278	0.022	0.068	0.182	0.020	0.193
0.022	0.028	0.034	0.020	0.023	0.102	0.028	0.018
0.088	0.236	0.145	0.287	0.186	0.088	0.108	0.058
0.075	0.200	0.044	0.043	0.034	0.225	0.273	0.060
0.145	0.176	0.023	0.022	0.051	0.039	0.041	0.123
0.144	0.032	0.028	0.037	0.024	0.157	0.035	0.145
0.110	0.063	0.057	0.062	0.061	0.058	0.153	0.067
0.034	0.041	0.184	0.208	0.285	0.023	0.029	0.023

To ensure the monolayer weights order was correct, the judgment matrix should be dealt with consistency test. Consistency should be tested as follows: Computing consistency index CI ($CI = \lambda_{max} - n/n-1$), where: λ_{max} was the eigenvalue of maximum, n represents for the number of the order of judgement matrix. If $CR < 0.1$, the consistency of the judgement matrix can be satisfied and so the order weights accepted.

Calculating consistency ratio $CR: CR = CI/RI$, the final results of AHP were validated by the random consistency ratio CR. If $CR < 0.1$, the results can meet the requirements. The values of λ_{max} , CI and the values of CR are shown in the Table 4, the values of CR are all less than 0.1, so the consistency test of the parameters was passed.

Table 4. λ_{max} of Judgement Matrix and Corresponding Consistency Test

	λ_{max}	C.I.	C.R.
A-B Matrix	3.080	0.040	0.069
B ₁ -C Matrix	3.009	0.005	0.009
B ₂ -C Matrix	2.000	0.000	0.000
B ₃ -C Matrix	3.000	0.000	0.000
C ₁ -D Matrix	11.710	0.071	0.047
C ₂ -D Matrix	11.969	0.097	0.064
C ₃ -D Matrix	11.750	0.075	0.049
C ₄ -D Matrix	11.853	0.085	0.056
C ₅ -D Matrix	11.915	0.091	0.060
C ₆ -D Matrix	11.509	0.051	0.034
C ₇ -D Matrix	11.587	0.059	0.039
C ₈ -D Matrix	11.667	0.067	0.044

Based on the assessment factor matrix and the monolayer weights matrix, the value of comprehensive assessment of the planting elements can be determined, the validation parameters ($C.I.= 0.075$, $R.I.=1.52$, $C.R.= 0.049 < 0.1$) were passed in the model, the results were shown in the Table 5.

Table 5. The Total order Weight Value of Hierarchy in AHP of 11 town/townships

Target Layer	Criterion Layer	Weight	Measure Layer	Object Layer	Total weight	Total Layer
planting elements assessment	Resource sub-system	0.694	Fertilizer consumption per sown area	Shiliwang township	0.060	10
			Pesticide consumption per sown area	Anren town	0.068	8
			Farmland Plastic Film consumption per sown area	Lunzhen town	0.062	9
	Information and energy sub-system	0.132	Agriculture information Level	Juzhen township	0.205	1
			Total Agricultural Machinery	Litun township	0.032	11
	Social-Economic sub-system	0.174	Power and energy information effective irrigation capacity	Fangsi town	0.135	2
			output ratio of planting industry	Xinzhai town	0.087	4
			Agricultural scale management	Xindian town	0.086	5
				Zhangzhuang town	0.084	6
				Liangjia town	0.078	7
				Shizhong subdistrict office	0.104	3

There was no doubt that AHP provided a scientific measure for analysis and decision making. Juzhen township, Fangsi town, Shizhong subdistrict office, Xinzhai town, Xindian town, Zhangzhuang town, Liangjia town, Anren town, Lunzhen town, Shiliwang township and Litun township, the weight above 11 townships/towns is 0.205, 0.135, 0.104, 0.087, 0.086, 0.084, 0.078, 0.068, 0.062, 0.060, 0.032 respectively, the weight value indicated that the planting elements dominance of 11 towns/townships is 0.205, 0.135, 0.104, 0.087, 0.086, 0.084, 0.078, 0.068, 0.062, 0.060 and 0.032, respectively.

4 Conclusions and Discussion

In a word, we drew conclusions that a set of reasonable indicator system in planting elements assessment was proposed on the township/town scale in this paper, it was suitable for processing by computers and was worth promoting. Furthermore, using AHP model, the paper constructed the hierarchical structure model of the planting elements assessment and calculated the factor weight of resource sub-system, information and energy sub-system and social-economic sub-system. Based on it, the planting elements dominance from the comprehensive assessment was Juzhen township, Fangsi town, Shizhong subdistrict office, Xinzhai town, Xindian town, Zhangzhuang town, Liangjia town, Anren town, Lunzhen town, Shiliwang township and Litun township. Obviously, the comprehensive assessment model of planting elements had preferable operability and practicability. It not only combined subjective evaluation with objective appraisal, but also qualitative with quantitative study, and fully considered of each assessment factor in system evaluation. Therefore, AHP method was scientific and reasonable to be used to evaluate the level of planting elements on country level.

References

1. Gaojun: Assessment and Technical Countermeasures of Ecological Safety of Cropping System in Suburban Region in Beijing—A Case Study in Shunyi County. China Agricultural University (2004)

2. Shi, C.: The Study of the Technology Path of the Efficient Using Water of the Piedmont of Mt. Taihang Shan in Hebei Province. Hebei Agricultural University (2012)
3. Zheng, Y.: Cultivated Land Fertility Evaluation and Planting Industry Layout in Tongzhou District of Beijing. Hebei Agricultural University (2012)
4. Liu, T.-S.: Research on the Appliation of Comparative Advantage Theory in Chinese Regional Farming. Hubei Agricultural Science 10, 1956–1959 (2012)
5. Jing, D., Li, D., Li, H., Zhang, Y.: Research on assessment method for rural information level based on AHP. In: Zhao, C., Li, D. (eds.) CCTA 2011. IFIP, vol. 293, pp. 125–134. Springer, Boston (2011)

The Monitoring of Rare Earths Mining from the Gannan Area of Southern China Using Remote Sensing Technology

Baoying Ye¹, Zhenghui Chen², Nisha Bao³, and Ying Li⁴

¹Institute of the Geology Survey, China University of Geosciences, Beijing, China

²Institute Mineral Resources, Chinese Academy of Geological Sciences, Beijing, China

³Institute for Geo-informatics & Digital Mine Research,

Northeast University, Shenyang, China

⁴Tianjin Institute of Geology and Mineral Resources, Tianjin, China

yeebaoying@gmail.com

Abstract. The weathering crust Elution-deposited Rare Earth is the peculiar and valuable source in China. The greatly mining activities in the south of GanZhou(Gannan) were occurred disorderly and illegally using the traditional extraction way, which brought out the dreadful environmental influence. In this study, the SPOT5 multi-spectral data was used to recognize and classify the destroyed land from mining activity. It was found that the most mining areas were located dispersedly, covered the area of 60.97km² in total with 524 sites, which accounted for 3.03% of the whole study area. There were 513 patches of destroyed area less than 1 km² distributed in the southwest of the study area. The results indicated that the mining integration should be concerned in this region and mining plan for further environmental protection.

Keywords: South of Ganzhou, Rare earth, Remote sense, Monitoring.

1 Introduction

Remote sensing and GIS technology play a key role in the study of Land use/cover change [1]. There were many researches focused on the environmental change from mining area using remote sensing data. These studies showed that satellite imagery can provide important information for mining environment and resolve controversies about future management directions [2-5].

There is a serious risk of chemical extraction from Weathering Crust Elution-deposited Rare Earth Ores that can make a major environmental damage in this area. Currently, the new technology has stepped into the third stage. In the first stage, the rare earth was separated using sodium chloride with oxalic acid as the precipitant. This process resulted in large amounts of wastewater contained high sodium chloride, which may pollute the surrounding soil and vegetation. Additionally, the residue of sodium chloride remained in the tailings would lead to soil salinization and affect the vegetation growth; In the second stage, sodium chloride was replaced by the ammonium sulfate as leaching solvent, which can reduce the soil pollution. However, the large-scale exploitation and depositing of ore body would result in the land destruction, water and soil loss[6]; In the third stage, the liquid was injected to

dissolve ore body directly without exploitation, and then rare earth elements were separated. However, this process had a risk of landslide [7-9].

Gannan is the mainly rare earth mining area in China. The high profit of the rare earth increases illegal mining in this area, which brings high environmental cost. As the large cover area of Weathering Crust Elution-deposited Rare Earth Ore, it is quite difficult to monitor and manage the whole area using traditional monitoring way based on field survey. The remote sensing technology has the capacity to acquire large area surface information and complete dynamic mining monitoring. Therefore, this study is aim to monitor rare earth mining in Gannan area using SPOT imagery, and acquire the information of dynamic exploitation process, we using manual interpretation method to discriminate the destroyed area. with the SPOT5 imagery, and filed surveying to confirm the result.

2 The Study Area

Gannan area of South China is rich in the rare earth sources. This study area was located in the west of Gannan (Figure1). The climate in this area is the tropical to

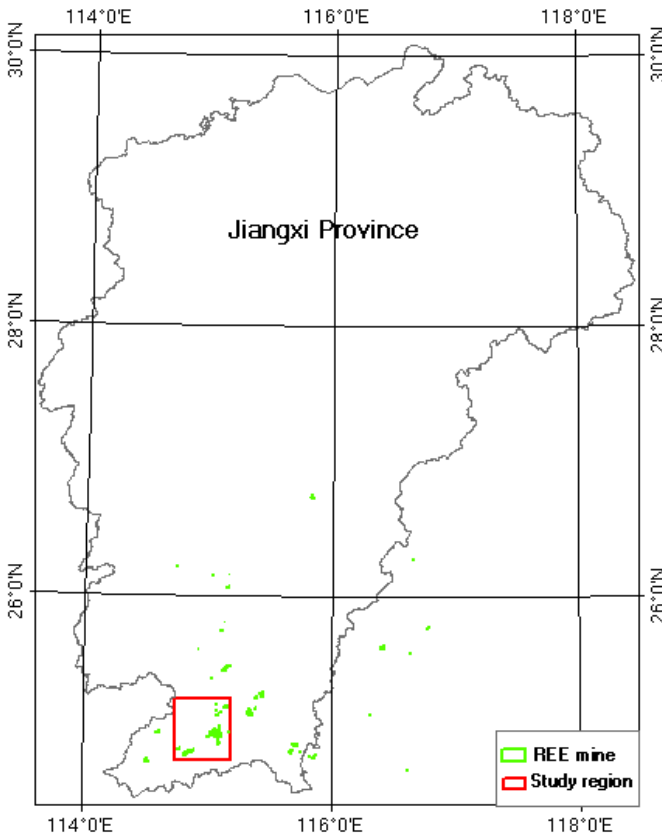


Fig. 1. The location of the study area in Gannan, China

subtropical. The wet and humid climate makes the flourishing plants, which is the source of the organic acid. It simulates the chemical weathering and formation of surface weathering crust. The rare earth is mainly from the weathering crust, even around 10 times higher than that from the base rock. This area is in the hilly country with elevation less than 550m. The topographic relief difference is 250m-260m. Gannan as the firstly mining area of rare earth exploitation has killed and polluted large area. Currently, there are dozens of active mining site in this area. The serious environmental issues are land degradation with vegetation removal and soil pollution.

3 Data and Method

In this study, the human interpretation was conducted to extract mining information from high resolution imagery, and then the data from field trip was used for accuracy assessment.

3.1 Data

Multi-spectral SPOT data with 10m resolution was used in this study, which acquired at 4th December 2010 with the dimap format. The ancillary data for image classification was Landsat/ETM data with 14.25m resolution and ASTER GRID DEM with 30m resolution (<http://gdex.cr.usgs.gov/gdex/>).

3.2 Ortho-rectification

As the landform of hilly country in this area, the mining site mostly located on the top of the hill. In order to target mining site accurately, the ortho-rectification of the imagery is necessary. Firstly, the band was composited by 412 for image interpretation. Furthermore, 21 ground control points were selected from ETM imagery. The ortho-rectification of SPOT5 imagery was conducted using bilinear interpolation resampling method based on the ERDAS's SPOT 5 orbital-pushbroom model. The average RMS error was below 1 pixel following ortho-rectification. As shown in the Figure 2, the SPOT 5 imagery covered the study area after ortho-rectification (Figure 2).

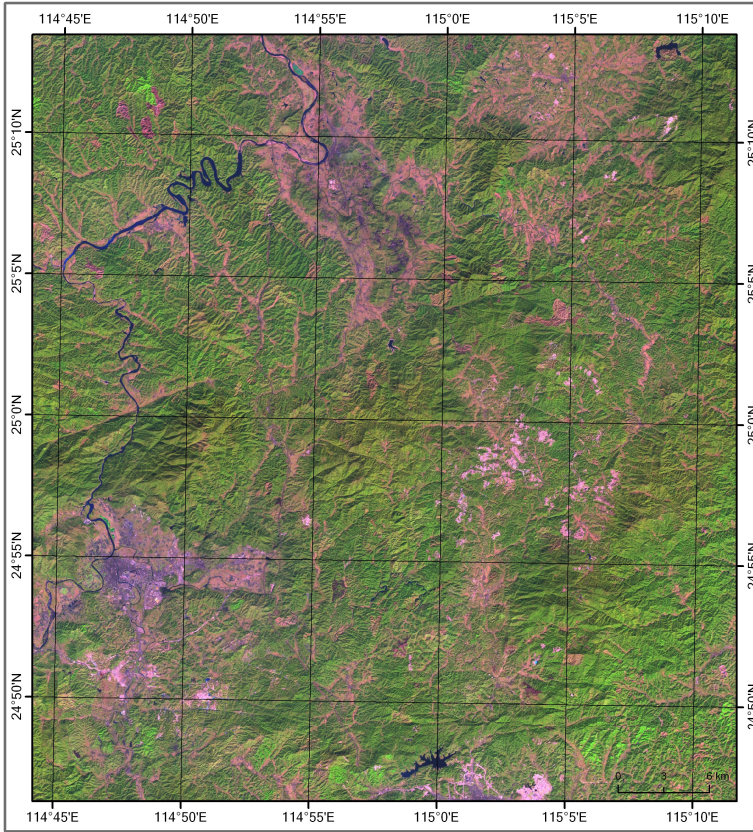


Fig. 2. The ortho-rectified SPOT5 imagery with 412 RGB combination covered study area

3.3 Image Interpretation Thumb

No matter traditional or advanced extraction technology, both ways would result in the land destruction or landslide, which would perform as the bare ground in the imagery. Given to the hilly country area, the land cover information with disturbed or destroyed by mining was easily identified in human interpretation, as shown in the Figure3. The target object was digitized and drew under ArcGIS10.0 from human interpretation. Each object was labeled by different land cover type. Topologic checking was conducted to confirm the classification result. The smallest size of object was 6 pixels by 6 pixels.

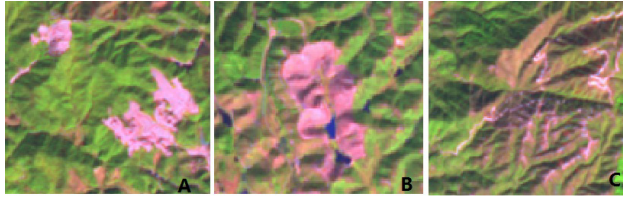


Fig. 3. The target object with pink color visualized in the imagery. A: The hill body was stripped; B: The vegetation was removed; C: The plants in the gully was destroyed.

4 Results and Analysis

The amount of patches in total was 524 with the area of 60.97km², which accounted for 3.03% in the study area. The largest patch size of destroyed area was 8.1km². The average patch size of destroyed area was around 1.30km². There were 513

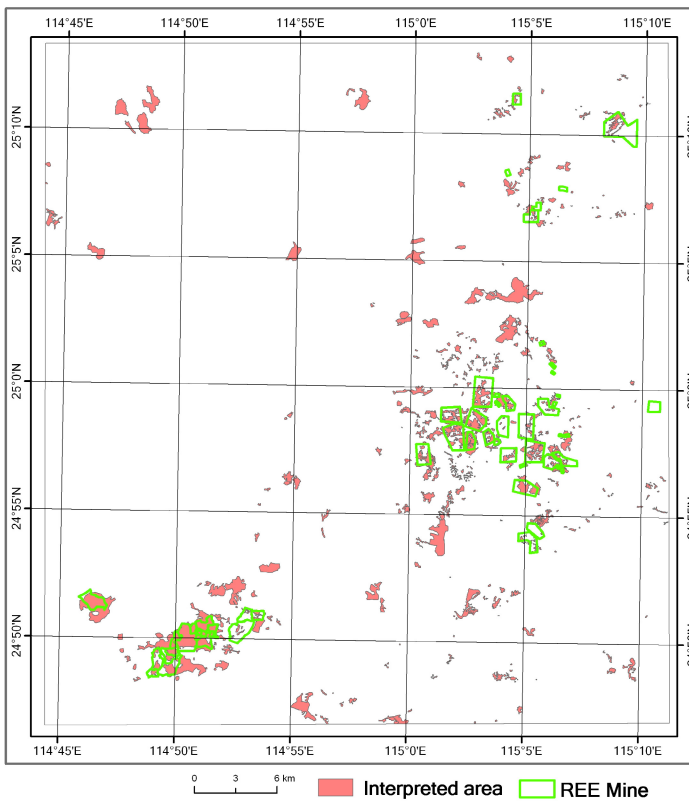


Fig. 4. The classified results by human interpretation. (REE mine: rare earth elements).

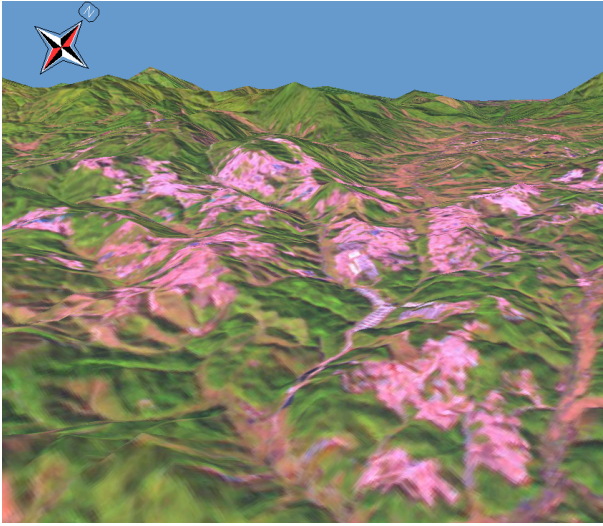


Fig. 5. 3D visualization in ArcGlobe

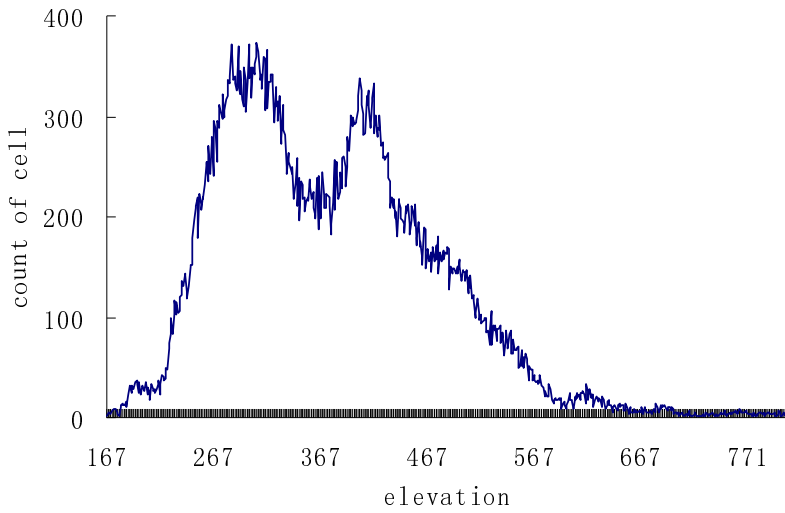


Fig. 6. The elevation distribution in mining area

patches of destroyed area less than 1km² distributed in the southwest of the study area. As shown in the Figure 4, the mining activities taken place at the east and south of this area, which corresponded to the classified results from the interpretation. The patches which represented the destroyed land cover can match the mining activities and mining lease.

The 3D analysis was conducted through ArcGlobe using SPOT and DEM data (Figure 5). Most REE mining activities mainly occurred on the top of the hill, which can be easily visualized from 3D imagery.

In order to analysis the landform of mining area, the interpreted polygons were converted to Grid by 30m resolution. Through overlaid with ASTERDEM, it was found that the elevation of the active mining area was between 300m to 500m, and the slope of that area was between 10 degree to 20 degree.

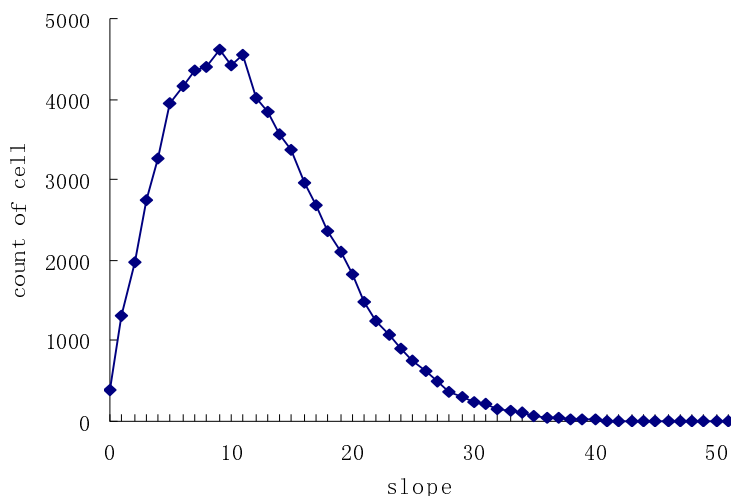


Fig. 7. The slope distribution in mining area

5 Field Survey

The field trip in the Quannan, Dingnan and Longnan district of Gannan area were taken on Nov. 2012 for the accuracy assessment. The photos collected from this trip showed that landform in this mining area was totally changed by exploitation and digging. As shown in the Figure8, the vegetation was removed and destroyed in the mining area, and the serious water and soil loss occurred in this area.



Fig. 8. The photos taken in Gannan mining area

6 Conclusion

Remote sensing has been a necessary and advanced technology in mining environmental monitoring, which can provide accurate, effective and comprehensive information for target object. The dynamic and update information from remote sensing technology can give a data support for Government and mining company to organize the environment rules and plan. Furthermore, high resolution imagery was required to acquire more detail information in mining area. Additionally, the small and disperse mining area should be integrated, which can be monitored and managed more easily and effectively.

References

1. Chen, H., Xu, X., Liu, Y.: Review of Researches on Remote Sensing Monitoring and Impact on Environment of Land Use/Cover Change. *Meteorological Science and Technology* 33(4), 289–294 (2005)
2. Bian, Z., Zhang, Y.: Land Use Changes in Xuzhou Coal Mining Area. *Acta Geographica Sinica* 61(4), 349–358 (2006)
3. Chen, L., Guo, D., Hu, Z., et al.: A Study on Remote Sensing Monitoring Land Use Change and Reclamation Measures of Subsidized Land in Xuzhou Coal Mining Area. *Progress In Geography* 23(2), 10–15 (2004)

4. Chen, H.-L., Chen, G., Guo, J.-Z.: The Application of Landsat TM for Ecological Environmental Monitoring in Mining Area. *Remote Sensing Information* (1), 31–34 (2004)
5. Wang, P., Liu, S.-F.: The detection of REE mine exploitation site change based on multi-temporal remote sensing images. *Remote Sensing for Land & Resources* 2, 65–68 (2007)
6. Lan, R.: The environmental problem and advice on Ion-adsorption Type Rare Earths Mineral. *Truth Seeking* (5), 174–175 (2004)
7. Chi, R.-A., Tian, J., Luo, X.-P.: The basic research on the weathered crust elution-deposited rare earth ores. *Nonferrous Metals Science and Engineering* 3(4), 1–13 (2012)
8. Liu, Y.: Water and soil loss and Treatment methods after Improved Rare Earth continuous mining technology. *Water Resources Development Research* 2(2), 30–32 (2002)
9. Zhao, J., Tang, X.-Z., Wu, C.: Status Quo of Mining and Recovering Technologies for Ion-absorbed Rare Earth Deposits in China. *Yunnan Metallurgy* 30(1), 11–14 (2001)

A Survey on Farmland Crop Information Acquisition

Danqin Yi and Haiyan Ji

College of Information and Electrical Engineering,
China Agricultural University, Beijing 100083, China
zita_zone@163.com, instru@cau.edu.cn

Abstract. The farmland crop information is the important foundation of developing fine agricultural practice. Crop information acquisition technologies have become the most effective means to increasing crop production and improving crop quality. In this paper, on the basis of introducing the characteristics of farmland crop data, different farmland crop information acquisition methods are surveyed in detail, sections need to be improved of these methods and related core technologies will be discussed. At last, this paper gives a table about crop information acquisition technology and sensing instrument systems applied in different levels (individual level, area level and wide-area level).

Keywords: precision agriculture (PA), crop information, information acquisition.

1 Introduction

All Food is the paramount necessity of human beings, and the essential material basis for any country on the way of development. China is a great agricultural country with large population, limited soil resources and traditional manual farming methods. With all these challenges, precision agriculture (PA) technologies have been used to improve field practices in crop production these years. PA provides a way to optimize agricultural production inputs, such as irrigation, fertilizing and spraying, based on farmland soil, environment and crop information at individual areas within a field, rather than applying uniform inputs across the entire field. In this way people can obtain not only the best economic benefits but also the ecological benefits.

The three main components involved in PA are information acquisition, data interpretation, and variable-rate application. The PA is an information-based technology. Only spatial information on field conditions as well as inputs and outputs of the field are accurately collected, can PA be successful [1]. The technology of farmland information acquisition directly affects the degree of agricultural informatization and the accuracy of agricultural production's decisions. How to get field soil, environment and crop information conveniently and quickly is the critical issue throughout the entire process of PA. Yet conventional acquisition method of farmland information, which mainly including traditional information retrieval methods and chemical diagnostic methods have many limitations. As to be known, appearance analysis method has strong subjectivity and poor accuracy; chemical

diagnosis is based on laboratory analysis of crop organizations, generally requires analyzing samples of crop, costs a lot of time, manpower and material resources [2]. The PA requires fast, real-time and positioning measurement. As the traditional crop information acquisition methods cannot meet the requirement of variable fertilization, we need to develop new methods, especially the technical method and sensing equipment can be used for fast acquisition of farmland information must be developed to meet the need of PA research and practice.

Farmland information can be divided into three parts: soil information, environment information, and crop information [3]. Soil information, including soil moisture, pH, organic matter content, conductivity, soil nutrients, and soil tillage resistance and etc. is the one of the main object of studying farmland information. Farmland environment information includes air temperature, humidity, light intensity, crop pests, and etc. Crop information includes crop growth information (such as canopy structure, leaf area index, plant height, etc.), crop nutrition information (including chlorophyll content, crop water status, nitrogen, phosphorus, potassium etc.) and some other information. Crop information is the most important index used in regulating plant growth, diagnosing crop nutrient deficiency, and predicting crop yields. All these information can make a contribution to agricultural land management and decision-making. High production, high-efficiency and modernizing agriculture can't become true without the help of all kinds of information.

In this paper, on the basis of introducing the characteristics of farmland data, different farmland crop information acquisition methods and related core technologies will be surveyed and discussed.

2 Characteristic of Farmland Crop Information

It is extremely important to instruct the agricultural production by knowing the crop it self's information. The farmland system is a very complicated ecology system, involves different kinds of factors. Even the crop itself is a complicated system. The collecting of crop data usually incurs the substantial costs and technologies [4]. To understand the characteristic of crop information fully is very necessary. There are the characteristic of farmland crop information. A) Spatiality. The production of crop is associated with spatial factors. Every farmland has its own geographic location and boundaries. Spatial data is usually used in generating different maps as coordinates. B) Complexity. Any agricultural system has huge factors include not only directly related factors but also indirectly related factors. Each factor contains its sub-factors. Farmland crop data can be collected from multiple sources such as onboard sensors, handheld devices, remote sensing, satellite, history material, etc. Categories of data are diverse, including text, number, image, sound, video, etc. C) Dynamics. All the information is changing all the time according to the time and space [5]. In-time acquisition of data is vital for PA. After all, all these factors increase the difficulty of getting agricultural crop data. People need to master high-tech and stable measurements or means to shield interference and obtain accurate data.

3 Crop Information Acquisition Methods

Crop information includes crop growth information, crop nutrition information, and some other information.

3.1 Crop Growth Information

Ground observation, remote sensing monitoring and model simulation are the main methods of monitor crop growth and development information. The leaf area index (LAI), canopy characterization, canopy structure, plant height and other growth factors are the main target be measured to monitor crop-growing status [6].

Remote sensing is becoming more and more popular for its unique advantages. M. Susan Moran et al. [7] successfully used aerial and satellite remote sensing data to inverse normalized difference vegetation index (NDVI) values, which can be used for diagnosis, estimation and production forecasting of large area crops [8]. Huang Jingfeng et al. [9] established Rice-SRS model to estimate the yield of rice with spectral normalized vegetation index obtained by NOAA/AVHRR satellite. Peng Xiao et al. [10] used the TM remote sensing image to obtain NDVI and inverse the LAI of rice. On the basis of domestic airborne imaging spectrum data and the spectral response of the synchronous sampling data, Yang Minhua et al [11] established wheat canopy physical and chemical parameters estimation model and realized the inversion of wheat canopy physical and chemical parameters through aerial hyper spectral remote sensing.

Infrared beam, ultrasonic, microelectrode constant current source technology and some other technologies can be used to monitor and analyze growing crops directly. Shimizu H et al. [12] used machine vision technology to non-contact measure three-dimensional growth information of crops. Zhao Chunjiang et al. [13] developed an instrument to inverse LAI, vegetation cover degree, biomass index to assess crop condition. This instrument uses the near-infrared and red characteristic bands, and detects the incident light and the reflected light of vegetation to get the NDVI (normalized difference vegetation index) values. Aziz S A et al. [14] studied ultrasonic sensing technology. They used it as one approach for corn plant canopy characterization. Lan Yubin et al. [15] developed a ground-based Multi-sensor fusion integration system, including a crop height sensor, a crop canopy analyzer for LAI, a NDVI sensor, a multispectral camera, and a hyper spectroradiometer to measure real-time crop conditions involve NDVI, biomass, crop canopy structure, and crop height. Qu Yonghua et al. [16] developed an automatic system designed on the basis of wireless sensors network (WSN) to collect crop structure parameters, like LAI and average leaf angle (ALA).

Plant height is an important parameter to be considered for management decision making. Plant height is a sensitive indicator to show plant health status and calculate yield potential in optimizing field inputs. Sui Ruixiu et al. [17] used ultrasonic sensors to develop a microcomputer-based measurement system to allow in-situ, non-destructive measurement for the morphological characteristics of bush-type plants. Searcy S W et al. [18] developed and field-tested an infrared beam sensor mounted on

a mechanical arm, using a “light curtain” for the cotton plant real-time height measurement. Tumbo S D et al. [19] successfully used ultrasonic sensors in the measurement of citrus tree volume. Ehsani M R et al. [20] investigated a laser-based sensor which can realize real-time estimate of plant volume. The sensor also performed well in measuring the biomass and LAI of a plant after being calibrated. Jones C L et al. [21] used ultrasonic distance sensing to realize plant height data collection, and estimated plant biomass using the product of top-view surface area of the plant. Sui Ruixiu et al. [22] used an ultrasonic sensor installed on a field vehicle such as a sprayer to scan the plant canopy and determine plant height in real time in situ. A plant height map was generated with the collected data by the sensor.

3.2 Crop Nutrition Information

For crop chlorophyll content nondestructive testing, MINOLTA company in Japan has produced a kind of Chlorophyll meter, which emit red light (about 650nm) and near infrared light (about 940nm) by the light emitting diode to the receiver through the leaf samples. The receiver receives the signals and transfers them into digital signals that will be used by the microprocessor to calculate the SPAD value. Yao Jiansong et al. [23] used visible-near infrared spectroscopy techniques to non-destructive test rape leaf chlorophyll content information. Liu Fei et al. [24] used visible/near infrared spectrum technology, quickly and accurately detected cucumber leaf SPAD value, which is helpful to the development of testing equipment.

Nitrogen is one of the most important factors that have a high impact on the production of crops. The main methods of monitoring nitrogen are remote sensing imaging, machine vision technology, spectrum analysis technology, Multi-spectral and hyperspectral imaging technology [25]. The remote sensing based crop nitrogen nutrition diagnosis, most people use remote sensing to inverse nitrogen concentration, nitrogen accumulation and other parameters which can determine crop nitrogen nutritional status [26]. He Yong et al. [2] developed a portable plant nutrients lossless tester to determine plant chlorophyll, water, nitrogen content quickly, non-destructive, and simultaneously. This instrument has a GPS and a wireless data transmission function. Combined with GIS software management system, large-scale crop nutrient content distribution map can be developed. Feng lei et al. [27] put the rape as the research object, used computer multi-spectral imaging technology for rapidly, accurately and non-destructive nitrogen diagnosis.

Crop water information collection is the basis of precision irrigation decision-making. It is a key for continuously, quickly, and precisely information collecting. Crop water information is helpful to develop advanced and reliable monitoring equipment. Crop water status information collection technologies of crop individual include infrared temperature method, leaf water potential, spectral method, etc. Regional crop water status information is mainly obtained through remote sensing methods, including thermal infrared remote sensing and microwave remote sensing methods [28]. Ji Haiyan et al. [29] used near-infrared spectroscopy, developed a living plant leaves water testing instrument which adopts ultra-low-power microprocessor MSP430 and new type of optical frequency conversion chip TSL230,

enabled field site fast non-destructive testing of crop leaf water content. Li Dongsheng et al. [30] developed the leaf temperature-measuring instrument, using infrared thermometry to measure leaf temperature to estimate leaf moisture state.

Canopy temperature relative to ambient air temperature is often used to assess plant stress caused by moisture deficit or high temperature [31] [32]. Continuous measurement of plant canopy temperature is useful in both research and agricultural production. James R. Mahana et al. [33] studied a low-cost infrared sensor based wireless temperature monitoring system, assessed the system's reliability and stability, and verified the feasibility of low-cost infrared temperature measurement system. O'Shaughnessy et al. [34] developed a wireless sensor system comprised mainly of infrared thermometer thermocouples located on a center pivot lateral and in the field below to monitor crop canopy temperatures. Daniel K. Fisher et al. [35] developed and constructed a low-cost microcontroller based system to monitor the temperature and the water status of crop. The system can realize automatic measurement of canopy temperature, soil temperature, air temperature, and soil moisture status in field. It includes a digital infrared temperature sensor, choose MLX90614 (Melexis, Concord, NH) infrared temperature module to get the plant canopy (leaf) temperature. The precision of the system is 0.3 degrees Celsius by experiments.

3.3 Others

Crop yield is the result of many factors, is the important data of the variable assignment management [36]. Commercialized grain yield monitor systems are mainly the AFS (advanced farming system) system (CASE IH Corporation, U.S.), the FieldStar system (AGCO Corporation, British), the Greenstar system (JohnDeree Corporation, USA), the PF (precision farming) system (AgLeader Corporation, USA), the production monitoring system of RDS, etc. All these systems are equipped with GPS positioning system, can automatically monitor crop production and make a crop yield map. Cereal production yield monitor sensor is the core of these systems, including the photoelectric volumetric flow sensor, the γ -ray impulse flow sensor and the impulse type flow sensor [3]. Some portable information collection and transmission systems have combined with GPS, GPRS or Zigbee technology, were built to obtain pictures, sounds, numbers, GPS information or any other data of field crops [37-40].

4 Discussions and Conclusions

4.1 Crop Information Acquisition

There have been many associated reports about rapid detection methods and instruments of the nitrogen content, chlorophyll content, and moisture content. And there are also some reports about detection methods of phosphorus and potassium content. But the report about crop trace information is less. This is mainly because the

main crop trace information is metal elements based, and their content is low. The ordinary sensing technology still not meets the requirements, and the use of spectrum and spectral imaging technologies doesn't directly react to metal element information.

4.2 The Core Technologies

- GPS

Farmland location information, which including latitude, longitude, shape and size of farmland, is mainly obtained through GPS (global positioning system). GPS technology is currently widely used in agricultural crop information acquisition systems, can be combined with crop information to make crop distribution map.

- Multi-sensor information fusion technology

Multi-sensor information fusion technology is a comprehensive automated information processing technology [41]. The use of real-time multi-sensor information fusion technology has become a new hot spot to simultaneously measure multiple parameters [42].

- Wireless communication technology

Wireless communication can be classified as long-distance communication (GSM, GPRS, etc.) and short-range communications (Bluetooth, Zigbee, RFID, etc.) [43]. GSM and GPRS, based on mobile communication network, can achieve remote agricultural information acquisition and monitoring. Wireless sensor networks, which has developed in recent years, integrate sensor technology, embedded technology, modern networking and wireless communication technology. It can achieve real-time data transmission via low-power short-range wireless communications technology (such as Wifi, Bluetooth, Zigbee, RFID, etc.). Farmland information self-organizing wireless sensor network system can be established.

- Multispectral / Hyperspectral imaging technology

As spectroscopic technique is easily affected by soil background, environment, crop canopy structure, the obtained spectrum signal is not able to completely react crops truthful information. Multispectral and hyperspectral imaging technology can make up for these shortcomings [2]. The researches about multispectral and hyperspectral imaging technology used in the crop phosphorus, potassium, and trace information are less. But there are already reports about multi-spectral imaging technology applied to detect the moisture content of crop leaves [44]. We had better establish the quantitative relationship between the spectral characteristics and crop growth/nutrition information and develop crop information equipment.

4.3 Conclusion

PA is an information-based technology. PA can use crop information in the farmland to control the arrangement of production inputs, maximize crop profit, and minimize environmental impact. Information acquisition and processing plays a very important role in PA. As shown in table 1, after understanding crop information acquisition methods, combined with the current situation and development trend, a structure about crop information acquisition technology and sensing instrument system is listed.

Table 1. Crop information acquisition technology and sensing instrument system structure

Level	Features of Object	applied technology innovation	Application characteristics
Individual	·Individual information for crops ·Farmland environmental factors interference	·Non-contact measurement ·The embedded system	·Quick and non-destructive detective ·Portable ·Handheld
Area	·Complicated environment ·Need location information	·Spectroscopy ·Multi-spectral imaging technology ·GPS	·Vehicular
Wide-area	·Spatiality ·Irregular shape of farmland	·Remote sensing technology ·Wireless sensor network	·Teletransmission

References

1. Wang, M.: Development of Precision Agriculture and Innovation of Engineering Technologies. Transactions of the Chinese Society of Agricultural Engineering 1 (1999)
2. He, Y., Zhao, C., Wu, D., Nie, P., Feng, L.: Fast detection technique and sensor instruments for crop-environment information: A review. Scientia Sinica, Informationis S1 (2010)
3. Wang, F., Zhang, S.: Research Progress of the Farming Information Collections Key Technologies on Precision Agriculture. Transactions of the Chinese Society for Agricultural Machinery 5 (2008)
4. Liu, X., Nelson, M., Ibrahim, M.: The Value of Information in Precision Farming. Paper of the Southern Agricultural Economics Association Annual Meeting (2008)
5. Duan, Y., Niu, X.: Research on Farmland Information Acquisition System Based on IoT. Advanced Materials Research (Volumes 532 - 533) (2012)
6. Zhang, G., Chen, H., Zhou, G.F., Ge, G.M.: A Survey on Crop growth dynamic monitoring technology. Chinese Meteorological Society 9 (2010)
7. A RADARSAT-2 Quad-Polarized Time Series for Monitoring Crop and Soil Conditions in Barrax, Spain. IEEE Transactions on Geoscience and Remote Sensing 50(4) (2012)
8. He, D., He, Y., Li, M., Hong, T.: Research Progress of Information Science-related Problems in Precision Agriculture. China Academic Journal Electronic Publishing House 01, 10–16 (2011)
9. Huang, J., Tang, S., Ousama, A., et al.: Rice yield estimation using remote sensing and simulation model. J. Zhejiang U Sci. A 3, 1862–1775 (2002)
10. Peng, X., Zhang, S.: Research on Rice Growth Status Based on NDVI and LAI. Remote Sensing Technology and Application 1 (2002)
11. Yang, M., Liu, L., Liu, T., et al.: Research on a Method to Retrieve Biophysical and Biochemical Parameters of Wheat Canopy with Hyperspectral Remote Sensing. Geodaetica Et Cartographic Sinica 4 (2002)
12. Shimizu, H., Heins, R.D.: Computer vision based system for plant growth analysis. Trans. ASAE 38, 958–964 (1995)

13. Zhao, C., Liu, L., Zhou, H., et al.: Development and application of a novel NDVI instrument. *Optical Technique* 30(3), 324–326, 329 (2004)
14. Aziz, S.A., Steward, B.L., Birrell, S.J., Shrestha, D.S., Kaspar, T.C.: Ultrasonic sensing for corn plant canopy characterization. ASAE Paper No. 041120. St. Joseph, Mich.: ASAE (2004)
15. Lan, Y., Zhang, H., Lacey, R., Hoffmann, W.C., Wu, W.: Development of an Integrated Sensor and Instrumentation System for Measuring Crop Conditions. *Agricultural Engineering International: CIGR Journal* (2009)
16. Qu, Y., Wang, J., Dong, J., et al.: Design and experiment of crop structural parameters automatic measurement system. *Transactions of the CSAE* 28(2), 160–165 (2012)
17. Sui, R., Wilkerson, J.B., Wilhelm, L.R., Tompkins, F.D.: A microcomputer-based morphometer for bush-type plants. *Computer and Electronics in Agriculture* 4, 43–58 (1989)
18. Searcy, S.W., Beck, A.D.: Real time assessment of cotton plant height. In: *Proceedings of Fifth International Conference on Precision Agriculture (CD)*, Bloomington, MN, USA (2000)
19. Tumbo, S.D., Salyani, M., Whitney, J.D., Wheaton, T.A., Miller, W.M.: Investigation of laser and ultrasonic ranging sensors for measurements of citrus canopy volume. *Applied Engineering in Agriculture* 18(3), 367–372 (2002)
20. Ehsani, M.R., Lang, L.: A sensor for rapid estimation of plant biomass. In: *Proc. the 6th Intl. Conf. on Precision Agri.*, Bloomington, MN, pp. 14–17 (July 2002)
21. Jones, C.L., Maness, N.O., Stone, M.L., Jayasekara, R.: Sonar and digital imagery for estimating crop biomass. ASAE Paper No. 043061. St. Joseph, Mich.: ASAE (2004)
22. Sui, R., Alex Thomasson, J., Ge, Y.: Development of Sensor Systems for Precision Agriculture in Cotton. *Int. J. Agric. & Biol. Eng.* 5(4), 1–14 (2012)
23. Yao, J., Yang, H., He, Y.: Nondestructive Detection of Rape Leaf Chlorophyll Level Based on Vis/NIR spectroscopy. *Journal of Zhejiang University (Agriculture and Life Sciences)* 4 (2009)
24. Liu, F., Wang, L., He, Y., Bao, Y.: Detection of SPAD Value of Cucumber Leaves Based on Visible/near Infrared Spectroscopy Technique. *Journal of Infrared and Millimeter Waves* 4 (2009)
25. Li, G., Zhu, L., Li, J.: Present Status of Research and Application of Non-destructive Measurement of Nitrogen Nutrition Diagnosis. *Heilongjiang Agricultural Sciences* 4, 127–129 (2008)
26. Chen, P., Sun, J., Wang, J., et al.: Using remote sensing technology for crop nitrogen diagnosis: status and trends. *Scientia Sinica (Informationis)*, S1 (2010)
27. Feng, L., Fang, H., Zhou, W., et al.: Nitrogen Stress Measurement of Canola Based on Multi-Spectral Charged Coupled Device Imaging Sensor. *Spectroscopy and Spectral Analysis* 9, 1749–1752 (2006)
28. Duan, A., Meng, Z.: Present Situation of Techniques and Equipments of Monitoring Crop Water Status. *Review of China Agricultural Science and Technology* 9(1), 6–14 (2007)
29. Hou, R., Ji, H., Rao, Z., et al.: Water detection instrument design for living leaves based on near infrared spectroscopy. *Transactions of the Chinese Society of Agricultural Engineering* S2 (2009)
30. Li, D., Guo, L., Guo, C., et al.: Development of leaf temperature measuring instrument and its application in plant leaf parameter measurement. *Transactions of the Chinese Society of Agricultural Engineering (Transactions of the CSAE)* 28(5), 139–144 (2012)

31. González-Dugo, M.P., Moran, M.S., Mateos, L., Bryant, R.: Canopy temperature variability as an indicator of crop water stress severity. *Irrigation Science* 24, 233–240 (2006)
32. Reynolds, M.P., Pierre, C.S., Saad, A.S.I., Vargas, M., Condon, A.G.: Evaluating potential genetic gains in wheat associated with stress-adaptive trait expression in elite genetic resources under drought and heat stress. *Crop Science* 47, 172–189 (2007)
33. Mahana, J.R., Conaty, W., Neilsen, J., Payton, P., Cox, S.B.: Field performance in agricultural settings of a wireless temperature monitoring system based on a low-cost infrared sensor. *Computers and Electronics in Agriculture* 71, 176–181 (2010)
34. O’Shaughnessy, S.A., Evett, S.R.: Developing Wireless Sensor Networks for Monitoring Crop Canopy Temperature Using a Moving Sprinkler System as a Platform. *Applied Engineering in Agriculture* 26(2) (2010)
35. Fisher, D.K., Kebede, H.: A low-cost microcontroller-based system to monitor crop temperature and water status. *Computers and Electronics in Agriculture* 74, 168–173 (2010)
36. Thylen, L., Murphy, D.P.L.: The control of errors in momentary yield data from combine harvesters. *Journal of Agriculture Engineering Research* 64(4), 271–278 (1996)
37. Kuang, Y., Xiao, M.: The Field Information Collection Apparatus. *Journal of Agricultural Mechanization Research* 8 (2010)
38. Cai, Y., Liu, G.: Development of portable system of field information collection and wireless transmission. In: Proceedings of Commemorate the Chinese Society of Agricultural Engineering was established 30 anniversary of Chinese Society of Agricultural Engineering 2009 Annual Conference, CSAE 2009 (2009)
39. Xu, X., Li, Z., Zhang, J.: The Design of Portable Cropland Information Collection Equipment Base on GPRS and GPS Technology. *Journal of Agricultural Mechanization Research* 8 (2008)
40. Zheng, X., et al.: Study on Design of Farmland Information Acquisition and Transmission System Based on ZigBee. *Journal of Anhui Agricultural Sciences* 6 (2003)
41. Li, X., Wang, W., Lei, T., et al.: Prospects of the application of multi-sensor information fusion techniques in agricultural engineering. *Transactions of the CSAE* 19(3), 10–12 (2003)
42. Han, C., Zhu, H.: Multi-sensor information fusion and automation. *Acta Automatica Sinica* (S1), 117–124 (2002)
43. Yang, W., Li, M., Wang, X.: Status quo and progress of data transmission and communication technology in field information acquisition. *Transactions of the CSAE* 24(5), 297–301 (2008)
44. Ramalingam, N., Ling, P.P., Derksen, B.C.: Background reflectance compensation and its effect on multispectral leaf surface moisture assessment. *Trans. ASAE* 48, 375–383 (2005)

Self-tuning PID-type Fuzzy Adaptive Control for CRAC in Datacenters

Junwen Deng¹, Liu Yang¹, Xinrong Cheng², and Wu Liu¹

¹ College of Engineering, China Agricultural University, Beijing 100083, China

² College of Information and Electrical Engineering,

China Agricultural University, Beijing 100083, China

{563106956,1151781485}@qq.com, yangliu@cau.edu.cn

Abstract. In order to eliminate the current negative condition of Automatic Computer Room Air-Conditioning (CRAC) system, self-tuning Fuzzy Logic Control (FLC) was designed and applied to fan speed in CRAC system. In this paper, we derive a thermodynamic model of a datacenter suitable for applying adaptive self-tuning PID-type fuzzy adaptive control theory. It combines the classic PID control strategy and fuzzy adaptive control theory. The classic PID control uses the error and rate of change of error as its inputs to control the temperature automatically, and the fuzzy logic controller is used in the self-tuning PID-type fuzzy control to tune the parameters of PID controller on-line by fuzzy control rules. Simulation and testing results show that the proposed self-tuning FLC method can achieve less steady-state error and short settling time in temperature control of datacenter.

Keywords: Air-Conditioning (CRAC) system, self-tuning Fuzzy control, adaptive control.

1 Introduction

Significant temperature pressure has been placed on traditional datacenters thermal management by increasing server power dissipation. Automatic Computer Room Air-Conditioning (CRAC) system improvement challenges have been steadily increasing over the past few years due to an increase in energy consumption and heat generation in datacenters. CRAC fan speeds have a significant effect on the recirculation flows in the datacenter, which are verified to be a major cause of inefficiency [1-3]. The energy needed for adjusting fan speed is much lower than the energy needed for adjusting the duty cycle of air compressor. For this reason, flexible design of CRAC fan speed optimization system supplying demand is substantially to reduce the energy consumption.

So far, classic control techniques, such as Proportional-Integral-Derivation (PID) controllers are still widely used in practice as they can be easily implemented, are low cost and reliable in harsh field condition. K_p , K_i and K_d parameters of PID were obtained to minimize the system error in many studies.

Recently, some complex control strategies based on classical control concepts have been proposed in attempts to improve the system performances. Salsbury described a feed forward control scheme based on a simplified physical model as a supplement of the conventional PI feedback control [4]. Kasahara et al. proposed a robust PID control scheme to deal with the model uncertainty caused by the changing characteristics of the plant [5]. Bi and Cai et al. developed an advanced auto-tuning PID controller for both temperature and pressure control [6].

Classic control schemes commonly use the first order or second order plus time delay models to represent process dynamics. The performances of these control schemes are limited when applied to CRAC process due to their inherent nonlinearity and time varying nature. To overcome these drawbacks, applications of intelligent control to CRAC system have drawn some interests. Some authors proposed fuzzy PID methods to improve performance of the control system. In Shayeghi H, Shayanfar HA, and Jalili's pervious papers [7] and [8], the authors proposed an improved control strategy based on fuzzy theory and genetic algorithm (GA) technique have been proposed. Fuzzy logic (FLC) of heating, ventilating and air-conditioning system was studied by Shan AJ, Krishnan N and Schmidt RR [7, 9]. The obtained results were comparing with those of PID control and these studies indicated that FLC had better result. However, the steady-state error was not totally eliminated. Existing work on thermal management in data centers, however, not take into account unexpected thermal anomalies and neglect the cost of control actions taken by the air conditioning system. This can lead to overheating of some spots. Obtaining better performances of the simulated systems became easier [10]. To eliminate this negative condition, self-tuning FLC was designed and applied to fan speed in CRAC system.

2 Related Work

In this paper, we derive a thermodynamic model of a data center suitable for applying adaptive self-tuning PID-type fuzzy adaptive control theory. We propose a novel control strategy based on this model. It combines the classic PID control strategy and fuzzy adaptive control theory. The classic PID control uses the error and rate of change of error as its inputs to control the temperature automatically and the fuzzy logic controller is used in the self-tuning PID-type fuzzy controller to tune the parameters of PID controller on-line by fuzzy control rules. It was shown that the usage of modeling and simulation methods for analyzing, testing and developing of CRAC systems decreases the design cost as well as the duration of the design process. Simulation and testing results show that the proposed self-tuning FLC method can achieve good performance in temperature control of datacenter.

3 The Thermal Model of the Datacenter

Fig.1 shows the layout of datacenter and location of a blade. Datacenter design plays an important role in the efficient thermal management. Chilled water CRAC units supply a raised floor plenum underneath the racks with cold air. Perforated tiles are located near the racks to transfer the cool supply air to the front of the racks.

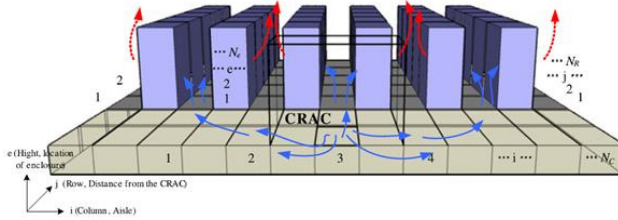


Fig. 1. The Layout of datacenter and location of a blade

As the CRAC system has featured such as considerable interference, non-linearity, large time delay, uncertainty and non-predicative, it is difficult to obtain the accurate mathematical model of thermodynamic in datacenter by considering all parameters. For this reason, we consider the following assumptions: According to the law of the energy conservation, the mathematical equation for datacenter thermal is as follows:

$$c_a v_a \rho_a \frac{dt_d}{dt} = c_a \rho_a f_a (t_d - t_a) - A_s \mu_s (t_s - t_d) + q_n + q_m \tag{1}$$

$$q_m = c_m m_m \frac{dt_m}{dt} = \mu_m A_m (t_m - t_d) \tag{2}$$

As most equipment in datacenter are made of irons, they have large coefficient of heat conductive, so we assume temperature variety rate has not much difference between equipment temperature variety rate.

$$\frac{d_m}{dt} = n_m \frac{dt_d}{dt} \tag{3}$$

If the fan motor heat dissipation is ignored, the equation (1) can be transferred to transfer function form as follows:

$$\begin{aligned} c_a v_a \rho_a s - c_m m_m n_m s - c_a \rho_a f_a t_d - A_s t_s \\ = -c_a \rho_a f_a t_a - A_s t_s \end{aligned} \tag{4}$$

If c is defined as CRAC hybrid equivalent thermal capacity as follows:

$$c = c_m m_m n_m - c_a v_a \rho_a \tag{5}$$

And R is defined as CRAC entire thermal resistance and R_s is defined as Surrounding walls, floor and roof thermal resistance as follows:

$$R_s = \frac{1}{A_s \mu_s} \tag{6}$$

After standard arrangement the result is as follows:

$$t_d(s) = \frac{k_d t_a(s)}{Ts + 1} + \frac{K_s t_s(s)}{Ts + 1} \tag{7}$$

The time constant and other parameters are as follows:

$$T = C * R \tag{8}$$

$$K_d = K * R \tag{9}$$

$$K_s = \frac{R}{R_s} \tag{10}$$

As the air heat transfer delay affects the datacenter temperature, consider delay time is, the equivalent transfer to be as follows:

$$t_d(s) = \frac{k_d t_a(s)}{Ts + 1} e^{-\tau s} + \frac{K_s t_s(s)}{Ts + 1} e^{-\tau s} \tag{11}$$

Setting the real-time temperature in the datacenter is 27, and the expected temperature in the datacenter is 20. The air flux of the datacenter was determined by the fan speed at end, Fan speed control is the core technology in Variable Air Volume (VAV) air condition system. It decides the liability and energy saving level of the CRAC system in the database. The fan speed is controlled by the open volume of the air condition. The transfer function of open volume to temperature can be expressed as an object of second-order inertial and net delay:

$$G(S) = \frac{10e^{-12s}}{(1 + 20s)(1 + 30s)} \tag{12}$$

The database CRAR system Mathematic Model is showed in figure 2. In the model, $U(t)$ is the output of the controller and $y(t)$ is the actual temperature of the database room.

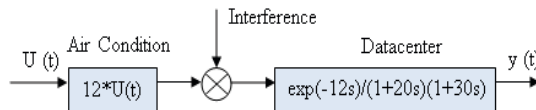


Fig. 2. CRAR System Mathematic Model

Table 1. Notation

Nomenclature	
C_a	Air specific heat [J/kg °C]
V_a	Air volume [m ³]
ρ_a	Air density [kg/m ³]
t_d	Real-time air temperature in dry test-bed [°C]
f_a	Fan air volume delivery [m ³ /s]
t_a	AGDR air temperature [°C]
t_s	Temperature of surroundings [°C]
t_m	Temperature of equipment [°C]
A_s	Area of surroundings [m ²]
μ_s	Coefficient of convective heat exchange between surrounding and air [w/(m ² °C)]
q_n	Fan motor heat dissipation [w]
q_m	Equipment heat dissipation [w]
c_m	Equipment specific heat [J/(kg °C)]
m_m	Equipment mass [kg]
μ_m	Coefficient of convective heat exchange between equipment and air [w/(m ² °C)]
A_m	Area of equipment [m ²]
n_m	Coefficient of dry test-bed temperature variety rate to equipment temperature [w/°C]
C	AGDR hybrid equivalent thermal capacity [F]
R	AGDG entire thermal resistance [Ω]
R_s	Surroundings thermal resistance [Ω]

4 Self-tuning PID-type Adaptive Control

The control system is optimized through the whole working range of the process and ensures a maximum of control loop quality by a very short response time of any alternation in the process and at a negligible overshooting of the process value during the control phase. The fuzzy controller showed enormous advantages in processed with intensive nonlinearity. An incremental fuzzy logic controller is used in the self-tuning PID-type fuzzy controller to tune the parameters of PID controller on-line by fuzzy control rules. The controller uses the error and rate of change of error as its inputs and can meet the desire of self-tuning parameters based on time-varying e and \dot{e} , and the output of the fuzzy controller is u .

$$u(k) = K_p e(k) + k_i \sum_{i=0}^k e(i) + k_d [e(k) - e(k-1)] \quad (14)$$

The database CRAR system Mathematic Model is showed in Fig.2. In the model, $U(t)$ is the output of the controller and $y(t)$ is the actual temperature of the database room. Where k_p is the controller gain.

$$K_d = \frac{k_p T}{T_i} \tag{15}$$

T is the sample time; T_i is the integral time parameter, T_d is the derivative time parameter [11]. The sub-block of language was given in the following manner: Positive Big (PB), Positive Middle (PM), Positive Small (PS), Zero (ZO), Negative Small (NS), Negative Middle (NM), Negative Big (NB).The output of the fuzzy systems is u . The fuzzy variables are defined for the rule base as: $(e, \dot{e}) = \{\text{the error, the variation of error}\}$, $\{\text{NB, NS, Z, PS, PB}\}$. $k_p, k_d, k_i = \{\text{the control parameters, Z, PS, PM, PB, PVB (Positive Very Big), [0,1], 1}\}$. Fig.3 shows the rule base fuzzy PID-type control and the rule K_i fuzzy.

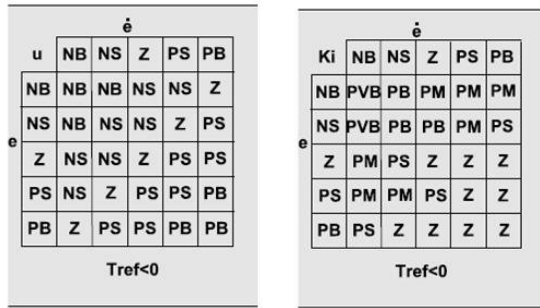


Fig. 3. (a) Shows the rule base fuzzy (b)Shows the rule K_i fuzzy

A membership function is a curve that defines how each point in the input space is mapped to a membership value (on degree of membership) between 0 and 1. In our study we will employ the trapezoidal membership functions for each fuzzy linguistic value of error e and the change rate of error \dot{e} showed in Fig.4.

By applying the self-tuning PID-type fuzzy adaptive controller, the control of the same CRAC system has been realized in order to compare of the control performance. The classical PID and FLC theories are combined in this study. The K_p, K_i, K_d values of PID parameters have adaptively been determined by using the dynamic FLC for each time-step. In this case, FLC has two inputs (e, \dot{e}) and three outputs (K_p, K_i, K_d) . The physical domain of the inputs (e, \dot{e}) is -1, -0.8, -0.6, -0.4, -0.2, 0, 0.2, 0.4, 0.6, 0.8,1 and that of the outputs (K_p, K_i, K_d) is 0, 0.1, 0.2,0.3, 0.4, 0.5, 0.6, 0.7, 0.8, 0.9, 1, selected again based on trial and error. Fig.5 shows the membership functions of output u .

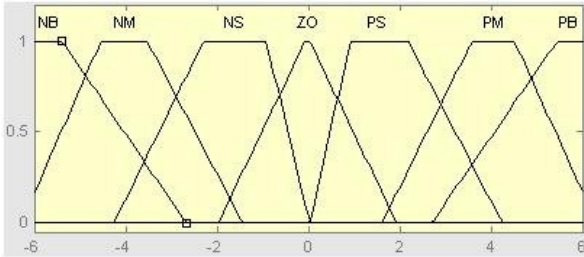


Fig. 4. The membership functions for the input e and \dot{e}

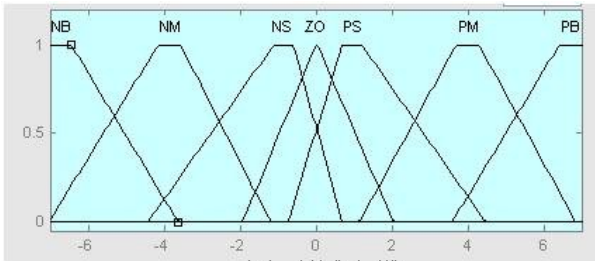


Fig. 5. The membership functions for the output u

5 The Numerical Simulation of the CRAC System

By using MATLAB/SIMULINK package program, the control, model and numerical simulation of CRAC fan system have been realized. The control diagram of CRAC fan system has been obtained by considering the input and output values of the device and the desired datacenter conditions. The obtained results have been presented in a graphical form. Every PID control system has its parameter range. It will result in unreliability and out of control if the parameters are out of the range. In the CRAC control system, the PID parameters are tuned by fuzzy inference. According to simulation, the tuning range of parameter K_p is between [25.4, 40.5], the tuning range of parameter K_i is between [0, 0.5] and the tuning range of parameter K_d is between [15.2, 20.6]. If the system is overshoot, first decrease the parameter K_p , then decrease the parameter K_i and in the end decrease the parameter K_d . If the system has long settling time, first decrease the parameter K_i , then decrease the parameter K_p and in the end decrease the parameter K_d . If the system has short settling time and High frequency fluctuations, first decrease the parameter K_d , then decrease the parameter K_p and in the end decrease the parameter K_i . The considered CRAC system controlled by the fuzzy-PID type and self-tuning PID-type fuzzy adaptive controller is shown in the block diagram Fig.6. T_{ref} is the desired reference temperature and T is the real temperature in datacenter. The PID parameters are tuned by adaptive fuzzy controller. Fig.6 shows the diagram of self-tuning fuzzy-PID control simulation system of CRAC fan. PID control model, fuzzy PID model [12] and self-tuning fuzzy-PID control model are respectively

established in the control link of the room temperature control and are contrasted through the MATLAB simulation [13]. Transferred discrete PID controller module from the sub-library of Simulink [14], after repeated experiments, took the ratio coefficient $K_p=171$, integral time constant $K_i=0.001$, differential time constant $K_d=10$ in PID control system [15]. The design idea of fuzzy-PID control is to find out the fuzzy relationship between 3 parameters of fuzzy- PID control and deviation e , change rate of deviation Δe , continuous detection e and calculation the Δe during the operation and online modified control parameters in accordance to the control principle, to meet the different requirements in different e and Δe , so that the controlled object has a good dynamic and static properties. We choose the set point to react based on the temperature in which ranges from 64.4F (18°C) to 80.6F (27°C).

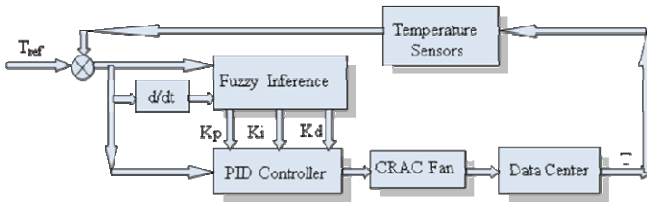


Fig. 6. The control diagram of CRAC fan system

Fig.7 shows the temperature control of datacenter when the classical PID, fuzzy-PD type and the self-tuning PID-type fuzzy adaptive controller are applied [16]. To simulate and compare facilitate the control model, set the supposed temperature for 25.5, simulate time for the 1500s.

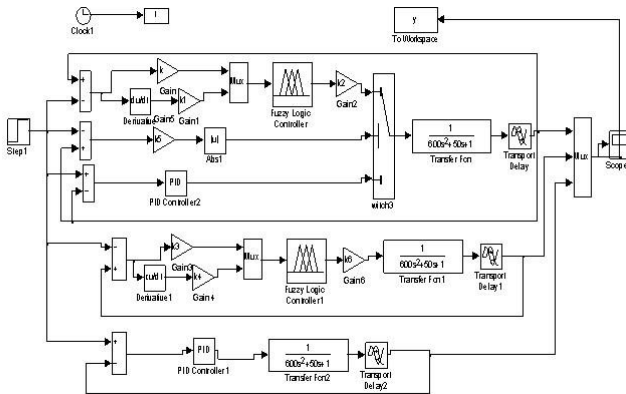


Fig. 7. The diagram of self-tuning fuzzy-PID control, fuzzy-PID control and PID control simulation

Fig.8 shows the simulation results: (1) PID control. More sensitive to interference [17], control is not satisfactory, with a large overshoot. The simulation found that there will be instability if the interference is too large. (2) General fuzzy-PID control.

Subjective the control rules, there is no self-learning function. The simulations found that the domain of fuzzy controller had been changed, required different parameters and bigger deviations in different given temperatures. (3) Self tuning Fuzzy-PID control. Self-tuning Fuzzy-PID control can achieve better control [18], shorter response time, small overshoot, and with good response performance and robustness, and can achieve better control.

The performance of the self-tuning PID-type fuzzy adaptive controller is the best among the others in terms of both the steady-state error and the settling time. There is no steady-state error [19] and the system reaches the desired reference temperature [20] while minimizing settling time. Although the fuzzy-PD type controller has no steady-state error, it has longer settling time. The classical PID controller has the worst performances.

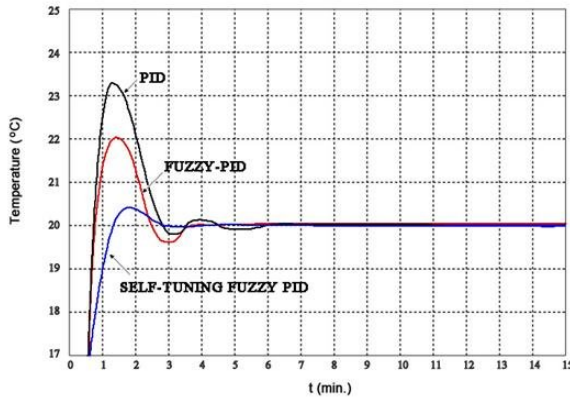


Fig. 8. The temperature control of datacenter

Fig.9 shows K_p - K_i - K_d variation of datacenter when the self-tuning PID-type fuzzy adaptive controller is applied.

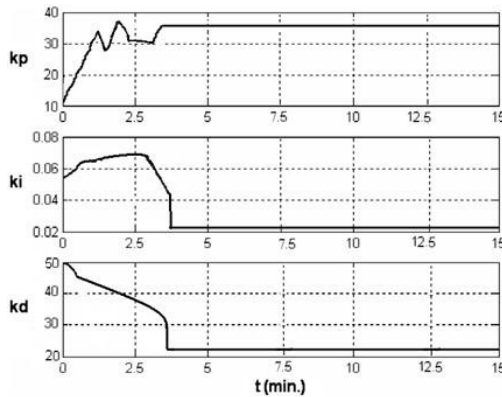


Fig. 9. Tuning trajectories of PID controller gains

6 Conclusion

Over the course of this study three types of CRAC fan speed controller were realized (and tested in the data center) by using MATLAB/SIMULINK pack-age program namely, the PID controller, the fuzzy-PD controller and self-tuning fuzzy PID controller. The result shows that the self-tuning fuzzy PID controller is the best among the others, in terms of both the steady-state error and the settling time.

References

1. Bash, C.E., Patel, C.D., Sharma, R.K.: Efficient Thermal Management of Data Centers Immediate and Long-Term Research Needs. *Intl. J. HVAC&R. Res.* (2003)
2. Boucher, T.D., Auslander, D.M.: Viability of Dynamic Cooling Control in a Data Center Environment (2004)
3. Lee, E.K., Kulkarni, I., Pompili, D., Parashar, M.: Proactive Thermal Management in Green Datacenter. *The Journal of Super-computing* (2010)
4. Salsbury, T.I.: A temperature controller for VAV air-handing units based on simplified physical models. *HVAC and R. Res.* (1998)
5. Kasahara, M., Matsuba, T., Boucherand, T.D., Auslander, D.M.: Design and tuning of robust PID controller for HVAC system (1999)
6. Bi, Q., Cai, W.-J., Wang, Q.-G.: Advanced controller auto-tuning and its application in HVAC system (2000)
7. Shayeghi, H., Shayanfar, H.A., Jalili, A.: Multi stage fuzzy PID power system automatic generation controller in the deregulated environment. *Energy Convers Manage* (2006)
8. Shayeghi, H., Jalili, A., Shayanfar, H.A.: Robust modified GA based multi-stage fuzzy LFC. *J Energy Convers Manage* (2007)
9. Schmidt, R.R.: Thermal profile of a high-density data center-methodology to thermally characterize a data center. *Trans Am Soc Heat RefrigAirCondEng, ASHRAE* (2004)
10. Schmidt, R.R., Karki, K.C., Patankar, S.V.: Raised floor computer data center: perforated tile flow rates for various tile layouts Thermal profile of a high-density data center-methodology to thermally characterize a data center. In: *Proc. of Intersociety Conference on Thermal Phenomena in Electronic Systems, ITherm* (2004)
11. Tao, Y.Y.H., New-style, G.Y.X.: PID control and application (2001)
12. Lei, L., Wang, H., Yu, Y.: Adaptive Fuzzy PID Control Method Based on Identification Structure. *International Journal of System and Control* (2006)
13. Yang, Y.: Application of MATLAB in PID Control Theory's teaching Reform. *Journal of Changshu Institute of Technology* (2009)
14. Wang, S., Jiang, W.: PID Tuning Based on MATLAB/Simulink. *Industry Control and Applications* (2009)
15. Lu, R.: Matter-element Modeling of Parallel Structure and Application about Extension PID Control Syetem. *Journal of Systems Science & Complexity* (2006)
16. Wang, L., Du, W.: Fuzzy self-tuning PID control of the operation temperatures in a two-staged membrane separation process. *Journal of Natrual Gas Chemistry* (2008)

17. Zi, B., Duan, B., Qiu, Y.: Fuzzy-PID control base on disturbance observer and its application. *Systems Engineering and Electronics* (2006)
18. Ma, Y., Liu, Y., Wang, C.: Design of Parameters Self-tuning Fuzzy PID Control for DC Motor. In: *The 2nd International Conference on Industrial Mechatronics and Automation (ICIMA 2010)* (2010)
19. Yu, Q.: Based on MATLAB's Analysis of Steady-State Error in Control System. *Journal of Changshu College* (2004)
20. Liu, Y.: Study on boiler temperature system PID controlbased on RBF neural network. *Journal of Baoji University of ArtsandSciences (Natural Science)* (2011)

Spatio-temporal Variability Analysis of Soil Volumetric Moisture Content on the Field Scale

Xueqin Tong, Yujian Yang^{*}, and Wei Dong

Science & Technology Information Institute of Shandong Academy of Agricultural Science
Number 202 Gongye North Road, Licheng District of Jinan,
250100, Shandong Province, P.R. China
yyj_tshkh@126.com

Abstract. The objective of this study was to explore spatio-temporal variability characteristic of soil volumetric moisture content (SVMC) during wheat and maize rotation system. In the article, SVMC was determined by the Time Domain Reflectometry (TDR), a total of 104 soil moisture content data from sampling sites were collected from the surface layer (0–20cm) at the experiment field (117°3'55.74"E, 36°43'8.99"N) with the support of grid-sampling method, sample measurements were implemented on June 3rd and on September 24th, 2009. On each sampling point, we inserted vertically TDR probe to monitor soil moisture. Each moisture measurement was geo-referenced using a Differential Global Positioning System (DGPS). The statistical analysis results showed that the SVMC range from 2.65 to 4.65 covered approximately percent 67% of the total samplings on June 3rd, which indicated the important effects on the total statistical distribution. Approximately percent 76% of the total samplings range from 45.4 to 55.4 on September 24th. To analyze the temporal variability of SVMC, we developed the comparison analysis results also indicated that the spatial pattern of SVMC clarified the fundamental complicated factors of the spatial structures and the comprehensive factors, and the exogenous variable decreased the effects on the spatial variability of SVMC from percent 70.9% to 54.9%, the random factors dominated the spatial variability of SVMC. The spatial distribution map of SVMC by Kriging interpolation was better to help us precisely and well understand the spatial distribution pattern of the SVMC of wheat-maize rotation system on the field scale.

Keywords: TDR, Spatio-temporal variability, Soil volumetric moisture content.

1 Introduction

Soil was inhomogeneous and continuous in nature, and its characteristics had the spatial structure. One of the challenges facing the adoption of precision agriculture (PA) technology was the identification of productivity-related variability of soil properties accurately and cost-effectively, the all-important work and base of precision agriculture was producing the spatial distribution map of soil property

^{*} Corresponding author.

content. The study of soil volumetric moisture content (SVMC), as one of soil properties, was the heated debate of soil-crop system, and was also the key factor connection with crop growth system [1]. Time domain reflectometry (TDR) was widely applied to measure soil electrical conductivity to infer SVMC. With a minimum of soil disturbance, TDR enabled to simultaneously estimate SVMC as well as electrical conductivity and was frequently applied as well in studies of solute transport in porous media[2]. Although SVMC was an important variable under soil-crop system framework, the spatio-temporal variability of SVMC had the less study from the correlation literatures, let alone analyze the SVMC variability on the field scale at home and abroad. The spatial variability of SVMC was developed from some researchers[2], mainly with statistical analysis and geostatistics, which were used in many domains, but the spatio-temporal analysis of SVMC was seldom studied on the field scale in recent years. Temporal stability of SVMC was a reflection of the temporal persistence of spatial SVMC patterns. Grayson et al. Vachaud et al [3]. found that soil texture was responsible for an observed high degree of temporal stability. Kachanoski & de Jong expanded the definition of temporal stability and correlated scale dependency of the temporal stability of SVMC [4]. From the new perspective, developing the comprehensive influence of SVMC to the spatial distribution of SVMC was the other significant objective. The amount of spatial variability as well as the spatial distribution of SVMC can have a critical impact on the irrigation status and management measure on the field scale. The research also showed that a starting point to characterize the structure and heterogeneity of SVMC fields was an examination of the spatial structure. Therefore, the objective of this study was to evaluate the efficiency of spatial statistical analysis and spatial distribution of SVMC during two-cropping for wheat and maize in one year, moreover, and the study explored the comparative analysis of the structure factors and complicated association factors in temporal scale impact on SVMC [5].

2 Material and Methodology

2.1 TDR Measurement Principle and Approaches

An overview of conceptual dielectric models for TDR application can be found in some literatures. TDR estimated the dielectric constant, in a soil matrix by measuring the propagation time of an electromagnetic wave (EM) sent from an EM pulse generator mounted on top of a coaxial cable, inserted into a soil matrix. EM waves propagate through the coaxial cable to the TDR probe, which was a rod made of stainless steel or brass. Part of the incident electromagnetic waves was reflected at the top of the probe because of the difference in impedance between cable and probe. The remainder of the wave propagated through the probe until it reached the end of the probe, where the wave was reflected. The round-trip time of the wave, from the beginning to the end of the probe was measured with an oscilloscope branched on the cable tester. For a homogeneous soil, volumetric water content is calculated by using a calibration curve. The curve was mathematically formulated in these literatures[6].

2.2 Data Acquisition of Soil Volumetric Moisture Content

SVMC was determined by TDR in the study. A total of 104 soil samplings about soil volumetric moisture content were collected from the surface layer (0–20cm) at the experiment field (117°3'55.74"E, 36°43'8.99"N) with the support of grid-sampling method, covering approximately 3 hm², located on the north shore of Xiaoqing River in Shandong province, P.R. China. Explanatory variables included environmental spatial datasets such as land use, drainage class were put forward to analyze. On each sampling point, we inserted vertically a triple wire TDR probe to monitor soil moisture, each moisture measurement was geo-referenced using a Differential Global Positioning System (DGPS), five moisture measurements were made within a 1-m diameter circle. The average reading for each point was computed as SVMC datum point. Sample measurements were implemented before wheat harvest on June 3rd, maize harvest on September 24th, in the latter sampling, the more validation points, and “maize 958” of maize cultivars was planted in the study area. The Kriging algorithm combined with GIS was applied on drawing the distributing map of SVMC and it also offered the theoretical foundation for the connection between studying SVMC and enhancing yield[7].

3 Results and Analysis

3.1 Statistical Characteristics of Soil Volumetric Moisture Content

The study explored the classical statistics analysis and developed the normality test of the variable based on Shapiro-wilk test in the normality of 0.05 incredile level. In general, Shapiro-Wilk normality test referred to the correlated documents. The classification of variance coefficient(C.V.), weak variation(C.V.<0.1), medieval variability (C.V.=0.1–1.0), strong variation(C.V.>1.0). Coefficient of variation of soil nutrients content, respectively.[8]C.V. of SVMC was 0.351, 0.105 in the two samplings, respectively, which belonged to the medieval variation, the mean value of the variable was 4.119, 50.739. In order to understand distribution characteristics of SVMC, we analyzed the frequency characteristics of the variable, the results referred to the Figure 1and Figure 2.

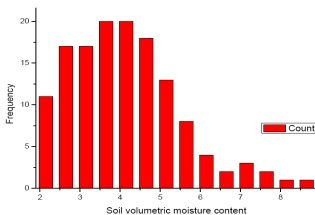


Fig. 1. The frequency characteristics of SVMC on June 3rd

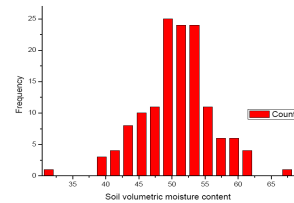


Fig. 2. The frequency characteristics of SVMC on September 24th

In the article, the study explored the frequency characteristics of SVMC on June 3rd and September 24th. The SVMC were divided into equal intervals ranging from low value to high value, the frequency statistics was developed for the variable, generally, sampling data falling on the interval boundary was considered of the high equal interval. As shown in Figure 1 and 2, the SVMC ranged from 2.65 to 4.65 covered approximately percent 67% of the total samplings on June 3rd, which indicated the important effects for the total statistical distribution. Approximately percent 76% of the total samplings ranged from 45.4 to 55.4 on September 24th, which responded to the whole statistical level. Normality distribution of the SVMC was the precondition of using interpolation to analyze SVMC feature, the normality was also developed in the study, the statistics characteristics of SVMC was illustrated about sampling data rather than the regional characteristics of the whole study area. Consequently, it is necessary to apply geostatistical methods together with GIS to solve this problem.

3.2 Geostatistical Characteristics of Soil Volumetric Moisture Content

Kriging Interpolation was the most common interpolation method in geostatistics. It was the method of optimized and precise estimation of partial variables in unobserved locations with application of original data and configuration of semi-variance function. The involved variables of semivariogram and the parameters of estimation accuracy provided the basic description of Kriging prediction, these variables and parameters was introduced in the other documents [8]. Such as nugget, sill, range, ME(Mean standardized error), ASE(Average standard error), RMSE(Root-mean-square error), MSE(Mean standard error) and RMSSE(Root-mean-square standardized error). The degree of spatial autocorrelation was described by the ratio of nugget and sill, the ratio of nugget and sill of soil volumetric moisture content was 0.709, 0.549 in the study, respectively. Results showed there was the medium spatial autocorrelation of SVMC. During the semivariogram model, the anisotropic change of SVMC was considered of 4.8 angel direction on June 3rd, good-fitness model was exponential model for the two times samplings of SVMC. From the Kriging results, for the sampling on June 3rd, ME equalled -0.020, RMSE equalled 3.844, ASE equalled 3.812, MSE equalled -0.007, RMSSE equalled 1.009. For the sampling on September 24th, ME equalled -0.018, RMSE equalled 1.359, ASE equalled 1.298, MSE equalled -0.028, RMSSE equalled 1.047. The prediction results from the two times sampling responded to the simulation accuracy. The evident change was presented in nugget, sill and range parameter of semivariogram model of SVMC, the ratio of nugget and sill of SVMC indicated that the random factors had an impact on the spatial variability of SVMC for the two times samplings, 70.9% and 54.9% of the total spatial variability, on June 3rd, the spatial results emphasized the rainfall and irrigation stochastic factors, but the samplings on Sep.24th, the exogenous variable decreased the effects on the spatial variability of SVMC from percent 70.9% to 54.9%, the random factors dominated the spatial variability of SVMC. The Kriging

algorithm combined with GIS was applied on drawing the distributing map of SVMC of different crops harvest stages and it also offered the theoretical foundation for the connection between studying SVMC and enhancing the yield. This study provided a systematic approach for estimating changes of SVMC at the regional scale. As shown in Figure 3 and Figure4, we concluded that the Kriging algorithm provided a practical spatial statistical tool for prediction and simulation of categorical soil moisture variable. For the two samplings (wheat harvest on June 3, maize harvest on September 24th, 2009), the comparison analysis results indicated that the spatial pattern of SVMC and also clarified the fundamental complicated factors of the spatial structures and the comprehensive factors from time-scale analysis.

The continued distribution of SVMC responded to the random factors and structure factors. The comparative results showed that the sensitivity of soil moisture holding-capacity which restricted the soil moisture content in the results. The high content regions of spatial surface on June 3rd located in the in the upper right corner, the spatial surface on September 24th measurement regions basically inherited the surface on June 3rd, the dominant factors were verified by the comparative analysis of the two times moisture content spatial distribution. Under the sensitivity, involvement of exogenous variable (such as stochastic rainfall factor, irrigation factor), SVMC in the surface layer can be resulted into change, but from a more stable changes, the distribution of high-value and low-value regions of SVMC were in touch with soil moisture-holding capacity. So the continued distribution of SVMC not only provided the foundation of the dynamic monitoring of the total distribution of soil water status, but also was the important part of soil water monitoring system.

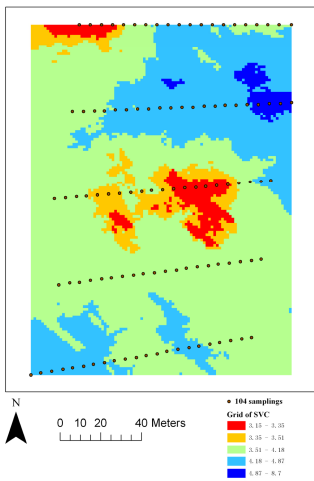


Fig. 3. The spatial variability of SVMC on June 3rd

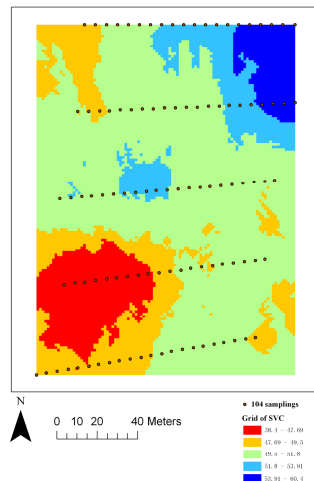


Fig. 4. The spatial variability of SVMC on Sep. 24th

4 Conclusions and Discussion

With the support of classical statistics, analysis results of 104 topsoil soil samplings indicated that the average content of SVMC, frequency analysis results showed that the SVMC ranged from 2.65 to 4.65 covered approximately percent 67% of the total samplings on June 3rd, approximately percent 76% of the total samplings ranged from 45.4 to 55.4 on September 24th, which responded to the whole statistical level. We concluded that the Kriging algorithm provided a practical spatial statistical tool for prediction and simulation of categorical soil moisture variable. For the twice samplings, the comparison analysis results showed that the spatial pattern of SVMC and also clarified the fundamental complicated factors of the spatial structures and the comprehensive factors from time-scale analysis. Making a better spatial distribution map of SVMC was of significance in promptly adjusting precise agriculture management like fertilization and irrigation, especially, the comparative study of the spatial variability of SVMC, which also offered the theoretical foundation for dynamic monitoring the connection between SVMC and the other variable, for example, crop yield. The spatial distribution map of SVMC by Kriging interpolation was better to help researchers precisely and well understand the spatial distribution of the SVMC located in the farmland of wheat-maize rotation system.

References

1. Yang, Y., Zhu, J., Zhao, C., Liu, S., Tong, X.: The spatial continuity study of NDVI based on Kriging and BPNN algorithm. *Mathematical and Computer Modelling* 54(3-4), 1138–1144 (2011)
2. Bechtel, A., Puttmann, W., Carlson, T.N., Ripley, D.A.: On the relation between NDVI, fractional vegetation cover, and leaf area index. *Remote Sensing Environment* 62(3), 241–252 (1997)
3. Verstraeten, W.W., Veroustraete, F., Feyen, J.: Assessment of Evapotranspiration and Soil Moisture Content Across Different Scales of Observation. *Sensors* 8, 70–117 (2008)
4. Aparicio, N., Villegas, D., Araus, J.L., Casades's, J., Royo, C.: Relationship between growth traits and spectral vegetation indices in durum wheat. *Crop Science* 42, 1547–1555 (2002)
5. Jian, Y., Hua, Z., Liu, S.: Spatial statistics of agronomy parameters and soil moisture content at the wheat jointing stage. *Transactions of the Chinese Society for Agricultural Machinery* 40, 159–164 (2009)
6. Yang, Y., Liu, S., Feng, W., Shang, M.: Comparison Study on the Spatial Estimation of Ji Wheat 22 Yield on the Precision Scale. *IEEE*, 576–579 (2011)
7. Yang, Y., Yang, J.: The trend variability of soil organic matter content in the salinity region of Yucheng city in Shandong Province. *Chinese Journal of Soil Science* 36(5), 647–651 (2005) (in Chinese)
8. Yang, Y., Tong, X., Zhu, J., Wang, D.: The Spatial Pattern Characteristic of soil Nutrients at the Field Scale. In: Li, D., Zhao, C. (eds.) *Computer and Computing Technologies in Agriculture*. IFIP AICT, vol. 293, pp. 125–134. Springer, Heidelberg (2009)

Taxonomy of Source Code Security Defects Based on Three-Dimension-Tree*

Zhang Yan^{1,2,**}, Dong Guowei², Guo Tao², and Yang Jianyu³

¹ School of Computer Science and Engineering, Beihang University, Beijing, China

² China Information Technology Security Evaluation Center, Beijing, China

³ China Agricultural University, College of Information and Electrical Engineering,
Beijing, China

zhangy@cse.buaa.edu.cn,

{donggw,guotao}@itsec.gov.cn, ycjyyang@126.com

Abstract. The authors present a new taxonomy for source code security defects based on three-dimension-tree, which considers the information of defect's cause, impact and representation synthetically. Case studies show that a sound system for classifying source code defects could be established with this taxonomy, and it is also good for the prevention and fixing of software vulnerabilities.

Keywords: three-dimension-tree, source code, security defect, taxonomy.

1 Introduction

Most security attacks are caused by the vulnerabilities of application system, and the defects that generated during software design and coding are the main source of them. Source code static analysis is an effective method for vulnerability reduction, because this method could consider the information of path widely and detect program's security defects automatically [1]. Generally, source code defects analysis includes lexical and syntax analysis, intermediate code generation and defect detection, as shown in Fig. 1. First, source code is compiled to Abstract Syntax Tree (AST) by lexical and syntax analyzer. Second, AST is transformed into Intermediate Representation (IR), such as Control Flow Graph (CFG), Call Graph (CF), and so on. Finally, IR is checked with defect detection rules and all kinds of analysis techniques, and the results are reported.

The construction of defect detection rule is an important step in above process, because the rule's description for detect affects analysis result directly. Classification of source code defects is helpful for the refinement of detection rules and the accuracy of analysis. Also, it is better for learning defects' nature and cause. Generally speaking, classification of source code defects is good for the prevention and fixing of new kinds of defects.

* This work was supported in part by the National Natural Science Foundation of China (90818021, 41171309).

** Corresponding author.

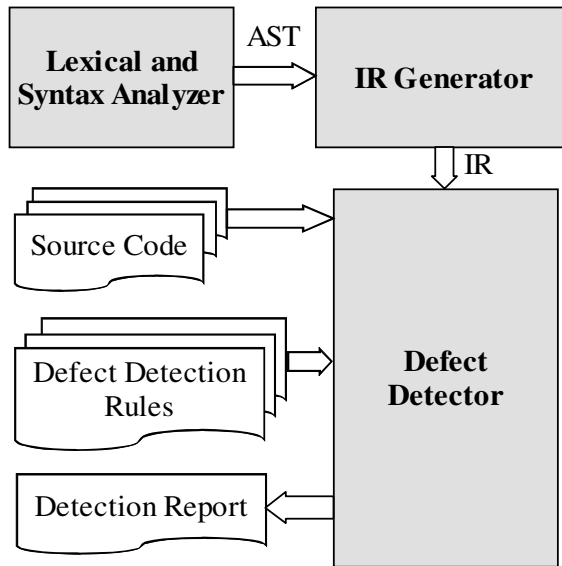


Fig. 1. Flow Graph of Source Code Defect Detection

At present, there is little taxonomy for source code defects, but the ones for software vulnerabilities are discussed by many researchers. In these works, vulnerabilities are sorted by cause [2-7], threat level [8], impact [4, 9-11], attack mode [5, 6, 11-15], fixing mode [10, 16], location [4, 5, 17], and so on. Although they involve most aspects of vulnerabilities, they are not suitable for source code defects. The main reason is that most of these methods only focus on one attribute of vulnerability.

In this article, we first introduce existing taxonomies of software vulnerabilities, and then present a kind of taxonomy for source code defects based on three-dimension-tree, which considers the information of defect's generation cause, impact and representation synthetically. At last, we sort the defects that are listed in CWE [18] and Fortify [19] with this taxonomy. Case studies show that a sound system for sorting source code defects could be established with this taxonomy, and it is also a guide for the prevention and fixing of software vulnerabilities.

This paper is organized as follow: in section 2, existing taxonomies of software vulnerabilities are introduced; in section 3, the taxonomy of source code defects based on three-dimension-tree is presented; in section 4, two case studies are given; in section 5, this paper is concluded.

2 Overview of Software Vulnerability Taxonomy

There are different definitions for software vulnerability as to different aspect, such as access control, state space, security strategy, etc [20]. Because of different requirement, existing taxonomies mostly focus on cause, impact, threat level, exploit mode, platform, and so on.

Introduction of Existing Taxonomies. As for Unix system, T. Aslam provided a taxonomy of functional errors based on cause [3]. He divided Unix errors into 4 kinds: design error, environment error, coding error, and configuration error. Design errors are issues that are generated during requirement analysis and software design; Environment errors are caused by the limitation of operation environment, such as errors that are result from compiler or OS defects; Coding errors mainly include synchronization errors, condition verification errors, etc; Configuration errors mainly include install location errors, install parameter errors and install permission errors.

F.B. Cohen presented an attack-mode-oriented taxonomy [12]. He analyzed more than 100 attack sets, and sort vulnerabilities into 18 categories: error and missing, unused value, implicit trustable attack, data spoofing, process bypass, distributed coordination attack, input overflow, Trojan horse, error after data integration, incomplete daemon, unreleased function use, misuse by attack, prohibit audit, failure lead by increasing system load, using network services and protocols, inter-process communication attack, race condition, improper default value.

I. Krsul provided impact-oriented taxonomy [9]. He pointed out that the impact of vulnerability could be divided into direct impact and indirect impact, and he sorted software vulnerabilities into data access, command execution, code execution and denial of service.

As to multi-factor taxonomy, C.E. Landwehr presented a vulnerability taxonomy based on source, time and location, in which source indicates Trojan horse, back door, logic bomb, etc; time refers to the parse that vulnerability takes place in software development life cycle, such as design, coding, maintenance; location means OS level, support software level or hardware level [5]. Upon this work, K. Jiwnani provided a taxonomy based on cause, location and impact for abstracting issues in software development [4]. In his method, cause indicates validation error, domain error, sequence or alias error, etc; Location refers to system initialization, memory management, process management or scheduling; Impact means unauthorized access, root or system access, denial of service, and so on.

D. Wenliang presented a vulnerability-life-cycle-based taxonomy [10]. He defined vulnerability life cycle as the process of “Import-Damage-Fixing”, and sorted vulnerabilities by cause, direct impact and fixing mode. Specifically, cause indicates input validation error, permission certificate error, sequence or alias error, etc; Direct impact refers to illegal code execution, illegal target change, illegal target resource access, denial of service, and so on; Fixing mode means entity false, entity missing, entity misplacing, entity error, etc.

CWE (Common Weakness Enumeration) is a defect dictionary provided by Mitre [18], which is used to provide a general criterion for identifying, reducing and preventing software defects. The last CWE version is 1.11, and it includes more than 800 kinds of defects. In CWE, defects are sorted into 3 classes, which are code defects environment defects and configuration defects, and the code defects includes executable code defects, source code defects and the defects that violates security design principle. Further, source code defects are divided into 14 subclasses: data handling, API abuse, security features, time and state, error handling, indicator of poor code quality, channel and path errors, handler errors, web problems, user interface

errors, initialization and cleanup errors, pointer issues, insufficient encapsulation. It's easy to see that the taxonomy for CWE's source code defects is based on cause.

Disadvantages of Existing Taxonomies. Based on the discussion above, we can see that there is little taxonomy for source code defects, and the ones for software vulnerability are not suitable for source code defects. The reasons are as follow:

(1) There is little taxonomy special for source code defects. Source code defects (or coding errors) are often defined as an independent category of software vulnerability, but are not divided deeply [3-5, 10]. In CWE, source code defects are only sorted into 14 simple classes [18];

(2) Some taxonomies could not be used for source code defects classification. For example, the ones based on attack mode or impact mostly consider the factors such as exploiting results [9, 12], which could not directly reflect the information of source code defects;

(3) Existing works could not reflect various aspects of defects. Most of them only consider one attribute of defect, such as cause, impact, which could only represent one aspect of defect. In addition, there are many overlaps between the categories that are generated by these methods. All of these are disbenefit for source code defect analysis.

3 Taxonomy of Source Code Defects with Three-Dimension-Tree

Classification Attributions of Source Code Defect. In order to regularize the process of source code defect analysis and provide wonderful defect detection rules, we research the taxonomy of source code defects. Based on the analysis above, vulnerabilities are sorted upon different attributes. Similarly, when classifying defects, we could also consider their attributes. After widely studying, we find that programmers often describe defects with their 6 attributes:

(1) Internal cause. This means the issues in source code that are generated during coding, such as the use of dangerous functions;

(2) Intended or unintended subjective cause. Intended defects are imported by developer deliberately, such as logic bomb and undeclared channel, and unintended defects are imported because of programmer's lack of the knowledge of secure coding;

(3) External cause. This attribute mainly focus on the issues generated by the call of external library, for which special environment should be considered;

(4) Impact of defects. This means the direct impact that is caused by source code defect, for example, buffer overflow;

(5) Issues arose in testing or execution. These are the error features that are shown in testing or running, such as I/O errors, calculation errors, logic errors, data handling errors, configuration errors, OS errors, interface errors, global variable errors, system crash, etc;

(6) Developing language. Some defects arise in special language. For example, J2EE configuration errors are special for Java.

We consider the complexity of defects, the extension of taxonomy and the 6 attributes above synthetically, and then provide 3 classification attributes for source code defects, which are cause, impact and representation:

- Cause. This attribute includes the internal, external and subjective causes of defect generation. We have concluded 9 classes of defects in this aspect, which are input issues and validation, API errors, access control and password fail, share and race, exception handle, unsafe code, boundary treatment, configuration errors, malicious code. Details are shown in Tab. 1.
- Impact. This attribute is the direct impact that defect produces. We have collected 9 classes and more than 30 subclasses of defects in this aspect, such as overflow, injection, manipulation, web attack, access control, leak, file system, deadlock, and denial of service. Details are shown in Tab. 2.
- Representation. This means the form that defect presents in source code, which could also be seen as the form of code with issue, and secure issues may arise when running this code. Of course, some representations are related with special language. We have summarized 13 classes and more than 150 subclasses of defects in this aspect, such as pretreatment, declaration and initialization, expression, integer, float, array, string, memory management, input and output, object oriented, concurrency, as shown in Tab. 3.

Taxonomy Based on Three- Dimension-Tree.We consider 3 attributes when sorting source code defects. That is, the category of a defect is decided by its cause, impact and representation. From Tab. 1, 2, 3, we can see that all of the 3 classification attributes satisfy multi-level containment, which could be described with tree structure. So we represent each attribute with a tree, and the set that includes all leaf nodes of one tree is also the set of corresponding attribute’s final categories. Details are shown in Fig. 2.

Definition (Three-Dimension-Tree Taxonomy). Let $Tree_{re}$, $Tree_{rt}$, and $Tree_{rp}$ be the trees that represent defect’s cause, impact and representation, and $child(n)$ the child node of node n in tree, if $Re=\{re|re\in Tree_{re}\} \wedge (child(re)== Null)\}$, $Rt=\{rt|rt\in Tree_{rt}\} \wedge (child(rt)==Null)\}$, and $Rp=\{rp|rp\in Tree_{rp}\} \wedge (child(rp)==Null)\}$, then $\{(a, b, c) | (a\in Re) \wedge (b\in Rt) \wedge (c\in Rp)\}$ is the set of defect categories that are generated by the Three-Dimension-Tree Taxonomy, and each (a, b, c) represents a category of defects.

Table 1. Causes of Defects

Cause	Intended	Malicious code	
	Unintended	Environment independent	Input issues and validation
			API errors
			Access control and password fail
			Share and race
			Exception handle
			Unsafe code
			Boundary treatment
	Environment dependent	Configuration errors	

Table 2. Impacts of Defects

Impact	Injection	SQL injection
		Command injection
		XML injection
	
	Overflow	Buffer overflow
		Integer overflow
	
	Manipulation	Path manipulation
		Configuration manipulation
	
	Access Control	Password crack
		Poor lock
		Race condition
	
	Leak	Resource leak
		Memory leak
		Information leak
	
	File system	File upload
		File include
	
	

Table 3. Representation of Defects

Representation	String Manipulation	Misjudgement of length of string
		Format string
		String iteration
	
	Semaphore	Single member field
		Semaphore handle
	
	Expression	Expression is always true
		Expression is always false
	
	Exception handle	Empty Catch block
		Unhandled exception
		Overly broad throws
	
	Math	Confusion of math operators
		Mix of mathematical type
		Divided by 0
	
	Constant	Unreasonable definition of constant
		Out of bounds
	
	

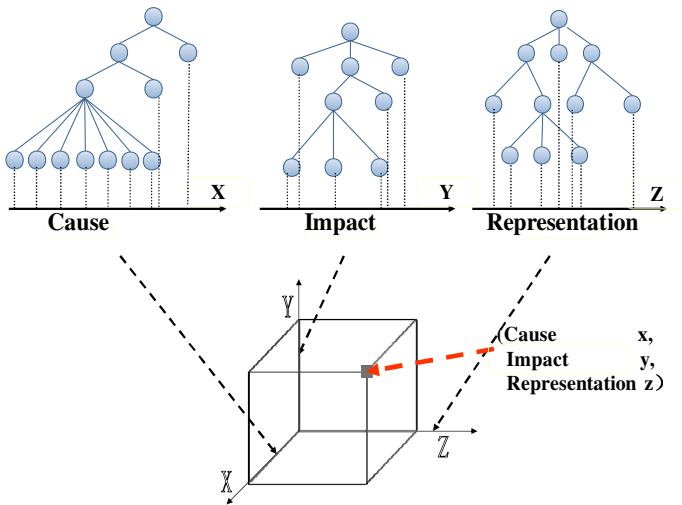


Fig. 2. Three-Dimension-Tree

As we see, this taxonomy could reflect the information and feature of defect in multi-aspects, which is good for the construction of defect detection rules. Besides, it is easy to extend categories in this method. When new defects come out, we should only insert 3 new nodes into 3 trees at suitable positions.

Nomenclature of Defect Categories. In this taxonomy, we name a kind of defects with a triple that includes the names of its corresponding cause, impact and representation, which is intuitive and applied. Defect’s features can be reflected by its name, which is good for defects’ modification and statistics. For example, we name the kind of defect that is described in code

```
#include <stdio.h>
int main(){
char fixed_buf[10];
sprintf(fixed_buf,"Very long format string\n");
return 0;
}
```

with (Input issues and validation, Buffer overflow, Array out of bounds in Sprintf()).

4 Case Study

Classification of CWE Defects. We classify about 110 items of source code defects listed in CWE with new taxonomy, and acquire 146 categories. Tab. 4 illuminates 12 of them. The second column indicates the item of defects that corresponding CWE ID denotes.

Following conclusions can be drawn from Tab. 4:

Table 4. 12 categories of CWE Defects

id	CWEID	Three-Dimension-Tree Taxonomy		
		Cause	Impact	Representation
1	113	Input issues and validation	HTTP response truncation	HTTP Cookie with incredible data
2	79	Input issues and validation	Cross-site scripting	
3	563	Unsafe code	Dead code	Unused variable
4	563	Unsafe code	Unsafe style	Coverage of independent increment
5	242, 676	API errors	Dangerous Function	Mac OS function
6	242, 676	API errors	Dangerous Function	Unix function
7	404	Unsafe code	False release	
8	404, 772	Boundary treatment	Unreleased Resource	File unclosed
9	103	Input issues and validation	Struts errors	validate() error
10	104	Input issues and validation	Struts errors	No inheritance of Validation
11	105	Input issues and validation	Struts errors	Missing Validator
12	590	Input issues and validation	Misuse of memory	Memory for free() isn’t provided by malloc()

(1) Defects’ detail information can be presented with new taxonomy. For example, the 1st category of defects is caused by input, and may import the impact of HTTP response truncation. It’s representation in code is one HTTP Cookie with incredible data. In addition, the 3rd and 4th categories are described as one item of defects in CWE (Code style and quality, ID is 563), but they are greatly different in impacts and representations, and these differences are embodied in new classification;

(2) The information about platform and language can be presented in new method. For example, the 5th and 6th categories are special for Mac OS and Unix respectively, while the 12th for C/C++;

(3) The attribute of representation in new taxonomy increases the intuition of defect. The 9th, 10th and 11th categories are all caused by input issues and validation, and all import Struts errors, but their representations are different, which are validate() error, no inheritance of Validation, and missing Validator. It's more intuitionistic.

Table 5. 10 categories of Fortify Defects

id	Fortify Defects	Three-Dimension-Tree Taxonomy		
		Cause	Impact	Representation
1	Cross-site scripting	Input issues and validation	Cross-site scripting	Poor Validation
2	Buffer overflow	Input issues and validation	Buffer overflow	Format String(%f/%F)
3	Dead code	Unsafe code	Dead code	Unused variable
4	SQL injection	Input issues and validation	SQL injection	Hibernate
5	Access control	Access control and password fail	Access control	Anonymous LDAP Bind
6	Race condition	Share and race	Race condition	File system access
7	Memory leak	Unsafe code	Memory leak	Memory redistribution
8	System information leak	Boundary treatment	System information leak	Missing Catch Block
9	J2EE misconfiguration	configuration errors	J2EE misconfiguration	Missing Error Handling
10	Object model violation	API errors	Object model violation	Just one of equals() and hashCode() Defined

Classification of Fortify Defects. Fortify is a famous tool for source code security analysis [19]. It could analyze programs in 19 languages. There are more than 300 items of defects in Fortify, and most of them are defined based on the description of defects in CWE and OWASP. We classify 86 items of them with new taxonomy, and get 194 categories. Tab. 5 lists 10 of them, and the set of defects that are described with 3 attributes in each line is only a subclass of Fortify defects in the same line. That is to say, classes derived from three-dimension-tree taxonomy are more refined.

5 Conclusion

In this paper, a new taxonomy for source code security defects based on three-dimension-tree is present, which considers the information of defect's cause, impact and representation synthetically. Case studies show that a sound system for classifying source code defects can be established with this taxonomy, and it is also good for the prevention and fixing of software vulnerabilities.

Upon existing works, we will continue refining classification attributes. The taxonomy in this paper is based on 9 kinds of causes, more than 30 kinds of impacts and more than 150 kinds of representations, but some defects could not be accurately defined, for example, the representations of the 2nd and 4th categories in Tab. 4 are blanks. Thus, our next goal is attributes refinement.

References

- [1] Mei, H., Wang, Q.X., Zhang, L., Wang, J.: Software Analysis: A Road Map. *Chinese Journal of Computers* 32(9), 1697–1710 (2009)
- [2] Piessens, F.: A Taxonomy of Causes of Software Vulnerabilities in Internet Software. In: *Proceedings of the 13th International Symposium on Software Reliability Engineering, ISSR 2002* (2002)
- [3] Aslam, T.: A Taxonomy of Security Faults in the Unix Operating System. Technique report TR-95-09, Department of Computer Science, Purdue University, West Lafayette, USA (1995)
- [4] Jiwnani, K., Zekowitz, M.: Susceptibility Matrix: A New Aid to Software Auditing. *IEEE Security and Privacy* 2(2), 16–21 (2004)
- [5] Landwehr, C.E., Bull, A.R., McDermott, J.P.: A Taxonomy of Computer Program Security Flaws with Examples. *ACM Computing Surveys* 26(3), 211–254 (1994)
- [6] Weber, S., Karger, P.A., Paradkar, A.: A Software Flaw Taxonomy: Aiming Tools at Security. In: *Proceedings of the 2005 Software Engineering for Secure Systems, SESS 2005* (2005)
- [7] Tsipenyuk, K., Chess, B., McGraw, G.: Seven Pernicious Kingdoms: A Taxonomy of Software Security Errors. *IEEE Security & Privacy* 3(6), 81–84 (2005)
- [8] Power, R.: *Current and Future Danger: A CSI Primer on Computer Crime and Information Warfare*. Computer Security Institute, San Francisco (1996)
- [9] Krsul, I., Spafford, E., Tripunitara, M.: Computer Vulnerability Analysis. Technique report TR- 47909-1398, Department of Computer Science, Purdue University, West Lafayette, USA (1998)
- [10] Wenliang, D., Mathur, A.P.: Categorization of Software Errors that Lead to Security Breaches. In: *Proceedings of the 21st National Information Systems Security Conference* (1998)
- [11] Bishop, M.: A Taxonomy of Unix System and Network Vulnerabilities. Technical Report CSE-95-8, Dept. of Computer Science, University of California at Davis, Davis (1995)
- [12] Cohen, F.B.: Information System Attacks: A Preliminary Classification Scheme. *Computers and Security* 16(1), 26–49 (1997)
- [13] Howard, J.D.: *An Analysis of Security Incidents on the Internet 1989-1995*. Carnegie Mellon University, Pittsburgh (1997)
- [14] Killourhy, K.S., Maxion, R.A., Tan, K.M.: A Defense-centric Taxonomy Based on Attack Manifestations. In: *Proceedings of the 34th IEEE/IFIP International Conference on Dependable Systems and Networks, DSN 2004* (2004)
- [15] Hansman, S., Hunt, R.: A Taxonomy of Network and Computer Attack. *Computers and Security* 24(1), 31–43 (2005)
- [16] DeMillo, R.A., Mathur, A.P.: A Grammar-based Fault Classification Scheme and Its Application to the Classification of the Errors of Tex. Technique report, Department of Computer Science, Purdue University, West Lafayette, USA (1995)

- [17] Bazaz, A., Arthur, A.J.D.: Towards a Taxonomy of Vulnerabilities. In: Proceedings of the 40th Annual Hawaii International Conference on System Science (2007)
- [18] Information on, <http://cwe.mitre.org/>
- [19] Information on, <http://www.fortify.com/>
- [20] Huang, M., Zeng, Q.K.: Research on Classification Attributes of Software Vulnerability. *Computer Engineering* 36(1), 184–186 (2010)

Path Recognition for Agricultural Robot Vision Navigation under Weed Environment

Peidong Wang, Zhijun Meng, ChangHai Luo, and Hebo Mei

Beijing Research Center for Intelligent Agricultural Equipment, Beijing 100097, China
{wangpd, mengzj, luoch, meihb}@nercita.org.cn

Abstract. In this paper, a path recognition method for agricultural robot vision navigation under weed environment is proposed. The vision navigation is based on color images sampled by a high speed camera. First, the crop and weed information is extracted using an appropriate color feature model to separate the green crop from background; then the image is thresholded, and the noise caused by weed is filtered by deleting small-area objects in the image; the navigation path is extracted through Hough transformation. Experiments are carried out in corn seedling field, and results show that the method can recognize navigation path correctly under weed environment.

Keywords: vision navigation, agricultural robot, weed noise filtration, path recognition.

1 Introduction

Autonomous agricultural robot has many applications such as environment information collection, seeding, fertilizing, spraying, etc. The goal of autonomous robot navigation is to control the trajectory of the robot and keep it along the driving path [1]. Computer vision based navigation has been widely researched recent years due to its advantages such as wide detection range, rich target information, good cost performance and flexibility [2-4].

The key to vision navigation is identifying crop automatically from the images and recognizing the navigation path [5]. Usually, the central line of the crop is extracted as the baseline for agricultural robot vision navigation. But the weed in the field will interfere with the crop information because it often has the same green color as the crop, and causes false navigation path recognition results [6]. Astrand has researched on weeding robot, and used two separate vision system, one is used for navigation and the other is used for weed recognition [7]. Zhao Bo uses neural network algorithm to classify the field environment [8]; the algorithm can classify the weed environment, but it's too time-consuming, and how to recognize the navigation path after environment classification is not specified. Xue Jinlin adopts a variable field-of-view method to guide an agricultural robot [9], which can improve the guiding performance at the end of a crop row. Dong Fuhong has built a row guidance system for an autonomous robot for white asparagus harvesting [10], but the system is specific to asparagus, thus lack of generosity.

In this paper, we propose a path recognition method for agricultural robot vision navigation under weed environment. The areas of the connected components in the image are calculated, and the noise caused by weed is filtered by deleting small-area objects in the image. Experimental results verify the correctness and performance of the proposed method.

2 Path Recognition Method

To recognize the path for agricultural robot vision navigation under weed environment, first we select an appropriate color feature model to extract the green crop and weed information from the image, and separate them from the background; then the image is thresholded, and the noise caused by weed is filtered by deleting small-area objects in the image; the navigation path is extracted through Hough transformation. The method is described in detail below.

2.1 Image Segmentation Based on Color Feature Model

The images used for vision navigation is captured by a color camera. We need to preprocess this image to get useful information [11]. In farmland environment, the crops which are used as guide targets are green, while the soil background is usually not green. In order to extract the crop information and eliminate background information, we need to select an appropriate color feature to raise the weight of the green channel of the color image. In this paper, the color feature model is chosen as below:

$$I = 2G - R - B \quad (1)$$

where R, G and B denotes the red, green and blue channel of the color image respectively. This color feature can raise the weight of the green channel, and enhance the contrast ratio with the non-green background.

After calculating the color feature I, a grayscale image is obtained. We segment the grayscale image using maximum between-class variance method to get a binary image BW for future processing.

2.2 Weed Interference Filtration

Due to the fact that weed has the same green color as the crop, there is still weed information remained on the binary image after image segmentation. The weed information may interfere with the useful crop information, and cause false navigation path recognition result. Therefore, we need to filter the weed interference.

In farmland field, the crops are always cluttered in line, while the weeds are scattered separately between crop lines in the field, and the weeds are usually smaller than crops. In the actual image, the crops are represented as connected regions with

big areas, while the weeds are represented as small-area objects. Therefore, we use small-area object deletion method to filter the weed interference. The steps of the method are as follows:

- 1) Determine the connected components in the binary image BW. The result is represented as C_i , where $i = 1, 2, \dots, N$;
- 2) Compute the area of each component, which is represented as S_i .
- 3) Remove small-area objects. The result is represented as: $L = \cup \{ C_i \mid S_i \geq P \}$, where P is the area threshold.

After eliminating the weed interference, the navigation path based on crop center line can be further extracted.

2.3 Navigation Path Extraction

The crop center line is regarded as the navigation path. In field environment, there may be crop line discontinuities due to miss-seeding. The Hough transformation is a global and robust line detection method, and can be used to find and link line segments in an image. Therefore, we adopt Hough transformation to extract the crop center line. The steps of the algorithm are as follows:

- 1) Calculate the image size.
- 2) Determine the size of the parameter space for Hough transformation based on image size, discretize the ρ - θ parameter space as many grids, where one grid represents an accumulator. Allocate memory for the grids.
- 3) For each point (x_i, y_i) in the image, substitute the discretized θ into $\rho = x_i \cos \theta + y_i \sin \theta$ to calculate the corresponding ρ , and the result falls on a specific grid; Add the accumulator corresponding to that grid by 1.
- 4) Detect the peak value of the accumulators. Estimate the correctness of the peak value detection through navigation path direction angle statistics.
- 5) Plot the navigation path in the image according to the detected peak value.

3 Experiment Verification and Results

To test and verify the method proposed in this paper, experiments are carried out in corn field with weed. The type of the camera used in the experiments is Monta G-125C from Allied Vision Technology Inc. The resolution of the camera is 1296*964, and the hardware interface of the camera is Gig E. The camera is fixed on Seekur robot made by MobileRobots Inc.

Figure 1(a) is an original color image obtained in corn field with weed. Figure 1(b) is the grayscale image obtained based on color feature model described in Section 2.1, from which we can see that the soil background is successful eliminated from the image after transformation, but the weed information is still remained between crop lines on the image, and this interferes with the useful crop information.



(a) Original color Image of corn field



(b) Image after grey level transformation

Fig. 1. Corn field images before and after grey level transformation

The binary image obtained by thresholding the grey scale image is shown in Figure 2(a), from which we can see the weed noise more clearly. Figure 2(b) shows the image after filtering the weed noise through small-area objects deletion, we can see that most of the weeds are eliminated from the image, only a few weed clutters are remained, but this does not affect the result of Hough transformation.



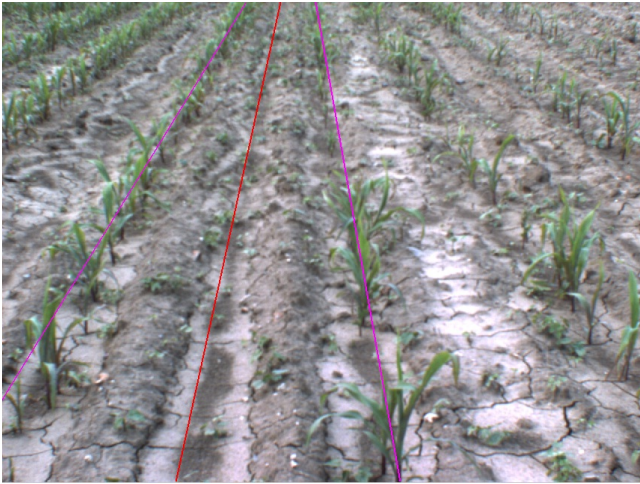
(a) Binary image after thresholding



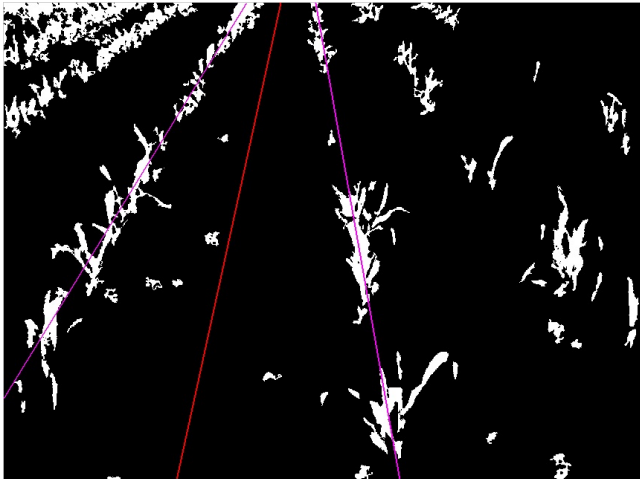
(b) Binary image after weed noise filtration.

Fig. 2. Binary images after thresholding and weed noise filtration

Figure 3 shows the crop center lines extracted through Hough transformation, and the navigation path calculated based on the crop center lines. The magenta lines represent crop center lines, and the red line represents the navigation path. The two crop lines around the image center are selected to calculate the navigation path. We can see that the crop center lines and the navigation path are correctly extracted. Similar experiments are carried out, and all of the results verify the correctness and performance of the proposed method.



(a) Navigation path shown in original image



(b) Navigation path shown in binary image.

Fig. 3. Navigation paths show in different images

4 Conclusions

Computer vision based robot navigation has been a major topic of discussion in precision agriculture, and path recognition under noise environment is a key factor to precise navigation. In this paper, we propose a path recognition method for agricultural robot vision navigation under weed environment. The soil background is eliminated by image segmentation based on color component. The weed noise is

filtered by deleting small-area objects in the binary image. The crop centerlines and navigation path are extracted through Hough transformation. Experimental results showed that most of the weed noise is eliminated from the field image. The path recognition method in this paper is practical and accurate for vision-based robot navigation.

The method proposed in this paper is aimed at straight-line navigation path, which is of little curvature. Further research will be focused on navigation paths with big curvature.

Acknowledgment. Funds for this research was provided by the National High Technology Research and Development Programs of China (863 Program), under Contract 2013AA040401 and Contract 2013AA102308.

References

1. Backman, J., Oksanen, T., Visala, A.: Navigation system for agricultural machines: Nonlinear Model Predictive path tracking. *Computers and Electronics in Agriculture* 82, 32–43 (2012)
2. Reid, J.F., Zhang, Q., Noguchi, N., et al.: Agricultural automatic guidance research in North America. *Computers and Electronics in Agriculture* 25, 155–167 (2000)
3. Keicher, R., Seufert, H.: Automatic guidance for agricultural vehicles in Europe. *Computers and Electronics in Agriculture* 25, 169–194 (2000)
4. Torii, T.: Research in autonomous agriculture vehicles in Japan. *Computers and Electronics in Agriculture* 25, 133–153 (2000)
5. Torii, T., et al.: Crop row tracking by an autonomous vehicle using machine vision. *JSAE* 62(5), 37–42 (2000)
6. Burgos-Artizzu, X.P., Ribeiro, A., Gujjarro, M., et al.: Real-time image processing for crop/weed discrimination in maize fields. *Computers and Electronics in Agriculture* 75, 337–346 (2011)
7. Astrand, B., Baerveldt, A.-J.: An agricultural mobile robot with vision-based perception for mechanical weed control. *Autonomous Robots* 13, 21–35 (2002)
8. Zhao, B., Wang, M., Mao, E., et al.: Recognition and classification for vision navigation application environment of agricultural vehicle. *Transactions of CSAM* 40(7), 166–170 (2009)
9. Xue, J.L., Zhang, L., Grift, T.E.: Variable field-of-view machine vision based row guidance of an agricultural robot. *Computers and Electronics in Agriculture* 84, 85–91 (2012)
10. Dong, F., Heinemann, W., Kasper, R.: Development of a row guidance system for an autonomous robot for white asparagus harvesting. *Computers and Electronics in Agriculture* 79, 216–225 (2011)
11. Pinto, F.A.C., Reid, J.F., Zhang, Q.: Vehicle guidance parameter determination from crop row images using principal component analysis. *Journal of Agricultural Engineering Research* 75(3), 257–264 (2000)

Application of LS-SVM and Variable Selection Methods on Predicting SSC of Nanfeng Mandarin Fruit

Tong Sun, Wenli Xu, Tian Hu, and Muhua Liu

College of Engineering, Jiangxi Agricultural University, 1225 Zhimin Street,
310045 Nanchang, P.R. China

{suntong980, xuwenli.1990}@163.com,
784643819@qq.com, suikelmh@sina.com

Abstract. The objective of this research was to investigate the performance of LS-SVM combined with several variable selection methods to assess soluble solids content (SSC) of Nanfeng mandarin fruit. Visible/near infrared (Vis/NIR) diffuse reflectance spectra of samples were acquired by a QualitySpec spectrometer in the wavelength range of 350~1800 nm. Four variable selection methods were conducted to select informative variables for SSC, and least squares-support vector machine (LS-SVM) with radial basis function (RBF) kernel was used to develop calibration models. The results indicate that four variable selection methods are useful and effective to select informative variables, and the results of LS-SVM with these variable selection methods are comparable to the results of full-spectrum partial least squares (PLS). Genetic algorithm (GA) combined with successive projections algorithm (SPA) is the best variable selection method among these four methods. The correlation coefficients and RMSEs in LS-SVM with GA-SPA model for calibration, validation and prediction sets are 0.935, 0.560%, 0.912, 0.631% and 0.933, 0.594%, respectively.

Keywords: Vis/NIR, LS-SVM, variable selection, soluble solids content, Nanfeng mandarin fruit.

1 Introduction

Soluble solids content (SSC) is one of the most important properties of fruits that match human's taste. In recent years, Visible /near infrared (Vis/NIR) spectroscopy has become a well-accepted method for SSC assessment of fruit because it works fast and non-destructively, allows no sample preparation and brings no environmental chemistry pollution. And it has been used to measure SSC in a variety of fruits such as mandarin fruit [1-2], apple [3-4], pear [5-6], kiwifruit [7-8], melon [9-10] and so on. Due to high resolution in modern spectroscopic instrument, the spectral data usually has hundreds or thousands wavelength variables, so contains substantial information. However, some of the information is useless or irrelevant to component properties, which will worsen the predictive ability of the model for component properties and should be eliminated. Recently, many variable selection methods were developed to eliminate irrelevant

information or variables, and reserve important information or variables. Ying et al. (2008) [11] used genetic algorithm (GA) method to select important variables for sugar content (SC) of apples, then developed calibration model by partial least squares (PLS). Compared to full-spectrum PLS, the root mean square error of prediction (RMSEP) in GA-PLS was decreased from 0.512% to 0.395%. Liu et al. (2009) [12] applied successive projections algorithm (SPA) to choose variables for organic acids of plum vinegar. Least squares-support vector machine (LS-SVM) was used to develop calibration models. The models developed by SPA-LS-SVM for organic acids were better than that of full-spectrum PLS. Sorol et al. (2010) [13] investigated PLS combined with several variable selection methods to assess Brix degrees of sugar cane juice, and GA-PLS obtained the best results. Wu et al. (2011) [14] reported that uninformative variable elimination (UVE) was necessary to conduct before SPA on spectra of dried laver for predicting protein content. The average improvement percentage of RPD (standard deviation/RMSEP) was 38.66%. Huang et al. (2011) [15] selected two important wavelength variables (431 nm, 976 nm) by SPA for total soluble solid contents (TSS) of mulberry fruit, and acceptable results were obtained. Sun et al. (2012) [16] applied competitive adaptive reweighted sampling (CARS) to sort important variables for SSC of navel oranges. The CARS-PLS model for SSC was better than other methods (UVE-PLS, SPA-PLS, full-spectrum PLS). Besides, there were other research works concerning variable selection in Vis/NIR application [17-19]. From above research papers, it can be found that variable selection will simplify models, and reduce predicted errors.

LS-SVM is an evolution of the standard support vector machine. It has the capability for both linear and nonlinear multivariate calibration, and can handle some latent nonlinear information existed in the spectral data [20](Suykens et al., 2002). Therefore, LS-SVM combined with several variable selection methods was proposed to assess SSC of Nanfeng mandarin fruit, with the purpose of developing a fast and accurate nonlinear model using important variables for quality assessment of Nanfeng mandarin fruit.

The objective of this research was to investigate the performance of LS-SVM combined with several variable selection methods to assess SSC of Nanfeng mandarin fruit. Calibration models developed by LS-SVM with different variable selection methods were compared to identify an optimal method for SSC assessment of Nanfeng mandarin fruit.

2 Experiments and Methods

2.1 Samples

A total of 280 Nanfeng mandarin fruits were purchased from a local fruit market and stored for 24 hours at about 20 °C and 60 % relative humidity (RH) to equilibrate before Vis/NIR spectra measurement. Samples were separated randomly into three sets: a calibration set (n=140), a validation set (n=70), and a prediction set (n=70), with the ratio of 2:1:1. In order to ensure the adaptability of the model, the calibration set contained the samples with the minimum and maximum values of SSC. Spectra collection and SSC determination of Nanfeng mandarin fruits were completed at the same day for same samples.

For SSC measurement, the pulp of Nanfeng mandarin fruit was macerated using a manual fruit squeezer after removing pericarp. And the filtered juice were used for SSC measurement with a hand-held refractometer (Atago Co. Ltd., Tokyo, Japan).

2.2 Spectra Acquisition

Diffuse reflectance spectra of Nanfeng mandarin fruits were acquired in the Vis/NIR system which consisted of a QualitySpec spectrometer (Analytical Spectral Devices, Inc., USA), light source, an optic fiber and a computer. The QualitySpec spectrometer was equipped with a Si detector (350~1000 nm) and an InGaAs detector (1000~1800 nm). The light source was tungsten quartz halogen lamp (4W/5.5V), and the color temperature was about 2901 K.

In this research, diffuse reflectance spectra of samples were acquired at two positions, and each position was acquired once. The average spectrum of each sample was used for further analysis. The positions of samples were put as the stalk-stem of fruit was perpendicular to horizontal plane, and one position was stalk up, another was stem up. A polytetrafluoethylene (PTFE) board was used to obtain reference spectrum prior to sample spectra acquisition. The integration time and scan number for reference and samples were both 136 ms and 2, respectively. Spectrometer parameters setting, spectra data obtaining and storing were carried out via the Indic software v4.0 (Analytical Spectral Devices, INC., USA). The measurement was expressed as $\log(1/R)$. R was percent reflectance of sample spectra.

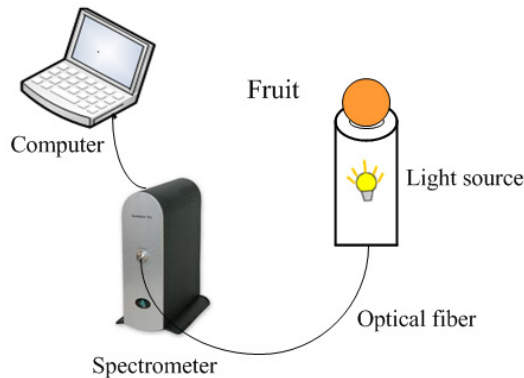


Fig. 1. Schematic diagram of Vis/NIR system

2.3 Variable Selection

2.3.1 UVE

Uninformative variable elimination (UVE) is a novel variable selection method based on stability analysis of regression coefficient [21]. The objective of UVE is to eliminate the variables that have no more useful information for modeling than noise. After reducing the uninformative variables, it can avoid a model to be over-fitting and improve model predictive ability. In the UVE algorithm, a noise matrix is appended to

instrumental response data for estimating the uninformative variables, and a PLS regression coefficient matrix $b = [b_1, \dots, b_p]$ is calculated from new matrix through leave-one-out cross validation. Then the stability value S of each variable can be calculated using equation (1). The large S value indicates the variable is more reliable and important for modeling. The variable whose S value is less than cut-off threshold will be realized as uninformative variable and eliminated. In this study, the cut-off threshold was set as 99% of maximal absolute S value of noise variables, and 1231 random variables (noise matrix) were added to spectral data.

$$s_j = \frac{\text{mean}(b_j)}{\text{std}(b_j)} \quad (1)$$

Where s_j is the reliability value of variable j , $\text{mean}(b_j)$ and $\text{std}(b_j)$ are the mean and standard deviation values of PLS regression coefficients of variable j .

2.3.2 GA

Genetic algorithm (GA) is an optimization method based on the principles of genetics and natural selection, and it has been successfully applied in the Vis/NIR spectroscopy for variable selection. The basic steps of GA algorithm are described as follows: first, a population of chromosomes is generated; second, PLS analysis is conducted and the fitness of each chromosome is calculated; third, chromosomes are chosen according to the fitness value; fourth, the chosen chromosomes are paired and reproduced by cross-over and mutation; then, step 2 to step 4 are repeated until the fitness reaches an acceptable value. The detailed principle of GA can be found in the literature [22-23]. In this study, the parameters of GA were set as follows: population size (30 chromosomes), probability of mutation (1%), probability of cross-over (50%), and number of runs (100).

2.3.3 SPA

Successive projections algorithm (SPA) is a novel forward variable selection algorithm for solving collinearity problems. In the SPA analysis, it has two phases. The first phase is to conduct projections on instrumental response data to generate subsets of variables. The second phase is to evaluate candidate subsets of variables obtained in the first phase by MLR according to root mean squared error of cross validation (RMSECV). And the best subsets of variables are obtained with the smallest RMSECV. The detailed principle of SPA can be found in the literature [24-25]. In this study, the parameters of minimum and maximum number of variables used in SPA were 1 and 30, respectively.

2.3.4 CARS

Competitive adaptive reweighted sampling (CARS) is a novel strategy for variable selection based on 'survival of the fittest' of Darwin's Evolution Theory. The absolute values of regression coefficients in PLS regression are used to evaluating the importance of each variable. In the CARS analysis, exponentially decreasing function based enforced wavelength selection and adaptive reweighted sampling (ARS) based

competitive wavelength selection are adopted to select the important variables. The detailed principle of CARS can be found in the literature [26]. In this study, the number of Monte Carlo sampling was set as 50, and 10-fold PLS cross validation was used to develop calibration model.

In the variable selection, UVE or GA was used to select wavelength variables for SSC of Nanfeng mandarin fruit first, then SPA or CARS was conducted to select wavelength variables based on the results of UVE or GA. So four combined variable selection methods (UVE-SPA, UVE-CARS, GA-SPA, GA-CARS) were used in this study, and conducted in the Matlab 7.6.0 (The MathWorks, Inc. USA).

2.4 LS-SVM

After variable selection, LS-SVM was used to develop calibration models for SSC of Nanfeng mandarin fruit. In order to evaluate the performance of LS-SVM with four variable selection methods, the results of LS-SVM were compared with the results of full-spectrum PLS.

In LS-SVM regression, radial basis function (RBF) kernel was used as the kernel function, simplex technique and leave one out cross-validation were used to find the optimal parameter values including regularization parameter γ and RBF kernel function parameter σ^2 . LS-SVM was conducted in the Matlab 7.6.0 (The MathWorks, Inc. USA).

3 Results and Discussion

3.1 Quality Attribute Distribution

The mean and standard deviation (S.D.) of SSC in all Nanfeng mandarin fruit were 14.45% and 1.59, respectively. Details of SSC statistic results for calibration, validation and prediction sets were presented in Table 1.

Table 1. Statistical results of soluble solids content of Nanfeng mandarin fruit in calibration, validation and prediction sets

<i>Parameter</i>	<i>Data set</i>	<i>Samples</i>	<i>Maximum</i>	<i>Minimum</i>	<i>Mean</i>	<i>S.D.</i>
SSC (%)	Calibration	140	18.6	10.4	14.43	1.58
	Validation	70	18.0	10.6	14.26	1.53
	Prediction	70	18.6	10.6	14.51	1.64

3.2 Spectral Analysis

Fig. 2 shows the Vis/NIR diffuse reflectance spectra of all Nanfeng mandarin fruit. From Fig. 2, it can be seen that there are obvious peaks and valleys in the wavelength range of 1000 nm~1800 nm, and spectra seem flat in the wavelength range of 350 nm~1000 nm. This is due to weak absorption in the wavelength range of 350 nm~1000 nm, and this wavelength range also contains useful information such as a third overtone stretch of CH and second and third overtones of OH (Shao et al., 2011). In the

wavelength range of 1000 nm~1800 nm, it develops peaks at about 1210 nm and 1465 nm, and develops valleys at 1100 nm, 1287 nm and 1676 nm. Besides, there are some noises at the two ends of spectra which lead to low signal/noise ratio, and the wavelength ranges of 350 nm~550 nm and 1780 nm~1800 nm are removed. So only wavelength range of 550 nm~1780 nm was used for further analysis, and there were 1231 wavelength variables in this wavelength range.

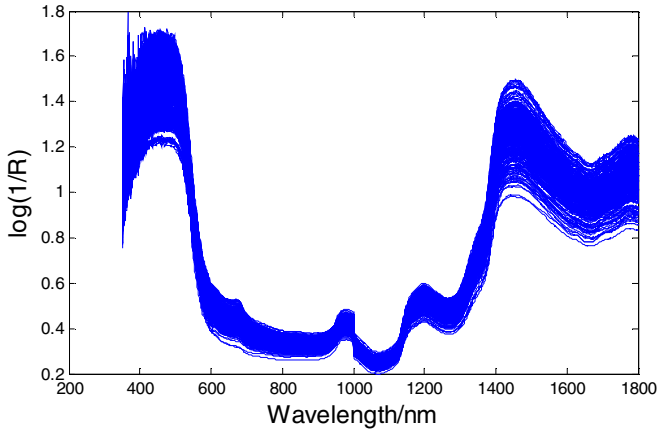


Fig. 2. Vis/NIR diffuse reflectance spectra of all Nanfeng mandarin fruit

3.3 Variable Selection

3.3.1 UVE-SPA

For UVE-SPA variable selection method, UVE was applied to select wavelength variables first, then SPA was conducted on the selected wavelength variables by UVE. Fig. 3 shows the stability results of each variable in the PLS model for SSC by UVE. In Fig. 3, the solid vertical line is the split line of wavelength variables and random variables, wavelength variables are at the left while random variables are at the right. Two dashed horizontal lines mean the upper and lower cutoffs for selecting wavelength variables. The variables beyond the cutoffs are realized as informative variables and reserved, while the variables between the cutoffs are realized as uninformative variables and eliminated. After UVE analysis, 151 variables were selected from 1231 variables for SSC.

Fig. 4 shows the root mean square error (RMSE) plot and selected variables by SPA for SSC of Nanfeng mandarin fruit based on the UVE analysis. From Fig. 4(a), it can be seen that the RMSE curve drops very quickly as the number of selected variables is increasing from seven to eight, ten to eleven and fifteen to eighteen. After that, the RMSE curve is level off with further increasing of the number of selected variables. Finally, twenty wavelength variables were chosen for SSC according to an F-test criterion with $\alpha=0.25$. Fig. 4(b) shows the distribution of the selected wavelength variables. From Fig. 4(b), it can be seen that most of the selected wavelength variables are near the peaks and valleys of spectrum.

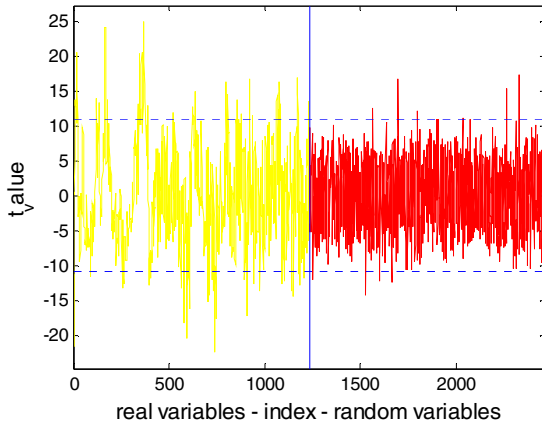
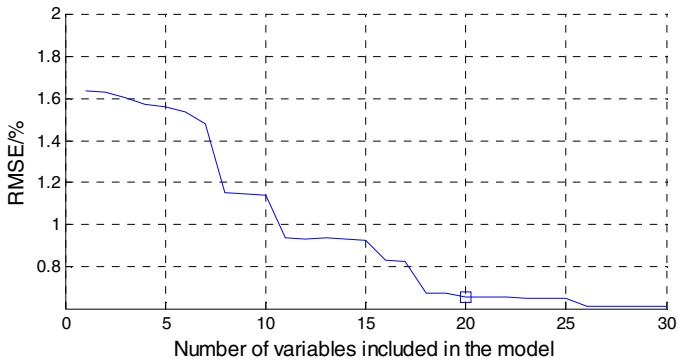
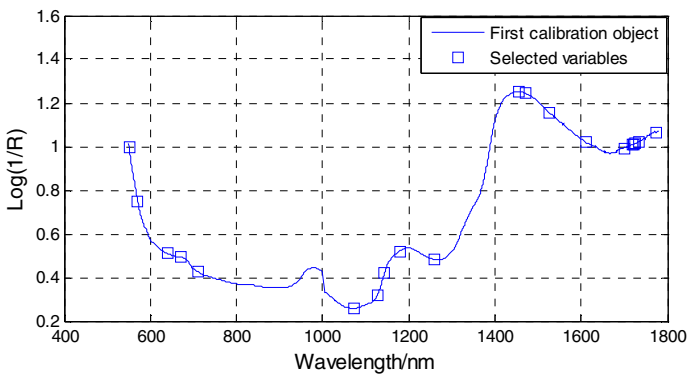


Fig. 3. Stability of each variable in the PLS model for SSC by UVE



(a)



(b)

Fig. 4. RMSE plot and selected variables by SPA based on UVE results: (a) RMSE plot; (b) Selected variables (shown in \square markers)

3.3.2 GA-SPA

Fig. 5 shows the results of GA variable selection for SSC of Nanfeng mandarin fruit. In Fig. 5, the solid horizontal line indicates the frequency cutoff for variable selection. The variables which frequency values are larger than frequency cutoff are realized as informative variables and reserved, and other variables are realized as uninformative variables and eliminated. After GA analysis, 137 variables were selected.

Fig. 6 shows the RMSE plot and selected variables by SPA based on GA results. From Fig. 6(a), it can be seen that the RMSE curve drops quickly as the number of selected variables is increasing from three to five, seven to eight, and fifteen to sixteen. The RMSE curve drops slowly as the number of selected variables is increasing from nine to fifteen, seventeen to twenty one. After that, the RMSE curve is level off with further increasing of the number of selected variables. And twenty one variables were selected at last. Fig. 6(b) shows the distribution of the selected variables for SSC by GA-SPA.

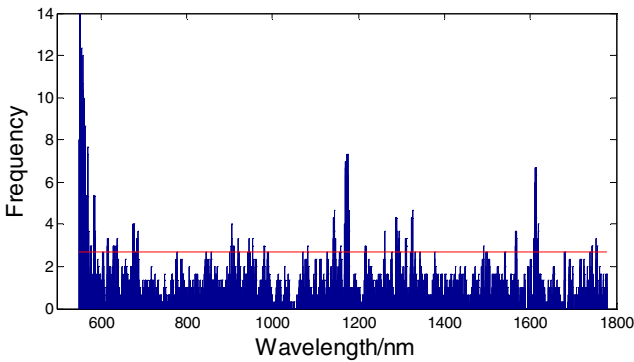
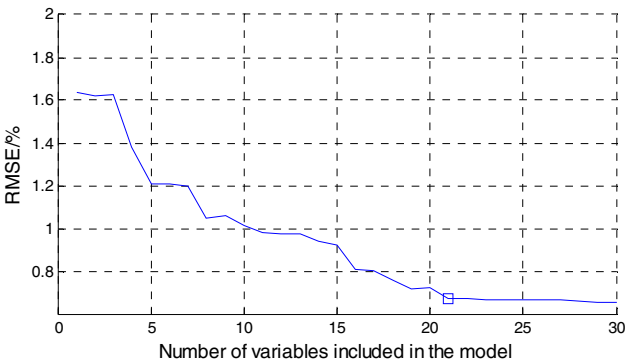
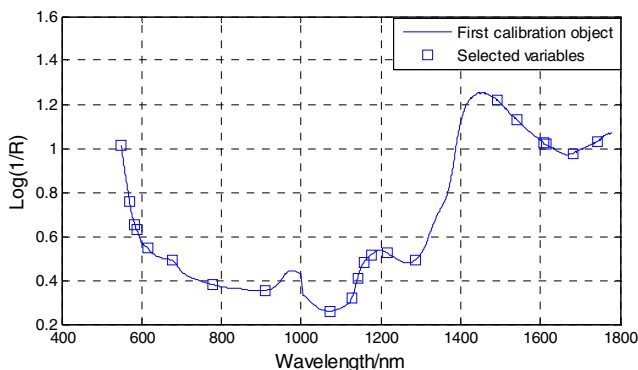


Fig. 5. Results of GA variable selection for SSC of Nanfeng mandarin fruit



(a)

Fig. 6. RMSE plot and selected variables by SPA based on GA results: (a) RMSE plot; (b) Selected variables (shown in \square markers)



(b)

Fig. 6. (Continued.)

3.3.3 UVE-CARS

In the UVE-CARS analysis, the same results of UVE in UVE-SPA were used, and CARS was conducted on the results of UVE. Fig. 7 shows the results CARS variable selection for SSC of Nanfeng mandarin fruit. From Fig. 7(a), it can be seen that the number of sampled variables decreases as the number of sampling runs increases, and the declining trend is from quick to slow. Fig. 7(b) shows the change of RMSECV with increasing of sampling runs. The RMSECV decreases slowly as the number of sampling runs is increasing from one to fifteen. After that, the RMSECV increases quickly with further increasing of sampling runs, this may indicate that some useful variables are eliminated during this process. Fig. 7(c) shows the change of regression coefficients of variables with increasing of sampling runs. The position of mark “*” means the minimum RMSECV, and the number of sampling runs is fifteen. Finally, twenty nine variables were selected. Fig. 8 shows the distribution of the selected wavelength variables for SSC by UVE-CARS.

3.3.4 GA-CARS

In the GA-CARS analysis, the same GA results in GA-SPA were used, and CARS was conducted on the results of GA. Fig. 9 shows the results of CARS variable selection based on GA results. From Fig. 9, it can be seen that the position of mark “*” is at twenty five sampling runs, and this indicates that the minimum RMSECV is obtained when the number of sampling runs is twenty five. According to the results of Fig. 9(a), seventeen variables were selected for SSC. Fig. 10 shows the distribution of the selected wavelength variables for SSC by GA-CARS.

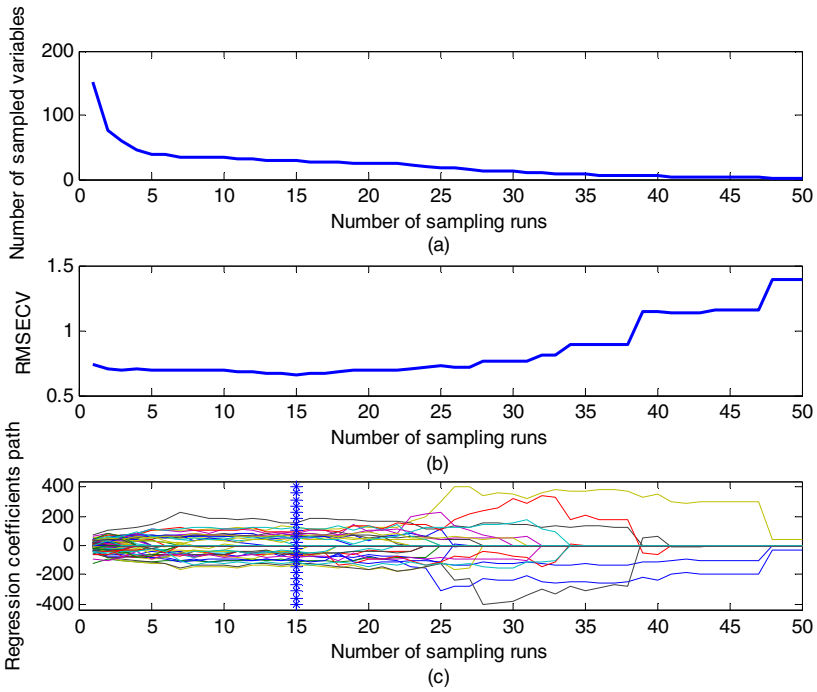


Fig. 7. Results of CARS variable selection based on UVE results: (a) Number of sampled variables; (b) RMSECV; (c) Regression coefficients path

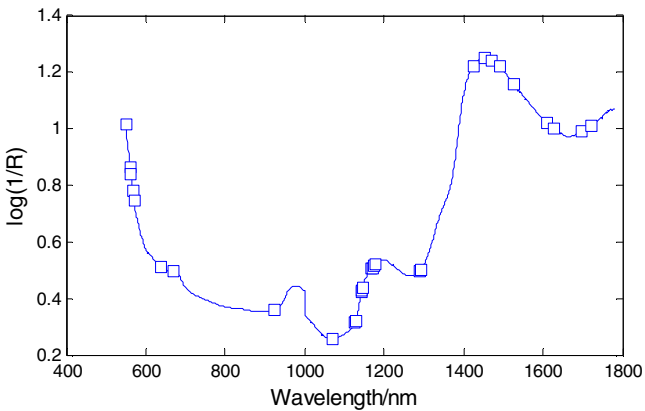


Fig. 8. Distribution of the selected wavelength variables for SSC by UVE-CARS

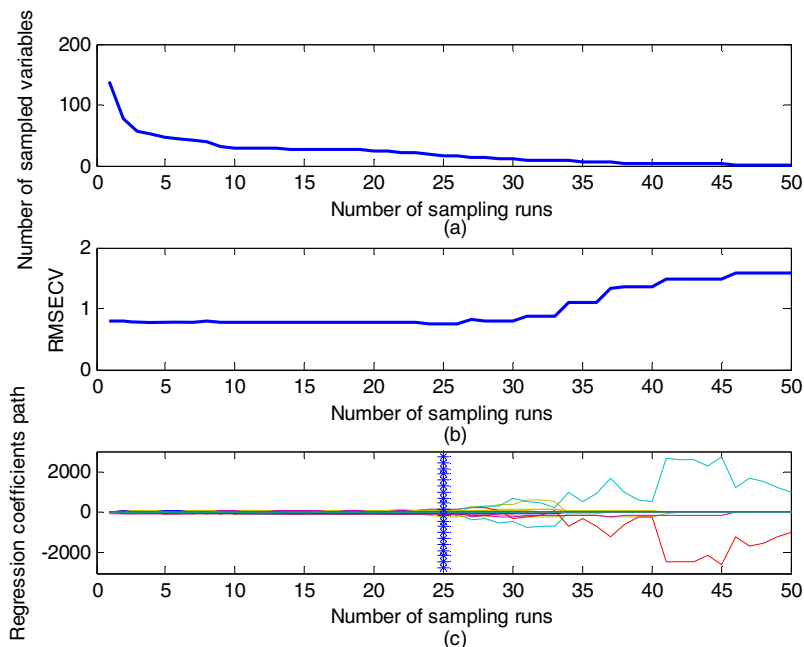


Fig. 9. Results of CARS variable selection based on GA results: (a) Number of sampled variables; (b) RMSECV; (c) Regression coefficients path

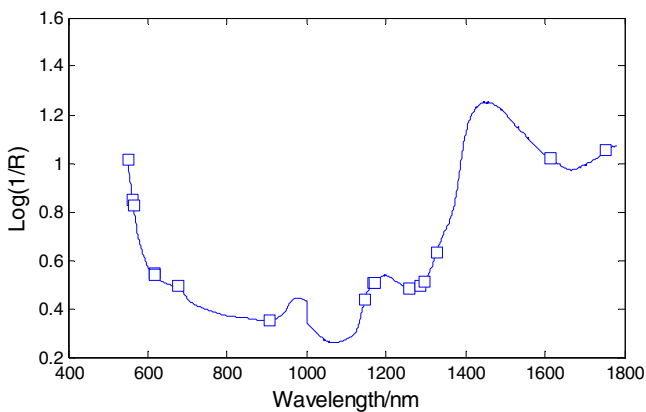


Fig. 10. Distribution of the selected wavelength variables for SSC by GA-CARS

3.4 LS-SVM

After variable selection, LS-SVM with RBF kernel was used to develop calibration models for SSC of Nanfeng mandarin fruit. Table 2 shows the results of LS-SVM and PLS regression for SSC of Nanfeng mandarin fruit. From table 2, it can be seen that

only about twenty variables are used in the LS-SVM (2% of the total number of variables), and 1231 variables are used in the PLS, while the results in LS-SVM models are comparable to the results of full-spectrum PLS model. This indicates that these four combined variable selection methods are useful and effective to eliminate uninformative variables and reserve informative variables.

For four combined variable selection methods, LS-SVM with GA-SPA obtains the best results, the correlation coefficients and RMSEs in the calibration, validation and prediction sets are 0.935, 0.560%, 0.912, 0.631% and 0.933, 0.594%, respectively. The worst results are obtained by LS-SVM with GA-CARS, and the correlation coefficients and RMSEs in the calibration, validation and prediction sets are 0.914, 0.641%, 0.836, 0.752% and 0.901, 0.716%, respectively. From above results, it can be concluded that GA-SPA is the best variable selection method among these four methods. This may due to that GA is suitable for eliminating uninformative variables and SPA is effective for selecting sensitive variables, so GA combined with SPA obtains the best results. For GA-CARS, the principles of GA and CARS are similar, this may be the reason why GA-CARS obtains the worst results. In order to evaluate the performance of LS-SVM models, the RPD (standard deviation/RMSEP) which has been defined as a measure of model performance [28] is introduced. The RPD values in the four LS-SVM models (UVE-SPA, GA-SPA, UVE-CARS, GA-CARS) are 2.67, 2.76, 2.44 and 2.29, respectively.

Table 2. Results of LS-SVM and PLS regression for SSC of Nanfeng mandarin fruit

<i>Method</i>	<i>Number</i> <i>of</i> <i>variable</i>	γ	σ^2	<i>Calibration</i>		<i>Validation</i>		<i>Prediction</i>	
				<i>r</i>	RMSEC	<i>r</i>	RMSEV	<i>r</i>	RMSEP
UVE-SPA	20	4.0e6	1.0e4	0.919	0.621	0.893	0.653	0.929	0.615
GA-SPA	21	1.6e10	5.0e7	0.935	0.560	0.912	0.631	0.933	0.594
UVE-CARS	29	6.8e10	4.3e7	0.910	0.651	0.862	0.699	0.912	0.671
GA-CARS	17	4.0e4	9.0e2	0.914	0.641	0.836	0.752	0.902	0.716
PLS	1231	---	---	0.919	0.619	0.897	0.649	0.901	0.710

4 Conclusions

The results demonstrate that four combined variable selection methods are useful and effective to select informative variables, and the results of LS-SVM with these combined variable selection methods are comparable to the results of full-spectrum PLS. GA-SPA is the best variable selection method among these four combined variable selection methods. The correlation coefficients and RMSEs in LS-SVM with GA-SPA model for calibration, validation and prediction sets are 0.935, 0.560%, 0.912, 0.631% and 0.933, 0.594%, respectively.

Acknowledgment. The authors gratefully acknowledge the financial support provided by the National Nature Science Foundation of China (No. 30972052), New Century Excellent Talents in Support of Ministry of Education Project (No. NCET090168) and Technology Foundation for Selected Overseas Chinese (2012).

References

1. Gómez, A.H., He, Y., Pereira, A.G.: Non-destructive measurement of acidity, soluble solids and firmness of satsuma mandarin using VIS/NIR-spectroscopy techniques. *Journal of Food Engineering* 77, 313–319 (2006)
2. Liu, Y., Sun, X., Zhang, H., et al.: Nondestructive measurement of internal quality of Nanfeng mandarin fruit by charge coupled device near infrared spectroscopy. *Computers and Electronics in Agriculture* 71S, S10–S14 (2010)
3. Fan, G., Zha, J., Du, R., et al.: Determination of soluble solids and firmness of apples by Vis/NIR transmittance. *Journal of Food Engineering* 93(4), 416–420 (2009)
4. Bertone, E., Venturello, A., Leardi, R., et al.: Prediction of the optimum harvest time of ‘Scarlet’ apples using DR-UV-Vis and NIR spectroscopy. *Postharvest Biology and Technology* 69, 15–23 (2012)
5. Sun, T., Lin, H., Xu, H., et al.: Effect of fruit moving speed on predicting soluble solids content of ‘Cuiguan’ pears (*Pomaceae pyrifolia* Nakai cv. Cuiguan) using PLS and LS-SVM regression. *Postharvest Biology and Technology* 51(1), 86–90 (2009)
6. Xu, H., Qi, B., Sun, T., et al.: Variable selection in visible and near-infrared spectra: Application to on-line determination of sugar content in pears. *Journal of Food Engineering* 109(1), 142–147 (2012)
7. McGlone, V.A., Clark, C.J., Jordan, R.B.: Comparing density and VNIR methods for predicting quality parameters of yellow-fleshed kiwifruit (*Actinidia chinensis*). *Postharvest Biology and Technology* 46(1), 1–9 (2007)
8. Moghimi, A., Aghkhani, M.H., Sazgarnia, A., et al.: Vis/NIR spectroscopy and chemometrics for the prediction of soluble solids content and acidity (pH) of kiwifruit. *Biosystems Engineering* 106(3), 295–302 (2010)
9. Flores, K., Sanchez, M.T., Perez-Marin, D.C., et al.: Prediction of total soluble solid content in intact and cut melons and watermelons using near infrared spectroscopy. *Journal of Near Infrared Spectroscopy* 16(2), 91–98 (2008)
10. Tian, H., Wang, C., Zhang, H., et al.: Measurement of soluble solids content in melon by transmittance spectroscopy. *Sensor Letters* 10(1-2), 570–573 (2012)
11. Ying, Y., Liu, Y.: Nondestructive measurement of internal quality in pear using genetic algorithms and FT-NIR spectroscopy. *Journal of Food Engineering* 84, 206–213 (2008)
12. Liu, F., He, Y.: Application of successive projections algorithm for variable selection to determine organic acids of plum vinegar. *Food Chemistry* 115, 1430–1436 (2009)
13. Sorol, N., Arancibia, E., Bortolato, S.A., et al.: Visible/near infrared-partial least-squares analysis of Brix in sugar cane juice: a test field for variable selection methods. *Chemometrics and Intelligent Laboratory Systems* 102, 100–109 (2010)
14. Wu, D., Chen, X., Zhu, X., et al.: Uninformative variable elimination for improvement of successive projections algorithm on spectral multivariable selection with different calibration algorithms for the rapid and non-destructive determination of protein content in dried laver. *Analytical Methods* 3, 1790–1796 (2011)

15. Huang, L., Wu, D., Jin, H., et al.: Internal quality determination of fruit with bumpy surface using visible and near infrared spectroscopy and chemometrics: A case study with mulberry fruit. *Biosystems Engineering* 109, 377–384 (2011)
16. Sun, T., Xu, W., Lin, J., et al.: Determination of Soluble Solids Content in Navel Oranges by Vis/NIR Semi-transmission Spectra Combined with CARS Method. *Spectroscopy and Spectral Analysis* 32(12), 3229–3233 (2012)
17. Chen, B., Meng, X., Wang, H.: Application of successive projections algorithm in optimising near infrared spectroscopic calibration model. *Journal of Instrumental Analysis* 26(1), 66–69 (2007)
18. Zou, X., Zhao, J., Huang, X., et al.: Use of FT-NIR spectrometry in non-invasive measurements of soluble solid contents (SSC) of ‘Fuji’ apple based on different PLS models. *Chemometrics and Intelligent Laboratory Systems* 87, 43–51 (2007)
19. Arakawa, M., Yamashita, Y., Funatsu, K.: Genetic algorithm-based wavelength selection method for spectral calibration. *Journal of Chemometrics* 25, 10–19 (2011)
20. Suykens, J.A.K., Van Gestel, T., De Brabanter, J., et al.: *Least Squares Support Vector Machines*. World Scientific, Singapore (2002)
21. Centner, V., Massart, D.L., de Noord, O.E., et al.: Elimination of uninformative variables for multivariate calibration. *Analytical Chemistry* 68(21), 3851–3858 (1996)
22. Leardi, R.: Application of genetic algorithm-PLS for feature selection in spectral data sets. *Journal of Chemometrics* 14, 643–655 (2000)
23. Leardi, R., Gonzalez, A.L.: Genetic algorithms applied to feature selection in PLS regression: how and when to use them. *Chemometrics and Intelligent Laboratory Systems* 41, 195–207 (1998)
24. Araújo, M.C.U., Saldanha, T.C.B., Galvão, R.K.H., et al.: The successive projections algorithm for variable selection in spectroscopic multicomponent analysis. *Chemometrics and Intelligent Laboratory Systems* 57(2), 65–73 (2001)
25. Galvão, R.K.H., Araújo, M.C.U., Fragoso, W.D., et al.: A variable elimination method to improve the parsimony of MLR models using the successive projections algorithm. *Chemometrics and Intelligent Laboratory Systems* 92(1), 83–91 (2008)
26. Li, H., Liang, Y., Xu, Q., et al.: Key wavelengths screening using competitive adaptive reweighted sampling method for multivariate calibration. *Analytica Chimica Acta* 648(1), 77–84 (2009)
27. Shao, Y., Bao, Y., He, Y.: Visible/near-infrared spectra for linear and nonlinear calibrations: a case to predict soluble solids contents and pH value in peach. *Food and Bioprocess Technology* 4(8), 1376–1383 (2011)
28. Williams, P.C., Sobering, D.C.: Comparison of commercial near infrared transmittance and reflectance instruments for analysis of whole grains and seeds. *Journal of Near Infrared Spectroscopy* 1, 25–32 (1993)

A Novel Robust Method for Automatic Detection of Traffic Sign

Bo Peng and Juan Wu

College of Information and Electrical Engineering, China Agricultural University,
Beijing, 100083, China
pengbo_cau@126

Abstract. Considering the requirement of high accuracy and robustness for traffic sign detection in real-world environments, this paper proposed a novel method for automatic detection of traffic sign. There are three main stages in the proposed algorithm: 1) segmentation by adaptive threshold in HSI color space to find the region of interest; 2) eliminate the noise present in the binary image and the small objects with morphological operations and mean filter; 3) contour extraction and curve fitting for a better contour by the least square method. Experimental results show a high success rate and demonstrate that the proposed framework is invariant to illumination, deformation, and partial occlusions.

Keywords: traffic sign, detection, morphology, contour extraction, fitting.

1 Introduction

Auto traffic sign detection is an essential part of advanced Driver Assistant System(DAS). Traffic signs provide warnings and instructions, having remarkable contrast with the background and characteristics like distinct shape and color. Being easily detected and recognized, traffic signs play an important role in safe driving. However, traffic signs are normally set in the right front side, resulting in the limitation of rotation quantity and geometric distortion. Therefore, traffic sign detection is facing a number of difficulties. (:) The illumination variations (including range of brightness, low visibility in twilight condition, fog weather and shadow, etc.), blurred images caused by car shaking, fuzzy signs, partial occlusion, as well as interferences of similar objects[1]. Both false detection of distractors and failure in detection of the real traffic signs could have negative effect on drivers. As a result, the high detection accuracy a key in the traffic sign detection.

There are three methods of traffic sign detection by locating the region of interests. The first method is color threshold segmentation. By using non-RGB color model to segment traffic sign, like HSV[2], CIECAM97[3], YUV[4], this method could minimize the effect of the glare, weak light or bad weather, such as fog. The second method is shape detection[5], such as using Hough transform[5]. However, it calls for massive calculation. The third method is detection based on feature (characteristics?), such as Haar feature[7], Hog feature[8][9], etc. In order to detect the red circle traffic

sign accurately under different real circumstances, this paper presents a robust traffic sign detection method. Three steps are involved: first of all, segment the image by threshold to get a binary image; Then eliminate the noise with morphological operations and mean filter. Finally, contour extraction and curve fitting for a better contour by the least square method.

2 Color Transformation

Color, which has high separability, is invariant in size and angle. By color segmentation of a traffic sign, we can detect its location in the image approximately. However, this method --- color threshold segmentation is easily affected by daylight, bringing problems like color reduction, light reflection and so on.

RGB color space model is the most intuitive color space. In this study, we transform RGB space model into HIS space model, since RGB space can be affected seriously by lightness and there are strong correlation among its three components. On the contrary, HIS color space model is visual uniform and consistent with human visualization. By using hue and saturation, it could eliminate the effect of illumination changes[10]. HIS color space model divides each pixel into hue, intensity and saturation. The transformation from RGB to HIS color space is as following:

$$H = 1 - \sqrt{3}(G - B)/[(R - G) + (R - B)] \quad (1)$$

$$S = 1 - \min(R, G, B)/(R + G + B) \quad (2)$$

$$I = (R + G + B)/3 \quad (3)$$

3 Noise Elimination

Noises could affect the detection accuracy by misleading the system into choosing the wrong targets. Therefore, it is important to suppress even eliminate the noises but still keep all the image details. Besides mean filter, this study also uses morphological erosion and dilation operation to eliminate the noises., and removes small sundries by setting aspect ratio afterwards. During the process, a dilation operation of the original image is first performed; and then-an erosion operation is used on the image when the contour is filled.; finally, the mean filter is used to smooth the image.

3.1 Mean Filter

Mean filter is a typical linear filtering algorithm. The basic principle is to construct a model on the target pixel in the image by adjacent pixels. Then the original pixel is replaced by the average value of pixels in the model. For example, a 3*3 filter model is constructed by 8 pixels around the target pixel.

3.2 Dilation and Erosion

Dilation and Erosion are two commonly used basic mathematics morphological operations. Dilation could fill the poles in the images as well as the dents on the edge. Erosion could not only reduce the size of original image, but also eliminate some small components in the image.

Suppose A represents a binary image while B stands for structural elements. A dilated by B is defined by formula (4) (shown below). Suppose Z represents two dimensional integer space. Each element of the set is a black or white pixel whose coordinate is (x,y). We focus on black pixels since this study turns objects into black while turning background into white. The rule of dilation is that, if a point of B falls in the area of A after one to one correspondence between the center of structural element B and each single points of A, this point will be turned into black. A dilated by B is represented by $A \oplus B$. According to figure. 1, after dilated by structural element circle, a dark blue square is turned into a light blue square with round corner.

$$A \oplus B = \{z | (\hat{B})_z \cap A \neq \emptyset\} \tag{4}$$

The definition of erosion is shown by formula (5). The result of B erode A is the full set of Z. The result will still falls in the area of A after B is translated the distance of Z. A eroded by B is represented by $A \ominus B$. Contrary to dilation, the rule of erosion is that, if all the points of B fall in the area of A after one to one correspondence between the center point of B and each single points of A, this point will be saved, otherwise it will be erased. According to figure 2, after eroded by structural element circle, the dark blue square is turned into the inside smaller light blue square.

$$A \ominus B = \{z | B_z \subseteq A\} \tag{5}$$

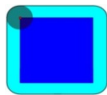


Fig. 1. Dilation Operation

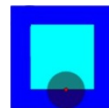


Fig. 2. Erosion Operation

3.3 Sundries Removal

Sundries removal aims at eliminating the small objects after image processing, by calculating the outline aspect ratio and the area of each small object. Take the circle traffic sign as an example. Considering factors like deformation and angel etc., which may affect removal process, we change the aspect ratio of the circle traffic sign from 1:1 to 0.8-1.3. If an object is beyond this range or its area is smaller than 1/500 of the whole image, we consider this object is unnecessary and can be eliminated. The same method can apply to other shape traffic signs, such as triangle, octagon as well as rectangle. By setting corresponding range, we can eliminate those small objects effectively and increase the detection accuracy.

4 Contour Extraction and Curve Fitting

In order to extract the sign contour clearly and accurately, this study uses an extraction method by merging Canny operator and Snake model[11]. In 1986, John Canny presented the very popular three criteria of detectors: good detection, good localization and only one response to a single edge. Based on the three criteria, he developed the optimal edge detection operator: Canny edge detection operator. The basic idea of Canny operator is to smoothing filter the original image by Gaussian filter., then to use Non-Maxima Suppression (NMS) to get the final edge image. Canny operator can achieve good localization accuracy. However, it could also cause fake edges and lost edges. Snake model is an active contour model which is brought by Kass in 1987. The principle of Snake model is that, by setting an initial curve around the target and moving the curve under both internal and external forces, the curve could finally converge to the real contour when it reaches the lowest energy. Snake model can achieve a closed contour. However, it lacks of good localization. As a result, the merge of Canny operator and Snake model is an effective way to solve the problems during contour extraction.

The images of traffic sign could lose certain information for some reasons, such as occlusions, which have negative effect on localization. Therefore, in this study, the curve fitting was done by least square method. The principle of least square method is to find a optimal matching function for a set of data by minimizing the sum of error squares. It uses the simplest way to get some absolutely unknowable truth value with minimum sum of error squares[12]. As a result, in the case of round traffic sign, we could use the least square method to fit circle center and radius by minimizing the sum of error squares.

5 Results and Discussion

5.1 Results

Detecting real images by the method mentioned above., Figure 3 shows the major steps of the detection process. Figure 3(a) is the original image; The green circle in Figure (f) shows the detection result, from which we can tell that the traffic sign has been detected clearly and accurately.

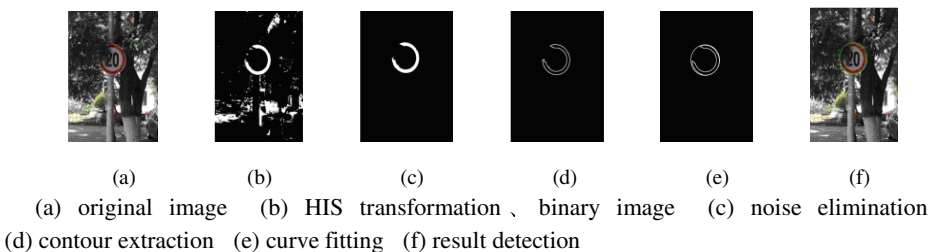


Fig. 3. The Detection Process of Real Traffic Sign



Fig. 4. Detection Results under different conditions

The experiment takes pictures of real images under different lightness and weather conditions. Running on 1G internal memory computer, the result shows that: During the day, the detection accuracy of the red circle traffic sign is above 98% and the False Positive Probability(FPP) is less than 2%. While taking the same sign during the night, the detection accuracy can still reach 96% with 4% False Positive Probability(FPP). By detecting the red circle traffic sign accurately, this result demonstrates that our new method could solve problems brought by illumination variation, deformation, rotation as well as occlusion and detect the traffic sign effectively.

5.2 Discussion

Without considering color segmentation, some different signs can look the same when turned into grey. Therefore, it is necessary to take color into account for traffic sign detection. The method based on color segmentation is fast and intuitive, however, it could be affected by illumination variation. Considering this, this study transforms RGB color space into HIS color space, which is robust and insensitive to illumination variation. This method could bring about high costs of calculation since the transformation is nonlinear. However, we can avoid this problem effectively by calculating space transformation in advance and saving it into look-up table. The limitation of this method, is that it is not robust to color and can be susceptible to interference from other objects with similar color.

Mean filter has a good effect on eliminating Gaussian noises. However since all the pixels are averaged during the process, the details of the image will be obscured. The erosion operation can erase the boundary points effectively and make the contour more converging and clear, while dilation operation can fill the spaces among the regions effectively and increase the continuity of the image. The difficulty of erosion and dilation operation is to choose structural elements. Choosing structural elements of small size can keep details of the contour but lose the efficiency in eliminating noises. While the effect of choosing structural elements of large size is just the opposite. In order to obtain more useful information, we can choose structural elements with protrusion shape, such as square, cross, etc, while the circle structural elements have minor effect on contour quality.

The contour extraction method of merging Canny operator and Snake model has high stabilization and localization accuracy. Besides, it could avoid the interference from fake edges and also fix the broken edges. The least square method has high robustness, solving problems like shape incomplete due to occlusions effectively during curve fitting.

6 Conclusion

This study proposes a novel, robust method of traffic sign detection. This method is insensitive to illumination variations and can avoid being affected by occlusion, rotation, deformation, etc to some extent. Based on the study of red circle traffic sign, this method segments red region threshold and gets the binary image in the first place by transforming the RGB color space into HIS color space. Then by eliminating noises with morphological operator and mean filter, as well as contour extraction and curve fitting, this method could effectively reduce the False Positive Probability(FPP) and achieve an accurate localization of the red circle traffic sign and any other real images. Experiments demonstrate that this algorithm has high rate of success, good localization accuracy, as well as high robustness to illumination variation, deformation and partial occlusions.

References

1. Ren, F., Huang, J., Jiang, R., Klette, R.: General Traffic Sign Recognition by Feature Matching. In: Proceedings of the 24th International Conference on Image and Vision Computing, New Zealand, pp. 409–414. IEEE, Wellington (2009)
2. Malik, R., Khurshid, J., Ahmad, S.: Road sign detection and recognition using color segmentation, shape analysis and template matching. In: Proceedings of International Conference on Machine Learning and Cybernetics 2007, pp. 3556–3560. IEEE, Hong Kong (2007)
3. Gao, X.W., Podladchikova, L., Shaposhnikov, D., et al.: Recognition of traffic signs based on their color and shape features extracted using human vision models. *Journal of Visual Communication and Image Representation* 17(4), 675–685 (2006)
4. Miiura, J., Kanda, T., Nakatani, S., et al.: An active vision system for on-line traffic sign recognition. *IEICE Transactions on Information and Systems* E85-D(11), 1784–1792 (2002)
5. Belaroussi, R., Tarel, J.P.: Angle vertex and bisector geometric model for triangular road sign detection. In: Proceedings of Workshop on Applications of Computer Vision 2009, pp. 1–7. IEEE, Snowbird (2009)
6. Wang, Y., Shi, M., Wu, T.: A Method of Fast and Robust For Traffic Sign Recognition. In: Proceedings of the Fifth International Conference on Image and Graphics 2009, pp. 891–895. IEEE, Xi'an (2009)
7. Bahlmann, C., Zhu, Y., Ramesh, V., et al.: A system for traffic sign detection, tracking, and recognition using color, shape, and motion information. In: Proceedings IEEE Intelligent Vehicles Symposium 2005, pp. 255–260. IEEE, Las Vegas (2005)
8. Creusen, I.M., Wihnhoven, R.G.J., Herbschleb, E., et al.: Color exploitation in HOG-based traffic sign detection. In: Proceeding of the 17th IEEE International Conference on Image Processing 2010, pp. 2669–2672. IEEE, Hong Kong (2010)
9. Overett, G., Petersson, L.: Large-scale sign detection using HOG feature variants. In: Proceeding of IEEE Intelligent Vehicles Symposium, pp. 326–331. IEEE, Baden-Baden (2011)
10. Fleyeh, H.: Shadow and Highlight Invariant Color Segmentation Algorithm for Traffic Signs. In: Proceeding of IEEE Conference on Cybernetics and Intelligent System 2006, pp. 1–7. IEEE, Bangkok (2006)
11. Zhang, Y., Sun, H.-Y., Sun, L.-J., Sun, X.-G.: Combination of active contour with passive edge detection in contour extraction. *Computer Engineering and Applications* 45(26), 160–162 (2009)

The Vulnerability Assessment Method for Beijing Agricultural Drought

Lingmiao Huang, Peiling Yang, and Shumei Ren

College of Water Resources & Civil Engineering, China Agricultural University,
Beijing 100083, China
huanglingmiao@cau.edu.cn, {yangpeiling, renshumei}@126.com

Abstract. Drought is a major disaster which Beijing agricultural systems faced with, build drought warning mechanism we need in-depth analysis the causes and mechanism of the drought to provide a basis for scientific disaster reduction and prevention. VAM vulnerability assessment method, selected 15 factors represent drought exposure, sensitivity and adaptive capacity, based on improved analytic hierarchy process to determine the weight of each factors, use K-means clustering algorithm to generate the drought vulnerability index system of research district. Draw vulnerability zoning map based on ArcGIS.

Keywords: Vulnerability, Assessment, Index System, VAM, Agricultural Drought.

1 Introduction

The risk of natural disasters is a result of natural disasters together with vulnerability, the level of loss risk is directly related with social vulnerability, to a great extent, decided by the vulnerability of hazard bearing [1]. Agricultural drought vulnerability means the property and status of agricultural production which is sensitive to drought and easily threatens by drought, as well as caused loss [2]. The impact factors of drought vulnerability are multifaceted [3].

Several scholars study on drought vulnerability in recent years, they focus on establishing drought vulnerability system based on a set of indicators. Liu Lanfang et al. [4] select nine indicators: precipitation, evaporation, the level of irrigation works and so on to evaluate vulnerability of agricultural drought in Hunan province. Wang Xiaohong et al.[5] develop a risk assessment model for agricultural drought, which includes the occurrence probability of drought, capacity of drought prevention, percentage of planting area, etc. Ni Shenghai et al. [6] select seven indicators to evaluate the Chinese agricultural drought vulnerability, according to the three elements, water resources characteristics, agriculture suffering drought and forming drought disaster circumstance and drought relief ability of water conservancies' facilities of the every locality, Wang Jingai et al.[7] obtains the distributional laws between the agricultural hazard- affected bodies and the centers of drought disaster in China based on regional combination of the hazard – formation factors with hazard - affected bodies. select three counties as typical hazard - affected bodies, i. e. the

rainfed field (Xinghe County) , the irrigated field (Xingtai County) & the paddy field (Dingcheng County) , set up a vulnerability diagnosis index system of agricultural drought disaster and put forward a regional assessment model of agricultural drought vulnerability, including the frangibility-adaptability model of the rainfed field , the production - living pressure model of the irrigated field and the water demand - supply model of the paddy field. Qiu Lin et al. [8] present threshold value of grade interval of estimation for vulnerability of agricultural drought in Hengyang city. According to variable fuzzy set theory, the variable fuzzy analysis method of multiple attribute and grades was proposed for quantitative estimation for vulnerability of agricultural drought disaster. Chen Ping, Chen Xiaoling, [9] select fourteen indicators representing exposure, sensitivity and adaptive capacity to droughts respectively. The weights of the indicators were calculated by analytic hierarchy process. Then using the composite index approach these indicators were combined into a drought vulnerability index of agricultural system by a linear aggregation. On the basis of the relationship between the drought vulnerability and exposure, sensitivity and adaptive capability, some suggestions for the drought hazard management in the future were proposed. Simelton et al. [10] identify socio-economic indicators associated with sensitivity and resilience to drought for each of China's main grain crops (rice, wheat and corn). Provincial harvest and rainfall data (1961–2001) are used to calculate an annual “crop-drought vulnerability index”. Leads us to propose a series of drought-vulnerability typologies based on the extent to which land, labor, capital, agricultural technology, and infrastructure buffer or exacerbate the effect of a drought event.

We commonly used drought index to indicate the degree of drought [11], however, it needs combine with drought vulnerability to accurately reflect drought risk. Yi Zhengjie et al.[12] built a farm soil moisture balance model together with simulation of soil moisture during crop's growth stages. In this way soil moisture simulation and drought degree evaluation are united to conduct dynamic evaluation of agricultural drought, which provides a handy and feasible method of real-time dynamic evaluation of agricultural drought through soil moisture simulation. Many scholars also have taken study on drought assessment of winter wheat in northern China. Wang Suyan et al.[13] based on understanding influence of water on the productive potentialities of winter wheat in semi-humid, semi-arid areas of northern China under natural climate condition, the “correction step by step” is used to calculate photosynthesis potential productivity, photo-temperature productivity and climate productive potentialities. Analysis the dynamic changes of winter wheat water and climate production potential in north China during the past 40 years. Sun Ning, Feng Liping et al.[14] Based on validation of two crop growth models (W heat SM and APSIM-W heat) for the winter wheat yield simulation of Beijing. Zhang Wenzong et al. [15] present a methodology for risk assessment and division of winter wheat drought hazard in Hebei Province, including the concept, calculation method and regional distribution of the disaster risk index. Also discussed the average decreasing rate, the disaster prevention and mitigation measures of dry year with different intensities and loses in different kind of risk areas.

During the growth period of winter wheat in northern winter wheat region, precipitation is mostly less than 250 millimeter. Along a gradient that sees increased aridity from south to north. In Beijing-Tianjin area, the precipitation has been less than 150 millimeter. But the water demand for the growth period was about 350–500 millimeter and the

demand for critical period was 200~250 millimeter, lack of 300 millimeter water [16]. The growth period of winter wheat in Beijing start from late September to mid-June [17], the rainfall of Beijing area is generally concentrated in the June to August, appear the phenomenon of precipitation and growth period of winter wheat water requirement dislocation, drought is a direct threat to stable and high yield of winter wheat, even has a serious impact on the socio-economic. It is urgent to carry out the study on Beijing drought vulnerability and reduce drought disasters.

The aim of this paper is to develop and apply a quantitative approach to agricultural drought vulnerability assessment within Beijing to identify which of the country's regions and districts are most vulnerable to drought. To achieve this aim, the study objectives are:

a) To establish an index system for the assessment of agricultural drought based on the three elements of drought vulnerability;

b) To select 15 factors represent drought exposure, sensitivity and adaptive capacity, based on improved analytic hierarchy process to evaluate the exposure, adaptive capacity and sensitivity of Beijing's eleven regions and the districts within the most vulnerable regions;

2 Materials and Methods

2.1 Study Area

Beijing is located in the longitude of $115^{\circ} 20'$ to $117^{\circ} 30'$ and the latitude of $39^{\circ} 25'$ to 41° . About 150km distance to the west of Bohai, located in the northwest edge of the North China Plain, the city's total area is 16410.54km^2 , mountain area account for 62%, and about 38% of the areas are plains. Beijing is surrounded by the Taihang Mountains and Yanshan Mountains in its western and northern, its southeast is a plain. The terrain is higher in the west; north and northeast, while inclined to the south and southeast.

The populations of Beijing are about 20 million; multi-year average precipitation is 585mm, the city's total water resources are 2.308 billionm^3 , however, water resources per capita are only 107m^3 , water resources are very scarce. From the history of drought disasters in Beijing, Beijing's drought is divided into three categories: spring drought, the early summer drought, summer drought. In recent years, the drought frequent occurred in Beijing, except the lower droughts loss rate during the year 1990 to 1998, since 1999, the drought loss rates were at high value. The impact of drought on agriculture was very big, evaluating and predicting spatial distribution of a given period of the potential risks of agricultural systems in Beijing which affected by the drought is particularly important to provide the basis for scientific disaster prevention and mitigation.

2.2 Research Method

In this paper, using VAM vulnerability assessment methods [18], the three elements of vulnerability classified as exposure, sensitivity, and adaptive capacity. Exposure

represent that system experience a degree of drought stress, it is related to the intensity, frequency and duration of the drought; sensitivity is the extent of agricultural system elements susceptible to the effects of drought; adaptive capacity is the behavior that stakeholders in the agricultural system taking to reduce the effects of drought in the pre-disaster and after disaster. The results of exposure, sensitivity, and adaptive capacity Co-expressed as drought vulnerability.

Using the formula [1]

$$V = f(E, S, A) \tag{1}$$

By the composite indicator method, the vulnerability results can be expressed as various indicators and the linear plus of their corresponding weights:

$$V = \sum_{i=1}^n I_i \times w_i + \sum_{l=1}^m I_l \times w_l + \sum_{r=1}^s I_r \times w_r \tag{2}$$

In the formula (1), V is drought vulnerability indicator of the evaluation unit; E is drought exposure indicator; S is drought sensitivity indicator; A is drought adaptability indicator. There are respectively multiplied by the evaluation indicator scores that belonging to the three elements and the corresponding weight of evaluation indicator. The I_i , I_l , I_r are the score of evaluation indicator i , l , r ; w_i , w_l , w_r are the weight value of the evaluation indicator i , l , r .

2.2.1 Establishment of the Evaluation Indicator System

Select representative sub-elements from the three elements: exposure, sensitivity and adaptive capacity in order to refine the three elements. this article focus on Beijing agricultural drought vulnerability, Beijing's high incidence of drought period was consistent with the growth of winter wheat, so the index system of this article mainly focus on considering the difference value between evaporation and rainfall in the winter wheat planting period and the proportion of winter wheat growth.

Table 1. List of drought vulnerability indicators

Element	Evaluation indicators	The explain of evaluation indicators	Data sources	Time
Exposure (E)	Difference value between evaporation and rainfall/mm(+)	Reflects the degree of crop water demand is satisfied	China Meteorological Data Sharing Network	
	Average elevation/m(+)	Elevation is positively related to water abstraction difficulty during the drought period	International Scientific Database (90 meter resolution data)	2010
	Average slope/° (+)	The slope affect soil water retention capacity, increasing the severe drought period irrigation difficulty		

Table 1. (Continued.)

	The river network density/ (km/km ²) (-)	Lack of precipitation, surface runoff is a major water sources of production and living		
	Forest coverage /% (-)	Influence the climate of the area and the conservation of rainfall		
	The irrigation index (-)	The proportion of effective irrigation area in the total area of cultivated land		
	Winter wheat planting ratio (+)	The proportion of winter wheat acreage in the total cultivated area		
Sensitivity (S)	Proportion of agricultural population(+)	The agricultural population groups are most sensitive to drought	Regional Statistical Yearbook of Beijing	2010
	Facilities agricultural area ratio(-)	The proportion of facilities agricultural area in the total cultivated area		
	Multiple cropping indicator (+)	Indicator of the degree of cultivated land use		
	Grain yield per unit area/ (t/hm ²)(-)	The lower, the more serious the impact of drought decrease yields, the more sensitive to drought		
	Rural electricity consumption/10 ⁴ kwh(-)	Reflect the level of the rural economy, as well as the time and the frequency use of agricultural machinery		
Adaptive capacity (A)	Net income of rural residents/Yuan(-)	Income determines the drought disaster recovery capabilities	Regional Statistical Yearbook of Beijing	2010
	Arable land per capita/hm2(-)	The performance of the population effect and the pressure of land		
	Agricultural power in unit of arable land / (w/hm ²) (-)	Manifest the level of mechanization of agricultural production, but also reflect the size of the irrigation mechanical power during drought period		

Note: The table "+" and "-" represent the various evaluation and drought vulnerability positive or negative correlation (partial indicators refer to Chen Ping [29] indicator system)

2.2.2 The Processing of Indicator Data

1) Difference value between evaporation and rainfall

Study area's main agricultural drought duration was the growth period of winter wheat from October to the second year of June. Firstly, reference crop evapotranspiration ET_0 use Penman formula recommended by Food and Agriculture Organization of the United Nations. Calculating the difference value between evaporation and rainfall in 16 meteorological stations of the study area, secondly, use ArcGIS regression kriging spatial interpolation to deal with the data to get the 90meter \times 90meter raster map of difference value between evaporation and rainfall in the whole study area. Thirdly, count the average value of the difference value between evaporation and rainfall in each evaluation unit.

2) Natural element indicators

The average elevation and average slope value in the evaluation unit were calculated by DEM image and slope map through ArcGIS. The drainage density values in evaluation unit was the intersection of the river vector layers and administrative boundaries vector layers in the study area by ArcGIS, then open the property sheet to sum its rivers' total length in each evaluation unit, latter, divided by the evaluation unit area.

2.2.3 Indicators Quantify and Weight Calculations

Analytic Hierarchy Process (AHP) is a method of evaluation and decision-making which is a combination of qualitative and quantitative analysis, quantitative analysis of the person's qualitative subjective judgment, making variety of heterogeneous data integration, it is a currently widely used to determine the weight. However, using AHP to build a judgment matrix will be a certain degree of subjectivity because the experts' judgment of the relative importance of the indicators varies different, while insufficient application of existing quantitative information is also an obvious inadequacy. Therefore, we can use the improved analytic hierarchy process method to calculate the weight of drought vulnerability indicators. Firstly, divide the evaluation behavior into three levels. Target layer is evaluation of vulnerabilities; criterion level is three drought vulnerability factors (exposure, sensitivity, adaptive capacity); lowest level is index layer which belonged to the upper evaluation indicators.

Assume that there are n number indicators involved in the evaluation, $N = \{1, 2, \dots, n\}$, P is an indicator of vulnerability standard evaluation set, according to study of this article, P have 5 elements, that is any indicator divided as the five clustering by the standard. The X_{ab} is the maximum membership grade of an indicator, according to the principle of maximum membership grade; the indicator is belonging to b clustering. The clustering level of X_{ab} which is maximum membership grade of an indicator belonging worse, the indicator of vulnerability is worse, the greater it caused vulnerability impact on the criterion level.

When two indicators are at the same level in criteria layer, the vulnerability impact on criteria layer are of equal importance; when the index i is at worse vulnerability clustering level when compared with index j , then consider that index i cause greater vulnerability impact on the criterion level than the index j . So:

- $d_{ij} = \begin{cases} 9 & \text{The degree of vulnerability of the index } i \text{ is four levels lower than the index } j \\ 7 & \text{The degree of vulnerability of the index } i \text{ is three levels lower than the index } j \\ 5 & \text{The degree of vulnerability of the index } i \text{ is two levels lower than the index } j \\ 3 & \text{The degree of vulnerability of the index } i \text{ is one level lower than the index } j \\ 1 & \text{The degree of vulnerability of the index } i \text{ is the same as the index } j \\ (1/3) & \text{The degree of vulnerability of the index } j \text{ is one level lower than the index } i \\ (1/5) & \text{The degree of vulnerability of the index } j \text{ is two levels lower than index } i \\ (1/7) & \text{The degree of vulnerability of index } j \text{ is three levels lower than the index } i \\ (1/9) & \text{The degree of vulnerability of index } j \text{ is four levels lower than the index } i \end{cases}$

Finally, use the K-means algorithm for the discretization of each index data indicators. The data is divided into five levels, making assignments for each indicator positive correlation with vulnerability assigned as 2,4,6,8,10; negatively correlated with vulnerability assigned as 10,8,6,4,2.

3 Results and Analysis

Making the weight of exposure, sensitivity and adaptive capacity in the criterion level equal. Using improved analytic hierarchy process to calculate the weight of the drought vulnerability indicators, and vulnerability evaluation results of all districts and counties in Beijing are shown in Table 2 and Table 3. View from the comprehensive weight of each indicator, Agricultural power in unit of arable land, the river network density, difference value between evaporation and rainfall, the three indicators have more important impact on target layer in drought vulnerability.

Table 2. Hierarchical structure and indicator weights of vulnerability evaluation (Consistency has passed the examination)

Target layer	Criterion level		Index layer		Comprehensive weight
	Element	Single-layer weight	Element	Single-layer weight	
Drought vulnerability	Exposure (E)	1/3	Difference value between evaporation and rainfall/mm(+)	0.3534	0.1178
			Average elevation/m(+)	0.1176	0.0392
			Average slope/ ^o (+)	0.1755	0.0585
	Sensitivity (S)	1/3	The river network density/(km/km ²) (-)	0.3534	0.1178
			Forest coverage /% (-)	0.092	0.0307
			The irrigation Index (-)	0.1495	0.0498
			Winter wheat planting ratio (+)	0.1123	0.0374

Table 2. (Continued.)

Adaptive capacity (A)	1/3	Proportion of agricultural population(+)	0.2803	0.0934
		Facilities agricultural area ratio(-)	0.1061	0.0354
		Multiple cropping index (+)	0.1061	0.0354
		Grain yield per unit area/ (t/hm ²)(-)	0.1538	0.0513
		Rural electricity consumption/10 ⁴ kwh(-)	0.114	0.038
		Net income of rural residents/Yuan(-)	0.1701	0.0567
		Arable land per capita/hm2(-)	0.2537	0.0846
		Agricultural power in unit of arable land / (w/hm ²) (-)	0.4623	0.1541

Table 3. Vulnerability assessment of districts and counties in Beijing (Exposure element index assessment result)

Evaluation index	Difference value between evaporation and rainfall	Average elevation	Average slope	The river network density	Element index result
Daxing	1.178	0.0784	0.117	0.4712	1.8446
Miyun	0.7068	0.2352	0.585	0.9424	2.4694
Pinggu	0.7068	0.0784	0.585	0.9424	2.3126
Yanqing	0.2356	0.392	0.468	1.178	2.2736
Huairou	0.7068	0.392	0.351	0.9424	2.3922
Tongzhou	1.178	0.0784	0.351	0.7068	2.3142
Changping	0.4712	0.1568	0.117	0.9424	1.6874
Shunyi	0.7068	0.0784	0.468	0.9424	2.1956
Mengtougou	0.2356	0.3136	0.234	0.4712	1.2544
Fengtai	0.9424	0.0784	0.468	0.2356	1.7244
Fangshan	0.2356	0.1568	0.234	0.9424	1.5688

(Sensitivity element index assessment result)

Table 3. (Continued.)

Evaluation index	Forest coverage	The irrigation Index	Winter wheat planting ratio	Proportion of agricultural population	Facilities agricultural area ratio	Multiple cropping index	Grain yield per unit area	Element index result
Daxing	0.307	0.0996	0.0748	0.5604	0.1416	0.354	0.1026	1.64
Miyun	0.0614	0.3984	0.2992	0.1868	0.354	0.2124	0.3078	1.82
Pinggu	0.0614	0.0996	0.2244	0.5604	0.354	0.354	0.1026	1.7564
Yanqing	0.1228	0.2988	0.374	0.3736	0.354	0.1416	0.4104	2.0752
Huairou	0.1842	0.1992	0.374	0.3736	0.2832	0.2124	0.2052	1.8318
Tongzhou	0.307	0.0996	0.1496	0.7472	0.1416	0.2832	0.2052	1.9334
Changping	0.1842	0.1992	0.2244	0.3736	0.0708	0.0708	0.513	1.636
Shunyi	0.307	0.0996	0.0748	0.934	0.1416	0.354	0.1026	2.0136
Mengtougou	0.2456	0.498	0.2992	0.1868	0.0708	0.354	0.513	2.1674
Fengtai	0.2456	0.2988	0.1496	0.1868	0.0708	0.0708	0.513	1.5354
Fangshan	0.2456	0.1992	0.2992	0.3736	0.2124	0.2124	0.3078	1.8502

(Adaptive capacity element index assessment result)

Evaluation index	Rural electricity consumption	Net income of rural residents	Arable land per capita	Agricultural power in unit of arable land	Element index result
Daxing	0.152	0.3402	0.6768	0.9246	2.0936
Miyun	0.38	0.567	0.3384	1.2328	2.5182
Pinggu	0.228	0.4536	0.6768	0.3082	1.6666
Yanqing	0.38	0.567	0.1692	1.541	2.6572
Huairou	0.304	0.4536	0.6768	0.3082	1.7426
Tongzhou	0.076	0.2268	0.6768	1.541	2.5206
Changping	0.076	0.3402	0.846	1.541	2.8032
Shunyi	0.152	0.1134	0.5076	0.9246	1.6976
Mengtougou	0.38	0.2268	0.846	1.2328	2.6856
Fengtai	0.076	0.1134	0.846	0.6164	1.6518
Fangshan	0.152	0.3402	0.6768	0.6164	1.7854

(Vulnerability assessment result)

Name of district	Daxing	Miyun	Pinggu	Yanqing	Huairou	Tongzhou
Vulnerability assessment result	5.5782	6.8076	5.7356	7.006	5.9666	6.7682
Name of district	Changping	Shunyi	Mengtougou	Fengtai	Fangshan	
Vulnerability assessment result	6.1266	5.9068	6.1074	4.9116	5.2044	

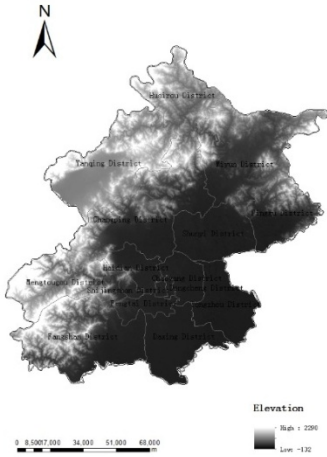


Fig. 1. Topography and administrative divisions of Beijing

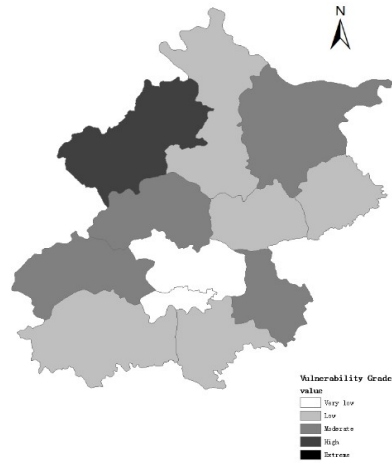


Fig. 2. The distribution of vulnerability grade

Beijing's topography and administrative divisions are shown in Figure 1. The level of vulnerability distribution is shown in Figure 2.

4 Conclusions

In this study, use the drought vulnerability assessment which considers three main factors. First, VAM is an effective method for analyze vulnerability of the various elements, VAM assessment methods is better at determining the impact factors of drought vulnerability, in order to analyze the area which may frequently occur drought. Prevent or reduce disaster losses before the drought had occurred.

However, using AHP to build a judgment matrix will be a certain degree of subjectivity because the experts' judgment of the relative importance of the indicators varies different, while insufficient application of existing quantitative information is also an obvious inadequacy. When using the improved analytic hierarchy process method to calculate the weight of drought vulnerability indicators, can avoid judgment matrix randomness which varies from person to person. This method is more objectivity, very stability, simple and easy to calculate. Using K-means algorithm to making index data discretization, can avoid the disadvantages of equal-width interval method which is too simple and easily influenced by the amount of data. Index data discretization has directly impact on the assignment of the index data and the accuracy of the final vulnerability assessment. Therefore, a suitable discretization method is particularly important.

Look at the result of index system for drought vulnerability assessment, the exposure index of Miyun, Pinggu, Huairou, Tongzhou are higher, indicating that the four districts experienced larger degree of drought stress. The sensitivity index of

Mentougou, Shunyi, Yanqing are higher, suggesting that in the three districts, the extent of agricultural system elements susceptible to the effects of drought are larger. Adaptive capacity index of Changping, Yanqing, Mentougou, Miyun are higher, showing that when these four districts occurred drought, the capability of stakeholders in the agricultural system taking measures to reduce the effects of drought in the pre-disaster and after disaster are poor. Integrate the three elements, the greater drought vulnerability districts are Yanqing, Miyun, Tongzhou, Mentougou and Changping.

References

1. Blaikie, P.M.: At risk: natural hazards, people's vulnerability, and disasters. Psychology Press (1994)
2. Keyantash, J., Dracup, J.A.: The quantification of drought: an evaluation of drought indices. *Bulletin of the American Meteorological Society* 83(8), 1167–1180 (2002)
3. Wilhelmi, O.V., Wilhite, D.A.: Assessing vulnerability to agricultural drought: A Nebraska case study. *Natural Hazards* 25(1), 37–58 (2002)
4. Liu, L., Liu, S., Liu, P., et al.: Synthetic analysis and quantitative estimation of the agricultural vulnerability to drought disaster in Hunan Province. *Journal of Natural Disasters* 11(4), 78–83 (2002) (in Chinese with English abstract)
5. Wang, X., Qiao, Y., Shen, R.: Drought risk assessment model for irrigation region. *Advances in Water Science* (1), 121–130 (2003) (in Chinese with English abstract)
6. Ni, S., Gu, Y., Wang, H.: Study on frangibility zoning of agricultural drought in China. *Advances in Water Science* (5), 705–709 (2005) (in Chinese with English abstract)
7. Wang, J., Shang, Y., Su, Y., et al.: A vulnerability diagnosis of agricultural drought disasters and regional sustainable development in China. *Journal of Beijing Normal University: Social Science Edition* (3), 130–137 (2005) (in Chinese with English abstract)
8. Qiu, L., Wang, W., Chen, S.: Quantitative estimation for vulnerability of agricultural drought disaster using variable fuzzy analysis method. *Transactions of the CSAE* 27(suppl. 2), 61–65 (2011) (in Chinese with English abstract)
9. Chen, P., Chen, X.: Evaluating drought vulnerability of agricultural system in Poyang Lake Ecological Economic Zone, China. *Transactions of the CSAE* 27(8), 8–13 (2011) (in Chinese with English abstract)
10. Simelton, E., Fraser, E.D.G., Termansen, M., et al.: Typologies of crop-drought vulnerability: an empirical analysis of the socio-economic factors that influence the sensitivity and resilience to drought of three major food crops in China (1961–2001). *Environmental Science & Policy* 12(4), 438–452 (2009)
11. Quiring, S.M., Papakryiakou, T.N.: An evaluation of agricultural drought indices for the Canadian prairies. *Agricultural and Forest Meteorology* 118(1-2), 49–62 (2003)
12. Yin, Z., Huang, W., Chen, J.: Dynamic evaluation of agricultural drought based on soil moisture simulation. *Journal of Irrigation and Drainage* 3, 5–8 (2009) (in Chinese with English abstract)
13. Wang, S., Huo, Z., Li, S., et al.: Water deficiency and climatic productive potentialities of winter wheat in north of China: study on its dynamic change in recent 40 years. *Journal of Natural Disasters* 1, 121–130 (2003) (in Chinese with English abstract)
14. Sun, N., Feng, L.: Assessing the climatic risk to crop yield of winter wheat using crop growth models. *Transactions of the CSAE* 21(2), 106–110 (2005) (in Chinese with English abstract)

15. Zhang, W., Zhao, C., Kang, X.: Study on methodology for risk assessment and division of winter wheat drought hazard in Hebei province. *Agricultural Research in the Arid Areas* 2, 10–16 (2009) (in Chinese with English abstract)
16. Wang, S.: Risk assessment and regionalization study on winter wheat drought in north of china. China Agricultural University (2004)
17. Zhang, C.: Study of the evaluate and zone methods on winter wheat drought risk based on GIS in Jing-Jin-JI region. Hebei Normal University (2010)
18. Fontaine, M.M., Steinemann, A.C.: Assessing vulnerability to natural hazards: impact-based method and application to drought in Washington State. *Natural Hazards Review* 10(1), 11–18 (2009)

Application of Modbus Protocol Based on μ C /TCP/IP in Water Saving Irrigation in Facility Agricultural

Jin-lei Li, Wen-gang Zheng, Chang-jun Shen, and Ke-wu Wang

Beijing Research Center of Intelligent Equipment for Agriculture, Beijing 100097, China

Abstract. As long as the deepen application of the Intelligent equipment technology in the Water Saving Irrigation, a hot topics in research is coming out, that is how to increase the proportion of the efficiency and output for the high tech facility in manufacture. The Modbus protocol based on u C/TCP/IP will play an important role in the Water Saving Irrigation application system, comparing to the others, it has such advantages of the Reliability of communication technology and real-time performance. After analyzing components of Modbus/TCP protocol, we applied it on real-time u C/OS-II kernel and ARM7 software and hardware and hardware environment with Modbus frame embedded in TCP frame. Test results show that Modbus/TCP protocol can achieve industrial standards. The protocol realizes the interconnection of control network and information network and has a broad application prospect in the agricultural water saving irrigation.

Keywords: Modbus/TCP, u C/OS-II, ARM7, real-time, water saving irrigation.

1 Introduction

In recent years, the industrial communication technology has been widely used in the field of agricultural water-saving irrigation. Current direction of development of agricultural water-saving irrigation is that transmitting irrigation data through the network, scientific and reasonable control of irrigation, and improve the comprehensive utilization of agricultural water resources. The specific application process has the following prolems: The first one is that the ways of irrigation data transmission mode is single, so standardized task is difficult to realize. The second problem is the real-time and reliability performance of information transmission is not good, unnecessary water waste exist in irrigation areas due to the poor efficiency and low reliability of information transmission [1,2].

Communication technology plays an important role in agricultural irrigation. In recent years, a few methods of network communication are widely used in agricultural water-saving irrigation applications. For instance, set an external serial server irrigation controller, or simply via Ethernet TCP/IP protocol transmission, etc. Although these methods have lots of advantages, such as interoperability, anti-interference ability and good real-time, but the defects of these ways can not be ignored. For example, communicate through an external serial server not merely engenders large power consumption, poor stability, low reliability but also generates additional costs.

However, transmission through TCP/IP protocol also leads to network insecurity occasionally [6,7].

Since 1970s, the Modbus protocol has been widely used in different areas, it's host/slave-machine communication way perfectly meet the requirement of deterministic. In our system, we combine the Modbus protocol with the TCP/IP protocol by inserting Modbus frame into the TCP frame. Since Modbus protocol has a large number of node installing, it's very suitable for irrigation controllers that require a lot of control valves. That is one of the reasons why Modbus possesses a high performance and low cost in the field of agricultural water-saving irrigation. Modbus is an truly open and ideal solution for agricultural water-saving irrigation. The effectiveness can be verified by experiment and its value can be proved in practical applications.

In this paper, aiming at the actual situation shortcomings of the current domestic agricultural water-saving irrigation, applied the industrial Ethernet technology to the agricultural water saving irrigation, and embedded the Modbus protocol into uC/TCP/IP, and a communication which is not only low power consumption and low-cost but also high compatibility has been realized. The problems of multiplicity and incompatibly of Field-bus standard, less accuracy and limited real time have been solved.

2 System Structure and Function

According to specific application, the system is based on the embedded Modbus/TCP/IP system structure. Essentially, the system structure is usually shown as that in Figure 1.

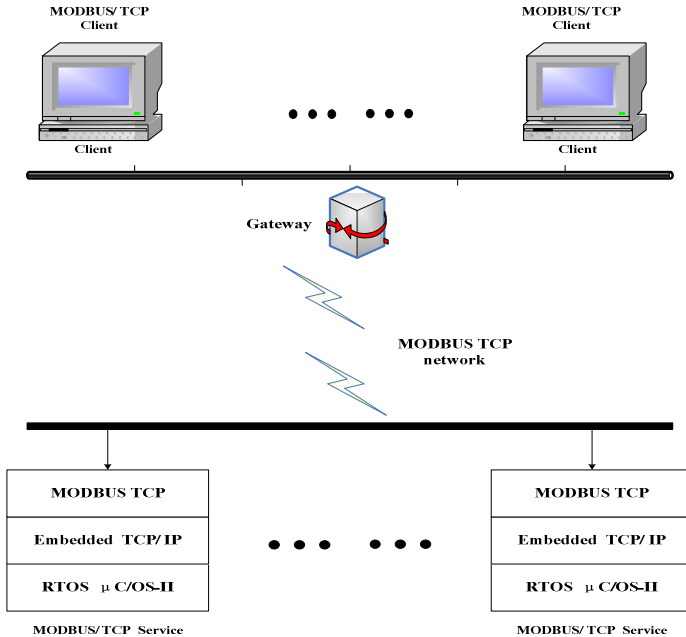


Fig. 1. The structure of MODBUS /TCP

The typical ways of the system are as follows: Irrigation control station Based on the Modbus/TCP as a server, a computer or embedded devices with the Modbus/TCP stack as a client. The client and the server are connected through the gateway, network interconnection equipment. Users can use the PC Modbus/TCP software on the PC client to exchange data with irrigation control station.

3 Hardware Design of Network Interface

The system structure is shown as that in Figure 2, the Ethernet Controller mainly composed of 5 parts. There are the microprocessor MCU, Ethernet physical layer interface chip DP83848, the RJ45 module used for cable connecting, 25MHz clock source, and the status LED lights which indicates the status of the connection. In our system, we use LPC2387 as the microprocessor, whose RAM memorizer of 64K and nominal operating frequency of 72MHz can provide abundant resources for μ C / TCP/IP transplantation [11]. In addition, the LPC2387 is capable of providing 10M/100Mbps Ethernet access in both half-duplex and full-duplex mode, with the built-in Ethernet MAC controller. Which can support Reduced Media Independent Interface, RMII and Buffered DMA Interface, BDI. We chosed DP83848C which is made by National Semiconductor as the Ethernet physical layer interface chip. It can easily connect with the MCU(LPC2387) with three kinds of interface mode(MII/RMII/SNI),and we chose RMII.

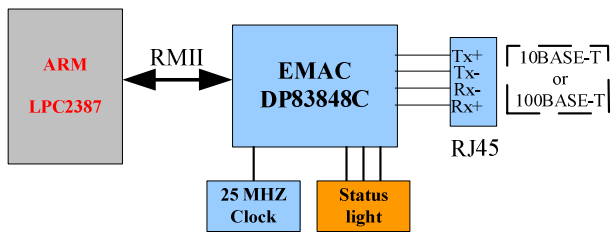


Fig. 2. Overall block diagram of system

Ethernet controller control the network DP83848C by a simplified and independent Media Interface, RMII interface. MAC chip outputs differential signal to the RJ45 port. When the cable access network mouth, the green LED light indicates connection, and the yellow LED light indicates data interchange. The circuit structure of this module is shown as that in Figure 3.

Channel 13: the channel consists RMII interface and MII interface. RMII Interface:CRS(P1.8),RX_ER(P1.14),RXD0(P1.9),RXD1(P1.10),TX_EN(P1.4),TXD0 (P1.0),TXD1(P1.1),REF_CLK(P1.15).MII Interface:MDC(P1.16),MDIO(P1.17).

Channel 14: The channel includes TX+,TX-,RX+,RX-,a total of two of the differential signal.

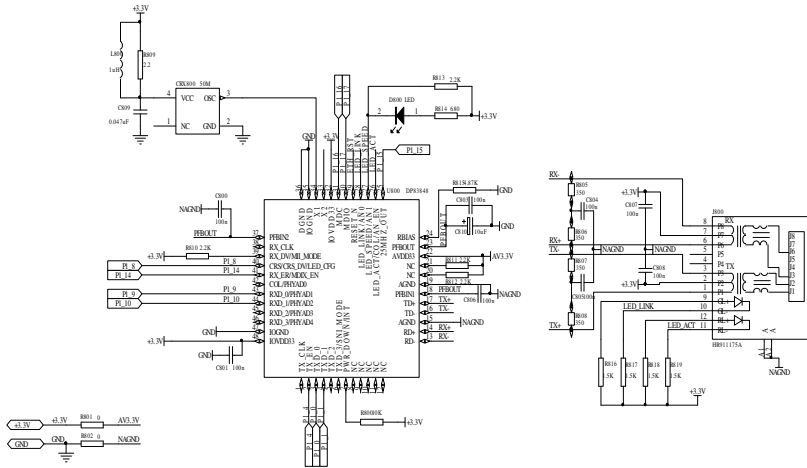


Fig. 3. U800 is the MAC module(DP83848). The microprocessor (LPC2387) connect with DP83848 with the RMI interface (P1.8,P1.14,P1.9,P1.10,P1.4,P1.0,P1.1); JP800 is the RJ45 module. The DP83848 connect with RJ45 with RX+,RX-, TX+,TX-.

4 The Software Design

4.1 The Transplant System of μC / OS-II

The transplant system of μC / OS-II operating system use μC / OS-II as the ROTs. So transplant μC / OS-II to hardware platform is the first thing to go before using μC / TCP/IP protocol stack, and generally speaking, it is related to four documents. There are OS_CPU_A.ASM,OS_CPU.H,OS_CPU.C.C which associated with the processor, and application-related OS_CFG.H. In our system, we use V2.84, the latest version of μC / OS-II.

4.2 The μC /TCP/IP Transplantation

The μC /TCP/IP is to achieve the most important and centralized protocols of TCP/IP. Including IP, ARP, ICMP, UDP, TCP and BSD Socket invocation interface. μC /TCP/IP include the following protocol module, NIC, ARP, IP, ICMP, UDP and TCP. At present, μC /TCP/IP can only support Interface Controller in ethernet,referred to NIC(Network Interface Controllers).And in our system it is DP83848. μC /TCP/IP operate as two tasks of μC /OS-II, Rx Task and Tmr Task. Rx_Task in charge of process the data packet received by NIC, if the data packet is needed by the present application layer, Rx_Task will put the data packet from network layer to application layer through TCP-IP protocol; and Tmr_Task is to manage all of the time delays related to TCP-IP protocol. During the μC /OS-II transplantation process, the user needs to realize the following functions:

- (1) interrupt service function NetNIC_ISR_Handler(), initialization and increate the interrupt nesting in IRQ.S

(2) interrupt handler `NetNIC_ISR_Handler()`, remove the CPU interrupt flag, send a semaphore and call the related function

(3) operating system function: It's achieved in `net_os.c`, which involves a large number of the μ C / OS-II-related operations function. This document provides a interface from TCP-IP protocol to the uC/OS-II operating system. If you want to migrate to a different operating system, the user can change `net_os.h / c` file. In RTOS Layer, tasks should be completed in three aspects: the establishment of `Rx_Task` and `Tmr_Task`, establish time control service functions, the establishment of 10 semaphores, as shown in Table 1.

Table 1. The semaphores created to transplant uC/TCPIP

serial number	semaphore
1	NetOS-InitSignalPtr
2	NetOS-LockPtr
3	NetOS-NIC-TxRdySignalPtr
4	NetOS-IF-RxQ-SignalPtr
5	NetOS-Sock-ConnReqSignalPtr
6	NetOS-Sock-ConnAcceptQ_Signal
7	NetOS-Sock-ConnCloseSignalPtr
8	NetOS-Sock-RxQ-SignalPtr
9	NetOS-IP-RxQ-SignalPtr
10	NetOS-TCP-RxQ-SignalPtr

4.3 Driver Programming in NIC

(1) Initialization. The whole initialization is consist of processor-related MCU initialization and PHY initialization. And the process includes:

```
static void EMAC_Init (NET_ERR *perr)
{
    NetBSP_Phy_HW_Init ();
    /*hardware reset initialization, configure IO, we use RMII.*/
    MAC1 = MAC1_RESET_TX |
    MAC1_RESET_MCS_TX |
    MAC1_RESET_RX |
    MAC1_RESET_MCS_RX |
    MAC1_RESET_SIM |
    MAC1_RESET_SOFT;
    /*confugure MCU ethernet register */
    NetNIC_PhyInit (perr);
    if (*perr==NET_PHY_ERR_RESET_TIMEOUT)
    {
        return ;
    }
}
```

/*initialize PHY (DP83848), First, reset PHY, and then read the ID of PHY to make sure that it has been reset successfully, and finally to the PHY control register assignment, set the data transfer rate, the default adaptive mode */

```

MAXF = 0x600;
/*configure register of TCP frame length, reset value is 0x600, the maximum
length is 1536 bits */
for (i = 0; i < 7; i++)
{
if ((clk_freq / MII_Dividers[i][0]) <= 25)
{
MCFG = MII_Dividers[i][1];
break;
}
SA0 = (NetIF_MAC_Addr[5] << 8) |
      (NetIF_MAC_Addr[4]);
SA1 = (NetIF_MAC_Addr[3] << 8) |
      (NetIF_MAC_Addr[2]);
SA2 = (NetIF_MAC_Addr[1] << 8) |
      (NetIF_MAC_Addr[0]);
EMAC_TxEn();
EMAC_RxEn();
}

```

4.4 Modbus/TCP Protocol Implementation

Modbus protocol defines a simple Protocol Data Unit(PDU), which has nothing to do with the basic communication. It consists a one byte function code and a variable length data. Unlike the standard Modbus frame, the Modbus/TCP frame embeds Modbus ADU into TCP for further transmission. Addressing and verification by the TCP/IP protocol, there is no necessity to recheck. What we need is to add a MBAP composed by seven bytes in order to identify the Modbus ADU. The MBAP can be divided into four parts, the detailed description as shown in table 2.

Table 2. Message header description of MBAP

region	Length	Description
Business unit ID	2bits	Modbus protocol request/response the ID of transaction process
Protocol ID	2bits	0=Modbus
Length	2bits	Uint ID and data length
Uint ID	1bits	The identification number of serial link or other bus to connect from the station

Function code that must carry on the operation, which is divided into a 16-bit word operation, such as 03 represent for maintaining a register operation, and 16 means multiple registers has to be written. The maximum data in Data domain is 248 bytes, and the specific format associated with functional code. In practice, the client sends the request data which shows the starting address of the register and the register number, meanwhile, the server respond with the number of operating registers and the status value of the register in a certain number.

The overall process in our system is as follows: The irrigation controller as a server waiting for the PC client to connect. The user can manage the irrigation controller with the software on computer when connected the them with reticle.

4.5 Modbus/TCP Protocol Communication Test and Results Analysis

Test results show that the first frame delay basically maintain within 1.3 ms, the last frame delay basically keep within 1.2 ms. The Result Indicates that 300 frames/second is normal processing speed of Modbus/TCP.

Table 3. The test results

sending rate (frame/second)	PC to irrigation controller			
	The first delay(ms)	frame	frame	The last frame delay(ms)
10	1.205			1.084
50	1.253			1.091
100	1.204			1.196
150	1.194			1.200
200	1.202			1.033
300	Frame lost			Frame lost

5 Summarization

Through a wholly analysis to the actual demand of current water-saving irrigation agriculture, then get a research of the Modbus/TCP protocol in facilities construction and Embedded System. The design of NIC and Modbus/TCP here have three advantages as follows: 1. Combining the Modbus/TCP technology and embedded system makes the Ethernet controller realize the real-time efficiency 2. The Modbus/TCP protocol here solve the multiplicity and incompatibly of field-bus standard 3. Successfully remove the μ C/OS-II format software, making the system high throughput data transferring, also solving the problems during operations to the complex control system, then low down the cost, more practically.

References

1. Proakis, J.G., Salehi, M.: Communication systems engineering. Prentice Hall, Upper Saddle River (2001)
2. Cook, D.J., Das, S.K.: Smart environments: technologies, protocols, and applications, vol. 11(5), pp. 13–46. John Wiley and Sons, Hoboken (2005)
3. Jia, X., Wang, C., Qiao, X.: Drive of wireless smart terminal and touch-screen human-machine interface for field irrigation (9), 8–12 (2008)
4. Can, A., Saban, S.: Application of Wireless Sensor Networks with GIS on the Soil Moisture Distribution Mapping. In: Photo Electricity Testing Technology, Ostrava, vol. 25, p. 8. Machinery Industry Press, Beijing (2005)

5. Sun, Z., Zhao, W., Liang, J., Du, K., Zhang, Y.: Design and application of greenhouse remote automatic control system based on GPRS and WEB. *Control & Automation* (2010)
6. Texas Modbus-IDA. Modbus Messaging on TCP/IP implementation Guide V1.0b, <http://www.modbus.org> (October 24, 2006)
7. Stevens, W.R.: TCP/IP Illustrated Chapter 1: Protocol
8. Tong, W.M., Xu, R., Lin, J.B.: Design of Ethernet Experimental System Based on LPC2478. *Low Voltage Apparatus* (22) (2011)
9. Jing, S.: Implement of Network Interface Communication Apply μC /TCP - IP Based on Ethernet Controller LAN91C111 12(6) (2010)
10. Yang, Z.Y., Zhang, Y., Zhang, K.L., Sun, Z.H.: Software Adaptive Fault-tolerance Method in Embedded Multiprocessor Environment. *Computer Measurement & Control* 20(6) (2012)
11. Sun, Y.H.: Research on Embedded Protocol Modbus/TCP/IP Conversion Module 5(6) (2008)

The Soil Heavy Metal Information Accurate Collection and Evaluation about *Lycium Barbarum* Cultivation in Western China

Ming Xiao^{1,2}, Wenjun Yang², Ze Zhang¹, Xianglin Tang¹, Xin Lv^{1,*},
and Dezhao Chi²

¹ Shihezi University Agriculture College, Xinjiang 832000 China

² Qinghai Agriculture and Forestry Academy of Sciences, Qinghai 810016 China
{mhmdxiao, ndyxiaozhun}@163.com, {273160043, 123452741}@qq.com
lxshz@126.com, qaafcdz@sina.com

Abstract. We selected two small sections of *Lycium Barbarum* cropland at Nuomuhong Farm in the Qaidam basin, western China: one had been farmed for only one year (original land), and the other had been farmed for many years (farm land). We tested surface soil samples for their content and distribution of six heavy metals (Cd, Zn, Pb, Cu, As, and Cr). All six heavy metals appeared at medium levels in samples from both sections of cropland. We conducted an interpolation analysis and drew a spatial distribution map based on the inverse distance weight (IDW) method. The distribution graph revealed a relatively consistent distribution of the six heavy metals in soil samples, a different gradation in the original land, and areas of higher values in the farm land. These findings suggest that the soil had been polluted. According to the Pollution-Free Food Standard and the Green Food Standard, we calculated the integrate pollution index using the Nemerow index method to check whether the levels met Pollution-Free food Standard and Green Food Standards. The values were 0.5 and 0.7 (defined as 'clean') in samples from the original land, but were 0.6 and 0.9 in samples from the farm land, which may be considered excessive.

Keywords: assessment, heavy metal pollution, standard, *Lycium barbarum*, Qaidam.

1 Introduction

Under heavy metal pollution, crop soils may exhibit latency, chronicity, irreversibility, and have strong toxic properties and abiotic degradation. This is an important challenge for producers of high-quality agricultural products and researchers in the fields such as edaphology, resource environmental protection, and agricultural product quality safety. Investigations of spatial variations in heavy metals, which are important to evaluating soil environmental quality and heavy metal pollution, involve analyzing spatial features

* Corresponding author.

including the content of heavy metals, along with any changes, trends, and spatial variation in those metals[1]. Recently, researchers have combined geographic statistics with geographic information system (GIS) data to analyze regional environmental processes. Mingkai Qu, Weidong Li and Chuanrong Zhang has assessed the spatial distribution and uncertainty of the potential ecological risks of heavy metals in soil using sequential Gaussian simulation (SGS) and the Hakanson potential ecological risk index (PERI) in Wuhan, China. Results show that the potential ecological risks of Cr, Cu, Pb, and Zn are relatively low in the study area, but Cd indeed reaches a serious level that deserves much attention and essential treatment[2]. Linsen Zhang, Jun Liang, Chunlin Wu *et al.* evaluated the contents of As Pb Cr Cd and Cu in an apple-planting region in Shanxi province using a method that incorporated a single pollution index and a comprehensive pollution index according the Green Food Standard, show that the heavy metals were not accumulated gradually in old apple orchards and all meet the standards[3]. Gailin Wu, like li, Mingde Hao *et al.* on the basis of the integrate pollution index of heavy metal research proposed fertilizer application should pay attention to the content of heavy metals in fertilizer, a reasonable choice, in order to avoid the contamination of the soil environment[4]. Xia Huang, Tingxuan Li and Haiying Yu. used a signal pollution index and the Nemerow composite index to evaluate the heavy metals risk, and the results show that there was Cd contamination in greenhouse topsoils in Shouang Shandong Province[5].

The Qaidam basin, located on the Tibetan Plateau, is a closed region and few studies have assessed environmental effects in the area of reclamation. No studies have investigated the spatial variation in heavy metals or their potential pollution risk in soils in the planting region of *Lycium barbarum* (common names: goqi berry, wolfberry, medlar).

2 Experiments and Methods

2.1 Experimental Samples

2.1.1 Study Area Overview

The Qaidam Basin is located on the edge of the Tibetan Plateau, surrounded by the Kunlun, Qilian, and Altun Mountains. Nuomuhong Farm is located southeast of the basin at altitudes ranging from 2700~3000 m. It is irrigated by snow waters from the Kunlun Mountains, which enables oasis farming. The area is cold and dry with little rainfall, abundant sunlight, and large differences between daytime and nighttime temperatures. Soil in the area has PH values ranging from 7.8~8.2. Because the area is mostly sandy loam and has few plant diseases and insect pests, it is suitable for growing *L. barbarum*, and the *L. barbarum* produced in this area is famous for its quality and is quite valuable [6].

2.1.2 Soil Sample Collection, Tests, and Data Processing

Sample Collection: Samples were collected based on the following guiding principles: Select cultivated farmland in flat areas (avoid depressions or mounds). Try to avoid non-representative areas, e.g., those that have been altered by human activity or where soil has greatly eroded. Do not collect samples from areas currently being fertilized. Try to collect samples 30 days before or after fertilization.

The farm land field was a rectangular area of 660 m × 510 m, and the original land was a rectangular area of 400 m × 330 m. We adopted the grid soil sampling method and selected samples at 100 m × 50 m intervals. A dot in each interval served as a center point; we randomly selected five points, each with a 3 m radius. We then took a 20 cm × 20 cm × 20 cm cube of soil from each point. From these samples, we took 1 kg from each and created a mixed sample by equally mixing the 1 kg samples from all the sites. The samples were taken to our lab for analysis. We recorded the fixed position sampling point coordinates using GPS. In order to prevent sample contamination, we did not let the samples touch metal containers during sample collection, preservation, and processing.

Sample Testing: Stones, grass roots, and other plant residues were removed from the samples, which were left to dry in a ventilated room. Samples were then filtered using a 100 mesh sieve (150 μm mesh size). A MILESTONE brand microwave digestion instrument was used, along with an inductively coupled plasma emission spectrometer.

The testing method involved using 7 ml (top grade and pure) concentrated nitric acid, 2 ml (top grade and pure) hydrogen peroxide, and 2 ml (top grade and pure) hydrofluoric acid. Standard substances of these chemicals were purchased from the National Standard Substance Center; for the standard curve, we used three density gradients of 0, 0.5, and 1 and a unit of mg/l.

2.2.3 Data Processing

The data were entered into Excel and subjected to the inverse distance weighting (IDW) method. A spatial analysis was conducted and the results were presented using ARCGIS9.3.

2.2.4 Heavy Metal Soil Pollution Assessment Method

Single pollution index evaluation: For the evaluation, $P_i = C_i/S_i$, where P_i is the i single pollution index of a pollutant, C_i is the i actual measurement, and S_i is the evaluation standard for the pollutant. The evaluation standard was calculated separately in accordance with the industrial standards of “Pollution-Free Food standard” (NY/T 5249-2004) [7] (Table 1), and “Green Food Standard” (NY/T 391-2000) [8] (Table 2). Values of $P_i < 1$ for As, Hg, Cd, Cr, and Pb indicate that the soil is not polluted, and the sample meets environmental standards. If one or more elements has a value of $P_i > 1$, the soil is polluted and does not meet environmental standard.

Table 1. Pollution-Free Food standard (NY/T 5249-2004). Heavy metals: mg/kg

Item	Grade level			
	Grade I		Grade II	
	Background	<6.5	6.5~7.5	>7.5
Cd≤	0.20	0.30	0.30	0.60
Hg≤	0.15	0.30	0.50	1.0
As≤	15	40	30	25
Cu≤	/	150	200	200
Pb≤	35	250	300	350
Cr≤	90	150	200	250
Zn≤	100	200	250	300

Table 2. Green Food Standard (NY/T 391-2000). Heavy metals: mg/kg

Farming condition	Dry field			Paddy field		
	<6.5	6.5-7.5	>7.5	<6.5	6.5-7.5	>7.5
PH	<6.5	6.5-7.5	>7.5	<6.5	6.5-7.5	>7.5
Cd≤	0.30	0.30	0.40	0.30	0.30	0.40
Hg≤	0.25	0.30	0.35	0.30	0.40	0.40
As≤	25	20	20	20	20	15
Pb≤	50	50	50	50	50	50
Cr≤	120	120	120	120	120	120
Cu≤	50	60	60	50	60	60

Nemerow pollution index evaluation: In $P_N = ((P_i^2 + P_0^2) / 2)^{1/2}$, P_N is the Nemerow composite index, P_i is the average pollution index for the soil, and P_0 is the maximum pollution index of the soil. As shown in (Table 3), soil quality is determined by changes in the P_N value and crops are affected by the degree and accumulation of pollutants.

Table 3. Nemerow composite index as evaluation standard

Degree	index	Pollution status	Pollution level
I	$P_N \leq 0.7$	safe	clean
II	$0.7 < P_N \leq 1.0$	caution	potentially unclean
III	$1.0 < P_N \leq 2.0$	mild contamination	pollution over limit
IV	$2.0 < P_N \leq 3.0$	mid-level pollution	soil, crops subject to severe pollution
V	$P_N > 3.0$	heavy pollution	soil, crops subject to heavy pollution

3 Results and Discussion

3.1 Analysis of Heavy Metal Content in Samples

Table 4 lists the heavy metal contents in 22 surface soil samples taken from original cropland. The variable coefficient reflects the average variable degree of sampling points in the total sample. Generally, 10%~100% exhibited medium variation: the variable coefficient for Cu in samples from original land reached a maximum of 61.48%, and the variable coefficient for As reached a minimum of 8.45%. The heavy metals can be arranged from maximum to minimum degree of variation as follows: Cd, Zn, Pb, Cu, As, and Cr.

Table 4. Descriptive statistics for heavy metal contents from original land

Element	Min (mg/kg)	Max (mg/kg)	Mean (mg/kg)	SD	CV(%)	Skew- ness	Kurtosis
As	0	26.40	15.47	8.45	8.45	-0.318	-0.689
Cd	0.14	0.42	0.30	0.077	25.49	-0.847	0.095
Cr	18.24	56.34	48.16	8.19	17.01	-2.507	8.265
Cu	13.44	90.12	28.16	17.66	61.48	2.447	6.572
Pb	5.76	28.49	13.38	4.92	36.80	1.380	3.287
Zn	30.08	61.90	44.84	9.28	20.70	0.471	-0.767

Table 5 lists the heavy metal contents in 50 surface soil samples taken from farm land. The variable coefficient reflects the average variable degree of sampling points in the total sample. The variable coefficient for Cd reached a maximum of 34.74%, and the variable coefficient for Cr reached a minimum of 6.15%. The heavy metals can be arranged from maximum to minimum degree of variation as follows: Cd, Zn, Pb, Cu, As, and Cr. Comparison between the two kinds of farmland reveals that the variable coefficients of Cr, Cu, Pb, and Zn decrease over time, but the variable coefficient of Cd increases significantly after years of farming.

Table 5. Descriptive statistics for heavy metal contents from farm land

Element	Min (mg/kg)	Max (mg/kg)	Mean (mg/kg)	SD	CV(%)	Skew- ness	Kurtosis
As	11.53	18.34	14.50	1.45	10.13	0.235	0.064
Cd	0.19	1.23	0.43	0.15	35.09	3.165	16.817
Cr	41.78	58.12	47.13	2.90	6.21	0.896	2.709
Cu	19.97	34.20	25.51	2.59	10.26	0.893	2.839
Pb	18.19	34.18	22.17	2.28	10.39	2.775	14.466
Zn	56.58	108.29	69.18	8.47	12.37	2.194	8.012

3.2 Spatial Distribution Features of Heavy Metals in Soil

We used the inverse distance weighting (IDW) method to conduct an interpolation analysis and examine spatial variation in the soil pollutants. As shown in Fig. 1, As content in original soil was greater in the west than in the east, and As content in the southwest region is greater than the natural background value. Few regions reached the level II standard. Cd content in original soil was clearly greater in the southeast and northeast than in other regions. In most areas, Cd content in soil was greater than the natural background value: in some areas values were greater than 0.40 and reached the level II standard. Cr content in original soil was less than the natural background value, with considerable spatial variation in the north and southwest regions. Cu content in original soil was highest in most north and northeast areas and the highest point was 90.12 mg/kg, but far lower than the level II standard and did not exceed the natural

background value. Spatial variation in Pb content in original land tended to be greater in the north than in the south, and tended to change gradually. Zn content was less than the natural background value, and spatial variations revealed that content tended to be higher in the west than in the east. Zn content was very high in some northeast areas.

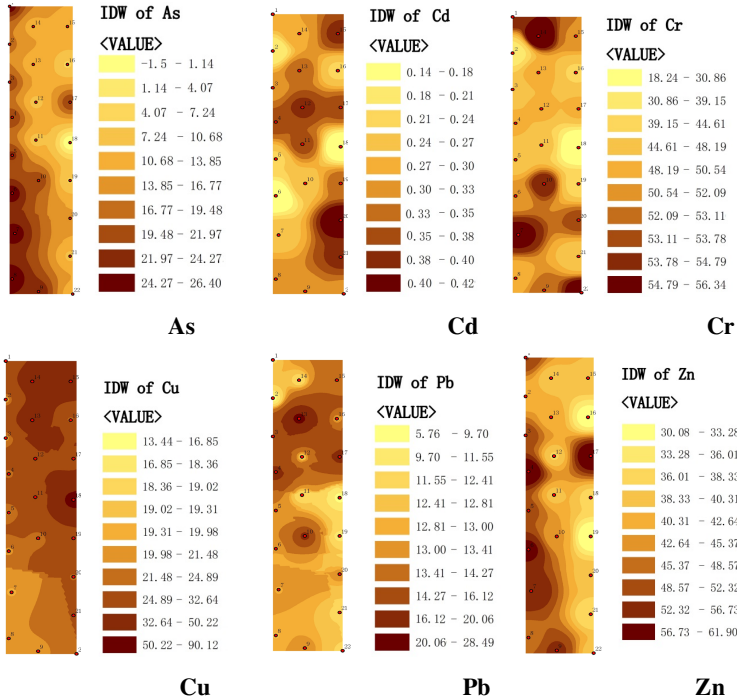


Fig. 1. The heavy metals content in soil and spatial variation in original land

Fig. 2 shows that As content in farm land was lower than the natural background value; only a few southwest and northwest regions reached the level II standard. Overall Cd content was greater than the natural background value, with most regions reaching the level II standard. The contents of Cr, Cu, and Zn in farm land exhibited a scattered spatial distribution. Generally, the comparisons revealed that in original land, spatial variation was very similar for all heavy metals, gradation levels differed, and the natural status of soil was relative stable. In farm land, heavy metal content exceeded the standard and differed greatly in quantity: Cr, As, Zn, Pb, and Cu contents were all more than 1.2~1.7 times higher than normal, and Cd content was nearly 5 times the normal value. These findings indicate that farm land has been polluted.

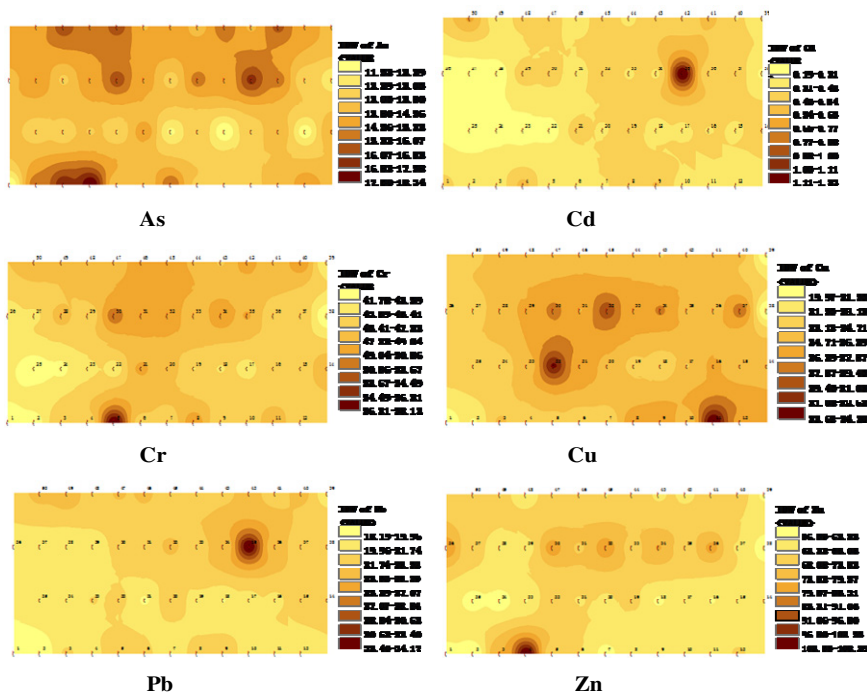


Fig. 2. The heavy metals content in soil and spatial variation in farm land

3.3 Soil Heavy Metal Pollution Assessment

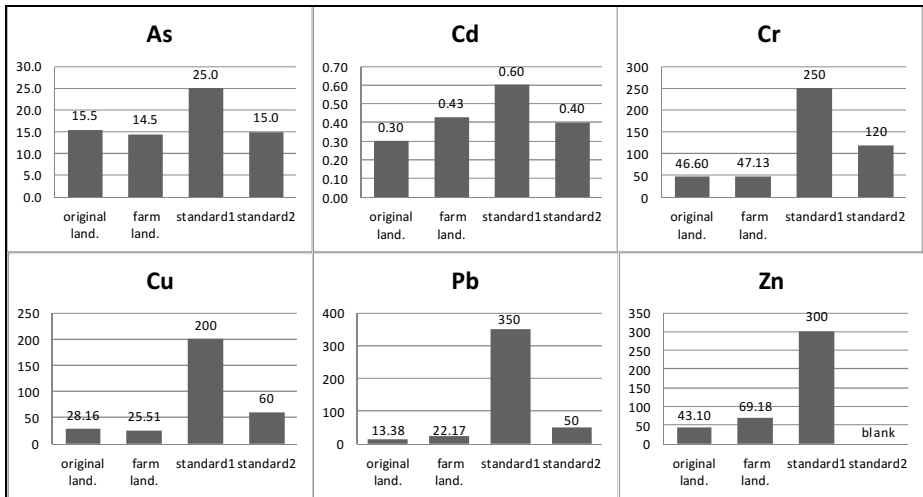
3.3.1 Soil Heavy Metal Contents Compared with the Standards

The As from the original land and farm land are both meet to the Green Food standard, but more less than the Pollution-Free Food standard; the Cr、Cu、Pb and Zn, from the original land and farm land are all far less than the Pollution-Free Food standard, and less than the Green Food standard (there is not Limited value for the Zn in the Green Food standard); the Cd is only 0.30 mg/kg in original land, both less than the two standards, but it rise to 0.43 mg/kg in farm land, increased 43%, over the Green Food standard, show that there is accumulation of Cd in farm land(see Fig. 3).

Unit:mg/kg

3.3.2 The Superscalar Rate of Soil Heavy Metal According Different Standards

In original land 4 samples exceed the Pollution-free Food Standard and 18 samples exceed Green Food Standard of As, the rate were 10% and 45% (Table 6). In farm land 31 samples exceed Green Food Standard of Cd, the rate is 62% (Table 7), show that there is accumulation of Cd in farm land.



(Standard1= Pollution-Free Food standard, standard2= Green Food standard)

Fig. 3. Comparison of soil heavy metals contents according to different standards

Table 6. The superscalar rate of soil heavy metal in original land

heavy meatal	samples	Pollution-free Food Standard		Green Food Standard	
		Superscalar	Superscalar rate(%)	Superscalar	Superscalar rate(%)
As	22	4	18	10	45
Cd	22	0	0	1	5
Cr	22	0	0	0	0
Cu	22	0	0	1	5
Pb	22	0	0	0	0
Zn	22	0	0	/	/

Table 7. The superscalar rate of soil heavy metal in farm land

heavy meatal	samples	Pollution-free Food Standard		Green Food Standard	
		Superscalar	Superscalar rate(%)	Superscalar	Superscalar rate(%)
As	50	0	0	0	0
Cd	50	2	4	31	62
Cr	50	0	0	0	0
Cu	50	0	0	0	0
Pb	50	0	0	0	0
Zn	50	0	0	/	/

3.3.3 Single Pollution Index Evaluation

With regard to upper limits for elements in the Pollution-Free Food Standard and the Green Food Standard, separate environmental evaluation criteria were used to calculate and analyze factors in the pollution index of heavy metals for soil samples taken from the two study areas. With regard to Pollution-Free Food Standard requirements, the pollution index was less than 1 in all samples from original land. This means that this area meets the Pollution-Free food standard for the six heavy metals investigated. With regard to the Green Food Standard, all pollution indices were also less than 1, indicating that this area also qualifies for the Green Food Standard (see Table 8).

Table 8. Single pollution index evaluation of soil heavy metal in original land

Heavy metal	Mean (mg/kg)	Pollution-Free food standards pollution index	Green Food Standard pollution index
As	15.47	0.62	0.77
Cd	0.30	0.50	0.75
Cr	46.60	0.19	0.39
Cu	28.16	0.14	0.47
Pb	13.38	0.04	0.27
Zn	43.10	0.14	/

With regard to upper limits for elements in the Pollution-Free Food Standard and the Green Food Standard, separate environmental evaluation criteria were again used to calculate and study analyze factors in the pollution index of heavy metals in 50 surface soil samples taken from farm land. With regard to the Pollution-Free Food Standard requirements, the maximum pollution index was 0.71 and the minimum was 0.06; because these values were less than 1 for all six heavy metals, this area meets Pollution-Free Food Standards. With regard to the Green Food Standard, five heavy metals had a pollution index less than 1, but the index for Cd was greater than 1, meaning that the soil is polluted and this area does not meet the Green Food Standards (see Table 9).

Table 9. Single pollution index evaluation of soil heavy metal in farm land

Heavy metal	Mean (mg/kg)	Pollution-Free food standards pollution index	Green Food Standard pollution index
As	14.50	0.58	0.72
Cd	0.43	0.71	1.06
Cr	47.13	0.19	0.39
Cu	25.51	0.13	0.43
Pb	22.17	0.06	0.44
Zn	69.18	0.23	/

3.3.4 Composite Pollution Index Evaluation

Composite Index is calculated based on Nemerow index method, and the Pollution-Free Food and the Green Food standards. According to the Pollution-Free Food and the Green Food standards the original land soil index were 0.5, 0.7, both in the “clean” level; the farm land were 0.6, 0.9, in the “clean” level according the Pollution-Free Food standard, in the “potentially unclean” leave according to the Green Food standard. (see Table 10).

Table 10. Nemerow index depend on different Standards (mg/kg)

		As	Cd	Cr	Cu	Pb	Zn	Mean	Max	Nemerow index
Pollution-free	Original land	0.62	0.5	0.19	0.14	0.04	0.14	0.27	0.62	0.5
	Farm land	0.58	0.71	0.19	0.13	0.06	0.23	0.32	0.71	0.6
Green food standard	Original land	0.77	0.75	0.39	0.47	0.27	/	0.53	0.77	0.7
	Original land	0.72	1.06	0.39	0.43	0.44	/	0.61	1.06	0.9

4 Conclusions

We analyzed data about six heavy metals (Cd, Zn, Pb, Cu, As, and Cr) and found that the Nuomuhong farm original land soil is pure and can comply with the Pollution-Free Food Standard and the Green Food Standard, but the farmland were subject to pollution during many years of farming, which resulted in heavy metal pollution, especially Cd pollution. Further research will be required to clarify the process of pollution.

We analyzed soil from two different areas of Nuomuhong Farm: original land and farm land, in terms of their heavy metal (Cd, Zn, Pb, Cu, As, and Cr) content. We used the Nemerow composite index to analyze and evaluate data. According to the Pollution-Free Food Standards, the soils in Nuomuhong Farm are all near or below excessive levels, and according to the Green Food Standard, original soil is all considered clean, whereas the farm land is at a borderline excessive level.

Acknowledgment. This research was funded by the Xinjiang Production and Construction Corps major science and technology program “precision agriculture and information on agricultural technology application and demonstration” (2007zx03). The authors would like to thank Prof. Dezhao Chi from Qinghai university for his good suggestion regarding article writing, and Dr. Hairong Lin from Shihezi university for her chemical analysis.

References

1. Bai, Y., Li, B., Hu, K.: Study on the space variable character of soil salt and its component in Huanghuaihai Plain. Soil Environmental Quality Standards (1999) (in Chinese)
2. Qu, M., Li, W., Zhang, C.: Spatial Distribution and Uncertainty Assessment of Potential Ecological Risks of Heavy Metals in Soil Using Sequential Gaussian Simulation. Human and Ecological Risk Assessment (2013)

3. Zhang, L., Liang, J., Wu, C., et al.: Evaluation and concentration of soil heavy metals in apple orchards in Shanxi province. *Journal of Fruit Science* 21(2), 103–105 (2004) (in Chinese)
4. Wu, G., Li, L., Hao, M., et al.: Effects of Long-term Fertilization on Heavy-metal Contents of Soil and Environmental Quality Evaluation. *Journal of Soil and Water Conservation* 6(24-3), 60–63 (2010) (in Chinese)
5. Huang, X., Li, T., Yu, H.: Risk assessments of heavy metals in typical greenhouse soils. *Plant Nutr. Fert. Sci.* 16(4), 833–839 (2010) (in Chinese)
6. Wu, G., Tang, H., Li, R.: The current situation of the development of Ningxia medlar in Qinghai. *Ningxia Agriculture and Forestry Science and Technology* 2, 62–63 (2008) (in Chinese)
7. Ministry of Agriculture of the People's Republic of China. Pollution-free food wolfberry production technology standard procedures-NY/T 5249–2004. Standards Press of China, Beijing (2004)
8. Ministry of Agriculture of the People's Republic of China. Environmental technical terms for green-food production area –NY/T 3912-2000. In: *Green-food Standard Collection*. pp. 86–90. Standards Press of China, Beijing (2003)

Research on the Optimization of Agricultural Supply Chain Based on Internet of Things

Guangsheng Zhang

Pinhu Campus, Jiaxing University, Pinhu, Zhejiang, 314200, China
zgs_88@163.com

Abstract. Technology of IOT which used in agricultural supply chain can help to improve operational efficiency and reduce supply chain costs. This paper analyzes the basic structure of agricultural supply chain, current status of the research, and summarizes major obstacles of the development process. The paper also describes application of IOT principle, as well as agricultural supply chain optimization approach based on internet of things, including agricultural production, processing, transportation and sales process. The results show that: integration and information management through IOT can reduce logistics costs and improve circulation efficiency and effectiveness. The government should develop policies to achieve agricultural internet of things, improve efficiency of agricultural supply chain operations.

Keywords: Internet of Things, Agricultural Supply Chain, Status Analysis, Optimization.

1 Introduction

The development of agriculture in China is backward. Farmers' income is low. The reasons are varied. One important reason is the circulation of agricultural supply chain is poor. Major agricultural supply chain process is from initial production to consumption of agricultural products. Among them, the core business is the main component, related to information flow, capital flow and logistics, etc. (main structure shown in Figure 1). Agricultural supply chain is characterized by many volume, broad area, the strong timing requirements of agricultural spending, more agricultural supply chain departments, more staff.

In recent years, agricultural supply chain has been developed rapidly. However, due to starting late, the development faces many difficulties, such as the backwardnesses of rural logistics infrastructure, low level of technology, lag agricultural supply chain standardization system and operation mode, weak administrative details and other issues, led to agricultural supply chain operational efficiency low. At present, optimization research of agricultural supply chain is less. As Wamba(2006)[1] used radio frequency identification (RFID) technology which be applied to the integrated food supply chain to replace bar code recognition technology , builded management information system. Bottani(2009)[2] used IOT to coordinate logistics and information flow, improve the integrated food supply chain management and reduce its cost. Thiesse(2009)[3] established a system through IOT, which assess the quality of agricultural products and processed products "from farmers to table". Li Jianwei(2011)[4] analyzed the specific application of

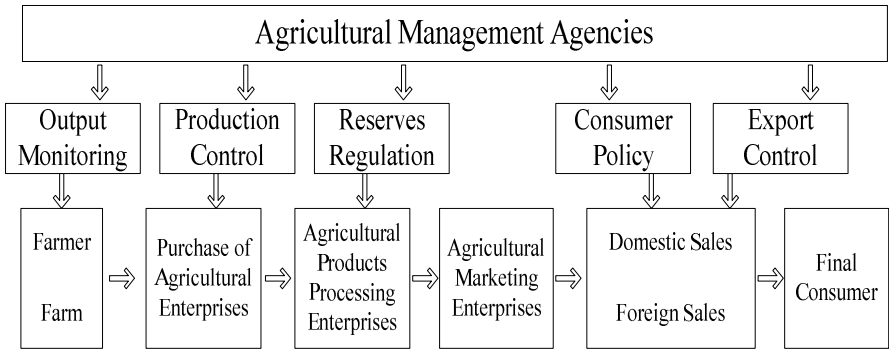


Fig. 1. Structure of Agricultural Supply Chain

IOT in agricultural production and farming, transportation, inventory, sales, and information management and other aspects. Liu Xuemei(2011)[5] analyzed the agricultural supply chain system according to recent incidents of food safety problems, effectively promoted the rapid development of agricultural supply chain. Zhou Hang(2011)[6] studied optimization of the food supply chain relies on IOT. Based on the above, we find that on agricultural supply chain research domestic and foreign scholars has focused on macro-level, multi-round concept, circulation system and other conditions and policy analysis, failed to put forward efficient optimization method. The rapid development of computer technology provides a solution to improve the efficiency of agricultural supply chain operations process. The development of IOT accelerates the progress of this trend.

2 Internet of Things

In 1999, MIT professor proposed IOT (Internet of Things). The purpose of IOT is to form a system of production and living smarter. IOT is defined as follows: through two-dimensional code reading equipment, radio frequency identification (RFID) devices, infrared sensors, global positioning systems and laser scanners and other information sensing device, according agreed protocol, it connects the Internet for information exchange and communication in order to achieve intelligent identify, locate, track, monitor and manage a network.

The structure of IOT can be divided into three layers: the perception layer, network layer and application layer. Perception layer is constituted by a variety of sensors, including temperature and humidity sensor, two-dimensional code label, RFID tags and readers, camera, GPS and other sensing terminals. Things perception layer is used to identify objects and collect information sources. Network layer is constituted by a variety of networks, including the Internet, wide network, network management systems and cloud computing platforms. It is the hub of things, responsible for transferring and processing information obtained by perception layer. IOT application layer is the interface of IOT and user. It combines with the industry needs to realize the intelligent application of IOT.

3 Optimization of Agricultural Supply Chain Based on IOT

3.1 Status Analysis

In recent years, our governments develop agricultural supply chains vigorously. The total amount of agricultural products logistics is growing. In the total social logistics, the importance of IOT is increasing, mainly reflected in the sensitivity to the customer, quality of life and social macro adjustment. From Figure 2 we can see that the total agricultural product logistics increased steadily year by year, as of 2010 reached 2.2355 trillion. However, the growth rate of agricultural logistics is relatively large, indicating that agricultural supply chain is vulnerable to be influenced by economic conditions and other external factors. The stability of the supply chain is poor.

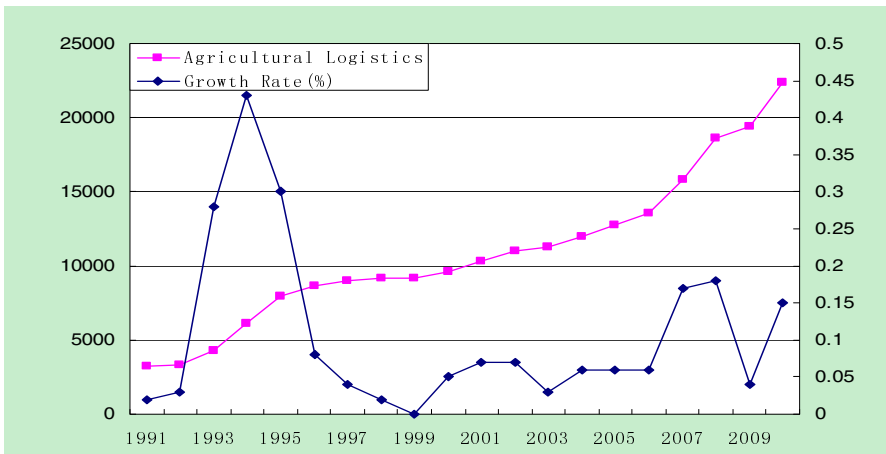


Fig. 2. Amount and Rate of Growth of Agricultural Product Logistics

Because development of agricultural supply chain is not perfect, its level of development is far behind developed countries. As shown in Table 1.

Table 1. Main Economic Indicators

	Cost	Loss rate	Processing Proportion	Value-added Processing	Proportion of Supermarket Sales
Developed Country	10%	5%	80%	1:4	80%~95%
China	40% (Food) 60% (Fruits and Vegetables)	15% (Food) 25% (Fruits and Vegetables)	10%	1:0.8	Less than 30%

3.2 Main Problems

In production, agricultural supply chain depends on natural conditions, environmental and human factors obviously. The Production is different from traditional industrial products and services; it has a universality and dispersion of consumption. Logistics is burdensome: Because diversity of market demands, this production led to a regional agricultural need in different areas. Perishability of agricultural products increases with distance and time, which limits the development of its circulation. Technology of agricultural logistics is backward: The rural logistics infrastructure and equipment are backward, technical conditions can not meet market demand. Given the low level of development of logistics technology, the level of mechanization of processing and packaging products is low and does not meet the conditions for the transport of agricultural products, processing, packaging, processing, and other terms. Uncertainty of market is big: Because agricultural production, consumption and market dispersion, we can not fully grasp market information, market volatility is a big settlement. In rural economic restructuring, the non-standard supply chain operations easily lead farmers to produce blindness. Input costs of agricultural supply chain are high: In order to ensure that products meet quality requirements of consumption and consumption, we need to take necessary measures in the circulation to strengthen asset specificity.

3.3 Applications of IOT in the Agricultural Supply Chain

The impact of IOT is enormous. Application of IOT can optimize agricultural supply chain facilities, inventory, transportation, information and procurement and other sectors, as well as manage agricultural production, transportation, consumption and other sectors, reduce supply chain costs, and achieve highly agile supply and fully integrated.

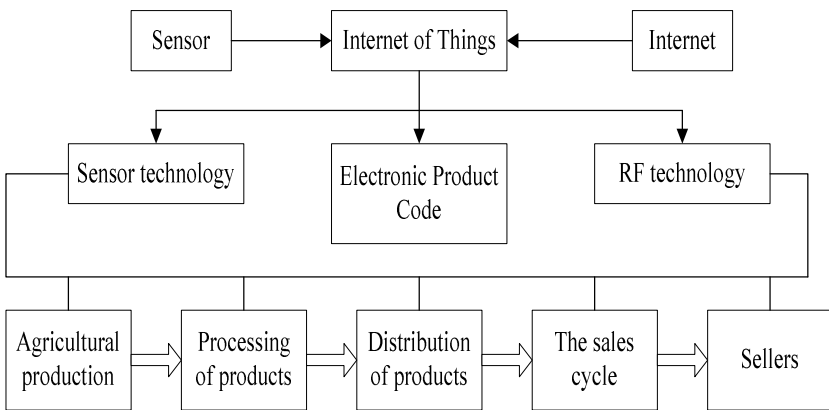


Fig. 3. Logistics Network Application in Agricultural Logistics

(1) Improve the overall construction of IOT: Putting IOT, sensor network, and internet together, using Sensor technology, electronic product code, radio frequency technology, we can accurately understand and grasp from procurement, manufacturing, handling, storage, transportation, distribution, sales to the service supply chain each link, reducing the agricultural supply chain in the “bullwhip effect” exists.

(2) The application in the process of production: IOT can solve problems that accord to the manufacturer’s requirements to operate, the operation is not higher transparency in traditional agricultural production. In the procurement of raw materials, IOT can tag encoding, establish database, and monitor products throughout the entire production process, including current temperature, humidity and the corresponding operators, all entered into the database to make it clear process prone to risks.

(3) The application in the process of transportation. IOT improves the efficiency of transportation greatly. First, this can realize visualization of the transport, agricultural transport vehicles are scheduled timely, try to avoid invalid transport. Second, the use of RFID tags can provide temperature monitoring, achieve agricultural vehicle dynamic perception, dynamic monitoring of the quality and safety of agricultural products. Again, IOT can dynamically acquire all cold storage inventory and in-transit traffic conditions in order to make transportation decisions science to achieve an effective cold chain logistics of agricultural products circulation.

(4) The application in the sales process: it reads information of product automatically through embedded tags using RFID, monitors the quantity and inventory quantity of goods, adds goods and deals expired products timely. The use of IOT can monitor the supply of goods and sales progress, determine the amount of purchase according to the proportion of sales. In the customer checkout time, we use radio frequency technology to shorten the time for the items of information literacy, improve the efficiency of the customer’s purchase and checkout.

(5) Application of the supply chain information transfer: For any one of the agricultural supply chain node enterprises, from the origin to the pin, using IOT you can understand the production of raw materials, processing conditions, who is responsible for inspection, storage warehouse, the current agricultural position, the current storage environment conditions and so on. IOT through effective information technology achieve a blending between man and agricultural.

4 Conclusions

This paper analyzes the basic structure of agricultural supply chain, current status of the research, and summarizes major obstacles of the development process. The paper also describes application of IOT principle, as well as agricultural supply chain optimization approach based on internet of things, including agricultural production, processing, transportation and sales process. It can promote the development of agricultural products logistics industry through modern agricultural logistics and networking technologies, change the practical problems of rural logistics problems. The government should develop policies to achieve agricultural IOT, specify IOT “perception of agriculture” direction, play an active role on the optimization of agricultural supply chain.

References

- [1] Fosso, W.S., Ygal, B., Lefebvre Louis, A., Elisabeth, L.: RFID technology and the EPC network as enablers of mobile business: a case study in a retail supply chain. *International Journal of Networking & Virtual Organisations*, 450–462 (2006)
- [2] Eleonora, B., Roberto, M., Andrea, V.: The impact of RFID and EPC network on the bullwhip effect in the Italian FMCG supply chain. *International Journal of Production Economics*, 426–432 (2009)
- [3] Frederic, T., Cosmin, C.: RFID data sharing in supply chains: What is the value of the EPC network? *International Journal of Electronic Business*, 21–43 (2009)
- [4] Li, J.: Research on the Optimization of Agricultural Supply Chain under the Background of Internet of Things. *Journal of Henan Agricultural Sciences* 8, 10–12 (2011)
- [5] Liu, X., Li, T.: Agricultural Supply Chain Risk. *Agricultural Economics* 1, 47–48 (2011)
- [6] Zhou, H., Sun, H.: The Research on Integrated Grain Supply Chain Management Based on Internet of Things. *Chinese Agricultural Science Bulletin* 7, 315–317 (2011)

Measurement and Study on Drying Shrinkage Characteristic of Tobacco Lamina Based on Computer Vision

Wenkui Zhu¹, Zhaogai Wang^{2,*}, Delong Xu^{1,3}, and Jinsong Du^{1,*}

¹Zhengzhou Tobacco Research Institute of CNTC, Zhengzhou 450001, China

²Institute of Agricultural Products Processing, Henan Academy of Agricultural Sciences, Zhengzhou 450002, China

³Jinan Cigarette Factory, Jinan 250104, China

{wkzhu79, dlxu88}@163.com, {zgwang1999, djsdxx}@126.com

Abstract. Accurate evaluation of shrinkage characteristic for tobacco lamina during drying process is important for optimizing tobacco primary process. The present work developed a detection and characterization method of shrinkage characteristic based on computer vision. Effect of types and dimensions of tobacco lamina on the shrinkage characteristic were investigated and shrinkage rate variation at different drying stages was also analyzed by this method. The results show that percentage reduction of area, which is obtained by detecting tobacco lamina area before and after drying, can be used to reflect the shrinkage characteristic of tobacco lamina. RSD of measurement results by this method is less than 6% under test conditions. Compared with upper tobacco leaf, middle tobacco leaf shows the higher shrinkage rate of 14.3%. Dimensions of tobacco lamina also have significant effect on its shrinkage characteristic. The larger size (up 30mm mesh) tobacco lamina shows a higher shrinkage rate. Shrinkage rate of tobacco lamina is closely related to moisture content variation during drying. The shrinkage of tobacco lamina during drying mainly occurs within the moisture content range of 20% to 14%.

Keywords: measurement, shrinkage characteristic, tobacco lamina, computer vision.

1 Introduction

Agricultural products processing widely involve the dehydration of materials by air drying. During drying process, one of the most common physical changes is the shape shrinkage, which is associated with the stresses caused by loss of water and heating in the pore structure of materials. Many literatures have reported drying shrinkage characteristics on various porous plant-based materials, such as vegetable, fruit, seeds and so on [1-7]. Due to the flexible skeleton structure of plant leaf, tobacco leaf as important economic crops is easier to shrinkage during drying in its primary process.

In the tobacco primary process, post-harvest tobacco leaf need to be broken into lamina, and then tobacco lamina is dehydrated by hot air drying. The area distribution

* Corresponding authors.

of tobacco lamina after drying is key quality index in tobacco primary processing, while which is directly affected by its shrinkage characteristic during drying. Therefore, accurate evaluation of tobacco lamina shrinkage characteristic is important for optimizing tobacco primary process. Generally, traditional sieving method is used to measure the distribution of tobacco lamina size before and after drying, then the difference of twice sieving results could indirectly reflect the drying shrinkage characteristic of tobacco lamina. However, sieving method is difficult to obtain the continuous distribution of tobacco lamina area. At the same time, its accuracy is also affected by tobacco lamina crush during mechanical sieving.

Due to the rapid development of image analysis technology, computer vision system has been more and more applied to the quality detection and classification of post-harvest agricultural products [8-14]. In the present work, the computer vision method was developed to measure drying shrinkage characteristic of tobacco lamina. And by this method, effect of types and dimensions of tobacco lamina on the shrinkage characteristic were investigated and shrinkage rate variation during drying was also analyzed.

2 Materials and Methods

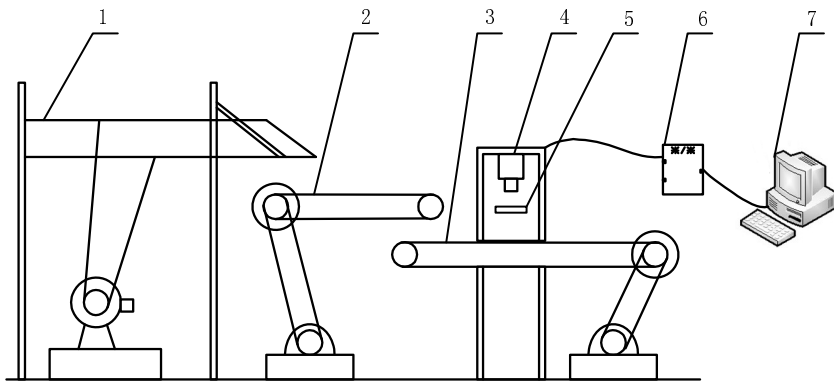
2.1 Tobacco Leaf Samples

The experimental materials used in the study included two types of flue cured tobacco lamina (a kind of upper tobacco leaf and a kind of middle tobacco leaf). Before experiment, moisture content of tobacco lamina was adjusted to 22% (on the wet basis) by adding a calculated amount of distilled water to sample. After adjusting the moisture content, they were put into isothermal and equal humidity equipment for 48h.

Dry processing of tobacco lamina sample was performed in a constant temperature and humidity oven. The drying air conditions are set at 80°C and 30% RH and sample is dehydrated from the moisture content 22% to 8% according to the actual drying technology in tobacco primary process.

2.2 Experimental Apparatus

The Fig. 1 shows the computer vision system designed for characterizing the drying shrinkage of tobacco lamina. The system mainly consists of sample distributing unit, image capture unit and image processing unit. Sample distributing unit uses two belts conveys with different speeds and a vibrating convey to realize the dispersed distribution of tobacco lamina on high speed belt. The vibrating convey is located before the lower speed belt conveys. Image capture unit above the high speed belt is set in a closed cabinet to avoid disturb from external light. The color line-scan digital camera (DALSA, SG-32-02K80) and linear LED light source are used in image capture unit. The camera has the maximum frame rate of 18 KHz and the resolution of 2048, and the corresponding image precision is up to 0.1mm². A computer with image analysis program acts as image processing unit.



1. Vibrating conveyor, 2. Low speed belt conveyor, 3. High speed belt conveyor, 4. Color line-scan digital camera, 5. Linear LED light source, 6. DA converter, 7. PC

Fig. 1. Diagram of computer vision system

Before the experiment, conveying speeds of two belts conveyers are set at 1m/s and 2m/s respectively, and speed of vibrating conveyor is set at 0.3 m/s. Tobacco lamina sample is paved on the vibrating conveyor which will loosen material adequately, and then transported to the low speed belt conveyor. After the low speed belt conveyor and high speed belt conveyor, the sample is distributed into single layer. The image of tobacco lamina on the high speed belt is continuously detected in real time by image capture unit and then analyzed by image processing unit.

2.3 Image Processing Methods

The image of tobacco lamina is collected and pretreated as the flow shown in Fig. 2. Collected color image was firstly transformed as gray level image. After image enhancing, median filter was used to remove the noise, then image binaryzation was carried by choosing proper threshold value. Edge and integrity of tobacco lamina image is close to the actual sample by using Presitt algorithm during boundary detection of image. Fig. 3 shows one of pretreated tobacco lamina image as well as its original image.

Pretreated image was further analyzed to obtain the characteristic values. The image area of each tobacco lamina as key characteristic value was calculated according to the number of image pixels points and area of each pixel point. Then the total area of sample measured can be obtained by summing image area of each tobacco lamina.

2.4 Evaluation of Shrinkage Characteristic

Total area of sample before and after drying was detected respectively according to the above image processing methods. The percentage reduction of tobacco lamina area is calculated by the following equation, which can be used to reflect the shrinkage characteristic of tobacco lamina during drying.

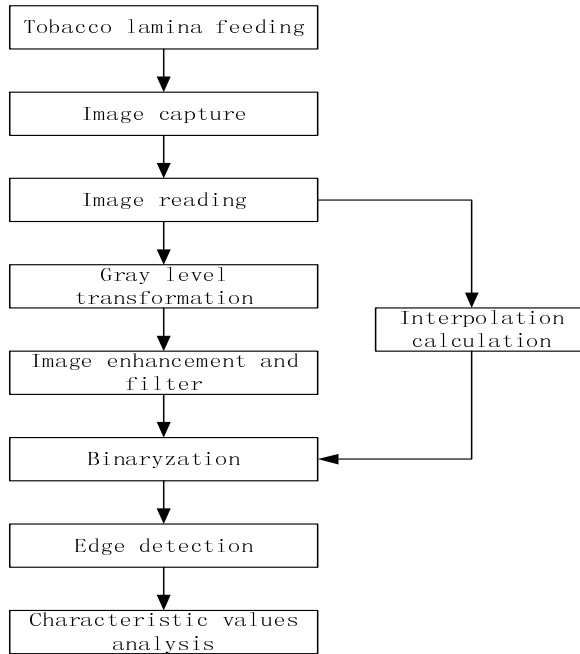
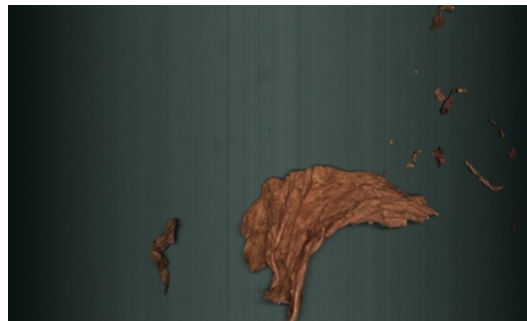
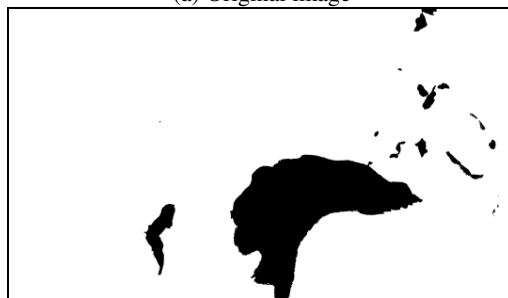


Fig. 2. The flow of image processing



(a) Original image



(b) Pretreated image

Fig. 3. Image of tobacco lamina

$$S = 1 - \frac{A_1}{A_0} \quad (1)$$

Where S is the shrinkage rate of tobacco lamina, A_1 is the total area of sample after drying and A_0 is the total area of sample before drying.

3 Results and Discussion

3.1 Accuracy Analysis of Measurement Method

In order to investigate the method accuracy for shrinkage rate measurement by computer vision, the repeated experiments were carried at different weight levels of sample tested. For each weight levels of tobacco lamina from 50g to 400g, 6 parallel samples were tested respectively to obtain the values of A_0 . After drying, the A_1 values of each sample were also tested. Table 1 showed the results of repeated experiments.

As can be seen from Table 1, the RSD of sample total area measured before and after drying is less than 2% for each weight levels of tobacco lamina. When the amount of sample measured is up to 200g, RSD of A_0 and A_1 is even less than 1%, which indicates a good reliability of test results for tobacco lamina area measurement by the computer vision system.

Table 1. Repeated experiment at different weight levels of sample

Experiment No.	50 g		100 g		200 g		300 g		400 g	
	A_0	A_1	A_0	A_1	A_0	A_1	A_0	A_1	A_0	A_1
1	14.16	12.38	28.1	23.99	55.43	47.94	83.34	70.52	117.04	100.59
2	14.1	12.53	27.89	24.33	56.2	47.54	83.13	70.63	117.51	100.88
3	14.05	12.31	28.89	23.99	56.15	47.87	82.57	70.11	117.92	100.69
4	13.69	12.47	28.16	23.64	56.07	48.13	82.24	70.8	117.74	101.08
5	13.89	12.48	28.18	24.14	55.67	48.09	82.24	71.15	117.26	101.02
6	14.52	12.37	27.6	24.23	55.71	48.24	82.26	71.2	117.22	101.77
Avg. (dm ²)	14.07	12.42	28.14	24.05	55.87	47.97	82.63	70.74	117.45	101.01
SD (dm ²)	0.28	0.08	0.43	0.24	0.31	0.30	0.49	0.41	0.34	0.42
RSD (%)	1.98	0.67	1.52	1.01	0.56	0.63	0.59	0.58	0.29	0.41

Shrinkage rates at different weight levels of sample tested were calculated according to the equation (1). The result is shown in Fig. 4. Standard deviation value of shrinkage rate varied from 0.02% to 0.005% with the increasing amount of tobacco lamina tested. When the amount of sample measured is up to 200g, shrinkage rate reached a stable level of 14% and its RSD is less than 6%. Considering this results, the sample amount for shrinkage rate measurement of tobacco lamina is choused at the level of 200g to ensure a proper measuring accuracy.

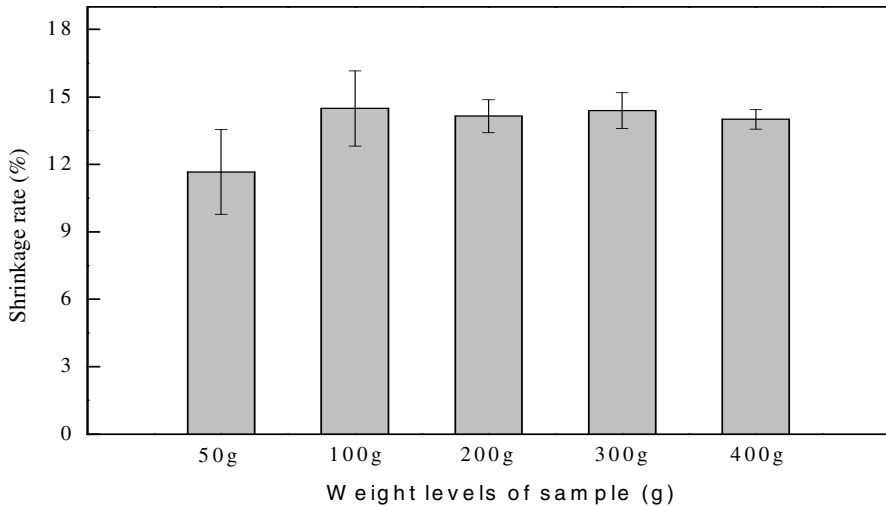


Fig. 4. Shrinkage rate of tobacco lamina at different amount of sample measured

3.2 Comparison of Shrinkage Characteristic for Different Tobacco Lamina

Based on the above measurement method, two types of tobacco lamina, including a kind of upper tobacco leaf and a kind of middle tobacco leaf, were analyzed to compare their drying shrinkage characteristic. The result can be seen in Fig. 5. Shrinkage rate of middle tobacco leaf during drying is 14.3%, while that of upper tobacco leaf is 11.9%. Higher shrinkage rate means more significant shrinkage characteristic for middle tobacco leaf during drying, which may be associated with its loose leaf structure than upper tobacco leaf.

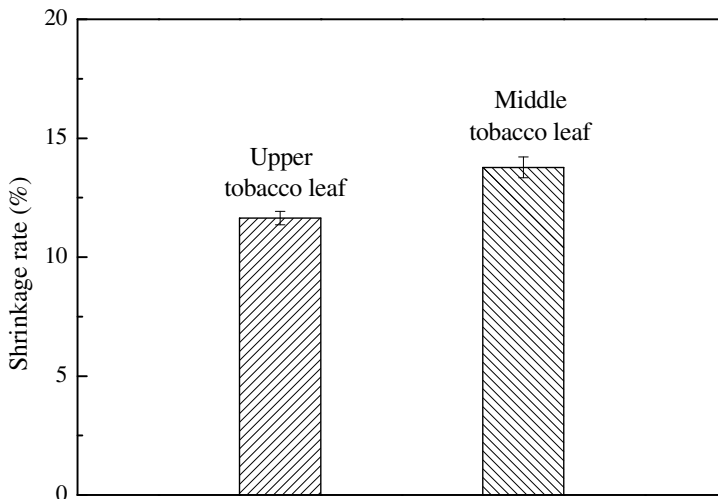


Fig. 5. Comparison of shrinkage rate for middle and upper tobacco lamina

In order to investigate the effect of different dimensions of tobacco lamina on its shrinkage characteristic, tobacco lamina was sieved into several parts with different dimensions, then area of each parts before and after drying were measured to obtain the shrinkage rate during drying. Table 2 presents the results for upper and middle tobacco leaf at the same drying conditions. It can be seen that the shrinkage rate increased with increasing the dimensions of tobacco lamina, especially for upper tobacco leaf. Shrinkage rate for the part of tobacco lamina under the mesh size of 10mm is only 6.44%, while for the part above the mesh size of 30mm is up to 13.82%. During drying process, both the internal structure contraction and the curing of leaf surface lead to area shrinkage of tobacco lamina. For the tobacco lamina with larger size, curing and deforming of leaf surface is easier to happen, which will result in more significant shrinkage of tobacco lamina area. This maybe can explain the effect of tobacco lamina dimensions on shrinkage rate.

Table 2. Effect of tobacco lamina dimensions on shrinkage characteristic

Sample Dimensions mm	Upper tobacco leaf			Middle tobacco leaf		
	A_0 dm ²	A_1 dm ²	S %	A_0 dm ²	A_1 dm ²	S %
<10	46.76	43.75	6.44	43.40	38.59	11.08
10-13.2	63.94	59.55	6.86	69.72	62.61	10.2
13.2-15	54.22	49.20	9.26	62.76	55.98	10.8
15-20	52.42	47.98	8.47	57.97	52.97	10.06
20-25	48.92	44.21	9.63	52.21	46.69	10.57
25-30	45.16	39.32	12.93	52.52	47.14	12.6
>30	46.51	40.08	13.82	52.01	45.08	13.32

3.3 Analysis of Shrinkage Rate Variation of Tobacco Lamina during Drying

Many previous literatures have shown that shrinkage characteristic of materials during drying is closely related with the variations of moisture content at different drying stages [15-18]. The shrinkage rate variation of tobacco lamina with its moisture content was also analyzed in the present work. The area of sample after drying were respectively measured when the moisture content of tobacco lamina decreased to 20%, 17%, 14% 11% and 8%, and the shrinkage rates of sample at different drying stages were obtained in Fig. 6.

For both upper and middle tobacco leaf, shrinkage rate of tobacco lamina increased with the decrease of moisture content during drying process. However, there is a more significant variation of shrinkage rate when moisture content of sample at the range of 20% to 14%. While at the moisture content range of 14% to 8%, shrinkage rate of sample only showed a little increase. For example, variations of shrinkage rate for middle tobacco leaf is about 6% when moisture content decreased from 20% to 14%, but that is only 1.3% when moisture content continuously decreased from 14% to 8%. It indicated that the shrinkage of tobacco lamina during drying mainly occurs at the initial drying stage. These results are benefit for optimization of the initial drying conditions to reduce the shrinkage rate of tobacco lamina.

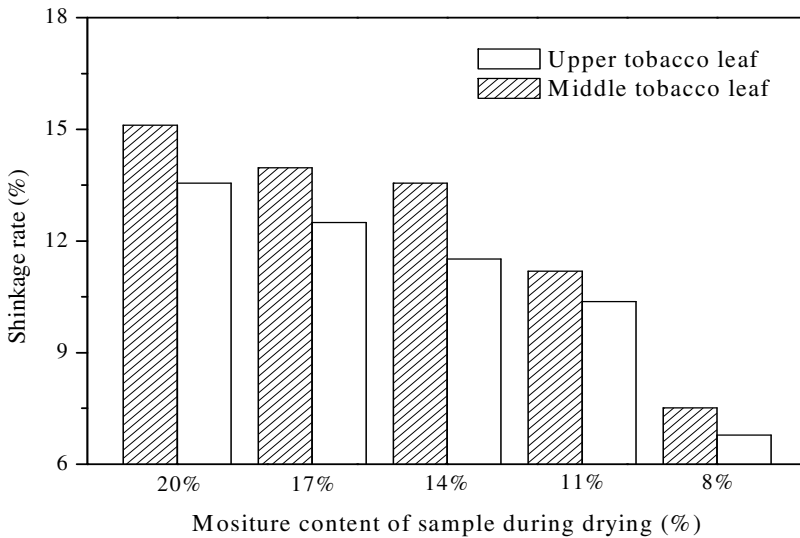


Fig. 6. Shrinkage rate variation of tobacco lamina during drying

4 Conclusion

Shrinkage characteristic during drying influences the area distribution of tobacco lamina, which is key quality index in tobacco primary processing. Accurate evaluation of tobacco lamina shrinkage characteristic is important for optimizing tobacco primary process. In the present work, a method based on computer vision was developed to measure drying shrinkage characteristic of tobacco lamina. By this method, effect of types and dimensions of tobacco lamina on the shrinkage characteristic were investigated and shrinkage rate variation of tobacco lamina during drying was also analyzed. The results showed that drying shrinkage characteristic can be reflected by shrinkage rate of tobacco lamina area, as is calculated by detecting the sample area before and after drying. RSD of shrinkage rate measured by this method is less than 6% under test conditions. Types and dimensions of tobacco lamina have significant effect on its shrinkage characteristic. Middle leaf had a higher shrinkage rate than upper leaf under the same drying conditions. While the larger size (up 30mm mesh) tobacco lamina also showed a higher shrinkage. Shrinkage rate of tobacco strips is closely related to moisture content variation during drying. The shrinkage of tobacco lamina during drying mainly occurs at the initial drying stage within the moisture content range of 20% to 14%.

Acknowledgment. Funds for this research was provided by the National Nature Science Foundation of China Plan Projects (31101373, 51306213).

References

1. Mayor, L., Moreira, R., Sereno, A.M.: Shrinkage, density, porosity and shape changes during dehydration of pumpkin (*Cucurbita pepo* L.) fruits. *Journal of Food Engineering* 103(1), 29–37 (2011)
2. Agnieszka, N., Adam, F., Alicja, Z.K., et al.: Drying kinetics and quality parameters of pumpkin slices dehydrated using different methods. *Journal of Food Engineering* 94(1), 14–20 (2009)
3. Mayor, L., Sereno, A.M.: Modeling shrinkage during convective drying of food materials: a review. *Journal of Food Engineering* 61(3), 373–386 (2004)
4. Cai, L., Shi, M.H.: Experimental study on shrinkage and rehydration of speed during drying process. *Journal of Southest University (English Edition)* (4), 343–346 (2003)
5. Maskan, M.: Drying, shrinkage and rehydration characteristics of kiwifruits during hot air and microwave drying. *Journal of Food Engineering* 48(2), 177–182 (2001)
6. Zhu, W.K., Yu, C.F., Li, B.: The Evolution of Moisture, Temperature, Density and Shrinkage Characteristics of Cut Tobacco during Cylinder Drying. In: 65th Tobacco Science Research Conference, USA, Kentucky (2011)
7. Zogzas, N.P., Maroulis, Z.B., Marinos, K.: Shrinkage and porosity of some vegetable during air drying. *Drying Technology* 12(7), 1653–1666 (1994)
8. Thomas, R., Marco, K.: Robotic harvesting of *Gerbera jamesonii* based on detection three dimensional modeling of cut flower pedicels. *Computers and Electronics in Agriculture* 66(1), 85–92 (2009)
9. Fernando, L.G., Gabriela, A.G., Jose, B., et al.: Automatic detection of skin defects in citrus fruits using a multivariate image analysis approach. *Computers and Electronics in Agriculture* 71(2), 189–197 (2010)
10. Zhang, L.B., Wang, Y., Yang, Q.H.: Kinematics and trajectory planning of a cucumber harvesting robot manipulator. *International Journal of Agricultural and Biological Engineering* 2(1), 17 (2009)
11. Riquelme, M.T., Barreiro, P., Ruiz-Altisent, M.: Olive classification according to external damage using image analysis. *Journal of Food Engineering* 87(3), 371–379 (2008)
12. Blasco, J., Cubero, S., Grmez-Sanchis, J.: Development of a machine for the automatic sorting of pomegranate (*Punica granatum*) arils based on computer vision. *Journal of Food Engineering* 90(1), 27 (2009)
13. Wan, Y.N.: Kernel handling performance of an automatic grain quality inspection system. *Transactions of the ASAE* 45(2), 369–377 (2002)
14. Wang, N., Zhang, N., Dowell, F.E.: Determining virtuousness of durum wheat using transmitted and reflected images. *Transactions of the ASAE* 48(1), 219–222 (2005)
15. Lang, W., Sokhansanj, S.: Bulk volume shrinkage during drying of wheat and canola. *Journal of Food Process Engineering* 16(4), 305–314 (1993)
16. Gabas, A.L., Menegalli, F.C., Telis-Romero, J.: Effect of chemical pretreatment on the physical properties of dehydrated grapes. *Drying Technology* 17(6), 1215–1226 (1999)
17. Reza, A., Mohammad, S., Jamal, A.: Evaluation of Concrete Drying Shrinkage Related to Moisture Loss. *ACI Materials Journal* 110(3), 269–278 (2013)
18. Yadollahinia, A., Latifi, A., Mahdavi, R.: New method for determination of potato slice shrinkage during drying. *Computers and Electronics in Agriculture* 65(2), 268–274 (2009)

Research of PID Algorithm for Valve Controlled Hydraulic Motor Variable Rate Fertilizer Control System

Liang Chunying^{1,2}, Wang Xi³, Ji Jianwei¹, Xu Qianhui², and Lü Peng²

¹ College of Information and Electrical Engineering, Shenyang Agricultural University, Shenyang 110161, China

² College of Information and Technology, Heilongjiang Bayi Agricultural University, Daqing 163319, China

³ College of Engineering Heilongjiang Bayi Agricultural University, Daqing 163319, China
{ndliangchunying, ndwangxi, xuqh2012, dqlvpeng}@163.com,
jianwei7879@hotmail.com

Abstract. In this system, the electromagnetic proportional valve is the actuator, and the valve controlled motor is controlled object, and the speed sensor is the feedback element, to send out the orders by industrial computer, to control the motor output speed by controller. According to the principle of the circuit and fluid mechanics, set up the mathematical model of the valve controlled hydraulic motor variable fertilization system. PID parameters tuning of system were performed by Ziegler-Nichols method, get the coefficient of increment algorithm. The step response of P, PI and PID of variable rate fertilization the system were studied by MATLAB/ SIMULINK, results show that: PID algorithm system, the overshoot was small, setting time was short, the number for oscillations was little compared with the P algorithm and PI algorithm, the dynamic performance of the system is excellent. The laboratory experiments results showed that: In the process of system operation, PID algorithm tracking speed was rapid, and steady-state error is smaller. Therefore, the electro-hydraulic proportional variable fertilization system with PID algorithm has good dynamic performance and steady state performance, and can meet the requirements of variable assignment.

Keywords: variable rate fertilizer, mathematical model, PID parameter tuning, valve controlled motor.

1 Introduction

Precision agriculture is the development direction of modern agriculture, variable fertilization is the most mature, the most widely used technique in precision agriculture. Variable control system is an important part of the variable machinery, it includes the following the speed regulation control way: electrically controlled mechanical Continuously Variable Transmission, electric control hydraulic motor, electric control step motor. Among them, the electric hydraulic system is widely used which has the characteristics of fast response, output power and high control accuracy, variables to adapt to the demand of large Variable Rate Fertilization. Electro-hydraulic proportional

valve control system for hydraulic motors in response to frequency of fast, short adjusting time, the dynamic characteristics of a good, high efficiency advantages [1-2], in the variable fertilization techniques are more and more widely used [3-7].

In recent years, precision agriculture variable rate fertilizer control strategy mainly around the PID control algorithm [8-12], fuzzy control rules [13-14] and the relevance vector machine [15] and other aspects of the research work commenced in improving the control system performance, increase precision fertilization made a lot of achievements and to promote the domestic development of intelligent variable fertilization seeder. Research process, due to the PID algorithm has the features of a simple structure, robustness and high reliability [16], has been widely used, however, PID parameter tuning is a complex optimization process that determines the performance of the control system, usually Engineering on tuning methods have decay curve method, Ziegler-Nichols step response method, ITSE optimal setting method, rapid titration and relay method and so on. This paper use of the analyzes of mechanism to establish the mathematical model of electro-hydraulic variable rate fertilization system, using Ziegler-Nichols method tuning PID controller parameters, and analysis parameters by testing the impact on system performance.

2 Compositions of Valve Controlled Hydraulic Motor Variable Rate Fertilizer Control System

Hydraulic Motor with variable rate fertilization system mainly consists of oil sources, electro-hydraulic proportional valves, hydraulic motors, variable rate fertilizer controllers, computers, and speed sensors and so on, as shown in Figure 1. Computer based on fertilizer prescription map given amount of fertilizer, compared with the

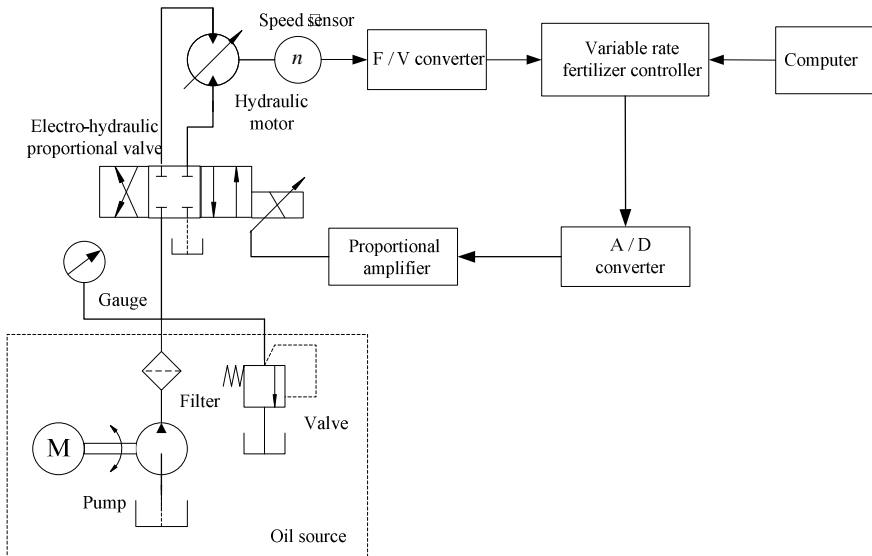


Fig. 1. Hydraulic Motor with variable rate fertilization system

speed sensor feedback, control algorithm based on the deviation adjusting armature voltage electro-hydraulic proportional valve, flow size change hydraulic motor speed, driven wheel speed changing of fertilizer to achieve variable rate fertilization.

3 The System Mathematical Model

The control system of variable rate fertilization through DGPS which is installed in tractor to determine the geographical position, transmitted this information to on-board computer for processing through the RS - 232 serial interface, it will find out the variable fertilization database through which corresponding the variable fertilization data and field position, transferred to the variable fertilization controller, Control the opening degree of hydraulic proportional valve, change the axis speed of soybean precision sowing machine, to realize the purpose of variable rate fertilization. The control system of variable rate fertilization system composition was shown in fig. 2.

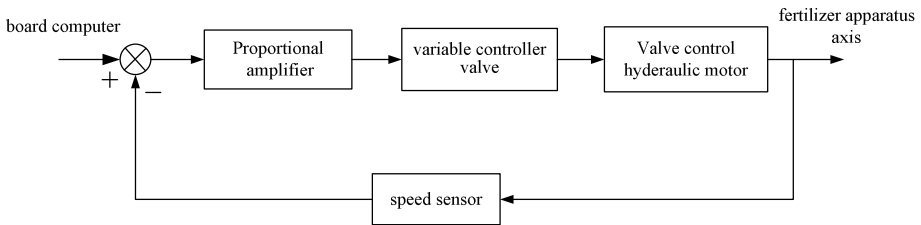


Fig. 2. Valve controlled hydraulic motor system composition

3.1 Transfer Function of Proportion Amplifier

Electro-Hydraulic Proportional Valve is current control type element, usually for the high output impedance voltage - current converter, the band width than hydraulic inherent frequency, can be regarded as amplification link, namely

$$K_a = \frac{I(s)}{U(s)} \tag{1}$$

Where $I(s)$ -Proportion amplifier output current;

$U(s)$ -Error voltage;

K_a -Proportion amplifier gain, $K_a = 0.3A/V$.

3.2 Transfer Function of Proportional Electromagnetic Valve

The system uses the electro-hydraulic proportional pressure pilot control valves, transfer function is second-order oscillation links:

$$G_v(s) = \frac{Q(s)}{I(s)} = \frac{K_q}{\frac{s^2}{\omega_v^2} + \frac{2\zeta_v s}{\omega_v} + 1} \quad (2)$$

Where $K_q = 1.87 \text{ m}^3 / \text{s} \cdot \text{A}$, $\omega_v = 335.2 \text{ rad} / \text{s}$, $\zeta_v = 0.57$

$Q(s)$ -flow of electro-hydraulic proportional valve when in the steady operating points, m^3/s ;

K_q -flow gain of electro-hydraulic proportional valve in the steady operating points;

ω_v -equivalent undamped natural frequency of electro-hydraulic proportional valve;

ζ_v - equivalent damping coefficient of electro-hydraulic proportional valve;

s - Laplace operator.

3.3 The Mathematical Model of Hydraulic Motor

1) Load Flux Function of Electro-Hydraulic Proportional Valve

$$Q_L = k_q x_v - k_c p_L \quad (3)$$

Where Q_L - load flux of electro-hydraulic proportional valve, m^3/s ;

x_v -displacement of proportional valves core, m;

p_L -Load pressure, Pa;

k_q -Flow gain, $\text{m}^3/\text{s} \cdot \text{A}$;

k_c -flow pressure coefficient of proportional valves, $\text{m}^5/\text{N} \cdot \text{s}$.

2) Flow Rate Continuation Equation of Proportional Valve

The load flux of the output to proportional valve, one part is used to promote a motor motion, another part is used to compensate the various leak of motor, another part is used to compensate flow of compressed. The characteristics of the hydraulic motor for the assumptions:

- (1) all hydraulic pipe is short and coarse, ignore pipe friction losses, ignore the fluid quality effect and pipeline dynamic effect;
- (2) motor oil and volume elastic modulus is constant;
- (3) hydraulic motor for internal and external leakage laminar flow;
- (4) consider liquid compressibility;
- (5) injection system as the constant-voltage source, oil supply pressure as constant.

According to the above assumptions can draw the continuous equation of flow of hydraulic pressure motor

$$Q_L = D_m \frac{d\theta}{dt} + C_{tm} p_L + \frac{V_m}{4\beta_e} \frac{dp_L}{dt} \quad (4)$$

Where Q_L -load flow, m^3/rad ;

D_m -theoretical displacement of hydraulic motor, m^3/rad ;

θ -angular displacement of hydraulic motor axis, rad;

C_m -total leakage coefficient of hydraulic motor, $m^5/\text{N} \cdot \text{m}$;

p_L -load pressure drop, N/m^2 ;

V_m -total volume of motor oil cavity, m^3 ;

β_e -integrated elastic modulus of system, N/m^3 .

3) Moment Equilibrium of Hydraulic Motor

Accord to the quality of motor axis and load, moving damping and spring force, and applied load force, according to Newton's second law can get equilibrium equation of piston force and load force.

$$T_g = D_m (p_1 - p_2) = D_m p_L = J_m \frac{d^2\theta}{dt^2} + B_m \frac{d\theta}{dt} + G\theta + T_L \quad (5)$$

Where T_g -theory torque produced by motor, $\text{N} \cdot \text{m}$;

J_m -total inertia of motor axis which is converted hydraulic motor axis and load, $\text{kg} \cdot \text{m}^2$;

B_m -viscosity damping coefficient of load and motor, $\text{N} \cdot \text{m} \cdot \text{s}/\text{rad}$;

G -torsion stiffness of elastic load, $\text{N} \cdot \text{m}/\text{rad}$;

T_L -acting on any external grinding load torque of motor axis, $\text{N} \cdot \text{m}$.

4) Transfer Function of Hydraulic Motor

$$Q_L(s) = k_q X_v(s) - k_c P_L(s) \quad (6)$$

$$Q_L(s) = D_m s \theta(s) + (C_m + \frac{V_m}{4\beta_e}) P_L(s) \quad (7)$$

$$T_g = D_m P_L(s) = (J_m s^2 + B_m s + G) \theta(s) + T_L(s) \quad (8)$$

To organize and simplified, ignored elastic load, ignored produce term of oil leakage and viscous damping, attainable:

$$\theta(s) = \frac{\frac{k_q}{D_m} x_v(s) - \frac{k_c + C_m}{D_m^2} \left[1 + \frac{V_m}{4\beta(k_c + C_m)} s \right] T_L(s)}{s \left(\frac{V_m J_m}{4\beta_e D_m^2} s^2 + \left[\frac{J_m (k_c + C_m)}{D_m^2} + \frac{B_m V_m}{4\beta_e D_m^2} \right] s + 1 \right)} \quad (9)$$

In order to simplify the analysis, some factors can be ignored in the condition of particularly use, especially the simplify or standardize characteristic equations. According to the system is mainly with inertial load, and the motor and load are rigidly connected, so elastic load can be neglected, namely $G = 0$, the pressure - coefficient ratio K_{ce} in all is very small, usually the load's viscous damper coefficient B_m generally are also small, the coupling effect of these two are smaller, namely $\frac{B_m K_{ce}}{D_m^2} \ll 1$, "(9)" can be simplified as:

$$\theta(s) = \frac{\frac{k_q}{D_m} x_v(s) - \frac{k_{ce}}{D_m^2} \left[1 + \frac{V_m}{4\beta_e k_{ce}} s \right] T_L(s)}{s \left(\frac{s^2}{\omega_h^2} + \frac{2\zeta_h}{\omega_h} s + 1 \right)} \quad (10)$$

Where $\omega_h = \sqrt{\frac{4\beta_e D_m^2}{V_t J_t}} = 183.6 \text{ rad/s}$, $\zeta_h = \frac{K_{ce}}{D_m} \sqrt{\frac{\beta_e J_t}{V_t}} = 0.12$

ω_h - undamped oscillation angular frequency;

ζ_h -Hydraulic damping ratio;

Flux near by point of stable state, according to“(10)” can get the transfer function of flux and external grinding load which is motor output angular displacement are:

$$\frac{\theta(s)}{Q(s)} = \frac{\frac{1}{D_m}}{s \left(\frac{s^2}{\omega_h^2} + \frac{2\zeta_h}{\omega_h} s + 1 \right)} \quad (11)$$

$$\frac{\theta(s)}{F_L(s)} = \frac{\frac{k_{ce}}{D_m^2} \left(1 + \frac{V}{4\beta_e K_{ce}} s \right)}{s \left(\frac{s^2}{\omega_h^2} + \frac{2\zeta_h}{\omega_h} s + 1 \right)} \quad (12)$$

The mathematical modeling of proportional valve was shown in fig. 3 below.

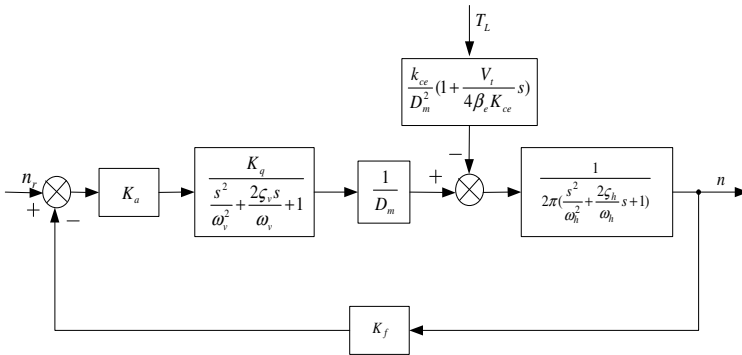


Fig. 3. The mathematical modeling of electro-hydraulic proportional valve control system

4 PID Parameters Setting

PID algorithm is one of the earliest control strategy, system error will be linear combination of the proportion, integral and differential of control signal, constitute the controlled object. The method is widely used in industrial process control Because of simple and good robustness and high reliability etc., PID strategy controller for:

$$u(t) = K_p [e(t) + \frac{1}{T_i} \int_0^t e(t) + T_D \frac{de(t)}{dt}] \tag{13}$$

Where $e(t)$ - Control deviation;

$u(t)$ - analog signals;

K_p - Percentage gain;

T_i - Integration time constant;

T_D -Differential time constant.

For Laplace transfer function for:

$$G(s) = \frac{U(s)}{E(s)} = K_p (1 + \frac{1}{T_i s} + T_d s) = K_p + K_i \frac{1}{s} + K_D s \tag{14}$$

There are some faults in the positional PID control arithmetic, first, it must to finish computing one $u(n)$, additvng $n+3$ times and multiplicativing 3 times, as well it will be increased following the time; second, it should to hold back the figure of $e(t)$ which come from sampling time, and it will occupied more memory space. This article use control increment method.

$$\Delta u(n) = u(n) - u(n - 1)$$

$$= K_p \{ [e(n) - e(n - 1)] + K_i e(n) + K_d [e(n) - 2e(n - 1) + e(n - 2)] \} \tag{15}$$

Where : K_p -proportional coefficient, $K_p = 0.6K_m$;

$$K_i \text{-integral coefficient, } K_i = \frac{K_p T}{0.5T_m} ;$$

$$K_d \text{-differential coefficient, } K_d = 0.125K_p T T_m ;$$

T_m - system constant amplitude oscillation gain;

K_m - oscillating period;

T - system sampling period.

And
$$\Delta u(n) = K_p (1 + K_i + K_d)e(n) - K_p (1 + 2K_d)e(n - 1) + K_p K_d e(n - 2)$$

$$= Ae(n) - Be(n - 1) + Ce(n - 2) \tag{16}$$

Where: Δu -PID increment of adjustment;

$e(n)$ -once before error;

$e(n - 1)$ -the first two times error;

$e(n - 2)$ -the first three times error.

$$A = K_p (1 + K_i + K_d) = K_p (1 + \frac{T}{T_i} + \frac{T_d}{T})$$

$$B = K_p (1 + 2K_d) = K_p (1 + \frac{2T_d}{T})$$

$$C = K_p K_d = \frac{2K_p T_d}{T} \tag{17}$$

System uses a tuning method named Nierkesi, turn the time integral coefficient of the controller to the largest ($T_i = \infty$), and zero the differential time coefficient ($T_d = 0$), adjusting the proportional gain increased gradually from 0 to increases gradually, amplitude of oscillation, and then write down the oscillating period $K_m = 0.955$, the system constant amplitude oscillation gain $T_m = 0.31s$, the system sampling period $T = 50ms$, and we can get:

$$K_p = 0.573, K_i = 0.1848, K_d = 0.0011;$$

$$A = 0.6795, B = 0.5742, C = 0.0006.$$

5 Simulation of Valve-Controlled Motor Velocity Control System

Simulink is an interactive model input and simulation environment launched by Math Works company, with a relatively independent function and use, it with the user interaction interface is based on Windows graphics programming method. Simulink is a can of dynamic system model, simulation and analysis package, it allows users to draw a series of charts to finish model work, and dynamically operation, the applicable to model of discrete and continuous, the mixture of both linear and nonlinear system, also support has a variety of sampling rate multi-rate system of Simulink provides customers with module base varied function module and is convenient for the user to the model simulation and analysis.

According to the established mathematical model, get valve control motor speed system PID control simulation charts, as fig. 4 shows:

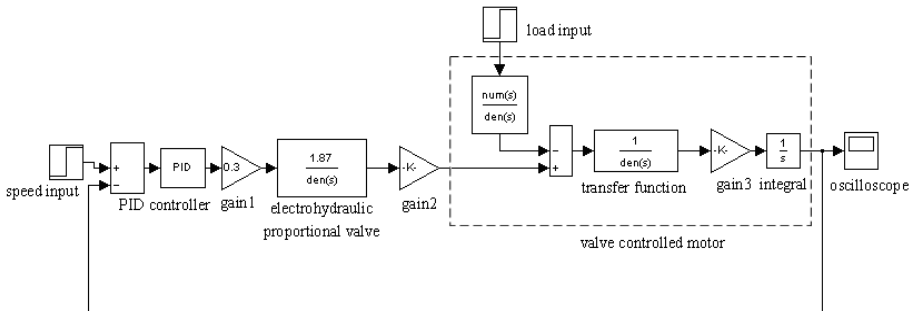


Fig. 4. Simulation charts of valve controlled motor system

Using P and PI control system speed simulation curve respectively as shown in figure 5 and figure 6, fig. 5 show that P control system overshoot is 78.38% and adjust time is 6.3 s, fig. 6 show that PI control system overshoot is 53.21% and adjust time is 3.75 s.

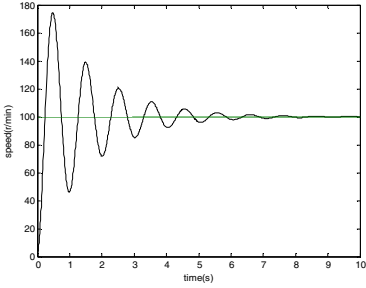


Fig. 5. P control system speed curve

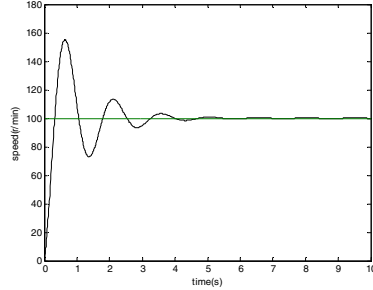


Fig. 6. PI control system speed curve

PID control system speed simulation curve fig. 7 shows that PID system overshoot is 27.92% and adjust time is 1.7 s. The test results show that the variable-rate fertilization control system with PID controller can restrain the vibration and decrease the intensity effectively. The PID controller is superior to the general P controller in the settling time, and the effect of control and adaptability, which accords with the design demand of the Variable-Rate Fertilization Control system completely.

6 Tracing Performance Test

Test verified system track results, test conditions: variable fertilization test bed; computer; BOPU data acquisition instrument; variable fertilization software. Step response curve of PI and PID system are respectively showed in fig. 9 and fig. 10 in the condition that the sampling frequency is 1KHz and given transmission ratio is 0.2. Fig. 9 show that overshoot of PI system is 31.5% and adjust time is 5.3 sec, however fig. 10 show that PID system overshoot is %, and adjust time is 2.7 s. The test results show that the variable-rate fertilization control system with fuzzy controller can restrain the vibration and decrease the intensity effectively, and the amplitude is reduced by 25%~30%. The fuzzy PID controller is superior to the general PID controller in the settling time, and the effect of control and adaptability, which accords with the design demand of the Variable-Rate Fertilization Control system completely.

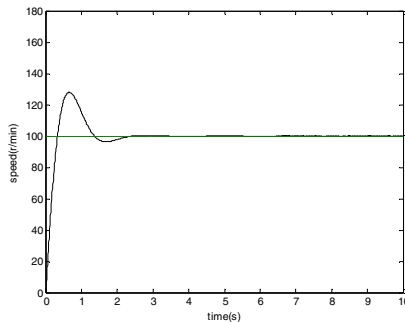


Fig. 7. PID control system speed curve

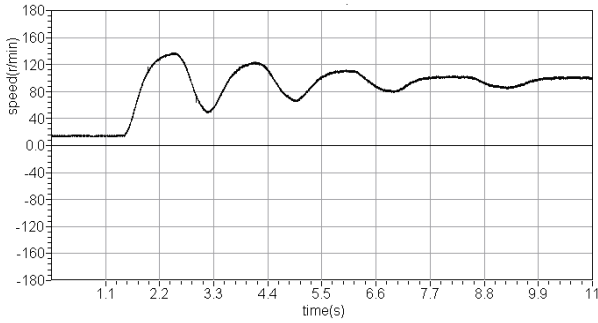


Fig. 8. PI system step response simulation

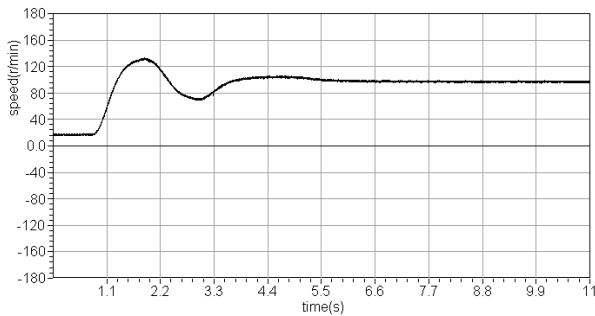


Fig. 9. PID system step response simulation

7 Conclusions

Use of MATLAB/SIMULINK simulation tools to achieve modeling of the variable rate fertilizing control system, the system with PID control strategy has high steady-state precision, fast dynamic response, small overshoot, strong anti-interference capability, can get good results. Carry the performance tests in the self-developed control system of variable-rate fertilization, test results and simulation results are basically consistent and achieve the expected goal.

Acknowledgment. Funds for this research was provided by national science and technology support plan major projects of china (2012BAD04B01, 2011BAD20B03, 2011BAD20B06), Science and Technology Project of education department of Heilongjiang province (12511355). The corresponding author is Prof. Ji Jianwei.

References

1. Hu, J., Yang, S., Zhang, L., et al.: Construct and Study Mathematical Model of Direct-acting Proportional Control Valve Hydraulic Pressure Motor. *Machine Building Automation* 38(3), 141–143 (2009)

2. Yanli, W.: Study on and Identification of Electro -hydraulic Proportional valve-Motor System, Chang'an University (2007)
3. Hui, Z., Li, S., Zhang, X., et al.: Development and performance of electro-hydraulic proportion control system of variable rate fertilizer. Transactions of the CSAE 26(2), 218–222 (2010) (in Chinese with English abstract)
4. Wang, X., Zhao, C., Meng, Z.: Design and experiment of variable rate fertilizer applicator. Transactions of the CSAE 20(5), 114–117 (2004)
5. Li, A., Wang, X., Wang, Z., et al.: Research about Variable Rate Fertilization Closed-loop Control System of Electro-hydraulic Speed. Chinese Agricultural Science Bulletin 25(7), 272–275 (2009)
6. Shao, L., Wang, X., Niu, X.Y., et al.: Design and experiment on PLC control system of variable rate fertilizer. Transactions of the Chinese Society of Agricultural Machinery 38(11), 84–87 (2007)
7. Fu, W., Meng, Z., Huang, W., et al.: Variable rate fertilizer control system based on CAN bus. Transactions of the CSAE 24(supp. 2), 127–132 (2008)
8. Chen, L., Huang, W., Meng, Z.: Design of Variable Rate Fertilization Controller Based on CAN Bus. Transactions of the Chinese Society of Agricultural Machinery 39(8), 101–105 (2008)
9. Zhang, H., Li, S., Zhang, X., et al.: Development and performance of electro-hydraulic proportion control system of variable rate fertilizer. Transactions of the CSAE 26(2), 218–222 (2010)
10. Meng, Z., Zhao, C., Liu, H.: Development and performance assessment of map-based variable rate granule application system. Journal of Jiangsu University 30(4), 338–342 (2009)
11. Fu, W., Meng, Z., Huang, W., et al.: Variable rate fertilizer control system based on CAN bus. Transactions of the CSAE, 24(supp. 2), 127–132 (2008)
12. Liang, C., Yi, S., Wang, X.: PID Control Strategy of the Variable Rate. Transactions of the Chinese Society of Agricultural Machinery Fertilization Control System 41(7), 157–162 (2010)
13. Shao, L., Wang, X., Niu, X.: Design and experiment on PLC control system of variable rate fertilizer. Transactions of the Chinese Society for Agricultural Machinery 38(11), 84–87 (2007)
14. Gu, Y., Yuan, J., Liu, C.: FIS-based method to generate bivariate control parameters regulation sequence for fertilization. Transactions of the CSAE 27(11), 134–139 (2011)
15. Yuan, J., Liu, C., Gu, Y.: Bivariate Fertilization Control Sequence Optimization Based on Relevance Vector Machine. Transactions of the Chinese Society of Agricultural Machinery (42), 184–190 (2011)
16. Niu, X.J., Wang, Y., Tang, J.: Optimization Parameters of PID Controller Parameters Based on Genetic Algorithm. Computer Simulation 11, 180–183 (2010)
17. Sun, L., Wang, F.: Research on variable rate seeding and fertilization technology. Journal of Northeast Agricultural University 40(3), 115–120 (2009)
18. Zhao, S., Ji, W.: Iterative learning control of electro-hydraulic proportional feeding system in slotting machine for metalbar cropping. International Journal of Machine Tools & Manufacture 45(7), 923–931 (2005)
19. Wu, Y., Zhang, D., Duan, S.: Iterative learning control on electro-hydraulic position servo systems of the pump-controlled cylinder. Journal of Taiyuan University of Science and Technology 27(4), 277–280 (2006)
20. Quan, L., Li, F., Wang, X.: Study on the efficiency of differential cylinder system driven with servo motor and constant pump. Proceedings of the CSEE 26(8), 93–98 (2006)

21. Niu, X., Qian, D., Wang, X., et al.: Research on control system of variable rate fertilizer applicator in precision agriculture based on NDVI. *Journal of Agricultural University of Hebei* 28(2), 94–98 (2005)
22. Zhang, Y., Gui, W.: Compensation for secondary uncertainty in electro-hydraulic servo system by gain adaptive sliding mode variable structure control. *Journal of Cent South University Technol.* 15(2), 256–263 (2008)
23. Tian, Y., Wu, S.: Theoretic analysis and experiment of valveless electro-hydraulic servo system. *China Mechanical Engineering* 14(21), 1822–1823 (2003)
24. Liu, J.K., Liu, Q., Er, L.J.: Zero phase error real time control for flight simulator servo system. *Chinese Journal of Mechanical Engineering* 17(1), 132–135 (2004)
25. Lin, C., Tang, Q., Tang, S.: The research and application prospect of precise fertilization techniques. *Journal of South China University of Tropical Agriculture* 12(2), 76–79 (2006)
26. Camp, C.R., Sadler, E.J., Evans, D.E.: Variable-rate, digitally controlled metering device. *Applied Engineering in Agriculture* 16(1), 39–44 (2000)
27. Hamson, S.J., Smith, L.A., Hanks, J.E.: Evaluation of Application Accuracy and Performance of a Hydraulically Operated Variable-Rate Aerial Application System. *Transactions of the ASABE* 52(3), 715–722 (2009)

OAPRS: An Online Agriculture Prescription Recommendation System

Qingtian Zeng, Zhichao Liang, Weijian Ni, and Hua Duan

College of Information Science and Engineering,
Shandong University of Science and Technology, Qingdao 266590, China
qtzeng@163.com

Abstract. Agriculture prescription can be targeted to solve problems in agricultural production for farmers, but in reality, agricultural technology personnel (ATP) or agricultural technology experts (ATE) are also short handed. So it is difficult to ensure that all farmers' issue is resolved and the existing agricultural technology websites just tidy up some common prescriptions, mostly without involving the personalized service. So this paper designed an online agriculture prescription recommendation system which realize three functions including the automatic question answering, recommendation for ATP or ATE and recommendation for similar users based on the construction of user interest model, the problem model and prescription model. Through this system the questions put forward by farmers can be solved timely and agricultural prescriptions can be better promoted and shared, which manifests that the system has great practical value.

Keywords: agriculture prescription, user interest model, Auto QA, personalized recommendation.

1 Introduction

Agricultural technology prescription is targeted solution for problems in agricultural production. In reality, ATP or ATE's manpower is not enough, so it is difficult to ensure that all farmers' issue is resolved timely. And most existing agricultural technology websites do not involve personalized recommendation even not give farmers entrance to ask questions. Such as the basic-level agro-technique extension information platform [1] developed jointly by Ministry of Science and Technology, Ministry of Agriculture and Chinese Academy of Agricultural Sciences and Chinese gardens online system [2].

User interest model is an important part of the personalized recommendation system. For example, [3] adopted behavior sequence and their relationships to express user interest model. [4] used ontology to represent user interest model and they recorded users' behavior information especially their method distinguished between short term and long term interest model. [5] used concept network to represent user interest model. [6] put forward a fine-grained user interest modeling method which could be divided into different small user interest classes. Mao et al. [7] built user interest model with

weighted semantic network. [8] constructed user interest model based on tree vector space model.

2 Recommendation Process of the System

Fig1 shows recommendation process of the system. The system includes a total of three roles: farmer, intelligent recommendation agent, ATP or ATE.

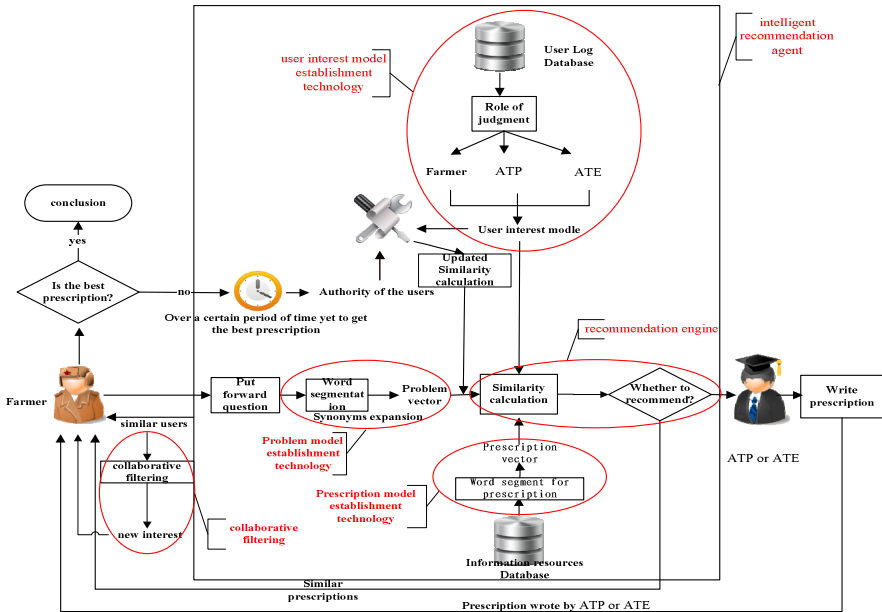


Fig. 1. Recommendation process of the system

The online agriculture prescription recommendation system has the following features:

- (1) Auto QA for prescription. Prescriptions with high similarity with the question will be pushed to the farmer after he or she fills the question.
- (2) Recommendation for ATP or ATE. ATP or ATE with high interest with the question will be recommended to the farmer after he or she filled the question.
- (3) Recommendation for similar users. Users with high similarity with the farmer and prescriptions of mutual interest of the farmer’s similar users will be recommended to the farmers when they login system and the farmers can view his or her similar users’ information.

3 Key Techniques of the System

The system includes four key techniques: (1) Model construction. It comprises user interest model establishment technology, problem model establishment technology, prescription model establishment technology. (2) Word segmentation algorithm. This article adopts forward maximum matching word segmentation algorithm to segment title and text of prescriptions and questions based on domain dictionary. Word segmentation algorithm is basic of model construction. (3) Similarity calculation method. The system determines whether or not to implement recommendation according to the size of similarity. Similarity calculation method is the core of the recommendation engine in Fig1. (4) Collaborative filtering. The system uses collaborative filtering to explore new interest from similar users for the farmer.

3.1 Model Construction

(1) User Interest Model

The system automatically records the user's behavior information such as questioning behavior, browsing behavior, retrieving behavior and collecting behavior etc. and sets different weights for different behaviors.

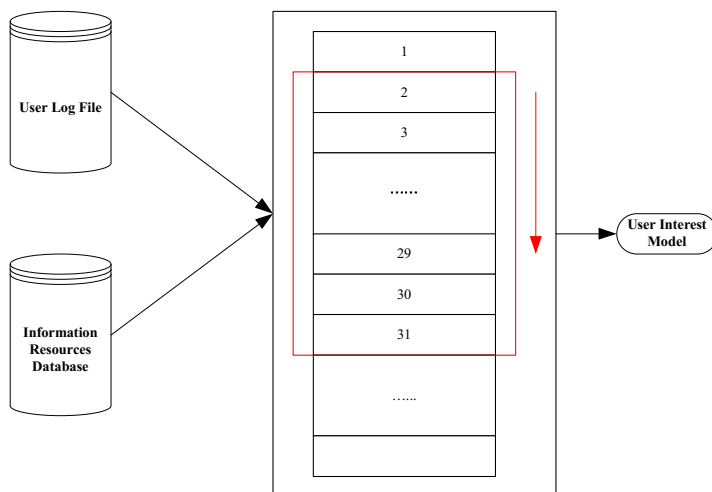


Fig. 2. Framework of data processing

Fig2 presents the framework of data processing. This article adopted window-type data processing method to mining user interest model.

The system has carried on word segmentation for the title and text of the prescription which is retrieved, browsed, collected and asked by users and then these keywords formed after word segmentation are stored into respective user log file. This article

statistically processes the data in the window and builds user interest model based on VSM (Vector Space Model). If the number of the interest node (key words) is n after statistical processing, the user interest model is expressed as following form:

$$U = \{f_1, f_2, \dots, f_n\} = \{(k_1, w_1), (k_2, w_2), \dots, (k_n, w_n)\} \quad (1)$$

Where $f_i(1 \leq i \leq n)$ represents i -th feature term of user interest model. $(k_i, w_i)(1 \leq i \leq n)$ represents i -th feature node of user interest model. $k_i(1 \leq i \leq n)$ represents i -th keyword. $w_i(1 \leq i \leq n)$ represents the weight of the keyword k_i .

In this paper, we use two different methods to indicate the weight of keyword. Firstly word frequency. If the number of occurrences of the keyword $k_i(1 \leq i \leq n)$ is $count_i$, computational formula of the $w_i(1 \leq i \leq n)$ is as following form:

$$w_i = \frac{count_i}{n} (1 \leq i \leq n) \quad (2)$$

Selectly $tf * idf$. $tf * idf$ comprises two parts. The first word-based feature is the term frequency (tf). This metric measures the importance of word t_i in document, i.e. mood, d_j with $n_{i,j}$ occurrences of the word in document d_j , divided by the sum of the number of occurrences of all words in document d_j .

$$tf_{i,j} = \frac{n_{i,j}}{\sum_k n_{k,j}} \quad (3)$$

The inverse document frequency (idf) measures the importance of the word with respect to a document.

$$idf_i = \log \frac{|D|}{|\{d_j : t_i \in d_j\}|} \quad (4)$$

Then $tf * idf$ is represented as the following form:

$$tf * idf_{i,j} = tf_{i,j} * idf_i \quad (5)$$

(2) Problem Model

This article builds problem model based on Vector Space Model. The system carries on word segmentation for the title and text of the question put forward by the farmer. If the number of keyword is n after statistical processing, the problem model is expressed as following form:

$$Q = \{qf_1, qf_2, \dots, qf_n\} = \{(qk_1, qw_1), (qk_2, qw_2), \dots, (qk_n, qw_n)\} \quad (6)$$

Where $qf_i(1 \leq i \leq n)$ represents i-th feature term of problem model. $(qk_i, qw_i)(1 \leq i \leq n)$ represents i-th feature node of problem model. $qk_i(1 \leq i \leq n)$ represents i-th keyword. $qw_i(1 \leq i \leq n)$ represents the weight of the keyword qk_i . qw_i is calculated as the formula (2) and formula (5).

(3) Prescription Model

This article builds prescription model based on Vector Space Model. The system carries on word segmentation for the title and text of prescriptions stored in information resources database. While in the processing of word segmentation, we also perform synonym extension by using “Ci Lin” and the number of occurrences of the synonym is respectively initialized to 1. If the number of keyword is n after statistical processing, the prescription model is expressed as following form:

$$P = \{pf_1, pf_2, \dots, pf_n\} = \{(pk_1, pw_1), (pk_2, pw_2), \dots, (pk_n, pw_n)\} \quad (7)$$

Where $pf_i(1 \leq i \leq n)$ represents i-th feature term of prescription model. $(pk_i, pw_i)(1 \leq i \leq n)$ represents i-th feature node of prescription model. $pk_i(1 \leq i \leq n)$ represents i-th keyword. $pw_i(1 \leq i \leq n)$ represents the weight of the keyword pk_i . pw_i is calculated as the formula (2) and formula (5).

3.2 Forward Maximum Matching Word Segmentation

Word segmentation algorithm is basis of the model construction. The domain dictionary adopted in this article is formed through training corpus in the field of agriculture and contains more than 60,000 vocabularies including 14 categories ranging from agricultural soils, agricultural meteorology, plant protection to forestry, aquaculture and so on. Algorithm 1 shows specific steps of forward maximum matching word segmentation algorithm.

Algorithm1. Forward maximum matching word segmentation algorithm

Input: *input_str* // a string need to be carried out word segmentation.

Output: *keywords* // an array storing the keywords.

Step1: *str = string.Empty* // a temporary variable for storing split word

position = 0 // a temporary variable for storing string's location

k = 0 // a temporary variable for storing matching scale's location

mm_length = 7 // maximum word length

Step2: If *position < input_str.Length*, go to Step3, if not, end the algorithm and return *keywords*

Step3: If *input_str.Length - position >= mm_length*, go to Step4, if not, go to Step9.

Step4: $Length = mm_length - k$, if $Length == 0$, go to Step5, if not, go to Step8.

Step5: $position ++$, $k = 0$ if

$input_str.Length - position \geq mm_length$, go to Step6, if not, go to Step7.

Step6: $str = input_str.SubString(position, mm_length)$.

Step7:

$str = input_str.SubString(position, input_str.Length - position)$.

Step8: $str = input_str.SubString(position, Length)$.

Step9: $Length = input_str.Length - position - k$, if $Length < 0$, $position ++$, $k = 0$; if not, $str = input_str.SubString(position, Length)$.

Step10: search str in the domain dictionary, if in the dictionary then go to Step11, if not, $k ++$.

Step11: if str is the stop word, nothing to do, if not, put str into $keywords$.

Step12: if $input_str.Length - position \geq mm_length$, $position += mm_length - k$, if not, $position += input_str.Length - position - k$.

Step13: $k = 0$, go to Step2.

3.3 Similarity Computing

In this article, we use vector cosine to measure the similarity between different models.

Based on formula (1) and formula (6), the similarity calculation formula between user interest model and question model is as follows:

$$sim(U, Q) = \frac{\sum_{i=1}^n w_i * qw_i}{\sqrt{\sum_{i=1}^n w_i^2} * \sqrt{\sum_{i=1}^n qw_i^2}} \quad (8)$$

If the farmer does not get a satisfactory prescription over a certain period of time, system will update the similarity calculation formula. We import authority of the ATP or ATE into the similarity calculation formula. We suppose that the number of the prescriptions filled by an ATP or ATE is w and the number of his or her prescriptions selected as the satisfactory prescription is m , then the authority calculation formula is:

$$Authority = \frac{m}{w} \quad (0 \leq m \leq w) \quad (9)$$

The updated similarity calculation formula between user interest model and problem model is:

$$sim(U, Q)' = \alpha Authority + (1 - \alpha) sim(U, Q) \quad (0.5 < \alpha \leq 1) \quad (10)$$

Based on formula (6) and formula (7), the similarity calculation formula between question model and prescription model is as follows:

$$sim(Q, P) = \frac{\sum_{i=1}^n qw_i * pw_i}{\sqrt{\sum_{i=1}^n qw_i^2} * \sqrt{\sum_{i=1}^n pw_i^2}} \tag{11}$$

Based on formula (1), the similarity calculation formula between user interest models is as follows:

$$sim(U, U') = \frac{\sum_{i=1}^n w_i * w'_i}{\sqrt{\sum_{i=1}^n w_i^2} * \sqrt{\sum_{i=1}^n w_i'^2}} \tag{12}$$

3.4 Collaborative Filtering

$C = \{U_1, U_2, \dots, U_n\}$ is the set of the users and $S = \{P_1, P_2, \dots, P_m\}$ is the set of the prescriptions. $r_{u,p}$ represents the degree of user u 's interest (similarity) in prescription P . $r_{u,p}$ is calculated through other similar users' interest in prescription P . \hat{U} is a user set with high similarity with user u . The function form of $r_{u,p}$ is as follows:

$$r_{u,p} = \frac{1}{N} \sum_{\hat{u} \in \hat{U}} r_{\hat{u},p} \tag{13}$$

Based on formula (1) and formula (7), the specific calculation formula of $r_{\hat{u},p}$ is as follows:

$$r_{\hat{u},p} = \frac{\sum_{i=1}^n w_i * pw_i}{\sqrt{\sum_{i=1}^n w_i^2} * \sqrt{\sum_{i=1}^n pw_i^2}} \tag{14}$$

Where N represents the count of the set \hat{U} . When $r_{u,p}$ is greater than the set threshold value, the system will carry on recommendation. In this way we can discover new interests for users.

3.5 Comparison between Word Frequency and $tf*idf$

In this article, we use two different indicators to indicate the weight of keyword. So we must compare the accuracy of two indicators. We recruit 150 system users to test the recommendation accuracy by using two different indicators. Those 150 system

users are divided into 5 groups, each group of number 10,20,30,40,50. If the users consider these prescriptions recommended by system as those they are interested in, so the recommendation is accurate. Fig3 presents the recommendation accuracy by using two different indicators and we can find that $tf*idf$ has better accuracy. So in the next system implementation, we use $tf*idf$ to indicate the weight of keyword.

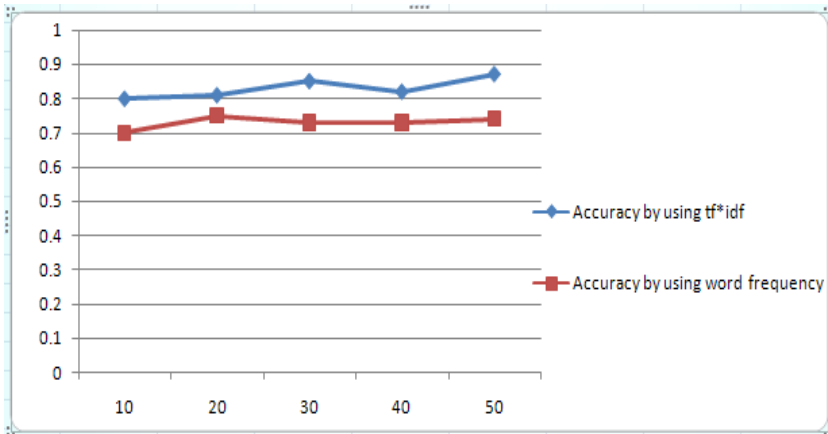



Fig. 3. Recommendation accuracy by using two different indicators

4 System Implementation

The system designed based on MVC (Model-View-Controller) model. The operating platform is Window XP or above versions and the browser is Firefox. System shown later in this article uses the data from 2013-5-1 to 2013-5-30, a total of 326 log files data. In this article, we only use recommended ATP or ATE to demonstrate our system.

4.1 View for Recommended ATP or ATE

Fig4 is the view for recommended ATP or ATE. The farmer fills title and text of the question and when he or she clicks the imagebutton , system returns a histogram for showing the recommended ATP or ATE. Horizontal axis of the histogram represents the name of the ATP or ATE and vertical axis represents interest with the question of the ATP or ATE. The farmer can online communicate with the ATP or ATE.

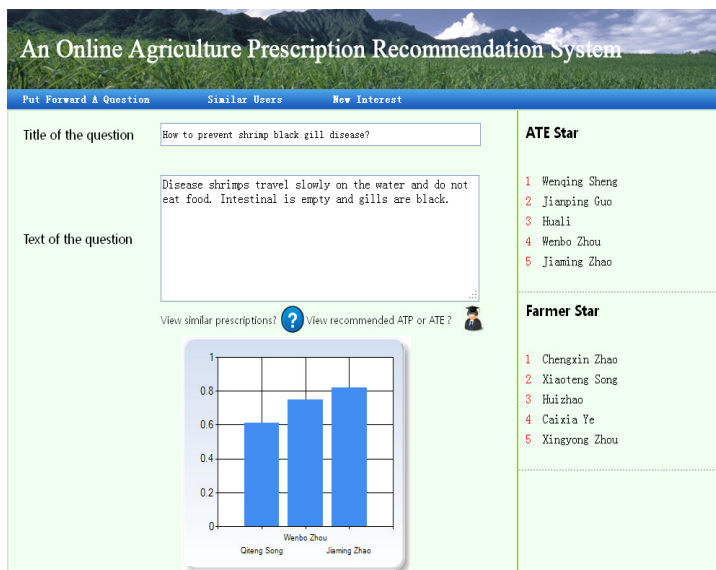


Fig. 4. Recommended ATP or ATE

5 Conclusion

This article designed and implemented an online agriculture prescription recommendation system. Farmers may find useful information in these recommended similar prescriptions to timely solve problems in the agricultural production. Farmers can view recommended ATP or ATE and online communicate with experts to get satisfactory prescriptions timely. What's more, the farmers can view similar users and find new interest from their similar users. The system provides a quick channel for farmers to seek prescriptions and provides useful agricultural information for farmers, which manifests that the system has great practical value.

We will continue to optimize the function of the system in the subsequent work such as get dynamic evolution process of the user interest model through the study of different periods of user interest model, which can predict user interest model over a period of time in the future to push timely and effective agricultural technique information for farmers.

Acknowledgements. This paper is supported partly by the NSFC (61170079 and 61202152); Special Fund for Agro-scientific Research in the Public Interest (201303107) and Special Fund for Fast Sharing of Science Paper in Net Era by CSTD(2012107); and Natural Science Foundation for Distinguished Young Scholars of Shandong and SDUST (201304 and 2010KYJQ101); and Sci. & Tech. Development Fund of Qingdao(13-1-4-153-jch). Excellent Young Scientist Foundation of Shandong Province (No.BS2012DX030); Higher Educational Science and Technology Program of Shandong Province(No.J12LN45), Postdoctoral Science Foundation of China (No. 2012M521363).

References

1. <http://www.farmers.org.cn/>
2. <http://zhibao.yuanlin.com/bchList.aspx>
3. Iglesias, J.A., Angelov, P.P.: Creating Evolving User Behavior Profiles Automatically. 10.1109/TKDE.2011 (2011)
4. Hawalah, A., Fasli, M.: A Multi-agent System Using Ontological User Profiles for Dynamic User Modelling. In: 2011 IEEE/WIC/ACM International Conference Web Intelligence and Intelligent Agent Technology (WI-IAT) (2011)
5. Kim, H.-J., Lee, S., Lee, B.-J.: Building Concept Network-Based User Profile for Personalized Web Search. 10.1109/ICIS.2010.56 (2010)
6. Tang, X., Zeng, Q.: Keyword clustering for user interest profiling refinement within paper recommender systems. *Journal of Systems and Software* 85(1), 87–101 (2012)
7. Mao, X., Xue, A., Ju, S.: A user interest building method based on weighted semantic net and effective information. *Application Research of Computers* 27(9) (2010)
8. Fei, H., Jiang, Y., Xu, L.: User interest model based on Tree Vector Space Model. *Computer Technology and Development* 19(5) (2009)

Study of Rice Identification during Early Season Using Multi-polarization TerraSAR-X Data

Lin Guo¹, Zhiyuan Pei¹, Shangjie Ma¹, Juanying Sun¹, and Jiali Shang²

¹ Chinese Academy of Agricultural Engineering, Ministry of Agriculture of China,
Beijing, 100105, China

² Research Branch, Agriculture and Agri-Food Canada, Ottawa, Ontario K1A-0C6, Canada
{guo_guolin,sunjuanying_my}@126.com, peizhiyuan@tom.com,
mashangjie@agri.gov.cn, shangj@agr.gc.ca

Abstract. The study of rice identification during early season aims to maintain cultivated area and distribution status of rice during its early season so as to provide decision support for agricultural management sectors to develop policies and measures, as well as important information for agricultural insurance sectors and agricultural products market. Multi-polarization TerraSAR-X data of Xuwen study site locating in Southern China were programmed during early season of early rice in the year of 2009. By means of comparing analysis, it is discovered that rice has more obvious identification features in jointing period and flowering period. Rice identification experiments are carried out using decision tree and object-oriented classification method. The results show that imagery acquired at the jointing period is more suitable for rice identification during the early season for a nationwide operational rice monitoring system.

Keywords: rice identification, early season, TerraSAR-X.

1 Introduction

Rice has the highest production and acreage of all grain crops in China. Most of China's paddy rice production is located in the southern provinces of the country where cloud cover and frequent rain severely limit opportunities for optical satellite acquisitions. Synthetic aperture radar (SAR) sensors are well suited for rice mapping with their ability to acquire data regardless of cloud cover. Scholars have used multi-temporal SAR data for rice identification and obtain good results[1-5].

Taking advantage of SAR data in transplanting period, heading period and early harvest period, Shao Yun and other researchers[6] measured distribution and acreage of rice in Zhaoqing, Guangdong Province, with the accuracy reaching 91%. By means of multi time-phase Radarsat-1 image and neural network method, Chen and McNairn[7] obtained the acreage of rice with producer accuracy mounting to 96%. Chen[8] took advantage of Multi-polarization ASAR data to measure the rice acreage in Southern China with accuracy of 81%.

However these satisfactory classifications were obtainable using multi-temporal data and coinciding with the end of the growing season. Early season estimates of acreages

are of significant interest for clients such as commodity brokers and marketing boards. In-season crop mapping and acreage estimates offer greater advantage.

Inoue and other researchers[9] found that SAR data of X-band is applicable to monitor early growing season of crop, yet more challenging to achieve. New Germany radar satellite provides possibility in rice identification in early stage with regard to working frequency range, polarization mode (multi-polarization and quad-polarization) and revisit cycle (11 days).

This study aims to determine the best time to acquire SAR data for rice mapping during its early season, determine the best rice growth stage to map rice, and develop the methods and procedure for rice mapping during early season. Thus in Xuwen, Guangdong study site, a time series of SAR data during early stage of early rice was obtained for this early season rice identification study. By comparing analysis of rice identification methods, the best period of rice identification during the early season was obtained, then the methods and procedures for rice mapping during the early season was developed.

2 Site Description

The Xuwen study site is located close to Leizhou City, Guangdong Province, China (20.88° N, 110.06° E). Being in central part of Leizhou Peninsula and northern part of tropical monsoon zone, the site is featured with abundant heat and rainfall, along with a large number of thunderstorms in summer. It has a terrain with high northwest part and low southeast part. Most of rice is planted in flat area, while a little portion is planted in the valleys. Apart from rice, there are also upland crops such as sugarcane and vegetables, and commercial crops such as watermelon and pineapple in flat area. There are eucalyptus, orchard and upland crop such as sugarcane in brae area.

Rice in the area is double cropped (two harvests per year). Due to separate management pattern, farmer's field management is relatively arbitrary with two main planting patterns - direct planting and transplanting. Meanwhile, the planting time span is quite long, so as to result in more obvious diversity in rice growing status during early age. In general cases, seeding period comes in mid-March, and the early-April is the transplanting stage. Tillering stage comes in the end of April and jointing stage comes in mid-May. June sees heading and flowering stage coming in the beginning of the month while mature period and harvest time in the end. Parcel of paddy field in study site is small with 100m long and 30m wide, and the weed echo on the ridge is quite obvious.

3 Data Acquisition

Four TerraSAR-X acquisitions were programmed during early growth period in early-rice of 2009. Data were collected in stripmap dual polarization mode with VV-VH polarizations with an incidence angle of 36.8° in an ascending orbit. Nominal spatial resolution of the stripmap product is 6 m. This resolution is well suited to the dimensions of the paddy fields typical of this study site. ①The planting situation is complex in March 27 with great variance. Direct seeding paddy fields were planted

and some early planted rice has emerged ; raising rice seedlings in transplanting fields was in operation with some fields in watering period awaiting for transplanting and some fields left unused without watering; some fields occupied by upland crops, such as hot pepper, would be transplanted with rice after harvest in the end of April. ②In April 18, most of the rice in direct planting field emerged and was in seeding establishment period, and would be in tillering period in about a week; most of transplanting field began to be transplanted, and some fields after upland crop harvest were in watering operation, while a little portion of fields with upland crop were still in harvest operation.③In May 10, rice in most of transplanting fields were in jointing period as transplanting operation was finished before the end of April. The general stem length was about 60cm and some rice has 45-50cm stem length due to late transplanting operation, while some rice had only 35cm stem length due to transplanting operation in the end of April after the harvest of upland crop. The growing variance was still obvious. ④In June 1, most of paddy fields were in flowering period with remaining discrepancies with regard to stem length and leaf coverage due to different planting mode and time. However, the growing situation tended to be the same with stem length of 90-110cm.

Field surveys were conducted close to the satellite acquisition dates. The contents of investigation contained: ① 41 ground control points were collected using a differential GPS with sub-meter accuracy. These ground control points were required to support ortho-correction of the imagery. ②Several ground samples were collected with crops types, location information and photos. At last 219 ground samples were selected through visual interpretation of remote sensing image. There were 219 screening samples in total with remote sensing images. These samples were divided into two groups randomly. One was used to train class rules while the other was used to evaluate the effect of rice identification.

4 Methods

In this study, details of the image processing methods were illustrated as follows. First step is Data acquisition and Pre-processing, include image data acquisition, field data acquisition and data preprocessing. Then by contrast analysis of the different imagery of VH and VV, the imagery with more obvious identification variance between rice and other major land cover types was selected. Next, the method and flow of classification was constructed for experiments of rice identification. At last the identification results of 4 temporally different images were obtained using above method and procedure, the best period of rice identification during early season was selected.

4.1 Data Acquisition and Preprocessing

To suppress speckle, the imagery was filtered using a 3 by 3 Lee filter. TerraSAR-X data were then converted to β^0 (dB). Ortho-correction was performed on both images using ground control points, DEM, and satellite ephemeris information. An RMS error under 1 pixel was achieved.

Backscatter is defined as radar cross section on unit area and could be obtained using formula (1), in which α_d represents the incident angle, K represents absolute calibration constant and A represents pixel brightness value β^0 . In backscattering images, the value of σ^0 is reflected by tonal brightness. Then different SAR data could be compared with each other.

$$\sigma^0 = \frac{\langle A^2 \rangle}{K} \sin(\alpha_d) \quad (1)$$

4.2 Data Analysis

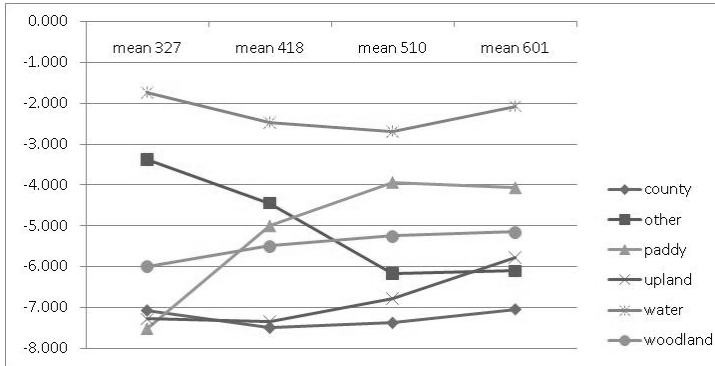
The paper acquired TerraSAR-X SM polarized images with dual polarization modes (VH and VV). The backscatter in dual-polarization mode contains more information for all land covers when comparing with single polarization mode. The interaction between radar wave and depolarization capacity of different polarization by land covers reflects attributive characters of different land cover types, such as dielectric properties, surface roughness, geometry form and direction, etc. Therefore, it is feasible for crop mapping using variation information of land covers in different polarization images. Calculate separately the difference imagery (Dvalue) of VH polarization and VV polarization backscattering coefficient for each TerraSAR-X data.

$$Dvalue = VH - VV \quad (2)$$

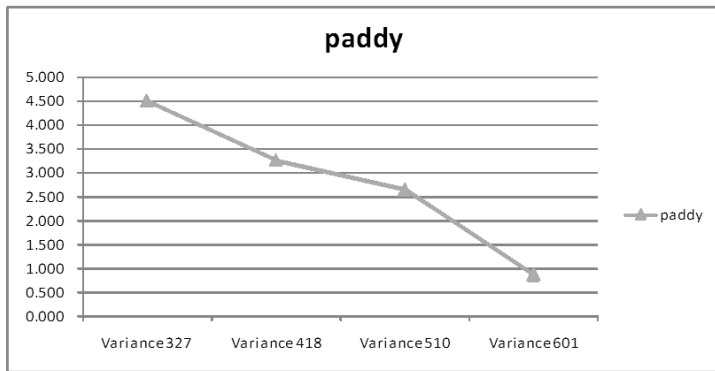
Based on the typical ground object samples, acquired through ground surveyed, the mean value and variance value of Dvalue for the dominant land cover types are provide in Table 1 and Figure 1. As shown in Table 1, we can see: ①The variance between rice and other land covers becomes greater as time passed by. On March 27, there was minimum variance between rice mean value and construction land and upland due to the variance of rice planting time and mode. There was still a portion of paddy field without being planted or transplanted. The variance between different surface features in May 10 and June 1 was relatively more obvious (See figure 1a). ②As time passed by, the variance value of rice gradually decreased, showing that the difference of rice growth brought about by planting mode and time gradually decreased, which was reflected in the figure as identification feature became more obvious and even (See figure 1b).

Table 1. Mean value of D-value

Class	March-27	April-18	May-10	June-1
Construction	-7.069	-7.502	-7.379	-7.043
Other	-3.369	-4.440	-6.173	-6.107
Paddy	-7.513	-5.009	-3.950	-4.078
Upland	-7.279	-7.342	-6.787	-5.782
Water	-1.746	-2.480	-2.696	-2.076
Woodland	-5.992	-5.497	-5.254	-5.153



(a) Mean value

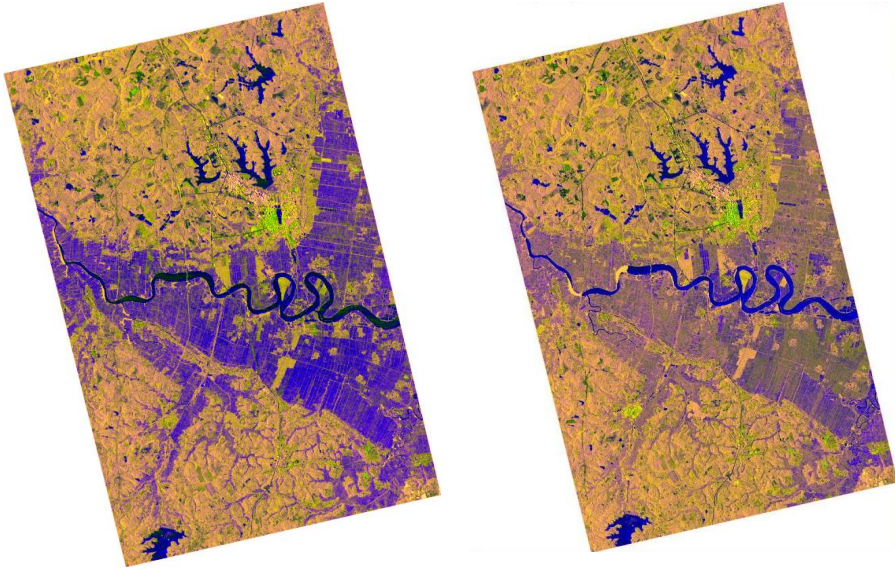


(b) Variance value

Fig. 1. The difference channel (VH-VV) temporal profile of typical ground objects

As analysis above, the backscatter on May 10 and June 1 showed more obvious features with regard to land cover separability and identification feature. Although the variance value of rice on May 10 was a little more than June 1, we can see from figure 2 that the variance still has obvious discrepancy with other land cover types, and the growth discrepancy brought by different rice planting mode was reflected by great variance.

The visual inspection of the two date TerraSAR-X data of May 10 and June 1 indicate relatively obvious identification features among land cover types. Even though rice showed multi-identification features, there was obvious separability between rice and other land covers.



(a) Colour composite constructed using data of May-10 (b) Colour composite constructed using data of June-1

Fig. 2. Colour composite constructed using TerraSAR-X data where red represents VH, green represents VV, and blue represents the difference channel (VH-VV)

4.3 Method and Flow of Rice Identification

In order to further analyze the rice identification effect of 4 temporally different images, the paper conducted rice identification experiments and obtained classification results of 4 temporally different images based on methods of object-oriented classification and decision tree. Classification procedure (Figure 3) contains image preprocessing (radiometric calibration, ortho-correction, speckle filtering, backscatter extraction), image segmentation, training/testing sample preparation, supervised decision tree extraction, classification based DT and accuracy assessment.

First, Image segmentation was applied to the three-channel image in order to clearly demarcate parcels (objects) of homogeneity[10-11]. Segmentation was completed using eCognition® Definies Imaging[12]. Next, knowledge conclusion study and rule acquisition were separately realized using training sample information of every land cover type via See5 software, and relative statistics information of VH and VV's backscattering coefficient and D-value was taken as classification feature to create decision tree (DT). Then DT was defined in eCognition to obtain classification results. The classification accuracy was tested using independent test samples.

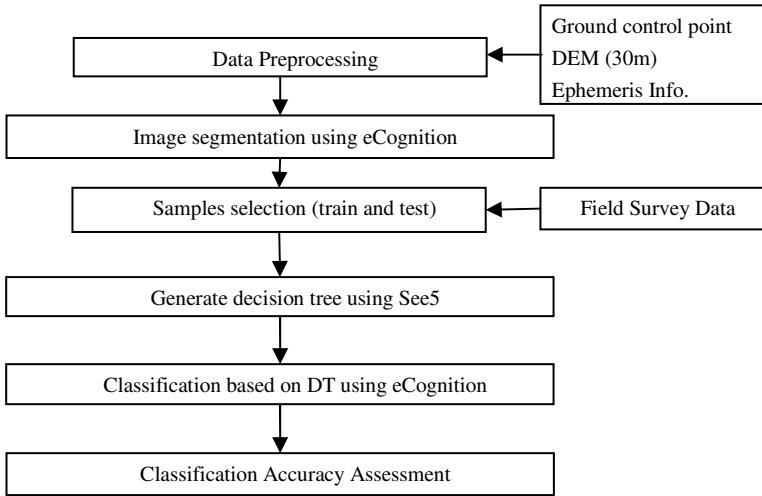


Fig. 3. Colour composite constructed using TerraSAR-X data where red represents VH, green represents VV, and blue represents the difference channel (VH-VV)

5 Results and Analysis

The entire study site was classified into 6 classes, including paddy rice, water, construction land, upland, woodland and other. Field surveyed sample data was settled according to this classification system (Table 2). We can see that the quantity distribution of every class sample was quite mean, in which construction land and water had little variation and little proportion in study site, while paddy and upland were major study objectives and had great variations as time passed by with more sample points. Sample set was divided into two parts randomly. As the quantities of training samples and validation sample were basically the same, the classification effect could be efficiently estimated.

Table 2. Ground survey data composition of different land covers

Classes	Train Samples	Test Samples	Total Number of Fields Surveyed
Paddy	17	23	40
Water	18	15	33
Construction land	17	16	33
Upland	21	24	45
Woodland	17	16	33
Other	17	18	35
Total Number	107	112	219

The 4 temporally images were processed and classified using the above method and procedures. Rice identification results were distinguished point by point using ground surveyed validation samples, and error matrix[13] could be created (Table 3).

Table 3. Ground survey data composition of different land covers

Class	Paddy	Water	Construction land	Upland	Woodland	Other	Overall Accuracy
User's Accuracy							
6-1	100.0%	93.8%	92.9%	80.0%	81.3%	77.8%	87.4%
5-10	91.7%	93.3%	93.3%	76.0%	76.5%	87.5%	85.7%
4-18	81.8%	100.0%	70.6%	65.4%	66.7%	76.5%	75.7%
3-27	84.2%	100.0%	65.0%	59.3%	60.0%	58.8%	69.6%
Producer's Accuracy							Kappa
6-1	95.7%	100.0%	86.7%	83.3%	81.3%	77.8%	0.85
5-10	95.7%	93.3%	87.5%	79.2%	81.3%	77.8%	0.83
4-18	78.3%	93.3%	80.0%	73.9%	62.5%	68.4%	0.71
3-27	69.6%	93.3%	81.3%	66.7%	56.3%	55.6%	0.63

We can see:

(1) The image of June 1 had the best classification result, most of the paddies was in the flowering period; The image of May 10 was the second best, in which most paddies were in the jointing period; March 27 and April 18 produced poorer results.

(2) Although the image of May 10 had lower accuracies than that of June 1, its overall accuracy, rice producer accuracy and user accuracy all achieved 85%; as its acquisition was about 20 days ahead of June 1, it also could achieve effective identification of paddies in the study site in spite of a slightly lower classification accuracy (a decrease of 1.7%).

From the above analysis, the image in June 1 had the best classification effect, in which period most of paddy was in flowering period; the image in May 10 took the second place, in which most paddy was in jointing period; March 27 and April 18 had inefficient effect. Although the image in May 10 had less efficient classification effect than that in June 1, its overall accuracy, rice producer accuracy and user accuracy all achieved 85%; as its acquisition was about 20 days ahead of June 1, it also could achieve effective identification on paddy in the study site in spite of classification accuracy decreasing by 1.7%. Considering the accuracy and timeliness, the image of May 10 is more suitable, and its accuracy estimation matrix is listed (Table 4).

Table 4. Xuwen study site classification result on May-10

Fields Surveyed	Classification Result						Sum	Producer's Accuracy
	Paddy	Water	Construction land	Upland	Woodland	Other		
Paddy	22	1	0	0	0	0	23	95.7%
Water	1	14	0	0	0	0	15	93.3%
Construction land	0	0	14	1	1	0	16	87.5%
Upland	1	0	1	19	2	1	24	79.2%
Woodland	0	0	0	2	13	1	16	81.3%
Other	0	0	0	3	1	14	18	77.8%
Sum	24	15	17	24	16	16	112	---
User's Accuracy	91.7%	93.3%	93.3%	76.0%	76.5%	87.5%	Overall Accuracy	85.7%

(1) Paddy, water and construction land have good identification effect as their producer accuracy and user accuracy both reached 85%.

(2) Upland had less efficient producer accuracy and user accuracy, mixing up with woodland and other surface feature. The possible reason was upland crop in flat area, such as sugarcane, dispersed over many hills besides in flat areas, which might cause confusion with eucalyptus seedlings.

(3) Classification combination (Table 5) was conducted based on image classification. The surface features were combined into “paddy” and “other” with obtainable rice identification accuracy of 97.3%.

Table 5. Rice identification result on May-10

Fields Surveyed	Classification Result			Producer's Accuracy
	Paddy	Other	Sum	
Paddy	22	1	23	95.7%
Other	2	87	89	97.8%
Sum	24	88	112	---
User's Accuracy	91.7%	98.9%	Overall Accuracy	97.3%

6 Conclusions and Discussion

(1) By using a decision tree and object-oriented classification method, TerraSAR-X data at the jointing period can achieve accurate rice identification in the early season with an accuracy of 97.3%.

(2) The images at the seeding period and tillering period had poorer results. The accuracies were not sufficient to fulfil requirements for rice mapping. Both the images at the jointing period and flowering produced good classification accuracies, the flowering period having the best result but providing maps later in the season. Considering the accuracy and timeliness, imagery acquired at the jointing period is more suitable for rice identification during the early season for a nationwide operational rice monitoring system.

Acknowledgment. This study is supported by the project named High Resolution Multi-load Cooperative Agricultural Applied Technology Study which number is GF13/15-311-003. We also thank Infoterra Asia Pacific(EADS-China) for the technical support.

References

1. Holecz, F., Dwyer, E., Monaco, S., Schmid, B., Frei, U.: An Operational Rice Field Mapping Tool Using Space Borne SAR Data. In: ERS-ENVISAT Symposium, Göteborg (October 2000)
2. Toan, T.L., Ribbes, F., Wang, L.-F., Floury, N., Ding, K.-H., Kong, J.A., Fujita, M., Kurosu, T.: CESBIO Toulouse. Rice Crop Mapping and Monitoring Using ERS-1 Data Based on Experiment and Modeling Results. *IEEE Trans. Geosci Remote Sensing* 35(1), 41–56 (1997)
3. Zhang, P., Shen, S., Li, B., Wang, X.: Studies on rice polarization backscatter signatures and rice mapping methodology. *Jiangsu Agricultural Sciences* 1, 148–152 (2006)
4. Guo, L., Pei, Z., Zhang, S., et al.: Rice identification using TerraSAR-X data. In: Proc. SPIE, vol. 8203, pp. 82030J-1–82030J-7 (2010)
5. Pei, Z., Zhang, S., Guo, L., et al.: Rice identification and change detection using TerraSAR-X data. *Canadian Journal of Remote Sensing* 37(1), 151–156 (2011)
6. Shao, Y., Guo, H., Fan, X., Liu, H.: Studies on Rice Backscatter Signatures in Time Domain and Its Applications. *Journal of Remote Sensing* 5(5), 340–345 (2001)
7. Chen, C., McNairn, H.: A Neural Network Integrated Approach for Rice Crop Monitoring. *International Journal of Remote Sensing* 27(7), 1367–1393 (2006)
8. Chen, J., Lin, H., Pei, Z.: Application of ENVISAT ASAR Data in Mapping Rice Crop Growth in Southern China. *IEEE Geosciences and Remote Sensing Letters* 4(3), 431–435 (2007)
9. Inoue, Y., Kurosu, T., Maeno, H., Uratsuka, S., Kozu, T., Dabrowska-Zielinska, K., Qi, J.: Season-long Daily Measurements of Multi-frequency (Ka, Ku, X, C, and L) and Full-polarization Backscatter Signatures over Paddy Rice Field and Their Relationship with Biological Variables. *Remote Sensing of Environment* 81(2-3), 194–204 (2002)

10. Benz, U.C., Peter, H., Gregor, W.: Multi-resolution Object-oriented Fuzzy Analysis of Remote Sensing Data for GIS-ready Information. *ISPRS Journal of Photogrammetry & Remote Sensing* 58, 239–258 (2004)
11. Guo, L., Pei, Z., Wu, Q., Liu, Y., Zhao, Z.: Application of Method and Process of Object-oriented Land Use-cover Classification Using Remote Sensing Images. *Transactions of the Chinese Society of Agricultural Engineering* 26(7), 194–198 (2010)
12. Definiens Imaging. eCognition User Guide. Definiens Imaging GmbH, Munich (2010), <http://www.definiensimaging.com/product.htm>
13. Foody, G.M.: Status of Land Cover Classification Accuracy Assessment. *Remote Sensing of Environment* 80, 185–201 (2002)

Color Image Segmentation in RGB Color Space Based on Color Saliency

Chen Zhang¹, Wenzhu Yang^{1,*}, Zhaohai Liu¹, Daoliang Li², Yingyi Chen²,
and Zhenbo Li²

¹ College of Mathematics and Computer Science, Hebei University, Baoding 071002, P.R. China

² College of Information and Electrical Engineering, China Agriculture University,
Beijing 100083, P.R. China
wenzhuyang@163.com

Abstract. It is difficult to separate the foreign fiber objects in a captured color image from the background accurately. To solve this problem, this paper presents a new approach for color image segmentation in RGB color space based on color saliency. Firstly, the captured RGB color image was separated to R, G and B color channels, and the color information for each channel was calculated. Secondly, the R saliency for each pixel in the R channel, the G saliency for each pixel in the G channel, and the B saliency for each pixel in the B channel was calculated respectively. Then comprehensive saliency map was obtained by the weighted R, G and B saliency. The weights for the R, G and B saliency were determined by the corresponding color information of each color channel. At last, the foreign fiber targets were separated out from the comprehensive saliency map using a threshold method. The results indicate that the proposed method can segment out the foreign fiber objects from the color image accurately.

Keywords: Color image segmentation, RGB color space, Color saliency, Foreign fiber targets, Comprehensive saliency map, Threshold method.

1 Introduction

Foreign fibers in cotton, such as hairs, plastic, polypropylene twines, affect the quality of the final cotton textile products seriously[1-4]. So they should be removed before spinning. Automated Visual Inspection is the state-of-the-art technology for picking out the foreign fibers from cotton lint. Image segmentation is one of the most important stage for foreign fiber detection. But it is very difficult to separate the foreign fiber objects in a captured color image from the background accurately. Nowadays, many methods for gray image segmentation are studied and widely used in many applications. Even the color image, will be transformed into gray image firstly[5-6], and then segmented using these methods developed for gray image segmentation.

* Corresponding author.

However, these methods fail to make full use of the color information to perform accurate segmentation[7-8]. So color image segmentation is one of the hot spot in image processing.

Image segmentation is one of the key techniques in image processing and machine vision system, and it is the first step in image analysis and pattern recognition. The aim of image segmentation is to partition an image into meaningful connected components. Nowadays, various image segmentation methods are available and some of them are used for foreign fiber recognition.

It is very difficult to separate the foreign fiber targets from the background using traditional image segmentation methods due to the inhomogeneous background brightness and variety of foreign fibers in different colors and shapes. So it is high time for us to solve this problem to improve the image segmentation accuracy. Visual attention based image processing method is one of the state-of-the-art methods and has been successfully used for object detection.

Scientists took considerable time and efforts to study the human visual attention system[9] in order to segment the targets automatically. Saliency map was firstly introduced by Koch and Ullman. For human vision, color information is important in a image, and the sensitive degree is different from one image to another. Itti proposed a color image segmentation method based on visual attention and saliency map[10], but the segmentation efficiency is not high. Hou introduced a new construction method of saliency map based on spectral residual[11]. Due to its simplicity and high efficiency, it has been widely used in many applications[12-14].

This paper presents a color image segmentation method based on RGB comprehensive saliency. Color information in a color image is vital to the human vision, so we consider red, green and blue value as the color information. We can obtain R, G, B information saliency map separately from the correspond channel. According to the different color information, we give different weights to different saliency map, and then, the comprehensive saliency map is created. We used a threshold method to realize the separation of target and background. The aim of this paper is to develop a method which can be employed in the AVI system to detect the foreign fibers precisely and quickly. The paper is organized as follows. We present the materials and methods in Section 2. We describe the experiments carried out to validate the performance of the proposed method for the task of foreign fiber detection in Section 3. Finally, we conclude this work in Section 4.

2 Materials and Methods

We chose feather, hair, plastic and polypropylene twine as typical foreign fibers in this research. An AVI system in our lab, as shown in Fig. 1, is used to capture the live color images of the foreign fibers.

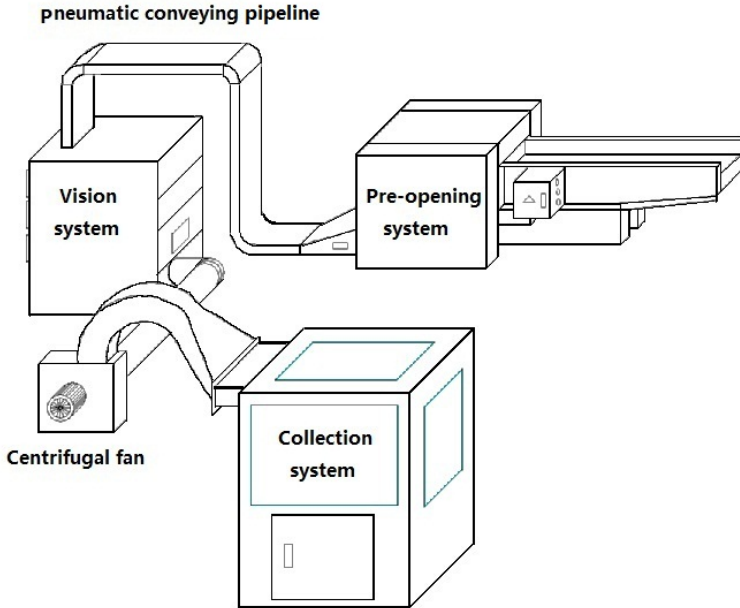


Fig. 1. Outline of the AVI system

The AVI system mainly consists of three sub-systems: a cotton lint pre-opening system, a visual inspection system and a cotton lint collection system. The compact cotton lint with foreign fibers was firstly pre-opened in the pre-opening system to make it loose. Then the loosed cotton lint was transferred to the visual inspection system. In the vision system, color images of foreign fibers were captured by line-scan camera, and analyzed in the computer. After the inspection finished, the cotton lint was collected and stored in the collection system.

2.1 Image Acquisition

Live color images of foreign fibers were captured by a line-scan camera in the vision system. The camera we used is a Piranha line scan color camera with 4096 resolution. It was set to internal exposure mode working at 10 KHz frequency. Live scanned lines were collected by an image acquisition board (X64-CL Express, CORECO, Canada) and stored in an image buffer. The frame size was set to 128 lines, so the image resolution in this application was 128×4096 pixels. Some sample images with different type of foreign fibers were shown as Fig. 2.

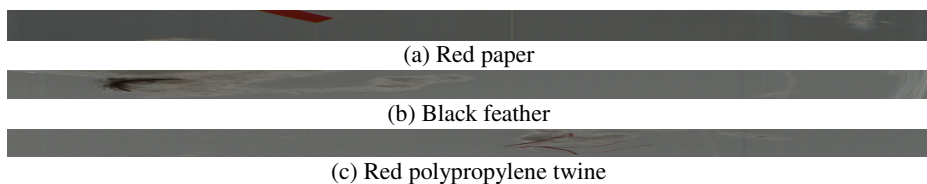


Fig. 2. Foreign fiber images

In the first image, a piece of red paper was in it. In the second image, we can seize black feather as the foreign fiber. In the third image, a piece of red polypropylene twine was found.

2.2 The Frame of the Method

Foreign fiber images we obtained were color images, and different images have different color information. We can divide a RGB color image into R channel, G channel and B channel. Because of R information, G information and B information varying from one image to another, the visual feeling about different channel is different. If the amount of R information is greater than the other two channels' information, the human is more sensitive to the R information. If the amount of G information is the largest, the human is more sensitive to the G information. It is the same for B information. According to the amount of R information, G information and B information, we can determine the weight of R saliency, G saliency and B saliency. Thus, we can form a comprehensive saliency map, and we use a threshold method in order to do the segmentation between the target and the background. The frame of the proposed method was shown in Fig. 3.

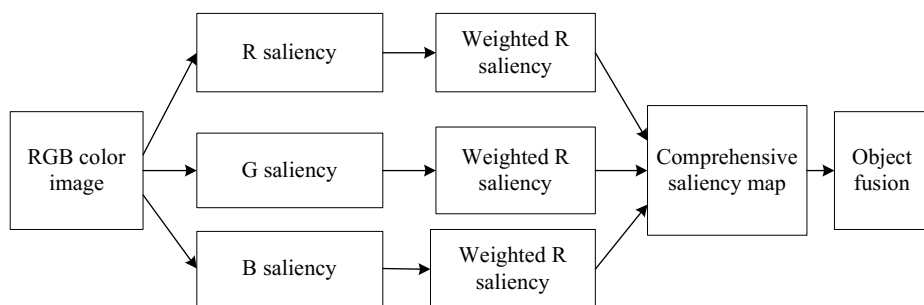


Fig. 3. The frame of the proposed method

2.3 Channel Information Calculation

The input color image I is a RGB color image whose resolution is $M*N*3$ pixels. M and N are the number of rows and columns. Let $R(i, j)$, $G(i, j)$ and $B(i, j)$ represent each channel information respectively, where i represents the abscissa of a pix, j represents

the ordinate of a pix. Let S_r, S_g, S_b be the sum of the R, G, B information respectively, and let M_r, M_g, M_b be the mean of the R, G, B information respectively.

$$S_r = \sum_{i=1}^M \sum_{j=1}^N R(i, j) \quad (1)$$

$$S_g = \sum_{i=1}^M \sum_{j=1}^N G(i, j) \quad (2)$$

$$S_b = \sum_{i=1}^M \sum_{j=1}^N B(i, j) \quad (3)$$

$$M_r = S_r / (M * N) \quad (4)$$

$$M_g = S_g / (M * N) \quad (5)$$

$$M_b = S_b / (M * N) \quad (6)$$

2.4 Color Saliency Calculation

The saliency of one channel information can be obtained by computing the absolute difference of the color feature with the mean color feature value. Let L_r, L_g, L_b present the corresponding color information saliency, and the formulae are as below.

$$L_r(i, j) = abs(R(i, j) - M_r) \quad (7)$$

$$L_g(i, j) = abs(G(i, j) - M_g) \quad (8)$$

$$L_b(i, j) = abs(B(i, j) - M_b) \quad (9)$$

2.5 Weights Determination

The weight for each color saliency depends on the amount of R information, G information, and B information. A larger amount of R information indicates that the R characteristics is more important for human visual perception, and a larger amount of G

information presents that the G characteristics is more important for human visual perception. It is the same for B information. Let W_1, W_2, W_3 represent the weight of each channel saliency. We can calculate them by the following formulae.

$$W_1 = M_r / (M_r + M_g + M_b) \quad (10)$$

$$W_2 = M_g / (M_r + M_g + M_b) \quad (11)$$

$$W_3 = M_b / (M_r + M_g + M_b) \quad (12)$$

2.6 The Comprehensive Saliency Map Calculation

After working out the weights, we can obtain the comprehensive saliency map by using the formula below.

$$S(i, j) = W_1 * L_r(i, j) + W_2 * L_g(i, j) + W_3 * L_b(i, j) \quad (13)$$

2.7 Foreign Fiber Objects Detection and Fusion

We can use a threshold method to distinguish the foreign fiber objects from the background. Let T be the threshold. When $S(i, j)$ is greater than T , we regard $\text{pix}(i, j)$ as a pixel in the foreign fiber object, while $S(i, j)$ is smaller than T , we think $\text{pix}(i, j)$ as a pixel in the background.

$$O(i, j) = \begin{cases} 0, & S(i, j) < T \\ 1, & S(i, j) \geq T \end{cases} \quad (14)$$

2.8 Algorithm Implementation

Step1: calculate the color feature R, G and B respectively.

Step2: calculate the channel information M_r, M_g and M_b respectively.

Step3: calculate the weight for each channel saliency based on M_r, M_g and M_b .

Step4: calculate the channel saliency map L_r, L_g and L_b respectively.

Step5: Obtain the comprehensive saliency map S according to the weights and the channel saliency maps.

Step6: Segment the targets by using a threshold method to get the final object O .

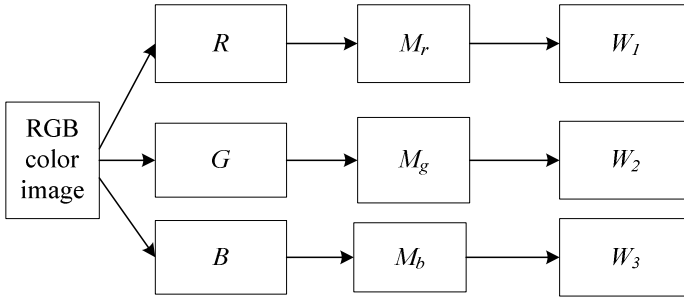


Fig. 4. The process of weights calculation

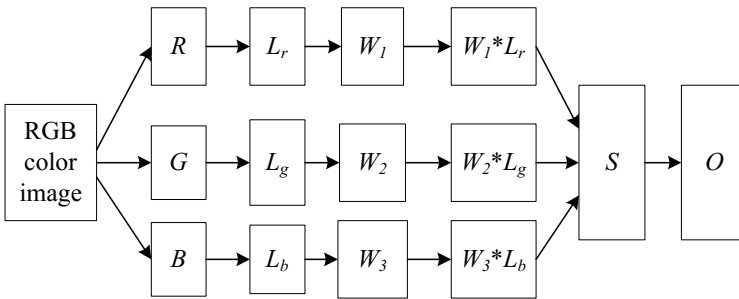


Fig. 5. The process of the Image segmentation method

3 Results and Discussion

The images we used in the experiment are live images captured by the AVI system. The algorithm was implemented in Matlab 7.0, and the operation system is Window XP.

A large amount of color images of foreign fibers were used to test the proposed method. The processing results of polypropylene twine were shown below. In this experiment, the human visual attention is associated with the whole image’s color information. The red color is dominant in the whole image, so we think red is the most important color for human visual feeling in this image of polypropylene twine. Thus, we raise the weight of red color saliency map in our experiment.

The processing results of black hair obtained by the proposed method were shown in Fig. 6. In this test, the human visual attention is associated with the whole image’s color. M_r and M_g larger than M_b , so red and green are regarded as the both important color for human visual feeling. Thus, we raise the weight of red and green color saliency map.

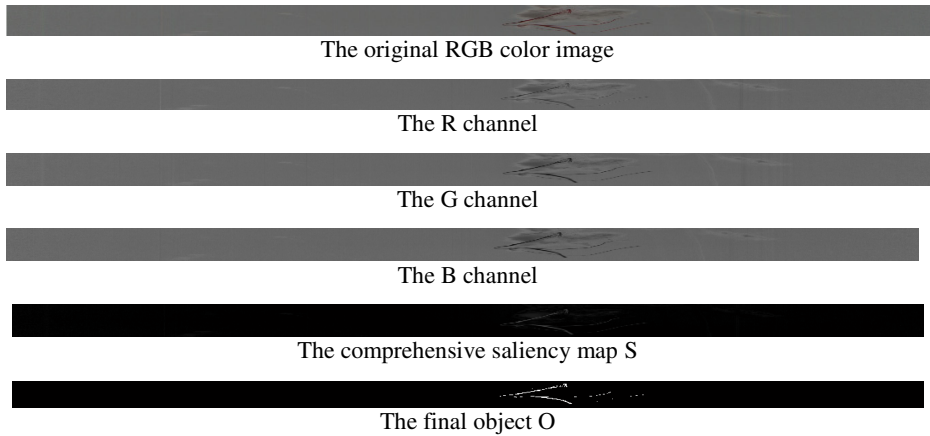


Fig. 6. The results of the segmentation of polypropylene twine

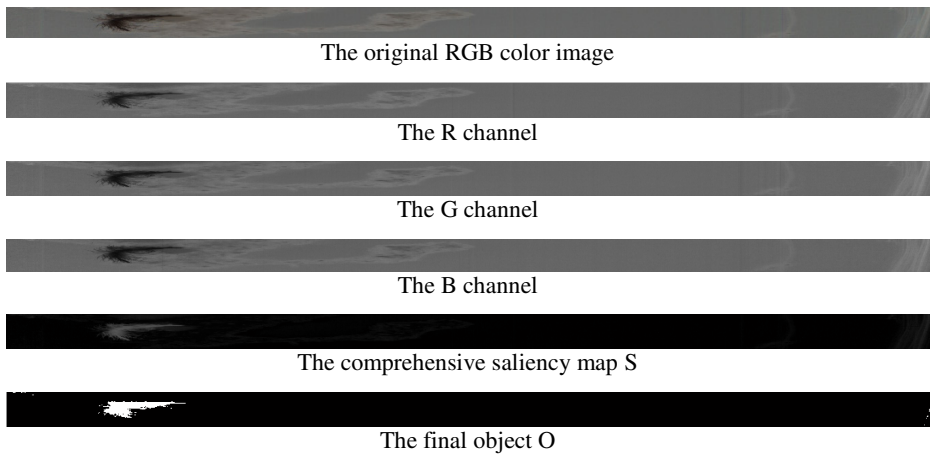

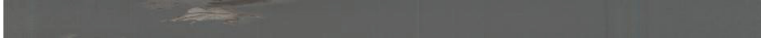

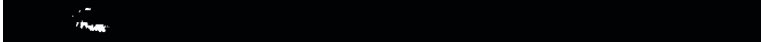







Fig. 7. The results of the segmentation of black feather

Compared with the spectral residual method, our method can get better flexibility. We use the color information in a color image to determine the saliency map dynamically. We use a threshold method to separate out the target. In our experiment, T was set to 0.115. The spectral residual method can not segment all the selected images in our experiment, while our method can get accurate segmentation, as shown in Table 1.

In our experiments, we use empirical value as the threshold, which can make the method simple and fast. The Otsu's algorithm has the problem in segmentation in our image, because of the low contrast ratio between the foreign fiber objects and the background. So we use the empirical value as the threshold in order to promote the segmentation accuracy.

Table 1. The comparison of the segmentation method

Original RGB image		(A1) black feather
		(B1) plastic film
		(C1) polypropylene twine
Spectral residual		(A2) the result of black feather
		(B2) the result of plastic film
		(C2) the result of polypropylene twine
our method		(A3) the result of black feather
		(B3) the result of plastic film
		(C3) the result of polypropylene twine

4 Conclusion

A new approach for color image segmentation in RGB color space based on color saliency was proposed. The amount of R, G and B color information was firstly calculated, and the weight of each channel saliency map was determined according to the corresponding color information. And then, the comprehensive saliency map was obtained. Finally, the foreign fiber targets were segmented out from the comprehensive saliency map. The results indicate that the proposed approach is consistent with the

human visual perception characteristics and can get accurate foreign fiber objects from the captured color images.

The threshold for comprehensive saliency map segmentation is empirical value. How to segment the foreign fiber images automatically will be researched in our future work.

Acknowledgements. The authors thank The Ministry of Science and Technology of the People's Republic of China (2013DFA11320, 2013BAK07B04), National Natural Science Foundation of China (31228016), Hebei University (2010-207), Key Laboratory of Modern Precision Agriculture System Integration Research Centre of the Education Ministry in China Agriculture university (X11-01), Hebei Education Department (Q2012063), and Hebei Science and Technology Department (12210133), for their financial support, and China Agriculture University for providing the testing environment.

References

1. Yang, W.Z., Li, D.L., Wei, X.H., Kang, Y.G., Li, F.T.: An automated visual inspection system for foreign fiber detection in lint. In: IEEE GCIS, pp. 364–368 (2009)
2. Yang, W., Lu, S., Wang, S., Li, D.: Fast recognition of foreign fibers in cotton lint using machine vision. *Mathematical and Computer Modelling* 54, 877–882 (2011)
3. Yang, W.-Z., Li, D.-L., Zhu, L.: A New Approach for Image Processing in Foreign Fiber Detection. *Computers and Electronics in Agriculture* 68(1), 68–77 (2009)
4. Yang, W., Li, D., Wang, S., Lu, S., Yang, J.: Saliency map basee color image segmentation for foreign fiber detection. *Mathematics and Computer Modelling* 58, 846–852 (2013)
5. Ye, Q.-X., Wen, G., Wang, W.-Q., et al.: A Color Image Segmentation Algorithm by Using Color and Spatial Information. *Journal of Software* 15(4), 522–530 (2004)
6. Bao, Q.-L.: Color Image Segmentation Based on HSV Color Space. *Software Guide* 9(7), 171 (2010)
7. Zhao, J.-X., Wang, J.: Color I mage Edge Detection Based on Subdivision of RGB Space. *Optoelectronic Technology* 29(3), 171–173 (2009)
8. Han, X.-W., Yang, Z., Li, Y.-P., et al.: A Method for Color Image Segmentation Based on Color Similarity Coefficient. *Journal of Shenyang University* 26(6), 14–17 (2004)
9. Zhang, H.-W., Zheng, Y.-F., Zhang, Q.-R.: Color Image Segmentation Based on Visual Attention Mechanism. *Computer Engineer and Application* 47(10), 154–157 (2011)
10. Itti, L., Koch, C., Niebur, E.: A model of saliency-based visual attention for rapid scene analysis. *IEEE Transactions on Pattern Analysis and Machine Intelligence* 20(11), 1254–1259 (1998)
11. Hou, X.-D., Zhang, L.-Q.: Saliency Detection: A Spectral Residual Approach. In: *Proceedings of The IEEE Conference on Computer Vision and Pattern Recognition*, pp. 1–8 (2007)
12. Stas, G., Lih, Z.-M., Ayellet, T.: Context-Aware Saliency Detection. *IEEE Transactions Pattern Analysis and Machine Intelligence* 34(10), 1915–1926 (2012)
13. Shi, H., Yang, Y.: A Computational Model of Visual Attention Based on Saliency Maps. *Applied Mathematics and Computation* 188, 1671–1677 (2007)
14. Hang, S., Yu, Y.: A computational model of visual attention based on saliency maps. *Applied Mathematics and Computation* 18(2), 1671–1677 (2007)

Water-Landscape-Ecological Relationship and the Optimized Irrigation Strategy for Green-Roof Plants in Beijing, a Case Study for *Euonymus japonicus*

Caiyuan Wang², Peiling Yang^{1,*}, Yunkai Li¹, and Shumei Ren¹

¹ College of Water Conservancy & Civil Engineering, China Agricultural University, Beijing 100083, China

yangpeiling@126.com

² Beijing Hydrological Station, Beijing, 100089, China

Abstract. Carbon sequestration and O₂ release due to the rapid development of urban greenland could be beneficial for the global implementation of energy saving and CO₂ emission reduction, however, this poses another question that increased the demand for irrigation becomes a concern for the sustainable utilization of water resources, especially for Beijing, with the scarcity of land and water resources for Greenland. *E.japonicus*, as one of typical green-roof plants, has the advantages of alleviating the effect of heat island and improving microclimate environment. However, it needs to make clear that how the physiological performance of *E.japonicus* treated with different water stresses including full irrigation (CK) (90%-100%FC), low water stress (LWS) (75%-85%FC), moderate water stress (MWS) (65%-75%FC), and serious water stress (SWS) (50%-60%FC) is, and landscape function and ecological serves function are also considered as integrated indicators to selecting optimization irrigation strategy in this study. The results showed that the photosynthetic rate, transpiration rate, stomatal conductance and water use efficiency of *E.japonicus* were in the order of LWS>MWS>SWS in three treatments of water stress. Moreover, the photosynthetic rate, transpiration rate, stomatal conductance and water use efficiency under LWS were 1.55%、3.3%、4.13%、7.1% higher compared to CK, respectively. Higher leaf area and chlorophyll content were also measured under the treatment of LWS. In terms of ecological serves function, carbon sequestration and oxygen release, and cooling and humidity were lessening with the soil moisture reducing which express the positive correlation relationship. but the differences was no significant. The LWS(75%-85%FC) stimulated the growth of *E.japonicus*, and effectively regulated the distribution of the assimilation object to chlorophyll and that for the growth of leaves. Besides, it played a significant role in ecological environment. Therefore, the LWS (75%-85%FC) is the optimal water-saving irrigation model.

Keywords: green-roof landscape function, ecological serves function, the optimal irrigation model.

* Corresponding author.

1 Introduction

The development of the world economy and urbanization resulted in increasing carbon dioxide emissions annually, which further caused global warming (King, C.D., 1995). Based on this serious problem, it is urgent to implement energy saving, reduce CO₂ emission, take the path of low carbon economy, and develop low carbon cities. Greenland has important self-purification capacity in the urban ecosystem, which is not only the primary producer of the urban ecosystem, but also the regulator of the ecological balance in the urban ecosystem. Greenland of certain quantity and quality could not only beautify the urban landscape and city appearance, but also serve as effective means of reducing and purifying the urban environment pollution (Jian-feng Li, 2010; Yang J, 2008; Fujii S, 2005; Yang J, 2005; Jim CY, 2007). With the implementation of global energy-saving, large area of urban Greenland have been developed, which directly resulted in increasing water consumption, the expansion of greenland area, and rocketing energy consumption. However, due to the shortages of water resources, land resources and energy resources in Beijing, the rapid development of Greenland aggravated the serious shortages. The study of green-roof and green plant water-saving could not only save large amounts of water, alleviate the tension of groundwater overexploitation as a result of surface water shortage, reduce the energy consumption by groundwater exploitation, but also to a large extent alleviate the serious problem of scarce usable Greenland in Beijing.

The natural condition is harsh in Beijing. Drought, less rain and larger evaporation cause water deficiency on soil. Green plants has some drought resistance ability. Researchers had done many works on the drought resistance of green plants under different control levels of soil moisture. But these studies mainly concentrated on the growth characteristics of plants (Djekoun, A., 1991; Heckathorn.S.A.,1997; Widodo,W.,2003; Subramanian,V.B.,1990; Wenting Zhang, Meizhi Mu, Huatian Wang. et al.,2009; Caiyuan Wang, Peiling Yang, Lu lu. et al.,2010; Jinmei Zhao, He Zhou, Jicheng Guo. et al, 2007; Wenting Zhang, Fuqiang Liu, Huatian Wang. et al.,2008; Yan Li, 2009). Moreover, farm crops were mainly selected as the objective of their studies, the yield of crops and the quality of fruit were taken as the most concerned indicator. But for of green plants, we focus on their landscape function and ecological functions in the afforestation of cities without regard to the yield of crops and the quality of fruit. Based on this, we must change the former idea for green plants irrigation study. Under water stress condition, it is necessary to find an optimal irrigation model by taking the combined effects of water-landscape-ecology into consideration, set up the reasonable soil moisture control level, and therefore provide theoretical basis for city afforestation and its irrigation management.

Therefore, with pot experiments and *E.japonicus* taken as the measured object, this paper studied the inadequate irrigation model with full consideration of water-landscape-ecology and the physiological response, which provided a theoretical basis for the management of green-roof plants under inadequate irrigation condition.

2 Materials and Methods

2.1 Experiment Materials

The selected *E.japonicus* was one of the typical green shrubs in Beijing. The experiment was conducted in College of Water Conservancy & Civil Engineering, China

Agricultural University (39°56'N, 116°17'E). The weather of experimental site is a warm sub-humid continental monsoon climate, with the average temperature of 12.8°C, annual effective accumulative temperature of 4500°C, frost-free period of 189d, annual rainfall of 450-650mm, and annual evaporation of 1835.8mm. *E.japonicus* was transplanted to flower pots in March 2009. Those pots were 26.5cm in height and 35cm in diameter. Three small holes were made at the bottom of the pots in order to maintain the permeability of soil and prevent water accumulating on the pot floor. The soil samples were collected from the experimental field of the China Agriculture University. After air drying and sieving into 2 mm mesh, the soil was packed to a bulk density of 1.35g/cm³, and left 5cm height below the pot top brim to avoid water overflow. The soil weight of each pot was 15.47kg. During the experiment, the soil moisture condition was controlled by weight method. For better survival rate of *E.japonicus*, all seedlings were fully irrigated within a month after transplanting, and rooting powder was applied which would help the roots grow rapidly.

2.2 Experiment Design

The experiment was designed by four soil moisture condition treatments with six replications: Full irrigation (90%-100%FC), Light water-stress (75%-85%FC), Middle water-stress (65%-75%FC), Severe water-stress (50%-60%FC). During the experiment process, with climate changes, the plants were irrigated to upper limit in every treatments when the soil moisture reached the lower limit of setting beforehand or was close to the lower limit. and made the soil moisture maintain between upper limit and low limit every treatment. For the sake of accuracy, water was irrigated by using the beakers of 400ml and 100ml. Before irrigating, a small tray was put under each pot, so that there would be water leaking from the gap between soil and the pot. Then water seepage was repoured into the pots slowly to ensure appropriate soil moisture for each treatment.

2.3 Observation Index and Measurement Method

Leaf area was measured 5 times by vitro method with 30 days interval between consecutive two x measurements. Total 30 leaves were taken from growth well leaves and fixed above the graph paper, then scanned by MRS-2400U2 scanner. The leaf area of scanning leaves was calculated by the AutoCAD software. The growth of leaves was measured by the weighing method in vitro, the whole shrub was divided into three parts: the upper, middle and lower and cut down, then each part leaves were measured the weight with the balance that the accuracy of balance was 0.01g.

The photosynthetic rate (Pn), transpiration rate (Tr), and stomatal conductance (gs) of leaf were measured by the CI-340 photosynthesis system the typical sunny day.was chose between two irrigation and measured once every 2 hours from 8:00-18:00. During the measurement, six leaves were selected from growth well leaves., according to the different positions of seedlings ,which divided into three parts: the upper, middle and low.

We chose the typical sunny day to measure chlorophyll in 10:00am by the SPAD-502 chlorophyll meter which was product in German. During the measurement, five growth well leaves were chose from the top of canopy.

2.4 Characterization of Landscape Function

As green plants of urban, the landscape function was particularly important. The landscape function of green plants mainly embodied in the size of leaves, sparse degree of leaves and leaves color.

Leaf area reflected the size of leaf, calculated as equation(1):

Total leaves area:

$$S_1 = S_2 \times W_1 / W_2 \quad (1)$$

Where S_1 is the total leaves area, cm^2 ; S_2 is the leaves area of scanning, cm^2 ; W_1 is the total fresh weight of leaves, g; W_2 is the leaves fresh weight of scanning, g.

Leaf area index(LAI) reflected the sparse degree of leaves, calculated as equation(2):

Leaf area index(LAI):

$$\text{LAI} = S_1 / \pi r^2 \quad (2)$$

Where LAI is the leaf area index; S_1 is the total leaves area, cm^2 ; r is the average canopy radius, cm.

In this text, leaf color was expressed by chlorophyll content. For evergreen shrub species, the higher chlorophyll content, the better Landscape function.

2.5 Characterization of Ecosystem Service Function

2.5.1 Fixing Carbon and Releasing Oxygen

The assimilation of plants enclosed the area of the net photosynthesis and the horizontal axis of time in the diurnal variation curve of plants' photosynthesis.

In this basis, we assumed that the net photosynthesis was P, the formula for calculating the net photosynthesis as follow:

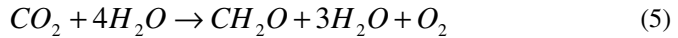
$$P = \sum_{i=1}^j [(P_{i+1} + P_i) \div 2 \times (t_{i+1} - t_i) \times 3600 \div 1000] \quad (3)$$

Where P is the total assimilation in the sampling day, $\text{mmol} \cdot \text{m}^{-2} \cdot \text{d}^{-1}$, P_i is the instantaneous photosynthetic of the measured point, P_{i+1} is the instantaneous photosynthetic of the next measured point, $\mu\text{mol} \cdot \text{m}^{-2} \cdot \text{s}^{-1}$; t_i is the instantaneous time of the measured point, t_{i+1} is the instantaneous time of the next measured point, h; j is the times of measuring; 3600 is 3600 seconds every hour; 1000 is 1000 μmol .

The total assimilation converted to amount of fixing CO_2 :

$$W_{\text{CO}_2} = P \cdot 44 / 1000 \quad (4)$$

Where 44 is molar mass of CO_2 , $\text{g} \cdot \text{mol}^{-1}$, W_{CO_2} is that per unit area of leaf fix CO_2 quality, $\text{g} \cdot \text{m}^{-2} \cdot \text{d}^{-1}$. According to the reaction equation of photosynthesis:



the rate of trees release oxygen is:

$$W_{O_2} = P \cdot 32 / 1000 \quad (6)$$

Unit is $g \cdot m^{-2} \cdot d^{-1}$

2.5.2 Cooling and Humidification

Cooling and humidifier based on the transpiration rate, and the formula for calculating:

$$E = \sum_{i=1}^j [(e_{i+1} + e_i) \div 2 \times (t_{i+1} - t_i) \times 3600 \div 1000] \quad (7)$$

Where E is the total transpiration in the test day, $mmol/(m^2 \cdot s)$; e_i is instantaneous rate of transpiration of the initial measured point. e_{i+1} is the instantaneous rate of transpiration of the next measured point ($\mu mol/(m^2 \cdot s)$); t_i is the instantaneous time of the initial measured point, t_{i+1} is the instantaneous time of the next measured point, h; j is the period of measuring;

$$W_{H_2O} = E \times 18 \quad (8)$$

Where 18 is molar mass of H₂O.

We assumed that *E.japonicus* absorbed heat per square meter leaves in the day as Q, due to transpiration of water, then

$$Q = W_{H_2O} \times L \quad (9)$$

Where Q is absorbing heat unit area every day, $kJ/(m^2 \cdot d)$; L is evaporation consumption of heat transfer coefficient ($L = 2495 - 2.38t$, t is the temperature of measured day).

3 Results and Analysis

3.1 The Effect on Photosynthetic Rate, Transpiration Rate, Stomatal Conductance in Different Controlling Level of Soil Moisture

During the experiment, the photosynthetic rate, transpiration rate and stomatal conductance of different leaves positions of *E.japonicus* were measured in different time. The results (table 1) showed that there were no negative relation between the photosynthetic rate, transpiration rate stomatal conductance and increasing water content On September, photosynthetic characteristics for MWS treatment (75%-85%FC) were performing better than other treatments, indicating that the differences in the demand for water and the ability to adapt in different time, due

to *E.japonicus* physiological regulation. Transpiration rate showed a single peak along with the solar radiation, temperature, humidity and other climate factors (Fig. 1). Photosynthetic rate showed a single peak in the full water supply, but the photosynthetic rate showed a "lunch break" phenomenon at midday under water stress condition. Stomatal conductance reached the maximum in all treatments in the morning.

Table 1. The effect on the photosynthetic characteristics in different water treatments

Time	parameters	treatments			
		CK	LWS	MWS	SWS
2010	photosynthetic (Pn) ($\mu\text{mol}\cdot\text{m}^{-2}\cdot\text{s}^{-1}$)	4.40±1.63a	4.34±1.33a	4.03±1.39a	3.36±1.35b
	Transpiration (Tr) ($\text{mmol}/\text{m}^2/\text{s}$)	0.92±0.44a	0.89±0.38a	0.88±0.36a	0.73±0.41b
	Stomatal conductance (Gs) ($\text{mmol}/\text{m}^2/\text{s}$)	33.90±16.1a	32.81±13.95b	32.09±13.22b	25.37±11.07b
	Water use efficiency (WUE) ($\mu\text{molCO}_2/\text{mmolH}_2\text{O}$)	6.16±4.31a	5.31±2.02b	5.14±2.12b	4.98±2.18b
	photosynthetic (Pn) ($\mu\text{mol}\cdot\text{m}^{-2}\cdot\text{s}^{-1}$)	4.51±1.28a	4.44±1.40ab	3.90±0.97bc	3.40±1.33c
2009	Transpiration (Tr) ($\text{mmol}/\text{m}^2/\text{s}$)	0.91±0.40a	0.94±0.37a	0.86±0.38ab	0.75±0.33b
	Stomatal conductance (Gs) ($\text{mmol}/\text{m}^2/\text{s}$)	34.36±15.64a	35.78±16.26ab	28.74±9.30bc	26.63±12.49c
	Water use efficiency (WUE) ($\mu\text{molCO}_2/\text{mmolH}_2\text{O}$)	5.53±1.98a	5.14±1.84ab	5.07±1.99ab	4.89±1.91b

Data followed by different letters (a, b, c) within same columns at same stage are significantly different at $P_{0.05}$ level; values are Mean±S.E. of each treatment.

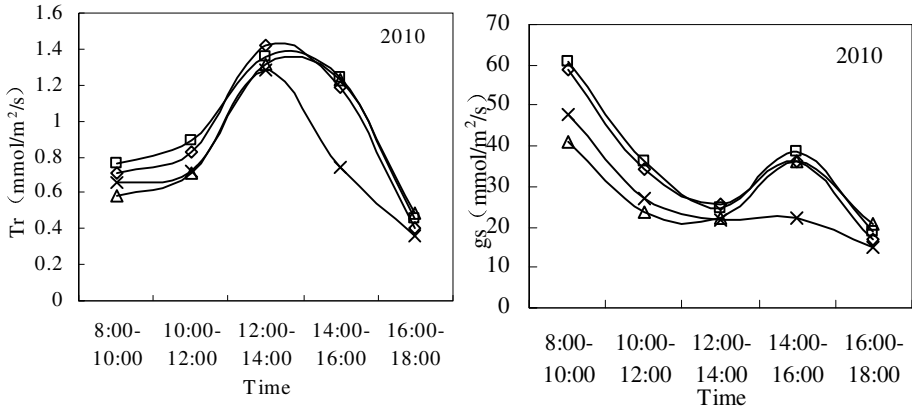


Fig. 1. The change process of the photosynthetic rate, transpiration, stomatal conductance in different time

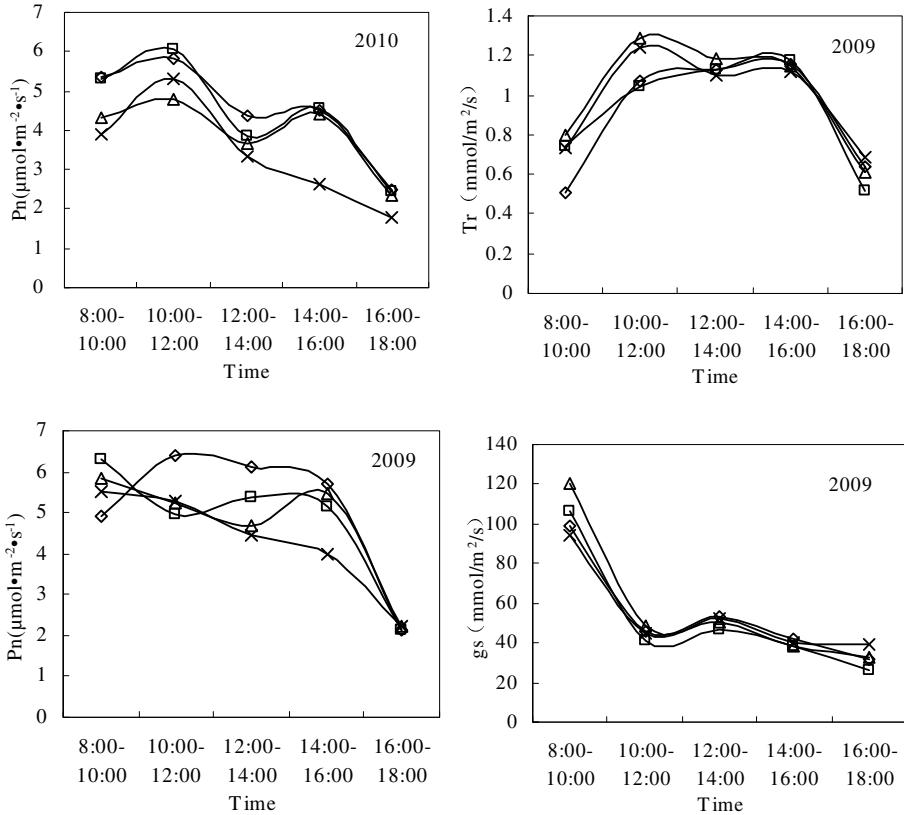


Fig. 1. (Continued.)

3.2 The Effect on Landscape Function and Ecosystem Services Function for *E. japonicus* in Different Control Level of Soil Moisture

3.2.1 Landscape Function

E. japonicus was the typical green plant in Beijing, which played an important role in the beautification of the city. In this paper, we evaluated the landscape function of *E. japonicus* with four parameters in different control levels of soil moisture, which were leaf area, leaf area index, leaf growth and chlorophyll.

As table 2 shown, leaf area, leaf area index, leaf growth and chlorophyll performed differently under various control levels of soil moisture. The leaf area, leaf area index, leaf growth and chlorophyll of the SWS treatment were less than other treatments. The result showed that (50%-60%FC) didn't provide enough water of normal growth of *E. japonicus*, which would restrain the growth of *E. japonicus*, such as sparse growth of leaves and smaller total leaves area. However, when the soil moisture was (75%-85%FC), leaves growth and the total leaves area were the optimal,

suggesting that (75%-85%FC) was the optimal soil moisture for the growth of *E.japonicus*, meanwhile, leaf growth showed flourish characteristics. The sizes of leaf area and leaf growth of the mid and low part of *E.japonicus* were quite important for appreciation as the green plants. Small and sparse leaf had an apparently impact on the landscape function of *E.japonicus*.

Table 2. The parameter of landscape function in different treatment

parameter	treatment				
	CK	LWS	MWS	SWS	
The total leaf area (cm ²)	951.84±73.64b	1026.14±71.85a	898.17±36.16bc	841.96±79.32c	
Leaf area index	0.24	0.44	0.43	0.28	
Amount of leaf growth (g)	up	53.18	73.04	48.08	46.68
	mid	109.78	127.92	123.53	45.03
chlorophyll (SPAD)	67.6±3.6b	75.4±5.4b	68.0±2.9a	65.2±2.4a	

Data followed by different letters (a, b, c) within same columns at same stage are significantly different at $P_{0.05}$ level; values are Mean±S. E. of each treatment.

3.2.2 Ecological Effects

The amount of carbon fixation and oxygen releasing, cooling and humidification of *E.japonicus* were showed in Table 3 under different treatments. We could see differences which was not significant each treatment through the variance analysis for data. Through comparing between different treatments, In 2009 and 2010, the amount of carbon fixation of the CK treatment is higher 8.68%, 10.53%, 17.93% and -1.42%, 8.59%, 30.21% than LWS, MWS, SWS treatment respectively; the amount of oxygen releasing of the CK treatment is higher 8.72%, 10.75%, 17.91% and 0.24%, 10.48%, 32.15% than LWS, MWS, SWS treatment respectively; the amount of cooling of the CK treatment is higher -0.83%, 5.94%, 7.13% and 4.19%, 4.54%, 25.95% than LWS, MWS, SWS treatment respectively; the amount of humidification of the CK treatment is higher -0.82%、5.94%、7.13% 和 4.19%、4.54%、25.95% than LWS, MWS, SWS treatment respectively; From data what mentioned above, the ecological of *E.japonicus* is lessening with the soil moisture reducing.

3.3 The Relation of Water-Landscape-Ecological

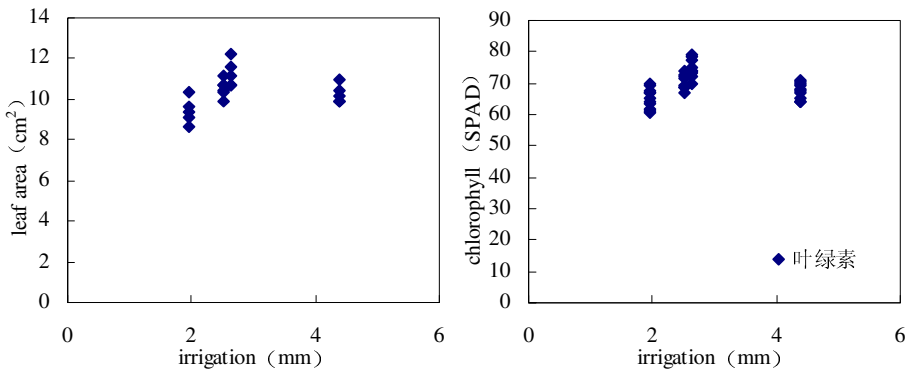
3.3.1 The Relation between Water and Landscape

Leaf color and size of leaf area of green plant were particularly important for appreciation. The paper analyzed the relation between leaf area and water, chlorophyll and water (Fig 2). The result showed that leaf color and leaf area of *E.japonicus* had a high relationship with soil moisture. There was not a linear relation between Chlorophyll content and leaf area. When the soil was too wet or too dry, it was bad for the growth of *E.japonicus*, which affected the landscape function of *E.japonicus*.

Table 3. The effect of ecosystem in different control levels of soil moisture

Time	parameters	treatments			
		CK	LWS	MWS	SWS
2010	Carbon fixation (g·m ⁻² ·d ⁻¹)	5.56±1.06a	5.64±0.27a	5.12±0.84a	4.27±0.49b
	Oxygen release (g·m ⁻² ·d ⁻¹)	4.11±0.77a	4.10±0.2a	3.72±0.61a	3.11±0.36b
	Humidification [mg/(m ² ·s)]	522.79±85.03a	501.77±27.91a	500.11±58.05a	415.08±73.56a
	Cooling (J/(m ² ·d))	1272.55±206.98a	1221.38±67.94a	1217.34±141.38a	1010.36±179.04b
2009	Carbon fixation (g·m ⁻² ·d ⁻¹)	6.51±0.83a	5.99±2.04a	5.89±1.74a	5.52±1.36a
	Oxygen release (g·m ⁻² ·d ⁻¹)	4.74±0.60a	4.36±1.49a	4.28±1.27a	4.02±0.99a
	Humidification [mg/(m ² ·s)]	545.15±121.76a	549.68±150.65a	514.58±123.22a	508.86±36.58a
	Cooling (J/(m ² ·d))	1328.68±296.76a	1339.74±367.19a	1254.19±300.33a	1240.24±89.14a

Data followed by different letters (a,b,c)within same columns at same stage are significantly different at $P_{0.05}$ level;values are Mean±S.E.of each treatment



(a) the relation of water and chlorophyll (b) the relation of water and leaf area

Fig. 2. The relation of water and landscape

3.3.2 The Relation between Water and Ecological

The ecological effects of *E.japonicus* under different water control level of soil moisture were obtained by calculating the amount of carbon fixation and oxygen release, cooling and humidification of *E.japonicus*. As Fig. 3 shown, carbon sequestration and oxygen release, and cooling and humidity were lessening with the soil moisture reducing which express the positive correlation relationship. but the

differences was no significant The results showed that the increasing or decreasing the amount of irrigation didn't produce fundamental influence on ecological service function.

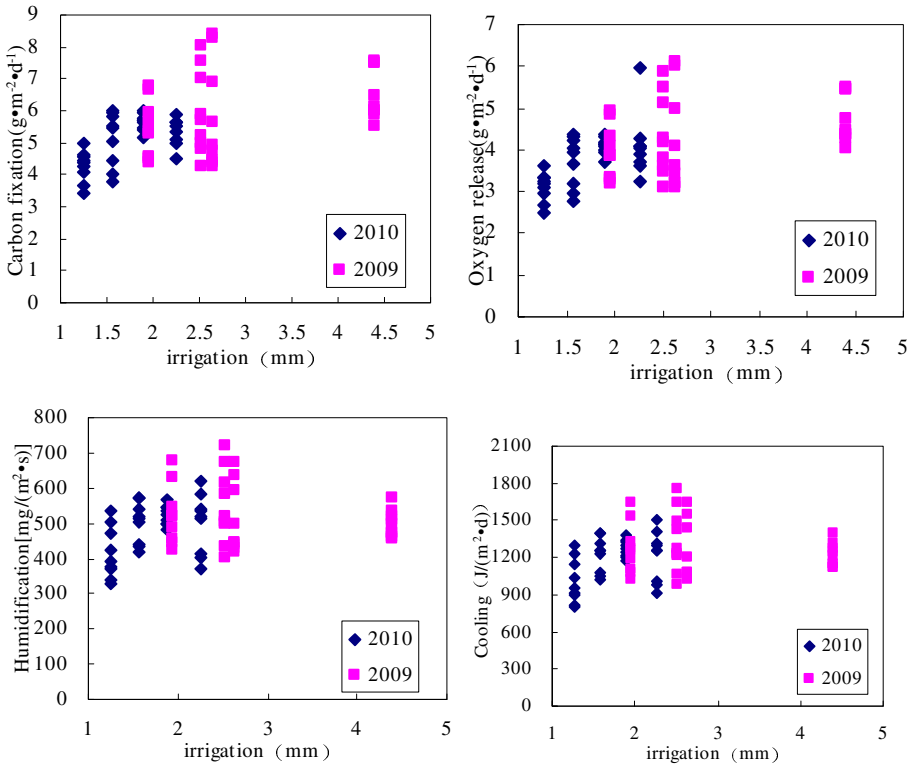


Fig. 3. The relation of water and ecological

4 Discussion

As the regulator of ecosystem, Greenland plays the role of improving the urban environment in the urban landscape, as well as beautifying the urban area (Nowak DJ, 2006). The global implementation of energy saving and CO2 emission reduction gave impetus to the rapid development of urban Greenland. The rapid development of Greenland largely aggravated the shortages of water resources, land resources and energy resources. In this paper we studied the relationships between water and landscape, between water and ecological function under different soil water stress conditions and the reasonable control level of soil moisture, which had great significance for alleviating the serious shortage of water resource and energy resource, constructing low-carbon city, and protecting the ecological environment.

The results showed that the optimal soil moisture was (75%-85%FC) (FC means field capacity). The conclusion could be explained by landscape function and

ecological service function: As for the landscape function, in this study, leaf area, leaf growth and chlorophyll content were used as the measuring standard for landscape functions of *E. japonicus* with leaf area reflecting the size of plant leaves, Leaf blade growth increment reflecting the extent of the growth sparse, and Chlorophyll content reflecting the green degree of leaves. By measuring the leaf area, leaf growth and chlorophyll, we analyzed the landscape features of *E. japonicus* with different control levels of soil moisture. The research showed that leaf growth, leaf area and chlorophyll of *E. japonicus* were inhibited in serious water stress. It also showed that the serious water stress could not meet the need of water for *E. japonicus*'s self-growth and exceeded its self-bearing capacity, causing the "dwarf" phenomenon of leaf growth with the yellow-green color. The growth of *E. japonicus* was better with the soil moisture of (75%-85%FC) than the case under other treatments. The result showed that in order to gain growth *E. japonicus* made necessary adjustment in terms of soil moisture through its own physiological regulation system, which synthesized extremely full nutrients for self-growth. Besides, leaf growth, leaf area and chlorophyll content reached the optimal level, which made the landscape function was sufficiently realized as the typical urban green shrub species. In the ecological aspect, this study used carbon fixation and oxygen releasing, cooling and humidification of *E. japonicus* as the measurement criteria. By analyzing carbon fixation and oxygen releasing, cooling and humidification, the result showed that there were no significant differences in carbon fixation and oxygen releasing, as well as in cooling and humidification with different control levels of soil moisture. The phenomenon showed that *E. japonicus* assigned more nutrients from soil absorbing to the photosynthetic mechanism through self regulation under water stress condition, so that it maintained better ability of absorbing CO₂.

This study also showed that the stomatal conductance was the largest in the morning for different treatments by analyzing the photosynthetic rate, transpiration rate and stomatal conductance of different leaf position. The explanation of the phenomenon was as follows: due to self-regulation of *E. japonicus*, the physiological activity was weaker at night. After a night's "sleep", with supplying its own body with the needed nutrients and it exchanged with outside and the channel of the exchange was stomatal. So the stomatal opened larger. Jiachou Chen and Yongqiang Zhang obtained similar conclusions, who studied peanuts and wheat (CHEN jiazhou, 2005; Zhang YQ, 2001). This study provided further evidence for the fact that the stomatal conductance are abnormally large in the morning. Photosynthetic rate showed a downward trend in the morning, and sustained low at noon, but the decline was slowdown. The explanation of the phenomenon was as follows: The serious water stress caused photosynthetic rate to decrease significantly, which may be caused by non-stomatal factors. Leaf had higher intercellular CO₂ concentration, which caused the disruption of respiratory system, and therefore resulted in the physical activity decreasing, hindering the transportation and distribution of photosynthetic products, and finally showed the photosynthetic rate decreasing. The solar radiation was quite strong at noon, when the leaves captured the excitation energy to exceed carbon assimilation capacity. The extra light energy was dissipated, causing light energy utilization efficiency low and made photosynthetic rate decrease (Muller P, 2001). On the other hand, temperature and photosynthetic rate were positively correlated in a certain temperature range. With the rise of temperature, the photosynthetic rate also rises. The optimal activation temperature of the key

enzyme Rubisco of photosynthetic was 25~30°C, which activity directly affected photosynthesis (Salvucci M E, 1986). When the leaf temperature was over-high, it was detrimental to their photosynthesis. Light and temperature conditions affect the supply of soil moisture, which also plays an important role in controlling leaf gas exchange (Yang C, 1998). This also explains why photosynthesis appeared the rising trend in the afternoon.

As this study was related to the physical aspects of plants and *E.japonicus* was evergreen shrub, we could not have a very in-depth study in a short time and recommended a long-term observation for the typical shrubs species to further understand the landscape function and ecosystem service function of urban greening plants. In the study, there were other limitations. we only chose clear days to measure the landscape function and ecosystem service function, but it is recommended to measure the landscape function and ecosystem service function according to different weather conditions (clear days, cloudy days, rainy days).

5 Conclusion

(1) In the vegetative nutrition growth and physiological control aspect, the LWS (75%-85%FC) caused the water-deficit on the plant root, adjusted photosynthetic products to allocate to different tissues and organs to improve the growth and physiological characteristics of *E. japonicus*. In the process of water use controlling aspect, the LWS (75%-85%FC) induced the protection mechanism of *E.japonicus* leaves, reduced plant water consumption of luxury and improved water use efficiency under the no obvious reduction of photosynthetic rate condition.

(2) In the Landscape function aspect, landscape feature and leaf area, leaf growth, chlorophyll content of *E.japonicus* showed a positive correlation. Larger leaf area, the more lush leaf growth and higher chlorophyll content, green plants performance the better landscape functions. (75%-85%FC) stimulated the growth of *E.japonicus*, adjusted the roots to absorb nutrients from the soil in the regulation of plants. Through measuring and studying leaf area, leaf growth and chlorophyll, based on the consideration of agricultural water-saving and landscape features, (75%-85%FC) was the optimal soil moisture.

(3) In the Ecological benefits aspect, carbon sequestration and oxygen release, and cooling and humidity were lessening with the soil moisture reducing which express the positive correlation relationship. the ecological effect of *E.japonicus* was not obvious under different control levels of soil moisture, different treatments did not show a significant difference. Based on consideration of agricultural water-saving and ecological benefits, we could be considered that the optimal soil moisture content was (75%-85%FC).

Therefore, the research based on comprehensive consideration of agricultural water-saving, landscape features, ecological benefits. Preliminary view was that the LWS (75%-85%FC) was the optimal irrigation pattern of *E.japonicus*.

Acknowledgements. The work is supported by the National science and technology support plan of China(2007BAD88B09-06).

References

- [1] Keeling, C.D., Whorf, T.P., Wahlen, M., van der Plicht, J.: Interannual extremes in the rate of rise of atmospheric carbon dioxide sine. *Nature* 375, 660–670 (1995)
- [2] Li, J.-F., Wai, O.W.H., Li, Y.S., et al.: Effect of green roof on ambient CO₂ concentration. *Building and Environment* 45, 2644–2651 (2010)
- [3] Yang, J., Yu, Q., Gong, P.: Quantifying air pollution removal by green roofs in Chicago. *Atmospheric Environment* 42, 7266–7273 (2008)
- [4] Fujii, S., Cha, H., Kagi, N., Miyamura, H., Kim, Y.S.: Effect on air pollutant removal by plant absorption and adsorption. *Building and Environment* 40, 105–112 (2005)
- [5] Yang, J., McBride, J., Zhou, J.X., Sun, Z.Y.: The urban forest in Beijing and its role in air pollution reduction. *Urban Forest & Urban Greening* 3, 65–78 (2005)
- [6] Jim, C.Y., Chen, W.Y.: Assessing the ecosystem service of air pollutant removal by urban trees in Guangzhou(China). *Journal of Environmental Management* 88, 665–673 (2007)
- [7] Djekoun, A., Planchon, C.: Water status effect on dinitrogen fixation and photosynthesis in soybean. *Agron. J.* 83, 316–322 (1991)
- [8] Heckathorn, S.A., De Lucia, E.H., Zielinski, R.E.: The contribution of drought-related decreases in foliar nitrogen concentration to decreases in photosynthetic capacity during and after drought in prairie grasses. *Plant Physiology* 101, 173–782 (1997)
- [9] Widodo, W., Vu, J.C.V., Boote, K.J., Baker, J.T., Allen, L.H.: Elevated growth CO₂ delays drought saress and accelerates recovery of rice leaf photosynthesis. *Exp. Bot.* 49, 259–272 (2003)
- [10] Subramanian, V.B., Maheswari, M.: Stomatal conductance, photosynthesis and transpiration in green gran during, and after relief of water stress. *Ind. J. Exp. Biol.* 28, 542–544 (1990)
- [11] Zhang, W., Mu, M., Wang., H., et al.: Physiological response of three garden plants to drought stress. In: National Ph.D. Candidates Academic Conference (2009)
- [12] Wang, C., Yang, P., Lu., L., et al.: Study on effect of different water environment on the growth of *Ligustrum vicaryi*. *Beijing Water* (3), 17–20 (2010)
- [13] Zhao, J., Zhou, H., Guo, J., et al.: Change of photosynthetic capacity of alfalfa under different water- stress intensity during branching. *Chinese Journal of Grassland* 29(2), 41–44 (2007)
- [14] Zhang, W., Liu, F., Wang, H., et al.: Study on drought resistance of two plants of urban Greenland: *hemerocallis fulva* and *Zoysia japonica*. *Chinese Agricultural Science Bulletin* 24(8), 327–331 (2008)
- [15] Li, Y.: Effects of water stress on physiological and biochemical characteristics of three ground cover plants. Inner Mongolia Agricultural University (2009)
- [16] Nowak, D.J., Crane, D.E., Stevens, J.C.: Air pollution removal by urban trees and shrubs in the United States. *Urban Forestry & Urban Greening* 4, 115–123 (2006)
- [17] Chen, J., Lv, G., He, Y.: Effects of soil water status on gas exchange of peanut and early rice leaves. *China. Journal. Apply. Ecol.* 16(1), 105–110 (2005)
- [18] Zhang, Y.Q., Jiang, J.: Effect s of leaf water physiological ecology process of winter wheat on soil water stress condition. *Arid Zone Research* 18(1), 57–61 (2001)
- [19] Muller, P., Li, X.P., Niyogit, K.K.: Non-photochemical quenching A response to excess light energy. *Plant Physiology* 125, 1558–1566 (2001)
- [20] Salvucci, M.E., Portis, A.R., Ogren, W.L.: Light and CO₂ response of ribulose-1,5-bisphosphate carboxylase/oxygenase activation in *Arabidopsis* leaves. *Plant Physiology* 80, 655–659 (1986)
- [21] Yang, C., Yang, L.: Plasticity of clonal modules of *Leymus chinensis* in response to different environment. *Chin. J. Appl. Ecol.* 9(3), 265 (1998)

Design and Implementation of Agro-technical Extension Information System Based on Cloud Storage

Leifeng Guo^{1,2}, Wensheng Wang^{1,2}, Yong Yang^{1,2}, and Zhiguo Sun^{1,2}

¹ Agricultural Information Institute of Chinese Academy of Agricultural Sciences,
Beijing 100081, China

² Key Laboratory of Digital Agricultural Early-Warning Technology, Ministry of Agriculture,
P.R. China, Beijing 100081

{guoleifeng, wangwensheng}@caas.cn, wheatblue@163.com,
sunbox.cn@qq.com

Abstract. In order to solve the problems of low efficiency and backward methods in the agro-technical extension activities, this paper designed an agro-technical extension information system based on cloud storage technology. This paper studied the key technologies, such as cloud storage service engine, cloud storage management node and cloud storage data node and designed the overall architecture of the agro-technical extension information system based on cloud storage technology. The application results demonstrate that this system has significantly improved the agro-technical extension service levels and cloud storage can greatly improve data storage capacity of the agricultural extension information system.

Keywords: cloud storage, agro-technical extension, information system.

1 Introduction

Under the condition of much people in little land and the shortage of land resource, the fundamental way to ensure national food security is how to convert the achievements in scientific research into productive forces and the key lies in how to innovative grass-root agro-technical extension. Currently, the main problems in grass-root agro-technical extension system are as follows [1]: First, the means and methods of agricultural extension need innovation urgently, "one mouth with two legs" promotion model is still the mainstream; Second, the management of agro-technical extension needs to be improved, how to evaluate the effectiveness of the extension is also very difficult; Third, technicians need to raise their quality and ability, overall aging, outdated knowledge, single profession are big problems among the technicians, they need to raise their quality and ability immediately.

The agro-technical extension information service system based on modern information technology, providing agro-technical consulting, expert consultation, training services, extension logs, dynamic scheduling and other functions, can effectively solve the problems which farmers encountered during the agriculture production and management activity[1]. However, the amount of user data in the agro-technical extension information system is large with a rapid data growth.

The traditional storage solutions on mass data storage and resources dynamically expanding have certain difficulties.

Cloud storage, which is based on virtualization, distributed, clustering technology, provides consistent access to data storage and business functions through unified management and scheduling over the various types of network storage devices[2]. Generally speaking, cloud storage has the following characteristics [3]: more storage space, better scalability, higher performance, and massive concurrent access.

In order to satisfy the requirements of massive data in the agro-technical extension information system, this paper introduced cloud storage and studied the key technologies of cloud storage, such as cloud storage service engine, cloud storage management node and cloud storage data nodes. Finally, this paper designed and realized agro-technical extension information system based on cloud storage.

2 Previous Work

The studies [4] on agricultural extension informatization were started early in our country, many of them focused on the collection or storage of the agro-technical extension resources. To achieve adequate information sharing, somebody [5] built a unified platform to collect information about agro-technical extension with the help of modern information technology. To provide better services for the agricultural extension workers, somebody [6] built a database about practical agricultural techniques with a large capacity. In 2009, Agricultural Information Institute [7] of CAAS carried out the research on agricultural extension informatization based on 3G technology and established a national information platform for grassroots agricultural extension. The use of cloud computing technology to solve the problems of agricultural extension informatization is still relatively rare.

3 Key Technologies

3.1 Service Engine

Cloud storage service engine [8] is the power unit of cloud storage system, providing the underlying support for the service node. It got the metadata information of data's specific location from the cloud storage management node, then directly read data from the storage node through the data transmission channel. The service engine meets the response speed of data processing and can quickly locate the target data nodes as index is supported by the cloud storage management nodes. Cloud storage service engine is the hub of the entire cloud storage system and needs to configure high-performance hardware.

Cloud storage service engine provides services such as resource management, object storage, database, etc. The support of concurrent access to multiple services is achieved through the expansion of service engine nodes.

3.2 Management Nodes

Cloud storage management node [8] is responsible for the management and monitoring of storage resource in the entire system, including metadata management, storage node failure handling, data redundancy, real-time data migration, etc. To schedule and manage easily, cloud storage management node will regularly collect data information from the data nodes, then reports the data storage location information to the service engine.

Cloud storage management node provides services such as metadata management, domain management, table space management, etc. It is responsible for the resource allocation, resource monitor and the automatic discovery and deployment of domain.

3.3 Data Nodes

Cloud storage data node [4] is the main component of cloud storage system and is responsible for data storage on its own node. Under the scheduling of the management node, data node implements cross-node data redundant and data recovery and provides storage resources to the entire system supporting the business system.

Cloud storage data nodes can startup, initialize and shutdown; supporting various fault alarm; supporting data query, insert, and delete; supporting synchronization of data copies, data recovery; copies statistics of resources and so on.

4 System Design

The entire system consists of the application layer, the interface layer and the storage layer [9]. Application layer is geared to the needs of grass-root agricultural technician by providing logs, video, voice, conferencing and other information services; Interface layer provides the interfaces to access the underlying storage resources, such as containers interfaces, directories interfaces, files interfaces and so on; Storage layer provides virtualized storage resources services to the application layer through cloud storage service engine, cloud storage management node and cloud storage data node.

4.1 Application Layer

(1) Design of Service System

To realize the functions of information exchanges, knowledge sharing and other business services, service system takes the grass-root agricultural technician as the core, focusing on active participation, self-learning, independent innovation. It includes the following subsystems: micro-blog communication subsystem, agro-technical blog subsystem, interest communication subsystem, remote video diagnostic consultation subsystem, on-demand courseware subsystem, agro-technical network library subsystem, diagnose prescription subsystem and so on.

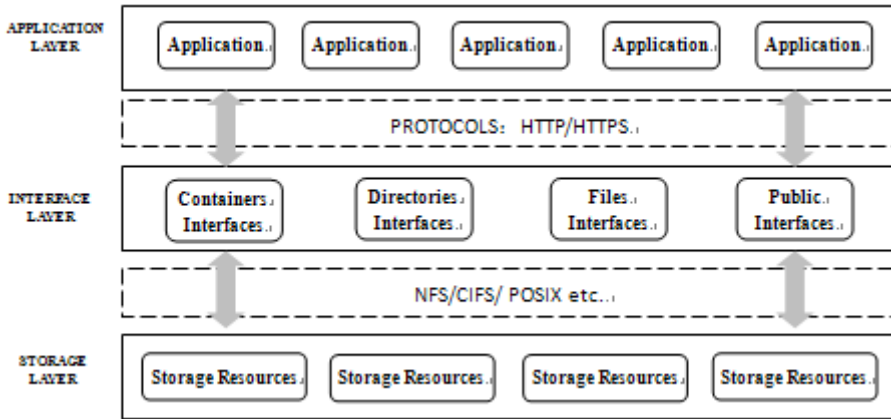


Fig. 1. Architecture of System

(2) Design of Management System

Management system used WEBGIS technologies to position agricultural technician, providing management and performance appraisal to agricultural technician and agricultural experts. It includes the following subsystems: agricultural technician management subsystem, agricultural technician work load statistics subsystem, agricultural expert management subsystem, agricultural technician performance management subsystem and so on.

(3) Design of Information Collection System

Information collection system directionally gathers specific agricultural situation information focused on different times and different regions, such as the coverage of crop, the situation of crop pests and animal diseases, the market supply and demand of agriculture products and materials etc. It includes the following subsystems: macro data acquisition subsystem, agriculture emergencies acquisition subsystem, significant agricultural situation directional collection subsystem, agricultural products marketing information acquisition subsystem, networking terminal acquisition subsystem and so on.

4.2 Interface Layer

Interface layer provides object storage services for the application layer through load balancing and web services, such as REST (Representational State Transfer) access interface. The interface to request resource service is divided into four categories based on the operating resources.

Container: Container consists of container name, container properties, metadata, storage policy and ACL (access control list). Containers are virtual carriers of storage objects in the directory service system and it virtually divides up the entire directory space. Name is the unique identity for a container. Each container can set metadata, ACL and storage strategy.

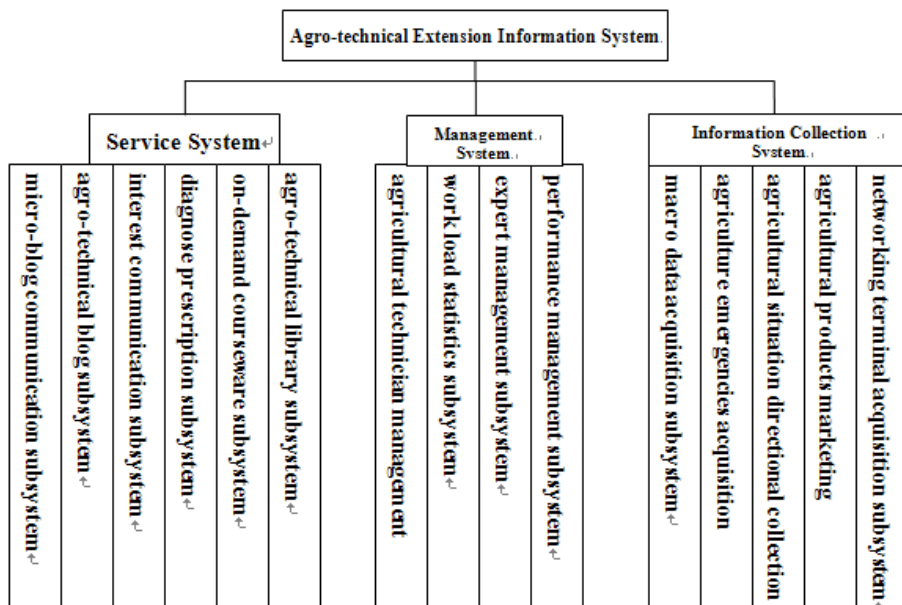


Fig. 2. Structure of Business Functions

Directory: Each directory can be viewed as an object in the container, directory path information is identified by object URI (Universal Resource Identifier) tag. Directory is comprised of attribute, metadata, access control lists.

File: In the container, each file can be viewed as an object and the location information can be identified by the object identifier URI tag. File is also comprised of file attributes, metadata, access control lists and entity data.

Public class: public class interface focused on the common characteristics of containers, directories and files, such as setting of user-defined metadata over file / directory; access of user-defined metadata over files / directory; obtain of the attributes about file / directory; search of file / directory; browse of the recycle bin; restore of the recycle bin; delete / empty of the recycle bin.

4.3 Storage Layer

Storage layer uses two differential pairs to transfer management data and user data, adapted master-slave mode. Cloud storage service engine called management data from cloud storage management node to access and control the data nodes directly; cloud storage management node manages the data nodes through the metadata.

Cloud storage service engine utilizes metadata information of specific data storage location providing by cloud storage management system, then interact directly with the storage nodes through the data transmission channel to read and write data. Cloud

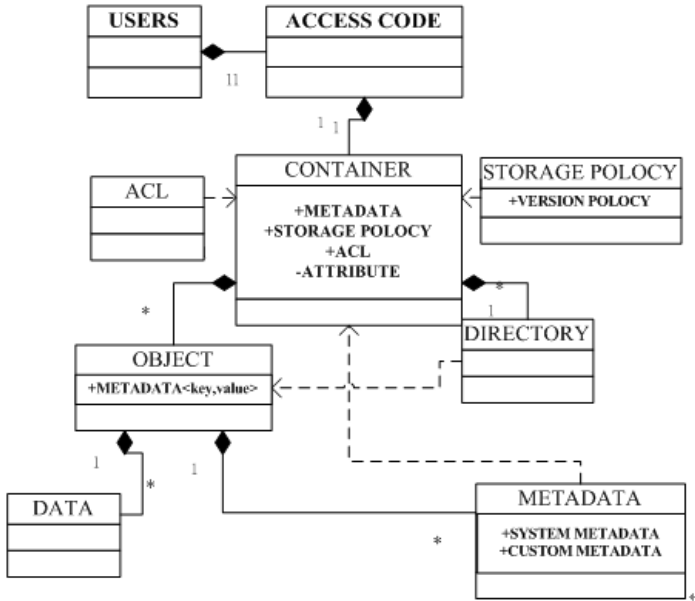


Fig. 3. Model of Interface

storage service engine provides data object access interface, such as containers, directories, files, and so on. It satisfies data storage needs for the videos, images, documents in the application layer.

Cloud storage management system periodically collects status data, resources data from data node. With the help of metadata nodes, it has a unified management to all data nodes, then reports the information, such as the physical location of the node, the available space, to the cloud storage service engine real-time. The support to index in the cloud storage management system can help cloud storage service engine quickly locate the target data nodes and meet the response speed of data processing.

Distributed file system is installed in the data nodes to virtualize physical storage resources to unified logical storage resources. Data nodes provide logical storage resources to the cloud storage service engine and report the corresponding relationship of the physical and logical storage resources to the cloud storage management node. Data is stored on the nodes as objects. After processing with a certain algorithm, data is distributed to many nodes and this increase system reliability and load balancing capabilities. Data nodes also support the expansion of storage nodes and redundancy.

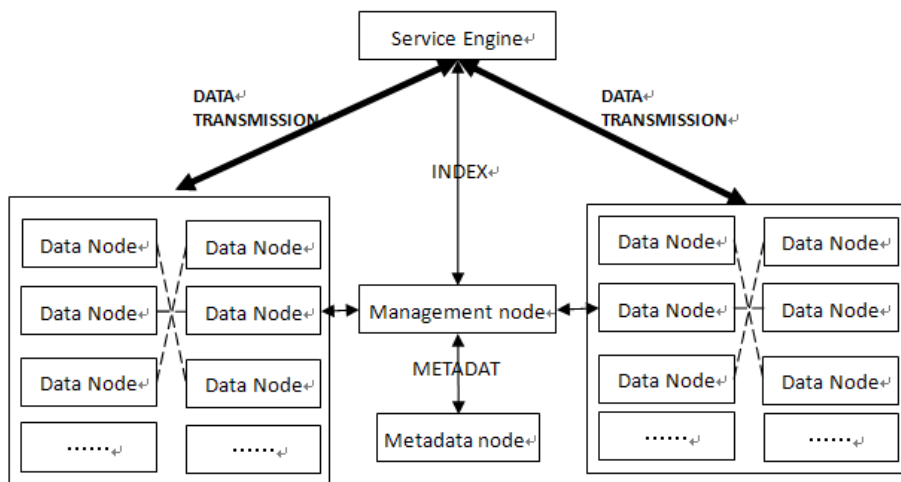


Fig. 4. Architecture of Cloud Storage

5 Implementation

Application layer system employs Struts2 + Spring + Hibernate framework and is divided into the presentation layer, business logic layer, data access layer. It includes functional modules, such as agricultural advice, diagnosis prescription, marketing logs, promotion maps, expert consultation, exchange of experiences, training courseware, agricultural information gathering, disaster submit etc. Cloud storage resources includes four cloud storage service engines, one cloud storage management node, two data nodes, two metadata nodes. With a mechanism of multiple data copies, cloud storage resources provide a total storage capacity of 50T.



Fig. 5. Home Page of Agro-technical Extension System

Agro-technical knowledge module provides agricultural technology about planting, breeding, production and processing etc. It has more than 100,000 data records.



Fig. 6. Module of Agro-technical Knowledge

Agricultural video module provides videos, courseware concerning field crops, livestock, disease prevention, aquaculture, fruit growing, vegetable growing, fish processing and so on, the number of videos in the current system is over 5000.



Fig. 7. Module of Agricultural Video

Currently, focused on the grass-root agricultural technician, the application and demonstration of this system has been carried out in Miyun, Daxing Beijing, Xinghua Jiangsu, Luohe Henan and other places. This system has greatly improved the extension capacity and service level of the agricultural technician and brought a good demonstration effect.

6 Conclusions

Fewer resources and lower efficiency are big problems in the agro-technical extension information system. To meet the requirements of mass data storage, dynamic expansion, resource conservation in the agro-technical extension information system, this paper introduced cloud storage technology to store data. Cloud storage is a scalable, highly reliable storage mode, supporting mass data storage and resource dynamic expansion.

From the adoption of cloud storage technology, the following conclusions can be drawn: 1) Data storage capacity of business systems can be greatly improved; 2) Since multiple copies of data store, data security is guaranteed; 3) The stability of the system is improved as the interface layer is adopted.

Acknowledgment. This paper is supported by National Science and Technology Support Program “Key Technologies for Agricultural Field Information Comprehensive Sensing and Rural extension”(2011BAD21B01).

References

1. Wang, W.: Build information platform with 3G technology and innovative grassroots agro-technical extension system. *World Telecommunications*, 41–44 (2011) (in Chinese)
2. Dan, F.: Network storage key technology of research and progress. *Mobile Communications* 33(11), 35–39 (2009)
3. Liu, S.: Discussion of the Cloud Storage Model Based on the Network. *Bulletin of Science and Technology* 28(10), 206–209 (2012)
4. Luo, C., Sun, S.: Promoting Informationization of Agrotechnical Extending in Beijing Suburb by Using Infomation Technology. *Journal of Library and Information Sciences in Agriculture* 15(1), 5–7 (2004)
5. Yan, Z.: Build Agricultural Extension Information Collection Platform, Promote the Development of Agricultural Extension Information. *China Agricultural Technology Extension* 25(10), 12–13 (2009)
6. Lu, W., Li, X.: Construction of a Database on Agro-technology Consultation for Nationwide Grassroots Agricultural Extension Agricultural Information Platform. *China Science and Technology Achievements* 2, 38–39 (2013)
7. Wang, W.: The Study and Integration of Key Technologies on Agricultural Extension Information based on 3G Technology. *China Science and Technology Achievements* 8, 66 (2011)
8. Guo, L.: Research on prototype system design and application theory of agricultural scientific research cloud (2011)
9. Bian, G., Gao, S., Shao, B.: Security structure of cloud storage based on dispersal. *Journal of Xi’an JiaoTong University* 45(4), 41–45 (2011)
10. Guo, L., Wang, W.: Design of platform for agricultural research and innovation information service based on cloud computing. *Journal of Anhui Agricultural Sciences* 41(7), 3203–3205 (2013)
11. Chen, L., Qi, W., Qi, Y.: Atmospheric monitoring network system based on cloud computing. *Journal of Computer Applications* 32(5), 1415–1417 (2012)
12. Wang, D., Song, Y., Zhu, Y.: Information platform of smart grid based on cloud computing. *Automation of Electric Power Systems* 34(22), 7–12 (2010)
13. Li, A., Pan, Y.: Management and spatial decision support system of farmland environment based on SaaS mode. *Transactions of the CSAE* 24(supp.2), 63–67 (2008)
14. Peng, Y., Wan, J., Wu, N.: A distributed storage and service platform based on cloud computing for exploration in the oil region. *Journal of Computer Research and Development* 48(suppl.), 224–228 (2011)

Analyzing Thermal Infrared Image Characteristics of Maize Seedling Stage

Zilong Chen^{1,2}, Dazhou Zhu², Xiangrong Ren³, Hua Cong³, Cheng Wang²,
and Chunjiang Zhao^{1,2}

¹ College of Information Engineering, Capital Normal University, BeiJing 100048, China

² Beijing Research Center of Intelligent Equipment for Agriculture, BeiJing 100097, China

³ Synthetic Proving Ground of Xinjiang Academy of Agricultural Science, Urumqi 830000, China

{504304574, 99869388}@qq.com,

{zhudz,wangc,zhaocj}@nercita.org.cn, conghua@xaas.ac.cn

Abstract. The temperature of crop leaf is closely related to leaf respiration, transpiration and its drought resistance. The rapid measurement of crop temperature is of great significance for breeding and agricultural cultivation management. The traditional infrared thermometer can only obtain the single point temperature. In this study, a high sensitive thermal infrared imager was used for recording the leaf temperature distribution of maize seedling stage. The temperature distribution of 5 different drought resistance varieties of maize in both normal water and drought stress treatment were analyzed. It turned out that there were obvious differences in temperature for different leaf position. The average temperature in the middle part of the leaf is 0.94°C higher than the leaf apex and 0.81°C higher than the leaf base. The results also showed that the leaf temperature is higher than that of the stem. And the average temperature of the whole blade is 24.07°C, which is higher than the background soil temperature (19.53°C). For the same maize variety, the leaf temperature of drought stress treatment is higher than that of normal water treatment. It was also found that the temperature of maize with good drought resistance is higher than that of the bad one, furthermore, the better the higher. The results above showed that the characteristics of temperature distribution in crops could be effectively obtained by using thermal infrared images, which also provided potential for the rapid identification of crop drought resistance.

Keywords: thermal infrared imaging, temperature, corn, drought resistance, image processing.

1 Introduction

Global warming has given rise to increasingly pressing drought. In China, the arid and semi-arid regions account for 52.5% of the land area, seriously affecting the development of agriculture [1]. From 1950 to 2007, the drought-led average annual losses of grains in China reached 15.8 billion kg, making up for over 60% of all natural disasters [2]. The growth of maize is threatened by the severe drought. For transpiration, leaf blades of plants control the inflow and effusion of moisture by controlling the size

of stomata. Changes in transpiration intensity determine the heat loss degree on the blade surface, thus leading to the changes of blade temperature [3]. Under normal circumstances, the blade temperature of plants maintains a relatively stable state through dehydration from transpiration. Under external stress like drought, the variation of blade temperature can be used to detect the stress conditions of plants [4].

The traditional temperature measurements are mainly carried out by the infrared thermometer. But this approach can only realize spot measurement rather than the assay on temperature distribution of a specific area. The increasingly sensitive infrared imaging system provides feasibility for the studies on blade stomata changes through the observation of surface temperature variation of blades [5]. The principle of the thermal infrared imaging technology is as follows: different absorption and reflection of various substances exposed under rays with different wavelengths can be reflected on temperature variation. This property can be used in the detection of temperature variation of maize blade. Compared with conventional ways, it presented advantages of speedy, efficient and convenient operation. Stomatal conductance from the thermal imaging measurement update showed satisfying correlation with that from conventional porometer [6]. By changing the intensity of the irrigation, times of crop temperature variation can be counted. The infrared thermal imaging can be used to assay the stomatal conductance of crops [7].

In China, scholars like Liu found that when under the threats of drought, temperature variation of blades can effectively reflect the drought resistance of maize in the seedling stage. The blade temperature difference can be used as the preliminary indicator of the screening of drought resistance [8-9]; canopy temperature showed great correlation with leaf water potential of rice, setting percentage and biomass. Higher temperature leads to smaller indicator. Jones conducted remote sensing study on the infrared thermal imaging of crop canopy, so as to quantitatively analyze the reactions of crops on water stress [10]. Sirault applied infrared thermal imaging to quantitatively analyze the permeability of wheat and barley under the salt stress [11]. Qiu introduced a reference dry blade (without transpiration), and applied the plant transpiration conversion coefficient to assay the environmental stress around watermelon, tomato and lettuce and other plants, including conditions of hydropenia and high temperature [12]. Takai discovered that the canopy temperature difference between sunny days and cloudy days can be used to estimate the subtle changes in stomatal conductance of rice [13].

Studies at home and abroad achieved fruitful findings in the research of crop temperature. The contrastive analysis in the above studies was conducted based on leaf temperature and the conventional drought resistance parameters. In this study, blade temperature distribution characteristics of maize canopy were analyzed based on thermal infrared image to study on the temperature distribution characteristics at different leaf positions of different blades. In addition, different drought-resistant maize species were processed with water treatment to analyze the temperature variation of plants after the treatment of drought stress and to explore into the relationship between thermal infrared image characteristics of seedling stage and maize drought resistance.

2 Experiments and Methods

2.1 Experimental Material

Five maize species suitable for cultivation in the north were selected, namely, Kuancheng 60(KC 60), Jingdan 68(JD 68), Jingke 528(JK 528), Dantiannuo No.3(DTN 3) and Yinnuo No.1(YN 1). With the query of species description from breeding units and breeding experts, the features of species were shown in Table 1.

Table 1. Information of different maize species

Species	Drought resistance	Breeding Places
KC 60	Good	Kuancheng Seed Co., Ltd, Hebei Province
JD 68	Good	Maize Research Center, Beijing Academy of Agriculture and Forestry Sciences
JK 528	Good	Maize Research Center, Beijing Academy of Agriculture and Forestry Sciences
DTN 3	Poor	Horticulture Institute, Dandong Academy of Agricultural Sciences
YN 1	Poor	Key Laboratory of Beijing Municipal Agricultural Application Technologies

2.2 Experimental Design and Plantation Management

The experiment was conducted in the solar greenhouse of Beijing Academy of Agriculture and Forestry. Flower pots with the aperture diameter of 25cm and depth of 15cm were selected, which were filled with 5kg of soils from fields. Quality corn seeds were selected and sowed in one cavity per pot with two seeds in one cavity. Each species was sowed for 10 pots so it was 50 pots. 2.0g of compound fertilizer carbonate diamine was applied. To the seedling stage, the final singling of seedlings with consistent growth length was made as 1 plant per pot. After sowing, timely ventilation, illumination, watering and fertilization were conducted according to the greenhouse maize management.

A control group was set in the experiment. In the early seedling stage (15 days after sowing, with the twin leaves), drought stress was conducted. 5 pots of each species of maize seedlings stopped watering, taken as the experiment group. The other 5 pots were watered regularly as the control group.

2.3 Infrared Image Acquisition

The experimental image acquisition device uses a high-resolution portable infrared thermal imaging instrument (VarioCam). The detector type: UFPA; Spectral range: 7.5 to 14 μ m; thermal sensitivity: at 30 $^{\circ}$ C, the thermal sensitivity < 0.065 $^{\circ}$ C; Frame frequency: 50/60Hz; infrared image: 384x288 pixels.

20d after sowing, we started the image acquisition. Acquisition time: 8:00am and 14:30pm in sunny days were selected until maize plants died under drought stress. When photographing, the thermal infrared imager was placed on the top of maize plants, keeping the lens perpendicular to the ground (about 0.5 to 0.8m from the top). The focal length and camera lens position was adjusted so that the canopy image can be clear and recognized. Thermal infrared images of all plants were taken, coded and preserved.

In the experiment, 5 infrared images were collected on October 17, 19, 23, 25 and 31, 2012. The weather during the experiment was sunny with the temperature varying from 28 to 33°C.

2.4 Infrared Image Processing

The original image acquired by the infrared camera was .IRB file, and different colors in the image represented different pixel values. Pixels of different colors show different temperature values. At 8: 00 a.m., as the plant leaves went through no illumination at low temperatures overnight, the plant temperature was almost consistent, no showing distinct differences. Hence, the infrared image taken in the afternoon was selected for analysis.

The IRBIS image processing software was used. First, the target image was opened on IRBIS 3. Color distribution of the image was adjusted through the scale calibration plate, so that the maize in the image was obviously separated from objects in the background to facilitate the processing. According to different shapes of blades, oval, round, or self-crossed circle was selected under the measurement label to circle the specific area of the leaves or stems. The maximum, minimum and average temperature in the circled region was read so as to obtain the temperature information of different blades at different leaf positions. The extracted temperature information was then recorded in the table.

3 Results and Discussion

3.1 Temperature Distribution Characteristics of Maize at the Seedling Stage

Seedling stage of maize refers to the stage from germinating to elongation. The seedling stage of maize is a crucial stage for the differentiation and growth of roots, stems, leaves and other vegetative organs and the differentiation of tassels. In this stage, less moisture was needed. Yet, water stress would lead to poor seedling development, influencing the later nutrition absorption and reproductive growth, and eventually reducing the production [14]. Thus, it can be seen that some characters of the maize at the seedling stage were closely related with the drought resistance of maize. In this study, the temperature distribution characteristics of maize canopy were studied and the relationship between thermal infrared image characteristics at the seedling stage and drought resistance of maize was discussed.

Infrared images acquired at 2:30 p.m. on October 31, 2012 were selected. Fig. 1 shows the thermal infrared image of a maize plant at the seedling stage. Three blades of the leaf canopy were analyzed with the measurement function of the software. In this study, we measured the temperature of leaf apex, leaf center and leaf base, with the data unit of °C and the precision of 0.01°C. The right side of the figure shows the scale plate. Different colors show the corresponding temperature range. Before each measurement, the scale plate was adjusted so that the blade color can be easily distinguished compared with the color of background objects so that the measurement region can be found precisely.

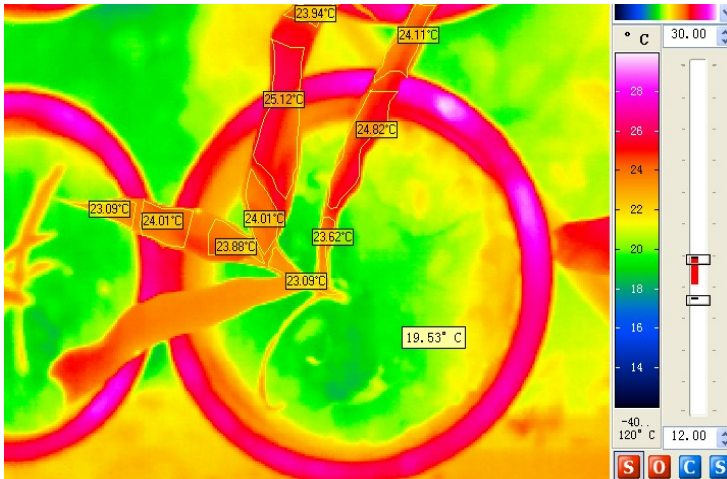


Fig. 1. Infrared Image Processing of Maize at the Seedling Stage

As shown in Fig. 1, the average temperature of three blades at different leaf positions was recorded in Table 1. It should be noted while circling that the circled area should be smaller than leaves so as to ensure that the circled areas were a part of the leaves. The average blade temperature was measured. Each small area was formed by several pixels. The size of circled area will influence the second digit of the temperature while the accuracy has met the requirements.

Table 2. Average Temperature of Different Blades at Different Blade Positions

Average Temp. (°C)	leaf apex	leaf center	leaf base
Blade 1	23.09	24.01	23.88
Blade 2	23.94	25.12	24.01
Blade 3	24.11	24.82	23.62
Average Temp.	23.71	24.65	23.84
Soil Temp.		19.53	
Stalk Temp.		23.09	

As can be seen from Table 2, for the temperature of each maize leaf, leaf center > leaf base > leaf apex. The average temperature of leaf center was higher than that of leaf apex by 0.94°C, while that of leaf center was higher than that of leaf base by 0.81°C. The plant temperature was much higher than soils in the pot (19.53°C). The stem temperature (23.09°C) was lower than leaves.

Transpiration and respiration affect the airflow and water flow in the leaves of plants. For moisture, with temperature variation, plants will carry out according self-regulation to offset the impact from water stress, and to adapt to the environment change so as to maintain the development and growth. The changes were reflected on the temperature variation of plant leaves. In this experiment, it was found that the temperature at different leaf positions in the maize canopy at the seedling stage showed the following regularities: leaf apex < leaf base < leaf center (as shown in Table 2). In the normal growth, the leaf shape of maize was arched, and the middle of the leaf was facing the sun, receiving most of the sun irradiation and high temperature; two ends of leaves received less sun irradiation and temperature. With the control over the open and closure of stomata, plants can control the moisture diffusion, thus enlarging the biomass of plants. The mechanism stems from the plant adaptation to drought, which is conducive to maintaining the normal growth and metabolism of plants.

3.2 The Maize Temperature Difference between the Watering Group and the Drought Stress Group

Infrared images acquired at 2:30 p.m. on October 31, 2012 were selected, when the leaves under the drought stress showed wilting. In image processing, the self-crossed way was used to circle the canopy leaves of various species in two groups. The average temperature of leaves was recorded in the following table.

Table 3. Average temperature in the watering group and the drought group

Species	Group	1	2	3	4	5	Avera
KC 60	the watering	24.25	25.81	25.56	25.69	25.15	25.292
	the drought	25.94	26.38	26.40	26.80	26.22	26.348
JD 68	the watering	25.58	25.20	25.47	24.17	25.45	25.174
	the drought	26.64	26.67	25.77	25.92	26.25	26.25
JK 528	the watering	25.19	25.34	24.96	24.82	24.68	24.998
	the drought	26.51	25.47	25.41	25.34	25.08	25.562
DTN 3	the watering	25.52	25.28	24.82	25.28	24.72	25.124
	the drought	25.80	25.34	25.35	25.03	25.13	25.33
YN 1	the watering	24.84	24.89	24.73	24.96	24.10	24.704
	the drought	24.58	25.62	24.32	24.65	24.17	24.668

To better demonstrate the temperature differences, the table was showed in the following curve graph:

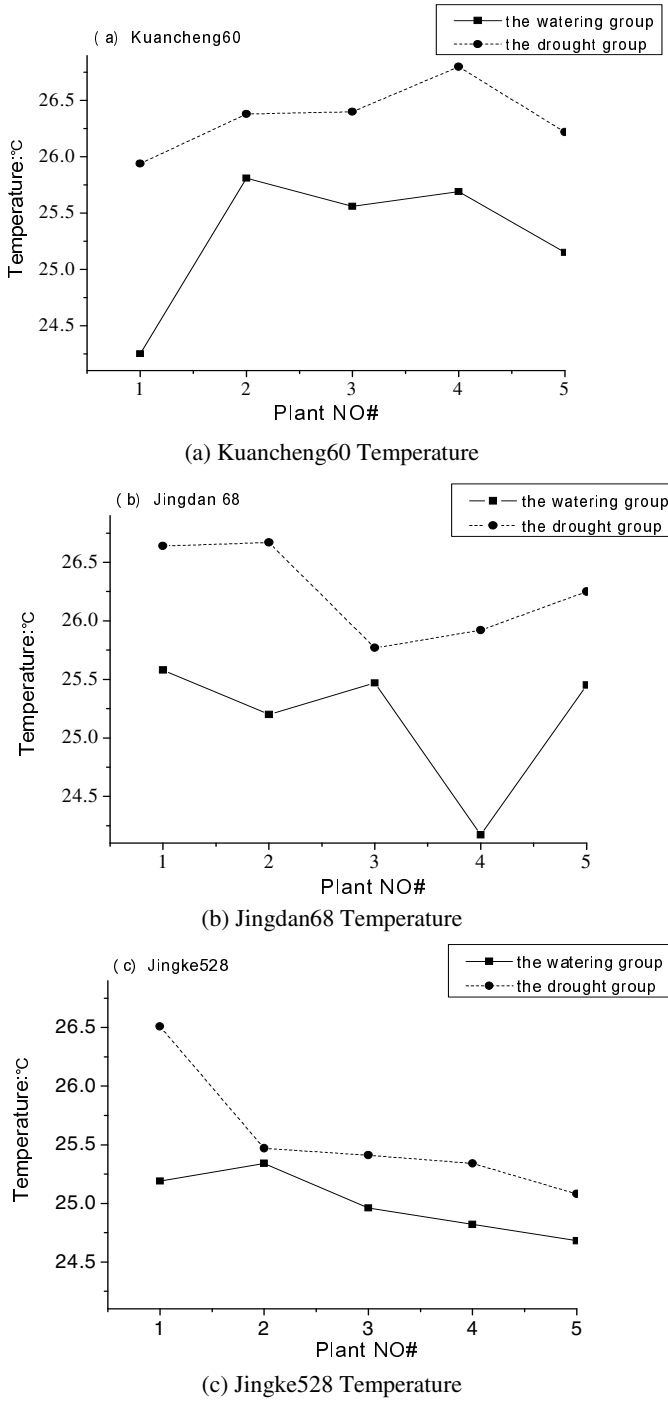
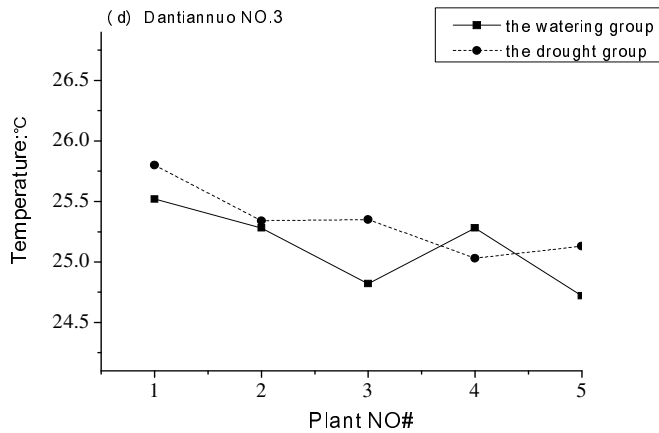
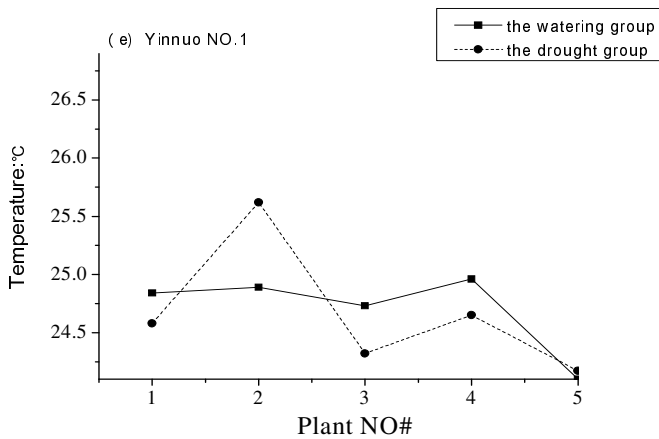


Fig. 2. Temperature Comparison between the Watering Group and the Drought Group



(d) Dantiannuo NO.3 Temperature



(e) Yinnuo NO.1 Temperature

Fig. 2. (Continued.)

It can be seen from the above figures that at the seedling stage of the five maize varieties, the average temperature of canopy leaf under drought stress (25.63°C) was higher than that in the watering group (25.06°C).

Under drought stress, the composition and structure of the plant plasma membrane has undergone significant changes. The cell membrane permeability was damaged so that cells cannot be divided and grow. In addition, stomata on the surface were closed, which influenced photosynthesis, the normal growth and development of plants and eventually lower yields [15].

In the experiment, two groups of water treatment were set for the simulation of the arid geographical environment in the north of China. 10 pots of each species were planted. Five pots were not watered under drought stress and the rest were watered. After that, infrared images were acquired, coded and preserved. The images were processed and the average temperature of canopy leaf was extracted. As shown in Fig. 2 that for different maize species at the seedling stage, the blade temperature in the drought group was higher than that of the watering group. Under drought stress, plants will resist drought stress within a certain range through a series of measures, mainly including stomatal regulation, osmotic adjustment, reactive oxygen removal, the protective effect of specific molecules and plant hormones regulation etc. 15. The direct reaction of plants to drought signal is to adjust the size of the stomatal aperture so as to prevent water loss. Under regular watering, maize stomata will be at the on-state and the water loss maintains the status quo. Under the drought stress, the water loss was much less compared with that with regular watering. Meanwhile, water loss will reduce the heat of leaves and lower the temperature. That is, the thermal loss under the drought stress was less than that under the watering. Hence, the blade temperature under the drought stress was lower than that in the watering group.

3.3 Temperature Difference between Drought-Resistant Plants and Non-drought Resisting Plants under the Normal Condition of Watering

Infrared images acquired at 2:30 p.m. on October 31, 2012 were selected, and temperature of plants in the watering group was extracted as the following table 4.

Table 4. Average temperature of canopy leaf of different varieties at seedling stage in the watering group

Species\Temp.	1	2	3	4	5	Aver Temp.
KC 60	26.33	27.49	27.60	27.62	27.76	27.36
JD 68	26.73	27.25	27.12	27.40	27.30	27.16
JK 528	27.02	26.88	26.57	26.98	27.06	26.902
DTN 3	26.86	26.24	26.37	26.63	26.30	26.48
YN 1	26.50	26.35	26.32	26.42	25.64	26.246

To better demonstrate the temperature differences, the table was showed in Fig.3.

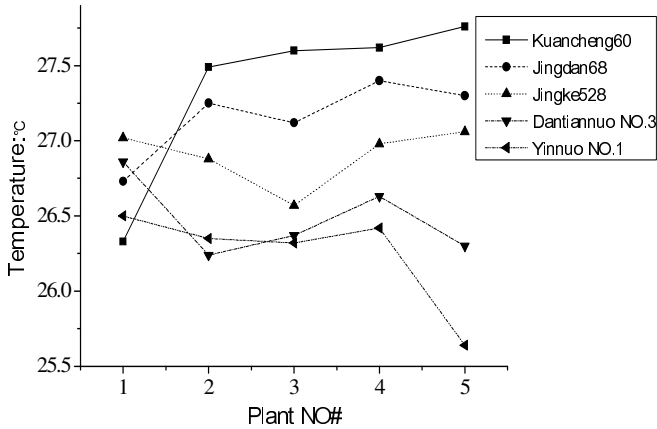


Fig. 3. The graph of the temperature in the watering group

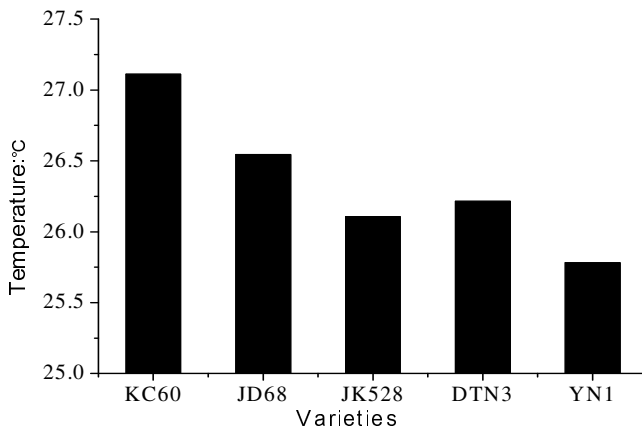


Fig. 4. Bar graph of average temperature in the watering group

From the above chart, in the watering group, plants with good drought resistance had higher blade temperature than those with poor drought resistance. The better the drought resistance, the higher the temperature of blades will be given the normal conditions.

3.4 Temperature Difference between Drought-Resistant Plants and Non-drought Resisting Plants under the Drought Stress

Infrared images acquired at 2:30 p.m. on October 31, 2012 were selected, and temperature of plants in the drought group was extracted as the following table 5.

Table 5. Average temperature of canopy leaf of different species at seedling stage in the drought group

Species \ Temp.	1	2	3	4	5	Aver Temp.
KC 60	27.51	27.69	27.01	27.04	26.31	27.112
JD 68	27.68	26.60	26.19	26.29	25.97	26.546
JK 528	27.09	26.24	25.91	25.90	25.39	26.106
DTN 3	26.70	26.36	26.21	26.22	25.59	26.216
YN 1	25.91	25.88	25.95	25.47	25.70	25.782

To better demonstrate the temperature differences, the table was showed in Fig.6.

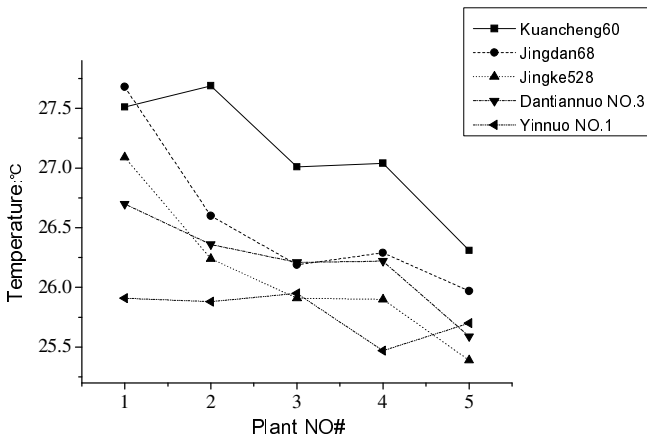


Fig. 5. The graph of the temperature in the drought group

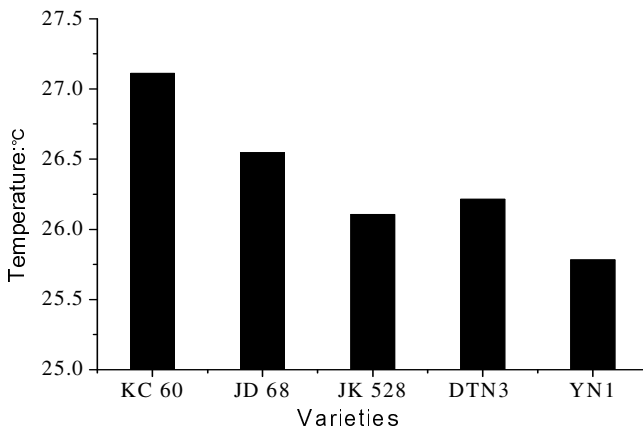


Fig. 6. Bar graph of average temperature in the drought group

From the above chart, in the drought group, plants with good drought resistance had higher blade temperature than those with poor drought resistance. The better the drought resistance, the higher the temperature of blades will be given the normal conditions.

Drought is the main limiting factor in maize growth. Different maize species present different reactions under water stress [16-20]. In this experiment, five maize species suitable for cultivation in the north were selected, and infrared images of plants of different species at the seedling stage were acquired. As can be seen from Figure 4, in the watering group, plants with good drought resistance had higher blade temperature than those with poor drought resistance, that is, Kuancheng 60 > Jingdan 68 > Jingke 528 > Dantiannuo No.3 > Yinnuo No.1, which formed a positive correlation with the drought resistance; as seen from Figure 6, the positive correlation with the drought resistance was also formed under drought stress. Thus, given different water treatment, temperature of canopy blade of plants with good drought resistance was higher than that with poor drought resistance. The above analysis presented that temperature of canopy blade of plants at the seedling stage can reflect the drought resistance of plants, which was demonstrated in the different controlling capacities of plants with different drought resistance over the stomatal conductance. Plants with good drought resistance have stronger control over transpiration through stomata opening and closing. As less moisture was taken away by transpiration, the temperature was eventually elevated.

4 Conclusions

Thermal infrared images of temperature distribution of maize at the seedling stage shows distinct features. Temperature distribution characteristics of different leaf positions reflect the growth of plants, and can provide significant guidance for secondary prevention and control of diseases and pests and timely spraying fertilizer. Temperature characteristics of species with different drought resistance can be used as the preliminary identification of the drought resistance of maize at the seedling stage. Average temperature of canopy leaves can be used as a reference indicator to identify the drought resistance of maize. It is a new approach to apply thermal infrared imaging technology in the research of maize and to use digital image processing technology with the temperature as the parameter to show the maize features at the seedling stage in the breeding, screening and growth detection of plants with drought resistance.

To sum up, it is feasible to use thermal infrared imager to acquire maize image at the seedling stage and analyze distribution characteristics of blade temperature to predict the drought resistance of plants. Compared with conventional ways of detecting the plant drought resistance, this approach is fast, efficient and convenient.

This approach can analyze and evaluate the drought resistance of different maize species, thus providing a fast judgment and filtering maize species with properties of water-saving, high yield and high drought resistance. This is of great importance and meanings to alleviate the drought in the current Northern China and improve the current food and water shortage in China.

Acknowledgment. This research was financially supported by Natural Science Foundation of China (31201125) and Beijing Nova Program (Z111105054511051).

References

1. Yang, G., Luo, X.: Effects on Traits of Corn Hybrids under Drought at the Different Growing Stages. *Journal of maize Science* 12, 23–26 (2004)
2. Li, Y., Wang, C., et al.: The engineering technique for agricultural drought and their application. *Engineering Sciences* 13(9), 85–88 (2012)
3. Lourtie, E., Bonnet, M., et al.: New glyphosate screening technique by infrared thermometry [*]. In: Fourth International Symposium on Adjuvants for Agrochemicals, Australia, pp. 297–302 (1995)
4. Laury, C., Dominique, V.D.S.: Imaging techniques in early detection of plants stress. *Trends in Plant Science* 5(11), 495–501 (2000)
5. Leinonen, I., Jones, H.G.: Combining thermal and visible imagery for estimating canopy temperature and identifying plant stress. *Journal of Experimental Botany* 55(401), 1423–1431 (2004)
6. Jones, H.G.: The use of thermography for quantitative studies of spatial and temporal variation of stomatal conductance over leaf surfaces. *Plant Cell Environment* 22, 1043–1055 (1999)
7. Bajons, P., Klinger, G., et al.: Determination of stomatal conductance by means of infrared thermography. *Infrared Physics & Technology*, 429–439 (2005)
8. Liu, Y., Ding, J., Subhash, C., et al.: Identification of Maize Drought-Tolerance at Seedling Stage Based on Leaf Temperature Using Infrared Thermography. *Scientia Agricultura Sinica* 42(6), 2192–2201 (2009)
9. Zhang, X., Chen, W., et al.: Canopy-air Temperature Difference of Rice in Key Water Requirement Periods. *Journal of Irrigation and Drainage* 30(4), 80–82 (2011)
10. Jones, H.G., Rachid, S., Loveys, R.B., et al.: Thermal infrared imaging of crop canopies for the remote diagnosis and quantification of plant responses to water stress in the field. *Functional Plant Biology* 36, 987–989 (2009)
11. Sirault, X.R.R., James, R.A., et al.: A new screening method for osmotic component of salinity tolerance in cereals using infrared thermography. *Functional Plant Biology* 36, 970–977 (2009)
12. Qiu, G., Kenji, O., et al.: An infrared-based coefficient to screen plant environmental stress: concept, test and applications. *Functional Plant Biology* 36, 990–997 (2009)
13. Toshiyuki, Yano, M., et al.: Canopy temperature on clear and cloudy days can be used to estimate varietal differences in stomatal conductance in rice [J]. *Field Crops Research*, 2009.
14. Li, Z., Xu, W., et al.: Discuss on Evaluating Method to Drought-resistance of Maize in Seedling Stage. *Journal of Maize Science* 12(2), 73–75 (2004)
15. Huang, S.: Harm by drought and mechanism of drought resistance of plant. *Journal of Anhui Agriculture Science* 37(22), 10370–10372 (2009)
16. Bi, S., Yongde, Z., et al.: Drought Resistance of Different Maize Varieties in Germination Stage. *Guizhou Agricultural Sciences* (2005)
17. Wang, B., Cui, R., et al.: Identification of peanut drought-tolerance at seedling stage using infrared thermography. *Chinese Journal of Oil Crop Sciences* 33(6), 632–636 (2011)
18. Liu, Y.: Application of Infrared Thermography in the Research of Plant Mechanism Response to Drought. *Chinese Agriculture Science Bulletin* 28(3), 17–22 (2012)
19. Zhao, T., Guo, B., et al.: The Study of Stomatal Conductance Estimation of *Populus deltoids* Bartr.x *Populus ussuriensis* Kom. By Infrared Thermography. *Chinese Agriculture Science Bulletin* 28(31), 65–70 (2012)
20. Wang, X., Chen, S., et al.: Application of Near Infrared Reflectance Spectroscopy in Determination of Drought Resistance of Winter Wheat. *Journal of Hebei Agriculture Science* (2011)

Modeling Design and Application of Low-Temperature Plasma Treatment Test Stand for Seeds before Sowing

Changyong Shao^{1,2}, Yong You¹, Guanghui Wang¹, Zhiqin Wang¹, Yan Li²,
Lijing Zhao², Xin Tang³, Liangdong Liu¹, and Decheng Wang^{1,4,*}

¹ College of Engineering, China Agricultural University, Beijing 10083, P.R. China

² Shandong Province Seeds Group, Jinan 250100, P.R. China

³ Shandong Agricultural and Engineering College, Jinan 250100, P.R. China

⁴ Key Lab of Soil-Machine-Plant System of Chinese Agriculture Ministry, Beijing 10083, P.R. China

{wdc, shaochangyong}@cau.edu.cn

Abstract. Stimulation with a low-temperature plasma (LTP) can improve the seed germination and seed adaptability to the environment. This technology has been applied in practice, but the study level of mechanism involved is still limited. Moreover, the treatment devices in using are quite simple. The paper focuses on the modeling design and application of the LTP treatment test stand for seeds before sowing. Numerous experimental LTP treatment on crop seeds and forage grass seeds will be conducted to find out the optimal dose used in the treatment. Another advanced method of this modeling is data collecting and intelligent monitoring system designed in, therefore all key process parameters can be under control during treatment period. At the same time, the modeling design will provide technical support for large-scale manufacturing of seed treatment devices.

Keywords: digital intelligence, Low-temperature Plasma(LTP), seeds treatment before sowing, development trend.

Studies show that the application of high quality, specially prepared seed is an important, yet still underestimated, yield-forming factor in the cultivation of many species of agricultural plants. Chemical methods are frequently applied in the treatment of seeds prior to sowing, but these methods are recognised as harmful to the environment because they are not selective in respect of nature lives although the agro-chemicals introduced are often very efficient. Nowadays, more and more physical methods (such as low-temperature plasma (LTP), magnetic technology, bio-frequency spectrum irradiation, solar power) have attributed to the pre-sowing treatment of seeds [1,2,3,4,5] which are commonly regarded as being friendlier to the environment.

* Corresponding author.

1 Introduction

The main objectives of this article are to prove the effect of low-temperature plasma treatment on seed germination and seedling, including vigor and rate of germination, root system, resistance to disease and drought, plant quality, maturity and yield; to design a modeling of low-temperature plasma treatment test stand for crop seeds and forage seeds. A scientific parameters of the technology system will be established for this stand, which will play an important role in the analysis and selection of treatment dose for different crop seeds, data collecting and intelligent monitoring system is the other major part of the test stand making all key parameters under supervision and control. Such kind of treatment devices can be produced in a large scale once the LTP test stand in the article is established and proved reliable.

Physical agriculture technology is the application of physical methods in agriculture and has been studied since the 1970s, many researchers wrote articles about this. Mr. Yin reported that low temperature plasma technology was utilized in biological applications in Russia, but there had been little research into the mechanisms involved [6]. According to Zhang, plasma seed treatment represented a new technology which could activate endogenous substances in the seeds, leading to improvements in the rate of seed germination, crop resistance, crop yield and an earlier maturity date [7]. According to Ms. Xu and Mr. Chen, plasma processing could be applied to the principle of space breeding and seed treatment with plasma energy and alternating inductance would stimulate the seeds potential and improve their vigor and strength [8]. Mr. Liu hypothesized that this technology narrowed the differences between individual seeds [9]. Mr. Li believed that plasma energy could separate oxygen molecules in the air and form ozone. Bacteria attached to the surface of seeds would be disinfected under the action of both plasma and ozone [10]. Laboratory tests have confirmed that for low plasma energy and a limited treatment time, no variations occur in the treated seeds and no character changes are observed during the plant growth period of the treated seeds [11].

As the mechanism of low-temperature plasma effect on seeds is not very clear, and the LTP processing device is quite simple now (Figure 1), it becomes impossible to use this technology and devices in a large scale. However, this question also make low-temperature plasma treatment before seed sowing become into a very attractive project to explore, a large number of lab tests have been done in lab and small open field by the authors, all results prove that plants show better characteristics in terms of germination, root system, resistance to drought and diseases, early maturity and yield after their seeds well treated by a suitable dose of low-temperature plasma (LTP).

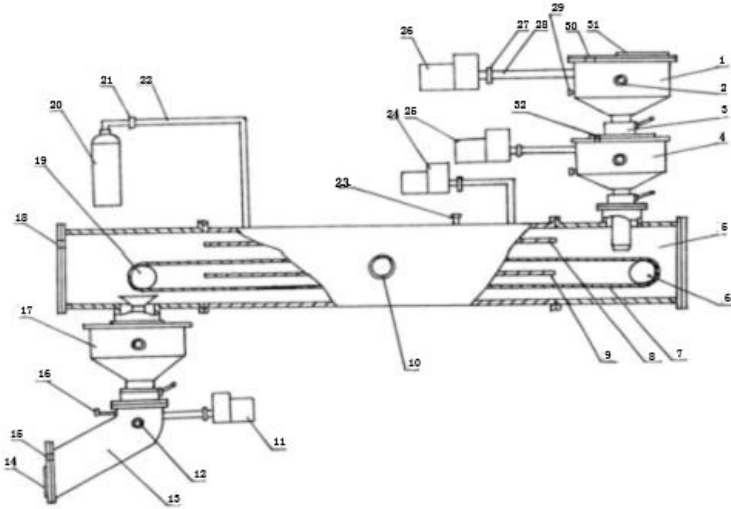


Fig. 1. Diagram of low-temperature plasma test stand device

1, Feeder compartment I; 2, Detector tube I; 3, Butterfly gate; 4, Feeder compartment II; 5, Feeder compartment III; 6, Driven wheel; 7, Transmission belt; 8, Top crown; 9, Bottom crown; 10, Detector tubeII; 11, Vacuum air pump I; 12, Detector tube III; 13, Feeder compartment IV; 14, Discharge port; 15, Thermocouple gauge tube I; 16, Deflating valve I; 17, Feeder compartment V; 18, Thermocouple gauge tube II; 19, Driver wheel; 20, Gas tank; 21, Gate; 22, Inlet pipe; 23, Deflating valve II; 24, Vacuum air pump II; 25, Vacuum air pump III; 26, Vacuum air pump IV; 27, Electromagnetic relief valve; 28, Vacuum tube; 29, Deflating valve III; 30, Thermocouple gauge tube III; 31, Feed cap; 32, Thermocouple gauge tube IV.

2 Key Points Focused in the Article

Shao Changyong (2012) pointed out that digital intelligent would be the development trend of the plasma seed processing device. To meet with this trend, the article focuses on two parts as following:

Firstly, the effects of different dose of LTP treatment on different crop seeds should be studied to find out the most appropriate dose applied in treatment. Secondly, increase stability of the LTP platform and carry out that data acquirement and signal analysis with computer, perfect the LTP system, achieve safety and reliable operation.

3 Contents and Objectives Decomposed

3.1 Contents of the Research

(1) General design. To study and summarize all scientific reports and articles concerned worldwide, clarify the basic function of LTP treatment devices for seeds and define the designs for both test stand and Experiment involved.

(2) Study on the design of LTP test device. This design composed by two parts: design of hardware and design of software. Hardware part will be responsible for technical treatment of LTP, while software part will charge of data collecting, supervising, controlling in the treatment period, and provide technical support for the intelligent devices in the future.

(3) Find out the appropriate dose of LTP. 30 different crop seeds and forage seed with low germination will be treated by different doze of LTP in our study, germination rate of treated and untreated seeds will be compared, finally to find out the relationship between characters of seeds and the treatment doze of LTP

(4) Communication between soft system and PC Visual Basic language will be used in software system design, and the communication between software system and PC will be realized through serial circuit.

3.2 Research Goal

(1) To submit more study results in the LTP research field. Take certain corp seeds and forage seed as the research targets whose biological germinations are poor, the article believes that find out the most ideal treatment dose can solve the technical barrier of promoting LTP treatment devices into the agricultural application.

(2) To provide craft and technical parameters for the research of technology integration. Integration of seed processing, mechanics engineering, computers and informations is the development trend of agricultural technology , the article is trying to establish such a reliable ,intelligent model of LTP treatment device on the ground of massive experiments and to provide craft and technical parameters for the upgrading of seed treatment devices.

4 Research Plan

4.1 Research Methods

As many discipline involved in the project, six methods will be used in the research:

- (1) Method of scientific literature review and survey analysis
- (2) Method of survey analysis and experiment
- (3) Method of experimental and positive research
- (4) Method of agronomy research and agricultural engineering research
- (5) Method of hardware design and software design
- (6) Method of general design and each module design

4.2 Technical Route

The route of modeling design and application of the LTP treatment test stand is shown in figure 2.

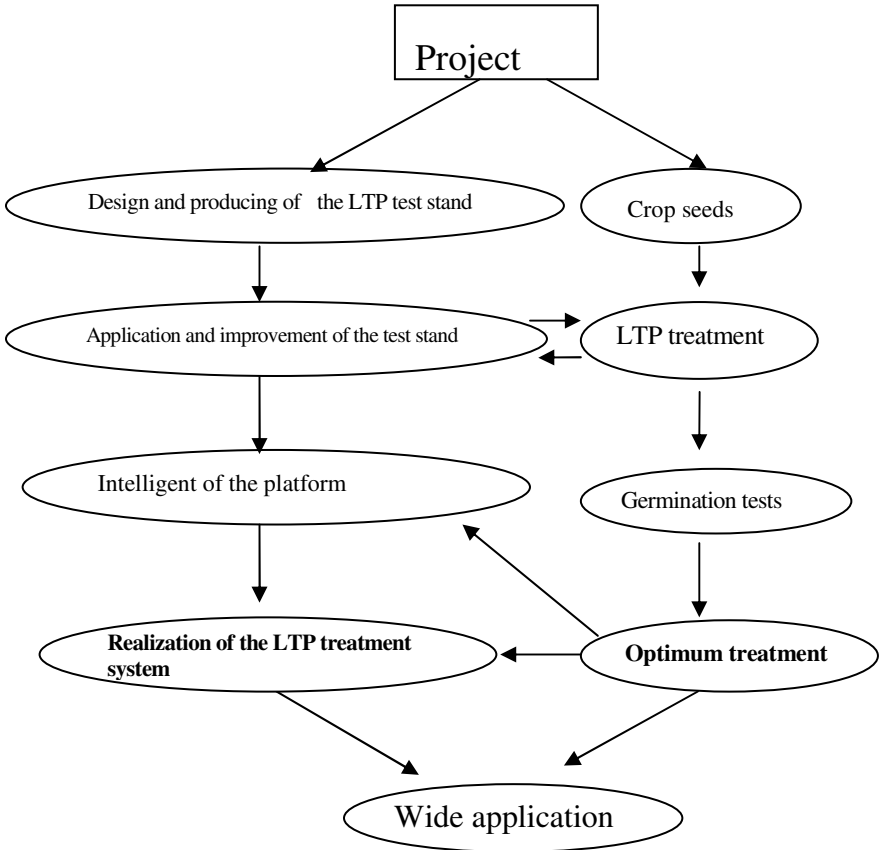


Fig. 2. LTP treatment system design

4.3 Scheme of the Experiments

4.3.1 Sample Seeds for the Experiments

All sample seeds are chosen from crop seeds and forage grass seeds, whose natural germinations are poor but uniform in size with good viability.

4.3.2 Treatment Dose of LTP

Healthy and uniform seeds will be counted and treated with various LTP strength (0, 10, 20, 40, 60, 80, 100, 120, 140, 160, 200, 220, 240, 260, 280, 300, 320, 340, 360, 380, 400W).

4.3.3 Germination Test

Germination test for vegetable seeds and small forage grass seeds: treated seeds will be placed in petri dish with two-layer filter paper at the bottom, 100seeds in each petri dish, and 4ml steamed water added in the dish to keep fine moisture. Germination test of the treated seeds will be done in the incubator with suitable temperature along with a check test. Each test will be repeated four times to confirm the repeatability of the results.

Germination test for grain seeds and large-size forage grass seeds: 50 treated seeds will be placed in petri dish with 120gr sterile sands at the bottom and 30gr sands on the top of the seeds for coverage, 30ml water will be dripped in, petri dish will be put on a light culture shelf, light period will be 12hours. The lid of petri dish should be uncovered after 3days, 10ml water is designed to drip in every 2 hour to keep sufficient water supply. Each test will be repeated four times and a check test is also added in.

Determination method of the germination

The germination rate is defined as the percentage of seeds that germinate in a specified short time (ST), the time in the test is specified as the days from the day of the first cotyledons breaking out from the seed coats or covered sands to the day that no new cotyledons coming out in 3days. These are calculated as follows:

Vigor of germination(%) = (Number of seeds germinated in ST days/total number of seeds) × 100%.

Rate of germination(%) = (Number of seeds germinated /total number of seeds) × 100%.

4.3.4 Determination of the Optimal Dose of LTP Treatment for Various Species Seeds

After germination test, the data of optimal intensity of LTP treatment for various species seeds will be got, list them in the following table:

Table 1. Optimal intensity of LTP treatment for seeds

Crop varieties	V1	V2	V3	V4	V5	V6	V7	V8
Intensity of LTP treatment (W)	W1	W2	W3	W4	W5	W6	W7	W8

4.3.5 Software Design and Communication with PC

Modularization method for designing software program will be based on the determination of optimal doses of LTP treatment for different seeds and construction of LTP treatment technology system, and it is in favour of extending and debugging a new function (Figure 3). The system and communications software will be programmed with the Windows XP operating system and for most stand-alone PC users, the interface is friendly and easy to operate.

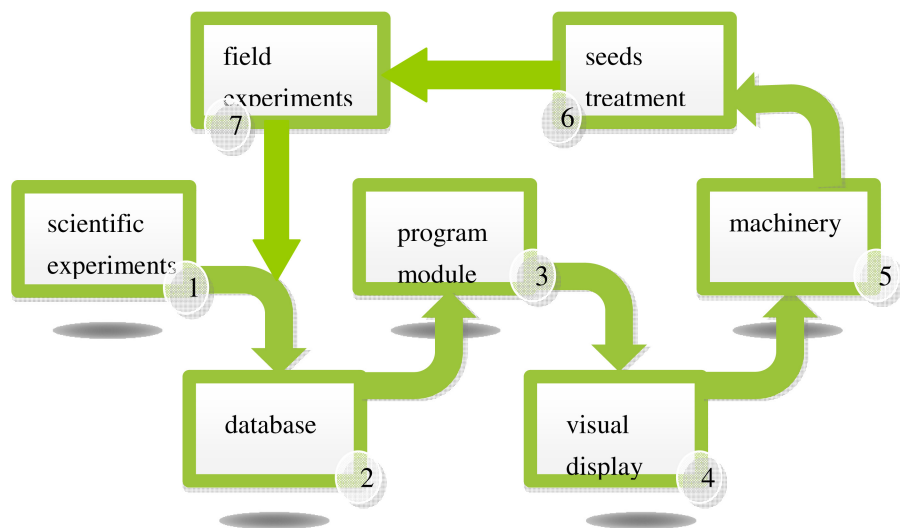


Fig. 3. Software programme design flowchart

5 Conclusions

(1) The paper try to establish a modeling of LTP treatment test stand for seeds before sowing, aiming at realizing a intelligent control of treatment dose, processing operation, supervision, data collecting and information feedback during the whole treatment.

(2) The paper try to determinate the optimal doses of LHP treatment and other key technical parameters for LTP treatment, finally find out the technical access to the research and development of LTP treatment machinery.

LTP treatment , as one of the effective physical methods for preparing seed, has an significant meaning to stimulate the potential energy of seeds, an intelligent LTP treatment device will meet this requirement. As an technologies integration of computer, machinery and serial communication, the new improved LTP treatment researched in this paper will be more stable and effective. It will be the development trend in agriculture industry and has a widely applied prospects.

Acknowledgment. The study was supported by Special Fund for Agro-scientific Research in the Public Interest (201203024) and the Fundamental Research Funds for the Central Universities(NO.2013QJ019).

References

1. Phirke, P.S., Kudbe, A.B., Umbarkar, S.P.: The influence of magnetic field on plant growth. Seed Science and Technology 24(2), 375–392 (1996)
2. Pietruszewski, S.: Effect of magnetic seed treatment on yield of wheat. Seed Science and Technology 21(3), 621–626 (1993)

3. Podleoeny, J.: The effect pre-sowing treatment of laser light on morphological features formation and white lupine yielding. In: *Lupin, An Ancient Crop for the New Millenium*. Department of Agronomy and Soils, Alabama Agric. Expt. Stn. and Auburn University, pp. 388–390 (1999)
4. Shao, C., Wang, D., Tang, X., et al.: Stimulating effects of magnetized arc plasma of different intensities on the germination of old spinach seeds. *Mathematical and Computer Modelling* 58(3-4), 808–812 (2013)
5. Shao, C., Fang, X., Tang, X., et al.: Effects of low-temperature plasma on seed germination characteristics of green onion. *Transactions of the Chinese Society for Agricultural Machinery* 44(6), 212–216 (2013) (in Chinese with an English abstract)
6. Yin, M.: *Research of magnetized arc plasma on seeds biological effects*. Dalian University of Technology, Dalian (2006) (in Chinese)
7. Zhang, Y., Zhang, J., Wang, Q.: The application of physical methods in sugar beet seed treatment. *China Beet and Sugar* (2), 20–22 (2005) (in Chinese)
8. Xu, Z., Chen, B., Wei, Z.: Various seed treatments on corn yield. *Agricultural science & Technology and Equipment* (4), 15–16 (2011) (in Chinese)
9. Liu, S., Ouyang, X., Nie, R.: Application status and development trend of the physical methods in the crop seed treatment. *Crop Research* 5(2), 520–524 (2007) (in Chinese)
10. Li, R.: Plasma machine seed treatment technology. *North Rice* 4(4), 52–53 (2010) (in Chinese)
11. Fu, S., Zhang, F., Li, J., et al.: Several physical techniques in agriculture and Prospects. *Agricultural Mechanization Research* (1), 36–38 (2006) (in Chinese)

Research on Rapid Identification Method of Buckwheat Varieties by Near-Infrared Spectroscopy Technique

Fenghua Wang¹, Ju Yang¹, Zhiyong Xi¹, and Hailong Zhu²

¹ Faculty of Modern Agricultural Engineering, Kunming University of Science and Technology, Kunming 650500

² Engineering Training Center, Kunming University of Science and Technology, Kunming 650500

wangfenghua018@163.com, {372086956, 315314518, 81065885}@qq.com

Abstract. In order to achieve the rapid identification of buckwheat varieties, and avoid buckwheat varieties mixtures, eight buckwheat varieties from different origins were identified by principal component analysis and support vector machines based on near-infrared spectroscopy. First, the buckwheat spectral information of the 120 samples have been collected using FieldSpec 3 spectrometer, and preprocessing through smooth + Multiplicative Scatter Correction (+MSC), a total of 120 sets were divided into 80 training sets and 40 prediction sets. After the principal component analysis, based on the binary tree support vector machine theory, the spectral information identification model of buckwheat varieties have been established and verified by LIBSVM package in MATLAB software. The results showed that the classification accuracy rate averaged 92.5% for eight different kinds of buckwheat by using near-infrared spectroscopy combined with principal component analysis and support vector machine. A new method for buckwheat varieties identification has been provided.

Keywords: Near infrared spectroscopy, Buckwheat, PCA, SVM, Variety identification.

1 Introduction

Buckwheat, mainly located in the alpine areas of the Loess plateau and the plateau mountains of Yunnan, Guizhou and Sichuan. It has a high nutritional and health value, known as the food treasures of "Medicine-Food"[1]. It also known as the triangle wheat, black wheat, belongs to the genus of dicotyledonous Polygonaceae, family of Fagopyrum Mill, mainly have two cultivar of buckwheat is Sweet Buckwheat (*Fagopyrum esculentum* Moench) and Tartary Buckwheat (*Fagopyrum tararicum* Gaerth). Therefore, the quality detection and the varieties identification of buckwheat has a very important significance in buckwheat planting, the deep processing industries and the quality improvement of buckwheat.

Near infrared spectroscopy analysis have the advantages of fast analysis without any pretreatment, no pollution, no damage, multi-component analysis, good reproducibility and suitable for online analysis, etc., which can be use to carry on the

qualitative or quantitative analysis by spectral data of the full spectrum or multi wavelength, and it is widely used in agricultural product quality testing and varieties identification [2-7]. Traditional identification method of buckwheat varieties is chemical method, it is cumbersome and destructive for buckwheat samples, and it is very useful to study a rapid nondestructive method for varieties identifying.

Without losing the main message, principal component analysis (PCA) can select fewer new variables to replace the original variables and resolve the overlapping bands which can not be analyzed, which is a mathematical method widely used in spectrum analysis [8]. Support vector machine (SVM) is a statistical theory learning algorithm, it has the advantages of high convergence speed and high accuracy than other classification algorithm, and it has been widely applied in the quality inspection of agricultural products and species identification [9]. However, the data indivisibility often appeared in multi-class prediction problems by using SVM. Therefore, this article uses principal component analysis combined with binary tree support vector machine to establish the NIR prediction model of different buckwheat varieties, to achieve the identification of buckwheat species.

2 Materials and Methods

2.1 Instruments and Materials

The spectral information was collected by FieldSpec3 spectrometer which made in U.S. ASD (Analytical Spectral Device) company.

Seven kinds of tartary buckwheat and a sweet buckwheat from Yunnan, Shanxi, Sichuan province in China were selected. They are Kunming tartary buckwheat, Luxi tartary buckwheat, Zhaotong tartary buckwheat No. 1 and No.2, Shanxi tartary buckwheat Y16, Xichang tartary buckwheat, Dali tartary buckwheat and Dali sweet buckwheat, a total of eight kinds of representative buckwheat varieties, each buckwheat selected 15 samples, a total of 120 samples. Each sample was air-dried, eliminating Impurities, particle size and consistent uniformity, and all samples were bagging sealing for spare use.

2.2 Acquisition of the Buckwheat Spectral Information

Buckwheat spectral data have been collected in outside, the test device was consist of computer, spectrometer, reflectance probe using the interior illuminant, calibration whiteboard, etc. and the Spectrometer selected FieldSpec 3 spectrometer, the sampling range is 350-2500 nm, spectral sampling interval is 1.4nm, and the resolution is 3nm. In the experiment, the 120 buckwheat samples were placed in the glass petri dish with the dimension of 90mm diameter, 15mm thickness respectively, put the reflectance probe close to the surface of the samples, and collected the sample spectral data using the

reflection mode. 15 repetitions and 10 times scanning for each sample, and then the average processing have been carried on using Viewspec pro software provided by ASD, and converted it to absorbance by $\log [I / R]$. Then the spectral data have been exported as ASCII format and processed with ASD View Spec Pro, Unscramble9.7, SPSS16.0 and MATLAB software. Buckwheat near-infrared spectroscopy absorbance graph are shown in Figure 1. The abscissa is the wavelength (nm), and the vertical axis is an absorbance $\log [I / R]$.

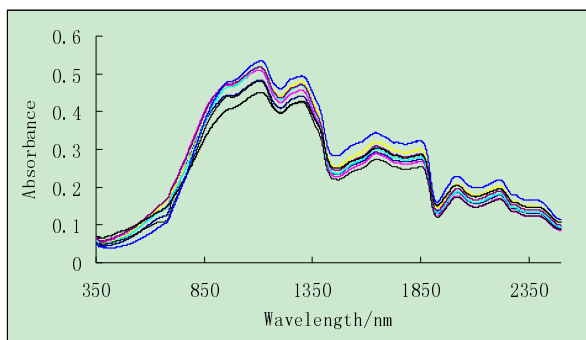


Fig. 1. Absorbance graph of buckwheat near-infrared spectroscopy

2.3 Multi-class SVM Classification Based on Binary Tree

Support vector machine is a machine learning algorithm based on the structural risk minimization (SRM) principle of statistical learning theory. For the positive and negative training samples, a hyperplane with the maximum interval has been obtained. As for the non-linear data sets, the training samples will be mapped into a high dimensional data space, to find a hyperplane in the feature space, and separate the positive and negative samples in a maximum possible [10].

Originally, SVM was designed for binary classification problems. This paper is a multi-class classification problem, using SVM classification method which based on binary tree for classification. For K types training samples, need to train $K-1$ support vector machine. In the first support vector machine, the first type sample as the positive training sample, and the 2,3 ..., K types of training samples as negative training samples SVM1. In the i support vector machine, the sample i as the positive training sample, and the $i+1, i+2$..., K types of training samples as the negative training samples SVM i , until the $K-1$ sample as the positive sample of the $K-1$ SVM, and the K type sample as the negative sample training SVM ($K-1$) [11], multi-class SVM classification process of binary tree as Figure 2:

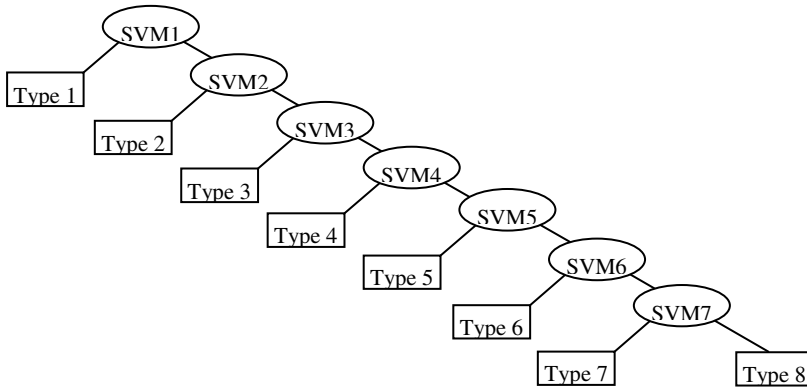


Fig. 2. SVM classification process

3 Experimental Results and Analysis

3.1 Data Preprocessing

The collected NIR spectroscopy is often influenced by high-frequency random noise, baseline drift, uneven sample and light scattering, so the spectral preprocessing is needed. Compared with different pretreatment methods, the average smoothing method was used in preprocessing of near infrared spectroscopy, the choice of the smoothing window size was 3, then multiplicative scatter correction (MSC) treatment was used, and it is good to filter high frequency noise generated by various factors.

3.2 Principal Components Extraction Based on Principal Component Analysis

The 120 samples were randomly divided into the prediction set and the validation set with 80 and 40 samples respectively. Sample spectral bands from 350 to 2500 nm, there are 2151 data in total. Computational complexity is large when using the full spectrum of computing. And due to the weak spectral information of some regional samples, the composition of the sample or the nature is lack of correlation. The principal component analysis is an effective method for data mining, it can translate the original multiple-wavelength variables into fewer new variables. These new variables are mutually independent, and it can synthetical reflect the information of original multiple-wavelength variables. [7,8]. The prediction set and the validation set were principal component analysis respectively by SPSS software, and the accumulative reliabilities of the first 7 principal components are shown in Table 1.

Table 1. Accumulative reliabilities of the first 7 PC s

Principal component	Accumulative reliabilities of prediction set/%	Accumulative reliabilities of validation set/%
PC_01	64.918	63.800
PC_02	89.035	88.092
PC_03	97.266	97.074
PC_04	98.973	98.857
PC_05	99.499	99.415
PC_06	99.865	99.836
PC_07	99.912	99.887

3.3 Buckwheat Varieties Identification Based on LIBSVM

The data arrangement have been carried on according to the multi-class SVM binary tree classification principle, and converted into a data set of .mat file for LIBSVM package. The dataset used in LIBSVM must have the attributes matrix and labels: the first column as a label, and the two to eight columns as property matrix. In 80 training sets, the 1st species tagged 1, and the rest are -1, the property matrix is representative of the principal component of each kinds of buckwheat, the attribute matrix as input, and the label as output. Based on the model, identified the No. 1 sample of the 40 samples of prediction sets; then identified the 70 training sets of the other species for the No. 2 species, and labeled No. 2 species as 1, the rest are -1 for modeling, and identified the 35 training sets for the No. 2 species; Until the SVM training for No. 7 sample, identified eight buckwheat varieties from different origin.

Through several tests the LIBSVM model parameters have been obtained, and the set as follows: Set Model Type: C-SVC, model parameter settings is $-S=0$ $-C=1$, Kernel function type: polynomial kernel function: $(\gamma * u^* * v + \text{coef0})^{\text{degree}}$, Therefore, $-t = 2$

1) To establish the model by using svmtrain:

model = svmtrain(train_label, train_data, '-s 0 -t 2 -c 1 -g 0.1');

Input: [train_data training set attribute matrix, the size is $n * m$, n represents the number of samples, m represents the number of attributes (dimensions), the data type is double; train_label is the training set labels, the size is $n * 1$, n represents the number of samples, and the data type is double]

2) To make predictions by using svmpredict:

[predictlabel,accuracy]=svmpredict(testdatalabel,testdata,model)

Input: [test_data is the test set attribute matrix, the size is $N * m$, N represents the number of the test sample set, m represents the number of attributes (dimensions), the data type is double; test_label is the test set labels, the size is $N * 1$, N represents the number of samples, data type is double]

In this paper, eight kinds of buckwheat samples were classified, and 7 support vector machine were needed to be trained: training set recognition rate of the first support vector machine is 98.75%, and the recognition rate of prediction set is 100%.

Accuracy = 98.75% (79/80) (classification),

Accuracy1= 100% (5/5) (classification) ;

The remaining 7 types buckwheat prediction identification were: 100%、80%、100%、80%、80%、100% and 100%。 The average recognition rate of the eight buckwheat varieties is 92.5%.

4 Conclusion

In this paper eight varieties of buckwheat from different origins were identified using near-infrared spectroscopy combined with principal component analysis and binary tree multi-class SVM classification methods. The buckwheat varieties spectral information identification model have been established by LIBSVM package in MATLAB software. The average accuracy rate of eight different types of buckwheat is 92.5%. The results showed that near infrared spectroscopy combined with principal component analysis and support vector machine algorithm for buckwheat spectral information modeling can be achieved to identify buckwheat species.

Acknowledgment. Funds for this research was provided by Yunnan Province application basis surface research projects (Item number: 2010ZC028), Kunming University of Science and Technology Analysis and Testing Fund (Item Number: 2011432, 2011436).

References

1. Kayashita, J., Shimaoka, I., Nakajoh, M., et al.: Consumption of a buckwheat protein extract retards 7,12-Dimethylbenz[alpha] anthracene-induced mammary carcinogenesis in rats. *Bioscience Biotechnology Biochemistry* 63(10), 1837–1839 (1999)
2. Wang, D., Ma, Z., Pan, L., et al.: Research on the Quantitative Determination of Lime in Wheat Flour by Near-Infrared Spectroscopy. *Spectroscopy and Spectral Analysis* 33(1), 69–73 (2013)
3. Zhang, Q., Zhang, J.: Region Selecting Methods of Near Infrared Wavelength Based on Wavelet Transform. *Transactions of the Chinese society for Agricultural Machinery* 41(2), 138–142 (2010)
4. Zhou, Z., Zhang, Y., He, Y., et al.: Method for Rapid Discrimination of Varieties of Rice using Visible NIR Spectroscopy. *Transactions of the Chinese Society of Agricultural Engineering* 25(8), 131–135 (2009)
5. Su, X., Zhang, X., Jiao, B., et al.: Determination of Geographical Origin of Navel Orange by Near Infrared spectroscopy. *Transactions of the Chinese Society of Agricultural Engineering* 28(15), 240–245 (2012)
6. Xi, Z., Wang, F.: Research Progress of Grain Quality Nondestructive Testing Methods. *Science and Technology of Food Industry* (15), 394–396, 400 (2012)
7. Wang, F., Yang, J., Zhu, H., Xi, Z.: Research of Determination Method of Starch and Protein Content in Buckwheat by Mid-Infrared Spectroscopy. In: Li, D., Chen, Y. (eds.) *Computer and Computing Technologies in Agriculture VI, Part II. IFIP AICT*, vol. 393, pp. 248–254. Springer, Heidelberg (2013)
8. Zhang, H., Zhang, S., Wang, F., et al.: Study on Fast Discrimination of Seabuckthorn Juice Varieties Using Visible-Nir Spectroscopy. *Acta Optica Sinica* 30(2), 574–578 (2010)

9. Wang, F., Zhu, H.G.Z.: Progress of Near-infrared Spectral Data Modeling Method. *Agricultural Engineering* 1(1), 56–61 (2011)
10. Zhang, T., Ding, Y.: Protein Structural Class Prediction with Binary Tree-Based Support Vector Machines. *Journal of Biomedical Engineering* 25(4), 921–924 (2008)
11. Lv, X., Li, L., Cao, W.: SVM Multi-class Classification based on Binary tree. *Information Technology* (4), 1–3 (2008)

The Characteristic of Hyperspectral Image of Wheat Seeds during Sprouting

Jiayu Chen^{1,2}, Honghui Chen³, Xiaodong Wang¹, Chunhua Yu¹, Cheng Wang¹,
and Dazhou Zhu^{1,*}

¹ Beijing Research Center of Intelligent Equipment for Agriculture, BeiJing 100097,
P.R. China

² School of Communication, Shandong Normal University, Jinan, 250014, P.R. China

³ Accounting School, Shandong Institute of Commerce and Technology, Jinan, 250103,
P.R. China

zhudz@nercita.org.cn

Abstract. The pre-harvest sprouting of wheat have significant influence for its quality and yield, therefore the fast detection of sprouting extent of wheat is very important for breeding and producing. In this study, the hyperspectral images of these seeds were collected by a near infrared hyperspectral imaging system, the wavelength of which was 850-1700 nm after wheat germination experiment at 0h, 12h, 24h, and 48h. The original light intensity of embryo and endosperm were extracted, and were then changed to reflectivity for later analysis. The image and spectral information of wheat with different parts, different varieties and different sprouting extent were compared. The results showed that after 12h sprouting, the reflectivity of embryo was lower than that of endosperm for the same seed, this is mainly due to the water and fat content of embryo was higher than the endosperm portions. For the same varieties of wheat seed at the germination of 12h, 24h and 48h, in the wavelength range of 870-1300 nm, the reflectivity increased with the increase of sprouting time, it was related to the changes of its internal content of fat in the seed germination process. At 1400nm, the reflectivity of sprouted wheat seeds were all lower than that of dry seeds, it was related to the rise of internal water content in the process of seed germination. Due to differences in seed water absorption and sprouting resistance, for different varieties of wheat seeds, its spectral characteristics are also different. The presented indicated that hyperspectral imaging could reflect the characteristics of sprouted wheat seeds, which provide some basis for explore the sprouting index by hyperspectral imaging.

Keywords: hyperspectral imaging, pre-harvest sprouting, wheat, seed.

1 Introduction

Pre-harvest Sprouting (Shorted for PHS) refers to the sprouting phenomenon if encountered rainy days or in a humid environment before harvest, and is mainly occurs in the drippy regions in the harvest season(Xiao et al., 2004). There are two main pre-harvest sprouting endanger frequent and severe areas in China: one includes

* Corresponding author.

Jiangsu and Anhui provinces which is south of the Huai River, most place of Hubei province and middle gluten and weak gluten wheat in the middle and lower reaches of the Yangtze River area of the south of Henan Province. The other includes strong gluten wheat area in northeast involved North, East of Heilongjiang province, Neimenggu Daxinganling and other regions (Zhu et al., 2010). Wheat pre-harvest sprouting is a climate disasters around the world-wide, it will cause a series of physiological processes, such as the increasing of α -amylase and other hydrolyses activity, cause the kernels internal storage material decompose in advance, severely affected the quality of the kernels (Zhao et al., 2009). Besides, pre-harvest sprouting also affect wheat yield and breeding value, cause large losses to agricultural production. So, achieving the detection of pre-harvest sprouting characteristics, cultivating wheat varieties with resistance to preharvest sprouting characteristics, improving the quality of wheat is an important task of the current breeding work.

There are three traditional methods to detect the resistance of wheat pre-harvest sprouting: the field natural identification method of extended harvesting, whole ear germination experiments and seed germination experiments, of which the main methods to detect the resistance of wheat pre-harvest sprouting are whole ear germination experiments and seed germination experiments. Currently, there are three technical means of wheat pre-harvest sprouting resistance detection, of which are biochemical measurement method, molecular detection method and visual method (Yang et al., 2007). Biochemical measurement method and molecular detection have flaws of complex operation, labor-intensive, costly and time consuming, destructive, visual method is susceptible to subjective factors and is difficult to detect status of early germination.

With the development of photovoltaic technology, try to take advantage of the various photoelectric detection technology to achieve the rapid detection of pre-harvest sprouting. Cheng Fang use machine vision technology to get the image of germinated rice seeds, and then use the corresponding image processing algorithm to obtain rice contour characteristic parameters, establish BP neural network model to achieve the recognition of healthy rice and buds valley rice. This method can identify germinated seeds which has the obvious appearance changes, but it is difficult to extract effective features of spike germinating seeds which are small opening (Cheng et al., 2007). Neethirajan and others get the X-ray images of healthy and sprouted kernels at the same time using Soft X-ray technology, extract 55 image features including gray level modeling and histogram from the scanned images, use neural network model to identify healthy and sprouted kernels with the recognition rate of 95% and 90% (Neethirajan et al., 2007). But the X-ray technology has a certain amount of radiation hazards to the human body, so, explore a fast and non-destructive method to detect pre-harvest sprouting imperative.

Hyperspectral imaging technology is the integration of spectroscopic techniques and imaging technology, it can obtain spectral information and image information at the same time. Hyperspectral image contains a lot of information, it can not only get its external morphology information using image information but also can get their internal composition information with spectral information. In terms of agricultural applications, hyperspectral imaging technology has been widely used in the diagnosis

of crop information (Wang et al., 2011), non-destructive testing of fruit quality (Hong et al., 2007) and other aspects. The application of hyperspectral imaging technique for seed testing, scholars have conducted a lot of exploration. Cogdill and others using Near-infrared spectral images to predict the moisture and oil content of a single corn kernels. Partial least squares(PLS) regression and principal components regression(PCR) were used to develop predictive calibrations for moisture and oil content, the moisture calibration achieved a best standard error of cross-validation(SECV) of 1.20%,the best oil calibration achieved an SECV of 1.38% (Cogdill et al., 2005). Xing and others use hyperspectral imaging system (1000–2500 nm) to collect single kernel map information, use Partial Least Square regression to predict the α -amylase activity of individual wheat kernels, the correlation coefficient can be 0.73, this method to separate wheat kernels with high α -amylase activity level from those with low α -amylase activity giving an accuracy of above 80%(Xing et al., 2009).Singh and others collect the map of healthy wheat seeds and germination of wheat seeds in the range of 1000-1600nm using NIR hyperspectral imaging system, develop the discriminant classifier model to identify healthy and germinated seeds, the discriminant classifiers gave maximum accuracy of 98.3% (Singh et al., 2009). The above research have shown the feasibility of hyperspectral imaging technology in wheat germination test, this study aims to collect the map of seeds in different parts, different germination periods, different varieties of wheat seeds using the hyperspectral imaging system, analyze of the changes in the spectral characteristics in depth, laying the foundation for selection of pre - harvest sprouting resistance.

2 Materials and Methods

2.1 Sample Preparation and Processing

Select eight different varieties of winter wheat, respectively Jingdong 8, Jing411, Zhongmai175, Nongda211,Zhongmai16, Jingdong 18, Nongda3432 and Nongda3291. Retrieve ten wheat ears of each species from the field, and hand-strip them for wheat grains after washing, air drying and burr picking. Each variety of 120 wheat seeds and divided into four parts, each part of 30 wheat seeds for the germination experiment. The seed germination time of four parts respectively are 0h, 12h, 24h, 48h, which 0h for the original dry seeds. The specific germination method is: repeatedly wash the wheat grains with tap water and put them in the 5% NaClO solution to conduct the disinfection for 5 minutes; then repeatedly wash them again by distilled water, encase them into the Petri dish lined with two layers of filter paper, and then add an appropriate amount of distilled water for the sprouting experiment. The seed germination hyperspectral information should be acquired after a certain period of time of the sprouting experiment. First, use absorbent paper to suck the excess water on the seed surface, to reduce the impact of water on the experimental data. At the same time to collect hyperspectral image of seed, using a color camera to obtain seed RGB image for subsequent comparative analysis between machine vision imaging results and spectrometer imaging results.

2.2 Hyperspectral Imaging System

The hyperspectral imaging acquisition system used in this study is mainly composed of Near-infrared imaging spectrometer, halogen light source, guides, sample platform, motion controller and computer. The experimental apparatus shown in Fig. 1. This Near-infrared imaging spectrometer was the InGaAs array of near-infrared spectrometer, which size is 250×190×160 mm, spectral range was 850-1700nm, spectral resolution was 2.7nm, spatial resolution was 0.25 mm. The power of the halogen light source is 50W, spectral range was 400-3000nm.

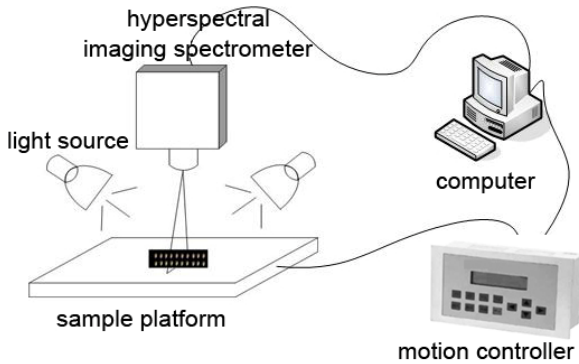


Fig. 1. Diagram of the experimental apparatus

2.3 The Acquisition of Wheat Seed Hyperspectral Image

Before the data acquisition, use the black cotton cloth to cover the sample stage of the hyperspectral imaging system in order to reduce the impact of the background noise. Take 30 germinated wheat seeds each time, make the ventral furrow downward, and uniformly tile on a black background sample stage in single-layer. Ensure the Interior for the darkroom environment and avoid interference from other light sources when do the experiment. Using halogen light source irradiation on germination of seed samples, and collected the hyperspectral image information of seed germination at 0h, 12h, 24h, 48h respectively. The vertical height of the sample to the spectrometer lens is 31cm, motor speed is 28.264mm/s, the height of the halogen light source is 24cm, integration time of imaging spectrometer is 18ms, the frame rate is 50fps. when setting up various other parameters of hyperspectral imaging system, collecting the data. Use the BaSO₄ Board as a standard reference Board.

2.4 Data Processing

Hyperspectral data collected was the original intensity value of the point for each pixel, using ENVI software to extract the average intensity value of image for the region of interest, compare with the simultaneous determination of the whiteboard spectrum, calculate a spectral reflectance of the object, as follows:

$$\text{Ref}_{\text{object}} = \left(\text{Rad}_{\text{object}} / \text{Rad}_{\text{whiteboard}} \right) \times \text{Ref}_{\text{whiteboard}} \times 100\% \quad (1)$$

Where, $\text{Ref}_{\text{object}}$ represented spectral intensity data of object obtained by whiteboard reflectance; $\text{Rad}_{\text{object}}$ represented measured by spectrometer; $\text{Rad}_{\text{whiteboard}}$ represented radiance of whiteboard measured by spectrometer; $\text{Ref}_{\text{whiteboard}}$ represented known reflectance ratio of whiteboard.

3 Results and Analysis

3.1 Comparative Analysis between Hyperspectral Image and Machine Vision Image of the Germinated Wheat Seed

Extract the hyperspectral image of seeds at 1300nm (see in Fig. 2), compared with RGB color image which was taken with the use of machine vision. As can be seen from figure 2: The picture of germination seed which was acquired using machine vision has higher resolution, the area of the protrusion, can be more clearly seen. The pictures taken using hyperspectral imaging spectrometer are grayscale image, have low resolution, but to seeds which were germinate more obvious, was able to identify the germinated part from hyperspectral image with naked eye. Therefore, as to seed morphology, the hyperspectral imaging systems generally had low resolution, so the identification was not as good as the machine vision. But, in the process of seed germination, especially early germination the morphological change of the seed is small at the same time there are more internal changes of biochemical composition, therefore, using spectral information is expected to be a more accurate analysis of seed germination characteristics. Hyperspectral image data contains spectral information and image information at the same time, use the image processing technology to extract reflectance spectra of specific area of the seed, then use the spectroscopic techniques to analyze the spectral differences, can achieve the map effect, get more refined analysis of the characteristics of seed germination.

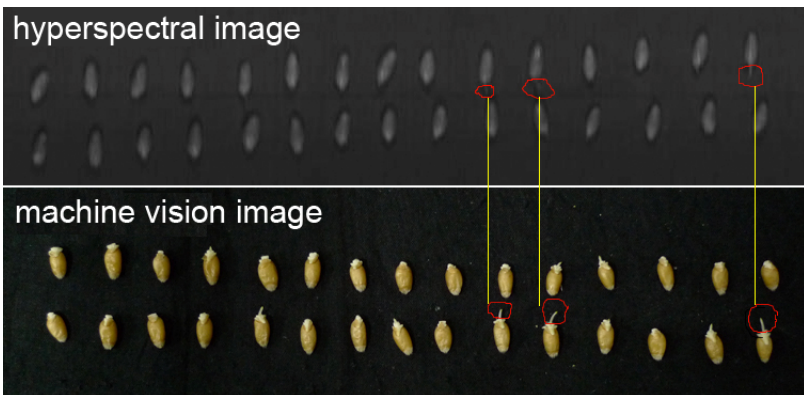


Fig. 2. Hyperspectral image and machine vision image of germination wheat seeds

3.2 The Analysis of Spectral Characteristics of the Region of Germinated Wheat Seed Embryo and Endosperm

Wheat seed is mainly composed of the embryo and endosperm, there are mainly three large storage material in the endosperm: carbohydrates, proteins and lipids, although the embryo part was a small part of the wheat, it were rich in protein, lysine, soluble sugar, fat and vitamins. In this study, we extracted the average spectrum of the embryo and endosperm of wheat kernel which was at the germination of 12h, and then fine analyzed the spectral absorption characteristics of the different regions. In the wavelength range of 870-1700 nm, the endosperm reflectance spectra was higher than that of the embryo portion(see in Fig. 3). This band contains three characteristic reflection valley, respectively are 885 nm, 1149nm and 1381nm, These three wavelengths respectively corresponding to the characteristic absorption wavelength of the water of 970nm, 1450nm and characteristic absorption wavelength of the fat at 1200nm, but the occurrence of the offset, this is mainly because that the wheat kernel is mixture, its various components within the spectral absorption occurs superimposed, therefore may lead to a spectral absorption peak position offset. As the water and fat content in the embryo is higher than the endosperm portions and therefore the spectral reflectance is lower than the reflectance of the endosperm.

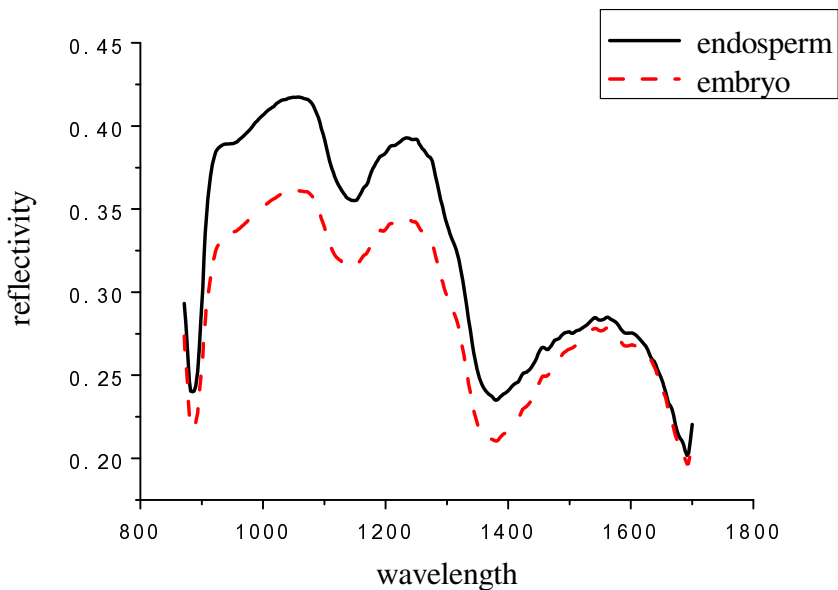


Fig. 3. The spectrum wheat seed in the germination of embryo and endosperm at 12h

3.3 Average Spectrum Analysis of Wheat Embryo at Different Germination Period

Collect the hyperspectral image after wheat germination experiment at 0h, 12h, 24h, 48h of 8 species, extract the original average intensity value of all varieties of wheat germ region, and then change it to reflectivity, calculate the average spectrum of different germination period of wheat germ (see in Fig. 5). It can be seen from the figure, at the germination of 12h, 24h and 48h, in the wavelength range of 870-1300 nm, the reflectivity increased with the increase of sprouting time, this band contains a reflection valley at 1149 nm which is the characteristic absorption of fat. So, the spectral reflectance within the range of this band change with time of germination may be related to the breakdown of fat, the embryo contains a lot of fat, with the increase in the degree of germination, fat gradually break down and reduced, causing the reflectivity increased gradually.

At 1400nm, the reflectivity of sprouted wheat seeds embryo at 12h, 24h, 48h were all lower than that of dry seeds, the main reason is that the band was in the vicinity of the water absorption band, in the germination process, the seed will absorb water, so the water content of the dry seed embryo is lower than the water content of the seed which is germinated. Furthermore, the reflectivity of sprouted wheat seeds embryo at 12h is lower than that of 24h and 48h, it may be due to before radicle grow, as a result of seeds imbibition of water, the water content is gradually increasing, so the reflectivity is at lowest. When the seed germinate arrive a certain state, rupture occurred because of embryos protrusion, water overflows which lead to water content gradually reduce, so, the reflectivity gradually increased.

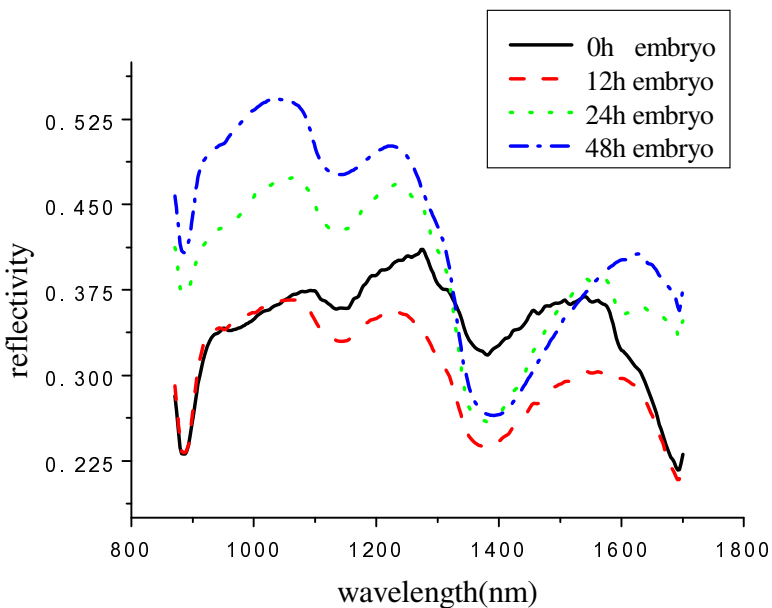


Fig. 4. The average spectrum of the embryo of 8 varieties of wheat at the same period

3.4 Average Spectrum Analysis of Wheat Embryo of Different Varieties in the Germination Process

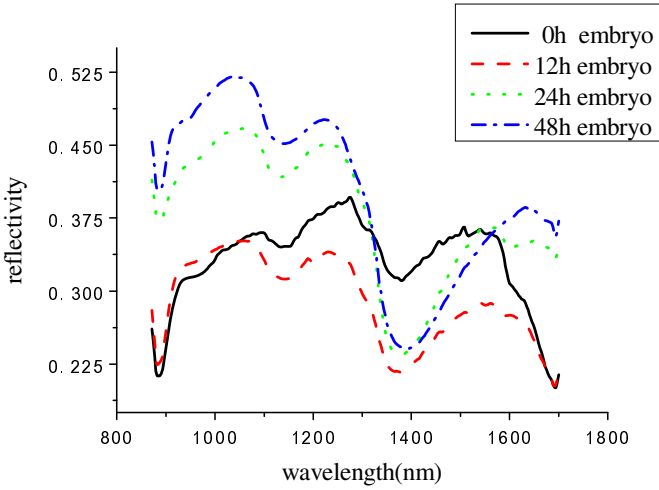
With hyperspectral images collected of wheat seed in different varieties, different times, extract the average spectrum of 30 wheat seed kernels of each variety to analyze the spectrum variation of the different varieties of wheat kernel embryo after the wheat seed germination experiment at 0h, 12h, 24h and 48h (see in Fig. 5). It can be seen from the figure:

From 12h, 24h to 48h, with the increase of germination time, at the wavelength range of 870-1300 nm, the reflectivity increased with the increase of sprouting time of all varieties except Nongda 3291. There are two reasons for this phenomenon: One is, the wavelength of 970nm is the water characteristic absorption, at the beginning of germination, mainly by imbibition of water, the water content is in a gradually increasing trend, when the seed germinate arrive a certain state, for embryos rupture, water overflows which lead to water content gradually reduce. So the germination time is longer, the reflectivity is higher. The second is the wavelength of 1200nm is the fat characteristic absorption, the embryo contains a lot of fat, with the increase of sprouting time, its internal fat hydrolysis under the action of the lipase, the fat content reduced, so, the reflectivity is higher.

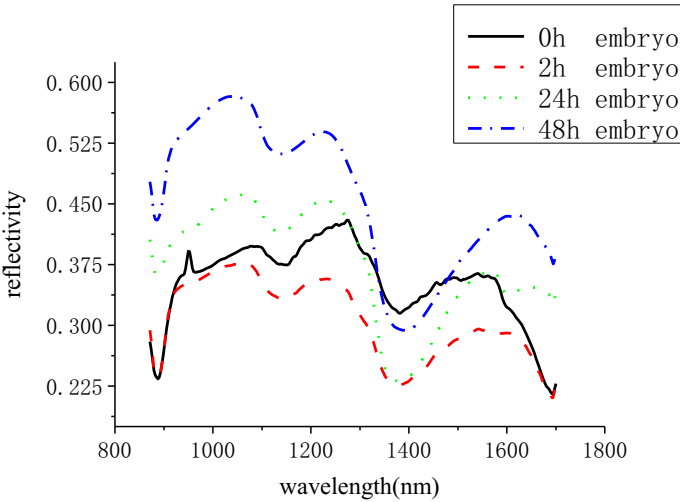
At 1400nm, the reflectivity of sprouted wheat seeds embryo at 12h is lower than that of 24h and 48h, but the reflectivity difference of sprouted wheat seeds embryo of Jing411 and Zhongmai175 at 12h and 24h is less than other varieties, illustrate that the water content of the two species in this two periods have little changes.

In the wavelength range of 870-1300 nm, not all the varieties reflectivity increases with the germination time prolonged, it mainly because it contains 1450nm for the center of the strong absorption band of water, this band of water absorption is stronger than 970nm for other components vulnerable influence the water absorption at 970nm, the band of 1450nm have absolute advantage of water absorption. For different varieties of seeds, due to different degrees of embryos ruptured, seed germination of spectral reflectance and gradual change of time with no obvious change with the seed germination time in the wavelength range of 1300-1700nm. Besides, the maximum reflectivity of Nongda3291 is 0.5, but other varieties of maximum reflectivity is larger than 0.52.

At 1400nm, the reflectivity of 12h sprouted wheat seeds were all lower than that of dry seeds. Further analysis revealed that: the reflectivity difference of 12h sprouted wheat seeds and dry seeds of Jingdong8, Jing411, Zhongmai175, Nongda211, Zhongmai16, Jingdong18, Nongda3432 and Nongda3291 respectively are 0.09627, 0.09095, 0.0727, 0.08479, 0.09405, 0.08849, 0.06057, 0.08739, but the difference of Zhongmai175 and Nongda3432 is smaller, it may be due to the capacity of water absorption is weaker than other varieties of the two varieties in the initial germination.

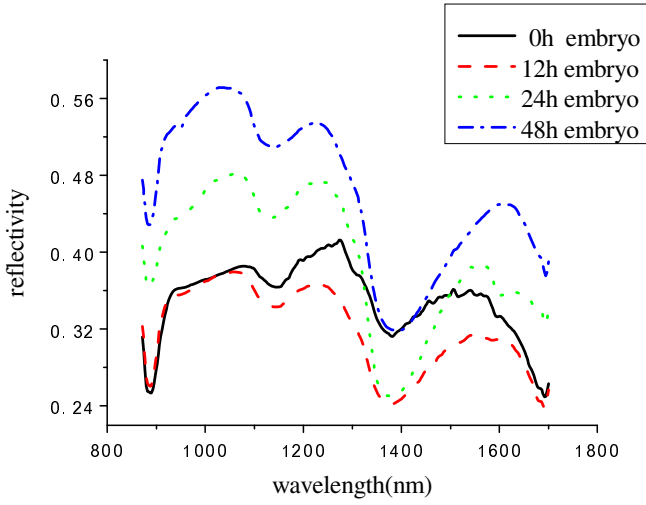


(a) Comparison chart of the average spectral reflectance of Jingdong8, different periods of wheat embryo

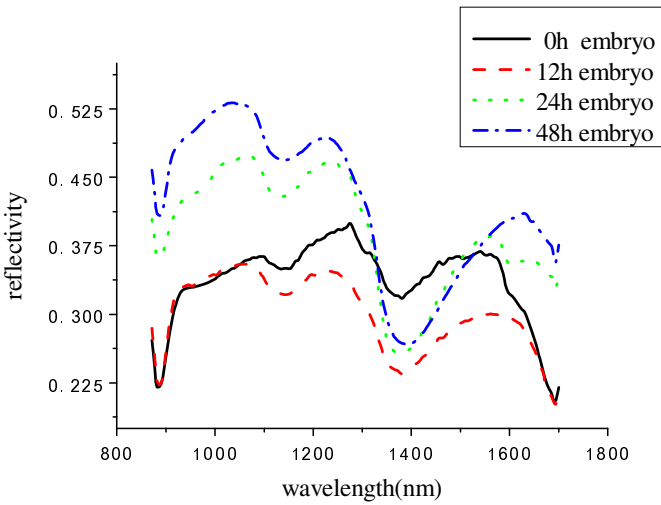


(b) Comparison chart of the average spectral reflectance of Jing411, different periods of wheat embryo

Fig. 5. Comparison chart of the average spectral reflectance of the same species, different periods of wheat embryo

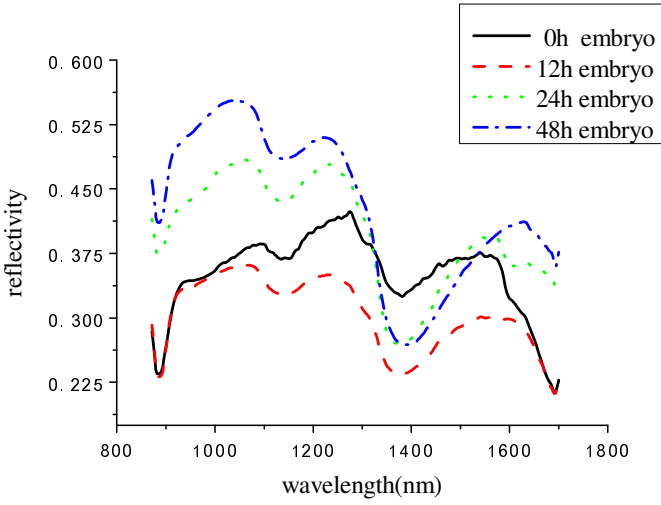


(c) Comparison chart of the average spectral reflectance of Zhongmai 175, different periods of wheat embryo

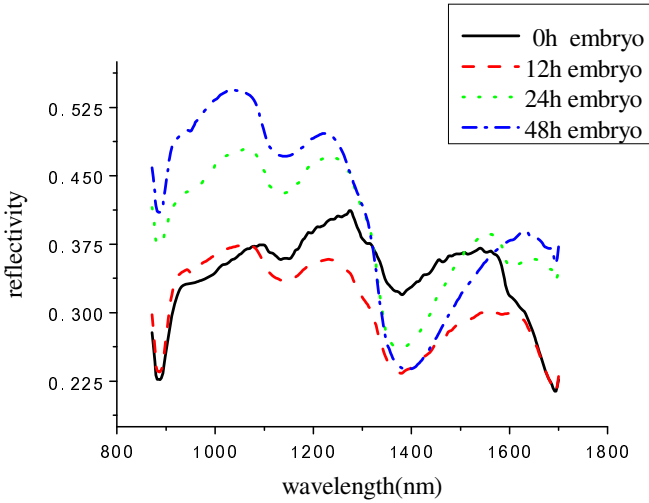


(d) Comparison chart of the average spectral reflectance of Nongda 211, different periods of wheat embryo

Fig. 5. (Continued.)

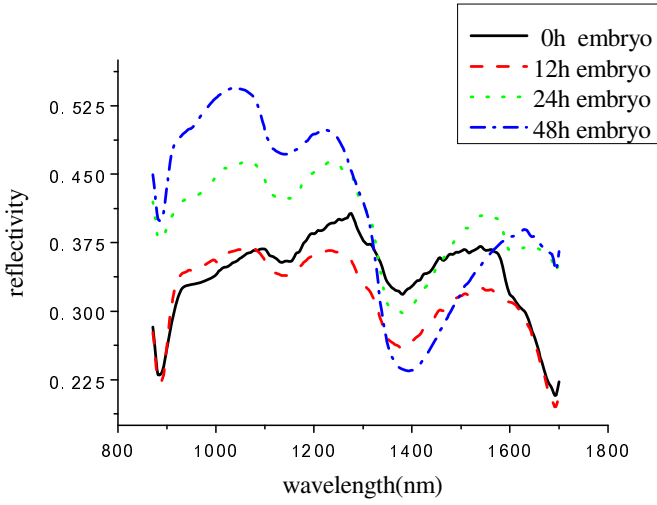


(e) Comparison chart of the average spectral reflectance of Zhongmai16, different periods of wheat embryo

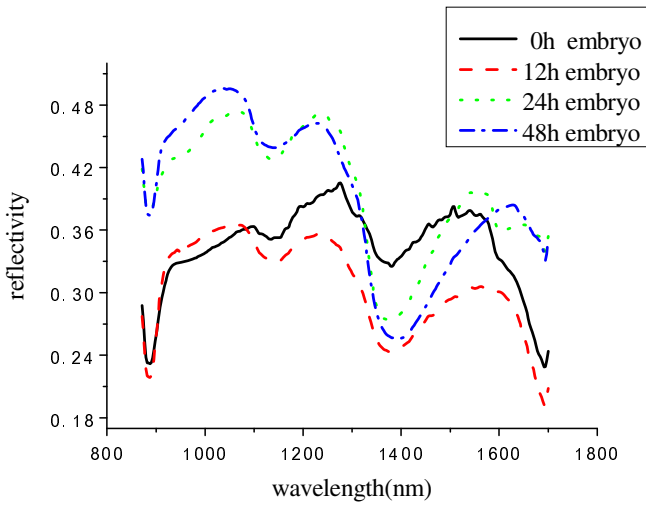


(f) Comparison chart of the average spectral reflectance of Jingdong18, different periods of wheat embryo

Fig. 5. (Continued.)



(g) Comparison chart of the average spectral reflectance of Nongda3432, different periods of wheat embryo



(h) Comparison chart of the average spectral reflectance of Nongda3291, different periods of wheat embryo

Fig. 5. (Continued.)

4 Conclusions

In this study, the hyperspectral images of these seeds were collected by a near infrared hyperspectral imaging system after wheat germination experiment at different times, select a region of interest and extract its average original light intensity values, and were changed to spectral intensity for later analysis. The results showed that after 12h sprouting, the reflectivity of embryo was lower than that of endosperm for the same seed, this is mainly due to the water and fat content of embryo was higher than the endosperm portions. For the same varieties of wheat seed at the germination of 12h, 24h and 48h, in the wavelength range of 870-1300 nm, the reflectivity increased with the increase of sprouting time, it was related to the changes of its internal content of fat in the seed germination process. At 1400nm, the reflectivity of sprouted wheat seeds were all lower than that of dry seeds, it was related to the rise of internal water content in the process of seed germination. Due to differences in seed water absorption and sprouting resistance, for different varieties of wheat seeds, its spectral characteristics are also different. Therefore, using hyperspectral imaging technology can reflect the spectral characteristics and internal changes of wheat germination process.

Acknowledgment. This project was funded by National Natural Science Foundation of China (31201125), Beijing Nova Program (Z111105054511051) and Beijing Academy of Agriculture and Forestry Youth Foundation (QN201107).

References

1. Xiao, S., Yan, C., Zhang, H., Sun, G.: *The Study on Wheat Pre-harvest Sprouting*, pp. 19–36. Publishing house of China Agricultural Science and Technology, Beijing (2004) (in Chinese)
2. Zhu, M., Zhang, R., Wang, B., Li, C., Zhu, X.: Wheat Pre-harvest Sprouting Physiology and Control Approaches. *Journal of Jinling Institute of Technology* 26(2), 49–54 (2010)
3. Zhao, T., Liu, Y., Deng, G., Yang, H., Pan, Z., Long, H., Yu, M.: Assessment of Methods Used in Testing Preharvest Sprouting Resistance in Hulled Barley. *Chinese Journal of Applied & Environmental Biology* 15(3), 380–384 (2009)
4. Yang, Y., Zhang, C., He, Z., Xia, L.: Advances on Resistance to Pre-harvest Sprouting in Wheat. *Journal of Plant Genetic Resources* 8(4), 503–509 (2007)
5. Cheng, F., Ying, Y.-B.: Inspection of germinated rice seed on panicle based on contour features. *Transactions of The Chinese Society of Agricultural Engineering* 20(5), 178–181 (2004)
6. Cheng, F.: Micro-observation of features of hybrid rice seed. *Journal of Zhejiang Agricultural University (Agric. & Life Sci.)* 29(2), 165–168 (2003)
7. Neethirajan, S., Jayas, D.S., Detlefsen, N.D.G.: of sprouted wheat kernels using soft X-ray image analysis. *Journal of Food Engineering* (2007)
8. Wang, K., Zhu, D., Zhang, D.-Y., Ma, Z., Huang, W.-J., Yang, G.-J., Wang, C.: Advance of the Imaging Spectral Technique in Diagnosis of the Information of Crop. *Spectroscopy and Spectral Analysis* 31(3), 589–594 (2011)

9. Hong, T., Li, Z., Wu, C., Liu, M., Qiao, J., Wang, N.: Review of hyperspectral image technology for non-destructive inspection of fruit quality. *Transactions of the Chinese Society of Agricultural Engineering* 23(11), 280–285 (2007)
10. Cogdill, R.P., Hurburgh Jr., C.R., Rippke, G.R.: Single-kernel maize analysis by near-infrared hyperspectral imaging. *Transactions of the ASAE* 47(1), 311–320 (2005)
11. Xing, J., Van Hung, P., Symons, S., Shahin, M., Hatcher, D.: Using a Short Wavelength Infrared (SWIR) hyperspectral imaging system to predict alpha amylase activity in individual Canadian western wheat kernels. *Sensing and Instrumentation for Food Quality and Safety* 3, 211–218 (2009)
12. Singh, C.B., Jayas, D.S., Paliwal, J., White, N.D.G.: Detection of Sprouted and Midge-Damaged Wheat Kernels Using Near-Infrared Hyperspectral Imaging. *Cereal Chemistry* 86(3), 256–260 (2009)
13. Vermeulena, P., Fernández, P.J.A., van Egmond, H.P., Dardennea, P., Baetena, V.: Online detection and quantification of ergot bodies in cereals using near infrared hyperspectral imaging. *Food Additives & Contaminants* 29(2), 232–240 (2012)
14. Yaping, Y., Xiao, C., Shihe, X.: Advances in the Study on Wheat Pre-harvest Sprouting. *Journal of Triticeae Crops* 23(3), 136–139 (2003)
15. Zhu, D., Wang, C., Pang, B.: Identification of Wheat Cultivars Based on the Hyperspectral Image of Single Seed. *Journal of Nanoelectronics and Optoelectronics* 7(2), 167–172 (2012)
16. Zhang, X., He, Y.: Rapid estimation of seed yield using hyperspectral images of oilseed rape leaves. *Industrial Crops and Products* 42, 416–420 (2013)
17. Yan, C.S., Zhang, H.P., Hai, L., Zhang, X.Y., Hu, L., Hu, H.Q., Pu, Z.J., Xiao, S.H.: Differences of Preharvest Sprouting Resistance among Chinese Wheat Cultivars. *Acta Agronomica Sinica* 32(4), 580–587 (2006)
18. Singh, C.B., Jayas, D.S., Paliwal, J., White, N.D.G.: Detection of insect-damaged wheat kernels using near-infrared hyperspectral imaging. *Journal of Stored Products Research* 45, 151–158 (2009)
19. Bauriegel, E., Giebel, A., Geyer, M., Schmidt, U., Herppich, W.B.: Early detection of Fusarium infection in wheat using hyper-spectral imaging. *Computers and Electronics in Agriculture* 75, 304–312 (2011)
20. Rodríguez-Pulido, F.J., Barbin, D.F., Dawen, S.: Grape seed characterization by NIR hyperspectral imaging. *Postharvest Biology and Technology* 76, 74–82 (2013)
21. Kong, W., Zhang, C., Liu, F., Nie, P., He, Y.: Rice Seed Cultivar Identification Using Near-Infrared Hyperspectral Imaging and Multivariate Data Analysis. *Sensors* 13, 8916–8927 (2013)
22. Vermeulen, P., Fernández, P.J.A., van Egmond, H.P., Zegers, J., Dardenne, P., Baeten, V.: Validation and transferability study of a method based on near-infrared hyperspectral imaging for the detection and quantification of ergot bodies in cereals. *Rapid Detection in Food and Feed* 405(24), 7765–7774 (2013)
23. Zhang, X., Liu, F., He, Y., Li, X.: Application of hyperspectral imaging and chemometric calibrations for variety discrimination of maize seeds. *Sensors* 12, 17234–17246 (2012)
24. Singh, C.B., Jayas, D.S., Paliwal, J., White, N.D.G.: Fungal Damage Detection in Wheat Using Short-Wave Near-Infrared Hyperspectral and Digital Colour Imaging. *International Journal of Food Properties* 15(1), 11–24 (2012)

Control Software Design of Plant Microscopic Ion Flow Detection Motion Device

Lulu He^{1,2}, Fubin Jiang², Dazhou Zhu³, Peichen Hou², Baozhu Yang⁴, Cheng Wang²,
and Jiuwen Zhang¹

¹ Information Science & Engineering, Lanzhou University, Lanzhou 730000, China

² Beijing Research Center for Information Technology in Agriculture, Beijing 100097, China

³ Beijing Research Center of Intelligent Equipment for Agriculture, Beijing 100097, China

⁴ Beijing PAIDE Science and Technology Development Co., Ltd., Beijing 100097, China

lulu_purple@163.com, jiangfubin0702@126.com,

{zhudz, houpc, yangbz, wangc}@nercita.org.cn, zhangjw@lzu.edu.cn

Abstract. To realize in vivo, real-time, non-invasive and in-situ detection analysis on the dynamic changes of ion flows in plant tissues, organs, cells and others under natural conditions, this paper designed three-dimensional electronic control motion platform of high-accuracy so as to realize the highly-accurate motion control in micron order and enable glass microelectrode to measure the plant tissues, organs and cells in its best state. The apparatus requires the portable design, so this paper chose the ion flow detection device with small size and high accuracy and micro integrative drive control module. Also graphical programming software LabVIEW was utilized to send serial port commands so as to realize the accurate and reciprocating motion of glass microelectrode at different positions and further accurately detect the plant microscopic dynamic ion flow parameter. The test showed that this control software could realize highly-accurate positioning of $0.6371\mu\text{m}/\text{step}$ in three-dimensional space and the software system could operate steadily, which provides strong supports for the plant microscopic ion flow detection.

Keywords: ion flow, LabVIEW, software control, accurate positioning.

1 Introduction

Same as the principles of non-invasive micro-test technique, plant microscopic ion flow detection technique is a new technique used to measure and study ion/ molecular flow. NMT (Non-invasive Micro-test Technique) is a general term of a wide mass of microelectrode techniques, including non-invasive scanning ion-selective electrode technique (SIET), which can obtain the ion or molecular flow inside and outside membrane of samples in premise of no destroy of test samples [1-2]. With profound three-dimensional measurement mode [3-4], this technique not only can measure the absolute concentration of ion/ molecular in stationary state but also can measure the motion rate and motion direction of plant samples. It has been widely used in the studies of plant cells and animal cells and also integrated with other microscopical techniques [5]. Some existing biological precise instruments have been used in the

plant ion flow detection by experts at home and abroad, for example, Non-invasive Micro-test System by USA Younger Company. Through the automatic control of computer and precision machinery and on the basis of ion flow velocity calculation principle in Fick law, this paper carried out three-dimensional, real-time and dynamic measurement under the condition of no contacting with test samples to obtain the information about ion/ molecular concentration, flow velocity and motion direction of samples. However, in consideration of the expensive cost, complex structure and wires, large size and immovability, this apparatus cannot be applied in the plant ion flow detection under natural conditions.

On the basis of the small-size ion flow detection motion device and hardware basis of micro integrative stepper motor drive control module, this design carried out virtual instrument development and design according to the concrete demands of ion flow data collection and motion mode. LabVIEW control software was utilized to send serial port commands to control stepper motor, which drives ion flow detection device to control the microelectrode. In this way, the accurate positioning in X, Y and Z directions can be realized and the gradient changes of ion concentration at different measurement points can be acquired. Furthermore, the absorption and diffusion rate and trend of certain target ions of the plant can be reflected. In this way, people can find the laws and characteristics of plant dynamic growth.

2 Control System Constitution of Motion Device

To satisfy the detection requirements of filed plant in-vivo ion flow, the apparatus shall be portable and have high accuracy and stability. To meet the above requirements, the designed control system in this paper is composed of four parts, upper computer, stepper motor drive control module, ion flow detection motion device and bundled control software of upper computer. Stepper motor drive control module consists of stepper motor drive control driver UIM242, control protocol converter UIM2501 and attached devices, which can connect multiple control drivers and realize the synchronous control of stepper motor by aid of its high integration level and micro and portable features. The ion flow detection motion device is respectively equipped with stepper motors in X, Y and Z directions, which converts the input pulses into corresponding angular displacements. Then through elaborate mechanical drive, they are converted into executive components of linear displacement and their input variables are impulse sequences and the output results are the corresponding angles or linear increments, whose rotations are operated in settled angle step by step [6-7]. The accuracy of this three-dimensional motion device can reach $0.094\mu\text{m}/\text{step}$, which can accurately positioning the sampling probe of ion flow detection motion device and control it to complete reciprocating motion. The bundled control software of upper computer owns sound human-computer interaction interface and good stability and portability.

3 Overall Design of Control System Software

This software system adopted LabVIEW virtual instrument development platform. The virtual instrument is the hardware platform which takes PC computer as the core and can be designed and defined by users. It has virtual panel and its core is software

technology [8]. Because LabVIEW software can provide many controls whose appearances are similar to traditional instruments, it is convenient to create user interface. Users can define and manufacture various kinds of instruments according to their own demands, so this design adopted LabVIEW development platform. Function library of graphical programming software LabVIEW includes data acquisition, GPIB, serial port control, data analysis, data display and storage. The programming of LabVIEW software control mode is so easy that users can construct the required instrument system. Furthermore, sound human-computer interaction interface makes the control more convenient and flexible [9-11].

Visual graphical programming language covers front panel and program chart. Front panel, similar to the operation panel of the instrument, includes knob, on/off keys and others. Program chart is the core of the software, which can be used to realize the functions of control software. The program execution sequence depends on the data flow direction [12].

The software is based on LabVIEW human-computer interaction interface, which can send control commands on stepper motor control driver to control instruments through interaction interface and obtain the equipment operational condition. To execute electrode three-dimensional motion control and data acquisition operation, the control software is composed of four parts, serial port command packaging, RS232 serial port protocol transmission, information feedback and control software interface program. Serial port command packaging packages hexadecimal character string command into modules that can be called conveniently. RS232 serial port protocol transmission can connect the command and instrument and send the data to the stepper motor drive control driver according to its specified communication mode. After receiving the control command, the stepper motor drive control driver will analyze the commands, complete the specified motions and return to hexadecimal character string. Information feedback module is specific to analyze the returned value character string and timely reflect the motion state of stepper motor. At the same time the limit sensors in each direction of the three-dimensional motion device analyze the feedback information to get the level fluctuation function of sensors and achieve motion protection. Control software interface program can provide the interaction interface which controls corresponding motions of ion flow detection motion device. Through this interface, users can complete all the operations of ion flow detection.

3.1 RS232 Serial Port Communication and Information Feedback

PC serial port has point-to-point communication with ion flow detection motion device and all commands are based on 7-digit standard ASCII commands of RS232 Protocol. Protocol converter control the subordinate control driver with high speed through CAN Protocol. In this way, serial port communication mode is adopted. The correctness of commands is related to the accuracy of experimental data acquisition. Wrong command may result in the damage of sampling probe of ion flow. To avoid this, information feedback module was designed in LabVIEW control software, which made it convenient for users to see the sent commands and analyze the feedback

information. In this way, the motion protection of ion flow detection motion device can be achieved.

LabVIEW provides powerful Virtual Instrument Software Architecture (VISA) library, which includes basic serial port operation functions such as serial port settings, serial port writing, serial port reading, serial port closing and so on [13]. To realize the serial port communication function, the serial port has been set as follows through serial port configuration functions. Baud rate = 9600; each byte includes one start bit, 8-bit data bits and one stop bit. There is no flow control and parity check bit. If time-out is over 10s, waiting time of 50ms is initiated. The serial port parameter configuration of both communication parties shall be same, or it will fail to work. Send the serial port commands in form of hexadecimal character string to the specific equipment of VISA resource name.

Wait for 50 ms delay before reading operation in order to determine the number of bytes in the receive buffer. Attribute nodes of Byte at Port return to the existing number of bytes in input buffer in order to guarantee the integrity of the received character string. Make use of reading function to read the data in the specific equipment of VISA resource name and the bytes of specific amount in the specific equipment. Then display the read data in the buffer as feedback information.

Feedback information is the information sent by control driver to upper computer. After receiving the command, the control driver will immediately send the confirmation message. If the command is wrong, it will not be executed. Once the required number of bytes actually read from the input buffer is finished or there is time-out error, this reading operation can be over.

3.2 Accurate Positioning of Ion Flow Detection Motion Device by LabVIEW Control

Plant microscopic ion flow detection experiment requires the three-dimensional microspur motion of microelectrode, which can enable the ion flow detection microelectrode to detect the ion absorption and release physiological properties of plant cells in optimum state. Therefore, the accurate positioning of ion flow detection motion device plays a vital role. This design adopted command-packaging motion control mode to respectively control the ion flow detection motion device in X, Y and Z directions so as to realize the highly-accurate positioning of ion flow detection motion device and support the relevant data collection of ion flow. Take motions in X axis as an example and its accurate positioning chart is shown as Fig. 1. The motions in Y axis and Z axis are similar to that in X axis.

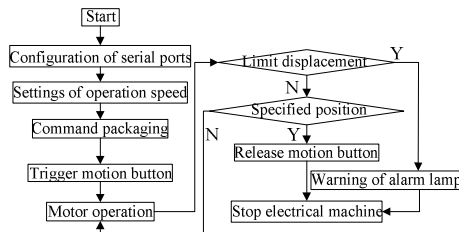


Fig. 1. Accurate positioning chart of stepper motor

First, the address of stepper motor control driver which receives commands shall be assigned. Commands include operation speed, enabling and stop. “+” in the operation speed command represents forward motion while “-” represents backward motion. The motion control button adopted the trigger mode of maintaining conversion until release. Selection function was used, so once the motion control was triggered, the motion enabling command could be triggered. After being released, execute the stop command “OFF” and realize the accurate positioning of the probe of ion flow detection motion device. Its real-time performance was good. After the serial port communication was over, device dialog handle must be closed and the serial port resources shall be released, or there would occur errors in serial port resource when the program is operates next time. The forward motion control program chart in X axis is shown as Fig. 2.

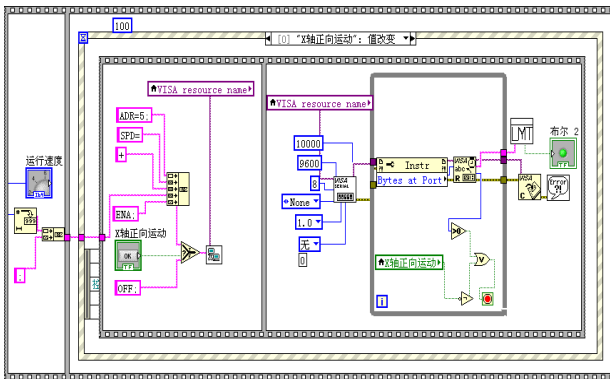


Fig. 2. Forward motion control program chart in X axis

3.2.1 Motion Control and Command Confirmation

Trigger forward motion button in X axis in the front panel and through serial port communication and information feedback subprogram, the confirmation information of the command can be received. Then determine whether the sent command is consistent with the user demands.

The message length is flexible and the maximum shall be 13 bytes. The feedback information is composed of the following parts, header, driver identification code, information identification code, information data and end mark.

- 1) Header represents the start of feedback information.
- 2) Driver identification code represents the site identification number of the control driver and the identification number of teach control driver is unique.
- 3) Information identification code indicates the attribute of the message.
- 4) Information data: control driver can immediately reply all the parameter information including the latest set one, read the feedback information and obtain the required parameter values through displacement.
- 5) End mark: the control driver adopts 0xFF as end mark to indicate the end of one message.

Input command is ADR=5; SPD=6000; ENA;, the aim is to enable X axis of control driver with identification number 5 to do enabling motion with speed of 6,000

pulses per second. After receiving the command, the control driver immediately displays the confirmation information, AA05 D0FF AA05 B500 2E70 FFAA 057F 0400 2E70 0000 0000 00FF. The meaning of the feedback information is as follows.

AA: command confirmation feedback.

05: specify the command object as the control driver with identification number 5.

D0: information identification code of driver site.

FF: end mark.

B5: information identification code of expected speed.

00 2E 70: rank according to 8-bit data byte, with high-order ahead and low-order behind, shown as Figure 3. Convert 7-bit data byte into 16-bit data through displacement and decimal system of 6,000. Namely the expected speed is 6,000 pulses per second, which is consistent with the user demands.

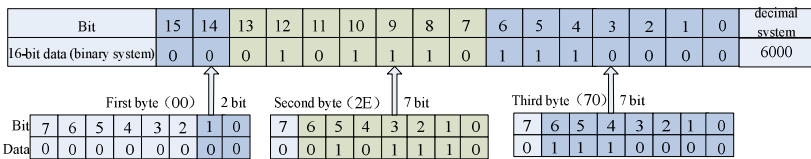


Fig. 3. Conversion of data byte

7F: synthetic byte, whose format is shown as table 1. The binary system of 7F is 01111111, which is one-to-one correspondence to the table. It can be converted that the stepper motor is forward enabling in form of 16-subdivision and automatically cut down the current when the motor stops.

Table 1. Synthetic byte in the feedback information

	7	6	5	4	3	2	1	0
Value	Unuse d=0	Cut current in half	Enablin g /off- lining	DIR directio n	Subdivision synchronizing and 15 represents the 16- subdivision.)	value	-1 (0 represents	

04: Current byte. Current value = actual current * 10. If Current value is 4, the actual current is 0.4 A. The actually set current is consistent with this.

00 2E 70: the expected speed is 6,000.

00 00 00 00 00: the expected displacement is not set. Convert 5 data bytes into 32-bit data to express the expected displacement. The conversion mode is similar to that of expected speed and here is not repeated.

3.2.2 Motion Protection

Ion flow detection motion device is precise instrument. The three dimensional motion displacement is expressed as X (slanted toward) =Y=Z≥26mm so as to protect the ion

flow detection motion device from damage due to exceeding the limited range. The stepper motor is equipped with limit sensors respectively at the forward and backward motions in X, Y and Z directions. How to determine whether the location of the stepper motor triggers the limit switch and after that how to control its motion state are the key techniques of motion protection of ion flow detection motion device. Therefore, this paper designed the motion protection subprogram and the limit program chart is shown as Fig. 4.

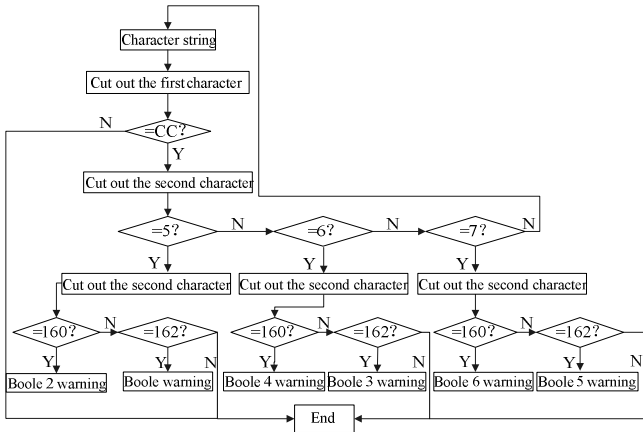


Fig. 4. Limit program chart

The limit sensor at both ends of ion flow detection motion device is connected with the sensor of stepper motor control driver. In this way, the event of sensor triggering occurs. The change notification of real-time state can response to the sensor event. There is feedback information in the reading buffer, which is still expressed in form of hexadecimal character string. Cut-out character string function is adopted to determine each byte. To prevent from the accident due to exceeding the limited displacement, once the limit sensor is triggered, immediately order the stepper motor to stop. Making use of the sensor event in the stepper motor control driver, when the limit sensor is at low level, the stepper motor stop working and the alarm lamp is lightened for warning.

The meanings of bytes are as follows.

- (1) The first byte corresponds to CC, expressing the state feedback information.
- (2) The second byte corresponds to one of 5, 6, or 7, namely the control driver identification codes respectively corresponding to X, Y and Z directions of ion flow detection motion device.
- (3) The third byte corresponds to A0 (whose decimal system is 160) and A2 (whose decimal system is 162), respectively representing that limit sensors of S1 and S2 are in the falling edge.

In case of forward motion of X axis, the feedback information displays character strings of four-byte, CC05 A0FF. The bytes can be converted that sensor S1 of control driver with site number of 5 is at low level, indicating that there is warning at

the forward motion of X axis and the corresponding Boole warning lamp is triggered. Finally, the stepper motor stops motion. The warning of the alarm lamp in the front panel of the main program is shown as Fig. 5. Two alarm lamps respectively set in X, Y and Z directions represent the forward limit and backward limit. In this way, the motion protection of ion flow detection device can be achieved.



Fig. 5. Front panel of limit warning

3.3 Reciprocating Motion of the Probe of Ion Flow Signals Controlled by LabVIEW

After the accurate positioning of the probe of ion flow detection motion device, in consideration of the practical application demands of plant ion flow detection experiment, this paper collected reciprocating motion of the probe through the control signals of ion flow detection motion device. During the process of reciprocating motion, the required experiment data by users were further studied and explored. The program chart of the reciprocating motion module is shown as Fig. 6.

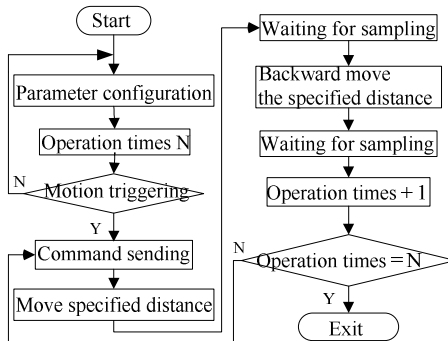


Fig. 6. Reciprocating motion chart

The front panel of reciprocating motion is shown as Fig. 7. Its function is to order the ion flow detection motion device to do the reciprocating motion from origin point to specified position and back the origin point again according to the set operation times in X axis. After setting the operation speed, operation times, waiting time of sampling, expected displacement increment and other parameters, trigger the start motion and the stepper motor starts to move. After it reaches the expected position, pause the waiting time of sampling and return to the origin point. In this way, reciprocating motion takes shape.



Fig. 7. Front panel of reciprocating motion

The sampling probe triggers forward motion and backward motion according to the set speed and displacement and after reaching the specified position, it waits for the sampling time. By setting the expected position as 0 and enabling command, the probe of ion flow sampling returns to the origin point again and completes one reciprocating motion. After the waiting time of sampling, which is same as that in the above procedure, the next reciprocating motion starts. Execute while loop for once and the operation times are taken as the cycle count of while loop. Until the set operation times set by users are completed and while loop is over, can it stops motion. Waiting time shall be calculated in the procedure. The motion time of stepper motor = displacement distance/operation speed. Procedure waiting time = operation time + sampling waiting time. The unit of operation time and sampling waiting time is second while that of procedure waiting time is millisecond. The conversion between these two units shall be carried out. Sampling waiting time can be set differently according to the experimental requirements of users.

Electric pulse signal received by stepper motor is converted into angle displacement or linear displacement. Through controlling the number of pulses, the angle displacement is controlled. In the plant microscopic ion flow detection experiment, ion flow detection motion device converts the motor power into linear motion. The reciprocating motion needs the microelectrode to accurately move to the

specified position and the length is of micron order. By aid of amplification factor k , angle displacement is converted into accurate distance length S . Because the eyepiece of microscope has a scale with $10\mu\text{m}/\text{square}$, people can test the precision through the relationship between pulses and real distance. The test results are showed as table 2.

Table 2. The datas of measuring the accuracy

Pulses (number)	Real distance 1 (μm)	Real distance 2 (μm)	Real distance 3 (μm)	Real distance 4 (μm)	Mean accuracy ($\mu\text{m}/\text{step}$)
10000	390	385	387	390	0.6208
5000	198	199	200	199	0.6368
2500	104	102	101	101	0.6538
Accuracy=0.6371 $\mu\text{m}/\text{step}$					

STP represented the relative displacement increment, defined with pulse count. In stepper motor control driver, 16 subdivision was executed, this experiment measured the stepper motor accuracy of $0.6371\mu\text{m}/\text{step}$, so $0.6371/16 * \text{STP} = S$, $\text{STP} = k * S$ was utilized. In this way, people can deduce that $0.6371/16 * k * S = S$. So $k=25$. The microscope imaging is showed as Fig. 8.

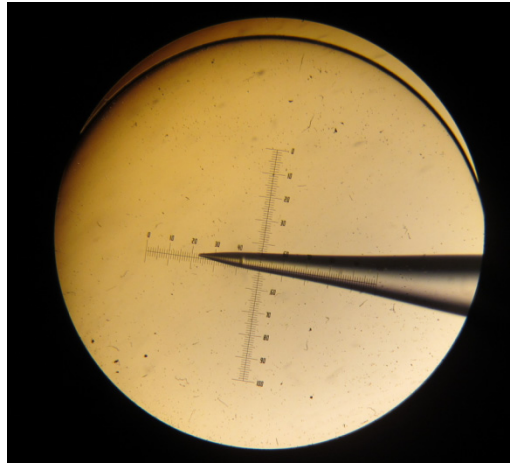


Fig. 8. The microscope imaging

4 Functional Test on the Control Software of Ion Flow Detection Motion Device

After set up the whole system, the functional test was carried out on the control software. The plant microscopic ion flow detection belongs to micro measurement, so

naked eyes cannot observe the displacement distance of probe microelectrode. Therefore, photoelectric microscope was adopted. Dividing rule is equipped on objective lens, with $10\mu\text{m}$ division value. Move the probe into the view distance and people could clearly observe the movement of the probe. Via multi-measurement average, we got the accuracy was $0.6371\mu\text{m}/\text{step}$. However, it is inevitable to generate errors. The reasons for errors are as follows. 1. The division value of photoelectric microscope is $10\mu\text{m}$, so the reading number in the measurement all were estimated numbers. 2. There existed accumulated errors during the mechanical rotation process but the accuracy of $0.6371\mu\text{m}/\text{step}$ still could satisfy the $2\mu\text{m}/\text{step}$ experimental requirement of plant ion flow detection. Also the motion device based on control software LabVIEW has sound real-time performance and stable performance.

5 Conclusions

By aid of LabVIEW development platform, the control on the motion device of plant microscopic ion flow detection is realized. The processing speed is fast and the real-time communication between GPIB and PC [14] can immediately feedback the motion information and have high accuracy and good real-time performance [15]. Three-dimensional microspur motion device based on this technique can satisfy the high requirements of precision measuring instrument and the control software can change control modes according to user demands at any time. The system can operate stably and have strong portability as well as accurate, flexible and portable features. However, the aesthetics of control software still need improvements. Repeated debugging and experimental detection as well as feedback of relevant experimenters are necessary for the improvement of the whole system. In this way, the usability of the software and the stability of the control software of plant microscopic ion flow detection motion device can be further improved and perfected.

Acknowledgment. Funds for this research was provided by the National key scientific instrument and equipment development project (2011YQ080052), Major national science and technology achievement transformation projects (finance construction [2012] No. 258) and Agricultural science and Technology Achievements Transformation Fund Project (2012GB2A00001).

References

1. Kunkel, J.G., Cordeiro, S., Yue, X., et al.: The use of non-invasive ion-selective microelectrode techniques for the study of plant development. In: Volkov, A.G. (ed.) *Plant Electrophysiology-Theory and Methods*, ch. V, pp. 109–137. Springer, Heidelberg (2005)
2. Xu, Y., Sun, T., Yin, L.: Application of non-invasive microsensing system to simultaneously measure both H^+ and O_2 fluxes around the pollen tube. *Journal of Integrative Plant Biology* 48(7), 823–831 (2006)

3. Yin, L., Yu, S., Yue, X.: Scanning ion-selective electrode technique and the application in higher plant research. *Progress in Natural Science* 16(3), 262–266 (2006)
4. Richardson, D.C., Richardson, J.S.: Teaching molecular 3-D literacy. *Biochemistry and Molecular Biology Education* 30, 21–26 (2002)
5. Ding, Y., Xu, Y.: Non-invasive micro-test technology and its applications in biology and medicine. *Physics* 36(7), 548–558 (2007)
6. Rahman, M.F., Poo, A.-N.: An Application Oriented Test Procedure for Designing Microstepping Step Motor Controllers. *IEEE Transactions On Industrial Electronics* 35(4), 542–546 (1988)
7. Zhou, L., Yang, S., Gao, X.: Modeling of stepper motor control system and running curve simulation. *Electric Machines And Control* 15(1), 20–25 (2011)
8. Long, H., Zhai, C., Liu, X., et al.: Testing system of step motors and drives based on virtual instrument. *Electric Machines And Control* 10(6), 553–557 (2006)
9. Li, J., Gao, W.: Design of Step Motor Control System Based on LabVIEW. *Science & Technology Information* 15, 85–86 (2010)
10. Jiang, J., Wu, B., Gao, J., et al.: Design of Stepper Motor Control by Virtual Instrumentation via Serial Interface. *Electronic Science and Technology* 25(8), 46–48 (2012)
11. Chen, D., Yao, C.: The design of PID control system based on LabVIEW for step motor. *Industrial Instrumentation & Automation* 15, 48–49 (2005)
12. Chen, F., Li, J., Ma, S., et al.: Design of Step Motor Control System Using LabVIEW. *Journal of Shanghai University (Natural Science Edition)* 12(1), 89–92 (2006)
13. Chen, Y., Yang, C., Cao, J., et al.: Energy normalized photon-stimulated discharge spectra of polymer dielectric film. *Electric Machines And Control* 13(First Edition), 41–51 (2009)
14. Gu, J., Qin, S., Jin, L., et al.: Experiment Study On The Resonant Frequency Of Usm Based On LabVIEW. *Proceedings of the CSEE* 23(8), 91–95 (2003)
15. Xiang, X., Xia, P., Yang, S., et al.: Real-time Digital Simulation of Control System with LabVIEW Simulation Interface Toolkit. In: *The 26th Chinese Control Conference*, Hunan, pp. 318–322 (2007)

Interactive Information Service Technology of Tea Industry Based on Demand-Driven

Xiaohui Shi and Tian'en Chen

National Engineering Research Center for Information Technology in Agriculture, Beijing
100097, China

{shixh, chente}@nercita.ogr.cn

Abstract. Information service technology is a bridge between user and information resource, also is the critical factor to weight the quality of information service. Focusing on the information service features of tea industry, the demand-driven and interaction of information service were emphasized in this paper. User and market as the major criterion for testing the quality of information service, the interactive information service mode based on the demand-driven was proposed to realize the maximum of information service value. Demands of users as the driving factor in the mode, introducing the interactive ideas of loop optimization on information demand and combining the push and feedback mechanism of information, the information service mechanism was further optimized to meet the actual demands of users.

Keywords: tea industry, demand-driven, interactive mode, information service.

1 Introduction

The main countries for tea production are in Asia, Africa and Oceania, but the most countries that have relative mature development in the field of agricultural informationization are mostly in Europe and America, and tea industry has lots of traditional factors, which lead to tea industry information service haven't got the real development, the research status of tea industry information service are almost blank around the world.

As we all know, China is the No.1 for tea tree acreage and No.2 for tea production, tea industry is always the traditional advantage industry[1]. However, comparing with our strong growth of tea industry, its information service is not suitable for meeting the actual demand. The existing tea industry information websites are almost lack of practicability, timeliness, traceability, predictability and sustainability, these actual issues made the information resource of tea industry difficult to be used constantly. But what are the basic reasons? Firstly, because of these characteristics such as regional difference, time difference, industry difference and user group difference of tea industry, the information cannot be found, selected and absorbed effectively if the information is not timely adjusted by information service provider; secondly, the professional and unified information service platform of tea industry has not formed,

which lead to the duplicated construction in information service websites of tea industry, one-sided information service content, lack of service characteristics and low service effectiveness.

In this paper, focusing on the issues existing in the information service of tea industry, based on analysis of information demand, combining the available and mature information service technologies, and introducing the interactive idea of loop optimization, the interactive information service mode of tea industry based on demand-driven has been presented for carrying out individualization service theory of tea industry.

2 Characteristics of Tea Industry Information Service

(1) Regionality

Agriculture influenced by climate, soil, humanity and surrounding is different from industry. There are two reasons lead to the regional differences: on the one hand, the differences between zonality and azonality of natural situation determine the fitness and range for agricultural biology to grow; one the other hand, social and economic condition determine the layout, structure, management mode of farming, forestry and animal husbandry, the direction of resource using, level of production and development. Tea industry as a part of agriculture, also has an obvious regionality. The differences in different tea production areas obviously present different tea varies, tea processing technologies, production and sales structure, tea-drink cultural, so the regionality of different tea production areas should be adequately considered.

(2) Seasonality

Tea tree is perennial woody, which has a total development cycle in whole life as well as yearly development cycle in one year. Tea tree's yearly development cycle refers to its growth and development progress in one year. Tea tree is both influenced by its growth characteristics and external environment situation, represents different growth characteristics in four seasons, such as bud's sprouting and pause, leaf's stretch and maturity, root's growth and death, blossom and fruiting. Tea information service must to provide timely information service in different period to ensure the commercial value of tea product.

(3) Comprehensiveness

Tea, which is a kind of economic crop with a high commodity, tea industry's information has obvious relevance. The comprehensiveness of information presents a piece of information may directly or indirectly have correlation and interaction with several pieces of information, so a piece of information usually is the synthesis of several kinds of information. High or low yield and high or low quality in elemental area determine the bud's quantity and raw material' quality, which also is determined by the development status of tea's shoots and having the reasonable tea tree's

cultivation and picking or not, and so on. It indicates that these related factors should be considered, providing reliable information service.

(4) Complexity

The tea industry's characteristic of being related with agriculture, industry and commerce lead to the close relationships which are constructed between rural and town, tea farmers and tea companies, links and links in tea industry chain. So that the "digital gap between urban and rural areas", the differences in the subjects of tea industry information service and information demands in every industry links must to be considered in tea industry information service. If information service is lack of pertinence, users will not find the information they are interested in and they need, which will seriously influence the quality of tea industry information service.

3 Analysis of User's Demand

The process of information consumption consists of information demand, information acquisition, information absorption and information creation, it indicates that the information consumption starts from information demand[2]. Along with the popularization of internet technologies, and expansion of scale and function of agricultural information system, user's demand presents dynamic characteristic and the price of demand's change presents nonlinear growth, so the analysis of information demand is more important. Whether the analysis of information demand is rational or not will decide the quality of information service.

3.1 Analysis of Information Demand for Different Tea Production Areas

In China, there are four areas of tea production in Jiangnan, Jiangbei, Huanan and Xinan respectively[3], because of obvious differences in geographical location, tea varieties, type of tea and soil environment (The brief introduction about four tea production areas of China was presented in table1). The existing differences, which contribute to form the individual information service for tea industry, are the basis for digging information demand. For example, some tea areas of Jiangbei usually not only are affected by late spring coldness between March to April but also autumn drought between August and September, which hinder the growth and development of tea tree and lead to protected tea became a better choice for tea planters in there. Obviously, users of tea production area of Jiangbei are more interested in information of cultivation and management related to protected tea, hence, the information service program that is suitable for tea production of Jiangbei must be established.

Table 1. Four tea production areas of china

Area of Tea production	Main type of tea	Main variety of tea	Temperature (°C)	Growth period (d)	Type of soil
Jiangnan	Green tea,	Shrub of	Annual	225 ~	Red soil is main part, yellow soil and yellow brown soil are small part
	Black tea,	middle-and-small-leaf	average 15~18.5	270	
	Oolong tea,	is main part,	The lowest — 5		
	White tea,	Arbor of	~ — 1		
	Dark tea,	middle-and-large-leaf	Extreme low —		
	Yellow tea	is small part	16~ — 8		
Jiangbei	Green tea	Shrub of middle-and-small-leaf	Annual average	180 ~	Yellow brown soil is main part, brown soil is small part
			15~16	225	
			The lowest — 7		
			~ — 3		
			Extreme low —		
			20~ — 6		
Huanan	Broken black tea	Arbor of large-leaf, Semi-arbor of middle leaf	Annual average	> 300	Latosol or lateritic red soil is main soil, yellow soil is small part
			20~29		
			The lowest		
			7~12		
	Pu'er tea		Extreme low —		
	Liubao tea		3~4		
Xinan	Black tea,	Shrub, small-arbor,	Annual average	200 ~	Lateritic red soil, yellow soil, hilly led soil and brown soil
	Green tea,	arbor	14~18.5	230	
	Borde-selling tea,		The lowest 4 ~		
	10				
	Scented-tea,		Extreme low —		
	Pu'er tea		3~4		

3.2 Analysis of Information Demand in Every Link of Industry Chain of Tea

Tea industry, which is one of agricultural industry, consists of cultivation, processing, storage, transportation and sale[4], forming a chain organization similarly. So the every link of industry chain of tea became the emphasis for analysis of information service demand. For example, in the link of tea cultivation, to obtain the tea variety information of multi-resistance and high-resistance is vital for tea cultivator to improve the quality of tea. It can be seen that the information about tea processing machine, tea logistics, tea import and export in the next three links is concerned by users, therefore, component elements and units of information demand of tea industry chain are the basis for searching information demand, and were analyzed primarily in figure 1.

Industry architecture unit		Information demand unit
Cultivation	Variety & propagation	Variety breeding, Variety match, Sexual multiplication, Vegetative Multiplication, etc.
	Construction of tea garden	Rejuvenation, Replanting, Soil improvement, etc.
	Soil management	Tillage, Water management, Fertilize, etc.
	Cultivation of tree crown	Pruning, Comprehensive maintenance for tree crown, etc.
	Safety production	Meteorological disaster and service, Safety production of non-pollution tea garden, etc.
	Picking tea	Picking standard, Storage of fresh leaf, Fresh-keeping of fresh leaf, etc.
Processing	Initial processing	Spreading, Withering, Rotating, Fermentation, etc.
	Precision processing	Dross elimination, Adjusting difference, Packaging, etc.
	Deep processing	Extraction of functional component, Tea liquid drink, Healthy tea, etc.
Storage & transportation	Storage & transportation of fresh leaf	Acceptance, Classification, etc.
	Storage and transportation of made tea	Storage device, Transportation, etc.
Sale	Domestic sale	Brand construction, Wholesale, Exhibition, etc.
	Exportation	International certification for quality safety, Ocean transport, etc.

Fig. 1. Information demand element partition of tea industry

3.3 Analysis of Information Demand of Service Subject in Tea Industry

Information service subject of tea industry consists of information supplier, information transportation carrier and information receptor, the latter two elements determine the diffusion of information and application of scientific and technological achievements for tea industry[5], which plays an important role in the system of information service. For example, information of tea cultivation has been paid more attention by the manager in planting base, large scale grower, scientific research institution and specialized cooperation organization respectively. In this study, there were four kinds of arrows, respectively pointing to four links of tea industry, which told us that different subjects had different information service demands in different links of industry chain of tea.

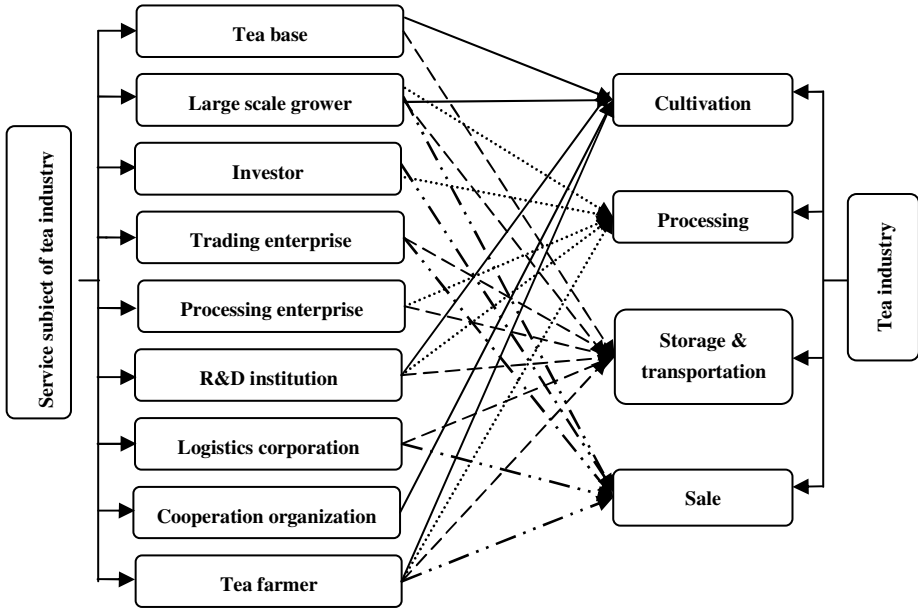


Fig. 2. Information demand matching between service subject and industry ring for tea industry

4 Interactive Information Service

Interactive information service is to realize personalized demand-oriented service through user platform interacting with user[6]. In this paper, based on some traditional technologies of information dissemination and acquisition, the interactive information service mode of tea industry has been established to emphasize the importance of demand-driven of user, close connection of push and feedback, loop optimization of demand and response, also carries out a guidance scheme of policy-making, directivity and strategy, and furthermore, manager will participate the system coordination when it is needed, to guarantee the complete mapping between demand layers and business layers, in that way, the personalized information demand of user can be meet and handle intelligently.

4.1 Key Technologies

(1) Information Pull technology

Information pull, a traditional way of information acquisition, means that user query information on the network with a purpose[7]. The process starts from sending a request to Web, then server will dealt with the received request and return the result needed by user, passively completing the task of data transport. Recently, search engine has become an important means of information acquisition in the process of information pull, and was praised as “information grasper”.

(2) Information push technology

Information push technology is a technology of information release and transportation, namely, through the corresponding technology standard and agreement, information can be obtained from information resource to meet the demand of user. In recent years, as a hotspot of network technology, push technology has become one of important means for agricultural information service[8].

(3) Information feedback mechanism

Information feedback is a portion of information returned to output side after all information starts from information resource and is passed to destination through channel. These characteristics of information feedback mechanism, such as pertinence, timeliness and continuity, directly represent the demand of user, also is real and effective basis for information provider to adjust the management decision, guaranteeing the quality of information. The newest results can be received by ways of online browse, mail subscription, SMS and so on.

(4) Information customization

Information customization is one of means for information acquisition, namely, the newest “dynamic” results can be “followed” through the customized network. In the process of information customization, first of all, information is provided for user after analysis, filter and integration which focus some characteristics of user, such as age, industry, level and interest and so on, the new demand of user will be fed back to center of service system to guarantee the pertinence of information service.

4.2 Mode of Interactive Information Service

After the study of information analysis of tea industry and key technologies of information service, the mode of interactive information service for tea industry has

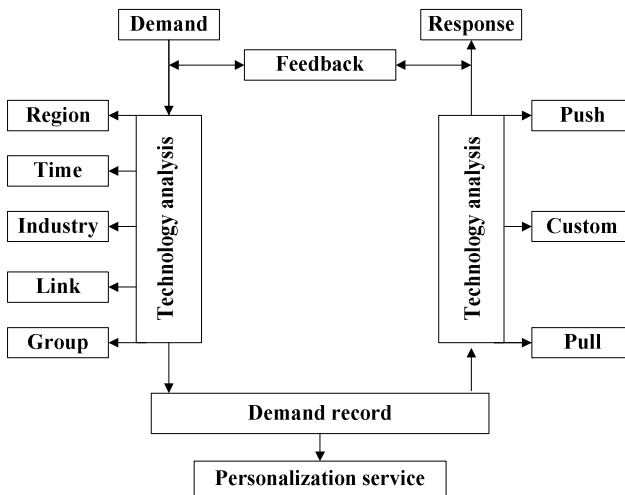


Fig. 3. Interactive information service mode for tea industry

been proposed to consider the characteristics of timeliness, accuracy, pertinent and availability in information service of tea industry.

(1) According to the features of region, time, industry, link and group, users have been classified by “static demand analysis” to formulate a primary scheme of information service. For example, where the user can be judged by the key information of registration, and which link of tea industry chain the user in also can be judged by the visit time of user.

(2) “Dynamic demand analysis” has been introduced based on the completed “static demand analysis”, namely, the contents of information service have been updated and integrated timely with the analysis of the visit record and feedback information, making users virtually participate the construction of information service system.

(3) Based on “static demand analysis” and “dynamic demand analysis”, information demand of user has constantly been responded by mature application of pull technology, push technology, customization technology and feedback technology. Information began with sending and ended with response, forming static information interaction loop mode, whether user is satisfied with the response to lead to stop or not.

5 Conclusions

In this paper, with the purpose of demand analysis of user, the differences in tea product areas, links of chain and service subject have gradually been carried out. Ultimately, interactive information service technology of tea industry based on demand-driven has been proposed, the main achievements and idea are represented as follow: (1) because of demand analysis was the basis for information construction in agriculture, the demand units involved in tea production areas, industry chain of tea and service subject of tea industry needed to be clearly presented; (2) interactive information service as one of personalized information service, which included pull, push and feedback of information, contributed to form the positive circle that established between users and constructors for tea industry information service; (3) the categorization in agricultural informationization construction showed professionalism and comprehensiveness, reflecting a significant trend for agricultural informationization construction. And the tea industry informationization construction meant that agricultural informationization construction works from the more general to the more specific, which will positively and vigorously promote information construction in other field of agriculture.

6 Discussion

(1) Shortage of information resource and disconnection of information service
Tea industry as one of the advantage and economic industry in China, always maintains the relative traditional operation method. Recently, every main tea production area has become aware the significance of tea industry informationization, and gradually built relative websites for tea industry information service, but the shortage in information resource didn't meet the every-growing information demand, especially the serious

disconnection between information service and user's demand has been seriously restricting the development of tea industry informationization.

(2) Based on information demand and emphasis on personalized service

Taking the tea information demand characteristics as the breakthrough point, based on the demand analysis of tea information service, the interactive information service model for tea industry has been proposed, namely, endeavoring to seek a personalized information service scheme according to the actual situation, which can effectively avoid the reconstruction and overbuild and is favorable for improve the quality of information service, finally contribute to the transformation from traditional agriculture to modern agriculture.

Acknowledgements. This paper is supported by a grant from National Science and Technology Support Program (2013BAD15B05).

References

1. Liu, C., Xu, M., Liu, P.: Path Analysis on the Development and Cultivation of the Tea Industry in China. *Resources Science* 33(12), 2376–2385 (2011)
2. Sun, L.-Y.: The General Situation of the Study on the Information Demand. *Sci.- Tech. Information Development & Economy* 16(13), 13–14 (2006)
3. Zhang, C.-Z., Ding, Z.: Techniques of Tea Counter-season Production in the Tea Production Areas of Jiangnan. *Nonwood Forest Research* 24(2), 55–58 (2006)
4. Li, J.-M., Zeng, F.-S., Tang, H.: *Abroad management of referential experience for agricultural production*. China Agriculture Press, Beijing (2007)
5. Chen, L.-P.: *Study on Channels and Patterns of Information Service in Rural Area*. Chinese Academy of Agricultural Science, Beijing (2006)
6. Deng, S.-L.: Analysis on Elements and Orientation of Interactive Information Service. *Information Studies: Theory and Application* 32(1), 18–21 (2009)
7. Wang, H., Chen, L., Zhang, L.: Information Pull and Push Technology. *Information Science* 22(12), 1440–1443 (2004)
8. Chen, C., Liao, G., Shi, X.: The Personalized Push Technology of Agriculture and Rural Information Service. *Chinese Agricultural Science Bulletin* 27(29), 151–156 (2011)

Design and Development of Intelligent Monitoring System for Plastic Tea Greenhouse

Fengyun Wang¹, Jiye Zheng¹, Lin Mei¹, Zhaotang Ding², Wenjie Feng¹,
and Lei Wang^{1,*}

¹S&T Information Engineering Research Center, Shandong Academy of Agricultural Sciences,
Jinan 250100, Shandong Province, P.R. China

²Tea Research Institute, Qingdao Agricultural University, Qingdao 266109, Shandong
Province, P.R. China

{wfylylily, jiyezheng, meilin670607, dztttea}@163.com,
fengwjcn@qq.com, nkywl@126.com

Abstract. The article studies the growth environment conditions of tea and puts forward a wireless intelligent monitoring system for plastic tea greenhouse. According to the environmental requirements of tea tree, this article firstly defines the environmental parameters for planting tea in the greenhouse, and then designs the hardware and software of the intelligent monitoring system of tea in the greenhouse, and finally concludes the characteristics of this system. Through the practical application in tea greenhouse, the system decreases the cost and workload of tea planting and improves the quality of tea so as to enhance the economic returns.

Keywords: Tea, Wireless, Greenhouse, Monitoring.

1 Introduction

Camellia sinensis (L.) belongs to evergreen plant in subtropics and mostly grows among forestry community in the evergreen broad leaf rainforest and monsoon forest. It grows under the forest canopy for long time and has formed the ecological habit of shade-humid-tolerance and diffused light hobby [1].

In order to meet the requirements of famous high-quality tea, tea tree is planted in plastic greenhouse in the north area of the Yangtze River in our country, especially in Shandong and Henan etc. The plastic tea greenhouse is a facility cultivation form to use plastic film covering the tea garden. It is a new type of cultivation techniques to make the picking time of tea earlier in winter and spring when the temperature is lower or in the tea area where is subject to damage of cold spell in later spring. The technique can shorten the winter dormancy time to make the tea tree sprout earlier,

* Corresponding author. Supported by: National science and technology support plan of P.R. China (2011BAD21B06), Key Applied Technological Innovation Project in Agriculture of Shandong Province: Key Technology Study and Application of Regulation and Control between Fertilizer and Water of Tea with Good Quality and High Yield.

add the picking turn of tea leaf and boost the shoot growth so as to improve the tea leaf yield. In addition, the technique controls the growth of tea tree through creating the suitable environmental conditions. Therefore it can be used to plant the tea in saline-alkali soil and desert etc non-cultivable land which can greatly improve the resource utilization rate of land, water and light [2] so as to realize the high yield, high quality, high efficiency and sustainable development of agriculture. The greenhouse cultivation of tea has become one of the basic modes for tea cultivation in north area of the Yangtze River [3].

In general, the quality of fresh tea leaf is directly decided by its ecological environment [4]. The change of environmental factors e.g. light intensity, air temperature and humidity and soil fertility etc will affect the growth and quality of tea leaf [5]. The plastic greenhouse belongs to the enclosed or semienclosed structure which can use the automation, computer, electronics etc technology to regulate and improve the temperature, humidity or light intensity etc parameters required by the growth of tea tree [6] to create the suitable growth conditions.

The wide use of wireless technology has made its application research in many national economy domains develop quickly since 1990s, especially the internet of things system based on zigbee wireless technology made it possible that the technology of precision agriculture was widely used for the production. In this article, a wireless intelligent monitoring system for plastic tea greenhouse based on zigbee is designed.

2 Environmental Parameters and Control Requirements for Tea Tree

2.1 Temperature

As a subtropical plant, the suitable temperature for tea tree is 17~25°C. Too high or too low temperature can cause the yield reduction of tea leaf even no yield. The temperature should be controlled at about 25°C in daytime and not less than 8°C in nighttime. When the temperature within the greenhouse rises to 25°C in winter or 30°C in spring, it should be cooled by ventilation. When the temperature lowers under 20°C, the ventilation port is closed to keep warm. In general, the ventilation port should be opened at about 10:00 am in fine day and closed at about 3:00 pm. When the temperature drops rapidly in nighttime, the straw mat should used to keep warm, if necessary, it is warmed by manual [7].

2.2 Humidity

The soil water content suitable to the growth of tea tree is 70~80%. If it exceeds 90%, the gas permeability of soil is bad which isn't beneficial to the growth of tea tree. The suitable air humidity within the greenhouse is 65~75% in daytime and about 80% in nighttime [8]. The ventilation opening lowers the air humidity and spray irrigation increases the air humidity.

2.3 Light Intensity

The photosynthetic rate, maximum photosynthetic rate and apparent quantum yield of cutting seeding of tea tree are up to the maximum values at 75% natural light intensity. The chlorophyll content lowers with the increasing of light intensity. The chlorophyll a/b increases with the increasing of light intensity. The new biomass is in line with the maximum photosynthetic which is up to the maximum value at 75% natural light intensity [9]. Because of sheltering of vertical shaft and arching within the greenhouse and weakening of light intensity caused by the reflecting, absorbing and refraction of transparent plastic etc, the light intensity within the greenhouse is only about 50% of natural light intensity which will affect the photosynthetic efficiency of tea leaf. Except for selecting apricus tea garden and using euphotic, anti-aging and antipollution transparent plastic film, artificial supplementary lighting is the most effective method that improves the light condition within the greenhouse in winter. The method is that use agricultural high pressure mercury lamp to illuminate the tea garden in the morning and evening in fine day or in cloudy day or in rainy day [10].

2.4 Carbon Dioxide

Carbon dioxide is the important matter for photosynthesis of tea tree. Carbon dioxide insufficient is the main limiting factor for yield and quality of tea leaf in plastic tea greenhouse. Before sunrise, the CO₂ concentration within the greenhouse is up to 0.05%~0.06% because of released CO₂ by respiration of tea tree, microbial activities in the soil and organism decomposition (the CO₂ concentration outside is ordinarily about 0.03% and stable). After sunrise, the CO₂ concentration within the greenhouse drops remarkably with the enhancement of photosynthesis of tea tree. If it isn't ventilated in sunny day, the CO₂ concentration even drops under 100μg/mL and the tea tree almost can't carry our photosynthesis. Therefore CO₂ fertilizer is applied within the greenhouse which can promote the photosynthesis of tea tree to improve the yield and quality of tea leaf. [11].

3 Intelligent Monitoring System Design

3.1 System Structure

In according to the environmental conditions and control requirements, the main environmental factors that affect the quality of tea are air temperature, air humidity, soil humidity, light intensity and CO₂ concentration. Therefore there are mainly four basic parameters. If necessary, the outdoor meteorological station (mainly including outdoor temperature, humidity, wind direction, wind speed, rainfall and light intensity) and video monitoring may be set. The output devices include ventilation port, straw mat (or cotton quilt), high pressure mercury lamp and CO₂ fertilizer distributor etc.

The system consists of wireless sensor networks (WSN), remote data transmission, monitoring center and wireless control output. The structure is shown in Fig. 1.

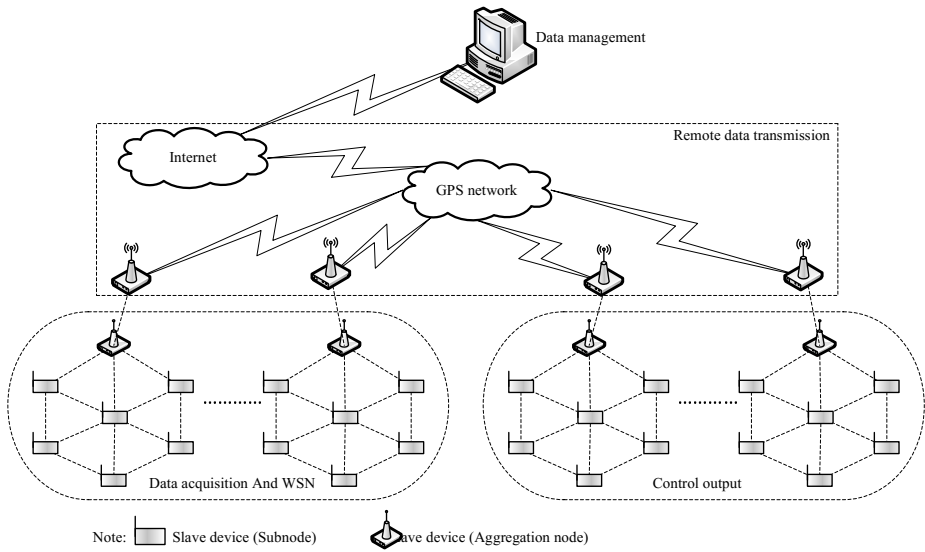


Fig. 1. Intelligent monitoring system structure

3.2 Wireless Sensor Networks

The wireless sensor networks mainly automatically acquire the air temperature, air humidity, soil humidity, light intensity, CO₂ concentration and video information etc and send the data to total node by zigbee network rapidly and reliably.

It consists of sensor, subnode and aggregation node. The sensor perceives the environmental information and has high stability, strong capacity of resisting disturbance, high measurement accuracy and rapid response speed etc features.

The subnode and the aggregation node adopt zigbee technology. It is a duplex wireless communication technology with close distance, low complexity, low power consumption, low speed and low cost. The technology is mainly used for the transmission of periodical data, intermittent data and data with long response time. Zigbee technology has the following features:

- Low power consumption. Two #5 dry cells can support one node working for 6~26 months, even longer, which is its outstanding advantage.
- Rapid response. It usually needs 15ms only from sleep mode to working mode (Bluetooth needs 3-10s) and the node only needs 30ms into the network which save the electric energy further.
- Large network capacity. It can adopt star, tree and net three network structures. One main node manages a number of subnodes, up to 254 subnodes. At the same time one main node can be managed by upper node. Therefore it can compose of 65000 nodes at the most.

Because the system for plastic tea greenhouse needs a few sensors and close communication distance, the network adopts star topology structure which algorithm is simple and can meet the monitoring requirements of tea garden to a large extent.

Considering the cost and performance, CC2530 is selected. It integrates the microprocessor module and a wireless transceiver module in one single chip. It has enhanced 8051 kernel with high speed, the latest zigbee 2007pro protocol, 2v-3.6v power supply range etc merits.

3.3 Remote Data Transmission

The data acquired from the sensors on site is sent to aggregation node by zigbee wireless communication technology. The aggregation node connects to the internet by GPRS network through which the data is sent to remote data monitoring center. At the same time, the order from monitoring center is sent to control devices by GPRS network so as to realize the remote intelligent monitoring for plastic tea greenhouse.

3.4 Monitoring Center

The monitoring center is the core of data management which realizes the analysis, processing, display, storage and output for acquired environmental data and releases it on the web. The monitoring software uses Microsoft visual basic 6.0 to develop and has the following functions:

- Collect and record temperature, humidity, light intensity and CO₂ concentration etc parameters, display them by digit, graph and image etc many modes and store them.
- Device state display. The system displays the running state of control device, e.g. the open or close of ventilation port etc.
- Set the alarm limit value of important parameters. When the value of alarmed parameter exceeds the limit, it will alarm automatically. The alarm mode includes multi-media sound-light alarm, network client alarm and mobile phone short message alarm etc.
- Set the control modes. The control modes include manual and automatic two modes. The automatic mode includes time control and condition control. When the control device needs start or stop at fixed time, e.g. roll up the straw mat at 10:00 am in winter, the time control mode may be selected. When the device is controlled by temperature or humidity etc parameters e.g. open the ventilation port for air temperature over 30°C, the condition control mode may be selected.
- History data display. It includes the history information of parameters, device state, alarm and control modes etc. The user can make a period of history data into curve to reflect the changes in plastic tea greenhouse.
- System configuration. It includes user management, communication set, parameter set, alarm value set, control conditions set, device set etc functions.

3.5 Control Output

The system adopts sectional-control strategy to decide the output. The sectional strategy uses different control algorithm in the deviation domain. Its block diagram is shown in Fig. 2.

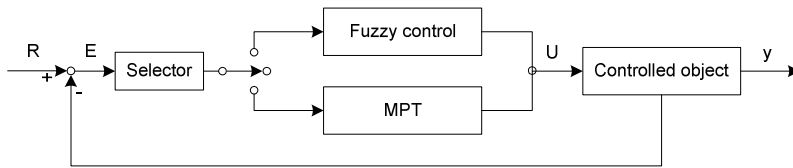


Fig. 2. Block diagram of sectional strategy

As shown in Fig. 2, when the deviation is larger than a certain domain, the fuzzy control is selected by operation mode selector to overcome integral saturation and confirm the output by fuzzy rules. When the deviation reduces within a certain domain, selector switches to MPT algorithm to decrease the overshooting during responding and eventually eliminate the residual. Therefore the sectional strategy integrates the merits of MPT algorithm and fuzzy control to improve the sensitivity and accuracy and obtain the ideal control effect [12].

The data is analyzed in according to the alarm set conditions and control algorithm. The result is sent to the control device or alarm device, e.g. ventilation port, straw mat, irrigating device and sound-light alarm device etc. For example, if the set value of air temperature is 25% within the greenhouse in winter for alarm and control, when the temperature rises to 25°C, the system decides the output through analysis, then the ventilation port is opened by the driven motor and the system sends out alarm signal. The alarm signal is reset by confirmation and when the temperature falls to 25°C, the ventilation port is closed.

4 Conclusion

The wireless intelligent monitoring system uses the latest wireless communication technology with micropower, digitalized temperature, humidity, light and CO₂ sensing technology to monitor the key points in tea garden which greatly reduces the workload and cost and forecasts the unsafe state in advance. The system can promote the production and management level, improve the state of tea tree growth and reduce the diseases and insect pests so as to regulate the growth period and enhance the economic performance.

References

1. Gong, X.F., Yu, Y.B., Xiao, B., Chen, C., Jin, S.: Effects of Different Cultivating Modes of Tea Gardens on Environment and Tea Quality. *Acta Botanica Boreali-Occidentalia Sinica* 28(12), 2485–2491 (2008)
2. Feng, M.X., Wang, P.S., Jiang, R.D.: Description on tea insect pests and diseases in Laoshan tea area of Shandong Province. *China Tea* 24(2), 14–15 (2002)
3. Chen, J.R.: Overview of Tea Garden Production Technology in Plastic Greenhouse. *Tea Science and Technology* (1), 12–14 (2012)

4. Shao, C.G., Yin, Z.X.: Research of Quality and Environmental Condition for Tea Leaf. *Journal of Tea Business* 21(4), 15–17 (1999)
5. Li, C.H., Wang, Y., Tang, X.B., Wang, Y.C.: The Effect of Different Eco-environment on the Quality of Famous Tea. *Southwest China Journal of Agricultural Sciences* 19(5), 946–948 (2006)
6. Wang, S.B.: Plastic Greenhouse Tea Garden's Management Technology. *Hubei Agricultural Sciences* 50(4), 754–758 (2011)
7. Guan, X.L., Zeng, L., Luo, L.Y.: Research Situation of Plastic Tea Greenhouse. *Fujian Tea* (4), 22–24 (2009)
8. Zheng, Y.Q.: Facility horticulture – Technical Points of Production Cultivation Management for Green Tea in North Area. *Agriculture & Technology* 25(2), 145–146 (2005)
9. Gu, B.J., Chang, J., Zeng, J.M., Wang, L.Y., Yuan, H.B., Ge, Y., Liao, J.X., Zhou, J., Cheng, H.: Under Greenhouse Manufacturing Administration Studies on the Optimal Irradiation for Tea Seedlings. *Journal of Tea Science* 26(1), 24–30 (2006)
10. Han, W.Y., Yu, Y.W., Wang, G.Q.: Synthetical Cultivation Technology of Plastic Tea Greenhouse. *China Tea* (6), 4–5 (1997)
11. Jin, J., Luo, Y.P.: Research Progress for Photosynthesis of Tea. *Tea Science and Technology* (1), 1–5 (2002)
12. Wang, F.Y., Mei, L., Feng, W.J., Wang, L., Wang, L.M., Ruan, H.J.: A Greenhouse Control with Sectional-control Strategy Based on MPT Intelligent Algorithm. In: Li, D., Chen, Y. (eds.) CCTA 2012, Part I. IFIP AICT, vol. 392, pp. 43–50. Springer, Heidelberg (2013)

Research on the Method of Simulating Knowledge Structure of the Information Searchers — Illustrated by the Case of Pomology Information Retrieval

Ding-feng Wu, Guo-min Zhou, Jian Wang, and Jian Wang,

Agricultural Information Institute of CAAS, Beijing 100081, China
zhougm@mail.caas.net.cn

Abstract. This paper reveals that the users of the pomology information retrieval system possess similar pomology knowledge structures after conducting questionnaire survey and interviews. Why such high consistency appears is explained by the comparison and analysis of the non-pomology-information-retrieval-system users. In the end, Based on the above conclusion, the method of simulating the searcher's professional knowledge structure by using the theory of pomology ontology is released in order to provide a theoretical exploration for the future information retrieval system, which will be more efficient and intelligent.

Keywords: pomology, information retrieval, users' knowledge structures, ontology.

1 Introduction

Nowadays, the way of researching information retrieval has already evolved from simply focusing on the statistical model and the mathematics algorithm to the stage that retrieval situation, user demand, task and social context are all concerned [1]. The knowledge structure of the searchers is very important among various contextual variables [2]. However, there is no final conclusion on how to actualize or utilize the knowledge structures of the users of information retrieval system [3]. The main reason remains in that there are huge differences between the knowledge structures of the searchers. It is likely that different searchers have largely diverged knowledge structures so that it is hard for the information retrieval system to get its search ability improved by taking advantage of this contextual variable [4].

Ontology is one of the hot issues of information science study. Ontology is defined as "Shared conceptualized explicit defined terminology" in information science and it is described as a set of domain concepts and the relations between them [5]. As an expression way of shared knowledge, ontology makes the knowledge understandable by computers. At the same time the ontology has the advantage of scalable architecture, high scalability and strong logical reasoning ability [6]. Domain ontology is a set of concepts and relations in a specific field [7]. So far, the pomology ontology is the most effective way of actualizing shared pomology knowledge [8].

Because of the independence and self-contained nature of the pomology knowledge structure and the pomology information searchers are often the researchers in or employees around the pomology field, there may be some rules in the knowledge structures of the users of pomology information retrieval system. With the demonstration and utilization of this regularity we may become successful in actualizing and utilizing the contextual variable of the searcher's knowledge structures, which can improve the efficiency of the search engines.

Bases its study on analyzing and exploring the theory and applications in the field, and carries out the experiment by questionnaires and interviews, this paper explored the information of the participants' pomology knowledge structure, and reveals that the pomology information searchers' professional knowledge structures are highly similar with each other. Based on the above conclusion, the method of expressing the searcher's professional knowledge structure by taking advantage of domain ontology is mentioned in order to provide a theoretical exploration for the future information retrieval system, which will be more efficient and intelligent.

2 Materials and Methods

The experiment mainly consists of questionnaires and individual interviews which have been conducted on two types of participants. One refers to the participants who conduct pomology information retrieval frequently, known as Test Group 1. The other refers to the ones who rarely conduct pomology information retrieval, known as Test Group 2. Online visual communication and face-to-face interviews are methods of testing the professional knowledge and skills of participants. By questioning, the pomology knowledge was extracted from the participant's words. By supplemented questionnaire surveys, the participant's pomology knowledge structure was reflected out.

Theoretically speaking, the investigation on the domain knowledge structures, which are often tree structures or net structures, can be carried out by traversing all the concepts. However, sample survey of some relatively important parts is adopted in the practice resulted from the obstacle that the concepts in pomology are too many to go through. The principles mentioned below should be followed when designing questions in the investigation.

Firstly, top concepts should all be selected in order to examine how firm the participant has grasped the knowledge in pomology. And at least one sub-concept should also be selected under each top concept for the same purpose.

Secondly, those concepts with the more relevant concepts in the concept map should be given higher priority as they are likely of more significance most of the time.

Thirdly, the concepts that appear frequently in the production practice should be taken since the investigation is aimed at the users of pomology information retrieval system.

Lastly, general concepts which belong to the nearest 2 or 3 layers to the root concepts should be focused on due to the habit that general concepts are usually used as key words when people conduct an information retrieval.

The principles of selecting concepts are showed in Fig 1. Top concepts like Concept 1, 2 and 3 should be selected in Fig 1 according to the selecting principles mentioned above. And Concept 4 as a common concept should also be selected. Concept 9 and 14

with relatively more relevant concepts should be selected accordingly. One of Concept 6, 7 and 8 should be selected in order to follow the first principle. Besides, the completeness of the investigation could be enhanced by the addition of some of the concepts between Concept 22 and Concept 62.

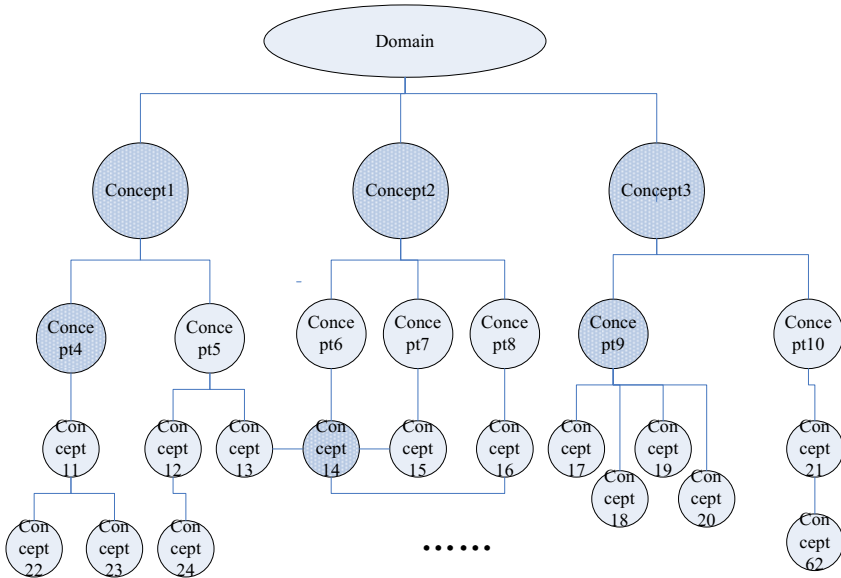


Fig. 1. The selection of important concept in knowledge structure

Based on the principles above mentioned, 43 of the 486 pomology concepts are selected and incorporated into the 25 questions in the questionnaires [9]. All questions are True or False items for the sake of objective analysis. Besides True or False options, a third option of No Idea is also counted in so as to avoid the coincidence that the participants who know nothing about the relevant knowledge choose a right answer by wild guess. A right answer will score while a wrong answer or a No Idea option won't. The questions in the questionnaire survey are listed in Table 1.

Table 1. The questions in the questionnaire survey

Concepts	Questions
pomiculture, fruit breeding, fruit tree protection, germ plasm resource of fruit trees, postharvest management	Pomology knowledge is divided into 5 parts known as pomiculture, fruit breeding, plant protection, germ plasm resource, and postharvest management.
fruit breeding	Fruit breeding is a kind of pomiculture knowledge.
fruit tree disease	Knowledge of fruit tree disease is part of pomiculture knowledge
identification of breed	Identification of breed refers to the work of deciding which breed a fruit tree belongs to.

Table 1. (Continued.)

breed	Knowledge of fruit tree breed belongs to fruit breeding knowledge.
stock	Stock is mentioned as a concept in fruit management.
transplant seedlings, full bearing age	Transplant seedlings are conducted during the full bearing age of the fruit trees.
apple preservation	Watering the apples before harvesting helps prevent the apples from going bad.
disease control of fruit trees, pest control, prevention and reduction of natural calamities	Fruit tree protection consists of disease control of fruit trees, pest control, and prevention and reduction of natural calamities like cold injury.
fruit management	Fruit management belongs to the concepts of fruit tree protection.
management of flowers and fruits	Management of flowers and fruits is pomiculture knowledge.
biological control	Biological control is an important topic in pomiculture research.
chemical control, integrated control	The disease and pest control of fruit trees can be divided into chemical control, integrated control, physical control, pesticide control and biological control.
pest control	Pest control is usually carried out in winter.
pruning of fruit trees	The pruning of fruit trees is done intensively in spring.
trimming and thinning of branches, pinching, twisting of tips	Methods of pruning of fruit trees involve trimming and thinning of branches, pinching, and twisting of tips.
fruit coloring	Fuji apples should be exposed to sufficient sunlight so that the fruits will maintain red.
apple canker	Apple canker is a commonly seen disease in apples.
apple anthracnose, apple ring rot	Apple anthracnose is also called apple ring rot because of the ring spots on the fruits.
Carposina niponensis Walsingham	Carposina niponensis Walsingham is not an apple tree pest for it only diets on peaches.
Red Fuji, Fuji	Red Fuji apple is one kind of Fuji apples.
cold resistance of fruit trees, apple industry district	Red Fuji apples are suitable to grow in northeast China in large areas due to their strong cold resistance.
management of rich water, base fertilizer, topdressing, composting	Fertilization of fruit trees consists of base fertilizer, topdressing, and composting.
growth period of fruit trees, phonological period of fruit trees	Growth period of fruit trees is also known as phonological period of fruit trees.
grafting, disease resistance of fruit trees, cold resistance of fruit trees	Grafting can create new varieties of nursery stocks but it has no evident influence on the improvement of disease and cold resistance of fruit trees.

3 Results and Analysis

The test participants who often conduct pomology information retrieval include science researchers of pomology working in laboratories, science researchers of promoting agricultural technologies in grass-root units and representatives of orchard workers, 16 in total. And there are another 15 participants who rarely conduct pomology information retrieval. The data of the questionnaire survey and the interview is listed in Table 2.

Table 2. The result of the questionnaire survey and the interview

Participants	Questionnaire scores	integrated analysis of questionnaires and interviews
Test Group 1: Participants who often conduct pomology information retrieval		
Participant 1	96	an experienced science researcher in pomology, working in the fields for years and possessing complete structures of knowledge
Participant 2	100	an experienced science researcher in pomology, working in the fields for years and possessing complete structures of knowledge
Participant 3	100	an experienced science researcher in pomology, working in the fields for years and possessing complete structures of knowledge
Participant 4	92	used to be an excellent science researcher in pomology, working as a manager and possessing complete structures of knowledge
Participant 5	96	used to be an excellent science researcher in pomology, working as a manager and possessing complete structures of knowledge
Participant 6	100	an experienced science researcher in pomology, working in the fields for years and possessing complete structures of knowledge
Participant 7	84	a middle-aged orchard worker, possessing complete structures of knowledge
Participant 8	92	used to be an excellent science researcher in pomology, working as a manager and possessing complete structures of knowledge
Participant 9	100	a doctoral student in pomology, focusing on cultivation and possessing complete structures of knowledge
Participant 10	100	a master student in pomology, focusing on cultivation and possessing complete structures of knowledge
Participant 11	96	a master student in pomology, focusing on breeding and possessing complete structures of knowledge
Participant 12	100	a young orchard worker specialized in pomology, possessing complete structures of knowledge

Table 2. (Continued.)

Participant 13	76	an old and experienced orchard worker with less complete structures of knowledge, or possibly facing difficulty in understanding the terms in the questionnaires
Participant 14	88	a middle-aged orchard worker, possessing complete structures of knowledge
Participant 15	96	a doctoral student in pomology, focusing on postharvest and possessing complete structures of knowledge
Participant 16	92	used to be an excellent science researcher in pomology, working as a manager and possessing complete structures of knowledge
<hr/>		
Test Group 2: Participants who rarely conduct pomology information retrieval		
Participant 17	16	being exposed to pomology knowledge in daily work at times and possessing little common sense or any structure of knowledge
Participant 18	64	an expert who comes into contact with pomology in his work often and has acquired much pomology knowledge, but with less complete structures of knowledge
Participant 19	12	having little professional knowledge in pomology, basing his answers on common sense of life
Participant 20	0	having little professional knowledge in pomology, basing his answers on common sense of life
Participant 21	16	having little professional knowledge in pomology, basing his answers on common sense of life
Participant 22	12	having little professional knowledge in pomology, basing his answers on common sense of life
Participant 23	48	having some common sense and a relative as an orchard worker, but with very incomplete structures of knowledge
Participant 24	20	being exposed to pomology knowledge in daily work at times and possessing little common sense or any structure of knowledge
Participant 25	16	having little professional knowledge in pomology, basing his answers on common sense of life
Participant 26	44	having filmed science and educational films in pomology in his early years of life, and accumulated much common sense of life in the years, but with less complete structures of knowledge
Participant 27	0	having little professional knowledge in pomology, basing his answers on common sense of life

Table 2. (Continued.)

Participant 28	24	being exposed to pomology knowledge in daily work at times and possessing little common sense or any structure of knowledge
Participant 29	32	having done research on topic concerning apples and possessing some common sense, but with very incomplete structures of knowledge
Participant 30	28	being exposed to pomology knowledge in daily work at times, and possessing little common sense and less complete structures of knowledge
Participant 31	8	having little professional knowledge in pomology, basing his answers on common sense of life

The analysis of the scores in the questionnaires turns out that the average score for Test Group 1 is 94.25, and that for Test Group 2 is 22.67. The standard deviation, the standard error and the range of the questionnaire scores of Test Group 1 and 2 are showed in Table. 3.

Table 3. The comparison of the questionnaire scores of two test groups

Test Group	standard deviation	standard error	range
Test Group 1	6.85	1.71	24
Test Group 2	17.99	4.65	64

The average score for Test Group 1 is 94.25 while that for Test Group 2 is 22.67, accounting for the fact that most of the participants from Test Group 1 possess relatively more complete structures of knowledge in pomology than those from Test Group 2 do. What is more, the participants from Test Group 2 are in lack of knowledge in pomology, let alone well formed knowledge structures. The standard deviation, the standard error and the range of the questionnaire scores all together indicate that the distribution of scores of the participants from Test Group 1 is centralized, which also means that these participants possess similar structures of knowledge in pomology.

Obviously, the conclusion can also be supported by the integrated analysis of the interviews and questionnaires. Generally speaking, the fact that the participants from Test Group 1 possess higher professional skills and relatively more complete professional knowledge, the knowledge structures of which tend to appear similar, is due to the elements that some of the participants have received years of professional training in pomology, some have abundant practical experience and have kept studying pomology, some have worked for years in the frontline of pomology research, and they are more connected with each other when they are at work, in daily life, studying and doing research, benefiting from numerous opportunities to communicate which are offered or supported by the government, such as Science and Technology Activities to the Country, the promotion of pomology knowledge by the local technicians of the agricultural technological station in the years, and the corporation maintained by the scientific research institutions and the orchard workers in near areas. On the contrary,

the similar degree of pomology knowledge of Test Group 2 is small due to that their professional backgrounds, educational backgrounds, interests and life experience are at variance with each other. It is true that some of these participants know a certain amount of pomology knowledge, while some almost know nothing. Therefore, it can be concluded that the participants from Test Group 2 lack professional knowledge as a whole, most of them possess very little common sense in pomology, and some have not formed complete knowledge structures in spite of their reasonable understanding of some of the pomology knowledge.

4 Conclusion

The above experiment has demonstrated that the professional knowledge structures of the users of the pomology search engines are highly similar to each other, which means they tend to converge at the acknowledgeable professional knowledge structures in pomology field. As domain ontology exactly expresses the collection of the structured acknowledgeable knowledge, it is feasible to simulate the knowledge structures of the users of pomology information retrieval system by pomology ontology.

References

- [1] Ingwersen, P., Jarvelin, K.: *The Turn Integration of Information Seeking and Retrieval in Context* (2005)
- [2] Kelly, D., Cool, C.: The effects of topic familiarity on information search behavior. In: Hersh, W., Marchionini, G. (eds.) *Proceedings of the Second ACM/IEEE Joint Conference on Digital Libraries (JCDL 2002)*, pp. 74–75. ACM, New York (2002)
- [3] Ingwersen, P., Jarvelin, K.: Information retrieval in context. In: Ingwersen, P., Belkin, N.J. (eds.) *Proceedings of the SIGIR 2004 Workshop on Information Retrieval in Context*, pp. 6–9. ACM, New York (2004)
- [4] Pennanen, M., Vakkari, P.: Students' cognition and information searching while preparing a research proposal. In: Bruce, H., Fidel, R., Ingwersen, P., Vakkari, P. (eds.) *Emerging Frameworks and Methods. Proceedings of the Fourth International Conference on Conceptions of Library and Information Science (CoLIS4)*, pp. 33–48. Libraries Unlimited, Seattle (2002)
- [5] Neches, R., Fikes, R.E., Gruber, T.R., et al.: Enabling Technology for Knowledge Sharing. *AI Magazine* 8(1), 36–56 (1991)
- [6] Lopez, V., Pasin, M., Motta, E.: AquaLog: An Ontology-Portable Question Answering System for the Semantic Web. In: *Proceedings of the 2nd European Semantic Web Conference*, pp. 91–126 (2005)
- [7] Meng, X.-X.: Special Issue – Agriculture Ontology. *Journal of Integrative Agriculture* 5(11) (2012)

Strategies for High Yield Inferred through Path Analysis of Major Economical Traits in Yongyou 8, a Hybrid Late Season Japonica Rice

Liu Weiming¹, Wang Enguo², Huang Shanyou³, and He Xianbiao³

¹Taizhou Vocational College of Science and Technology, Taizhou Zhejiang 318020

²Plant Protection Station of Linhai City, Linhai Zhejiang 317000

³Taizhou Institute of Agricultural Sciences, Linhai Zhejiang 317000
15157622288@139.com

Abstract. In order to further clarify the path to high yield cultivation techniques for Yongyou 8, a hybrid late season japonica rice line, we selected 65 sets of data from 11 sites in Zhejiang and Jiangsu Provinces between 2005 and 2011, analyzed profiles of panicle, kernel and weight in Yongyou 8. Through correlation, regression and path analysis, a technical strategy has been proposed for high yield Yongyou 8 cultivation: appropriate control of the number of effective tillers, focus on large panicles, with appropriate attention to seed setting rate and kernel weight.

Keywords: hybrid rice, Yongyou 8, yield trait, path analysis, technical strategy.

1 Introduction

Simple correlation[1-3] or multiple regression[4-7] analysis are often employed to study the relationship between plant main characters and crop yield often using. However, simple correlation cannot fully examine the relationship between variables, so that the results might have a certain one-sidedness (Ref??). Multivariate regression analysis, to a certain extent, can eliminate confusion between variables and reveal the real correlation of the independent variables with their dependent variables. The path analysis is able to effectively demonstrate a direct effect of the relevant variables on the outcome and to find out the indirect effect of casual factors on the affected factors, allowing comparison of the relative importance of various causal factors [8-10]. Such a comprehensive analysis will be a solid ground for improving yield cultivation techniques.

In order to determine cultivation strategies for high yield of intermediate to late season japonica rice, we explored the effect of major economical traits on yield[11-13]. Yongyou 8, an elite and late season cultivar, is often used as a three-strain hybrid rice line. In 2012, we collated 55 sets of data from 2005 to 2011 in 9 sites of Zhejiang and Jiangsu Provinces, to determine the relationships between traits and yield, performed regression, correlation and path analysis [14] for Yongyou 8. Later, we have gathered more economical trait data from various sites, and further analyzed the effects of major economical traits on yield of Yongyou 8.

2 Materials and Methods

2.1 Data Collection

Yongyou 8 is a 3-strain hybrid late season japonica rice line with moderate growth period, can be grown late season in areas where rice is harvested once or twice a year. Yongyou 8 has loose tillers, moderate tillering capability, high panicle bearing rate, large spikes, high seed setting rate, moderate lodging resistance. The quality of rice meets the national standard of second excellence grade.

Results from analysis of 65 sets of field data for 7 continuous years from 11 sites in the two Provinces (Table 1) indicate that the yield was negatively correlated with the number of effective tillers per unit area, but positively correlated with the number of total kernels, filled kernels per panicle and 1,000 kernel weight. The seed setting rate was the highest in paddies with a yield at 11250 kg/ha, followed by paddies with a yield at 8250 kg/hm².

Table 1. Characteristics of Panicle, Kernel and Weight Traits at Various Yield Level

Yield Level(kg/hm ²)	>11250	≤11250—>9750	≤9750—>8250	≤8250
No of Paddies	21	19	17	8
Effective Tillers(10 ⁴ /hm ²)	226.97	237.33	240.61	241.86
Total Kernels/Panicle	239.36	229.00	201.58	177.50
Filled Kernels/Panicle	204.85	173.04	155.68	146.64
Seed Setting Rate	85.39	75.83	77.89	83.00
1,000 Kernel Weight(g)	28.28	27.98	27.18	26.56
Mean Yield(kg/hm ²)	12633.09	10303.72	8953.82	8050.31

2.2 Method of Analysis

Sixty five sets of trait data were analyzed for correlation, regression and path to reveal the cultivation technical strategy to high yield.

3 Results and Analysis

3.1 Regression Analysis among Traits

As shown in Table 2, among five traits, yield is negatively correlated with the number of effective tillers not statistically insignificant though, and positively correlated with the remainder 4 traits very significantly. Further analysis of the five traits revealed that the number of effective tillers was negatively correlated at very significant level with total number of kernels per panicle, filled kernels and 1,000 kernel weight, weakly correlated with seed setting rate. The total number of kernels per panicle was very significantly correlated with filled kernels, 1,000 kernel weight, weakly negatively correlated with seed setting rate. Thus, relationships among the five traits are complex,

and their relationships with yield vary even negative. Thus, it is the key to understand how to coordinate traits with yield, how to focus on the main factor to fully explore the traits.

Table 2. Correlation Coefficients for Major Economic Traits

	x_2	x_3	x_4	x_5	Actual Yield
Effective Tillers	-0.7741**	-0.7156**	0.0237	-0.3460**	-0.1498
Total Kernels/panicle		0.8546**	-0.1880	0.6262**	0.4956**
Filled Kernels/Panicle			0.3390*	0.5340**	0.6982**
Seed Setting Rate				-0.1737	0.3835**
1,000 Kernel Weight					0.6378**

Note: * denoted difference at $\alpha = 0.05$. ** denotes deference at $\alpha = 0.01$.

3.2 Gradual Correlation Analysis

We analyzed 65 sets of data for traits by stepwise regression, maximized coefficient. The regression equation is

$$\hat{y} = -31504.81 + 34.81 x_1 + 46.75 x_3 - 38.49 x_4 + 810.23 x_5 \pm 754.78$$

Where,

x_1 = effective tillers, x_2 = kernels per panicle, x_3 = filled kernels per panicle, x_4 = seed setting rate, and x_5 = 1,000 kernel weight.

Through results of stepwise regression analysis, it can be seen that among the five traits, the total kernels per panicle did not contribute to yield. The ranges of the five traits were 1.7700~3.2850 million/hm², 149.60~288.90 kernels/panicle, 114.27~250.74 kernels/panicle, 65.50~89.20% and 25.30~29.32 g for x_1 , x_2 , x_3 , x_4 , x_5 , respectively. The range of yield (y) was 7665.00~13549.50 kg/hm².

Results of variance analysis indicated that the F value for the regression equation was 75.60 with $P < 0.01$. Analysis of partial correlation revealed that filled kernels per panicle ($r(y, x_3) = 0.7003$) had the largest contribution to yield, followed by effectively panicles ($r(y, x_1) = 0.6672$), weight per thousand kernel ($r(y, x_5) = 0.5888$) and seed setting rate ($r(y, x_4) = 0.2599$). But multiple regression analysis revealed the there are dependences among traits. Since there is colinearity between factors, it is hard to accurately estimate the contribution of each trait on the yield. Path analysis could effectively reveal the direct and indirect effect of these traits on the yield. Thus, path analysis was employed to determine the effect of major economic trait on yield.

3.3 Path Analysis

Based on stepwise regression analysis, four main factors were selected for path analysis to further clarify the importance of each trait on yield. Results showed that filled kernels per panicle had the largest effect on yield, followed by effective tillers, 1,000 kernel weight, and seed setting rate (Table 3).

Table 3. Path Coefficient Analysis

Factor	Direct Effect	Through x1	Through x3	Through x4	Through x5
Effective Tillers	0.6042		-0.6141	0.0036	-0.1435
Filled Kernels/Panicle	0.8581	-0.4324		0.0510	0.2214
Seed Setting Rate	0.1503	0.0143	0.2909		-0.0720
1,000 Kernel Weight	0.4147	-0.2091	0.4583	-0.0261	

The path coefficient due to direct effect of effective tillers was 0.06042. However, effective tillers had a large negative effect through filled kernels per panicle, as much as -0.6141, with small positive effect indirectly through seed setting rate and a small negative effect through the 1,000 kernel weight. The ultimate effect of effective tillers on yield was -0.1498. Thus, the number of effective tillers had a large effect on kernels per panicle. In order to increase the number of filled kernels per panicle, it is necessary to reduce the number of effective tillers.

The number of filled kernels per panicle had the largest direct effect on yield with a path coefficient as high as 0.8581. However, its negative indirect effect through the number of effective tillers was also as high as -0.4324 while its positive indirect effect through the weight per thousand kernel and seed setting rate was small, respectively being 0.2214 and 0.0510. Thus, the number of filled kernels per panicle has a combined effect 0.6982. Therefore, in high yield cultivation, it is extremely important to control the negative effect of the number of panicles through the number of filled kernels, focusing on produce large panicles.

The seed setting rate had the smallest direct coefficient, being 0.1503. Its positive indirect effect through the total number of kernels per panicle was higher, being 0.2909. Its indirect effects through the number of effective tillers and the 1,000 kernel weight were weak, being 0.0143 and 0.0720. Ultimately, the seed setting rate had a combine effect of 0.3835.

The 1,000 kernel weight had a direct path coefficient 0.4147. Its negative effects through the number of effective tillers and seed setting rate were respectively -0.2091 and -0.0261, but the positive indirect effect through the number of filled kernels was 0.4583. Therefore, the 1,000 kernel weight had a combined effect of 0.6378.

4 Discussion and Conclusion

Our analysis showed that the number of filled kernels had the greatest direct positive effect. The effect of seed setting rate and the 1,000 kernel weight were exerted indirectly through the positive effect of the number of filled kernels. The number of effective tillers was strongly negatively correlated with the number of total kernels, the number of filled kernels, and the weight of thousand kernels, and negatively correlated with yield. The total number of kernels per panicle was very significantly correlated with the number of filled kernels. Therefore, the technical strategy to high yield cultivation of Yongyou 8 is to appropriately control effective tillers, focus on large panicle, and pay attention to seed setting rate and kernel weight.

In the current study, results of analysis of five economic traits were somewhat different from previous report, not as previously reported negative correlation [13]. Through stepwise regression analysis, the total number of kernels per panicle fell out to be an important factor. Results of path analysis indicated that yield was affected most significantly by the number of filled kernels per panicle. This is consistent with the previous notion “to appropriate control the number of effective panicle, focus on large panicle and pay attention to kernel weight”. Data for this analysis is more inclusive, containing those collected from more sites, thus is more representative.

Yongyou 8 is an intermediate to late season rice line that can be cultivated in areas where rice is grown once or twice a year. This adaptive line has outstanding performance in Zhejiang and Jiangsu. Zhu has pointed out that Yongyou 8 has displayed a dynamic ultrahigh yield trend of “small at first, stable in the middle and strong at last”. An ultrahigh yield can be achieved by stabilizing the panicle number, focusing on large panicle, increasing the pool, strengthening the source, preventing lodging [15]. The current study has found that the large panicle character contributed the largest to ultrahigh yield of Yongyou 8. The number of kernels per panicle had a clear larger contribution to yield than other factors. Because the number of effective tillers was very strongly negatively correlated with the total number of kernels and the number of filled kernels, it is imperative to appropriately control the number of effective tillers.

References

1. Guo, Y.M., Mu, P., Liu, J.F.: Correlation analysis and QTL mapping of grain shape and grain weight in rice under upland and lowland environments. *Acta Agronomica Sinica* 33(1), 50–56 (2007)
2. Zeng, X.P., Li, Q.X., Lv, J.Q.: Canonical correlation analysis between quality and yield characters of hybrid rice. *Southwest China Journal of Agricultural Sciences* 19(6), 991–995 (2006)
3. Zhang, X.J., Xu, Z.J.: The correlation of rice yield and its components. *Journal of Shenyang Agricultural University* 34(5), 362–364 (2003)
4. Sun, C.M., Wang, Y.L.: Regressive analysis between leaf characters and yield factors in elongation stage in rice. *Journal of Yangzhou University (Agricultural and Life. Science Edition)* 26(2), 71–73 (2005)
5. Zhao, Y., Huang, F.K., Tong, X.L., Ling, B., Pang, X.F.: Secondary compounds in rice varieties resistant to *Nilaparvata lugens*. *Chinese Journal of Applied Ecology* 5(11), 2161–2164 (2004)
6. Zhang, Y.F., Wang, Y.L., Zhang, C.S., Dong, G.C., Yang, L.X., Huang, J.Y., Chen, P.F., Gong, K.C.: Differences of nitrogen absorption and utilization and their influences on grain yield of conventional Indica rice cultivars. *Jiangsu Journal of Agricultural Science* 22(4), 318–324 (2006)
7. Guo, L.B., Luo, L.J., Xing, Y.Z., Xu, C.G., Mei, H.W., Wang, Y.P., Yu, X.Q., Ying, C.S., Shi, C.H.: Genetic analysis and utilization of the important agronomic traits on Zhenshan97×Minghui 63 recombinant inbred lines(RIL) in rice (*Oryza sativa* L.). *Acta Agronomica Sinica* 28(5), 644–649 (2002)
8. Li, P.F., Yang, S.Q., Zhang, Y.H., Tian, H.P.: Analysis of main agronomic characters of rice in Ningxia. *Acta Agriculturae Boreali-occidentalis Sinica* 16(2), 33–36 (2007)

9. Cheng, Y.S., Liao, Y.P., He, X.Y., Chen, Z.M., Chen, Y.H.: Relevance and path analysis on harvest index and single yield and its composition factors of rice. *Guangdong Agricultural Sciences* (9), 36–38 (2006)
10. Wang, H.Z., Luo, W.X., Wang, Y.B.: Correlation and path analysis of economic characters of hybrid rice. *Seed* 23(12), 55–57 (2004)
11. Liu, W.M.: Correlation, Multiple Regression and path Analysis between Yield Traits and Yield on Intersubspecific Hybrid Rice. *Chinese Agricultural Science Bulletin* 25(1), 70–72 (2009)
12. Liu, W.M.: Analysis of high yield and efficiency technique in intersubspecific hybrid rice. *Journal of Agricultural Science and Technology* 3(11), 43–46 (2009)
13. Liu, W.M.: Study on the High Yield and High Efficiency Cultivation Technique of Indica-japonica Intersubspecific Hybrid Rice as Single-cropping Late Rice. *Hubei Agricultural Sciences* 18(50), 3684–3686 (2011)
14. Liu, W.M.: Analysis of High Yield and Efficiency Technique on Yongyou 8 Hybrid Rice. *Hybrid Rice* 28(2), 40–42 (2013)
15. Zhu, Y.Y., Sha, A.Q., Fan, B.G.: Formation Rule of Super-high-yielding and Cultural Techniques for Yongyou 8. *Jiangsu Agricultural Sciences* 40(2), 45–47 (2012)

Mathematical Modeling and Optimization of Schemes of Major Agronomic Factors for Hybrid Rice ‘Yongyou 17’

Liu Weiming¹ and Bao Zuda²

¹Taizhou Vocational College of Science & Technology, Zhejiang, Taizhou 318020

²Seed Management Station, JiaoJiang, TaiZhou, ZheJiang, Taizhou 318000

15157622288@139.com

Abstract. In this study, the computer aided modeling and optimization was used to select agronomic scheme of high yield and high net profit for a single-season late rice hybrid ‘Yongyou 17’. A field experiment with three agronomic factors including seedling age, planting density, pure N fertilizer rate were performed and the data were used to construct regression models using yield and net profit as the objective variables. Simulation of those models produced the optimum schemes consisting of seedling age, planting density and pure N fertilizer rate to achieve the highest yield and net profit.

Keywords: hybrid rice, agronomic scheme, mathematical model, model optimization, nitrogen fertilizer, seedling stage, planting density, yield, net profit.

1 Introduction

Nowadays, the optimal experimental design used has been widely used in agricultural studies [1-4]. Rotational combination design, the secondary saturated D-optimal design, and simplex lattice design were all applied in the studies for high-yield cultivation techniques in rice, sweet potatoes, corn, soybean, turmeric (*Dioscorea*) by this research group [5-10]. In this study, rotational combination design was used to conduct field trials for establishing a mathematical model for optimal management of the single-season rice hybrid ‘Yongyou 17’.

‘Yongyou 17’ is a three-line Indica-Japonica hybrid cultivar bred by the Crop Institute of Agricultural Academy of Zhejiang Province and Ningbao Seed Company, Ltd. The cultivar was registered in Zhejiang Province in 2012 (Zhe Registrar Rice 2012018). The cultivar has good stem strength; it is highly resistant to lodging. It has a medium growth period with nice pigment change during the late growth stage. The big panicles with dense grains produce high yield. The objective of this study was to determine the effects of major agronomic traits on yield and net profit of ‘Yongyou17’.

2 Materials and Methods

The field experiment was set up using the seedling age (x_1 , days), planting density (x_2 , cluster/hm²), pure N fertilizer rate (x_3 , kg/hm²) as the decision variables in a

tertiary quadratic general rotary design [11]. Table 1 contains the three decision variables, the treatment levels and the corresponding linear code. The yield and net profit were used as the objective variables.

Table 1. Decision variables and the treatment levels

Linear code	x_1	x_2	x_3
+1	30	202500	201.15
-1	18	127500	51.15
0	24	165000	126.15
+1.682	34	228075	252.30
-1.682	14	101925	0

Seedling age was controlled by sowing seeds at different dates (Table 1). Seeds sowed on May 26th, 30th, June 4th, 10th and 14th produced seedlings of 34, 30, 24, 18 and 14 days, respectively, at the transplanting date on June 28th. Single plant was planted per hole.

The size of each plot was 16 m² (3.2m x 5m). To prevent fertilizer from leaching into adjacent plots, the between plot area was covered with plastic film. In each plot, 450 kg/hm² of calcium phosphate was applied as base fertilizer. KCl (300 kg/hm²) was used in three applications at a ratio of 1:2:2, as base fertilizer, at 15 days post-transplanting, and panicle fertilizer. Pure N fertilizer rate was 252.30, 201.15, 126.15, 51.15 kg/hm². Nitrogen fertilizer was applied five times in a ratio of 4; 2; 2;1;1, as base fertilizer, 7 and 15 days after transplanting, flowering fertilizer, and seed set fertilizer. The field experiment was performed in 2012, in Shujiang district, Taizhou, Zhejiang. Except for the treatments, the experimental field was managed consistently.

3 Results and Analysis

According to the quadratic regression orthogonal rotation design principles, a regression mathematical model was obtained as follows:

$$\hat{y} = b_0 + \sum_{i=1}^3 b_i x_i + \sum_{i < j} b_{ij} x_i x_j + \sum_{i=1}^3 b_{ii} x_i^2 + \sigma$$

In which, (the Chinese words in the following formula should be changed to English word or letters)

$$\sigma = \sqrt{SS_{\text{剩}} / f_{\text{剩}}}$$

Based on the structure of the matrix and the obtained yield and net output of Yongyou 17, quadratic regression analyses were carried out focusing on the yield and profit.

3.1 Yield Result Analysis

Using the tertiary quadratic general rotary regression analysis, models for the three agronomic traits and yield were constructed as follows:

$$\hat{y}_1 = 12808.65 - 92.7 x_1 + 490.65 x_2 + 1247.55 x_3 - 56.25 x_1^2 - 415.2 x_2^2 - 688.35 x_3^2 - 97.35 x_1 x_2 + 333.6 x_1 x_3 - 13.35 x_2 x_3$$

$$(-1.682 \leq x_i \leq 1.682, \quad i = 1, 2, 3)$$

In the model, x_2 , x_3 , x_2^2 and x_3^2 are at the extremely significant level, and $x_1 x_3$ are at a significant level. The rest of variables are not significant ($\alpha=0.25$). To increase accuracy level, all the non-significant variables were excluded from the models. Then the regression model was rewritten as:

$$\hat{y}_1 = 12808.65 + 490.65 x_2 + 1247.55 x_3 - 415.2 x_2^2 - 688.35 x_3^2 + 333.6 x_1 x_3$$

$$(-1.682 \leq x_i \leq 1.682, \quad i = 1, 2, 3)$$

In this regression models, all the variables are significant, and the lack-of-fit sum of squares is not significant. These models should be very effective for simulation experiment.

Test of significance identified yield is mainly affected by planting density and pure N fertilizer rate, and seedling age has a smaller effect. When compared for interaction effect ($x_1 x_3$), it was found that the lower nitrogen fertilizer rate should be combined with younger seedlings, and higher fertilizer rate with older seedlings. In general, higher N fertilizer rate was correlated with higher yield. When seedling age and nitrogen fertilizer rate were set around treatment level 1, the yield was at the highest level.

3.2 Profit Result Analysis

In this study, rice, seedling, urea, KCl, and calcium phosphate were priced at 2.80 yuan /kg, 52 yuan/10,000 seedlings, 2.50 yuan/kg, 3.60 yuan/kg and 0.90 yuan/kg, respectively. When estimating the investment, only the cost of materials and supplies were included. After converting the net profit per plot into profit per hectare, a ternary quadratic general rotary regression model was constructed. After exclusion of variables that are not significant ($\alpha=0.25$), the regression model for net profit is described as follows:

$$\hat{y}_2 = 32565.60 + 1178.85 x_2 + 3085.50 x_3 - 1162.65 x_2^2 - 1927.35 x_3^2 + 934.05 x_1 x_3$$

$$(-1.682 \leq x_i \leq 1.682, \quad i = 1, 2, 3)$$

Test of significance showed that, same as in the yield model, x_2 , x_3 , x_2^2 , x_3^2 are extremely significant, and $x_1 x_3$ is at a significant level. The overall regression model is extremely significant. The relationship between the three agronomic factors and net profit is approximately the same as that in the yield model. Planting density and pure N fertilizer rate are the major factors influencing profit, while the effect from seedling

age is relatively small. The interaction effect of $x_1 x_3$ on net profit is also similar to that on yield. Lower nitrogen fertilizer rate combined with younger seedlings, and higher fertilizer rate with older seedlings should yield a higher net profit. The highest net profit was achieved when the seedling age and nitrogen rate were both set at around treatment level 1.

These results indicate that the three agronomic factors have a consistent effect on yield or net profit. Therefore agronomic schemes aimed at increasing yield also can produce high net profit. Then the optimum agronomic schemes for high yield and high profit were selected using computer simulation of the mathematical models described above.

4 Model Optimization

4.1 Optimization of the Agronomic Schemes for High Yield

The high yield agronomic schemes were selected using the yield regression model and selecting $(-1.682 \leq x_i \leq 1.682)$ as the region for constrain [12, 13]. Twenty-one schemes were found to produce a yield above 12900kg/hm² (Table 2). At the 95% confidence level, the value of x_1, x_2, x_3 each was 0.456-1.206 (26-31 days), 0.282-0.995 (175575-202305 clusters/hm²) and 1.148-1.437 (212.25-233.85 kg/hm²).

Table 2. Computer model using increasing yield as the objective variable

Level	x_1	Frequency	x_2	Frequency	x_3	Frequency
-1.682	0	0.000	0	0.000	0	0.000
-1.000	2	0.095	2	0.095	0	0.000
0.000	5	0.238	7	0.333	0	0.000
1.000	6	0.286	7	0.333	12	0.571
1.682	8	0.381	5	0.239	9	0.429

4.2 Model Optimization for High Net Profit

The high profit agronomic schemes were selected by simulating net profit regression model within the same constraint region as for yield. Sixteen schemes were found to produce a net profit exceeding 32700 yuan/ hm² (Table 3). The value for x_1, x_2, x_3 each (at 95% confidence level) was 0.479-1.368 (27-32 days), 0.257-0.999 (174638-202463 clusters/ hm²) and 1.058-1.368 (205.5-228.75 kg/ hm²). It can be seen that the similar values were selected for the three agronomic factors in the net profit schemes and those aimed at high yield.

Table 3. Computer modeling aimed at increasing the net profit

Level	x_1	Frequency	x_2	Frequency	x_3	Frequency
-1.682	0	0.000	0	0.000	0	0.000
-1.000	2	0.125	1	0.063	0	0.000
0.000	2	0.125	6	0.375	0	0.000
1.000	5	0.313	6	0.375	11	0.688
1.682	7	0.437	3	0.187	5	0.312

5 Conclusions

In this study, regression models were constructed to simulate the relationship between three agronomic factors (seedling age, planting density, pure N fertilizer rate) and the yield and net profit of single season hybrid rice 'Yongyou 17'. Model analysis indicates that yield and net profit have similar responses to the three agronomic factors. Among the three agronomic factors, planting density and pure N fertilizer rate have bigger effects whereas that from seedling age is relatively small. Production schemes were constructed using simulation of mathematical models integrating data from a field experiment. Under the production conditions used in this study, for 'Yongyou 17' to achieve high yield and high profit, the optimum scheme consists of the following conditions: seedling age of 26-30 days, planting density of 165000-180000 cluster/hm², pure N fertilizer rate of 210-225kg/hm².

References

1. Chen, Z.L., Cao, W., Tang, F.D., Huang, L.R., Li, L.D., Ai, J.: Effects of water and fertilizer coupling on seedling biomass of *Lespedeza bicolor* in sandy land of northwestern Liaoning province. *Journal of Northeast Forestry University* 39(1), 34-47 (2011)
2. Ruan, P.J., Ma, J., Mei, Y., Yang, Y.P.: Effect of different density and N-application rate on maize quality. *Chinese Agricultural Science Bulletin* 20(6), 147-149 (2004)
3. Gao, J., Zhang, Y.C.: Application of D-saturation optimum design in culture medium screening for micropropagation of virus-free tube potato. *Journal of Qinghai University (Nature Science)* 26(3), 24-26 (2008)
4. Liu, Y., Chi, D.Z., Ma, X.G.: Multiplication of subculture for Faba Bean (*Vicia faba* L.). *Journal of Qinghai University (Nature Science)* 26(5), 59-61 (2008)
5. Liu, W.M., Ye, A.M.: Study on optimization combination for intercropping spring corn with spring soybean. *Acta Agriculturae Zhejiangensis* 16(3), 131-135 (2004)
6. Liu, W.M., Wang, R.Z.: Study on fertilizer application techniques of annual *Dioscorea zingiberensis*. *Journal of Chinese Medicinal Materials* 29(4), 313-315 (2006)
7. Liu, W.M., Xu, J.: Research on the transplanting density and nitrogen application for Zhongzheyou 1 planted as single cropping late rice. *Hybrid Rice* 21(5), 50-53 (2006)
8. Liu, W.M., Yan, B.L., Zhao, Y.F., Wu, L.H.: Effect of planting density and rates of nitrogen and potassium fertilizers on yield and economic efficiency of sweet potato (cv. Zheshu 13). *Acta Agriculturae Zhejiangensis* 19(1), 55-59 (2007)

9. Liu, W.M., Wu, L.H.: Optimized test on comprehensive agronomic measures of Zheshu 13. Seed 26(4), 73–75 (2007)
10. Liu, W.M., Xi, T.W., Zhu, D.H., Zhu, S.L.: Comprehensive agronomic optimization for Zheqiu soybean 3. Bulletin of Science and Technology 23(3), 382–385 (2007)
11. Yang, D.: Experimental Design and Statistical Analysis, pp. 227–255. China Agriculture Press, Beijing (2002)
12. Liu, W.M., Yu, Z.Y.: Application of rotary regression experimental design in agronomy optimization experiment. Applied Probability and Statistics 3(3), 274–275 (1987)
13. Liu, W.M.: Application of regression design in the study of intercropping system of crops. Statistics and Management 25(5), 1–5 (2005)

Segmentation of Small Animal Computed Tomography Images Using Original CT Values and Converted Grayscale Values

Guoqiang Ma¹, Naixiang Li¹, and Xiaojuan Wang²

¹ Dept. of Computer Science & Information Engineering, Tianjin Agriculture University, Tianjin 300384, China

mgqwxj@163.com, linaixiang@tjau.edu.cn

² Library, Tianjin Agriculture University, Tianjin 300384, China
cwangxiaojuan6996@163.com

Abstract. Medical image segmentation is the foundation of normal and diseased tissue 3D visualization, operation simulation and visual operation. In this paper, we comprehensively use two values that represent the same object (body tissue), to segment by the same algorithm implementation. The original CT images are downloaded from the web source, the dog rib tumor CT scan image by GE medical systems, all the experiment of dataset of 312 thoracic CT scans. The core of the segmentation is k-means clustering algorithm. The segmentation process consisted of two phases: (1) convert CT value to JPG gray value or not use the original CT value as the data sets for clustering; (2) segmentation bone tissue using the new k-means clustering algorithm program which is implemented with MATLAB 2012a programming language and for two-dimensional data matrix directly. The experiment produced strikingly different results. These results may be indicating that not only the segmentation algorithm of CT image is important, but also the data for segmentation is important too.

Keywords: Image segmentation, Computed tomography, k-means clustering.

1 Introduction

Image segmentation is a challenging task in image analysis. Image segmentation plays important role in medical image. A large variety of methods of have been proposed in several years. Intracranial image segmentation techniques for CT images include semi automated region-growing [1], intensity threshold [2, 3], and automated level set methods [4, 5].

The process of grouping a set of physical or abstract objects into classes of similar objects is called clustering. A cluster is a collection of data objects that are similar to one another within the same cluster and are dissimilar to the objects in other clusters. Clustering algorithm is a kind of do not need training, unsupervised (unsupervised) statistical method. In a sense, clustering is a classification of self training. Because of the lack of training sample set, so the iterative clustering algorithm is performed on

the image classification and extraction of feature values. Among them, K-means [6], Fuzzy C-Means [7, 8], EM (Expectation-Maximization) and hierarchical clustering method [9, 10] is commonly used in clustering algorithms. K-means clustering algorithm calculate the current average of each class, then according to the new generation of mean pixel to reclassify (mean pixel in recent class), the new generation class iterative execution front steps.

In this paper, we propose a new processing framework draws on the existing techniques of k-means clustering algorithm and use the CT value for segmentation in CT images. The main algorithm is still using the K-means algorithm. The best contribution of this paper are: (1) completed a specialized MATLAB language program implementation of k-means clustering algorithm for CT images segmentation; (2) using the CT value of DICOM format files directly to calculate by k-means clustering algorithm for segmentation. The results show the segmentation quality is better than using the transformational grayscale values.

2 DICOM Format and Original CT Values

2.1 DICOM Format

DICOM (Digital Imaging and Communications in Medicine) is a standard for handling, storing, printing, and transmitting information in medical imaging. It includes a file format definition and a network communications protocol. A DICOM data object consists of a number of attributes, including items such as name, ID, etc., and also one special attribute containing the image pixel data (i.e. logically, the main object has no "header" as such: merely a list of attributes, including the pixel data). A single DICOM object can have only one attribute containing pixel data. For many modalities, this corresponds to a single image. But note that the attribute may contain multiple "frames", allowing storage of cine loops or other multi-frame data. The same basic format is used for all applications, including network and file usage, but when written to a file, usually a true "header" (containing copies of a few key attributes and details of the application which wrote it) is added.

2.2 CT Value

The characteristic of CT is able to distinguish the slight difference of human tissue densities; the standard is based on the body tissues of X-ray absorption coefficient (μ value) to decide. In order to calculate and convenience, the linear attenuation coefficient is divided into 2000 units, known as the CT value, unit of measurement called Hounsfield.

Using water as a value of 0, the upper bound of bone CT value is 1000; the lower air CT value is -1000. At present, most of the CT scanner has a range of 1000 or more than 2000. In fact, CT value is the corresponding X-ray value of the attenuation coefficient with the different human tissue in CT image. In the CT image, bone and air CT values were specified for upper and lower bounds. The calculation formula of CT value is shown in equation 1.

$$CT_Value(HU) = \frac{\mu_{tissue} - \mu_{water}}{\mu_{water}} \times 1000 \quad (1)$$

The CT values of normal human tissues, organs are shown in Table 1.

Table 1. CT values of normal human tissues

Classes	CT values(HU)
Water	0± 10
cerebrospinal fluid	3~8
plasma	3~14
edema	7~7
alba	25~32
ectocinerea	30~40
blood	13~32
clot	64~84
liver	50~70
spleen	50~65
pancreas	45~55
kidney	40~50
muscle	40~80
gallbladder	10~30
fat	-20~-80
calcification	80~300
atmosphere	<-200
bone	>+400

Matlab R2012a provides `dicominfo()` and `dicomread()` function, respectively, used to read DICOM format image file header data and metadata. For example, in the MATLAB R2012a command window input: `info=dicominfo('D:\ANONYMIZE2\DICOM7_000000.dcm')`, Running result will display detailed information about the file. Two parameters of these detailed information illustrate the transform relation of the record value and the real CT value, they are "RescaleIntercept" and "RescaleSlope". The conversional relation can be represented in equation 2.

$$CT_Value(HU) = pixel_value \times RescaleSlope + RescaleIntercept \quad (2)$$

CT_Value represents the real CT value of body tissue, $pixel_value$ represents the pixel value of a DICOM formatted CT image file, it can be read out by the `dicomread()` function.

2.3 DICOM Values Covered to Grayscale Values

Jpg/Jpeg is an efficient compression format, the file format is JPEG (Joint Photographic Experts Group) standard products. The depth image are 8bit, 12bit,

considering the human eye to gray level of sensory discrimination, the general use of the bit depth is 8bit, the 256 gray level. In the gray image in JPG format, each pixel value is the gray value, the range between 0~255.

Conversion principle is very simple, is to use the `dicomread()` function to read the CT value matrix from a DICOM formatted CT image file and converted to a numerical matrix of 0~255. The conversional relation can be represented in equation 3.

$$I_{gray} = \frac{(I_{CT} - \min(I_{CT})) \times 255}{\max(I_{CT}) - \min(I_{CT})} \quad (3)$$

I_{gray} represents the 256 gray level image matrix after conversion, I_{CT} represents the CT value matrix read by `dicomread()` function.

Matlab key codes of the conversion program are as follows:

```
I=dicomread(CT_file);
I_ct=double(I);
a=max(I_ct(:));
b=min(I_ct(:));
[x,y]=size(I_ct);
for j=1:y
    for i=1:x
        I_gray(i,j)=(I_ct(i,j)-b)*255/(a-b);
    end
end
imwrite(uint8(I_gray),jpg_filename,'jpg');
```

2.4 Matlab K-means Clustering Algorithm Program

K-means algorithm is a hard clustering algorithm, it is a typical of the objective function clustering method based on the prototype of representative which uses the distance summation of data points to the prototype (class center) as the optimum objective function, using the method for the extremism of function to get the iterative adjustment rules. The K-means algorithm uses the Euclidean distance as the similarity measure, it calculates an optimal classification of vector $V = (v_1, v_2, \dots, v_k)^T$ based on an initial clustering center, and keep the evaluation value J_c to a minimum. Algorithm often uses the error sum of squares function as the clustering criterion function, the squared error function is defined as $J_c = \sum_{i=1}^k \sum_{p \in C_i} \|p - M_i\|^2$. The parameter M_i represents the average of class C_i , the parameter p represents a point of class C_i .

We do not use the k-means function in the MATLAB statistics toolbox and write a new k-means clustering algorithm program specifically for CT image.

The process of k-means clustering algorithm is improved by iterative method. The input parameters are two, respectively is the JPG format image file name $I_filename$ and the number of clusters K ; output only corresponding class label matrix IDX_mar . The termination condition function program is that the objective function value of error square sum is no change. The actual amounts of code of this process are only 38 lines using MATLAB programming language.

The pseudo - code of the improved k-means function as follows.

```

1 Begin: $I\_filename='jpg\_file\_name';k='num\_class';$ 
2  $I=imread(I\_filename);$ 
3  $[m\ n]=size(I);$ 
4  $Flag=zeros(m,n);$ 
5  $ma=max(I);mi=min(I);$ 
6 Select  $k$  values as the center of initial  $K$  class from the  $mi$  to  $ma$  equidistantly
7  $J=0;$ 
8 For  $i=1$  to  $m*n$ 
9     For  $j=1$  to  $k$ 
10         Calculate the Euclidean distance from each point of  $I$  to  $K$  values of
class center
11         Save the minimum of  $K$  distance
12         make a kind of markers in  $Flag$  matrix
13     Next  $j$ 
14 Next  $i$ 
15 Calculate the error sum of squares
16 If  $Jc==J$ 
17     Results: marked matrix  $Flag$ 
18 End function: End
19 Else
20      $J=Jc$ 
21     According to the categories, recalculate the  $K$  centroid
22 Endif
23 Goto 8

```

The 256 gray levels JPG format image is segmented by the new k-means clustering algorithm program. This process is shown in Figure 1.

3 Materials and Method

The original CT images are downloaded from the web source, "DICOM7 medical image database", URL: <http://www.dicom7.com/>. The compression package is named for the "ANONYMIZE2", the dog rib tumor CT scan image by GE medical systems, all the experiment of dataset of 312 thoracic CT scans. The first step is converting the DICOM format images to JPG format images using the equation 1. The second step is segment the DICOM format images using CT values and the JPG images using gray values by the new k-means function.

The configuration of the computer used for experiments is with Intel Core Duo 3.33 GHz CPU, RAM Memory 2 GB, 32 bits Windows 7 ultimate; the algorithms are used MatLab2012a programming. We analysis the quality of segmentation results through observe segmentation result with the naked eye.

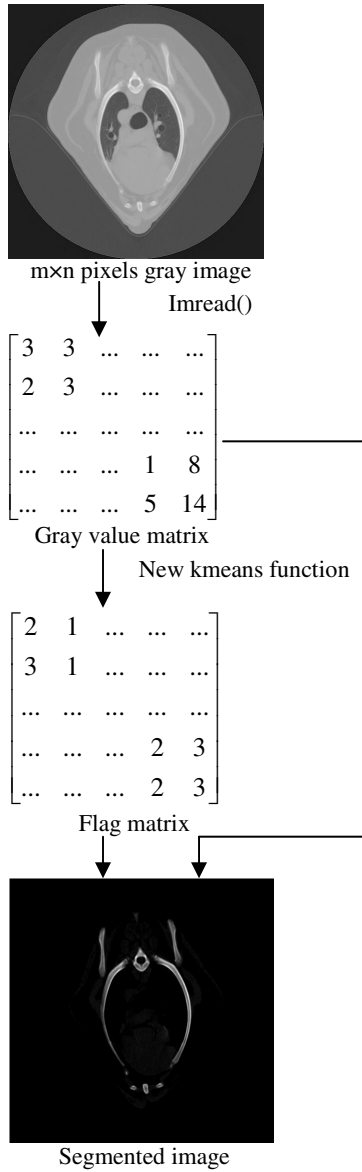

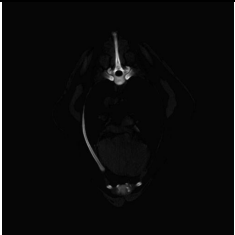
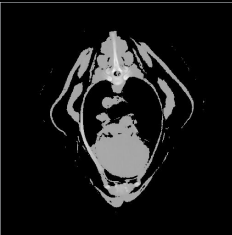

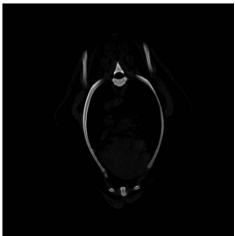
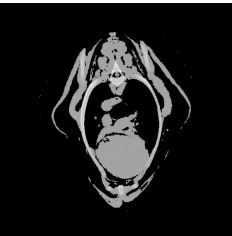
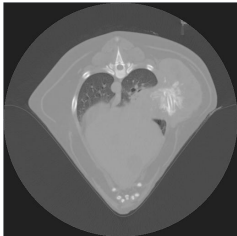
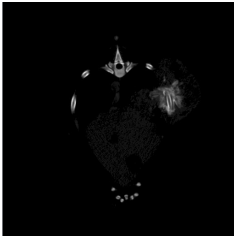
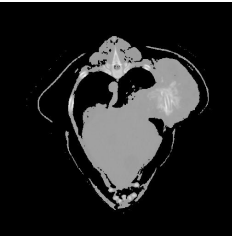


Fig. 1. Segmentation process of JPG image

4 Results

The analysis of computation complexity and comparison of implementation speed for the dog rib tumor segmentation shows that our algorithm takes about 1 second. From the visual effect of view by naked eye, the segmentation effect using of CT value is good to using the gray value by the same segmentation algorithm and the same program implementation. Three examples of segmentation results are shown in Table 2.

Table 2. Three examples of segmentation results

DICOM format files	Original CT images	Segment by CT value	Segment by gray value
DICOM7_000376			
DICOM7_000378			
DICOM7_000684			

5 Conclusions

We have presented a segmentation approach for CT images, which was demonstrated and validated using two dataset of the same CT image scans, consisting of 312 image volumes. The core of the segmentation is k-means clustering algorithm. The segmentation process consisted of two phases: (1) convert CT value to JPG gray value or not use the original CT value as the data sets for clustering; (2) segmentation bone tissue using the new k-means clustering algorithm program which is implemented with MATLAB 2012a programming language and for two-dimensional data matrix directly.

In this paper, we comprehensively use two values that represent the same object (body tissue), to segment by the same algorithm implementation. The experiment produced strikingly different results. These results may be indicating that the segmentation algorithm of CT image is important and the data for segmentation is important too. In other words, what kind of data can really represent the real thing? This could be a complex problem.

Acknowledgment. Funds for this research were provided by the Doctor Foundation of Tianjin Agriculture University, No.2012D09.

References

1. Kamdar, M.R., Gomez, R.A., Ascherman, J.A.: Intracranial volumes in a large series of healthy children. *Plast. Reconstr. Surg.* 124, 2072–2075 (2009)
2. Mardini, S., See, L.C., Lo, L.J., Salgado, C.J., Chen, Y.R.: Intracranial space, brain, and cerebrospinal fluid volume measurements obtained with the aid of three-dimensional computerized tomography in patients with and without Crouzon syndrome. *J. Neurosurg.* 103, 238–246 (2005)
3. Strik, H.M., et al.: Three-dimensional reconstruction and volumetry of intracranial haemorrhage and its mass effect. *Neuroradiology* 47, 417–424 (2005)
4. Jafarian, N., et al.: Automatic fontanel extraction from newborns' CT-images using a model based level set method. In: *Proc. 17th Iranian Conference of Biomedical Engineering (ICBME)*, Isfahan, November 3-4 (2010)
5. Kazemi, K., et al.: Automatic fontanel extraction from newborns' CT images using variational level set. In: Jiang, X., Petkov, N. (eds.) *CAIP 2009*. LNCS, vol. 5702, pp. 639–646. Springer, Heidelberg (2009)
6. Meena, A., Raja, K.: K Means Segmentation of Alzheimers Disease in PET scan datasets: An implementation. In: *International Joint Conference on Advances in Signal Processing and Information Technology, SPIT 2012*, pp. 158–162 (2012) ISSN: 1867-8211
7. Valvi, P., Shah, B., Shah, S.: Improved fuzzy c-mean algorithm for Medical Image segmentation. *International Journal of Engineering Research & Technology (IJERT)* 1(3) (May 2012) ISSN: 2278-0181
8. Ajala Funmilola, A., Oke, O.A., Adedeji, T.O., Alade, O.M., Adewusi, E.A.: Fuzzy k-c-means Clustering Algorithm for Medical Image Segmentation. *Journal of Information Engineering and Applications* 2(6), 2225–2506 (2012) ISSN 2225-0506 (online)
9. Lei, T., Sewchand, W.: Statistical approach to X-Ray CT imaging and its applications in image analysis – part II: A new stochastic model-based image segmentation technique for X-Ray CT image. *IEEE Transactions on Medical Image* 11(1), 62–69 (1992)
10. Liang, Z., MacFall, J.R., Harrington, D.P.: Parameter estimation and tissue segmentation from multispectral MR images. *IEEE Transactions on Medical Image* 13, 441–449 (1994)

Design and Implementation of Laiwu Black Information Management System Based on ExtJS

Chen Dong¹, Liu Pingzeng^{*}, Zhang Yunfan², and Ma Hongjian²

^{1,2} School of Information Science and Engineering, Shandong Agricultural University,
Taian 271018, China

¹ Beijing Research Center for Information Technology in Agriculture,
Beijing 100097, China

Abstract. Aimed at the problems of low level of informatization in LaiWu blackpig process and the old way of using paper for date storage, in order to speed upthe informatization development of the process, the LaiWu black pig information management system based on ExtJS is designed. In this paper, the design and realization of the system, as well as the open source framework is illustrated in detail, the ExtJS+SSH(Sturts+Spring+Hibernate)framework exploration model is put forward,and the separation of page and is realized. The result of system operation shows that not only the level of informatization in LaWu black pig process is improved, but also its maintainability and expandability are developed.

Keywords: ExtJS, Struts framework, Spring framework, Hibernate framework.

1 Introduction

LaiWu black pig is North China local pig breeds, belongs to one of the precious local pig breeds. which has a high rate of reproduction, feeding force, obvious heterosis, resistance to coarse resistance, tender meat mellow characteristics. In recent years, according to the characteristics of Laiwu pigs, Laiwu increased its conservation and utilization, but there are still many problems, such as the black pig rearing informatization level is not high, low efficiency of breeding information recording. In view of Laiwu black pig in conservation and optimization problems, in order to realize the local pig breed information, this paper shows that the information management system of Laiwu black pig. This system is developed for Laiwu black pig breeds unique information management system, with a single head black pig as the goal, to achieve uniform code on each head of black pig. In order to establish information management platform for Laiwu black pig, to provide complete information chain of pork traceability of Laiwu black pig.

Laiwu black pig information management system uses the most popular J2EE framework. The development technology of J2EE framework is becoming more and

^{*} Corresponding author.

more mature and perfect, the system running cost and performance more advantages than other architecture, the current more popular Struts+Spring+Hibernate (hereafter referred to as SSH) architecture provides complete, lightweight J2EE software development model, which makes Web application becomes more convenient. However, the Web system not only needs to have stability and robustness, also need to have a friendly user interface. At present, SSH in the presentation layer implementation is proposed, mainly lack of interaction mechanism and system background effectively in a JSP page Struts tags, the data interaction with the page can not be separated, resulting in system development process requires a large amount of JSP page, makes the system maintenance is more complicated; and change a tag of a page will cause to refresh the whole page, resulting in the presentation layer of the flexibility reducing network bandwidth, and to bring greater pressure.

Therefore, using appropriate AJAX framework in the overall architecture, not only can improve the system page development efficiency, but also can greatly increase the system interface and the user interaction. In recent years , the rapid development of ExtJS is an excellent AJAX framework, which provides a common component of almost all Web applications, can not only realize the beautiful user interface , and can realize efficient separation presentation layer and business logic layer separation by using the asynchronous interaction mechanism, which further increases the system maintainability.

The innovation of this paper lies in specially according to the growth characteristics of Laiwu black pig and the design and implementation of the information management system. And in the design of the system and puts forward some new ideas for the integration of Extjs and SSH framework, unified standard of Laiwu black swine model of information transmission in the system, to provide a strong guarantee for the establishment of Laiwu black pig traceability system.

2 Open Source Framework

2.1 Extjs

Ext JS is the leading standard for business-grade web application development. With over 100 examples, 1000 APIs, hundreds of components, a full documentation suite and built in themes, Ext JS provides the tools necessary to build robust desktop applications.

Compared to other AJAX framework, ExtJS is the biggest characteristic of supporting the built-in UI components of both beautiful and abundant , rather than through plug-ins. This makes the UI assembly more seamless cooperation. The ExtJS support Grids, TabPanel (multiple tags panel), Chart, Window, Tree, Layout Manager, ComboBox, Form, Toolbar, Menu, Templates and DataView, Panel etc.. These components make ExtJS not only is a JavaScript library, and a framework on real significance, can be satisfied with the large, complex Web application requirements.

Therefore, using ExtJS above advantages, not only can integrate Web system and SSH architecture well , and can reduce the burden on developers, and can achieve a high interactive system page.

2.2 SSH

A Web application system framework is divided into the presentation layer, control layer, business logic layer and data persistence layer . The SSH framework provides a complete lightweight J2EE software development model, in which struts is used as the presentation layer and control layer mainly framework, provide MVC control, all kinds of presentation layer labels and input validation and other functions, improve the efficiency of development.

Spring can effectively organize business logic layer object, easily with other said seamless integration framework, allowing the option to use a module which according to requirements; provides a unified interface for different data access technology, and the use of inversion of control (IoC) can be easily implemented bean assembly provides concise; AOP implementation of the transaction management.

Hibernate is a work in the persistence layer based on the object-relational mapping (ORM) open source framework, it provides lightweight object encapsulation of JDBC, and provides a powerful, fully object-oriented query language (HQL), so the Java programmer can freely according to the object-oriented way of thinking to manipulate the database. The data are encapsulated into object, reduces the complexity of the persistence layer, that developers can concentrate on the application, and not to care about the underlying database structure.

3 Analysis and Function of the System

Combined with the current Laiwu black pig growth, feeding and slaughter characteristics, this paper built the Laiwu black pig information management system suited to their characteristics; System manage information of Laiwu black pigs from birth to slaughter, including the Laiwu black pig breeding, slaughtering, warehousing information. To achieve unified management of black pig information, to provide complete information criterion for a black pig raising sales.

The system function module as shown in Figure 1:

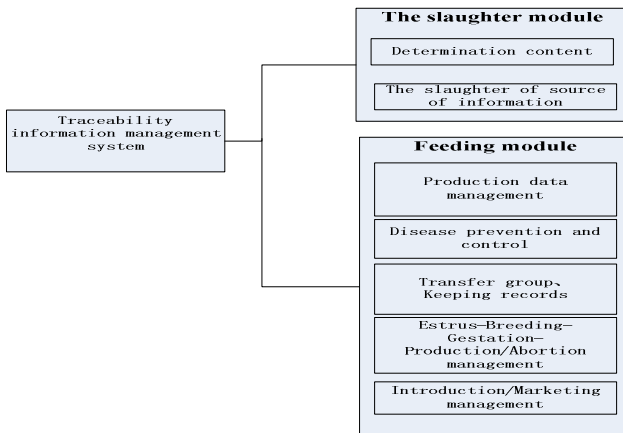


Fig. 1. Laiwu pig traceability information management system function module

4 System Implementation

Laiwu black pig in information management system base on the ExtJS3.4+Spring3+Hibernate version, debug browser is Firefox, auxiliary debugging tool is Firebug, the environment is prepared to install the Spket plugin for Myeclipse10.

4.1 System Framework

The system framework is shown in Figure 2, page display use Extjs framework, business logic control use Struts and Spring, data persistence use Hibernate. Interaction between Extjs and server is all Ajax requests, data exchange format is JSON. Injection of Bean use Spring Ioc technology. Struts realize control layer. The overall frame structure is clear, distinct, fully meet the requirements of system design.

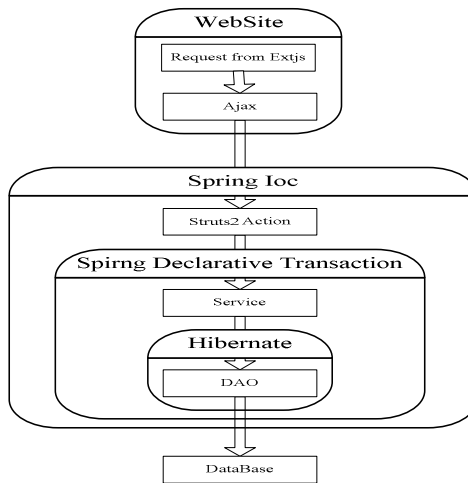


Fig. 2. System architecture

4.2 ExtJS View

4.2.1 Extjs Framework

As shown in Figure 3, the Extjs application architecture in Laiwu pig traceability information management system similar to the MVC structure, View layer is the presentation layer components, the main application of TreePanel, FormPanel, Grid and other components complete the display function; Controller layer is responsible for controlling the browser events, in the the View layer and Model layer as a bridge; Model layer is mainly responsible for data interaction.

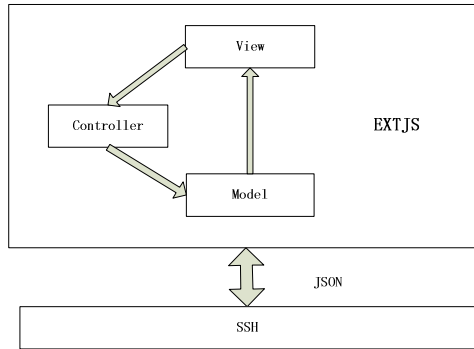


Fig. 3. Extjs application framework in Laiwu pig in the system

4.2.2 ExtJS Configure

UTF-8 code are used for data interaction between ExtJS frame and background. So the interface in the use of ExtJS programming, through the following settings can be for the Chinese character display:

```

<script
type=" text/javascript src="extjs/ext-lang-zh_CN.js"
defer=true charset="UTF-8">
</script>
  
```

4.2.3 Components Declaring and Layout

ExtJS UI library includes a variety of components, including TreePanel, FormPanel, GridPanel, Button components used in the system.

In the component declaration, make full use of the ExtJS object oriented thinking, set the constructor for the main components, in order to unify the style and save code, will set the basic properties in constructor. When use a component to the system,calling the constructor, instantiate of component object.

4.2.4 Data Interchange Format

ExtJS use AJAX to send data formats including XML and JSON (JavaScript Object Notation) format, the JSON format is recommended, the JSON is a lightweight data interchange format, easy for machines to parse and generate, lighter than XML, because JSON is a JavaScript native format, which means that the processing of JSON data in JavaScript does not require any special API or toolkit. So in Laiwu pig traceability system select JSON format as data transmission format.

As shown below, for example in the JSON data transmission system:

```

{"idTransforms":[{"cardid":"91800000120427","realid":"808027000000011"},
{"cardid":"91800000120428","realid":"808027000000012"},{"cardid":"91800000120431","realid":"808027000000015"},{"cardid":"91800000120432","realid":"808027000000016"}]}
  
```

4.2.5 Interactive Data Processing

Laiwu pig system using two kinds of interactive mode:

Using Store: Laiwu pig system data show almost all Ext.grid.GridPanel components, where use Store as a data storage object, it is responsible for the original data into objects of Ext.data.Record. Through the Ext.data.Store, obtain the background data and converts it into a form that can be used form.

Store has two parts: proxy and reader. Proxy is a data acquisition mode, reader refers to how to parse this data. Ext.data.Record is the most basic part of Ext.data.Store, the main function is to save the data. HttpProxy using the HTTP protocol,using the Ajax gain backstage data, it need to set the URL parameters. JsonReader is a JSON data reader, by Reader make data read out, it will get the corresponding data from JSON using the name parameter by default. The proxy and reader properties in store, JSON can be read into the Record instance, and then execute this.Store.load () to achieve the transition process. Finally, through instantiation of grid, generating and displaying tables, data will be presented to the front.

As shown in Fig. 4:



The screenshot shows the '莱芜猪产业链食品安全溯源系统' (Laiwu Pig Industry Chain IOT Trace System) interface. The main content is a table titled '猪高管理画板' (Pig Management Dashboard) with the following data:

猪高名	猪高管理	猪高类型	猪高地址
1011	100	产仔母猪	莱芜
1012	100	保胎猪	莱芜
1013	100	胎前母猪	莱芜
1014	100	产仔猪	莱芜
1015	100	公猪	莱芜
1016	100	母猪	莱芜
1017	100	产仔母猪	莱芜
1018	100	保胎猪	莱芜
1033	100	产仔猪	莱芜
1055	100	保胎猪	莱芜
1111	4	母猪	guanchang
123	120	产仔猪	23423
G1-1	3	母猪	猪场一排第一个
G1-10	3	母猪	猪场一排第十个
G1-2	3	母猪	猪场一排第二个
G1-3	3	母猪	猪场一排第三个

The interface also includes a sidebar menu with options like '日常系统', '猪高管理', '信息统计', and '系统管理'. The footer contains copyright information for 2012-2020 NDAU and the logo for LRACE.

Fig. 4. Laiwu pig system interface table example

Using Ajax:In data exchange, largely depends on the underlying implementation of Ajax. In order to unify the interface, the Ext package on the ajax, so the of Ajax in the Ext can be used between with different underlying implementation. Therefore, in Laiwu pig system, in addition to the application of Ext.data.Store and the backstage data exchange, another way is the application of Ext in Ajax.

Pigs in Laiwu system, all form submissions are used Ext.Ajax, calling the request function of Ext.Ajax, the argument is a JSON object. The URL parameter show that will access url of the background. The params indicates that sent to the background parameters, here use JSON objects. Method is request method, due to the transmission of a large amount of data, here use post. "success" parameter represents a callback function response after success."failure" parameter represents a callback function response after failure.

Note, here the response failure does not mean business database operations failure, but that HTTP returns 404 or 500 error. So in success method using the if statement to judge business failure, but failure method only judge HTTP response error.

4.3 Business Logic Layer and Data Persistence Layer

The data exchange layer is responsible for transmitting a request and receive the response in ExtJS, then Struts according to the configuration file (struts-config.xml) receiving a ActionServlet Request assigned to Action corresponding processing. In the business layer, Spring IoC container management service component is responsible for providing the business model component to Action, and also provides the transaction processing, the buffer pool, to enhance system performance and ensure the integrity of data. But in the persistence layer, object mapping and database interaction is dependent on Hibernate, DAO component request data, and return results.

5 Conclusions

According to the basic situation of Laiwu black pig industry design of Laiwu black pig information management system based on ExtJS, has the advantages of using ExtJS technology to make the system more friendly interface, reduces the coupling of the front page and back office processing layer, more conducive to the development and maintenance of the system; and the using of SSH framework, making the system more stable, structure more clear. System design of Laiwu black pig industry improves the information management level, simplify the feeding process, to ensure the integrity of the information of Laiwu black pig, Laiwu pig breeds make excellent brand construction entering a new level.

Acknowledgment. This research was supported by National Science and Technology Support Project of China (Grant No. 2013BAD15B05) all support is gratefully acknowledged.

References

1. Caulkins, J.P.: A method for managing access to web pages: Filtering by Statistical Classification (FSC) applied to text. *Decision Support Systems* 42(1) (2004)
2. Anonymous. Research and Markets; Professional JavaScript Frameworks: Prototype, YUI, ExtJS, Dojo and MooTools. *Computer Weekly News* (2009)
3. Niedermayer, A.: On platforms, incomplete contracts, and open source software. *International Journal of Industrial Organization* (2013)
4. Power, D.J.: Securing web services for deployment in health grids. *Future Generation Computer Systems* 22(5) (2005)
5. Pons, A.P.: Semantic prefetching objects of slower web site pages. *The Journal of Systems & Software* 79(12) (2006)

6. Jayashree, K.: Web Service Diagnoser Model for managing faults in web services. *Computer Standards & Interfaces* (2013)
7. Tahir, A.: A systematic review on the functional testing of semantic web services. *The Journal of Systems & Software* (2013)
8. Madhusudan, T.: A declarative approach to composing web services in dynamic environments. *Decision Support Systems* 41(2) (2004)
9. Bennett, S.: Implementing Web 2.0 technologies in higher education: A collective case study. *Computers & Education* 59(2) (2012)
10. Vantaggiato, A.: Automatic exams management with the Common Lisp HTTP Server. *Computer Networks and ISDN Systems* 30(1) (1998)

Fresh Tea Picking Robot Based on DSP

Heng Li¹, Chao Li¹, Liming Xu¹, Guangming Qin², Xin Lu¹, and Ying Zhao²

¹College of Engineering, China Agricultural University, QingHua East Road No.17, Beijing, China

²Nanjing Agricultural Machinery Research Institute, Nanjing 210014
{liheng06,xlmoffice}@126.com, caulc2012@163.com

Abstract. According to the tea cultivation conditions a 4 DOF gantry Cartesian coordinate tea-picking robot was designed. The picking gripper was used two fingers, driven by a servo to open and close. One finger was furnished a knife to cut the tea stem. The controlling system was based on TMS320F2812 DSP and was consisted of both C and assembly language. It was able to achieve serial communication, data processing and precise servo control. The tea picking robot work efficiency verification tests and linkage comparative test have been conducted in the indoor. The results show that the maximum operating frequency of motor drive system of X-axis, Y-axis and Z-axis were 173.61kHz, 58.59kHz and 24.40kHz respectively, and that two-axis linkage and three-axis linkage operation efficiency were 1957 times per hour and 2517 times per hour respectively.

Keywords: tea, picking robot, DSP, servo control, two-axis and three-axis linkage.

1 Introduction

The two main ways to pick tea are artificial picking and mechanical harvesting. But the artificial picking is labor intensive and highly cost, and the mechanical picking uses the method of cutting, so it has a high breakage rate and is harm to the tea trees. Also it makes the subsequent sorting more difficult and it is not suitable for picking famous tea. Robot application in this field in China or abroad is still in the blank. This paper developed a TMS320F2812 DSP controlled 4 DOF tea-picking robot which can pick various kinds of tea piece by piece. DSP is a high-performance microprocessor in digital signal processing and controlling, which has the character of high speed, high efficiency, strong anti-jamming capability and strong scalability. It can meet the high-speed and real-time demand.

2 The Picking Robot Mechanism Design

2.1 Tea Cultivation

In order to meet the needs of the job of the tea-picking robot, tea trees were specially cultivated. The tea garden space diagram was showed in Fig. 1. The ridge width of tea trees is 1.2m, the height is between 0.5m and 0.8m, and the row space is 1.5m. The robot works across in the tea ridge and goes forward with the caterpillar tractor.

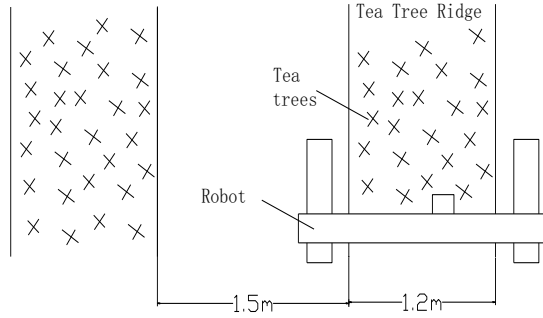
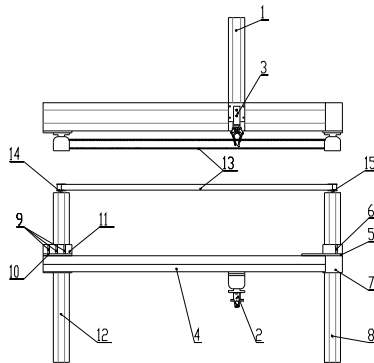


Fig. 1. The tea garden space diagram

2.2 Design of the Tea Picking Robot Mechanism

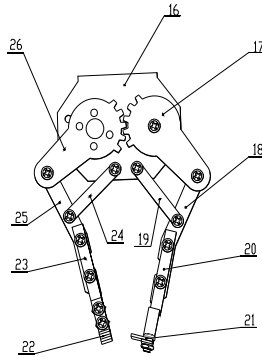
According to the dimensions of the tea ridge, a 4 DOF gantry Cartesian coordinate tea-picking robot was designed. The robot manipulator (Fig. 2 (a)) consisted of X1 slide, X2 slide, Y slide, Z slide, picking gripper, synchronous belt, synchronous belt pulley and some connecting plates. The effective stroke of X-axis, Y-axis and Z-axis are 500mm, 1300mm, and 200mm respectively. The Y-axis is connected across the two X-axis and the Z-axis is installed on the Y-axis. In order to ensure that X1-axis and X2-axis move synchronously the two axes are connected by a synchronous belt.

According to the specific requirements of the tea picking, a steering engine driven picking gripper was designed (Fig. 2 (b)), which was installed on Z-axis. The left gear of the gripper was connected and rotate with the rotating shaft of the steering engine. The right gear achieves the opposite direction of rotation through a gear pair with the left gear, and together with the four bar linkage mechanism (18,19,24,25) achieving the opening and closing of the gripper. When the blade and the blade pad installed on the front end of the two fingers meshing together, the tea can be cut down.



(a) Manipulator

Fig. 2. Tea Picking Robot mechanism



(b) Picking Gripper

1-Z slide;2-Picking gripper;3-Gripper fixed plate;4-Y slide;5-Right vertical mounting plate of Y slide;6-Right rib of Y slide;7-Right horizontal mounting plate;8-X2 slide(driven);9-Left rib of Y slide;10-Left vertical mounting plate of Y slide;11-Left horizontal mounting plate of Y slide;12-X1 slide(driving);13-Synchronous belt;14-Left synchronous pulley;15-Right synchronous pulley;16-Gripper bracket;17-Right gear of gripper;18-Right finger;19-Right connecting rod;20-Blade bracket;21-Blade;22-Blade pad;23-Bracker of blade pad;24-Left connecting rod;25-Left finger;26-Left gear of gripper(driving)

Fig. 2. (Continued.)

3 The Control System of the Tea Picking Robot

3.1 Hardware Components and Principle of DSP Control Board

The TMS320F2812 chip from TI company was selected to be the control chip. This chip is a 32-bit fixed-point DSP chip which is suitable for use in industrial control, motor control etc. It's running clock can reach 150MHz, and each instruction cycle is 6.67ns. It has 128k ×16-bit on-chip FLASH, 18k×16-bit SRAM and abundant peripheral interfaces. In order to reduce the difficulty of the system design, the mature development board QQ2812 was selected. This development board equipped with the F2812 chip and commonly used peripherals and interfaces. Fig. 3 shows the system function block diagram. The communication between the image processing unit and the DSP controller was achieved by RS232 serial port, transmitting the three-dimensional coordinate information of each plucking. According to the position gotten from image processing unit, the DSP can achieve the close-loop control of DC servo motor on X,Y and Z axis and the open-loop control of gripper steer engine.

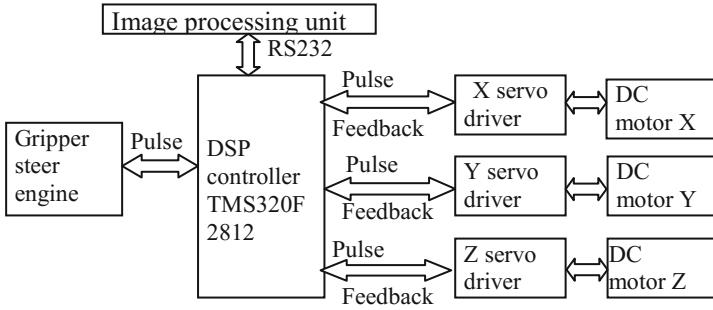


Fig. 3. System block diagram

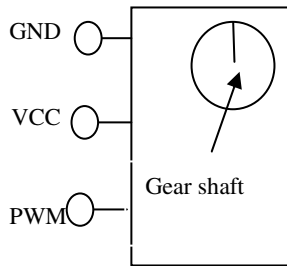


Fig. 4. Analog servo

3.2 Servo Control System

The structure of the analog servo was showed in Fig. 4, which was used in this system. The servo control signal is PWM signal, changing the duty cycle can change the angular position of the gear shaft of the servo. The DSP output two different duty cycle of the pulse signal corresponding to the gripper opening and closing state.

3.3 Motor Control System

This system has 3 DC servo motor whose model is MAX32. Due to the system’s mobile power and take energy issues into consideration, a small probability 20 W DC motor and gear reducer drive program was selected. After the DSP receive the txt data file from image processing unit, the data was specially processed and convert into the position information of the respective axes. Then DSP sent a certain number of pulse to control the motor to rotate a certain angle, so that the each axis can move to the specified location[4,5]. The control flow diagram of the servo motor was showed in Fig. 5. The motor control system was composed of three control loops which are current loop, velocity loop and position loop. Under the work condition each motor moves according to DSP’s construction, and through the three closed loop DSP can achieve high precision velocity control and position control[5,6].

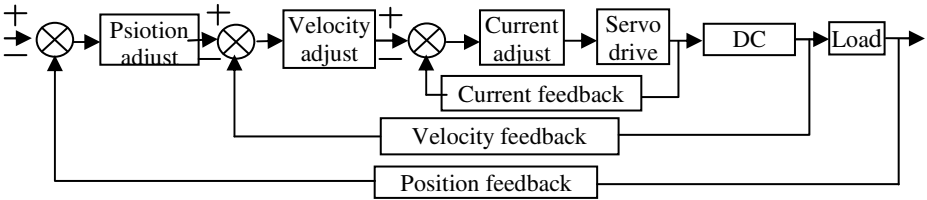


Fig. 5. Motor control block diagram

3.4 Software Design

The software was designed by CCS3.3(Code Composer Studio), using C language and assembly language to achieve all the function. The workflow was showed in Fig. 6. System is initialized after powered on, then steps into the communicating stage, receiving position data from the image processing unit, after which X, Y and Z axis move and the gripper close, picking the tea. Simultaneously, the blower work and the tea is drawn back into the collection box, completing a picking action. Then the system will detect whether all the position have been completed. It will go to next area ,if completed. Otherwise, it will go to the next position. After having been developed and debugged, the software was flashed into the FLASH memory of the DSP from the JTAG port via USB emulator[7,8,9]. Then it was copied to RAM when working to improve the running speed. After powered on, the system orderly calls concerning functions which contain initializing function, position initializing function – pos_init(), communicating function-data_read(), coordinate detecting fuction-pos_dect(), 5 action functions and 3 DSP counter overflow interrupt functions. Table 1 shows the main function and function description.

Table 1. Key functions and use

Function name	characteristic	Capability
Initialization()	Initializing function	Initializing concerned register
pos_init()	Task function	Each axis goes to original point
data_read()	Task function	Serial communication
pos_dect()	Task function	Detectingposition exceed the maximum stroke or not
move_xy(m,n)	Task function	X,Y move
z_down(m)	Task function	Z axis goes downward
paw_close()	Task function	Gripper closes
z_up()	Task function	Z axis goes upward
paw_open()	Task function	Gripper open
eva_t1pint_isr()	Interrupt function	X-axis position interrupt respond
eva_t2pint_isr()	Interrupt function	Y-axis position interrupt respond
evb_t3pint_isr()	Interrupt function	Z-axis position interrupt respond

3.5 Communication

This system uses standard RS232 interface as a means of communication(Fig. 7). After initializing, the DSP enter the serial communication routines waiting for the data stransmission from image processing unit. The DSP needs 4 bits decimal coordinates information, so a special processing method was used, which filters the received data and remains the thecharacters whose ASSIC value is between‘0’to‘9’, storing the valid chatacters in a structure in the format of every 4 characters a group as a 4-bit integer and using a particular 4-bit digits as a sign of the end of the data.

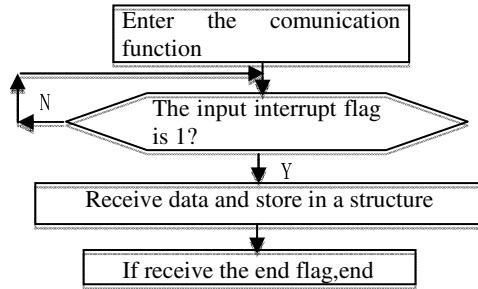


Fig. 6. Flowchart of serial communication

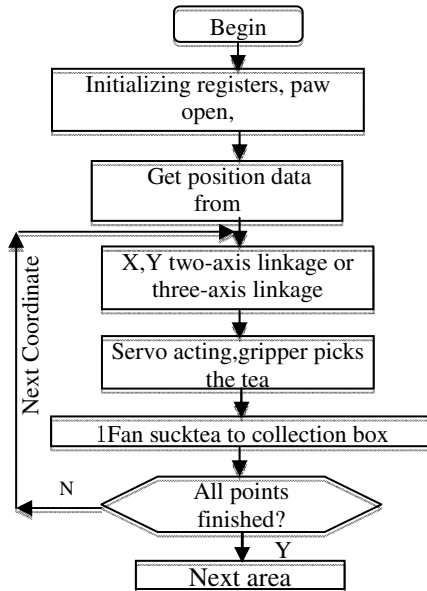
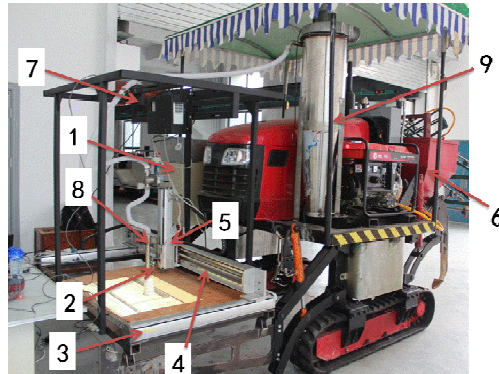


Fig. 7. Software flow chart

4 The Efficiency Analysis and Test of the Tea Picking Robot

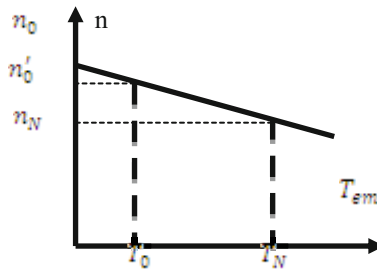
4.1 The Efficiency Principle Analysis of the Tea Picking Robot

The robot is showed in Fig. 8, which is consisted of control board, X silde, Y slide, Z slide, gripper etc. It is install on a crawler tractor when working. The picking speed of the robot detemines the final operating efficiency which is influenced by to factors, the software factor and the hardware factor.



1-control board, 2-gripper,3-X slide,4-Y slide,5-Z slide,6-crawler tractor,7-camera
8-suction tube 9-collecting box

Fig. 8. The whole system



n_0 —Ideal no load speed ; n'_0 -Actual load speed ; n_N -Rated speed; T_0 -No load torque
; T_N -Rated torque ; T_{em} -Load torque

Fig. 9. Mechanical characteristic curve of DC motor

4.2 Software Factor

The TMS320F2812 DSP has two event managers, each of which has two independent counter. Adjusting the upper limit value can change the overflow cycle, so as to achieve the purpose of changing the pulse frequency. Formular (1) is the output pulse frequency formular[9,10].

$$f = \frac{HSPCLK}{(TxPR+1)2^{TPS}} \quad (1)$$

f-output frequency; TxPR-overflow value of counter(x is 1,2,3 or 4); TPS-division factor of counter; HSPCLK-system clock pulse frequency.

4.3 Hardware Factor

The physical characteristics of the motor is another factor affecting the efficiency. Formular (2) is the DC motor speed formular and the mechanical characteristic curve of DC motor is showed in Fig. 9 [5].

$$n = \frac{U}{\phi C_e} - \frac{R}{\phi^2 C_e C_T} T_{em} = n_0 - \beta T_{em} \quad (2)$$

n_0 —Ideal no load speed ; β -Equivalent load curve slope ; T_{em} -Load torque ; U -Rated voltage ; ϕ -Excitation flux ; R -Armature resistance ; C_e -EMF constant; C_T -Asynchronous motor torque constant.

4.4 Test of the Tea Picking Robot

4.4.1 Maximum Working Test of the Motor System

1) Test purpose. In order to test the actual highest working speed, a operating frequency test was done.

2) Test method. When not connected to the image processing unit, the highest working speed of each motor system were tested by adjusting the output pulse frequency through the CCS software. The output frequency was changed by changing the value of TXPT in the initializing function. The word length of the DSP is 32 bits, and it's initialization value of the register is consisted of 4 hexadecimal numbers whose format is as following:

$$TXPR = 0x1234 \quad (3)$$

Aiming to test the minimum value of TXPR(corresponding to the maximum value of the output pulse frequency), change the second bit of the right number from the right to the left successively and compile and debug the software online, and then test whether the motor system can work normally[10].

3) Test results. The frequency test histogram obtained through 3 times of repeated tests was showed in Fig. 10. The test value of X-axis for each time were 173.53kHz,173.69kHz and 173.62kHz respectively. Correspondingly, the value of Y-axis were 58.61kHz,58.50kHz and 58.57kHz respectively, the value of Z-axis were 24.38kHz,24.44kHz and 24.51kHz respectively. Finally, the average highest frequency of X,Y and Z axis were 173.61kHz, 58.59kHz and 24.40kHz respectively.

4.5.3 Experimental Results and Analysis

The test was repeated three times to test the 10-point overall time. The experimental results were showed in Fig. 11. In the first set of test, the two-axis linkage total time was 18.41 seconds, and the three-axis linkage is 14.24 seconds. The second set of test results are 18.56 seconds and 14.37 seconds. The third set of test results are 18.32 seconds and 14.40 seconds respectively. By calculating the average value of overall time and the average time per time, the average picking time each time of two-axis and three-axis linkage are 1.84 seconds and 1.43 seconds respectively. Then the efficiency of each linkage can be determined. The two-axis sequence of operation is that X,Y axis move simultaneously, when arriveing the destination, the X axis moves, and after Z reaches the special location the gripper acts, then the Z axis goes back to original position. Characteristics of two-axis linkage is that the gripper moves up and down vertically which will not collide with the surrounding tea trees, but has a slower speed and relatively lower efficiency. The three-axis sequence of operation is that X,Y and Z axis move simultaneously, when arriveing the destination gripper acts, then X,Y and Z axis go to next position. Characteristics of three-axis linkage is that it has a higher speed, but may collide with the surrounding tea trees. Three-axis reduces the independent operation time of Z-axis, and the data obtained from experiments shows that these two action took 0.41 seconds. According to calculating the work frequency hourly, the two-axis linkage is 1957 times per hour and the three-axis linkage was 2517 times per hour, so the three-axis linkage has a obvious speed advantage.

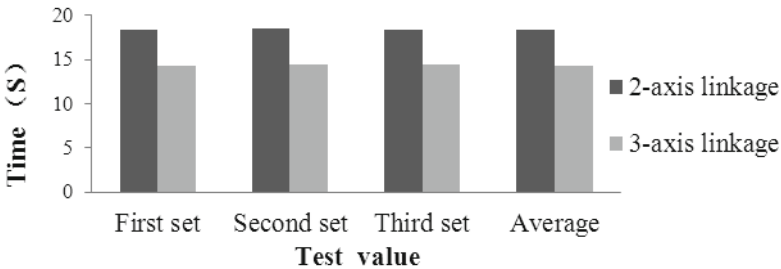


Fig. 11. Linked experimental result

5 Conclusions

Based on the tea cultivation conditions a TMS320F2812 DSP controled 4 DOF tea-picking robot was designed. Based on the experimental verification, the following conclusions were drawn:

- 1) A 4 DOF gantry Cartesian coordinate tea-picking robot was designed and a gripper who can pick and cut was designed. This robot can pick tea across the ridge whose structure could meet the basic operational requirements.
- 2) The high-performance TMS320F2812 DSP can achieve the real-time control, rapid response, and fast communication. It also can convert the coordinate positions into the number of pulses accurately, achieve the real-time interrupt response accurately, position the gripper accurately and achieve the close loop control of the robot.

3)The theoretical analysis of the working efficiency was finished in the indoor test, and the following factor affecting the working efficiency were found: the output pulse frequency, the ideal no load speed, the system damping, the load, the gear ratio of the redactor and the linkage form. The actual working frequency of the motor system was obtained through the frequency test which were 173.61kHz, 58.59kHz and 24.40kHz respectively. The linkage comparison test indicated that the operating sequence and linkage formate can be changed by changing the parameters of the control software, that the efficiency of two-axis linkage and three-axis linkage were 1967 times per hour and 2517 times per hour respectively.

4)The robot was only tested indoor, also need test in the field in the future.

Acknowledgements. This project was a “National scientific support project” in rural areas (2011BAD020B07-3) which was financially supported by the Department of Science and Technology of China. The Key Technology and Equipment Research and Development of Tea Work Robot (BE2011345) .

We gratefully acknowledge the help and support providers from The Ministry of Agriculture Nanjing Institute of agricultural mechanization, Yangzhou University and Nanjing Forestry University.

References

- [1] Wang, Y., Chen, A., Liu, X.: The rectangular coordinate robot control system. Light industry machinery, Ning Du Yunsheng high-tech research institute (fourth period 2010)
- [2] Kuwahara, J.H., Ono, Y., Nikaido, M., Matsumoto, T.: A Preceion Direct-Drive Robot ARM. Yokogawa Hokushin Electric Corporation, Corporate R & D, Musashino-shi
- [3] Zhou, G., Li, Z., Jiang, F.: DSP and CPLD-based open robot controller. Control Engineering, 84–86 (first period, 2006)
- [4] Lei, A.: Robot motion control software design. Master thesis, Southeast China University (2008)
- [5] Chen, L., Yan, Z., Liu, X.: Control Motors, 3rd edn. Xi'an Electronic and Science University Press, Xi'an (2000)
- [6] Zhang, B., Zhao, H., Yue, Y.: DSP-based stepper motor control system design. Instrument Technique and Sensor (8), 63–66 (2010)
- [7] Xu, X., Yu, J., Zhang, L.: Stepper motor multi-axis the DSP control system design. Mechanical and Electrical Product Development and Innovation 18(5), 110–112 (2006)
- [8] Tang, M.: The develop of ARM-based programmable controller. Nanjing University of Information Engineering, Nanjing (2007)
- [9] Wang, L., Zhang, S., Ma, C., Xu, Y., Qi, J.: ARM -based variable spraying control system design. Jilin University Key Laboratory of the Ministry of education (2010)
- [10] Ren, R., Zhou, L., Yao, G.: TMS320F2812 Source code analysis. Publishing House of electronics industry, China (2012)

Study on Cloud Service Mode of Agricultural Information Institutions

Xiaorong Yang^{1,*}, Neng-fu Xie^{1,*}, Dan Wang^{1,*}, and Li-hua Jiang^{1,*}

¹ Agriculture Information Institute, Chinese Academy of Agriculture sciences, Beijing, P.R. China

² Institute of Scientific and Technical Information of China, Beijing, P.R. China

³ China Machinery Industry Information & publication, Beijing, P.R. China
{yangxiaorong, xienengfu, wangdan01, jianglihua}@caas.cn

Abstract. As a new service mode, cloud services become the growth point of the service innovation of agricultural information institutions. This paper presents three-layer cloud service model of agricultural information institutions which includes infrastructure layer, automated management system layer and service layer from bottom to top. Based on this model, this paper studies the cloud service mode and construction content of agricultural information institutions from four angles of IaaS, PaaS, DaaS and SaaS. Finally, the cloud service mode facing internal member institutions and readers of the national science and Technology Library is designed to verify the cloud service model.

Keywords: cloud computing, cloud services, agricultural information institutions, service mode, IaaS, PaaS, DaaS, SaaS.

1 Introduction

With the development of cloud computing technology, the cloud service application research becomes a hot issue. As a cloud service guide, Google puts forward a complete set of distributed parallel cluster infrastructure according to the characteristics of the large scale network data. And Google provides a series of SaaS for individual users and enterprises including the Google search engine, Google maps, photos&videos sharing, social networks, Gmail, Google calendar, Google Apps Market place and so on. As a non-profit and the world's largest library cooperation organization, Online Computer Library Center (OCLC) launched the Web collaboration library management service cloud in April 23, 2009. And OCLC provides a full set of cloud computing library information management service such as joint cataloging, interlibrary loan, WorldCat.org, WorldCatLocal, Questionpoint, CONTENTdm, circulation management, procurement management, and copyright management. China Academic Library & Information System (CALIS) joined nearly 800 university libraries to open the SaaS including E read, current contents of western

* Key Laboratory of Agricultural Information Service Technology, Ministry of Agriculture, The People's Republic of China.

journals(CCC), unified authentication system (UAS), interlibrary loan (ILL), distributed collaborative virtual reference system (CVRS) and the unified data exchange system (UES) (Wenqing Wang et.al, 2009). Baidu Inc opens their own core cloud capabilities to provide a series of cloud services and products such as Personal cloud storage(PCS), Site App、mobile test cloud (MTC) and Baidu application engine (BAE) for the developers and users.

Agricultural information institutes own rich resources and strong talent team. And they should undertake the social responsibility to provide high quality and efficient service for agricultural users. To apply cloud computing technology, resource utilization and service efficiency will be enhanced obviously.

2 The Cloud Service Model of Agricultural Information Institutions

To design the cloud service model, agricultural information institutions should evaluate the existing software and hardware facilities, technical strength and financial support comprehensively. Three factors are very important for the cloud service hierarchy. Firstly, it should be guided by the principle of applicability, economy, maintainability, safety, reliability, scalability. Secondly, it should be based on the standards system. The last but not least, it should be supported by the operation maintenance and security system. The hierarchy includes infrastructure layer, automated management system layer and service layer from bottom to top. The relationship and structure are shown in figure 1.

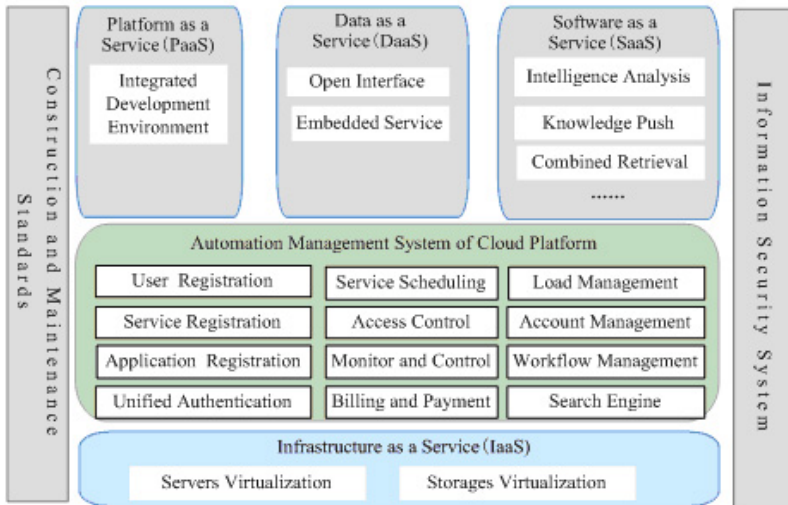


Fig. 1. The Cloud Service Model of Agricultural Information Institutions

The IaaS layer is the underlying structure of the three layer cloud service model. This layer consists of some hardware facilities such as the cloud computing cluster equipments, cloud storages, cloud network transmission equipments and cloud physical resource management servers. The server, database, memory, operating system, I/O equipment, storage and computing power become a virtual resource pool by virtualization technology. Thus the virtual resource pool can provide the resources on the basis of calculation, storage, network and a single operating system etc..

The automated management system layer is the underlying service based on IaaS. The layer includes a set of middleware service such as user registration, service scheduling, unified authentication, search engine, load management, unified authorization, log statistics and service register.

The service layer is a set of services based on IaaS layer and the automated management system layer. This layer consists of PaaS, DaaS and SaaS. PaaS provides the cloud application development platform which includes application development, application testing and application hosting. DaaS provides data service for users by the open interface. SaaS is a software application model which provides cloud application service by the Internet transmission (Chen Chen et.al, 2012).

3 The Cloud Service Mode and Construction Content of Agricultural Information Institutions

Cloud service requires not only depth investment in hardware and virtualization software but also high-level technical staff. So agricultural information institutions should be guided by the demand and focus on DaaS and SaaS.

3.1 Virtualization of Hardware Resources as IaaS to Improve Resource Utilization

For internal business, the existing hardware equipment should be deployed and managed by virtualization to provide a basic customized platform Including CPU, memory, storage, network resources etc.. Based on the platform, users can deploy and run the operating system and applications. Data center is responsible for hardware maintenance, resource allocation and operation monitoring. The construction mode of combining the business solutions and self-developed scheme should be adopted. Construction steps are proposed to implement step-by-step according to the demand of business and cloud computing technology study.

3.2 Building the Integrated Development Environment as PaaS to Improve the Management Efficiency

For internal developers, the integrated development environment based on virtualization should be built to manage unified development, storage, testing etc.. By integrating the procedures and tools including database, Web server, network storage space, package class libraries, third party application module, debugging tools, version control etc., developers can use the highly reusable architecture.

3.3 The Data Access by Opening Data Interface as DaaS to Produce the Advantage of Agricultural Information Resources

After many years of accumulation, agricultural information institutions have owned rich research achievements and information resources. Agricultural information institutions have also the social responsibility to help those public service institutions which have not full resources and sufficient funds in order to carry out effective information service and enhance the value and influence of information resources. Standard interface can be opened for the domestic public information service institutions or group users. Users can embed the information resources into their local information service platform by standard interface. The query submitted by the user can be dynamically mapped to local and remote information sources so as to achieve one-stop access to local resources and remote resources.

3.4 Opening Software as SaaS to Make Full Use of the Software Resources of Agricultural Information Institutions

Agricultural information institutions should play their technology advantage to provide the network software with independent intellectual property rights as renting services for the organizations which have not strong technical strength. SaaS can carry out from three aspects. Firstly, only software can be rented and databases are constructed by users own. For example, users can rent the web content management system, scientific research projects management systems etc.. Secondly, software and data can be rented together. This is using software based on databases. For example, users can rent the intelligence analysis system, knowledge service system etc.. Thirdly, several institutions establish the sharing system together. The one which owns stronger technical strength provides software and all institutions co-construct data resources. For example, many libraries carry out joint reference, the original offer, check by services and so on (Xiaobo Xiao et.al, 2012) .

4 Application Case

National science and technology library (NSTL) is a united service organization of national science libraries in various fields covering science, engineering, agriculture, medicine. After 10 years of development, NSTL has developed a number of application systems with independent intellectual property rights, more than 40 databases and 180 million records. With the development, the current main business of NSTL is stable (Xiaodong Qiao et.al, 2010). But new service mode is needed to improve the utilization and the competitiveness of resources, to reduce the maintenance cost of equipment and personnel, and to reduce the workload of system maintenance.

According to the existing conditions and future development goals, suitable cloud service mode based on the cloud service model of agricultural information institutions is designed for the internal member institutions and the readers. Firstly, IaaS is provided for internal business by virtualizing servers and storage devices. The third

phase system, traceback system, citation system, monitoring system can be deployed in a virtual machine to guarantee system continuity effectively. And new applications can be deployed quickly so as to improve work efficiency. Secondly, by establishing virtual centers and virtual service stations, integrated development and operation environment as PaaS is provided for 9 member institutions and 50 service stations all over the country. The management efficiency is improved greatly and the performance of NSTL platform is improved. Thirdly, DaaS is provided to public information organizations in china by the open standard interface. Thus the organizations whose resources are not full and funds are not sufficient can access to NSTL resources more conveniently. Forth, softwares with independent intellectual property rights are made full used as SaaS. Federal libraries can use information analysis tools and knowledge service tools based on federate databases.

5 Conclusions

As a new service mode, cloud services become the growth point of the service innovation of agricultural information institutions. However, limited by the technology, cloud platforms provided by the current domestic IT manufacturers need the same physical equipments in brand, machine model, configuration and so on. Thus the original brand equipment can be not used, which is contrary to the original intention of resources conservation of cloud computing. So cloud services should be guided by the demand and constructed in accordance with the principle of pilot first, implement step by step, steady transition, comprehensively promote. And the construction of talent team should be strengthened and specialized technical personnel should be fostered to keep track of the development of cloud computing technology sustainably so as to make technical preparations for large-scale cloud services.

Acknowledgment. Funds for this research was provided by project of national science and technology library “Research on cloud service mode and construction of cloud computing service platform for NSTL (2012XM02)”.

References

1. OCLC News release. OCLC announces strategy to move library management services to Web scale, April 23- May 15(2009), <http://www.oclc.org/news/release/200927.htm>
2. Qiao, X., Liang, B., Li, Y.: NSTL strategic positioning, the recent advances and future development planning. NSTL Special Issue for 10 Years (Digital Library Forum) (10), 11-17 (2010), <http://www.dlf.net.cn>
3. Wang, W., Chen, L.: The Model of CALIS Cloud Service Platform for Distributed Digital Libraries. *Journal of Academic Libraries* 4, 13-18 (2009)
4. Chen, C., Wu, W.: A Research on Cloud Services Pattern Architecture and Innovation for Digital Library Under Cloud Computing Environment. *Research on Library Science* 13, 70-74 (2012)
5. Xiao, X., Shao, J., Zhang, H.: The third Phase SaaS Platforms and Cloud Services of CALIS. *Library and Information Service Online* 3(52), 52-56 (2012)

Impact of Simulated Irrigation with Treated Wastewater and Saline-Sodic Solutions on Soil Hydraulic Conductivity, Pores Distribution and Fractal Dimension

Fangze Shang, Shumei Ren, Tian Zou, Peiling Yang, and Nuan Sun

College of Water Resources and Civil Engineering, China Agricultural University,
Beijing 100083, China

{shangfangze, renshumei, zoutian066, yangpeiling}@126.com,
aile007@yeah.net

Abstract. Irrigation with treated wastewater which has the characteristics of higher salt content, larger sodium adsorption ratio (SAR), and more organic matter and suspended particles can cause the deterioration of the soil environment. Ordinary water, treated wastewater, and saline-sodic solutions with SAR = 3, 10 and 20 ($\text{mmol}_c\cdot\text{L}^{-1}$)^{0.5}, respectively, were used as five irrigation water types, and the changes of soil saturated hydraulic conductivity (K_s), soil pores distribution, and soil pores single fractal dimension (D_m) were studied after simulated irrigation for 1 and 2 years with simulated irrigation systems, which consisted of soil bins and simulated evaporation systems. The results showed that soil K_s in the following descending order: CK > SAR3 > WW > SAR10 > SAR20, and the adverse effects on soil K_s caused by suspended solid particles and dissolved organic matter might play a more significant role than sodium in treated wastewater. The 0-5 cm soils had a smaller single soil pore area but larger pores quantity after simulated irrigation, the distribution of soil pores which was irrigated with treated wastewater had a smaller change compared with saline-sodic solutions treatments, and it showed the soil pores structure binary image was an effective method to analysis soil pores distribution. Soil D_m increased after simulated irrigation, and the smallest was the soil simulated irrigation with treated wastewater for 1 year, because the plugging and filling of suspended particles and dissolved organic matter in treated wastewater made the soil pores well distributed, but the soil D_m did not increase with increasing of SAR levels in irrigation waters. The relative SAR levels irrigation to soils and soil K_s had a good linear correlation relationship, while the relationship between soil D_m and the relative SAR levels irrigation to soils was very complicated. The soil D_m which calculated from soil binary images could not well reflect the hydraulic conductivity of saturated soil. Irrigation with treated wastewater had a greater effect on soil K_s than soil D_m , comparing with saline-sodic solutions which had the similar SAR value. It was suggested that the future research should consider both the horizontal and vertical directions of soil D_m to well reflect the soil K_s .

Keywords: treated wastewater, sodium adsorption ratio (SAR), soil saturated hydraulic conductivity (K_s), soil pore distribution, soil pore single fractal dimension (D_m), simulated irrigation.

1 Introduction

China is one of the world's 13 severe water shortage countries, and it is also a large agricultural country, thus the shortage of water resources and the huge consumption of water in agriculture becomes a contradiction. The use of treated wastewater for agricultural irrigation provided a way to solve this contradiction [1]. However, the use of treated wastewater can cause the deterioration of the soil environment, such as soil saturated hydraulic conductivity (K_s) decrease and soil pore structure change.

The treated wastewater had the characteristic of higher salt content, larger sodium adsorption ratio (SAR), and more organic matter and suspended particles. For soils irrigation with saline-sodic water, the swelling and dispersion of clay particles were two major mechanisms responsible for reduction in hydraulic conductivity, and the plugging of soil pores by dispersed clay particles was a major cause [2-5]. But for soils irrigation with treated wastewater, organic matter and suspended particles caused physical and biological plugging to soil pores, and had more complex effect to soil hydraulic conductivity [6-7]. Some studies showed that when salt concentration was smaller than flocculating value of soil clay particles, the main factors which affect soil K_s was the dispersion of soil clay particles, while salt concentration was larger than flocculating value of soil clay particles, the main factors affect soil K_s was the swelling of clay soil particles [8]. High SAR in irrigation water had different effects on different soils, and many studies showed it had a larger effect on loam soil than sandy soil [9-11], which meant that the swelling and dispersion of clay particles had positive correlation with salt content and SAR in soil solutions. However, Singh et al [12] showed that the increase of SAR did not necessarily cause the decrease of soil hydraulic conductivity, after irrigation with water of SAR = 20 and 40, the soil K_s reduced by 12% and 7%, respectively, and when irrigation water with high salinity and SAR, the hydraulic conductivity did not reduce significantly. Therefore, the relationship between the irrigation water with different SAR levels and soil K_s is still less known.

Irrigation with high SAR water may cause the change of soil pores, and fractal dimension is an important index that describes the soil pores. Mandelbort [13] first proposed fractal theory was a nonlinear science theory which description the system that very complicated but had the scale invariance, and laid the foundation for using fractal theory study soils. Tyler and Wheatcraft [14] first applied the fractal geometry method to study the soil physics, and showed that soil pore shape had fractal characteristics, thus could describe by the fractal dimension. Perrier et al [15] also showed that soil pores structure exist self-similar phenomena, and showed an obvious fractal characters. Many studies used fractal method to carry on various researches about soil pores [16-19]. Some studies used image analysis to study soil pores structure [20-21]. Single fractal dimension and multifractal dimension had their respective advantages and disadvantages, and the single fractal dimension could describe the soil pores on the whole [22-25]. However, the study on the impact of long-term irrigation with different SAR levels waters on soil K_s and the fractal dimension are less, and the relationship between irrigation water SAR, soil K_s and the fractal dimension are also less known.

To our knowledge, the relationship between irrigation water SAR, soil K_s and the fractal dimension are less studied, and the difference among ordinary water, treated wastewater and saline-sodic water on soil physical property are also less known. Thus, our objectives were: (1) to compare the impact of simulated irrigation with treated wastewater and saline-sodic solutions with different SAR levels on soil K_s , soil pores distribution and soil fractal dimension; (2) to explore the relationship between irrigation water SAR levels, soil K_s and fractal dimension.

2 Experiments and Methods

2.1 Simulated Irrigation Systems

The experiment was conducted in the experiment hall in the college of water resources and civil engineering of China Agricultural University during September to December, 2011. Simulated irrigation systems consisted of soil bins and simulated evaporation systems. The soil bins were built by clay soil, and daub cement on four sides of the soil bins, a total of five soil bins were built, and each had a length of 1.2 m, width of 1.2 m and high of 1.5 m. Waterproof adhesive were daubed at inside and the bottom of the soil bins, and form 1 mm thick waterproof layer. The soil bins bottom slope was 5^0 , from down to up laid permeable fabric and inverted filter at the bottom of soil bins, and the inverted filter was made by quartz sand. After laid permeable fabric and inverted filter, 40 cm thick sandy soil was filled, then 80 cm thick loam was filled. The sandy soils were taken from Daxing district of Beijing, and the loam were taken from Tongzhou district of Beijing. In order to ensure tightly compacted soil bins, the soils were first through the 2 mm screen and slightly wetted and carefully mixed before packing. The soil bins were subsequently packed layer by layer in increments of 2 cm according to the actual field soil bulk density. The initial physical and chemical properties of experiment soils were listed in table 1. Simulated evaporation systems were including the first support, electric fan, distribution box, the second support and 275 W infrared light bulbs that installed in the second support. The first support erected in the upper part of the soil bin, and electric fan hanging in the first support. The second support fixed in the first support, and located below of the electric fan, three infrared light bulbs fixed on the two second support, respectively, electric fan and infrared light bulbs connected with distribution box through the wire, respectively. Simulated irrigation systems schematic diagram were shown in Fig. 1.

Table 1. Initial physical and chemical properties of experiment soils

Soil types	pH	EC	Bulk density	Sand	Silt	Clay	Organic C
		($\text{dS}\cdot\text{m}^{-1}$)	($\text{g}\cdot\text{cm}^{-3}$)	%			
Loam	8.3	0.27	1.4	54.04	36.85	9.11	0.42
Sandy soil	8.4	0.25	1.4	88.48	8.13	3.39	0.19

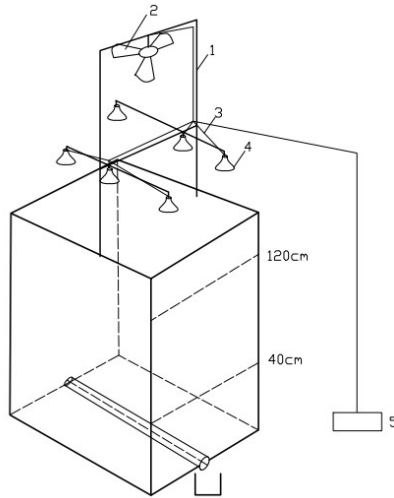


Fig. 1. Simulated irrigation systems schematic diagram (1: the first support; 2: the electric fan; 3: the second support; 4: the 275 w infrared light bulbs; 5: the distribution box)

2.2 Experimental Design

The treated wastewater was secondary precipitation water that taken from Qinghe sewage treatment plant of Beijing, ordinary water was tap water that taken from China Agricultural University. Using treated wastewater, ordinary water and deionized water to configurate five kinds of different SAR levels water. According to formula (1), quantitative NaCl and CaCl₂ (reagent grade) were added in deionized water to configurate saline-sodic solutions with SAR = 3, 10 and 20 (mmol_c·L⁻¹)^{0.5}, respectively. CK, WW, SAR3, SAR10 and SAR20 denoted ordinary water, treated wastewater, and saline-sodic solutions with SAR = 3, 10 and 20 (mmol_c·L⁻¹)^{0.5}, respectively. Relevant chemical characteristics of the five irrigation waters were presented in table 2. With reference to the winter wheat and summer corn irrigation quota in Beijing plain at normal rainfall, the winter wheat irrigation quota was 200 mm and 4 times irrigation, and the summer corn irrigation quota was 30 mm and 1 time irrigation in farmland, thus simulated irrigation water for each soil bin was 330 L for 1 year, irrigation water was 66 L at each soil bin at each time, and after 5 and 10 times irrigation, it means simulated irrigation for 1 and 2 years, respectively. After irrigation water for 66 L at each soil bin, electric fan opened 8 hours every day, and opened infrared light bulbs for 0.5 hour at the second, fourth, sixth and eighth day, respectively, 10 days later, irrigation with the same water again, a total of 10 times of cycle irrigation were conducted. After simulated irrigation for 1 and 2 years, sampling surface soil with cutting ring in order to measure soil K_s , three repetitions, and sampling 0-5 cm surface soil with density cutting ring to analysis soil fractal dimensions. CK-1, WW-1, SAR3-1, SAR10-1 and SAR20-1 denoted treatments that simulated irrigation for 1 year with ordinary water, treated wastewater, and saline-sodic solutions with SAR = 3, 10 and 20 (mmol_c·L⁻¹)^{0.5}, respectively, and CK-2,

WW-2, SAR3-2, SAR10-2 and SAR20-2 denoted treatments that simulated irrigation for 2 year with ordinary water, treated wastewater, and salt solutions with SAR = 3, 10 and 20 ($\text{mmol}_c\cdot\text{L}^{-1}$)^{0.5}, respectively.

$$\text{SAR} = \frac{\text{Na}^+}{\sqrt{\text{Ca}^{2+} / 2}} \quad (1)$$

Table 2. Important chemical characteristics of the five water types used during simulated irrigation

Parameter	Irrigation water type				
	CK	WW	SAR3	SAR10	SAR20
pH	7.84	7.78	8.2	7.56	7.02
EC($\text{dS}\cdot\text{m}^{-1}$)	713.5	994	965	1043	1245
SAR($\text{mmol}_c\cdot\text{L}^{-1}$) ^{0.5}	0.74	2.75	3	10	20
K ⁺ ($\text{mg}\cdot\text{L}^{-1}$)	8	8.91	0	0	0
Ca ²⁺ ($\text{mg}\cdot\text{L}^{-1}$)	52.36	96.59	286.93	83.25	25.27
Na ⁺ ($\text{mg}\cdot\text{L}^{-1}$)	14.5	106.13	282.55	497.25	558.35
Mg ²⁺ ($\text{mg}\cdot\text{L}^{-1}$)	18.91	40.66	0	0	0
Cl ⁻ ($\text{mg}\cdot\text{L}^{-1}$)	22.9	105	355	355	355
SO ₄ ²⁻ ($\text{mg}\cdot\text{L}^{-1}$)	75	104	0	0	0
HCO ₃ ⁻ ($\text{mg}\cdot\text{L}^{-1}$)	142	242	0	0	0
TSS ^a ($\text{mg}\cdot\text{L}^{-1}$)	3.5	21.3	0	0	0
BOD ^b ($\text{mg O}_2\text{ L}^{-1}$)	1.1	12.6	0	0	0
COD ^c ($\text{mg O}_2\text{ L}^{-1}$)	3.5	39.3	0	0	0

^aTSS = total suspended solids, ^bBOD = biological oxygen demand, ^cCOD = chemical oxygen demand

2.3 The Soil K_s Equation

In the measurement of soil K_s , the water flow was continuous, and the water temperature difference did not exceed 2⁰C, and could be considered as isothermal, thus the experiment met the requirement of Darcian law's laminar flow conditions, according to Darcian law formula (2), and combined with formula (3), we could launch soil K_s formula (4) in constant head:

$$q = K_s \frac{\Delta H}{L} \quad (2)$$

$$q = \frac{Q}{At} \quad (3)$$

$$K_s = \frac{QL}{A\Delta Ht} \quad (4)$$

Where q denoted water flux; K_s denoted soil saturated hydraulic conductivity; ΔH denoted total head of seepage path; L denoted straight line length of seepage path; Q denoted water volume; A denoted cross-sectional area of seepage and t denoted seepage time.

2.4 Soil Thin Section Preparation

The soil thin section was made in the laboratory in the college of Materials Science and Technology of China University of Geosciences (Beijing). Preparation of soil thin sections was undertaken using standard procedures adapted from the method described by Murphy [26] and Guan et al [20]. Use density cutting ring to get 0-5 cm surface soil samples, collected samples were dried at 60 °C-80 °C in drying oven until water was completely evaporated, then cooled the samples to 40 °C, and took out the samples, then cut the intermediate section, and using coarse sandy paper (120[#]) to polish the soil until the soil thickness was 1 cm, then heated the samples to about 80 °C, afterwards, put epoxy resin and triethanolamine into the beaker at the ratio of 10:1, and heated them as curing agent, then put the samples into the beaker, made curing agent to penetrate completely into the samples. After that, put the samples on plate glass and fine grinding to 2 mm with emery. Put chromic oxide and oxalic acid into the beaker at the ratio of 3:1, added distilled water, and stir well as polishing liquid, using this polishing liquid to polish samples. At the end of the whole process, a soil thin section with side length of 7 mm, and thickness of 2 mm was obtained.

2.5 Digital Image Acquisition

The digital images were made in National Nonferrous Metal and Electronic Material Analysis Test Centre in General Research Institute for Nonferrous Metals of China. The digital images were obtained using a JEOL JSM-6510 scanning electronic microscope (SEM), and its resolution is 3.0 nm, magnification is 5X-300000X. A JS-1600 Small ion sputtering apparatus was also used in combined with scanning electronic microscope (SEM). The whole electronic micrograph was enlarged 55 times, then chosen areas were enlarged 200, 2000 and 5000 times. These three magnifications were compared, and the 200 times image was chosen as the image best representing soil structure [20]. The digital form of the picture was a grey level picture.

2.6 Image Segmentation

The goal of the soil image segmentation was extraction parameters from soil particles and pores, and quantitative analysis. The average grey value of edge point pixel method as image segmentation threshold value was used [27], and then used global threshold method to segmentation grey image, and then converted the segmentation grey image to binary image. In the soil binary images, the soil pores was black and solid was white. The threshold value of soil images was shown in table 3.

Table 3. The threshold value of soil images

Type	Threshold value	Type	Threshold value
CS ^a	61	SAR3-1	53
CK-1	66	SAR3-2	78
CK-2	66	SAR10-1	54
WW-1	59	SAR10-2	54
WW-2	81	SAR20-1	54
		SAR20-2	74

^aCS = initial soil

2.7 Calculation Methods of Soil Single Fractal Dimension

Soil single fractal dimension (D_m) quantitative described the complexity of the soil fractal, and the characteristic of soil fractal. Small island method was used to calculate soil D_m . Mandelbrot et al [28] pointed:

$$\alpha_d(\varepsilon) = \frac{L^D(\varepsilon)}{A^2(\varepsilon)} \quad (5)$$

$$\log L(\varepsilon) = D \log \alpha_d(\varepsilon) + \frac{D}{2} \log A(\varepsilon) = C + \frac{D}{2} \log A(\varepsilon) \quad (6)$$

Where C was a constant, and $D_m = 2 * D / 2$ was the soil single fractal dimension [29].

3 Results and Discussion

3.1 Effects of Irrigation with Treated Wastewater and Saline-Sodic Solutions with Different SAR Levels on Soil K_s

Effect of different irrigation waters on soil K_s was shown in Fig. 2. It can be observed that after simulated irrigation for 1 and 2 years later, soil K_s in the following descending order: simulated irrigation with CK > SAR3 > WW > SAR10 > SAR20, which meant the irrigation water types and SAR levels in waters determined the soil K_s , but the irrigation frequency did not affects the soil K_s , and the soil K_s decrease amplitude of simulated irrigation for 2 years was smaller than 1 year. Compared with initial value of the soil K_s , after simulated irrigation for 1 year, the K_s of all treatments decreased significantly, because irrigation water caused the certain scour to surface soil and changed the soil structure. In the circumstance of irrigation water with the approximately equal SAR level, the soil K_s irrigation with treated wastewater was smaller than saline-sodic solutions, it might be the reason that the soil pores block caused by suspended solid particles, and the dispersion of soil caused by dissolved organic matter had a greater effect on soil structure than the dispersion of soil clay and aggregate caused by sodium in treated wastewater. The soil K_s irrigation with

saline-sodic solutions had the descending order: simulated irrigation with SAR3 > SAR10 > SAR20, and the higher level of SAR in irrigation solutions, the smaller of the soil K_s , and similar effects on soil hydraulic conductivity had been reported [8].

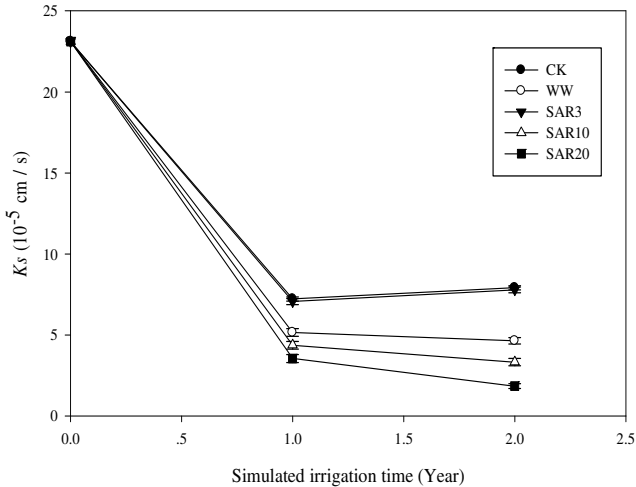


Fig. 2. Effects of irrigation waters on soil K_s

3.2 Effects of Irrigation with Treated Wastewater and Salin-Sodic Solutions with Different SAR Levels on Soil Pores Distribution

Soil binary images after simulated irrigation for 1 and 2 years was shown in Fig. 3. In the soil binary images, the soil pores was black and solid was white. CS was the soil initial binary image, it had the largest area of single soil pore and decreased gradually from outside to inside, but its pores quantity were increasing. CK-1 and CK-2 binary images had the similar soil pores distribution, and except for a few macro-pores, many pores had a small area, and the macro-pores unevenly distributed in the small pores. WW-1 and WW-2 binary images also had the similar soil pores distribution, most of the pores had the same area, but compared with WW-2, WW-1 binary image had a smaller average pores area. SAR3-1 and SAR3-2 binary images had a great difference in soil pores distribution, after simulated irrigation for 1 year, the soil pores distribution looked like continuous rolling mountains, but after simulated irrigation for 2 years, the single pore area of a few soil pores became larger. SAR10-1 and SAR10-2 binary images also had a great difference in soil pores distribution, compared with simulated irrigation for 1 year, all soil macro-pores disappeared after simulated irrigation for 2 years. As for SAR20-1 and SAR20-2 binary images, compared with simulated irrigation for 1 year, soil macro-pores quantity increased almost 2 times, and the distribution of soil pores was relatively more uniform. Different irrigation soils had different pores distribution characteristics, which was similar with the findings of Li et al [30]. In conclusion, CS binary image had the largest area of single soil pore but the smallest pores quantity, after simulated irrigation for 1 and 2 years, all soil binary images had a smaller single soil pore area

but larger pores quantity. The distribution of pores irrigation with ordinary water and treated wastewater had the similar pores distribution after simulated irrigation for 1 and 2 years, respectively. In soil binary images irrigation with saline-sodic solutions, simulated irrigation frequency affected the distribution of pores, and at the different SAR levels, the change trend with irrigation frequency were also difference.

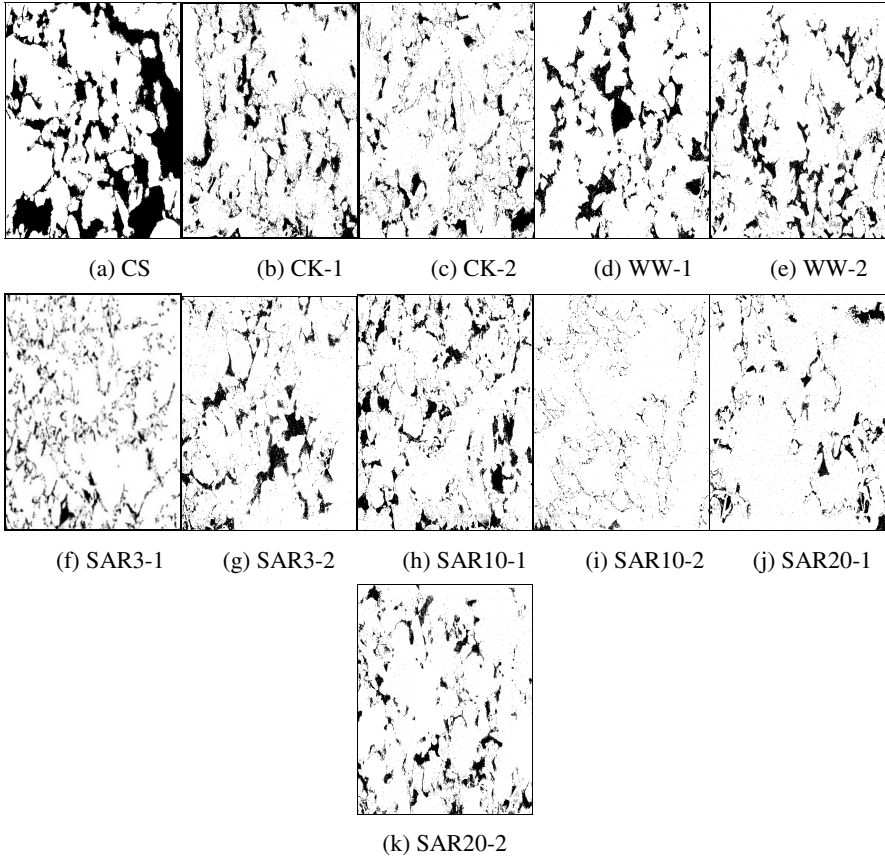


Fig. 3. The soil binary images (CS denoted initial binary image, -1 and -2 denoted soil binary image that simulated irrigation for 1 and 2 years, respectively, similarly hereinafter)

3.3 Effects of Irrigation with Treated Wastewater and Saline-Sodic Solutions with Different SAR Levels on Soil Pores Single Fractal Dimension

According to the formula (6), soil pores single fractal dimension (D_m) was twice as large as the slope of the double-log curve between $L(\varepsilon)$ and $A(\varepsilon)$. Soil D_m changed with different irrigation water was shown in Fig. 4. The slope of the fitting line (half of the D_m) in Fig. 4-CS was the smallest, the slope of the fitting lines were increased after simulated irrigation. Except for CK treatment, all other treatments had a larger slope after simulated irrigation for 2 years than 1 year. Except for the fitting line of

the CS and SAR10-2 had a R^2 with 0.891 and 0.835, respectively, all other treatments had a $R^2 \geq 0.900$, which meant $LogA(\varepsilon)$ and $LogL(\varepsilon)$ showed a good linear correlation relationship, and soil surface pores structure had a good self-similarity, namely fractal features. WW-1 and WW-2 had the biggest R^2 values, and simulated irrigation with treated wastewater had the best fitting effect.

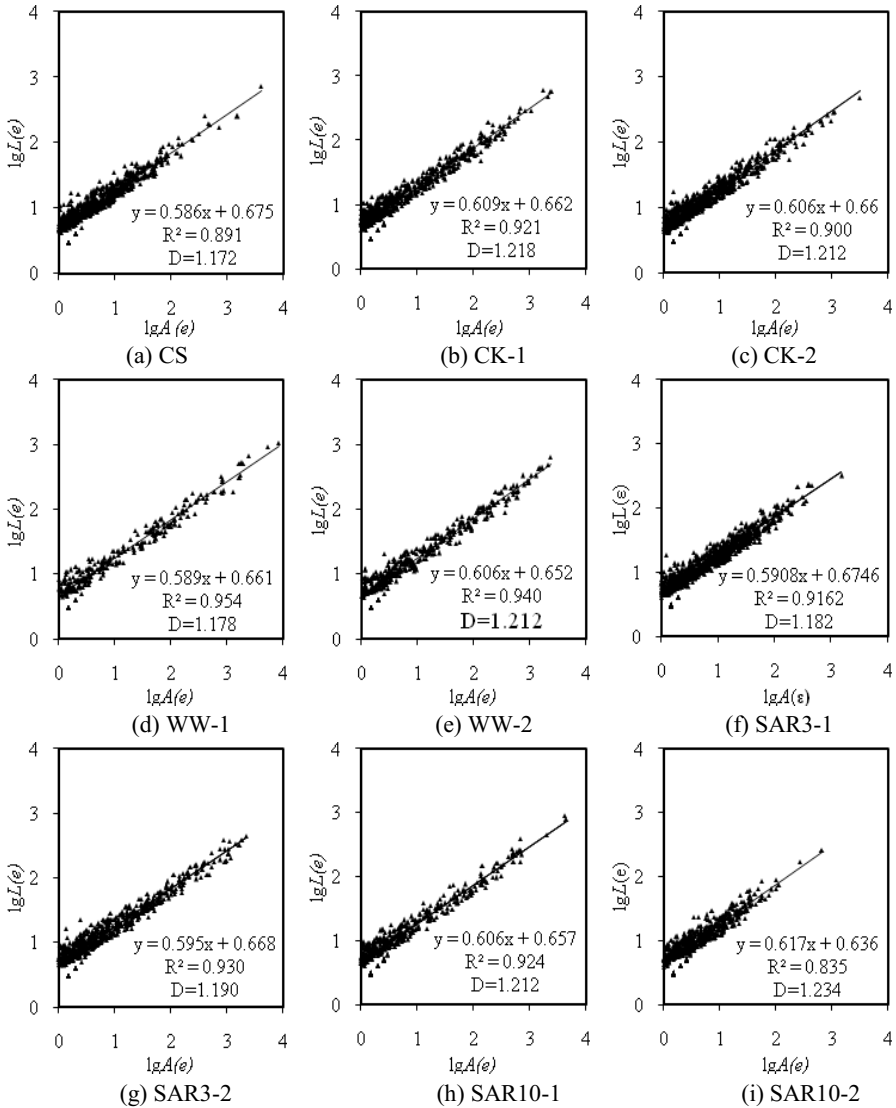


Fig. 4. Soil pores single fractal dimension (D_m) that based on digital image

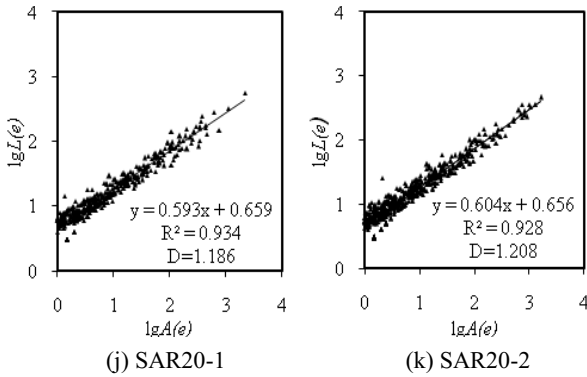


Fig. 4. (Continued.)

Soil D_m with different irrigation water and simulated irrigation time was shown in Fig. 5. Irrigation water changed the soil structure, and the soil D_m increased after simulated irrigation, which meant soil pores distribution became more complex. Except for CK treatment, soil D_m increased with the longer of simulated irrigation times. Soil D_m became the largest after simulated irrigation with ordinary water for 1 year, and irrigation with ordinary water caused the most serious erosion on surface soil. Soil D_m became the smallest after simulated irrigation with treated wastewater for 1 year, it might because the plugging and filling of suspended particles and dissolved organic matter in treated wastewater made the soil pore well-distributed. Among soils irrigation with saline-sodic solutions, SAR level of 10 had the largest soil D_m after simulated irrigation for 2 years, soil D_m did not increase with increasing SAR in irrigation waters. The accuracy of the soil D_m that obtained through the digital image analysis method depended on the discretion of resolution of grey scale image came from original soil thin section. In order to get more accuracy soil D_m , it was necessary to improve the discretion of resolution of soil thin section.

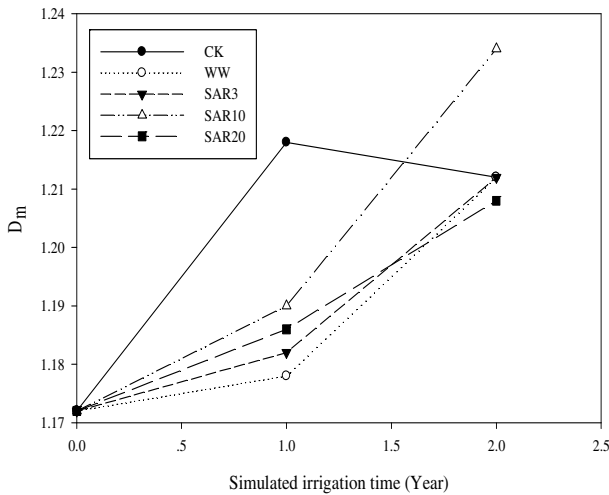


Fig. 5. Soil pores single fractal dimension (D_m) after simulated irrigation with different waters

3.4 The Correlation Relationship between Soil K_s , D_m , and Relative Values of SAR Irrigation to Soils

The correlation relationship between soil K_s , D_m and relative values of SAR irrigation to soils were shown in Fig. 6. The initial soil K_s and D_m data were not included in the Fig. 6. According to SAR levels in irrigation water and the time of simulated irrigation, the relative values of SAR irrigation to soils were set, and CK-1, CK-2, WW-1, WW-2, SAR3-1, SAR3-2, SAR10-1, SAR10-2, SAR20-1 and SAR20-2 was 0.74, 1.48, 2.75, 5.5, 3, 6, 10, 20, 20 and 40, respectively. The linear correlation relationship between soil K_s and the relative values of SAR was: $y (K_s) = -0.143x (SAR) + 6.855$, and $R^2 = 0.714$ (Fig. 6-A), which meant they had a good linear correlation relationship, and with the increase of SAR levels in irrigation waters and the longer of simulated irrigation times, the soil K_s linear decreased. The linear correlation relationship between soil D_m and the relative values of SAR was: $y (D_m) = 0.000x (SAR) + 1.200$, and $R^2 = 0.025$ (Fig. 6-B), which meant they had a very weak linear correlation relationship, and the relationship among soil D_m , the SAR levels of irrigation water and irrigation frequency were very complicated, the electrolyte concentration in saline-sodic water and special material in treated wastewater might all affect the soil D_m . The linear correlation relationship between soil D_m and the soil K_s was: $y (D_m) = 0.001x (K_s)^2 - 0.02x (K_s) + 1.247$, $R^2 = 0.142$ (Fig. 6-C), which meant they had a weak parabola correlation relationship. When used soil D_m represented soil pores structure of soil binary image based on the electron microscope scanning, it couldn't better reflect the relationship with soil K_s , because surface soil pores structure just reflected the distribution characteristics of soil pores on horizontal direction, and couldn't reflect the soil pores on the vertical direction.

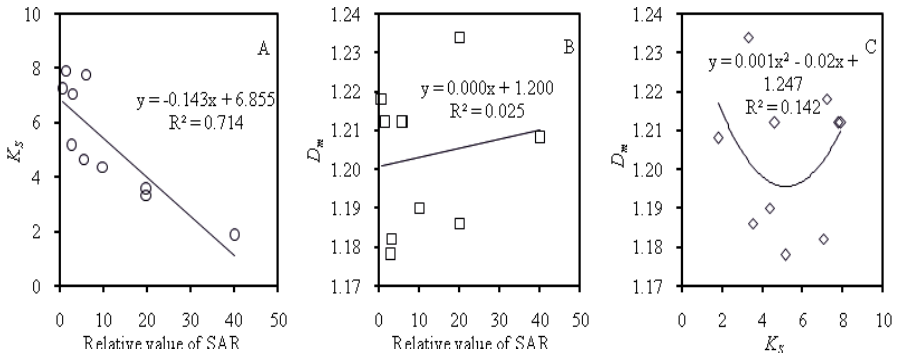


Fig. 6. The correlation relationship between soil K_s , D_m , and relative values of SAR in irrigation to soils (A: the correlation between the relative value of SAR and soil K_s ; B: the correlation between the relative value of SAR and soil D_m ; C: the correlation between soil K_s and D_m)

4 Conclusions

After simulated irrigation to soils in soil bins with ordinary water, treated wastewater and saline-sodic solutions with different SAR levels for 1 and 2 years, the results showed that soil K_s in the following descending order: simulated irrigation with CK > SAR3 > WW > SAR10 > SAR20, and the soil pores plugging caused by suspended solid particles, and the dispersion of soil caused by dissolved organic matter had a greater effect on soil structure than the dispersion of soil clay and aggregate caused by sodium in treated wastewater. After simulated irrigation, soils had a smaller single soil pore area but larger pores quantity, and the distribution of soil pores which was irrigated with treated wastewater had the similar pores distribution after simulated irrigation for 1 and 2 years, but for treatments irrigated by saline-sodic solutions, simulated irrigation frequency affected the distribution of pores, and with the difference of SAR levels, the change trend with time were also difference. The results also showed the soil pores structure binary image was an effective method to analysis soil pores. Soil D_m increased after simulated irrigation, and the smallest was the soil simulated irrigation with treated wastewater for 1 year, because the plugging and filling of suspended particles and dissolved organic matter in treated wastewater made the soil pore well-distributed, and the soil D_m did not increased with increasing of SAR in irrigation waters. Irrigation with treated wastewater had a greater effect on soil K_s than soil D_m , comparing with saline-sodic solutions which had the similar SAR. The relative values of SAR irrigation to soils and soil K_s had a good linear correlation relationship, while the soil D_m and the relative values of SAR irrigation to soils had a very weak linear correlation relationship. The soil D_m calculated from soil binary images could not well reflect the soil K_s , thus future research should consider both the horizontal and vertical directions of soil D_m to reflect the hydraulic conductivity of saturated soil.

Acknowledgment. Funds for this research was provided by the Public Welfare Project of Ministry of Water Resources of China (No.201101051), and the National Natural Science Foundation of China (No.51279204).

References

1. Yi, L., Jiao, W., Chen, X., et al.: An Overview of Reclaimed Water Reuse in China. *Journal of Environmental Sciences* 23(10), 1585–1593 (2011)
2. Minhas, P.S., Sharma, D.R.: Hydraulic Conductivity and Clay Dispersion as Affected by the Application Sequence of Saline and Simulated Rain Water. *Irrigation Science* 7(3), 158–167 (1986)
3. Minhas, P.S., Singh, Y.P., Chhabba, D.S., et al.: Changes in Hydraulic Conductivity of Soils Varying in Calcite Content under Cycles of Irrigation with Saline-Sodic and Simulated Rain Water. *Irrigation Science* 18(4), 199–203 (1999)
4. Sun, J., Kang, Y., Wan, S., et al.: Soil Salinity Management with Drip Irrigation and its Effects on Soil Hydraulic Properties in North China Coastal Saline Soils. *Agricultural Water Management* 115(4), 10–19 (2012)

5. Zhang, G., Chan, K.Y., Li, G.D., et al.: The Effects of Stubble Retention and Tillage Practices on Surface Soil Structure and Hydraulic Conductivity of a Loess Soil. *Acta Ecologica Sinica* 31(6), 298–302 (2011)
6. Gharaibeh, M.A., Eltaif, N.I., Al-Abdullah, B.: Impact of Field Application of Treated Wastewater on Hydraulic Properties of Vertisols. *Water, Air, and Soil Pollution* 184(1-4), 347–353 (2007)
7. Viviani, G., Iovino, M.: Wastewater Reuse Effects on Soil Hydraulic Conductivity. *Journal of Irrigation and Drainage Engineering* 130(6), 476–484 (2004)
8. Frenkel, H., Goertzen, J.O., Rhoades, J.D.: Effects of Clay Type and Content, Exchangeable Sodium Percentage, and Electrolyte Concentration on Clay Dispersion and Soil Hydraulic Conductivity. *Soil Science Society of America Journal* 42(1), 32–39 (1978)
9. Felhendler, R., Shainberg, I., Frenkel, H.: Dispersion and Hydraulic Conductivity of Soils in Mixed Solutions. In: *Proceedings of the Transition of the 10th International Congress of Soil Science*, pp. 103–112. Nauka Pub. House, Moscow (1974)
10. Lado, M., Ben-Hur, M.: Effects of Irrigation with Different Effluents on Saturated Hydraulic Conductivity of Arid and Semiarid Soils. *Soil Science Society of America Journal* 74(1), 23–32 (2010)
11. Mahdy, A.M.: Soil Properties and Wheat Growth and Nutrients as Affected by Compost Amendment under Saline Water Irrigation. *Pedosphere* 21(6), 773–781 (2011)
12. Singh, R.B., Minhas, P.S., Chauhan, C.P.S., et al.: Effect of High Salinity and SAR Waters on Salinization, Sodication and Yields of Pearl-Millet and Wheat. *Agricultural Water Management* 21(1-2), 93–105 (1992)
13. Mandelbort, B.B.: *The Fractal Geometry of Nature*, pp. 1–8. W. H. Freeman and Company, New York (1983)
14. Tyler, S.W., Wheatcraft, S.W.: Application of Fractal Mathematics to Soil Water Retention Estimation. *Soil Science Society of America Journal* 53(4), 987–996 (1989)
15. Perrier, E., Bird, N., Rieu, M.: Generalizing the Fractal Model of Soil Structure: The Pore-Solid Fractal Approach. *Geoderma* 88(3-4), 137–164 (1999)
16. Caruso, T., Barto, E.K., Siddiky, M.R.K., et al.: Are Power Laws that Estimate Fractal Dimension a Good Descriptor of Soil Structure and Its Link to Soil Biological Properties? *Soil Biology and Biochemistry* 43(2), 359–366 (2011)
17. Crawford, J.W., Pachepsky, Y.A., Rawls, W.J.: Integrating Processes in Soils Using Fractal Models. *Geoderma* 88(3-4), 103–107 (1999)
18. Dathe, A., Eins, S., Niemeyer, J., et al.: The Surface Fractal Dimension of the Soil-Pore Interface as Measured by Image Analysis. *Geoderma* 103(1-2), 203–229 (2001)
19. Zhao, S., Su, J., Yang, Y., et al.: A Fractal Method of Estimating Soil Structure Changes under Different Vegetations on Ziwuling Mountains of the Loess Plateau, China. *Agricultural Sciences in China* 5(7), 530–538 (2006)
20. Guan, X., Yang, P., Ren, S., et al.: Multifractal Analysis of Soil Structure under Long-Term Wastewater Irrigation Based on Digital Image Technology. *New Zealand Journal of Agricultural Research* 50(5), 789–796 (2007)
21. Vogel, H.J., Kretschmar, A.: Topological Characterization of Pore Space in Soil—Sample Preparation and Digital Image-Processing. *Geoderma* 73(1-2), 23–38 (1996)
22. Ahmadi, A., Neyshabouri, M.R., Rouhipour, H., et al.: Fractal Dimension of Soil Aggregates as an Index of Soil Erodibility. *Journal of Hydrology* 400(3-4), 305–311 (2011)
23. Bird, N., Díaz, M.C., Saa, A., et al.: Fractal and Multifractal Analysis of Pore-Scale Images of Soil. *Journal of Hydrology* 322(1-4), 211–219 (2006)

24. Dathe, A., Tarquis, A.M., Perrier, E.: Multifractal Analysis of the Pore-and Solid-Phases in Binary Two-Dimensional Images of Natural Porous Structures. *Geoderma* 134(3-4), 318–326 (2006)
25. Li, Y., Li, M., Horton, R.: Single and Joint Multifractal Analysis of Soil Particle Size Distributions. *Pedosphere* 21(1), 75–83 (2011)
26. Murphy, C.P.: *Thin Section Preparation of Soils and Sediments*, pp. 20–30. A. B. Academic Publishers, UK (1986)
27. Guan, X.: *The Quantitative Simulation of Soil Quality at Different Scales under the Reclaimed Water Irrigation*, pp. 42–45. China Agricultural University, Beijing (2009)
28. Mandelbrot, B.B., Passoja, D.E., Paullay, A.J.: Fractal Character of Fracture Surfaces of Metals. *Nature* 308(5961), 721–722 (1984)
29. Li, Y., Xu, T., OuYang, Z., et al.: Micromorphology of Macromolecular Superabsorbent Polymer and its Fractal Characteristics. *Journal of Applied Polymer Science* 113(6), 3510–3519 (2009)
30. Li, D., Velde, B., Zhang, T.: Study on Soil Pore Characteristics on Small Scale by Using Techniques of Serial Digital Images. *Acta Pedologica Sinica* 40(5), 521–528 (2003)

Author Index

- Bao, Nisha I-197
Bao, Zuda I-464
- Cai, Lixia II-89
Cao, Liying II-89, II-138
Cao, Weishi II-461
Chen, Congcong II-247
Chen, Dong I-478
Chen, Guifen II-89, II-138
Chen, Hang II-89
Chen, Honghui I-408
Chen, Huiping II-434
Chen, Jianshu I-32, I-41
Chen, Jiayu I-408
Chen, Jinliang II-10
Chen, Qingyu I-117
Chen, Tian'en I-434, II-34, II-177,
II-247, II-255
Chen, Yingyi I-348, II-523, II-534,
II-544
Chen, Yongjun II-282
Chen, Youjia II-222
Chen, Zhenghui I-197
Chen, Zilong I-380
Cheng, Shu-han I-152, I-160
Cheng, Xinrong I-215
Chi, Dezhao I-289
Cong, Hua I-380
Cui, Yuntao II-404
- Deng, Junwen I-215
Deng, Xiaohui II-50
Dian, Songyi II-513
Ding, Wen I-102
Ding, Zhaotang I-443
Dong, Guowei I-232
Dong, Jing II-34, II-177
Dong, Qin II-129
Dong, Wei I-226
Du, Jianjun II-290
Du, Jinsong I-306
Duan, Hua I-327
- Fa, Peng II-461
Fang, Chengjun I-168
- Fei, Biaoqing II-492
Feng, Wenjie I-61, I-443
Feng, Xianzhen II-381
Fränzel, Norbert II-552
Fu, Guohua I-10
Fu, Junqian II-50
Fu, Zetian II-453
- Gao, Wanlin II-404
Geng, Xia II-326
Gong, Zhenping I-25
Gu, Jihai I-16
Guo, Leifeng I-371, II-188
Guo, Lin I-337
Guo, Liqun II-114
Guo, Ping II-10
Guo, Tao I-232
Guo, Xinyu I-183, II-222, II-290
- Han, Ke II-478
Han, Nana II-70
Han, Xue II-434
He, Lu II-342
He, Lulu I-422
He, Xianbiao I-458
Hou, Lifan II-232
Hou, Peichen I-422
Hou, Xingjie II-1
Hu, Tian I-249
Hu, Xuelun II-523
Hua, Chunjian I-168
Hua, Su II-351
Huai, Heju II-165, II-198
Huang, Caojun II-478
Huang, Lijuan II-269
Huang, Lingmiao I-269, II-392
Huang, Shanyou I-458
Huang, Yan II-486
Huang, Zhenxiang II-114
- Ji, Haiyan I-206
Ji, Jianwei I-315
Jia, Honglei II-381
Jiang, Chong II-10
Jiang, Fubin I-422

- Jiang, Li-hua I-497, II-361
 Jiang, Meng I-152, I-160
 Jiang, Shuwen II-34
 Jin, Jianhua II-309
 Jin, Xiangyang I-16

 Kong, Qingfu I-61

 Li, Chao I-486
 Li, Chunan II-89
 Li, Cunjun II-165, II-198
 Li, Daoliang I-348, II-423, II-444,
 II-492, II-504
 Li, Heng I-486
 Li, Jingling I-117, I-190
 Li, Jin-lei I-281
 Li, Jun II-282
 Li, Lin I-175
 Li, Naixiang I-470
 Li, Shasha II-414
 Li, Shao-Ming I-175
 Li, Xinxing II-453
 Li, Xiufeng II-188
 Li, Yan I-69, I-393
 Li, Yang II-381
 Li, Ying I-197
 Li, Yunkai I-358
 Li, Zhenbo I-348
 Li, Zhongke I-90
 Li, Zhuo II-42
 Liang, Chunying I-315
 Liang, Taibo II-239
 Liang, Yong II-24, II-326, II-423
 Liang, Zhichao I-327
 Liu, Chen II-255
 Liu, Chunhong II-534
 Liu, Chunxi II-381
 Liu, Fengzhen II-212
 Liu, Hantao II-486
 Liu, Hao I-32, I-41
 Liu, Liangdong I-393
 Liu, Mei II-469
 Liu, Muhua I-249
 Liu, Pan II-269
 Liu, Pingzeng I-478
 Liu, Shuangxi II-444, II-461
 Liu, Tong II-469
 Liu, Tonghai II-42
 Liu, Weiming I-458, I-464
 Liu, Wu I-215

 Liu, Xianxi II-461
 Liu, Xiao II-10
 Liu, Xin I-160
 Liu, Xinhui II-381
 Liu, Xinyu II-232
 Liu, Yalin II-544
 Liu, Yande II-129
 Liu, Yueqin II-145
 Liu, Zhaohai I-348
 Liu, Zhe I-175
 Lü, Peng I-315
 Lu, Shenglian II-222
 Lu, Xin I-486
 Luo, ChangHai I-242
 Luo, Cheng II-42
 Lv, Xin I-289

 Ma, Guoqiang I-470
 Ma, Hongjian I-478
 Ma, Juncheng II-453
 Ma, Li II-138
 Ma, Shangjie I-337
 Ma, Yinchu I-102
 Mei, Hebo I-242
 Mei, Lin I-443
 Meng, Meng I-1
 Meng, Zhijun I-242
 Mu, Weisong II-351

 Ni, Weijian I-327, II-469

 Ouyang, Aiguo II-129

 Pang, Ming I-16
 Pei, Zhiyuan I-337
 Peng, Bo I-263, II-114
 Peng, Fa II-444, II-453, II-492

 Qi, Jiangtao II-381
 Qin, Guangming I-486
 Qin, Xiangyang II-198

 Ren, Shumei I-269, I-358, I-502, II-392
 Ren, Xiangrong I-380
 Ruan, Huaijun I-61, I-109, I-190

 Sang, Lingling II-370
 Schneider, Manuel II-552
 Shang, Fangze I-502
 Shang, Jiali I-337

- Shao, Changyong I-393
 Shen, Chang-jun I-281
 Shen, Lifeng II-504
 Shi, Leigang II-165, II-198
 Shi, Sijia I-25
 Shi, Xiaohui I-434
 Shi, Yanhua II-145
 Si, ChunJing I-52
 Sicheng, Jiang I-123
 Sun, Juanying I-337
 Sun, Li II-351
 Sun, Nuan I-502
 Sun, Qian II-24
 Sun, Shuhong I-69
 Sun, Tong I-249
 Sun, Zhiguo I-371, II-188
 Sun, Zhihui II-222
- Tan, Feng II-478
 Tan, Wei I-78
 Tan, Ying I-90
 Tang, Xianglin I-289
 Tang, Xin I-393
 Tang, Yan I-61, I-109
 Tao, Rong I-78
 Tao, Shishun II-282
 Teng, Guanghui II-42
 Tian, Zhihong II-434
 Ting, Huang I-123
 Tong, Xueqin I-109, I-226
- Wan, Yongshan II-212
 Wang, Baolin II-239
 Wang, Caiyuan I-358
 Wang, Cheng I-380, I-408, I-422
 Wang, Chengwen I-16
 Wang, Chuanyu I-183, II-290
 Wang, Cong II-34
 Wang, Dan I-497, II-79
 Wang, Decheng I-393
 Wang, Dengwei II-177
 Wang, Enguo I-458
 Wang, Fenghua I-401
 Wang, Fengyun I-61, I-443
 Wang, Guanghui I-393
 Wang, Hui I-16
 Wang, Jiabin I-1
 Wang, Jian I-145, I-450, II-158
 Wang, Jianlun I-32, I-41
 Wang, Jianwei II-239
- Wang, Jinbo II-404
 Wang, Jinfeng I-128, I-137
 Wang, Jinwu I-128, I-137
 Wang, Jinxing II-444, II-461
 Wang, Ke-wu I-281
 Wang, Lei I-190, I-443
 Wang, Lianzhi II-404
 Wang, Lili I-117
 Wang, Peidong I-242
 Wang, Shuting I-32, I-41
 Wang, Wensheng I-371, II-188
 Wang, Xi I-315
 Wang, Xiaodong I-408
 Wang, Xiaojuan I-470
 Wang, Xiguang II-61
 Wang, Xuechun II-282
 Wang, Yang II-444, II-453, II-492
 Wang, Yang-ren I-69, II-70, II-309,
 II-316
 Wang, Yaping II-129
 Wang, Yingbiao II-1
 Wang, Yonghao II-232
 Wang, Yubin II-434
 Wang, Yue II-138
 Wang, Zhaogai I-306
 Wang, Zhi-jun I-152, I-160
 Wang, Zhiqin I-393
 Wei, Yaoguang II-523, II-534, II-544
 Weichert, Frank II-552
 Weiskopf, André II-552
 Wen, Qian II-351
 Wen, Weiliang II-222
 Wu, Ding-feng I-145, I-450
 Wu, Juan I-263
 Wu, Qiulan II-326
 Wu, Sheng I-183, II-290
- Xi, Guiqing II-478
 Xi, Jiaqin II-239
 Xi, Zhiyong I-401
 Xiao, Boxiang I-183, II-290
 Xiao, Deqin II-50
 Xiao, Ming I-289
 Xie, Fangli II-158
 Xie, Guozhen II-247
 Xie, Neng-fu I-497, II-152, II-361
 Xu, Bin I-90
 Xu, Dan II-444, II-453, II-492
 Xu, Delong I-306
 Xu, Dongbo I-41

- Xu, Liming I-486, II-1
 Xu, Qianhui I-315
 Xu, Wenli I-249
 Xu, Xingzhen II-461
- Yang, Baozhu I-422
 Yang, Fang II-262
 Yang, Hao II-423
 Yang, Jianyu I-232
 Yang, Ju I-401
 Yang, Liu I-215
 Yang, Peiling I-269, I-358, I-502, II-392
 Yang, Senbin I-78
 Yang, Wenjun I-289
 Yang, Wenzhu I-348
 Yang, Xiaorong I-497, II-79
 Yang, Xinlun I-128
 Yang, Yong I-371, II-188
 Yang, Yongxi II-381
 Yang, Yujian I-109, I-117, I-190, I-226
 Ye, Baoying I-197
 Yi, Danqin I-206
 Yi, Tongchuan II-255
 Yin, Qisheng II-239
 You, Yong I-393
 Yu, Chunhua I-408
 Yu, Helong II-138
 Yu, Jian II-404
 Yu, Na II-342
 Yu, Ping II-98, II-301
 Yu, Ying II-165, II-198
 Yuan, Xiaoqing II-504
 Yun, Wenju II-370
- Zeng, Lihua II-453
 Zeng, Qingtian I-327, II-469
 Zhang, Changqing I-78
 Zhang, Chao II-370
 Zhang, Chen I-348
 Zhang, Chi II-247
 Zhang, Dongmei II-10
 Zhang, Fan II-534
 Zhang, Guangsheng I-300
- Zhang, Hong-bin II-361
 Zhang, Jie II-79, II-158
 Zhang, Jing II-158
 Zhang, Jiuwen I-422
 Zhang, Kun II-212
 Zhang, Licai II-523
 Zhang, Lingxian II-453
 Zhang, Ning II-145
 Zhang, Ruirui II-255
 Zhang, Xiaodong I-175
 Zhang, Xuefu II-152
 Zhang, Yan I-232
 Zhang, Yanling II-239
 Zhang, Yiding II-513
 Zhang, Yunfan I-478
 Zhang, Ze I-289
- Zhao, Chunjiang I-380
 Zhao, Dongmei II-98
 Zhao, Lijing I-393
 Zhao, Manquan II-145, II-486
 Zhao, Ming II-478
 Zhao, Wenxiang I-61, I-109
 Zhao, Xueguan II-1
 Zhao, Ying I-486
 Zhao, Zuliang I-175
 Zheng, Jiye I-443
 Zheng, Wen-gang I-281
 Zheng, Wensheng I-25
 Zheng, Xiaofei I-1
 Zhou, Guo-min I-450, II-158
 Zhou, Hanping II-239
 Zhou, Nan II-301
 Zhou, Qiuping I-10
 Zhou, Wei I-137
 Zhou, Xin-yang II-316
 Zhou, Zhijian II-351
- Zhu, Benjing II-212
 Zhu, Dazhou I-380, I-408, I-422
 Zhu, De-Hai I-175, II-370
 Zhu, Hailong I-401
 Zhu, Wenkui I-306
 Zou, Detang I-128, I-137
 Zou, Tian I-502